

**Molybdenum Mediated Synthesis of Pentathiepins – Potent Cytotoxic and Antimicrobial agents and Discovery of Novel Pd/PTABS Catalyst for The Synthesis of Pharmaceutically Relevant Drug Molecules via C–N, C–O, and C–S Cross-coupling**

I n a u g u r a l d i s s e r t a t i o n

zur

Erlangung des akademischen Grades eines  
Doktors der Naturwissenschaften (Dr. rer. nat.)

der

Mathematisch-Naturwissenschaftlichen Fakultät

der

Universität Greifswald

vorgelegt von

Bandaru Venkata Siva Sankar Murthy

geboren am 05 August 1985 in Indien

Greifswald, 2020

Dekan: Prof. Dr. Gerald Kerth

Gutachter: Prof. Dr. Carola Schulzke

Gutachter 1: Prof. Dr. Fuk Yee KWONG

Gutachter 2: Dr. Tatiana Besset

Tag der Promotion: 01-12-2020

*„Dream is not that which you see while sleeping, it is something that does not  
let you sleep “.*

*-APJ Abdul Kalam*

**Table of Content**

List of Abbreviations .....	xiv
<b>Chapter 1: Synthesis of novel heterocyclic fused pentathiepins and their cytotoxic and antimicrobial properties .....</b>	<b>1</b>
1.1 Introduction.....	1
1.1.1 Sulfur centered redox-networks and mechanistic pathways <i>in vivo</i> .....	1
1.1.2 Polysulfides: A particular class of bio-reductive drugs.....	3
1.1.3 Chemical reactivity of polysulfides and disulfides and biological significance .....	5
1.1.4 Reactive sulfur species: Pentathiepins.....	5
1.2 Biological significance of pentathiepins .....	6
1.3 Synthetic methodologies for pentathiepins .....	9
1.4 Overview.....	12
1.5 Results and Discussion .....	14
1.5.1 Quinoxalin fused pentathiepin family ( <b>7a-7f</b> ).....	14
1.5.2 Characterization of pentathiepins via NMR spectroscopy and mass spectrometry.	17
1.5.3 Pyrazine fused pentathiepin derivatives ( <b>10a-d</b> ).....	19
1.5.4 Imidazol-fused pentathiepin [8-ethoxy- [1,2,3,4,5]pentathiepino[6',7':3,4]pyrrolo[1,2-a]imidazo[2,1-c]pyrazine] ( <b>14</b> ).....	21
1.5.5 Pyridine fused pentathiepins ( <b>17a-b</b> ) .....	23
1.5.6 Nicotinamide fused pentathiepins ( <b>21a-21f</b> ) .....	23
1.5.7 Synthesis of 11-methoxy-2-(4-methoxyphenyl)-3H-[1,2,3,4,5] pentathiepino[6',7':3,4]pyrrolo[1,2-a]pyrrolo[2,3-e]pyrazine ( <b>25</b> ).....	25
1.5.8 Synthesis of 12-ethoxy-6a,6b-dihydro- [1,2,3,4,5]pentathiepino[6',7':3,4]pyrrolo[1,2-a]quinolone ( <b>28</b> ) .....	26
1.5.9 Synthesis of 3-benzyl-7-ethoxy-3H-[1,2,3,4,5]pentathiepino[6',7':3,4]pyrrolo[2,1- i]purine ( <b>33</b> ).....	28
1.5.10 Pyridine sulfanilamide pentathiepin derivatives ( <b>38a-e</b> ).....	29
1.6 X-ray crystal structure analysis.....	31
1.7 Mechanistic investigations.....	31
1.8 Biological investigations of novel pentathiepins .....	34
1.8.1 Oxidative stress and glutathione peroxidase .....	34
1.8.2 Biological activity of pyrrolo[1,2a]quinoxaline appended pentathiepins ( <b>7a-f</b> ) .....	37
1.8.3 Pyrazine fused pentathiepins' biological activity .....	41
1.8.4 Pyridine fused pentathiepins' biological activity .....	42

## Table of Content

1.8.5 Nicotinamide fused pentathiepins' biological activity .....	43
1.8.6 Biological activity of <b>25</b> , <b>28</b> , and <b>33</b> .....	46
1.8.7 Pyridine sulfonamide pentathiepins and their biological activity .....	49
1.8.8 Investigation of anti-microbial activity of novel pentathiepins in various pathogens. .....	50
1.9 Summary of biological activity of all investigated/novel pentathiepins.....	53
1.10 Conclusion .....	54
1.11 Experimental .....	57
1.11.1 Synthesis of precursors <b>3a-f</b> , <b>4a-f</b> , <b>12</b> , <b>A</b> , <b>B</b> , <b>19a-e</b> , <b>23</b> , <b>31</b> , <b>35</b> and <b>36a-e</b> .....	57
1.11.1.1. Synthesis of 7-methylquinoxalin-2(1H)-one ( <b>3b</b> ) and 6-methylquinoxalin- 2(1H)-one ( <b>3c</b> ) .....	57
1.11.1.2. Synthesis of 6-methyl-3-(trifluoromethyl)quinoxaline-2(1H)-one ( <b>3e</b> ) .....	58
1.11.1.3. Synthesis of 6, 7-dimethylquinoxalin-2(1H)-one ( <b>3d</b> ) .....	58
1.11.1.4. Synthesis of 6, 7-dimethyl-3-(trifluoromethyl)quinoxaline-2(1H)-one ( <b>3f</b> ) ...	58
1.11.1.5. Synthesis of 2-chloro-7-methylquinoxaline ( <b>4b</b> ) .....	59
1.11.1.6. Synthesis of 2-chloro-6-methylquinoxaline ( <b>4c</b> ) .....	59
1.11.1.7. Synthesis of 2-chloro-6-methyl-3-(trifluoromethyl)quinoxaline ( <b>4e</b> ).....	59
1.11.1.8. Synthesis of 2-chloro-6, 7-dimethylquinoxaline ( <b>4d</b> ) .....	59
1.11.1.9. Synthesis of 2-chloro-6, 7-dimethyl-3-(trifluoromethyl)quinoxaline ( <b>4f</b> ) .....	60
1.11.1.10. Synthesis of 6,8-dibromoimidazo[1,2-a]pyrazine ( <b>12</b> ).....	60
1.11.1.11. Synthesis of (4-fluorophenyl)(piperazin-1-yl)methanone ( <b>A</b> ) and 1- tosylpiperazine ( <b>B</b> ) .....	60
1.11.1.12. Synthesis of compounds <b>19a-e</b> .....	61
1.11.1.13. Synthesis of 2-bromo-6-(4-methoxyphenyl)-5H-pyrrolo[2,3-b]pyrazine ( <b>23</b> ) 62	
1.11.1.14. Synthesis of 9-benzyl-6-chloropurine ( <b>31</b> ) .....	62
1.11.1.15. Synthesis of 6-chloropyridine-3-sulfonyl chloride ( <b>35</b> ).....	63
1.11.1.16. 2-chloro-5-(piperidin-1-ylsulfonyl)pyridine ( <b>36a</b> ) .....	63
1.11.1.17. 4-((6-chloropyridin-3-yl)sulfonyl)morpholine ( <b>36b</b> ) .....	64
1.11.1.18. 6-chloro-N-[(2S)-3-methylbutan-2-yl]pyridine-3-sulfonamide ( <b>36c</b> ) .....	64
1.11.1.19. N-((3s,5s,7s)-adamantan-1-yl)-6-chloropyridine-3-sulfonamide ( <b>36d</b> ) .....	64
1.11.1.20. N-(benzo[d][1,3]dioxol-5-ylmethyl)-6-chloropyridine-3-sulfonamide ( <b>36e</b> ) 65	
1.11.1.21. N-benzyl-6-chloropyridine-3-sulfonamide ( <b>36f</b> ) .....	65

## Table of Content

1.11.2 General procedure for the Sonogashira cross-coupling-synthesis of <b>6a-f</b> , <b>9a-b</b> , <b>13</b> , <b>16a-b</b> , <b>20a-e</b> , <b>24</b> , <b>27</b> , <b>32</b> , <b>37a-f</b> .....	65
1.11.2.1. Synthesis of 2-(3,3-diethoxyprop-1-ynyl)-7-methylquinoxaline ( <b>6b</b> ) .....	65
1.11.2.2. Synthesis of 2-(3,3-diethoxyprop-1-ynyl)-6-methylquinoxaline ( <b>6c</b> ) .....	66
1.11.2.3. Synthesis of 2-(3,3-diethoxyprop-1-ynyl)-6-methyl-3-(trifluoromethyl)quinoxaline ( <b>6d</b> ).....	66
1.11.2.4. Synthesis of 2-(3,3-diethoxyprop-1-yn-1-yl)-6,7-dimethylquinoxaline ( <b>6e</b> )...	66
1.11.2.5. Synthesis of 2-(3,3-diethoxyprop-1-ynyl)-6,7-dimethyl-3-(trifluoromethyl)quinoxaline ( <b>6f</b> ) .....	67
1.11.2.6. 2-(3, 3-diethoxyprop-1-yn-1-yl)pyrazine ( <b>9a</b> ):.....	67
1.11.2.7. 2-(3, 3'-diethoxyprop-1-yn-1-yl)-3-ethoxypyrazine ( <b>9b</b> ):.....	67
1.11.2.8. Synthesis of 6-bromo-8-(3,3-diethoxyprop-1-yn-1-yl)imidazo[1,2-a]pyrazine ( <b>13</b> ) ..... ..67	
1.11.2.9. Synthesis of 2-(3, 3-diethoxyprop-1-yn-1-yl)pyridine ( <b>16a</b> ): .....	68
1.11.2.10. Synthesis of 1-(2-(3,3-diethoxyprop-1-yn-1-yl)pyridin-3-yl)ethan-1-one ( <b>16b</b> ): ..... .68	
1.11.2.11. Synthesis of (6-(3, 3-diethoxyprop-1-yn-1-yl)pyridin-3-yl)(piperidine-1-yl)methanone ( <b>20a</b> ).....	68
1.11.2.12. Synthesis of (6-(3,3-diethoxyprop-1-yn-1-yl)pyridin-3-yl)(morpholino)methanone ( <b>20b</b> ) .....	68
1.11.2.13. Synthesis of 6-(3,3-diethoxyprop-1-yn-1-yl)-N,N-diethylnicotinamide ( <b>20c</b> ) 69	
1.11.2.14. Synthesis of (4-(6-(3,3-diethoxyprop-1-yn-1-yl)nicotinoyl)piperazine-1-yl)(4-fluorophenyl)methanone ( <b>20d</b> ) .....	69
1.11.2.15. Synthesis of (6-(3,3-diethoxyprop-1-yn-1-yl)pyridin-3-yl)(4-tosylpiperazin-1-yl)methanone ( <b>20e</b> ).....	69
1.11.2.16. Synthesis of 2-(3,3-diethoxyprop-1-yn-1-yl)-6-(4-methoxyphenyl)-5H-pyrrolo[2,3-b]pyrazine ( <b>24</b> ) .....	69
1.11.2.17. Synthesis of 2-(3,3-diethoxyprop-1-yn-1-yl)quinolone ( <b>27</b> ) .....	69
1.11.2.18. Synthesis of 9-benzyl-6-(3,3-diethoxyprop-1-yn-1-yl)-9H-purine ( <b>32</b> ): .....	70
1.11.2.19. 2-(3,3-diethoxyprop-1-yn-1-yl)-5-(piperidin-1-ylsulfonyl)pyridine ( <b>37a</b> ):	70
1.11.2.20. 4-((6-(3,3-diethoxyprop-1-yn-1-yl)pyridin-3-yl)sulfonyl)morpholine ( <b>37b</b> ): 70	

## Table of Content

1.11.2.21.	6-(3,3-diethoxyprop-1-yn-1-yl)-N-[(2S)-3-methylbutan-2-yl]pyridine-3-sulfonamide ( <b>37c</b> ):	70
1.11.2.22.	N-((3s,5s,7s)-adamantan-1-yl)-6-(3,3-diethoxyprop-1-yn-1-yl)pyridine-3-sulfonamide ( <b>37d</b> ):	71
1.11.2.23.	N-(benzo[d][1,3]dioxol-5-ylmethyl)-6-(3,3-diethoxyprop-1-yn-1-yl)pyridine-3-sulfonamide ( <b>37e</b> ):	71
1.11.2.24.	N-benzyl-6-(3,3-diethoxyprop-1-yn-1-yl)pyridine-3-sulfonamide ( <b>37f</b> ):	71
1.11.3	Synthesis of pentathiepin derivatives <b>7a-f</b> , <b>10a-b</b> , <b>14</b> , <b>21a-e</b> , <b>25</b> , <b>28</b> , <b>38a-f</b>	71
1.11.3.1.	Synthesis of 12-ethoxy-2-methyl-[1,2,3,4,5]pentathiepino[6',7':3,4]pyrrolo[1,2-a]quinoxaline ( <b>7b</b> ):	72
1.11.3.2.	Synthesis of 6-methyl 10-ethoxy-pentathiepino-pyrrolo [1,2-a]quinoxaline ( <b>7c</b> )	72
1.11.3.3.	Synthesis of 6-methyl 10-ethoxy-3-(Trifluoromethyl)-pentathiepino-pyrrolo [1,2-a]quinoxaline ( <b>7e</b> )	72
1.11.3.4.	Synthesis of 12-ethoxy-2,3-dimethyl-[1,2,3,4,5]pentathiepino[6',7':3,4]pyrrolo[1,2-a]quinoxaline ( <b>7d</b> )	73
1.11.3.5.	Synthesis of 6, 7-dimethyl 10-ethoxy- 3-(trifluoromethyl)pentathiepino-pyrrolo [1,2-a]quinoxaline ( <b>7f</b> )	73
1.11.3.6.	11-ethoxy-[1,2,3,4,5]pentathiepino[6',7':3,4]pyrrolo[1,2-a]pyrazine ( <b>10a</b> )	73
1.11.3.7.	6,11-diethoxy-[1,2,3,4,5]pentathiepino[6',7':3,4]pyrrolo[1,2-a]pyrazine ( <b>10b</b> )	74
1.11.3.8.	Synthesis of 6-bromo-8-ethoxy-[1,2,3,4,5]pentathiepino[6',7':3,4]pyrrolo[1,2-a]imidazo[2,1-c]pyrazine ( <b>14</b> )	74
1.11.3.9.	6-ethoxy-[1,2,3,4,5]pentathiepino[6,7-a]indolizine ( <b>17a</b> )	74
1.11.3.10.	1-(6-ethoxy-[1,2,3,4,5]pentathiepino[6,7-a]indolizin-11-yl)ethan-1-one ( <b>17b</b> )	75
1.11.3.11.	(6-ethoxy-[1,2,3,4,5]pentathiepino[6,7-a]indolizin-9-yl)(piperidin-1-yl)methanone ( <b>21a</b> )	75
1.11.3.12.	(6-ethoxy-[1,2,3,4,5]pentathiepino[6,7-a]indolizin-9-yl)(morpholino)methanone ( <b>21b</b> )	75
1.11.3.13.	6-ethoxy-N,N-diethyl-[1,2,3,4,5]pentathiepino[6,7-a]indolizine-9-carboxamide ( <b>21c</b> )	76
1.11.3.14.	(6-ethoxy-[1,2,3,4,5]pentathiepino[6,7-a]indolizin-9-yl)(4-(4-fluorobenzoyl)piperazin-1-yl)methanone ( <b>21d</b> )	76
1.11.3.15.	(6-ethoxy-[1,2,3,4,5]pentathiepino[6,7-a]indolizin-9-yl)(4-tosylpiperazin-1-yl)methanone ( <b>21e</b> )	76

## Table of Content

1.11.3.16. Synthesis of 11-ethoxy-2-(4-methoxyphenyl)-3H-[1,2,3,4,5]pentathiepine[6',7':3,4]pyrrolo[1,2-a]pyrrolo[2,3-e]pyrazine (25).....	77
1.11.3.17. Synthesis of quinoline pentathiepin (28) .....	77
1.11.3.18. Synthesis of 3-benzyl-12-ethoxy-3H-[1,2,3,4,5]pentathiepine[6',7':4,5]pyrrolo[2,1-i]purine (33) .....	77
1.11.3.19. 6-ethoxy-9-(piperidin-1-ylsulfonyl)-[1,2,3,4,5]pentathiepine [6,7-a]indolizine (38a) .....	78
1.11.3.20. 4-((6-ethoxy-[1,2,3,4,5]pentathiepine[6,7-a]indolizine-9-yl)sulfonyl)morpholine (38b).....	78
1.11.3.21. 6-ethoxy-N-[(2S)3-methylbutan-2-yl]-[1,2,3,4,5]pentathiepine[6,7-a]indolizine-9-sulfonamide (38c) .....	79
1.11.3.22. N-((3s,5s,7s)-adamantan-1-yl)-6-ethoxy-[1,2,3,4,5]pentathiepine[6,7-a]indolizine-9-sulfonamide (38d) .....	79
1.11.3.23. N-(benzo[d][1,3]dioxol-5-ylmethyl)-6-ethoxy-[1,2,3,4,5]pentathiepine[6,7-a]indolizine-9-sulfonamide (38e) .....	80
1.11.3.24. N-benzyl-6-ethoxy-[1,2,3,4,5]pentathiepine [6,7-a]indolizine-9-sulfonamide (38f).....	80
<b>Chapter 2: Pd-catalyzed cross-coupling reactions in the synthesis of biologically relevant organic molecules – State of the art.....</b>	<b>82</b>
2.1. Background: Pd-catalyzed cross-coupling reactions .....	82
2.2. General mechanism for palladium catalysed cross-coupling reactions .....	85
2.3. Pd-catalyzed carbon-heteroatom cross-coupling reactions - mechanisms.....	86
2.3.1. Palladium catalyzed C–N bond formation.....	88
2.3.2. Palladium catalyzed C–O bond formation.....	96
2.3.3. Palladium catalyzed C–S bond formation.....	104
2.3.4. Palladium catalyzed C–P cross-coupling.....	109
2.4. Summary and prospective.....	112
<b>Chapter 3: The serendipitous discovery of the potent catalyst Pd/PTABS and application in C-X (X= N, O, S) cross-coupling of chloroheteroarenes under milder conditions.....</b>	<b>113</b>
3.1. The unexpected finding: acylation of chloroheteroarene and discovery of Pd/PTABS catalyst. .....	113
3.2. Pd/PTABS: Carbon-heteroatom (C–X, where X= N, O, and S) cross-coupling of chloroheteroarenes. ....	118



## Table of Content

3.3.	Pd/PTABS: The C–N cross-coupling of <i>chloroheteroarenes</i> with secondary amines at room temperature. ....	119
3.3.1.	Background.....	119
3.3.2.	Results and Discussion .....	120
3.3.3.	C–N cross-coupling reaction optimization .....	121
3.3.4.	Substrate scope development.....	123
3.4.	Pd/PTABS: The C–O cross-coupling of <i>chloroheteroarenes</i> with substituted phenols under milder conditions.....	131
3.4.1.	Background.....	131
3.4.2.	Results and discussion: C-O cross-coupling reaction optimization.....	132
3.4.3.	Substrate Scope development .....	134
3.5.	Pd/PTABS: The C–S cross-coupling of <i>chloroheteroarenes</i> with thiophenols and access to novel thioethers, sulfones and sulfoximines.....	144
3.5.1.	Background.....	144
3.5.2.	Results and discussion: C–S cross-coupling reaction optimization.....	145
3.5.3.	Substrate scope development.....	148
3.5.4.	Mechanistic Investigation and DFT (density-functional theory) studies.....	151
3.6.	Conclusion .....	155
3.7.	Experimental.....	157
	General.....	157
3.7.1.	Synthesis of PTA, PTABS, PTAPS, PTABX (X= Cl, Br, I) and PTABBn ....	157
3.7.2.	Pd/PTABS catalytic amination of <i>chloroheteroarenes</i> at ambient temperature. 160	
3.7.2.1.	2-(Pyrrolidine-1-yl)pyrazine ( <b>12a</b> ) .....	160
3.7.2.2.	2-Morpholinopyrazine ( <b>12b</b> ).....	160
3.7.2.3.	2-(Piperidin-1-yl)quinoxaline ( <b>12c</b> ) .....	160
3.7.2.4.	2-(Piperidin-1-yl)quinoxaline ( <b>12d</b> ).....	161
3.7.2.5.	2-Morpholinoquinoxaline ( <b>12e</b> ).....	161
3.7.2.6.	<i>N, N</i> -diethylquinoxalin-2-amine ( <b>12f</b> ).....	161
3.7.2.7.	8-(Piperidin-1-yl)imidazo[1,2- <i>a</i> ]pyrazine ( <b>12g</b> ).....	162
3.7.2.8.	8-(Pyrrolidin-1-yl)imidazo[1,2- <i>a</i> ]pyrazine ( <b>12h</b> ).....	162
3.7.2.9.	2-(Pyrrolidin-1-yl)benzo[ <i>d</i> ]oxazole ( <b>12i</b> ) .....	162
3.7.2.10.	<i>Tert</i> -butyl 4-(benzo[ <i>d</i> ]oxazol-2-yl)piperazine-1-carboxylate ( <b>12j</b> ) .....	163
3.7.2.11.	2-Morpholinobenzo[ <i>d</i> ]oxazole ( <b>12k</b> ).....	163

Table of Content

3.7.2.12.	2-(Piperidin-1-yl)benzo[d]oxazole ( <b>12l</b> ).....	163
3.7.2.13.	6-(Piperidin-1-yl)-9H-purine ( <b>12m</b> ) .....	164
3.7.2.14.	6-Morpholino-9H-purine ( <b>12n</b> ).....	164
3.7.2.15.	N, N'-diethyl-9H-purin-6-amine ( <b>12o</b> ) .....	164
3.7.2.16.	Tert-butyl 4-(9H-purin-6-yl)piperazine-1-carboxylate ( <b>12p</b> ) .....	164
3.7.2.17.	6-(Pyrrolidin-1-yl)-9H-purine ( <b>12q</b> ) .....	165
3.7.2.18.	7-Morpholino-4-(pentyloxy)pteridin-2-amine ( <b>12r</b> ) .....	165
3.7.2.19.	4-(Pentyloxy)-7-(piperidin-1-yl)pteridin-2-amine ( <b>12s</b> ) .....	165
3.7.2.20.	4-(Pentyloxy)-7-(pyrrolidin-1-yl)pteridin-2-amine ( <b>12t</b> ) .....	166
3.7.2.21.	Tert-butyl-4-(2-amino-4-(pentyloxy)pteridin-7-yl)piperazine-1-carboxylate ( <b>12u</b> ) .....	166
3.7.2.22.	2-Chloro-4-(pyrrolidin-1-yl)pyrimidine( <b>14a</b> ) .....	166
3.7.2.23.	2-Chloro-4-(piperidin-1-yl)pyrimidine ( <b>14b</b> ).....	167
3.7.2.24.	2-Chloro-4-morpholinopyrimidine ( <b>14c</b> ) .....	167
3.7.2.25.	Tert-butyl 4-(2-chloropyrimidin-4-yl)piperazine-1-carboxylate ( <b>14d</b> ).....	167
3.7.2.26.	2-Chloro-4-(4-tosylpiperazin-1-yl)pyrimidine ( <b>14e</b> ).....	167
3.7.2.27.	Di-tert-butyl 4,4'-(pyrimidine-2,4-diyl)bis(piperazine-1-carboxylate) ( <b>15</b> )	168
3.7.2.28.	2-(Hydroxymethyl)-5-(6-morpholino-9H-purin-9-yl)-tetrahydrofuran-3,4-diol ( <b>17a</b> ) .....	168
3.7.2.29.	2-(Hydroxymethyl)-5-(6-(piperidin-1-yl)-9H-purin-9-yl)-tetrahydrofuran-3,4- diol ( <b>17b</b> ) .....	169
3.7.2.30.	Tert-butyl4-(9-(3,4-dihydroxy-5-(hydroxymethyl)-tetrahydrofuran-2-yl)-9H- purin-6-yl)piperazine-1-carboxylate ( <b>17c</b> ).....	169
3.7.2.31.	6-Chloropyrimidine-2,4(1H, 3H)-dione ( <b>19</b> ) .....	169
3.7.2.32.	6-Chloro-1,3-dimethylpyrimidine-2,4(1H,3H)-dione ( <b>20</b> ).....	170
3.7.2.33.	1,3-Dimethyl-6-(piperidin-1-yl)pyrimidine-2,4(1H,3H)-dione ( <b>21a</b> ) .....	170
3.7.2.34.	Tert-butyl (R)-(1-(1,3-dimethyl-2,6-dioxo-1,2,3,6-tetrahydropyrimidin-4- yl)piperidin-3-yl)carbamate ( <b>21b</b> ).....	170
3.7.2.35.	Synthetic approach to Alogliptin:2-((6-Chloro-3-methyl-2,4-dioxo-3,4- dihydropyrimidin-1(2H)-yl)methyl)benzotrile ( <b>24</b> ) .....	171

## Table of Content

3.7.2.36.	<i>(R)</i> -2-((6-(3-Aminopiperidin-1-yl)-3-methyl-2,4-dioxo-3,4-dihydropyrimidin-1(2H)-yl)methyl)benzotrile ( <b>25</b> ) .....	171
3.7.3.	Pd/PTABS catalytic etherification of <i>chloroheteroarenes</i> at moderate temperatures. ..... 172	
3.7.3.1.	2-(4-Methoxyphenoxy)pyrazine ( <b>28a</b> ) .....	172
3.7.3.2.	2-(4-( <i>tert</i> -Butyl)phenoxy)pyrazine ( <b>28b</b> ).....	173
3.7.3.3.	2-(Naphthalen-2-yloxy)pyrazine ( <b>28c</b> ).....	173
3.7.3.4.	2-(Naphthalen-1-yloxy)pyrazine ( <b>28d</b> ).....	173
3.7.3.5.	2-(4-Methoxyphenoxy)benzo[d]oxazole ( <b>28e</b> ) .....	173
3.7.3.6.	2-(4- <i>tert</i> -Butylphenoxy)quinoxaline ( <b>28f</b> ).....	174
3.7.3.7.	2-(4-Methoxyphenoxy)quinoxaline ( <b>28g</b> ).....	174
3.7.3.8.	2-(Mesityloxy)quinoxaline ( <b>28h</b> ).....	174
3.7.3.9.	2-(3-Nitrophenoxy)quinoxaline ( <b>28i</b> ) .....	175
3.7.3.10.	2-(Quinolin-8-yloxy)benzo[d]thiazole ( <b>28j</b> ).....	175
3.7.3.11.	6-(Quinoxalin-2-yloxy)-2H-chromen-2-one ( <b>28k</b> ) .....	175
3.7.3.12.	2-(3, 5-Bis(trifluoromethyl)phenoxy)benzo[d]oxazole ( <b>28l</b> ).....	176
3.7.3.13.	2-(1-Bromonaphthalen-2-yloxy)quinoxaline ( <b>28m</b> ).....	176
3.7.3.14.	7-(4-Methoxyphenoxy)-4-(pentyl)pteridin-2-amine ( <b>28n</b> ).....	176
3.7.3.15.	2-(Pentafluorophenoxy)quinoxaline ( <b>28o</b> ).....	177
3.7.3.16.	2-(8-Bromonaphthalen-1-yloxy)benzo[d]oxazole ( <b>28p</b> ) .....	177
3.7.3.17.	2-(4-Allyl-2-methoxyphenoxy)benzo[d]thiazole ( <b>29a</b> ).....	177
3.7.3.18.	2-(4-Allyl-2-methoxyphenoxy)pyrazine ( <b>29b</b> ) .....	178
3.7.3.19.	2-(5-allyl-2-methoxyphenoxy)quinoxaline ( <b>29c</b> ).....	178
3.7.3.20.	Ethyl-2-(benzo[d]oxazol-2-ylamino)-3-(4-(benzo[d]oxazol-yloxy)phenyl)propanoate ( <b>29d</b> ) .....	178
3.7.3.21.	3-(Benzo[d]thiazol-2-yloxy)-13-methyl-6,7,8,9,11,12,13,14,15,16-decahydro-17H-cyclopenta[a]phenanthren-17-one ( <b>29e</b> ) .....	179
3.7.3.22.	13-Methyl-3-(pyrazin-2-yloxy)-6,7,8,9,11,12,13,14,15,16-decahydro-17H-cyclopentaphenanthren-17-one ( <b>29f</b> ) .....	179
3.7.3.23.	( <i>8R,9S,13S,14S</i> )-13-Methyl-3-(quinoxalin-2-yloxy)-6,7,8,9,11,12,13,14,15,16-decahydro-17H-cyclopenta[a]phenanthren-17-one ( <b>29g</b> )... 180	
3.7.3.24.	( <i>13S</i> )-3-(Benzo[d]oxazol-2-yloxy)-13-methyl-7,8,9,11,12,13,14,15,16,17-decahydro-6H-cyclopenta[a]phenanthren-17-ol ( <b>29h</b> ) .....	180

## Table of Content

3.7.3.25.	4-(4- <i>tert</i> -Butylphenoxy)-2-chloropyrimidine ( <b>31a</b> ).....	181
3.7.3.26.	2-Chloro-4-(4-methoxyphenoxy)pyrimidine ( <b>31b</b> ).....	181
3.7.3.27.	8-((2-Chloropyrimidin-4-yl)oxy)quinoline ( <b>31c</b> ).....	181
3.7.3.28.	(13 <i>S</i> )-2-(2-Chloropyrimidin-4-yloxy)-13-methyl-7, 8, 9, 11, 12, 13, 15, 16- octahydro-6 <i>H</i> -cyclopenta[ <i>a</i> ]phenanthren-17(14 <i>H</i> )-one ( <b>31d</b> ).....	182
3.7.3.29.	2-Chloro-4-(2-isopropyl-4-methylphenoxy)pyrimidine ( <b>31e</b> ).....	182
3.7.3.30.	2,4-bis(4-methoxyphenoxy)pyrimidine ( <b>32a</b> ).....	182
3.7.3.31.	2,4 (Di-estrogen)) pyrimidine ( <b>32b</b> ).....	183
3.7.3.32.	2-(6-(8-Bromonaphthalen-1-yloxy)-9 <i>H</i> -purin-9-yl)-5-(hydroxymethyl)- tetrahydrofuran-3,4-diol ( <b>34a</b> ).....	183
3.7.3.33.	2-(Hydroxymethyl)-5-(6-(4-methoxyphenoxy)-9 <i>H</i> -purin-9-yl)- tetrahydrofuran-3,4-diol ( <b>34b</b> ).....	184
3.7.3.34.	9-Ethyl-6-(2-isopropyl-5-methylphenoxy)-9 <i>H</i> -purine ( <b>34c</b> ).....	184
3.7.4.	Tandem Catalytic Processes Using the Pd/PTABS System.....	184
3.7.4.1.	2-(4-(Phenylethynyl)phenoxy)benzo[ <i>d</i> ]thiazole ( <b>35a</b> ).....	185
3.7.4.2.	2-(4-((4-Methoxyphenyl)ethynyl)phenoxy)benzo[ <i>d</i> ]thiazole ( <b>35b</b> ).....	185
3.7.4.3.	2-(4-( <i>p</i> -Tolylethynyl)phenoxy)benzo[ <i>d</i> ]thiazole ( <b>35c</b> ).....	186
3.7.4.4.	6-(4-(Benzo[ <i>d</i> ]thiazol-2-yloxy)phenyl)-3-(4-hydroxy-5- (hydroxymethyl)tetrahydrofuran-2 yl)furo[2,3- <i>d</i> ]pyrimidin-2(3 <i>H</i> )-one ( <b>36</b> ).....	186
3.7.5.	Pd/PTABS catalytic thioetherification of chloroheteroarenes at moderate temperatures.....	187
3.7.5.1.	2-(Phenylthio)pyrazine ( <b>41a</b> ).....	187
3.7.5.2.	2-(2,6-Dimethylphenylthio)pyrazine ( <b>41b</b> ).....	188
3.7.5.3.	2-(Pyrazin-2-ylthio)benzenamine ( <b>41c</b> ).....	188
3.7.5.4.	2-(Ethylthio)pyrazine ( <b>41d</b> ).....	188
3.7.5.5.	2-Admantanethiopyrazine ( <b>41e</b> ).....	189
3.7.5.6.	2-(Phenylthio)quinoxaline ( <b>41f</b> ).....	189
3.7.5.7.	2-(2,6-Dimethylphenylthio)quinoxaline ( <b>41g</b> ).....	189
3.7.5.8.	2-(Quinoxalin-2-ylthio)benzenamine ( <b>41h</b> ).....	190
3.7.5.9.	2-(Benzylthio)quinoxaline ( <b>41i</b> ).....	190
3.7.5.10.	2-( <i>sec</i> -Butylthio)quinoxaline ( <b>41j</b> ).....	191
3.7.5.11.	Admantanethio2- quinoxaline ( <b>41k</b> ).....	191
3.7.5.12.	2,4-Bis(phenylthio)pyrimidine ( <b>41l</b> ).....	191
3.7.5.13.	2,4-Bis( <i>sec</i> -butylthio)pyrimidine ( <b>41m</b> ).....	192

## Table of Content

3.7.5.14.	2,4,6-Tris(phenylthio)-1,3,5-triazine ( <b>41n</b> ).....	192
3.7.5.15.	(2R, 3R, 4S, 5R)-2-(Hydroxymethyl)-5-(6-(phenylthio)-9H-purin-9-yl)-tetrahydrofuran-3,4-diol ( <b>42a</b> ) .....	192
3.7.5.16.	6-(Phenylthio)-9H-purine ( <b>42b</b> ).....	193
3.7.5.17.	2-((3-Methyl-2,4-dioxo-6-(phenylthio)-3,4-dihydropyrimidin-1(2H)-yl)methyl)benzotrile ( <b>42c</b> ) .....	193
3.7.5.18.	2-((6-(sec-Butylthio)-3-methyl-2,4-dioxo-3,4-dihydropyrimidin-1(2H)-yl)methyl)benzotrile ( <b>42d</b> ) .....	193
3.7.5.19.	(2R, 3S, 4R, 5R)-2-(6-(Ethylthio)-9H-purin-9-yl)-5-(hydroxymethyl)-tetrahydrofuran-3,4-diol ( <b>42e</b> ) .....	194
3.7.5.20.	(2R, 3S, 4R, 5R)-2-(6-(sec-Butylthio)-9H-purin-9-yl)-5-(hydroxymethyl)-tetrahydrofuran-3,4-diol ( <b>42f</b> ).....	194
3.7.5.21.	(2R, 3R, 4S, 5R)-2-(6-(Adamantan-1-ylthio)-9H-purin-9-yl)-5-(hydroxymethyl)tetrahydrofuran-3,4-diol ( <b>42g</b> ).....	195
3.7.5.22.	2-(Phenylsulfonyl)quinoxaline ( <b>43</b> ).....	195
3.7.5.23.	Imino(phenyl)(quinoxalin-2-yl)-sulfanone ( <b>44</b> ) .....	196
3.7.5.24.	Azathiaprin ( <b>46</b> ) .....	196
3.8.	Molecular structures and X-ray single crystal diffraction data.....	197
3.9.	References.....	213
	List of Scientific Contributions.....	241
	Lebenslauf.....	244
	ACKNOWLEDGEMENT .....	245

## List of Abbreviations

ACN	Acetonitrile
APCI-MS	Ambient Temperature Chemical Ionization-Mass Spectrometry
Bcl-2	<i>B-cell lymphoma 2</i>
BINAP	2,2'-bis(diphenylphosphino)-1,1'-binaphthyl
BippyPhos	5-(di-tert-butylphosphino)-1', 3', 5'-triphenyl-1'H-[1,4]bipyrazole
BSA	Bovine Serumalbumin
CDI	1,1'-carbodiimidazole
CETP	Cholesterylester transfer protein
CHNS	Carbon Hydrogen Nitrogen Sulfur
CI	Confidence Interval
CyPf-t-Bu	(R)-1-[(SP)-2-(Dicyclohexylphosphino)ferrocenyl]ethyl-di-tert-butylphosphine
Cys	Cystein
DABCO	1,4-Diazabicyclo(2,2,2)octane
DavePhos	2-Dicyclohexylphosphino-2'-(N,N-dimethylamino)biphenyl
DCC	N,N'-Dicyclohexylcarbodiimid
DCM	Dichloromethane
DFT	Density function theory
DGAT1	Acyl-CoA: diacylglycerol acyltransferase
DIPEA	Di-isopropylethylamine

## List of Abbreviations

Dippf	1,1'-Bis(diisopropylphosphino)ferrocene
DMF	<i>N,N'</i> - dimethylformamide
DMSO	Dimethylsulfoxide
DNA	Deoxy Nucleic Acid
DPEphos	Bis[(2-diphenylphosphino)phenyl]ether
DPP-4	Dipeptylpeptidase-4
dppb	Butane-1,4-diylbis(diphenylphosphane)
dppf	1,1'-Bis(diphenylphosphino)ferrocene
dppp	1,3-Bis(diphenylphosphino)propan
EI-Ms	Electron Ionization-Mass Spectroscopy
ESI	Electro Spray Ionization
ESI-Ms	Electro Spray Ionization-Mass Spectroscopy
Et <sub>3</sub> N	Triethylamine
EtOAc	Ethyl acetate
FIV	Feline Immunodeficiency Virus
G6PD	Glucose-6-Phosphatdehydrogenase
GPx	Glutathione peroxidases
GR	Glutathione reductase
GSH	Glutathione
GSSG	Glutathionedisulfide
H <sub>2</sub> O <sub>2</sub>	Hydrogen peroxide

## List of Abbreviations

HBTU	3-[Bis(dimethylamino)methylumyl]-3H-benzotriazol-1-oxide hexafluorophosphate
HCT	Human COLORECTAL CARCINOMA cell line
HIV	Human Immunodeficiency Virus
HMTA	Hexamethylenetetramine
HO <sup>•</sup>	Hydroxide radical
HOCl	Hypochlorous acid
Hsp	Heat Shock protein
IC <sub>50</sub>	Half maximal inhibitory concentration
IC <sub>90</sub>	90% of maximal inhibition
KOAc	Potassium acetate
LiHMDS	Lithium bis(trimethylsilyl)amide
MEP	Molecular Electrostatic Potential
MIC	Minimum Inhibitory Concentration
MS	Mercaptosuccinic acid
MTT	3-(4,5-dimethylthiazol-2-yl)-2,5-diphenyltetrazolium bromide
NaO <sup>t</sup> Bu	Sodium tertiary butoxide
NHC	Nucleophilic Heterocyclic Carbene
NMR	Nuclear Magnetic Resonance
NO <sup>•</sup> , NO <sub>2</sub> <sup>•</sup>	Nitrogen monoxide and dioxide radicals
NPA	Natural Population Analysis



## List of Abbreviations

O <sub>2</sub> <sup>•-</sup>	Superoxide radical
ONOO	Peroxynitrite
P( <i>o</i> -tolyl) <sub>3</sub>	Tri- <i>ortho</i> -tolylphosphine
PhMe	Toulene
ppm	Parts per million
PTA	1,3,5- triaza-7-phosphaadmantane
PTABBn	1,3,5- triaza-7-phosphaadmantane benzaylbromide
PTABBr	1,3,5- triaza-7-phosphaadmantane butylbromide
PTABCl	1,3,5- triaza-7-phosphaadmantane butylchloride
PTABI	1,3,5- triaza-7-phosphaadmantane butyliodide
PTABS	1,3,5- triaza-7-phosphaadmantane butylsultonate
PTAPS	1,3,5- triaza-7-phosphaadmantane propylsultonate
QSAR	Quantitative Structure Activity Relationship
RNS	Reactive Nitrogen Species
ROS	Reactive Oxygen Species
rt	Room temperature
S <sub>8</sub>	Elemental Sulfur
Sec	Selenocystein
Se-OH	Selenic acid
SOD	Superoxide dismutase
SPhos	2-Dicyclohexylphosphino-2',6'-dimethoxybiphenyl

## List of Abbreviations

SynPhos	S-(-)-6,6'-Bis(diphenylphosphino)-2,2',3,3'-tetrahydro-5,5'-bi-1,4-benzodioxin
THPC	Tetrakis(hydroxymethyl)phosphonium chloride
TLC	Thin Layer Chromatography
Toco	$\alpha$ -tocopherol
TOF	Turnover frequency
TON	Turnover Numbers
UV	Ultra Violet
Xantphos	4,5-Bis(diphenylphosphino)-9,9-dimethylxanthene
Xphos	2-Dicyclohexylphosphino-2',4',6'-triisopropylbiphenyl
$\Delta G$	The Gibbs free energy

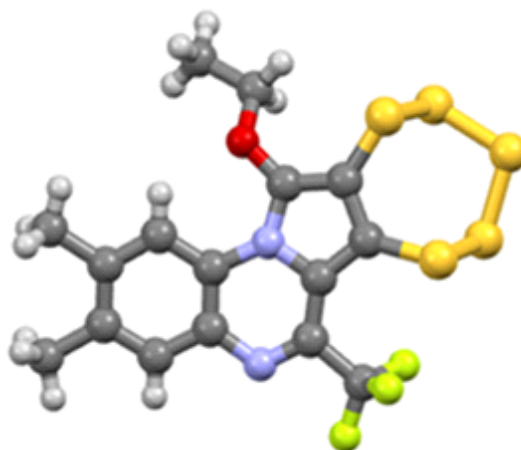
## Measurements and Units

cm	Centimeter ( $10^{-2}$ meter)
g	Gram
M	Molar
mg	Milligram ( $10^{-3}$ gram)
min	Minute
h	Hour
mL	Milliliter ( $10^{-3}$ liter)
mM	Millimolar ( $10^{-3}$ Molar)
$\mu\text{g}$	Microgram ( $10^{-6}$ gram)

## List of Abbreviations

$\mu\text{L}$	Microliter ( $10^{-6}$ liter)
$\mu\text{M}$	Micromolar ( $10^{-6}$ Molar)
nM	Nanomolar ( $10^{-9}$ Molar)
rpm	Rounds per minute
sec	Seconds
U	Units
$^{\circ}\text{C}$	Degrees centigrade
%	Percentage
ppm	Parts per million
mol%	Mole percentage
equiv.	Equivalents
m/z	Mass to charge ratio
Mp	Melting point

## Chapter 1: Synthesis of novel heterocyclic fused pentathiepins and their cytotoxic and antimicrobial properties



### 1.1 Introduction

Sulfur is the heteroatom most widely used in biomolecules after oxygen, phosphorous and nitrogen. Sulfur is exceptional due to its importance in biological redox processes and its rich functionality in a variety of critically important small molecules, peptides, proteins and enzymes. The sulfur-rich natural products found in plants, fungi, animals, and many other sources have shown unique biochemical features associated with coordination chemistry, catalysis and redox-chemistry.<sup>1-2</sup> Generally, in these natural extracts, sulfur might be present in the form of thiols, thiosulfonates, thiosulfonates, isothiocyanates, sulfoxides, sulfones and polysulfides (figure 1.1). Most of these derivatives are exhibiting antibacterial and anticancer properties, and therefore gained significant pharmacological attention.

#### 1.1.1 Sulfur centered redox-networks and mechanistic pathways *in vivo*

Sulfur participates preferably in atom exchange or electron transfer redox processes (e.g., GSH) under physiological conditions. Figure 1.1 illustrates a glimpse of the various sulfur based redox pathways *in vivo*.<sup>1</sup> Although such complex networks are being under continuous

exploration, the given snapshot provides a basic understanding of the complexity of redox-active sulfur species.

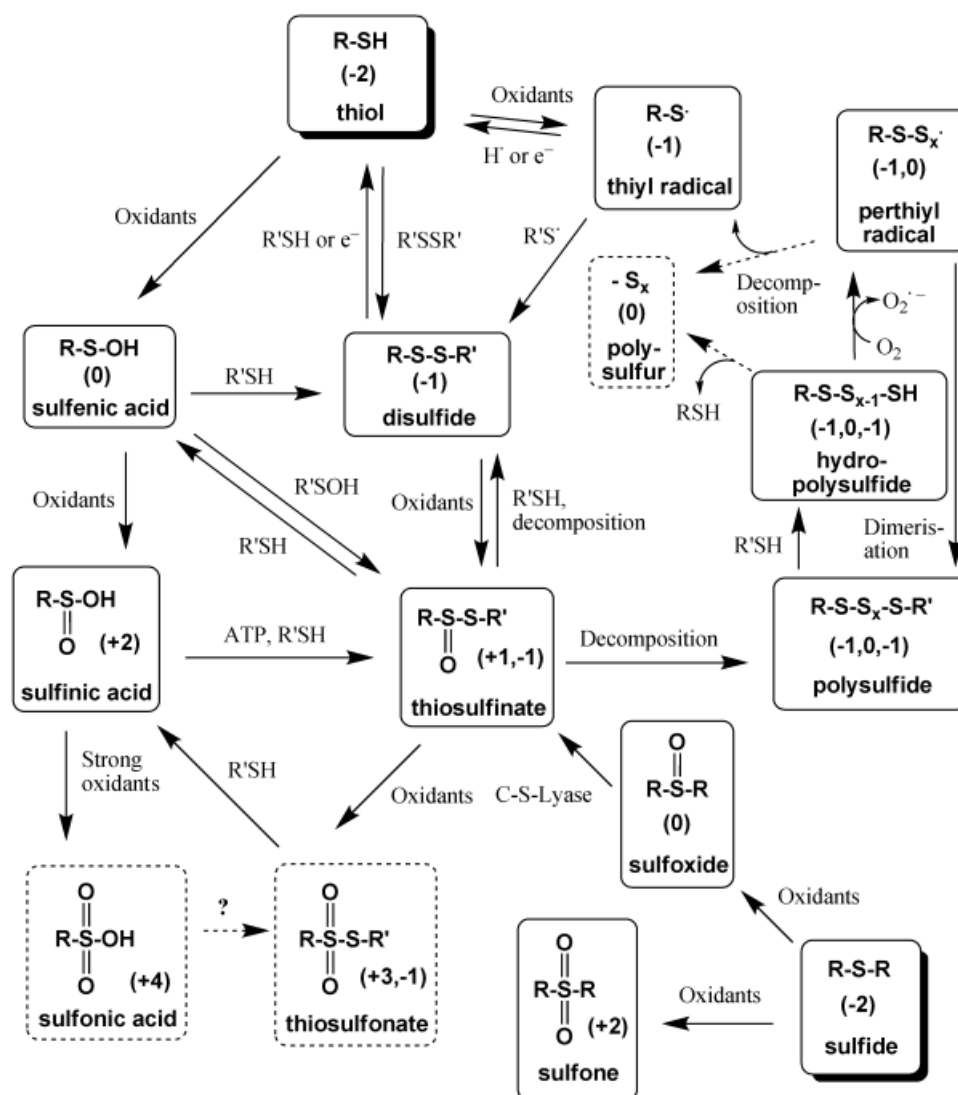


**Figure 1.1:** A summary of the sulfur redox network with various sulfur forms depicted with their formal oxidation states.<sup>1</sup>

Sulfur's catenation as well as its interchalcogen bond formation property and flexible oxidation states (-2 to +6), allow for its special biological redox-behaviour that is as of yet not entirely deciphered.<sup>1</sup> According to recent *in vitro* and *in vivo* studies on natural sulfur species it was speculated that sulfur could occur in more than ten different oxidation states under physiological conditions.<sup>2</sup> For example, sulfur is in -2 oxidation state in glutathione (GSH) and it can lose up to eight electrons to form sulfates (such as heparin sulfate  $\text{SO}_4^{2-}$  with oxidation state +6). Sulfur can also show fractional formal oxidation states. Numerous biologically relevant oxidative species such as thiyl radicals ( $\text{RS}\cdot$ ), sulfoxides ( $\text{RS(O)R}$ ), sulfones ( $\text{RS(O)}_2\text{R}$ ), sulfenic ( $\text{RSOH}$ ), sulfinic ( $\text{RS(O)OH}$ ) and sulfonic acids ( $\text{RS(O)}_2\text{OH}$ ) are known.

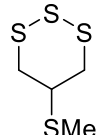
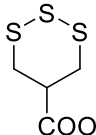
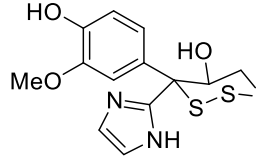
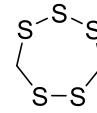
They exhibit distinct redox-active and radical generating properties. Additionally, the ring and chain-forming ability of sulfur further extended the library of species such as disulfides (RSSR), polysulfides (RS<sub>x</sub>R', x ≥ 3), thiosulfates (RS(O)SR'), thiosulfonates (RS(O)<sub>2</sub>SR'), hydropersulfides and hydropolysulfides (RS<sub>x</sub>H, x=2 and x ≥ 3 respectively).

The importance of sulfur in biology is due to: a) it's *in vivo* occupancy of various sulfur oxidation states, b) exhibiting numerous chemical forms for each oxidation state and c) the functional properties shown by these synthetic forms in addition to their redox activity. Preferably, cells frequently employ its metal binding and nucleophilic substitution properties to inhibit oxidative stressors (e.g., peroxides, hydroxide radicals, and peroxy nitriles), toxic metal ions and related substances. Figure 1.1 depicts redox-active species of sulfur, and the majority of them can be easily derived from thiol by simple oxidation and nucleophilic substitution. The redox mechanisms of these species include one and two-electron transfer reactions, hydride and oxygen transfer, thiol/disulfide exchanges, nucleophilic exchange and radical reactions.<sup>3</sup>

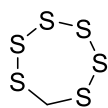
### 1.1.2 Polysulfides: A particular class of bio-reductive drugs

The polysulfides (RS<sub>n</sub>R' n ≥ 3) present in many plants and lower organisms and their unusual pro-drug activation mechanisms gained significant importance in biological studies.<sup>1</sup> Moreover, industrial applications of organic polysulfanes in high-pressure lubricants (as an additive),<sup>4</sup> in “Thiokol” rubber (vulcanized rubber) preparations, in cement and oil production are well established.<sup>5</sup> Notably, many sulfur-rich low molecular weight natural organopolysulfanes were discovered recently, and their intriguing structures and physiological activities are quite fascinating to explore. Interestingly, most of these isolated/identified biological materials from marine organisms and foods consist of chain-like or cyclic-organic polysulfanes (Table 1.1).<sup>6-7</sup>

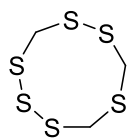
**Table 1.1:** Naturally occurring cyclic polysulfanes

 <p>5-methylthio-1,2,3-trithiane <i>Chara globularia</i> (green alga)<sup>8-9</sup></p>	 <p>5-carboxyl-1,2,3-trithiane <i>Asparagus officinalis</i><sup>10</sup></p>	 <p><i>Aplidium sp.D.</i> (ascidian)<sup>11</sup></p>	 <p>Lenthionin <i>Chondria</i> <i>California</i> (red Alga)<sup>6, 12-13</sup></p>
--	---	---	---

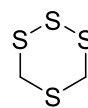
## Chapter 1: Pentathiepins



Hexathiepane  
*Lentinus edodes*<sup>14-16</sup>



Hexathionane



1,2,3,5- tetrathiane

	$n = 3; R^1=R^3=Me; R^2=CH_2OH; R^4 = CH_2Ph$ Sporidesmine E	<i>Fungus Pithomyces chartarum</i> <sup>17-18</sup>
3,6-Epipolythiopiperazine-2,5-dione	$n=4; R^1=R^3=Me; R^2=CH_2OH; R^4=CH_2Ph$ Sporidesmine G	<i>Penicillium turbatum</i> <sup>19</sup>
	R = H, Lissoclinotoxin A	<i>Lissoclinum perforatum</i> (ascidian) <sup>20</sup>
	R = Me; Varacin	<i>Lissoclinum vareau</i> <sup>21-23</sup>
	Lissoclinotoxin B	<i>Lissoclinum Perforatum</i> <sup>24</sup>

It was observed that the natural components in these organisms often contain R-S<sub>n</sub>-R type chain-like polysulfanes in which the chain length varies in between 2 to 6, while the organic moiety R could be a saturated or an unsaturated alkyl or aryl group. For example, the volatile oil extracted from *Asafetida* (*oleogum*) via steam distillation is abundant of 2-butyl-1-propenyldisulfane, 1-methylthiopropyl-1-propenyldisulfane and 2-butyl-3-methylthioallyldisulfane along with a few tri- and tetrasulfane derivatives.<sup>25</sup> In another example, calicheamicin  $\gamma_1$ <sup>126</sup> and the esperamicins A<sub>1</sub>, A<sub>2</sub> and A<sub>1b</sub><sup>27</sup> bear the MeSSS- group attached to complex natural product structures, and they are potent antitumor agents and antibiotics. Table 1.1 depicts a few important naturally occurring biologically active cyclic polysulfanes along with their extraction sources. Among all, the cyclic polysulfides extracted from the Far-Eastern *ascidian* genus *Lissoclinum* (varacin<sup>21</sup> and lissoclinotoxin-A<sup>28</sup>) and *polycitor* sp., (varacin A-C)<sup>29</sup> have shown high therapeutic potency. These types of seven-membered cyclic polysulfanes are named pentathiepins and the study of their derivatives is the central concept of this project.

### 1.1.3 Chemical reactivity of polysulfides and disulfides and biological significance

Polysulfides and disulfides differ significantly in their chemistry, as it was discussed in detail by Ralf Steudel in his review.<sup>30</sup> For example, the reaction of disulfides (RSSR) with GSH results in the mixed disulfide RSSG and RSH, whereas under the similar conditions polysulfides ( $RS_nR'$   $n \geq 3$ ) result in a mixture of di- or polysulfides ( $RS_nR'$   $n \geq 2$ ) along with hydroperdisulfide (RSSH) and hydropolysulfide ( $RS_nH$   $n \geq 3$ ).<sup>31-32</sup> The highly reducing hydroper- and poly-sulfides react readily with dioxygen ( $O_2$ ) in the cells under physiological conditions and form the superoxide radical ( $O_2^{\bullet}$ ) and  $RS_n^{\bullet}$  ( $n \geq 2$ ). The combination of  $RS_n^{\bullet}$  radicals generates a polysulfide RSSSR which further reacts with another equivalent of GSH to continue the catalytic cycle and produce further superoxide radicals. In the presence of superoxide dismutase (SOD) and copper or iron ions,  $O_2^{\bullet}$  is converted into hydrogen peroxide and reactive hydroxide radical ( $HO^{\bullet}$ ). Since  $HO^{\bullet}$  is known to cause cell apoptosis by modifying protein-membrane and DNA, the generation of superoxide radicals (catalytically or stoichiometrically) explains the toxicity of natural polysulfides. This phenomenon of superoxide radical generation is not observed with disulfides, which renders polysulfides more interesting from the biological and pharmacological point of view.

On the other hand, the diallyl trisulfide and diallyl tetrasulfide extracted from various natural sources such as garlic exhibit a broad spectrum of antimicrobial, antibacterial and antifungal activities.<sup>33-35</sup> In general, diallyl trisulfide induces cytotoxicity in cultured human prostate cancer cells via a mechanism involving  $O_2^{\bullet}$  formation and increasing the intercellular labile iron ion concentrations.<sup>36</sup> The cyclic trisulfide Lenthionine can be isolated together with polysulfide 1,2,3,4,5,6-hexatheipane from *Shiitake* mushrooms. Lenthionine was identified as potential antibacterial and antifungal agent, while the cyclic hexasulfide fraction was found biologically irrelevant.<sup>14</sup> The cyclic trisulfide, cis-5-hydroxy-4-(4'-hydroxy-3'-methoxyphenyl)-4-(2"-imidazolyl)-1,2,3-trithiane extracted from *Aplidium sp.* is active against P388 murine leukemia cells with an  $IC_{50}$  of 13  $\mu\text{g/mL}$  and also inhibits the Gram-positive bacterium *B. subtilis* and the fungus *C. albicans*.<sup>11</sup> Though the trisulfides mentioned above are exhibiting a pro-oxidant effect, it is crucial to consider that the reaction pathways *in vivo* are diverse, complex and additionally can also activate the antioxidant responses.<sup>37</sup>

### 1.1.4 Reactive sulfur species: Pentathiepins

The Hantzsch-Widman nomenclature system is used for naming the seven-membered organo polysulfide rings bearing five sulfur atoms and two carbon atoms. Accordingly, for the carbon-



carbon bond type, they are named as 1,2,3,4,5 pentathiepins (unsaturated) and pentathiepins (saturated).<sup>30</sup> Although Fehér synthesized the saturated and unsaturated forms of these organopolysulfides earlier in the years 1967-1971,<sup>38-39</sup> their biological relevance was only realized after twenty years with the isolation of natural antibiotics containing seven-membered polysulfur rings from marine organisms.<sup>40</sup> Compared to their saturated counterparts, pentathiepins have been gaining considerable interest as antitumor, antifungal and antiseptic drugs. The biological activity depends on their heterocyclic moiety.<sup>41</sup> Additionally, the high stability, the high inversion barrier energy of the chair conformation of the poly sulfur ring and its occurrence in Nature with potent biological activity motivated researchers for more comprehensive investigations. Besides, pentathiepins have found applications in industry as cathodic materials.<sup>40</sup> Recently, these compounds were realized as valuable starting materials for various synthetic organic processes for the preparation of sulfur-containing derivatives, such as 1,4-dithiines, 1,2,4,5-tetrathiocines, 1,2-dithiols and many others.<sup>40</sup>

### 1.2 Biological significance of pentathiepins

Varacin, lissoclinotoxin A, B and *N, N'*-dimethyl-5-(methylthio)varacin were the first naturally extracted pentathiepins from marine organisms (Figure 1.2).<sup>29</sup> Varacin isolated from marine *ascidian Lissoclinum vareau* was proven highly toxic towards human colon cancer HCT 116 with an IC<sub>90</sub> value of 0.05 µg/ml and also exhibited antimicrobial activity against *Bacillus subtilis* and *S.Aureus*.<sup>21</sup> Lissoclinotoxin A isolated from *Lissoclinum sp.* bearing a hydroxyl group at position-4 of the benzol ring has shown antimicrobial activity against *Staphylococcus aureus*.<sup>20</sup> The cyclic amine bearing lissoclinotoxin B isolated from *Lissoclinum perforatum* has shown similar biological activity against fish-pathogens *Aeromonas salmonicida* and *Vibrio anguillarum*.<sup>24</sup> Furthermore, the varacin analogues *N, N'*-dimethyl-5-(methylthio)varacin and 3,4-desmethylvaracin isolated from different *Lissoclinum* species have been identified as potential protein kinase C inhibitors.<sup>42</sup>

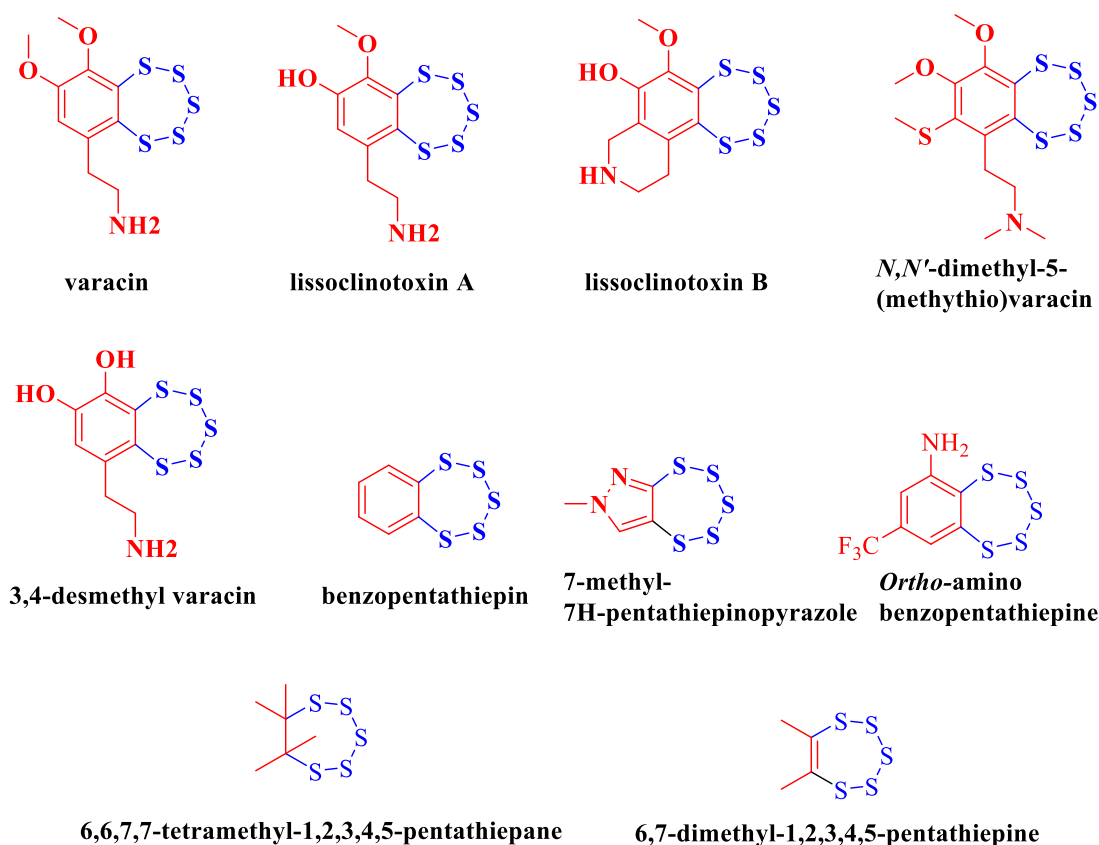


**Figure 1.2:** Natural pentasulfide species and synthetic mimics with significant biological relevance.

Additionally, various synthetic mimics were prepared. Interestingly, they also have shown equal potency, for example, 7-methyl-7H-[1,2,3,4,5]pentathiepinopyrazole synthesized by DuPont pharmaceuticals is patented for its fungicidal activity.<sup>43</sup> A trifluoromethyl substituted *ortho*-amino benzopentathiepin was recently reported as anticonvulsive and anxiolytic agent improving the emotional state during Alzheimer's disease.<sup>44</sup> Later, different heterocyclic fused pentathiepin analogues were prepared; however, their biological significance was not established (Figure 1.3).<sup>45-46</sup>

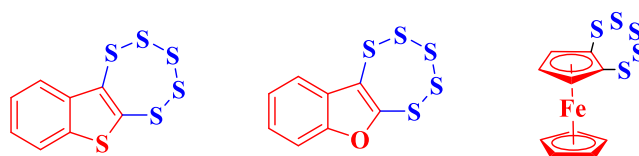


**Figure 1.3:** Fused heterocyclic and ferrocene based pentathiepins

Considering the superoxide radical generation ability of polysulfides in the presence of GSH (*vide supra*), Chatterji and Gates proposed a thiol dependent DNA-cleavage mechanism for 7-methylbenzopentathiepin (Figure 1.4).<sup>47</sup> In their experiments, strand breaks in supercoiled DNA-plasmids were observed upon incubation of pentathiepins with physiologically relevant

thiols (GSH, cysteine).<sup>48</sup> The formed superoxide was transformed to hydrogen peroxide via superoxide dismutase (SOD), which then undergoes the Fenton's reaction to produce a hydroxide radical, consequently inducing DNA damage.<sup>49</sup>

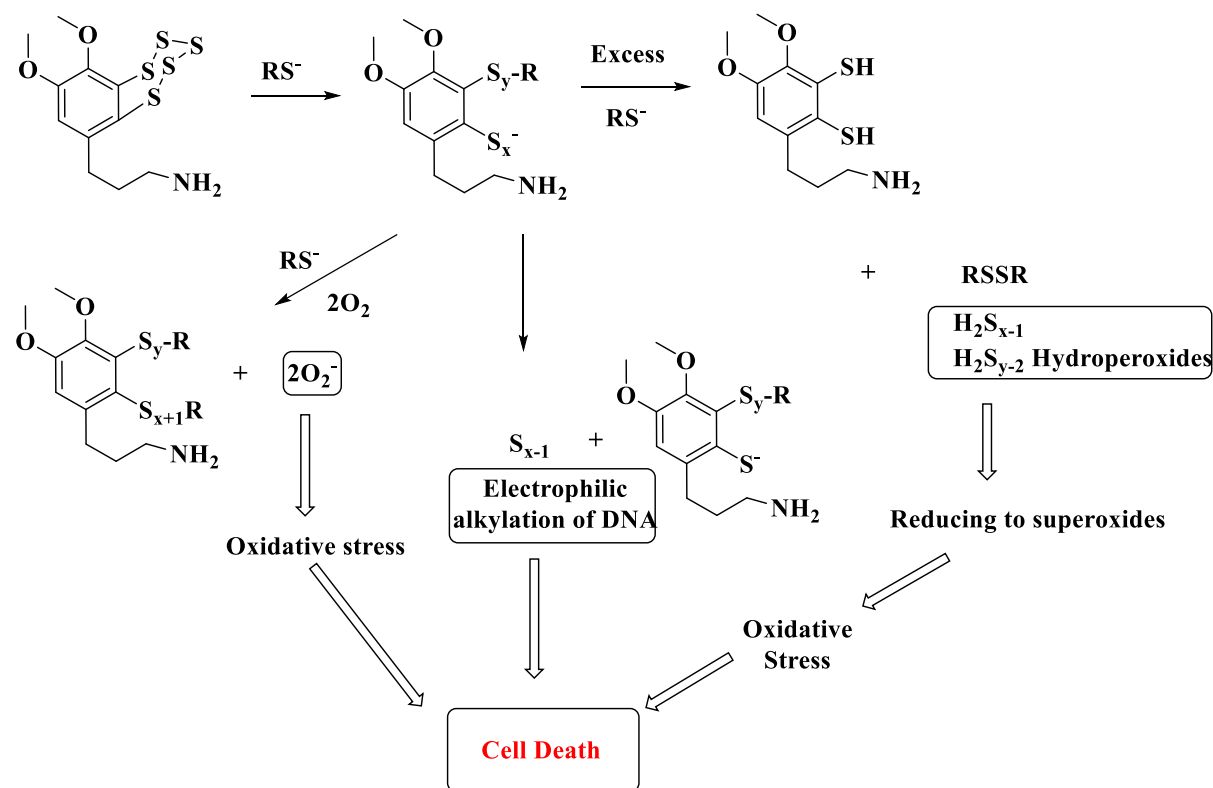


**Figure 1.4:** Biological activity of pentathiepins in the presence of an excess of physiological thiols and generation of superoxides.

Furthermore, the DNA-binding ability of varacin and subsequent enhancement of biological activity for a specific 2-mercaptoethanol concentration supports the proposed mechanism.<sup>49</sup>

However, the DFT investigations conducted by Greer and his co-workers on structural parameters and chemical reactivity of pentathiepins suggested that the in situ S<sub>3</sub> (reactive sulfur intermediate) fragmentation is vital in producing reactive oxygen species (ROS) (Figure 1.5).<sup>50</sup> Generally, natural pentathiepins contain a short alkylamine side chain in their backbone compared to their synthetic mimics. According to the computational and experimental data, the nucleophilic attack of a free amine (primary or secondary) on the S-1 position of the pentathiepin is an energetically low-lying process.<sup>50</sup> Furthermore, the S<sub>3</sub>-loss from pentathiepins was confirmed by trapping the reactive sulfur unit with norbornene. In contrast, the tertiary amines bind reversibly on S-1 of the pentathiepin moiety and do not facilitate the S<sub>3</sub>-unit cleavage. Based on these supportive results, authors proposed a valid mechanistic rationale for the queries such as, why a few pentathiepins were biologically more active than

others or about the precise role of the attached amine linkage. For example, the antimicrobial activity of benzopentathiepin-6-acetamides is in range of 1-16  $\mu\text{g/mL}$ , while the analogues derivative without the five-membered sulfur ring was inactive.<sup>41</sup> The quantitative structure activity relationship (QSAR) studies and molecular docking analysis further suggested bacterial DNA ligase binding properties for these classes of pentathiepins.<sup>41</sup>

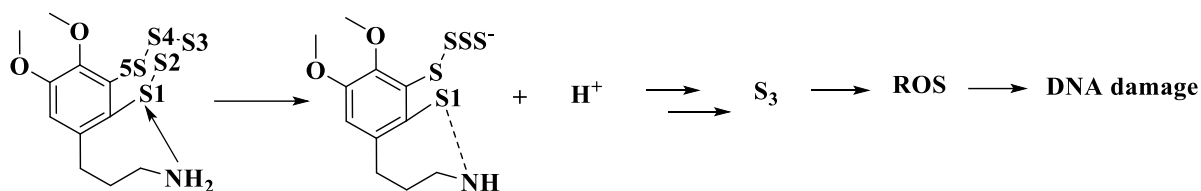


**Figure 1.5:** Biological activity of pentathiepin via nucleophilic amine triggered  $\text{S}_3$  unit loss.

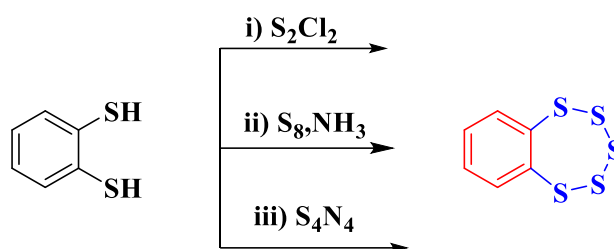
Recently reported thiophene- and pyrrole-substituted pentathiepins have shown high efficacy towards the nucleocapsid protein function of the feline immunodeficiency virus (FIV).<sup>51</sup> Notably, authors proposed an alternative mechanism to DNA cleavage, i.e., a potential zinc ejection mechanism. The cysteine unit from a zinc finger opens the pentathiepin sulfur ring via nucleophilic attack resulting in a protein-pentathiepin intermediate. The intermolecular rearrangement followed by an ejection of the zinc-pentathiepin complex leads to intramolecular disulfide bond formation between cysteine units in the protein.<sup>51</sup> However, conclusive mechanistic evidence for such type of process is yet to be disclosed.

In summary, the five-membered sulfur unit in the pentathiepin moiety, as well as their aromatic or heterocyclic units, is crucial for their biological relevance. Although different mechanisms were proposed, the distinct functional roles of polysulfides under specific physiological environments and consequent biological outcomes are yet to be studied in detail.

### 1.3 Synthetic methodologies for pentathiepins

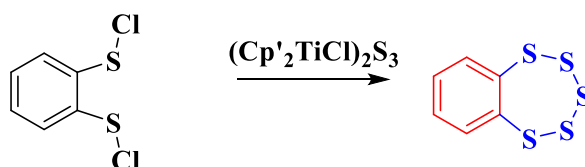
The heterocyclic pentathiepins such as indole or thiophene fused pentathiepins were proven to exhibit relevant biological activity.<sup>40</sup> However, there is a scarcity for an efficient synthetic procedure to furnish them. Only synthetic approaches for pentathiepins bearing the benzene moiety were explored frequently. Fehér's initial reports dated back to 1967, employed  $\text{S}_3\text{Cl}_2$  for the synthesis of cyclohexapentathiepane; procedures with more stable  $\text{S}_2\text{Cl}_2$  were introduced later to obtain improved isolated yields.<sup>39</sup> In 1970, Fehér synthesized benzopentathiepin in 80% isolated yield by employing optimized conditions with benzodithiol. The availability and the stability of the dithiol precursors, however, limit the general

applicability of this synthetic protocol for pentathiepins (Scheme 1.1(i)).<sup>38</sup> Later, Sato and co-workers reported the synthesis for functionalized varacin skeleton-based pentathiepins by reacting elemental sulfur with the respective dithiols in the presence of liquid ammonia at 20°C in a titanium autoclave (Scheme 1.1 (ii)).<sup>52</sup> However, highly substituted benzodithiols resulted in lower conversions while the benzo[d][1,2,3]trithiole was isolated as a major product. Later, a tetrasulfurtetranitride ( $S_4N_4$ ) mediated synthetic methodology for the preparation of pentathiepins from their respective dithiols was reported (Scheme 1.1 (iii)).<sup>40, 53</sup>



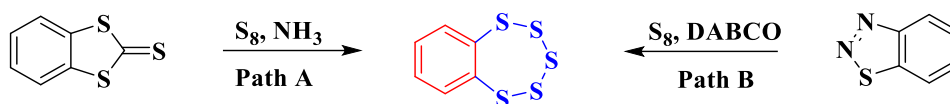
**Scheme 1.1:** Benzopentathiepin synthesis from benzene dithiol.

The insertion of the  $S_3$ -unit into benzene-1,2-bis-(sulfenyl chlorides) with chlorotitaniumtrisulfide was investigated for the first time by Steudel and co-workers for targeting pentathiepins (Scheme 1.2).<sup>54</sup>



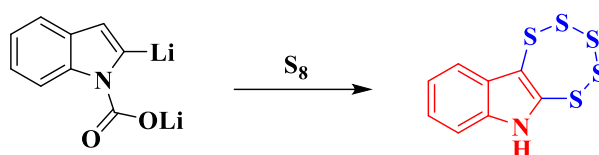
**Scheme 1.2:** Synthesis of benzopentathiepin from benzene-1,2-bis-(sulfenyl chloride).

Additionally, the pentathiepin preparation from protected dithiols, i.e., dithiole-2-thiones in the presence of elemental sulfur and liquid ammonia was reported (Scheme 1.3, path A).<sup>55</sup> However, the protocol lost its generality by failing the synthesis of 7-nitrobenzopentathiepin, and other derivatives substituted with electron-withdrawing groups. Similarly, Chenard and co-workers synthesized pentathiepins from benzothiadiazole and elemental sulfur in the presence of 1,4-Diazabicyclo(2,2,2)octane (DABCO) (Scheme 1.3, path B).<sup>56</sup> The observed enhanced activity was attributed to the employment of highly nucleophilic DABCO, presumably supporting the ring-opening of the thiadiazol moiety, consequently building the cyclic polysulfide ring. Moreover, by using this protocol heterocyclic fused derivative such as, pyrazolo- and dihydrofuran pentathiepins were prepared in quantitative yields.<sup>56</sup>



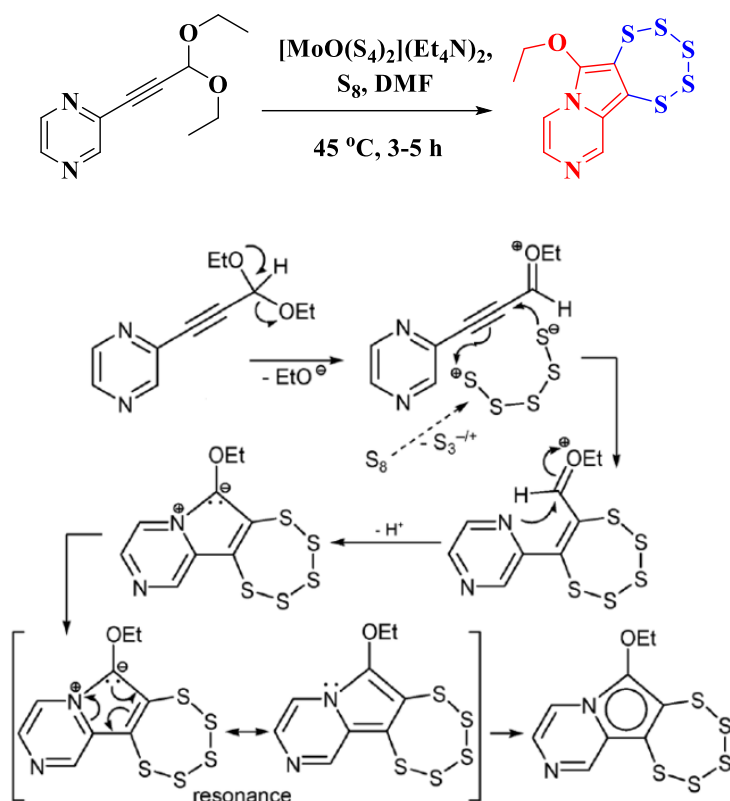
**Scheme 1.3:** Path A: Synthesis of pentathiepins from benzene dithio-2-thione; Path B: from thiadiazols

Bergman and co-workers developed an efficient synthetic methodology to obtain indole based pentathiepins via lithium mediated direct cyclosulfurization with elemental sulfur. This methodology was successfully applied in the synthesis of various heterocycle fused pentathiepins (Scheme 1.4).<sup>30, 40</sup>



**Scheme 1.4:** Synthesis of indole fused pentathiepin via lithiation/sulfurization.

Although numerous synthetic protocols were developed for the synthesis of a variety of pentathiepins, the majority of them suffer from limitations such as harsh reaction conditions, long durations of reactions as well as complex non-eco-friendly purification processes. In 2013, our group (Zubair et al.) developed a milder and well-tolerated protocol serendipitously, while investigating molybdenum coordination chemistry with heterocyclic alkynes.<sup>57</sup>



**Scheme 1.5:** Molybdenum mediated synthesis of pentathiepieno-pyrrolo[1,2-a]pyrazine. Plausible reaction mechanism for the formation of pentathiepieno-pyrrolo[1,2-a]pyrazine.<sup>57</sup>

The reaction of a *N*-heterocycle bearing di-ethoxy alkyne moiety (e.g., pyrazine, quinoxaline) with equimolar amounts of elemental sulfur in the presence of tetraethylammonium-oxobis(tetrathio)molybdate ( $[\text{MoO}(\text{S}_4)_2](\text{Et}_4\text{N})_2$ ) in either DMF or ACN at room temperature for 3 to 5 hrs resulted in novel heterocyclic pentathiepins (Scheme 1.5).<sup>57</sup>

Considering the zwitterionic nature of the  $\text{S}_5$ -unit, presumably generated from elemental sulfur ( $\text{S}_8$ ) under the reaction conditions, an addition on the alkyne moiety takes place followed by nitrogen driving the cyclization/aromatization and resulting in the pentathiepieno-[1,2-a]pyrazine.<sup>57</sup> However, detailed mechanistic investigations were essential to decipher molybdenum's role in the complete process. This was one of the aims of this PhD project, and more details are portrayed in the results and discussion section of this chapter.

## 1.4 Overview

This chapter describes the synthesis of various new families of heterocycle fused pentathiepins via the molybdenum mediated methodology, which was previously reported in our research group (Zubair et al.). Due optimizations of the process were made following the targeted heterocyclic pentathiepin properties. The central objectives of this project include extending

the library of heterocycle fused pentathiepins, optimization experiments to increase overall yields, as well as understanding the reaction mechanism of the molybdenum mediated process. The targeted families were categorized based on the heterocycle moiety fused to the pentathiepin rings, such as quinoxaline, pyrazine, pyridine, purine, imidazopyrazine, pyrrolopyrazine moieties and others. The biologically active heterocyclic scaffolds were preferably selected, and functional group modifications were performed to enhance the water solubility of the final products. Generally, the syntheses of the pentathiepin derivatives proceeded through multi-step organic synthesis; however, the Sonogashira cross-coupling and molybdenum mediated five-membered sulfur ring formation steps were common. The rack stable and commercial palladium (II) catalysts were employed for the Sonogashira cross-coupling to prepare corresponding 1,1'-diethoxy alkyne precursors. Subsequently, these alkyne precursors were transformed into the respective pentathiepins in the presence of  $[\text{MoO}(\text{S}_4)_2]$   $(\text{Et}_4\text{N})_2$  and elemental sulfur under  $\text{N}_2$  atmosphere. The crude mixtures of final products were purified by column chromatography, the  $^1\text{H}$ ,  $^{13}\text{C}$ ,  $^{19}\text{F}$ -NMR, APCI-MS, CHNS, and X-ray diffraction analysis techniques were used for complete characterization of final pentathiepins. It is worth to mention, that the  $^1\text{H}$  NMR spectra of methylene ( $-\text{CH}_2-$ ) protons of the ethoxy functional group are consistent in all synthesized pentathiepins, and later they were considered as fingerprint signals for these compounds. Furthermore, the attempt to understand the reaction mechanism of the molybdenum mediated process was made via performing same control experiments. Notably, the  $[\text{MoO}(\text{S}_4)_2]$   $(\text{Et}_4\text{N})_2$  complex was found crucial for the pentathiepin formation while other Mo(IV)/Mo(VI) sources such as  $\text{MoO}_2\text{S}_2$ ,  $\text{MoO}_4$  were unsuccessful. The  $[\text{Cu}(\text{S}_4)_2]$   $(\text{Ph}_4\text{P})_2$  complex was also investigated for the pentathiepin ring formation and observed to yield the desired pentathiepin in the initial screening.

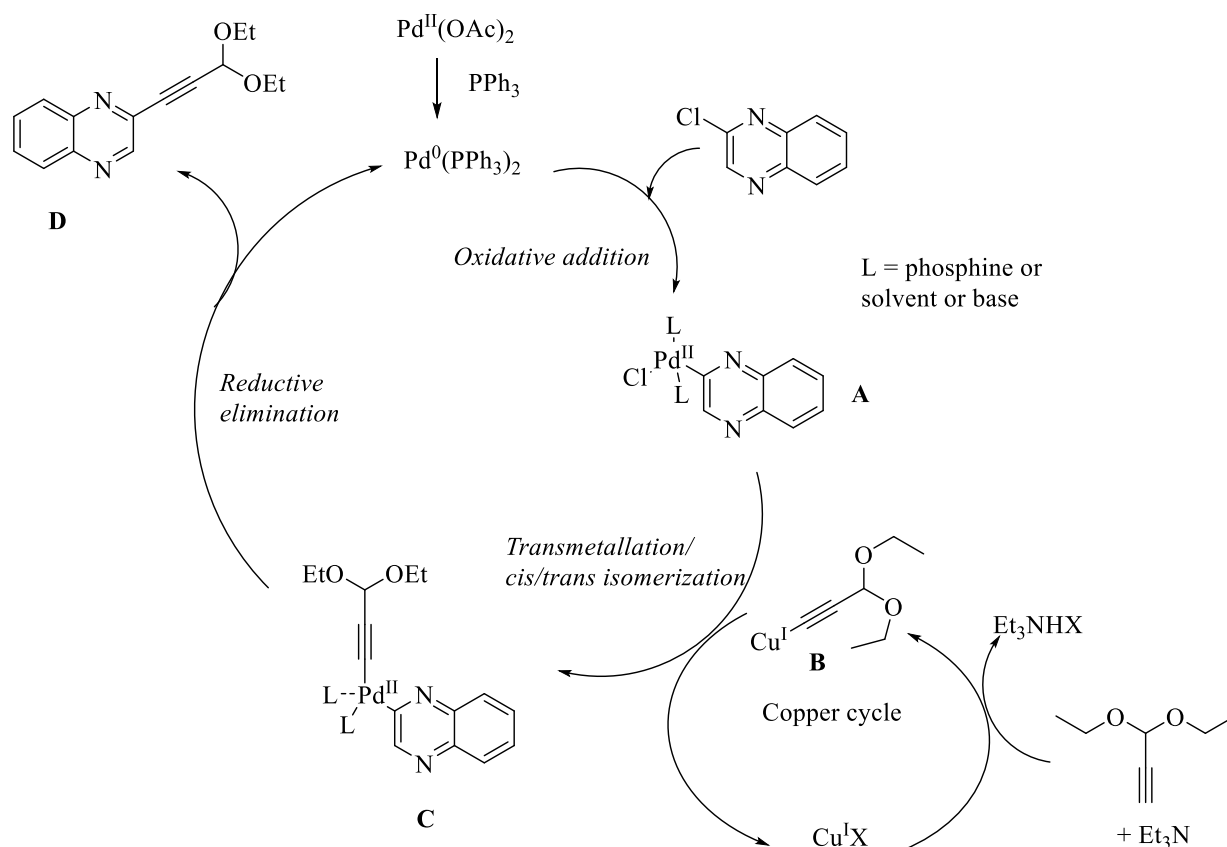
Also, the purified pentathiepin probes were investigated further for their biological relevance as anti-cancer and anti-microbial agents. Prof. Dr Bednarski and his co-workers made the cytotoxic evaluations, and the anti-microbial investigations were performed with the help of Dr Med. Bohnert at the University of Greifswald *Klinikum*. This chapter also lists same results from Mr. Jo Henry Judernatz's Master thesis and Ms. Hanna's Bachelor thesis. The contributions from the Master thesis added eight novel nicotinamide fused pentathiepin to the library as well as their anti-cancer and anti-microbial activity results as discussed. Similarly, the GPx1 enzyme inhibition properties and cytotoxicity of two pentathiepins from the Bachelor student are also described in the larger context of this chapter.



## 1.5 Results and Discussion

### 1.5.1 Quinoxaline fused pentathiepin family (7a-7f)

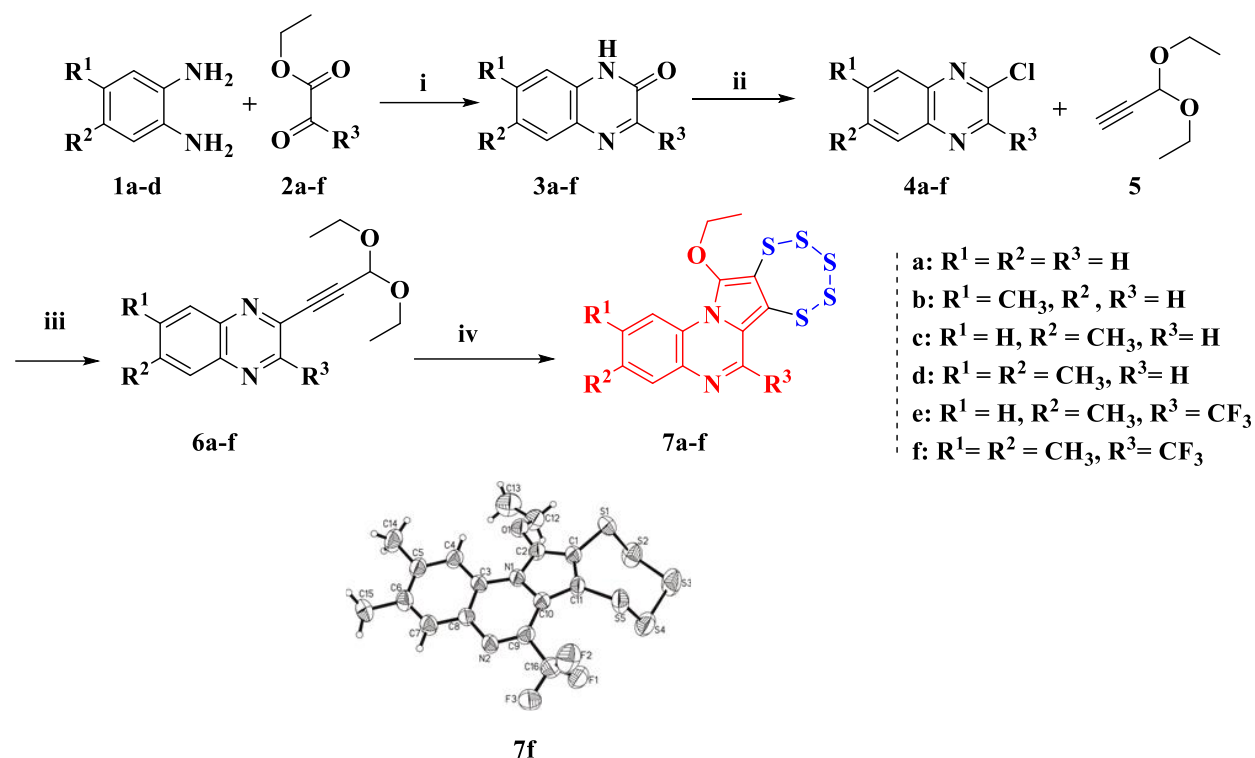
In the beginning of the PhD project, various chloro-substituted quinoxaline derivatives were synthesized according to the known literature procedure.<sup>57</sup> The reactions of 1,2-phenylenediamine (1a) or 5-methyl-1,2-phenylenediamine (1b) 4-methyl-1,2-phenylenediamine (1c) or 4,5-dimethyl-1,2-phenylenediamine (1d) with ethyl glyoxylate (2a-f) resulted in quinoxaline-2-one (3a) or 7-methylquinoxalin-2-one (3b) or 6-methyl quinoxaline-2-one (3c) or 6,7-dimethyl quinoxaline-2-one (3d), respectively. Similarly, trifluoromethyl substituted ethyl glyoxylate (2e-f) was employed to synthesize 6-methyl-3-trifluoromethyl quinoxaline-2-one (3e) or 6,7-dimethyl-3-trifluoromethyl quinoxaline-2-one (3f). Subsequent refluxing of compounds 3a-f in neat POCl<sub>3</sub> for 3-6 hrs resulted in the conversion of amide into chloro-derivatives, 2-chloroquinoxaline (4a) or 7-methyl-2-chloroquinoxalin (4b) or 6-methyl-2-chloroquinoxalin (4c) or 6,7-dimethyl-2-chloroquinoxalin (4d) or 6-methyl-3-trifluoromethyl-2-chloroquinoxalin (4e) or 6,7-dimethyl-3-trifluoromethyl-2-chloroquinoxalin (4f), respectively. The chloro-substituted derivatives 4a-f were employed as electrophilic coupling partners in the Sonogashira cross-coupling with 3,3'-diethoxy-propyne (5) in the presence of palladium catalyst to produce respective ethoxy-substituted alkynyl quinoxaline (6a-6f) in moderate to good isolated yields. All Sonogashira coupling reactions were conducted under a strict inert atmosphere regime in DMF or acetonitrile solvents. The crude coupling alkynyl products were obtained after solvent extraction followed by solvent evaporation, and final purification by column chromatography in 10-30% ethyl acetate/hexane mobile phase to yield air-stable pure compounds (6a-f).



**Scheme 1.6:** The Sonogashira cross-coupling reaction mechanism involved in the synthesis of compound **6a** as example.

In general, the Sonogashira coupling constitutes a multi-metallic catalysis involving Pd(II) pre-catalyst and Cu(I) as supporting catalyst (Scheme 1.6). The activated Pd(0) species will be generated *in situ* in the presence of phosphine ligand or solvent, which subsequently activates the C–halogen bond of the aryl(hetero)halide via oxidative addition (**A**). Simultaneously, the co-catalyst CuI reacts with an alkyne in the presence of the base triethylamine to produce a copper(I)acetylide intermediate (**B**), which undergoes *trans*-metalation with the previous *in situ* formed palladium oxidative adduct (**A**) (Ar-Pd(II)(L)<sub>2</sub>-X) and regenerates the Cu(I)-halogen complex. The palladium intermediate **C** (Ar-Pd(II)L<sub>2</sub>-Alkyne) formed after *transmetalation*, and *cis-trans* isomerization undergoes a reductive elimination to produce the respective aryl alkyne (**D**) as coupled product and redirects the Pd(0) species back to the catalytic cycle (Scheme 1.6).

Standard spectroscopic methods were applied to characterize the purified alkyne derivatives **6a-f**. Most of the compounds were isolated as dark brown oils at room temperature which solidified upon cooling to -20°C. The <sup>1</sup>H and <sup>13</sup>C NMR spectra of compounds **6a-f** along with the <sup>19</sup>F NMR of compounds **6e** and **6f** were recorded in CDCl<sub>3</sub>. In the <sup>1</sup>H NMR, the signals for the aromatic protons of the quinoxaline moiety of **6a-f** were found between 7.85–8.92 ppm.

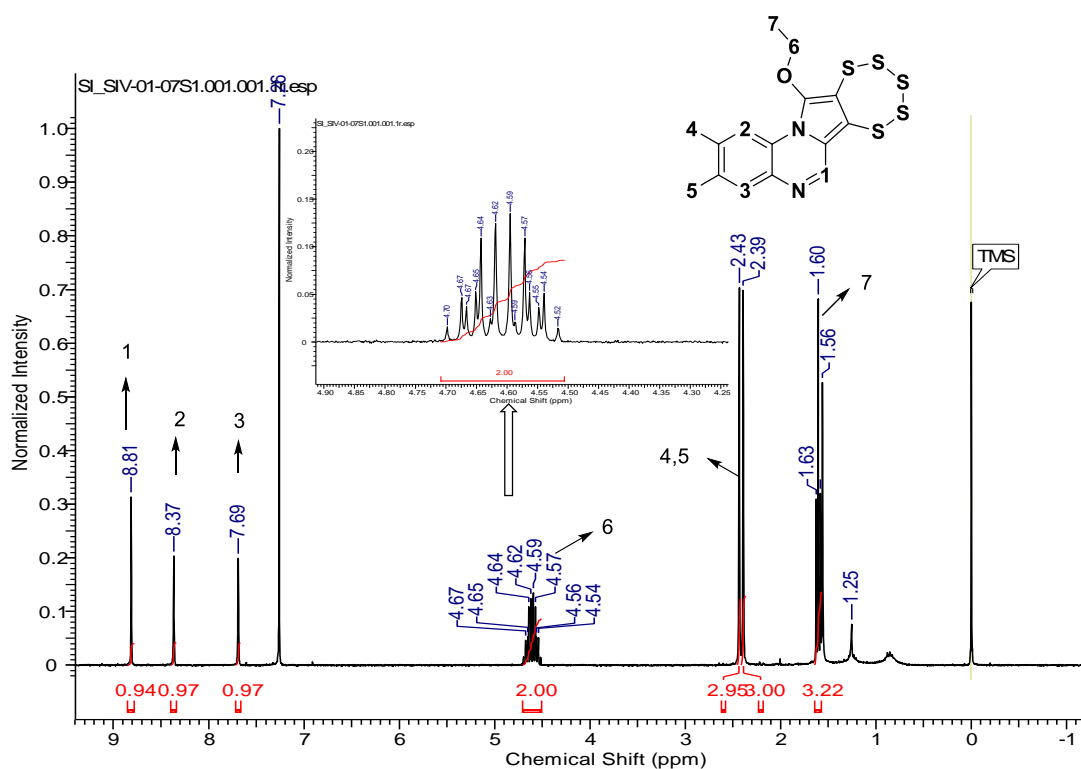


**Scheme 1.7:** Synthesis of quinoxaline fused pentathiepins: i) EtOH, 2 h, reflux; ii) POCl<sub>3</sub>, 2 h, reflux; iii) 1 mol% Pd(OAc)<sub>2</sub>, 5 mol% PPh<sub>3</sub>, 5 mol% CuI, 3 equiv. Et<sub>3</sub>N, CH<sub>3</sub>CN or DMF, 6 h, reflux; iv) [MoO(S<sub>4</sub>)<sub>2</sub>].(Et<sub>3</sub>N)<sub>2</sub> 0.5 equiv., 1 equiv. S<sub>8</sub>, DMF, 15 h, rt.

The characteristic signals in the range of 5.58-5.60 ppm were consistently observed in all aryl alkynes for the quaternary methine carbons (EtO-CH-OEt). Additionally, singlets at 2.54 ppm were observed for -CH<sub>3</sub> protons in compounds **6b-6f** and <sup>19</sup>F NMR show the signal at -66.14 ppm for the -CF<sub>3</sub> group in compounds **6e** and **6f**. Two signals in between 3.52-3.45 ppm and 1.22-1.10 ppm were observed in all compounds and were assigned to methylene (-O-CH<sub>2</sub>-CH<sub>3</sub>) and methyl (-O-CH<sub>2</sub>-CH<sub>3</sub>) groups of the ethoxy moieties, respectively. Furthermore, signals observed in the range of 91.1-77.0 ppm in the <sup>13</sup>C NMR were assigned to the alkyne linkage to the aromatic unit in **6a-f** and the presence of the CF<sub>3</sub> substituent in compounds **6e** and **6f** resulted in the typical C-F coupling pattern around 128.0-129.6 ppm. The molecular mass and the respective fragmentations for the compounds **6a-f** were analyzed by ambient temperature chemical ionization mass spectrometry (APCI-MS). Subsequently, reacting these fully characterized alkyne precursors **6a-f** with one equivalent of elemental sulfur (S<sub>8</sub>) in the presence of 0.5 equiv. (Et<sub>3</sub>N)<sub>2</sub> [MoO(S<sub>4</sub>)<sub>2</sub>] (Mo-precursor) complex in DMF at room temperature for 15 hrs resulted in the targeted quinoxaline-pentathiepins (**7a-f**) in moderate to good isolated yields (30-56%) (Scheme 1.7). The progress of the reaction was monitored via thin-layer chromatography (TLC). After the completion of reaction the crude products, were purified by column chromatography to yield bright lemon yellow amorphous solids.

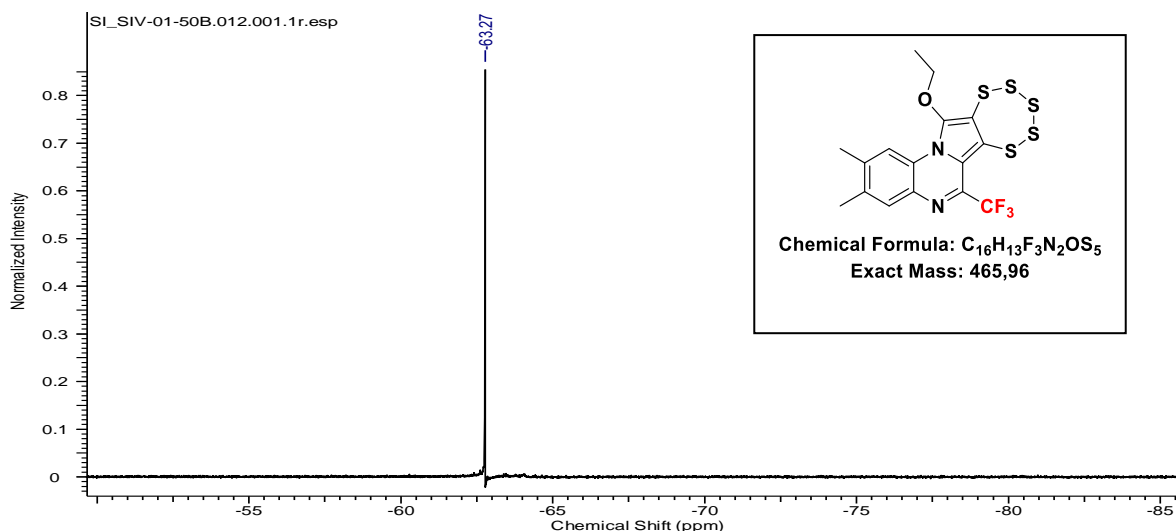
### 1.5.2 Characterization of pentathiepins via NMR spectroscopy and mass spectrometry

The  $^1\text{H}$ ,  $^{13}\text{C}$  NMR and  $^{19}\text{F}$  NMR measurements were performed for purified samples (**7a-f**) in  $\text{CDCl}_3$ . Interestingly, the  $^1\text{H}$  NMR consistently exhibited a multiplet splitting pattern for all tested pentathiepins with the integration of 2H at 4.56-4.71 ppm, which was attributed to the methylene protons ( $-\text{CH}_2-$ ) of the ethoxy functionality (Figure 1.6). The splitting patterns are of the  $\text{ABX}_3$  type, which can be considered as an indirect proof for the presence of the five-membered sulfur ring entity (pentathiepin).<sup>28, 40</sup>

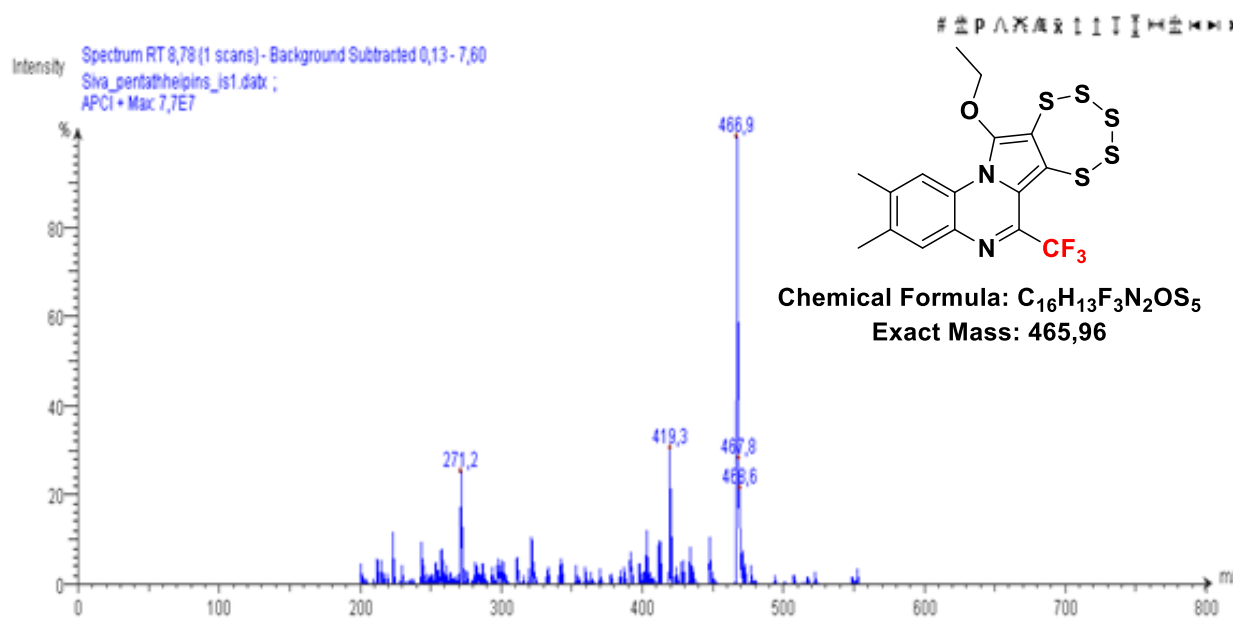


**Figure 1.6:**  $^1\text{H}$  NMR spectrum for compound **7c** (intra: the  $\text{AA}'\text{BB}'$  type of splitting for the  $-\text{CH}_2-$  protons of the ethoxy functional group)

The typical slow inversion rate of the sulfur ring is due to a high inversion energy barrier of 30 kcal/mol.<sup>40</sup> The half-chair transition state of the sulfur ring during an inversion process is highly energy-intensive, while the  $3sp^3$  lone pair containing sulfur orbitals repel each other.<sup>28</sup> Thus, an asymmetry to the molecule is induced. Such type of induced asymmetry causes the  $-\text{CH}_2$  protons to behave as diastereotopic and in consequence yielding a pair of chemically non-equivalent protons resulting complex splitting pattern in the  $^1\text{H}$  NMR.

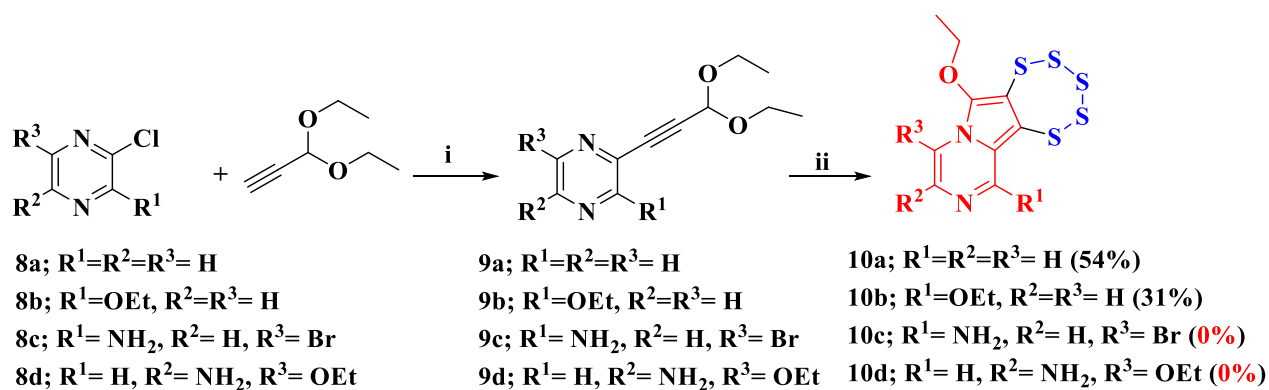
Figure 1.7:  $^{19}\text{F}$ -NMR for compound **7f**.

Additionally, the  $^{13}\text{C}$  NMR spectra of compounds **7a-f** gave signals for the C-S linkage in between the ranges of 115.8-117.2 ppm in agreement with previously reported data.<sup>57</sup> The  $^{19}\text{F}$ -NMR of  $\text{CF}_3$  bearing pentathiepins **7e** and **7f** have shown a downfield shift of 3 to 4 ppm ( $\delta$ : -63.27 ppm) in comparison to their alkyne congeners, presumably due to the perturbations in electron density around the  $\text{CF}_3$  moiety (Figure 1.7). The APCI-MS analysis of all final products **7a-f** showed the molecular ion [M] and/or [M+H] peaks, and in Figure 1.8 the APCI-MS spectra for compound **7f** is depicted as an example. Furthermore, the molecular structure of **7f** was confirmed by X-ray single-crystal structural analysis.

Figure 1.8: APCI-MS spectra for the compounds **7f**.

## 1.5.3 Pyrazine fused pentathiepin derivatives (10a-d)

Considering the biological significance of pyrazine scaffolds in various active pharmaceutical ingredients, we extended the application of the molybdenum mediated protocol to prepare pyrazine appended pentathiepins. In this process, the 2-chloropyrazine substituted starting substrates (**8a-8d**) were taken to the Sonogashira cross-coupling with 3,3'-diethoxy-propyne in the presence of the Pd(II)/Cu(I) multi-catalytic system resulting in the corresponding cross-coupled products **9a-d** in quantitative yields. Subsequently, the alkyne precursors **9a-d** are reacted with elemental sulfur in the presence of the Mo(IV) complex to form the corresponding ring-closed pentathiepin products. However, while compounds **9a** and **9b** were successfully converted to the respective pentathiepin derivatives, the amine substituted pyrazine substrates failed and resulted in unidentified complex mixtures. Presumably, the amine substitution adjacent to a pyrazine 'N'-atom established a suitable chelating pocket for the Mo(IV) center; consequently, the triple bond activation was hindered, and the expected ring-closing process was completely impaired.<sup>58</sup>



**Scheme 1.8:** Synthesis of pyrazine fused pentathiepins; i) Pd(OAc)<sub>2</sub>, 1 mol%, PPh<sub>3</sub>, 5 mol%, CuI, 5 mol%, Et<sub>3</sub>N 3 equiv., CH<sub>3</sub>CN or DMF, 6 h, reflux; ii) [MoO(S<sub>4</sub>)<sub>2</sub>].(Et<sub>3</sub>N)<sub>2</sub> 0.5 equiv., 1 equiv. S<sub>8</sub>, DMF, 15 h, rt.

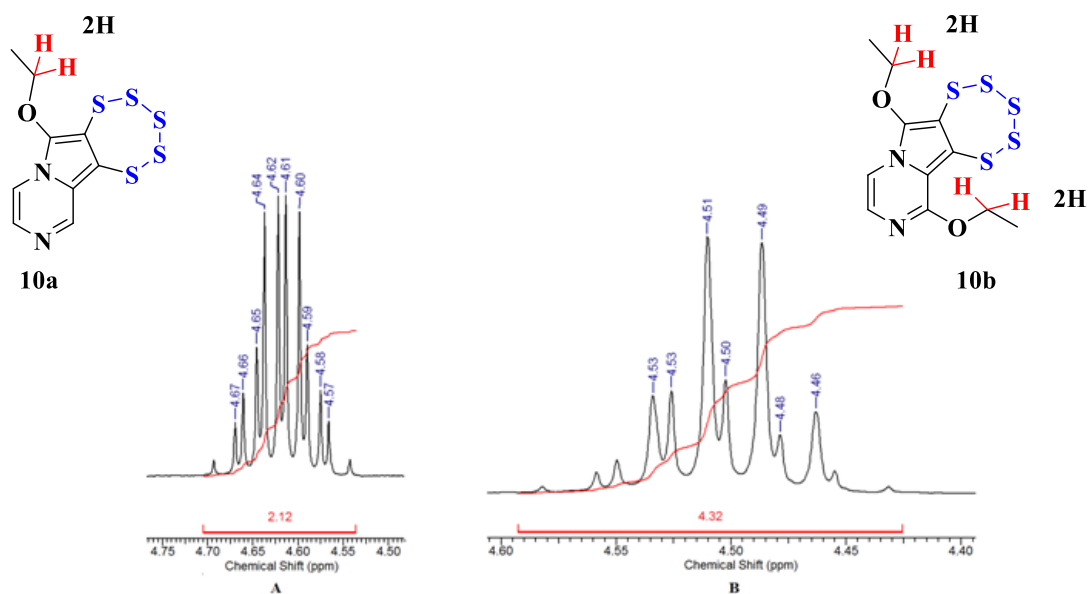


**Figure 1.9:** A: Typical AA'BB' splitting of  $-\text{CH}_2-$  protons (2H) observed for **10a**, B: AA'BB' splitting of  $-\text{CH}_2-$  protons (4H) observed for **10b**.

The crude products **10a** and **10b** were purified by column chromatography in 5% EtOAc/hexane mixture and isolated in 54% and 31% yields, respectively (Scheme 1.8). The final products were characterized by  $^1\text{H}$ ,  $^{13}\text{C}$  and APCI-MS methods. Single-crystal X-ray structural analysis confirmed the molecular structures of **10a** and **10b**.<sup>57</sup> The typical  $-\text{CH}_2-$  multiplet splitting between  $\delta$ : 4.5-4.7 ppm was observed for both **10a** and **10b** (Figure 1.9A & 1.9B) which confirms the presence of the five-membered sulfur moiety in the compounds. In figure 1.10, the molecular structures of compounds **10a**, **10b** as well as the APCI-MS spectra for compound **10b** are depicted. The molecular ion peak at 365.2 m/z is denoted as [M+H] signal of the final product.

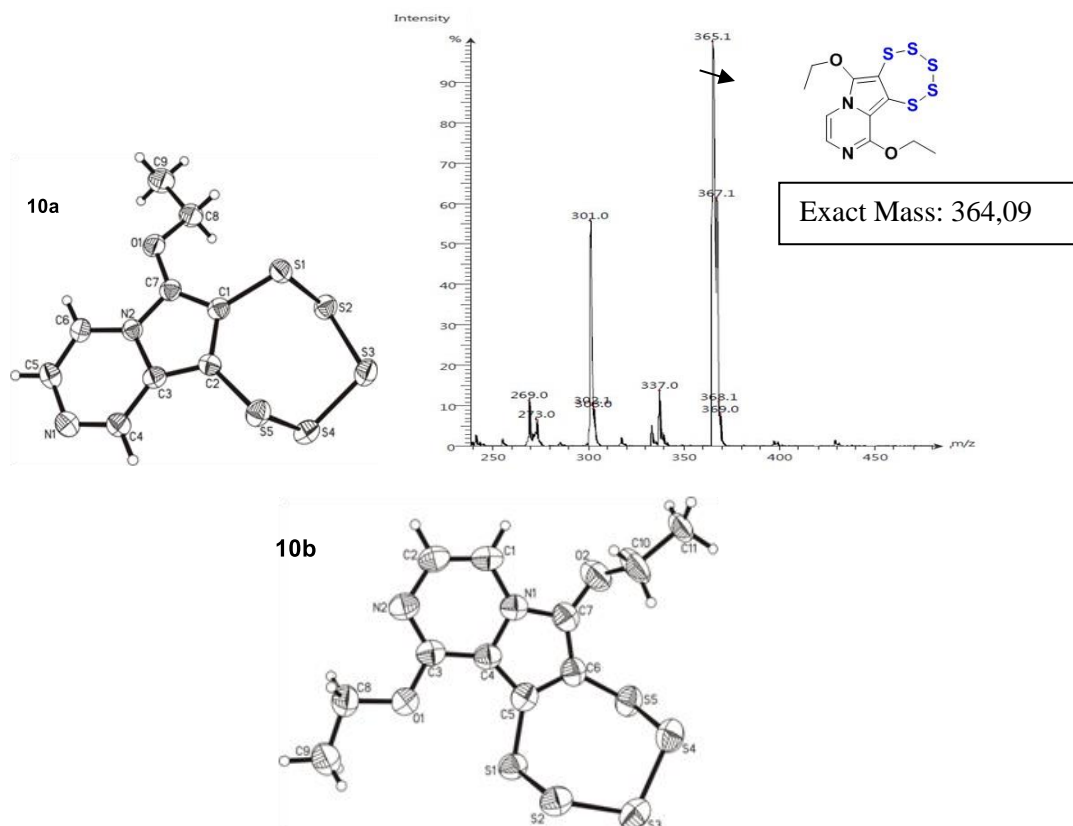
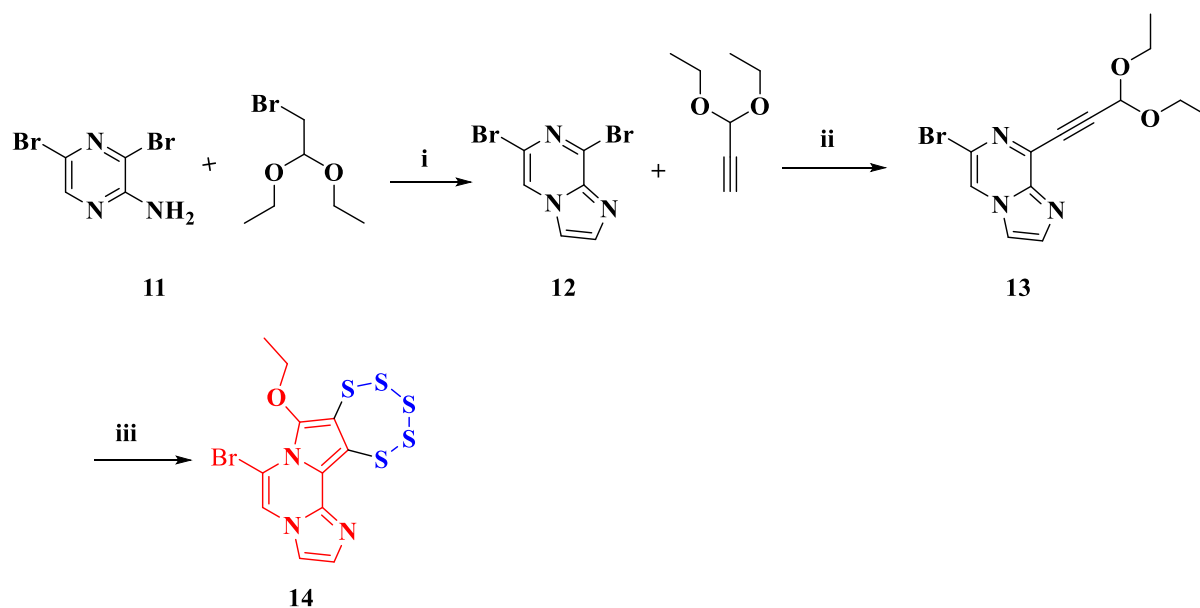


**Figure 1.10:** Molecular structures of compounds **10a**, **10b**; APCI-MS spectrum for compound **10b**.

#### 1.5.4 Imidazol-fused pentathiepin [8-ethoxy-[1,2,3,4,5]pentathiepino[6',7':3,4]pyrrolo[1,2-a]imidazo[2,1-c]pyrazine] (**14**)

Imidazo[1,2-a]pyrazine structural moieties are known active biological units in many drug molecules such as Zolpidem, Zaleplon and many others.<sup>59</sup> Due to the synthetic feasibility of these scaffolds in combination with potent biological significance, a pentathiepin derivative fused to the imidazolo-pyrazine unit was envisaged. The imidazo[2,1-a]pyrazine derivative **12** was synthesized from 2,6-dibromo-3-amino-pyrazine (**11**) by reaction with bromoacetaldehyde diethoxy acetal under reflux conditions for 4 hrs in a H<sub>2</sub>O/THF mixture.<sup>60</sup>





**Scheme 1.9:** Synthesis of 8-ethoxy-[1,2,3,4,5]pentathiepinopyrrolo[1,2-a]imidazo[2,1-c]pyrazine; i) H<sub>2</sub>O/THF reflux, 4 h, 94%, ii) Pd(PPh<sub>3</sub>)<sub>2</sub>Cl<sub>2</sub> 2 mol%, CuI 3 mol%, 3equiv. Et<sub>3</sub>N, CH<sub>3</sub>CN, 80 °C, 6 h; iii) [MoO(S<sub>4</sub>)<sub>2</sub>]·(Et<sub>4</sub>N)<sub>2</sub> 0.5 equiv., 1 equiv. S<sub>8</sub>, DMF, 50 °C, 2 h.

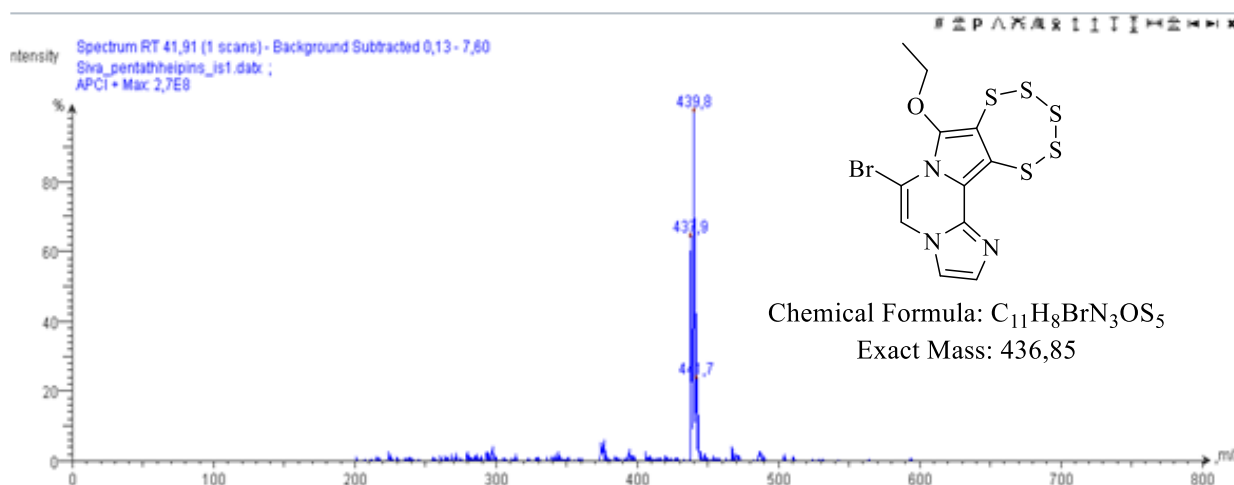
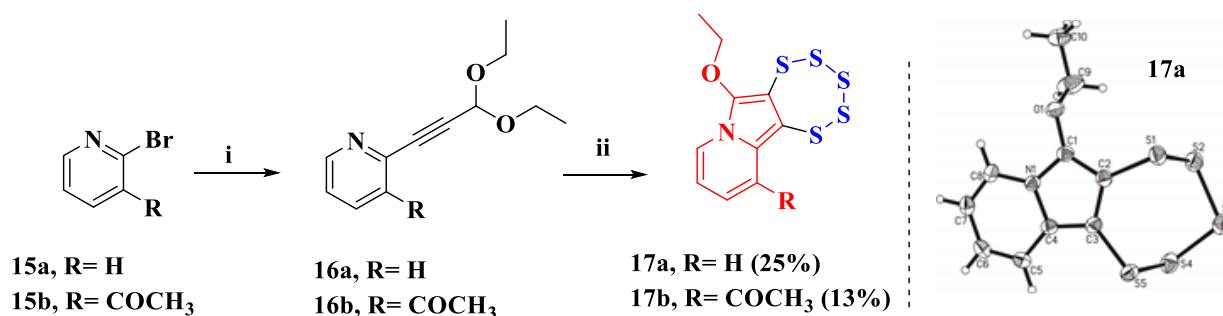


**Figure 1.11:** APCI-MS spectrum for compound **14**.

The resultant off white solid **12** was taken further to the regular sequence of the Pd(II)-catalyzed Sonogashira coupling followed by Mo(IV)-mediated ring-closing steps and resulted in the targeted 8-ethoxy-[1,2,3,4,5]pentathiepinopyrrolo[1,2-a]imidazo[2,1-c]pyrazine (**14**) in 28% isolated yields after column purification (Scheme 1.9). <sup>1</sup>H, <sup>13</sup>C-NMR, APCI-MS experiments characterized the final product, and the composition was confirmed by CHNS analysis. Figure 1.11 shows the APCI-MS spectrum for compound **14**, where the molecular ion peaks at 436 m/z [M] and 437 m/z [M+H], 438 m/z [M+2H] were observed.

### 1.5.5 Pyridine fused pentathiepins (17a-b)

In the next phase, we aimed to prepare pyridine appended pentathiepin derivatives. The 3-substituted 2-bromo pyridine derivatives **15a-b** were coupled with 3,3'- diethoxy propyne in the presence of the Pd(OAc)<sub>2</sub> and CuI multi-catalytic system (Sonogashira conditions) resulting in the alkyne precursors **16a** and **16b** in quantitative yields as brown solids (Scheme 1.10). The purified fractions of these alkyne precursors were further reacted with elemental sulfur in the presence of the Mo(IV) complex resulting in ring-closing and leading to the formation of novel pyridine pentathiepin derivatives. The crude reaction mixtures were purified by column chromatography in 5-10% EtOAc/hexane yielding the desired products **17a** and **17b** in 25% and 13% yields, respectively (Scheme 1.10). <sup>1</sup>H, <sup>13</sup>C, APCI-MS experiments characterized the final products, and their elemental composition was confirmed by CHNS analysis. The molecular structure of compound **17a** was further confirmed by single-crystal X-ray structural analysis (Scheme 1.10).



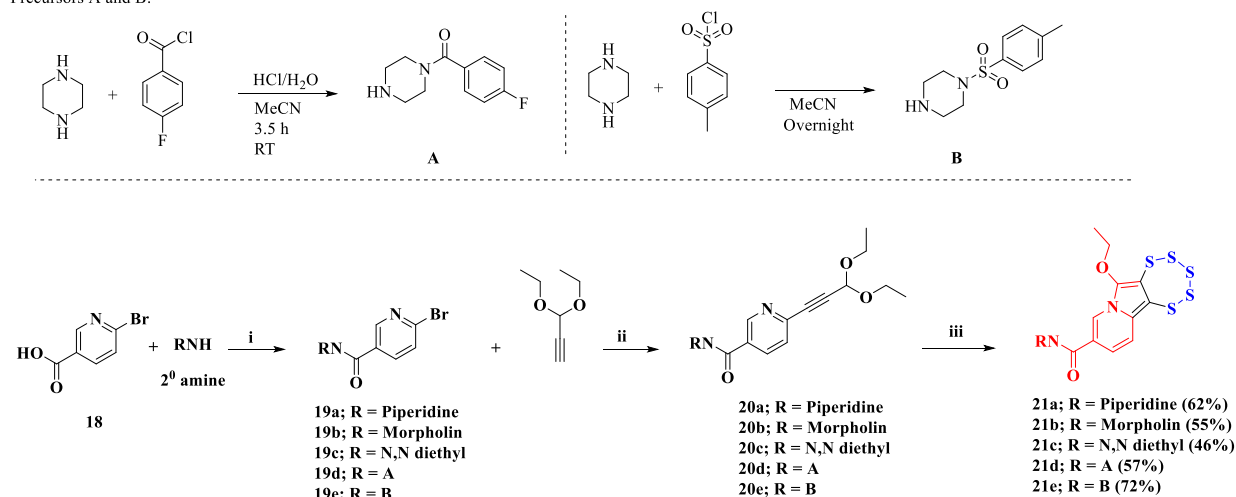
**Scheme 1.10:** i) 3,3'-diethoxy propyne, Pd(OAc)<sub>2</sub> 2 mol%, CuI 3 mol%, 3 equiv. Et<sub>3</sub>N, CH<sub>3</sub>CN, 80 °C, 6 h; ii) [MoO(S<sub>2</sub>)<sub>4</sub>].(Et<sub>4</sub>N)<sub>2</sub> 0.5 equiv., 1 equiv. S<sub>8</sub>, DMF, 15 h, rt.

### 1.5.6 Nicotinamide fused pentathiepins (21a-21f)

After the success with the pyridine scaffold, next novel pentathiepins fused to a nicotinamide backbone were envisioned. The nicotinamide backbone is a crucial building block in various anti-microbial agents (e.g. Niacin), and its efficacy was well established in anti-Mycobacterium tuberculosis therapies already back in 1945.<sup>61-62</sup> Moreover, in 1991 the efficacy of nicotinamide treatment in human immunodeficiency virus (HIV) research was first comprehensively reviewed.<sup>63</sup> Therefore, we presumed that incorporating a physiologically active pentathiepin moiety into the nicotinamide backbone enhances the medicinal properties of the resultant species as well as their water solubility.

## Chapter 1: Pentathiepins

Precursors A and B:



**Scheme 1.11:** i) HBTU, DIPEA, 0 °C to rt, 18 h; ii) Pd(PPh<sub>3</sub>)<sub>2</sub>Cl<sub>2</sub> 5mol%, CuI 5 mol%, 10 equiv. Et<sub>3</sub>N, DMF, 18 h, rt; iii) [MoO(S<sub>2</sub>)<sub>4</sub>].(Et<sub>4</sub>N)<sub>2</sub> 0.5 equiv., 1 equiv. S<sub>8</sub>, DMF, 15 h, rt.

Initially, the respective nicotinamide derivatives were synthesized according to the literature procedure of Lange et al.<sup>64</sup> The piperazine was protected either with acetyl or with sulfonyl chlorides and the resultant corresponding secondary amine precursors **A** and **B** were used in the following reactions (Scheme 1.11). Subsequently, 6-bromo nicotinic acid (**18**) was reacted with various secondary amines such as piperidine, morpholine, *N,N'*-diethylamine, and protected piperazines (**A** and **B**) in the presence of 3-[Bis(dimethylamino)methyl]iumyl]-3H-benzotriazol-1-oxide hexafluorophosphate (HBTU) and base diisopropylethylamine (DIPEA) at low temperatures to yield the respective peptide derivatives **19a-19e**. These nicotinamide derivatives **19a-19e** were further taken into the sequential reactions of the palladium-catalyzed Sonogashira cross-coupling (**20a-e**) followed by Mo(IV)-mediated ring-closing steps resulting in the desired novel nicotinamide fused pentathiepins **21a-e** in good yields (Scheme 1.11). The final structures of the compounds were confirmed by <sup>1</sup>H, <sup>13</sup>C, <sup>19</sup>F- NMR, APCI-MS and CHNS investigations. The molecular structures of the compounds **21a**, **21b**, and **21c** were further confirmed by single-crystal X-ray diffraction analysis (Figure 1.12).

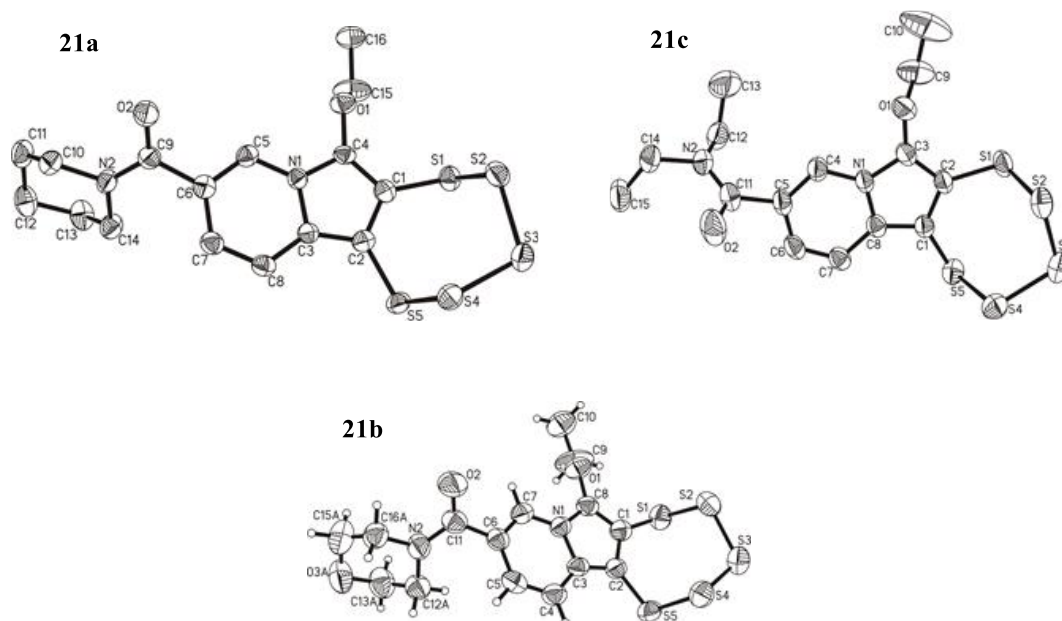
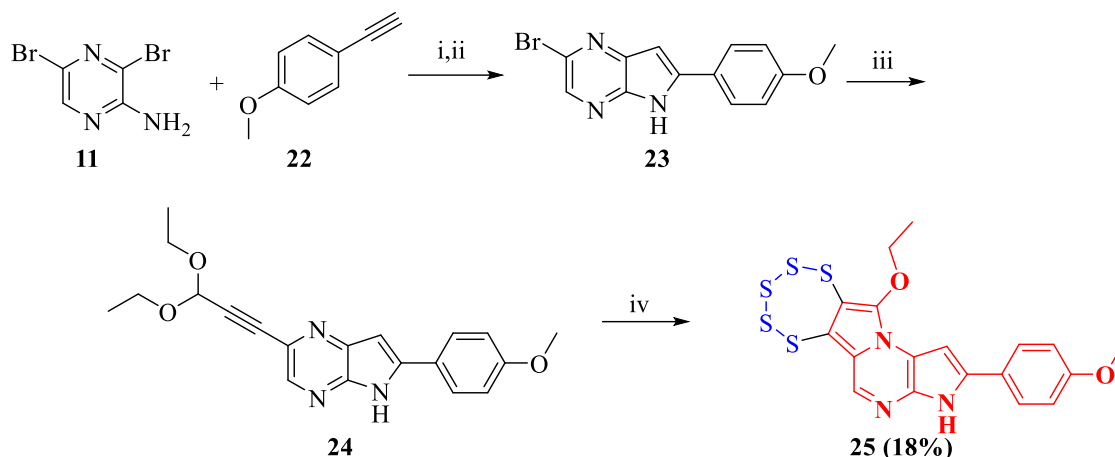


**Figure 1.12:** The molecular structures of compounds **21a**, **21b** and **21c** shown with ellipsoids at the 50% level. H-atoms in **21a** and **21c** were omitted for clarity reasons.

### 1.5.7 Synthesis of 11-methoxy-2-(4-methoxyphenyl)-3H-[1,2,3,4,5]pentathiepino[6',7':3,4]pyrrolo[1,2-a]pyrrolo[2,3-e]pyrazine (**25**)

Aryl substituted pyrrolo-pyrazine scaffolds are biologically significant chromophores and have been employed in nucleoside labeling chemistry.<sup>65</sup> Moreover, these scaffolds were widely applied as protein kinase inhibitors in neurodegenerative and proliferative disorders.<sup>66</sup> Considering the chromophore property and physiological importance of this moiety, we expected that having a pentathiepin ring fused to the chromophore's pyrrolo-pyrazine backbone would facilitate the fluorescence based tracking of the active species inside the cell as well as possibly add further physiological activity.

Compound **25** was synthesized from 2,6-dibromo-3-amino-pyrazine (**11**) via two sequential Sonogashira cross-coupling steps. Initially, the cross-coupling of compound **11** with alkyne synthon **22** in the presence of the Pd(II)/Cu(I) catalytic system resulted in the Sonogashira product. The resultant crude reaction mixture was subsequently taken to the ring-closing step in the presence of base sodium hydride to result in the pyrrolo-pyrazine unit (**23**). Compound **23** was isolated in 78 % yield after column purification.

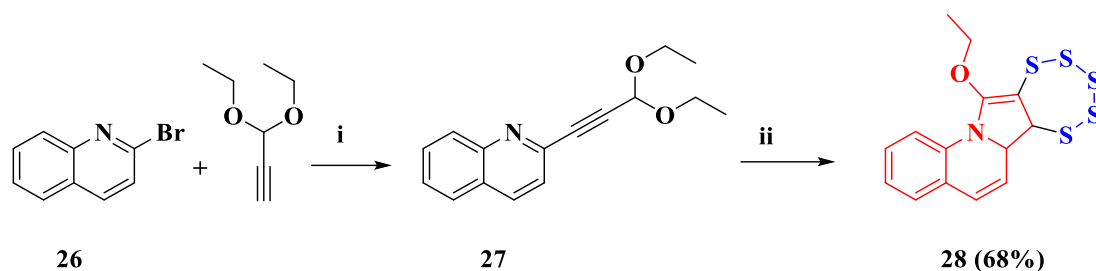


**Scheme 1.12:** Synthesis of 11-methoxy-2-(4-methoxyphenyl)-3H-[1,2,3,4,5]pentathiepino[6',7':3,4]pyrrolo[1,2-a]pyrrolo[2,3-e]pyrazine; i) Pd(OAc)<sub>2</sub> 5 mol%, PPh<sub>3</sub> 7 mol%, 6 mol% CuI, Et<sub>3</sub>N, 3 equiv., CH<sub>3</sub>CN, 80 °C, overnight; ii) NaH, dry THF, 60 °C, 18 h, 78% (two steps) iii) Pd(PPh<sub>3</sub>)<sub>2</sub>Cl<sub>2</sub> 5 mol%, 3 mol% CuI, Et<sub>3</sub>N 3 equiv., DMF, rt, overnight; iv) [MoO(S<sub>4</sub>)<sub>2</sub>].(Et<sub>3</sub>N)<sub>2</sub> 0.5 equiv., S<sub>8</sub> 1 equiv., DMF, 50 °C, 15 h.

Compound **23** exhibits fluorescence on the TLC plate under a UV lamp at 356 nm irradiation. The fluorescent compound **23** was further coupled with 3,3'-diethoxy-propyne under the Sonogashira reaction conditions, followed by ring-closing by the molybdenum complex resulting in the targeted fluorescent pentathiepin derivative (**25**) as red solid in 18% isolated yield after column chromatography purification (35% EtOAc/hexane) (Scheme 1.12). The low yields are attributed to the pyrrolo-pyrazine moiety chelating pocket, which possibly competes with the molybdenum activation of alkyne  $\pi$ -coordination. The purified sample was characterized comprehensively by <sup>1</sup>H, <sup>13</sup>C-NMR, APCI-MS and CHNS analytical methods.

### 1.5.8 Synthesis of 12-ethoxy-6a,6b-dihydro-[1,2,3,4,5]pentathiepino[6',7':3,4]pyrrolo[1,2-a]quinolone (**28**)

Quinoline is a crucial scaffold in medicinal chemistry as its functional modifications have derived biologically important molecules which exhibited enhanced activities through different mechanisms. They predominantly act as growth inhibitors, angiogenesis inhibitors apoptosis inducers, and nuclear receptor modulators.<sup>67-70</sup> In addition, a quinolone backbone is frequently seen in HIV integrase inhibitors,<sup>71</sup> antibacterial,<sup>72-73</sup> antitumour,<sup>74-76</sup> antimalarial,<sup>77</sup> and antifungal/herbicidal agents.<sup>78</sup> Moreover, camptothecin-I is a well-known natural quinolone alkaloid with well-established anticancer property.<sup>79</sup>



**Scheme 1.13:** i) Pd(PPh<sub>3</sub>)<sub>2</sub>Cl<sub>2</sub> 2 mol%, 3 mol% of CuI, 3 equiv. DIPEA, DMF, rt, overnight; ii) [MoO(S<sub>4</sub>)<sub>2</sub>].(Et<sub>3</sub>N)<sub>2</sub> 0.5 equiv., S<sub>8</sub> 1 equiv., DMF, 60 °C, 4 h.

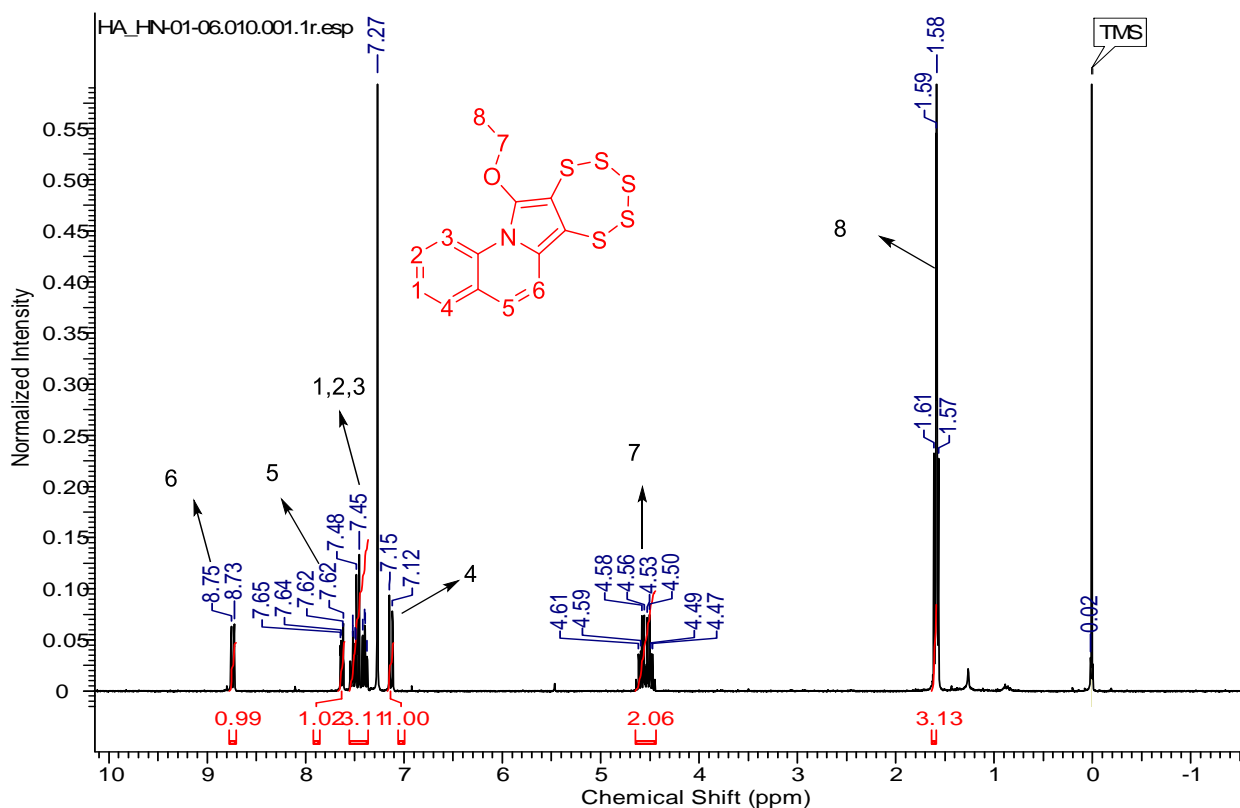
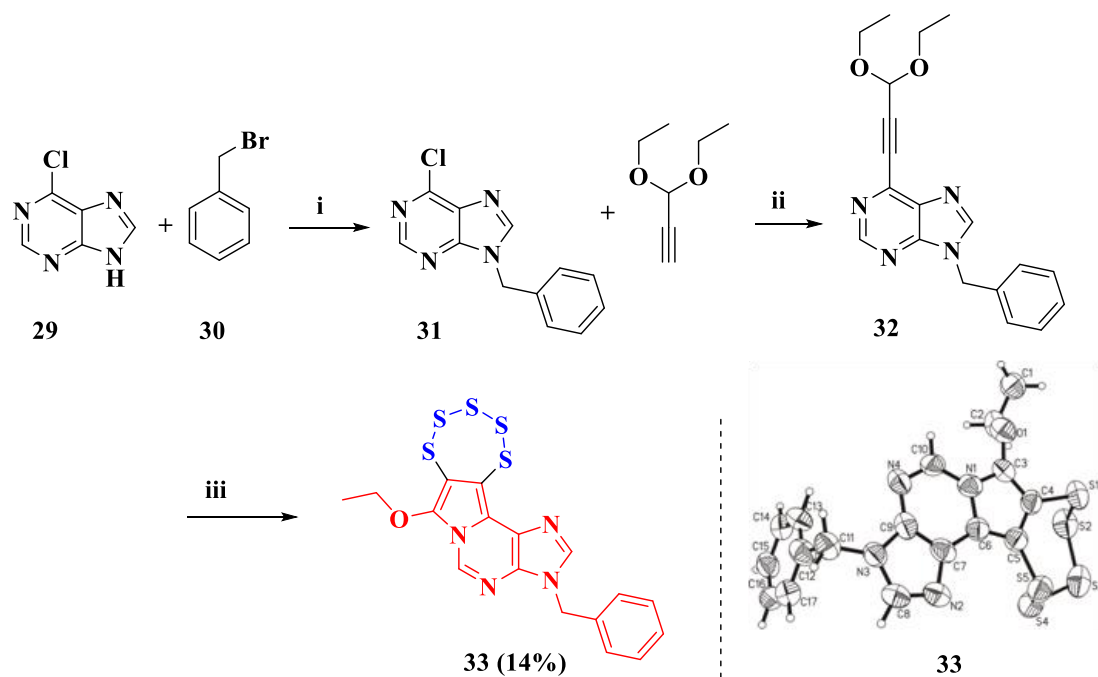


**Figure 1.13:** <sup>1</sup>H NMR spectrum of compound **28**.

Therefore, a quinolone fused pentathiepin was targeted. During this process, 2-bromoquinoline was reacted with 3,3'-diethoxy-propyne under Sonogashira conditions to result in coupled product **27** in quantitative yields. The subsequent reaction of **27** with elemental sulfur in the presence of 0.5 equivalents of Mo(IV)-complex gave the desired 12-ethoxy-6a,6b-dihydro-[1,2,3,4,5]pentathiepino[6',7':3,4]pyrrolo[1,2-a]quinolone (**28**) in 68% isolated yields after column purification (Scheme 1.13). The finished product was identified by <sup>1</sup>H, <sup>13</sup>C-NMR, APCI-MS analysis and the composition of the pentathiepin was confirmed by CHNS analysis. Figure 1.13 depicts the <sup>1</sup>H-NMR spectrum for compound **28**, and the respective protons are assigned.

### 1.5.9 Synthesis of 3-benzyl-7-ethoxy-3H-[1,2,3,4,5]pentathiepino[6',7':3,4]pyrrolo[2,1-i]purine (33)

Moieties derived from the nucleobase purine gained significant importance in medicinal chemistry. For example, the purine based drug olomoucine and its derivatives are potent cyclin dependent kinase protein (CDK) inhibitors, where they selectively bind the ATP pockets of the proteins.<sup>80</sup>



**Scheme 1.14:** i) 3 equiv.  $K_2CO_3$ , DMF, rt, overnight; ii)  $Pd(PPh_3)_2Cl_2$  5 mol%, CuI 6 mol%, 3 equiv.  $Et_3N$ , DMF, rt, overnight; iii)  $[MoO(S_4)_2]$ ,  $(Et_3N)_2$  0.5 equiv.,  $S_8$  1 equiv., DMF, 50 °C, 15 h.

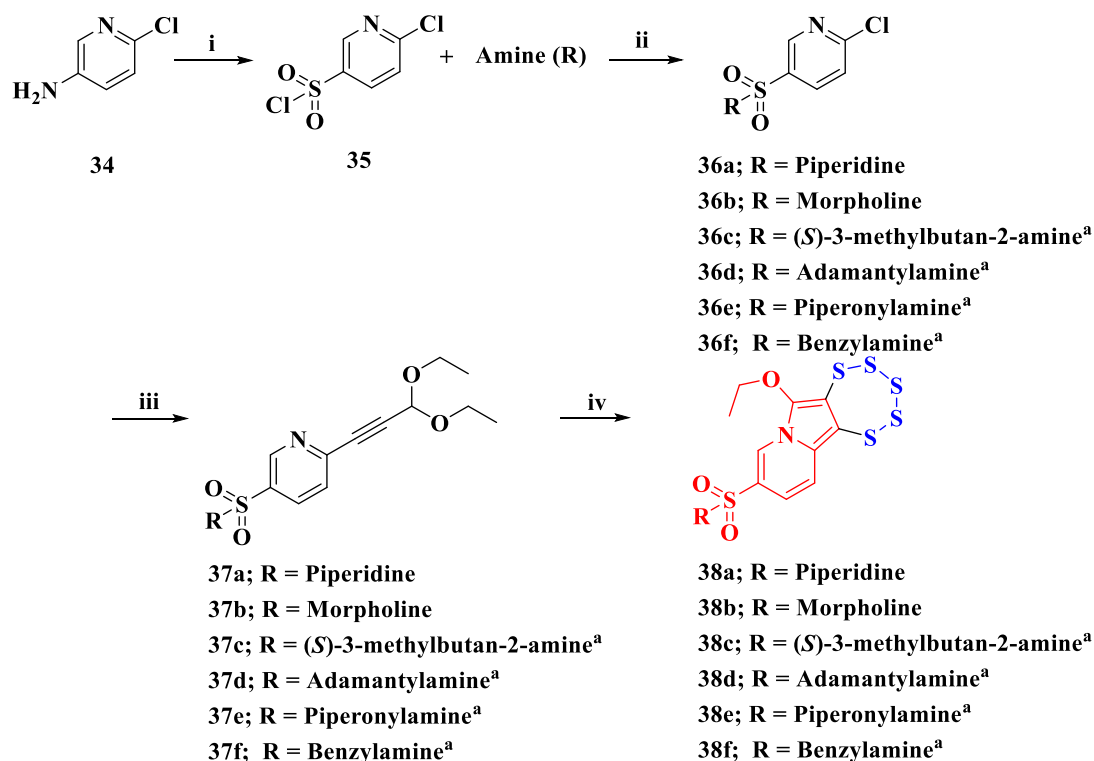
Purine fused pentathiepins were, therefore, targeted in order to develop novel potent cytotoxic agents. Thus, 6-chloro-9H-purine (**29**) was reacted with benzyl bromide in the presence of base potassium carbonate ( $K_2CO_3$ ) for protecting the N-9 position of the purine ring in 9-benzyl-6-chloropurine (**31**) (Scheme 1.14).

The resultant product **31** was identified by APCI-MS analysis, where the major peak was observed at 245.4 m/z  $[M+H]$  which is in perfect agreement with the theoretical value of 244.68 m/z. Subsequently, compound **31** was coupled with 3,3'-diethoxy-1-propyne via a palladium-catalyzed Sonogashira reaction giving compound **32**. The crude product was taken further to  $[MoO(S_4)_2](Et_3N)_2$  mediated ring-closing with elemental sulfur to furnish the respective 3-benzyl-12-ethoxy-3H-[1,2,3,4,5]pentathie-pino[6',7':4,5]pyrrolo[2,1-i]purine (**33**) (Scheme 1.14).<sup>57</sup> The purified fractions were isolated after column chromatography (5-25% EtOAc/hexane) in 14% yield as a yellow solid. Further, the chemical structure of compound

**33** was confirmed by  $^1\text{H}$ ,  $^{13}\text{C}$ -NMR, APCI-MS and CHNS analytical methods. The final molecular structure was identified by single-crystal X-ray structural determination (Scheme 1.14).

### 1.5.10 Pyridine sulfanilamide pentathiepin derivatives (38a-e)

The sulfonamide side chains are well known for their biological activity; specifically, they are vital components in numerous various antibiotics. In general, sulfonamide antibiotics intercede in bacterial folic acid synthesis via inhibiting the dihydropteroic acid synthesis, which is a progenitor of folic acid.<sup>81</sup> Consequently, inactive folic acid accumulation results in the termination of bacterial growth. We envisioned that the combination of an anti-bacterial effect with the production of oxidative stress via the pentathiepin moiety could enhance the antibiotic properties of the resultant drug molecule, thus provide highly active antibiotics. Besides, the sulfonamide scaffolds could probably increase the hydrophilicity of the resultant molecule, which is presumably, advantageous as the parent pentathiepin has low water solubility.



**Scheme 1.15:** i)  $\text{SO}_2$ ,  $\text{NaNO}_2$ ,  $\text{HCl}$ ,  $0\text{ }^\circ\text{C}$ , 1h, ii) DIPEA,  $\text{DCM}$ ,  $0\text{ }^\circ\text{C}$  to rt, 2-4 h, iii)  $\text{Pd}(\text{PPh}_3)_2\text{Cl}_2$  2 mol% ( $^t\text{Pd}(\text{OAc})_2$  2 mol%, XPhos 5 mol%),  $\text{CuI}$  3 mol%, 3 equiv.  $\text{Et}_3\text{N}$ ,  $\text{CH}_3\text{CN}$ ,  $80\text{ }^\circ\text{C}$ , 2-6 h, iv)  $[\text{MoO}(\text{S}_4)_2] \cdot (\text{Et}_4\text{N})_2$  0.5 equiv.,  $\text{S}_8$  1 equiv.,  $\text{DMF}$ ,  $50\text{ }^\circ\text{C}$ , 2 h.

Initially, 6-chloropyridin-3-sulfonyl chloride (**35**) was prepared by the reaction of 6-chloropyridin-3-amine (**34**) with sodium nitrate ( $\text{NaNO}_2$ ) and  $\text{HCl}$  in a freshly prepared sulfur dioxide solution ( $\text{SO}_2$ ) at  $0\text{ }^\circ\text{C}$  (Scheme 1.15).  $^1\text{H}$  and  $^{13}\text{C}$  NMR confirmed the resultant



product. Then compound **35** was reacted with a primary or secondary amine under alkaline conditions, using *N,N*-diisopropylethylamine (Hünig's base) at 0 °C resulting in **36a-f**. Subsequently, the chloro function of compounds **36a-f** was exchanged by 3,3'-diethoxy-1-propyne via Sonogashira coupling. Sonogashira coupled products (**37a-f**) were confirmed by mass spectrometry and utilized for the next step without isolation in order to avoid product loss prior to the final pentathiepin formation.

Piperidine substituted derivative **37a** was, however, characterized by  $^1\text{H}$  NMR and  $^{13}\text{C}$  NMR. The  $^{13}\text{C}$  NMR signals at  $\delta$ : 83 ppm and 87.6 ppm are in agreement with literature reported values, which confirms the presence of the triple (alkyne) bond in **37a**.<sup>82</sup>

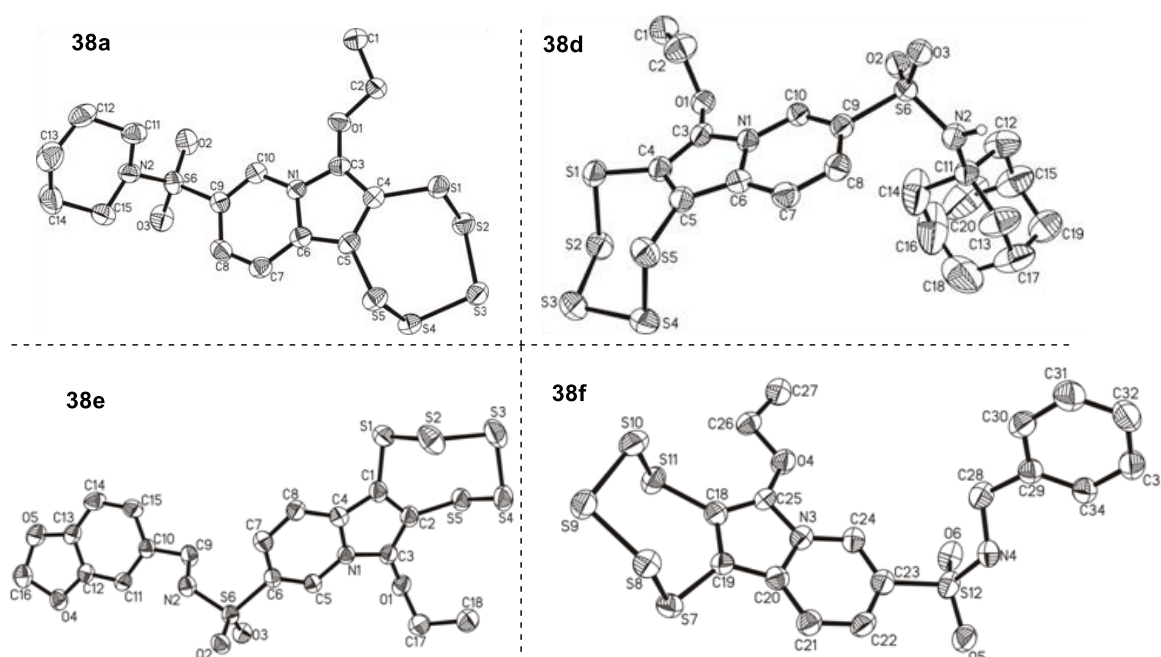


**Figure 1.14:** Molecular structures of compounds **38a**, **38d**, **38e**, **38f** with ellipsoids at the 50% level.

Finally, the six novel sulfonamide bearing pentathiepins (**38a-f**) were synthesized according to the established protocol, and purified fractions were isolated in reasonable quantities. The products were characterized by APCI-MS,  $^1\text{H}$ ,  $^{13}\text{C}$ -NMR, elemental analysis (CHNS) and, in parts, by X-ray crystal structure analysis (**38a**, **38d**, **38e** and **38f** in Figure 1.14).

Notably, in previous reports, in the mass spectra of pentathiepin derivatives the  $[\text{M}-\text{S}_2]^+$  ion peak was prominently detected with high intensity, while the  $[\text{M}+\text{H}]^+$  peaks were rather minimal or absent.<sup>83</sup> In contrast, for all pentathiepin derivatives synthesized via Mo(IV)-mediated procedure we observed the  $[\text{M}+\text{H}]^+$  signal as significant peak along with all possible fragmentations such as  $[\text{M}-\text{S}_2]^+$ ,  $[\text{M}-\text{S}_3]^+$  and others. In most of the previously reported data

the electron ionization (EI-MS) method was employed, which is a rather hard ionization method which possibly facilitates an extensive fragmentation of pentathiepins. The employment of a soft ionization methodology as atmospheric pressure chemical ionization (APCI-MS) was efficient in identifying the  $[M+H]^+$  peak as dominant species due to less predominant fragmentation.<sup>84</sup>

### 1.6 X-ray crystal structure analysis

Twelve pentathiepins were evidenced by single-crystal X-ray diffraction analysis in addition to the standard  $^1\text{H}$ ,  $^{13}\text{C}$ ,  $^{19}\text{F}$ -NMR, MS and CHNS measurements. Although a few disorders in substituent functional groups or aromatic systems were observed, the overall quality of the crystal data is good. Most importantly, the obtained molecular crystal structures allowed to perform a comparative crystallographic analysis. In general, the chair conformation of the pentathiepin (polysulfur unit) is thermodynamically favorable according to the previously reported pentathiepin crystal structures.<sup>83</sup> The bond lengths and bond angles of twelve pentathiepin moieties are summarized in table 1.2 and table 1.3. The average bond distance between sulfur atoms, (2.05-2.06 Å) is in agreement with the canonical S–S bond distance in cyclooctasulfur  $\text{S}_8$  (2.051 Å).<sup>83, 85</sup> Interestingly, S–C bond lengths between 1.73 and 1.75 Å were observed, which are between the  $sp^2$  hybridized S–C single bond length (1.81 Å) and S=C double bond length (1.6 Å). The decreased bond distances of S–C connections could be due to the fused five-membered aromatic system, which might interact with lone pair sulfur  $p$ -orbitals of adjacent S atoms and thereby enhances the stability of pentathiepin ring. The S–S bond angles were ranging between 102.72° to 105.26° degrees and S–C bond angles averaging between 126.8° to 127.4°, which were in agreement with literature known values for  $\text{S}_6$  and  $\text{S}_8$  scaffolds.<sup>85, 87</sup>

### 1.7 Mechanistic investigations

All aforementioned pentathiepin derivatives were synthesized by the  $(\text{Et}_4\text{N})_2[\text{Mo}^{\text{IV}}\text{O}(\text{S}_4)_2]$  mediated procedure in the presence of elemental sulfur.<sup>86 57</sup> Originally, it was attempted to synthesize molybdenum dithiolene complexes from the alkyne precursors by reaction with  $(\text{Et}_4\text{N})_2[\text{Mo}^{\text{IV}}\text{O}(\text{S}_4)_2]$ . However, the first thereby isolated product was surprisingly identified as a novel *N*-heterocyclic pentathiepin. As pentathiepins are biologically active molecules<sup>40</sup> research in this field was continued leading to further various heterocycle fused pentathiepin derivatives. A plausible mechanism for pentathiepin formation was reported in our initial communication.<sup>57</sup> The importance of utilizing alkyne precursors bearing two diethoxy

functional groups (protected aldehyde) was well established earlier by Zubair et al. by conducting several control experiments. The alkyne precursors without the diethoxy moiety, in fact, results in corresponding Mo(IV) bis-dithiolene complexes, instead of pentathiepins.

However, open questions with respect to the role of  $(\text{Et}_4\text{N})_2[\text{Mo}^{\text{IV}}\text{O}(\text{S}_4)_2]$  species in the reaction mechanism prompted us to perform additional investigations. Pentathiepin formation was never observed when  $(\text{Et}_4\text{N})_2[\text{Mo}^{\text{IV}}\text{O}(\text{S}_4)_2]$  was replaced by other Mo(IV) precursors such as  $(\text{Et}_4\text{N})_2[\text{MoO}_2\text{S}_2]$ ,  $\text{K}_3\text{Na}[\text{MoO}_2(\text{CN})_4]$  or only in the presence of excess elemental sulfur. This suggests that the  $(\text{Et}_4\text{N})_2[\text{Mo}^{\text{IV}}\text{O}(\text{S}_4)_2]$  complex plays a dual role: activating the triple bond and engaging in a redox reaction with elemental sulfur. Accordingly,  $\text{S}_8$  might be reduced to an  $\text{S}_5^{2-}$  fragment while Mo(IV) is oxidized to Mo(VI) bound to the remaining  $\text{S}_3$  fragment. In the course of the ongoing reaction, elemental sulfur is formed, probably at least partly from the  $\text{S}_4^{2-}$  ligands of the original complex, and released while re-reducing molybdenum to the Mo(IV) complex. The regeneration of the Mo(IV) complex was confirmed as red  $(\text{Et}_4\text{N})_2[\text{Mo}^{\text{IV}}\text{O}(\text{S}_4)_2]$  crystals were isolated from the crude reaction mixture after completion of the pentathiepin formation (Figure 1.15). Although the current protocol well tolerates a variety of fused heterocycles, the competitive coordination effect of Mo(IV) toward the alkyne triple bond ( $\pi$ -donor) and chelating ligands ( $\sigma$ -donors or  $\pi$ -donor) is limiting the substrate scope. As an alternative, a similar copper complex  $(\text{PPh}_4)_2[\text{Cu}(\text{S}_4)_2]$  was prepared according to the previously reported literature procedure.<sup>87</sup> The employment of copper metal complex in pyridine fused pentathiepin (**17a**) synthesis instead of Mo(IV) precursor in the presence of sulfur was successful and interestingly the reaction completed within 2 h with improved overall yield of 52%. The developed copper-mediated procedure is currently under investigation with challenging substrates like purines, pyrazino[2,3-b]pyrazine and others. We believe such type of protocol will be highly advantageous in accessing new classes of pentathiepin molecules.

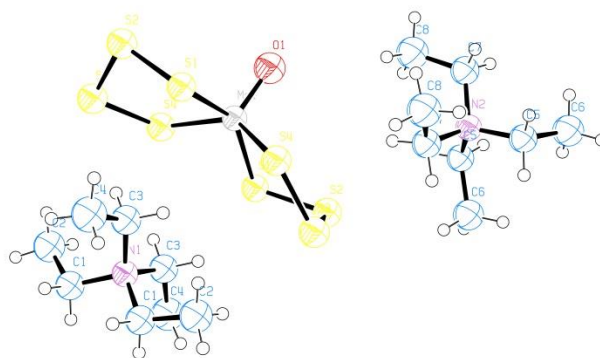


**Figure 1.15:**  $(\text{Et}_4\text{N})_2[\text{Mo}^{\text{IV}}\text{O}(\text{S}_4)_2]$  molecular structure determined by single-crystal X-ray analysis with ellipsoids at 50% level.

Table 1.2: S–S and C–S bond lengths in Å for pentathiepin moieties.

Bond distance in Å (pentathiepin)														
Atom 1	Atom 2	7f	10a	10b	17a	21a	21b	21c	33	38a	38d	38e	38f	Ø
S1	S2	2.052	2.058	2.061	2.061	2.062	2.055	2.057	2.062	2.058	2.055	2.057	2.061	<b>2.059</b>
S2	S3	2.043	2.054	2.05	2.06	2.055	2.049	2.048	2.053	2.058	2.049	2.045	2.048	<b>2.050</b>
S3	S4	2.049	2.049	2.057	2.048	2.051	2.045	2.046	2.050	2.043	2.056	2.054	2.055	<b>2.053</b>
S4	S5	2.055	2.061	2.056	2.067	2.074	2.068	2.067	2.071	2.070	2.063	2.051	2.060	<b>2.062</b>
S5	C1	1.733	1.734	1.734	1.732	1.733	1.734	1.735	1.727	1.732	1.737	1.734	1.740	<b>1.734</b>
C2	S1	1.749	1.756	1.744	1.748	1.747	1.746	1.741	1.756	1.754	1.749	1.735	1.745	<b>1.747</b>

Table 1.3: Bond angles of the pentathiepin moieties.

Bond angles in °														
Atoms	7f	10a	10b	17a	21a	21b	21c	33	38a	38d	38e	38f	Ø	
C1-S1-S2	103.48	103.56	102.71	103.29	102.36	102.43	102.42	102.76	101.74	102.09	103.53	103.51	<b>102.72</b>	
S1-S2-S3	104.67	104.77	103.74	104.91	104.45	105.00	104.66	104.8	106.04	105.69	106.59	104.69	<b>105.26</b>	
S2-S3-S4	104.44	104.47	104.33	104.93	104.85	104.25	105.33	104.84	104.85	104.57	103.49	104.52	<b>104.43</b>	
S3-S4-S5	104.31	104.09	105	104.86	104.32	104.14	104.53	104	104.33	103.2	102.82	103.73	<b>103.85</b>	
S4-S5-C2	103.61	103.17	102.84	103.57	103.36	104.25	102.74	102.25	102.77	103.11	103.52	103.92	<b>103.07</b>	
S5-C2-C1	127.05	128.8	125.29	128.03	127.0	128.14	126.4	127.25	127.36	128.69	128.7	127.15	<b>127.41</b>	

## 1.8 Biological investigations of novel pentathiepins

### 1.8.1 Oxidative stress and glutathione peroxidase

Cells use reducing or oxidizing mechanisms to maintain an appropriate balance. The predominance of any reducing or oxidizing metabolism in organisms that cannot be controlled by the cell results in reductive or oxidative stress.<sup>88</sup> In consequence, alterations in membranes, proteins and genetic material occur, and that provokes the initiation of apoptosis or necrosis and finally the destruction of the cell.<sup>89</sup> In general, oxidative stress is characterized by the increased presence of highly reactive oxygen and nitrogen species, called ROS (reactive oxygen species) and RNS (reactive nitrogen species).<sup>90</sup> The main reactive oxidizing species include various radicals such as the superoxide radical ( $O_2^{\cdot-}$ ), the hydroxyl radical ( $OH^{\cdot}$ ), nitrogen monoxide and dioxide ( $NO^{\cdot-}$ ;  $NO_2^{\cdot}$ ) and some non-radicals such as hydrogen peroxide ( $H_2O_2$ ), hypochlorous acid (HOCl) and peroxynitrite (ONOO).<sup>90</sup> Besides their toxic effects, these reactive species also behave like messenger substances in the organism in low concentrations. ROS were proven vital for cell proliferation, and apoptosis.<sup>91</sup> ROS occur under normal metabolic reactions, especially in the mitochondria and peroxisomes. Superoxide radicals are generated in the mitochondria, then disproportionate to  $H_2O_2$  and  $O_2$  catalyzed by mitochondrial superoxide dismutase (SOD).<sup>92-94</sup> The resultant  $H_2O_2$  may be reduced to a hydroxide ion and a hydroxyl radical via the iron-dependent Fenton's reaction.<sup>95-96</sup> ROS can also occur via necessary enzyme associated processes. For example, ROS can be produced by various cytochrome P450 isoforms, oxidases such as xanthine and NADPH oxidases,<sup>97</sup> and nitrogen monoxide synthases.<sup>98</sup> ROS also arise from viral infections<sup>99</sup> and UV radiation.<sup>100</sup>

The hydroxyl radicals generated by the Fenton's reaction are the most aggressive ROS. They can actively interact with biomolecules, and consequently have a far-reaching influence on their functionalities. For example, strand breaks of DNA are induced by oxidation and lipid peroxidation strongly influences membrane fluidity. Therefore, cells need mechanisms to detoxify emerging ROS. The endogenous and exogenous antioxidant molecules such as ascorbic acid,  $\alpha$ -tocopherol (Toco) and glutathione (GSH) are known to act as radical scavengers or as reducing agents. Alternatively, other enzymatic systems are also performing the detoxification of ROS, namely, SOD, catalases and glutathione peroxidases (GPx) which catalytically break down ROS.<sup>101-102</sup>

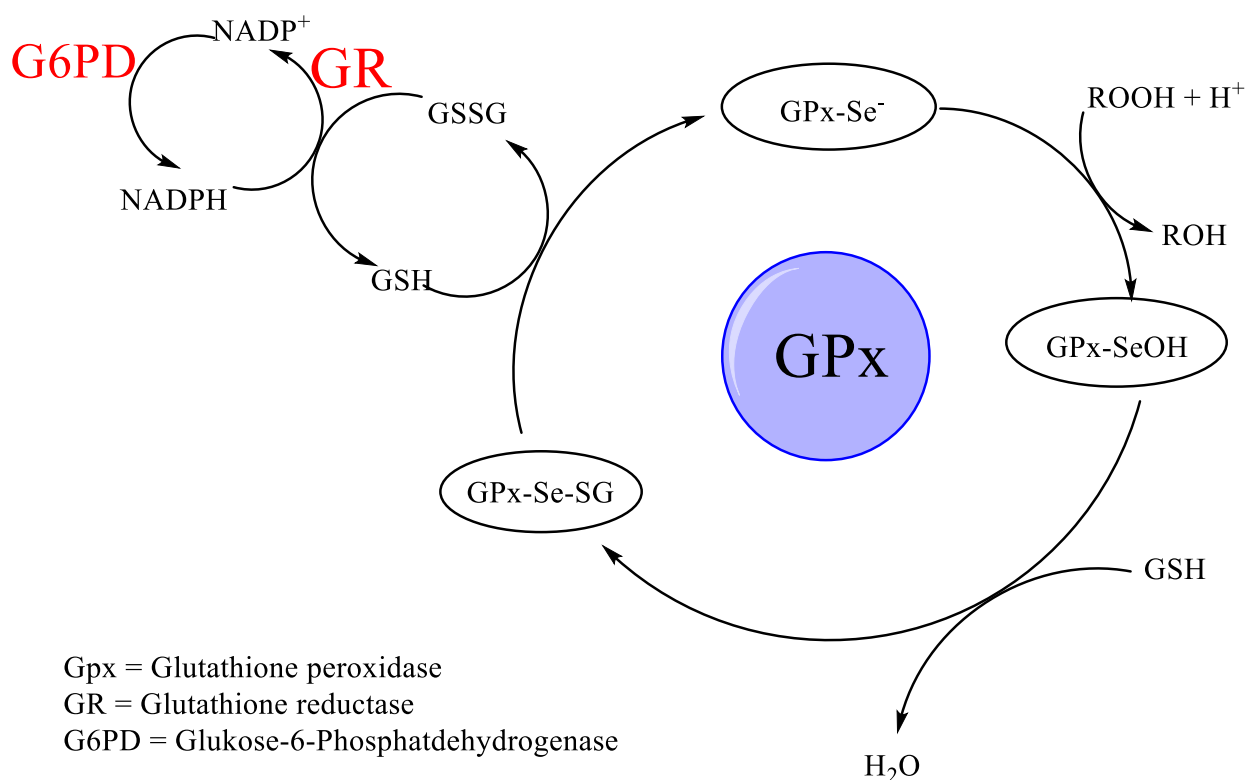


**Figure 1.16:** The enzymatic inactivation mechanism of peroxides by the GPx-1 enzyme.

As general transfer ROS, increasing concentrations of  $\text{H}_2\text{O}_2$  can cause damage in cells. The glutathione peroxidases (GPx) as necessary antioxidative enzymes efficiently break down intracellular  $\text{H}_2\text{O}_2$  and organic peroxides. The GPx enzymes use two glutathione (GSH) molecules and oxidise them to the disulfide (GSSG) while reducing  $\text{H}_2\text{O}_2$  or the organic peroxide to either water or the corresponding alcohol, respectively. Eight GPx isoenzymes are known, of which GPx-1, -2, -3, -4 and -6 have the rare amino acid selenocysteine in their active centres, whereas the other isoenzymes carry cysteine.<sup>103</sup> Selenocysteine can be deprotonated at physiological pH value, while Cys is undissociated due to the pKa difference (SeCys: pKa = 5.2; Cys: pKa = 8.4).<sup>104</sup> Thus, under physiological conditions, the SeCys exists as selenolate ( $\text{Se}^-$ ), which can subsequently be oxidized to selenic acid (Se-OH) by peroxides. One equivalent of GSH is then able to reduce the selenic acid, creating a GSselenate intermediate. Due to the nucleophilic attack of another equivalent of GSH, the selenium recovers its original selenolate form via the formation of GSSG and the catalytic cycle of the GPx is completed (Figure 1.16). The reduced GSH can then be recovered from GSSG by glutathione reductase (GR), which utilizes the oxidation of NADPH, to  $\text{NADP}^+$ . The circulations of the glucose-6-phosphate dehydrogenase or the pentose-phosphate pathway recover NADPH, subsequently regulating the GPx redox process (Figure 1.16).

The role of GPx in tumor development as well as in tumor progression has been controversial.<sup>105-106 107-108</sup> In general, the anti-oxidative activity of GPx-isoenzymes is associated with a positive effect for organisms. However, polymorphisms of GPx1 caused a reduced effect of the GPx; consequently, excessive ROS levels in the cells then act on the DNA and thus promote a higher risk in cancer progression for malignant lung, breast and prostate diseases.<sup>109-111</sup> On the other hand, it is described that high GPx1 activity in malignant diseases can cause a poor prognosis.<sup>112-113</sup> In many instances, the literature supports that with positive regulation of the GPx1, various tumour cells can develop resistance to chemotherapy.<sup>114</sup> By inhibiting the activity of GPx1, these resistant cells could be made available again for cytostatical treatment.<sup>115</sup> Thus, the development of GPx inhibitors could offer a promising avenue to novel anticancer drugs.

Only a few inhibitors for GPx1 have been identified to date, all having relatively low specificity and sensitivity. Mercaptosuccinic acid (MS) is a well-characterized inhibitor of the GPx1 along with other mercaptans such as tiopronin.<sup>116</sup> These thiols are believed to inhibit the mechanism by first reacting with the selenocysteine in the enzyme active site to an oxidised selen-thiol intermediate.<sup>117</sup> Gold- and mercury compounds like auranofin, gold(I)thioglucose and methylmercury also have GPx inhibitory activity. The high effectivity of these compounds to GPx1 is attributed to the avid affinity of gold and mercury to thiols and selenols. However, this high affinity also minimizes selectivity. These compounds are also known to act as potent inhibitors of the glutathione reductase and the thioredoxin reductase.<sup>118-120</sup>

The rich history of polysulfane moieties as anti-cancer, antibiotic, and anti-fungal agents and their role in many biological redox processes inspired us to investigate novel pentathiepins for their biological significance.<sup>21 29 28</sup> The origin for cytotoxicity could be their ability to cleave DNA via an oxidative type mechanism and this mechanism is generally well accepted.<sup>121-123</sup>

In the current work, we have synthesized twenty-five novel pentathiepins possessing various heterocyclic rings and evaluated them as potential GPx1 inhibitors. Additionally, the cytotoxic potential of the compounds to kill cancer cells in vitro was assessed. These results show that pentathiepins have more diverse effects on the cellular systems than expected. The GPx1 enzyme inhibition and anti-cancer activity investigations were conducted together with cooperation partner Prof. Dr Bednarski and his co-workers at the Institute of Pharmaceutical Biology, University Greifswald. In these studies, the pentathiepins bearing various heterocyclic scaffolds such as quinoxaline (**7a-f**), pyrazine (**10a-b**), pyridine (**17a-b**), nicotinamide (**21a-e**), pyrrolo-pyrazine (**25**), quinoline (**28**), purine (**33**), and pyridine sulfonamide (**38a-f**)

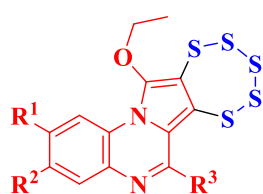
derivatives were employed. The individual results of GPx1 inhibition, cell proliferation or viability data ( $IC_{50}$  concentrations) are discussed for each class of pentathiepin. The GPx1 enzyme inhibition and cytotoxicity experiments for compounds **28** and **17b** were performed by Ms. Marutz (Bachelor thesis). Similarly, the anti-cancer activity of compounds **33**, and **38a-f** was investigated by Mr. Jo Henry Judernatz (Master thesis), and the respective results are included in the following summary.

Also, the anti-microbial activity of pentathiepins **7e-f**, **10a-b**, **17a**, **21d-e**, **33**, and **38a-f** was tested in gram-positive *S.aureus*, gram-negative *E.coli* microorganisms, and their minimum inhibitory concentrations (MIC) were established. Finally, the pentathiepins **21d-e**, **33**, and **38a-f** were verified further for their anti-fungal properties against two *Candida* stems, namely *C.albicans* and *C.glabrata* fungi. The anti-microbial and anti-fungal screening experiments were conducted at the University of Greifswald, Klinikum with the help of cooperation partner Dr. Med. Bohnert and his co-workers.

### 1.8.2 Biological activity of pyrrolo[1,2a]quinoxaline appended pentathiepins (**7a-f**)

#### *GPx1 enzyme inhibition activity*

The pentathiepin derivatives' (**7a-f**) potential inhibition properties were initially screened by using the Gpx1 enzyme extracted from inexpensive bovine erythrocytes.<sup>116</sup> Inhibition potencies of the compounds were ranked by their  $IC_{50}$  values; i.e.,  $IC_{50}$  is "the concentration of a substance that causes a defined inhibition and it is the median concentration that causes 50 % inhibition"<sup>116</sup> (Figure 1.17). The  $IC_{50}$  values of the pentathiepins and mercaptosuccinate (MS) against bovine GPx1 are summarized in table 1.4. All of the tested pentathiepins, regardless of the substitutions on the quinoxaline scaffold, showed a significant GPx1 inhibition, ranging from 3.76  $\mu$ M down to 0.47  $\mu$ M.



- 7a:  $R^1 = R^2 = R^3 = H$   
 7b:  $R^1 = CH_3, R^2, R^3 = H$   
 7c:  $R^1 = H, R^2 = CH_3, R^3 = H$   
 7d:  $R^1 = H, R^2 = CH_3, R^3 = CF_3$   
 7e:  $R^1 = R^2 = CH_3, R^3 = H$   
 7f:  $R^1 = R^2 = CH_3, R^3 = CF_3$

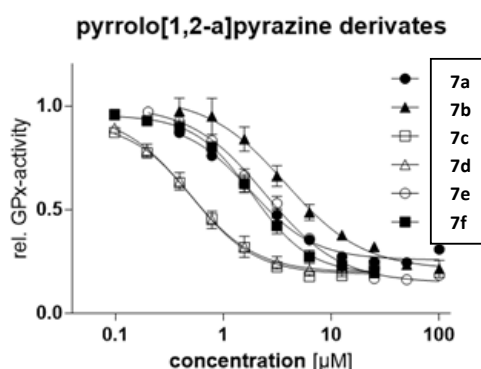




**Figure 1.17:** Rel. dose-inhibition curves of bovine GPx-1 inhibited by pentathiepins [mean  $\pm$  SD; n>4].<sup>116</sup>**Table 1.4:** Inhibition of bovine erythrocyte GPx1 by mercaptosuccinate (MS) and pentathiepins, reported as an average of IC<sub>50</sub>-values [confidence interval (CI) 95%; n>3]

Compound	IC <sub>50</sub> [ $\mu$ M]	CI 95% [ $\mu$ M]
<b>Mercaptosuccinic acid (MS)</b>	5.86	4.21–8.14
<b>7a</b>	1.76	1.39–2.24
<b>7b</b>	3.76	2.88–4.89
<b>7c</b>	0.52	0.45–0.61
<b>7d</b>	0.47	0.38–0.59
<b>7e</b>	2.44	2.17–2.75
<b>7f</b>	1.86	1.67–2.04

All tested quinoxaline fused pentathiepins have shown higher potency than the known Gpx1 inhibitor mercaptosuccinic acid (MS) which has an IC<sub>50</sub> of 5.86  $\mu$ M in the same assay. Specifically, the trifluoro substituted pentathiepin **7d** has shown an approximately twelve-fold higher inhibition than MS (Table 1.4). Interestingly, the position of a methyl substituent in *para* to nitrogen of the pyrrole in **7d** is having a higher potency compared to its *meta*-substituted congener **7b**. On the other hand, also the unsubstituted derivative **7a** is more effectively inhibiting Gpx1 enzyme compared to **7b**. Substituting 6 (*para*), 7 (*meta*) positions of the quinoxaline with methyl yielding the bis-methyl derivative **7e** results in a dramatic loss of potency. A trifluoromethyl-substituent at position R<sup>3</sup> has no noticeable effect on inhibitory potency; for example, the Gpx1 inhibition is better in **7c** and **7d** than the di-methylated trifluoromethylation derivative (**7f**).

Pentathiepins **7c** and **7d** differ only by CF<sub>3</sub> substitution at R<sup>3</sup> and both have comparably good potency. Additionally, the possible inhibition of glutathione reductase (GR) from yeast was examined for all the pentathiepins (**7a-f**), and no inhibition at relevant concentrations was identified. Also, no inhibition of bovine catalase and rat thioredoxin reductase was found for compounds **7e** at concentrations that inhibit GPx. These experimental results demonstrate the high selective potency of pentathiepins derivatives (**7a-f**) towards Gpx1 enzyme inhibition.

***Cytotoxicity and cell proliferation in various cancer cell lines in crystal violet assay***

The cytotoxicity of pentathiepins was determined by using the crystal violet proliferation assay. The determination for **7a**, **7c**, **7d** and **7f** was not possible unfortunately due to their low solubility in the aqueous environment. The IC<sub>50</sub> concentration for **7b** was also not entirely successful as precipitation of crystals was observed after examination of the cells under a microscope. The IC<sub>50</sub> values for the inhibition of proliferation for **7b** and **7e** are in the range of 2.0–7.5 μM. Table 1.5 depicts the corresponding values.

**Table 1.5:** IC<sub>50</sub> concentrations [μM] for inhibition of proliferation for pentathiepins **7b** and **7e** in various cancer cell lines. Incubation time 96 h; n>4; n.d. = not determined.

Cancer cell line	<b>7b</b> (IC <sub>50</sub> [μM])	<b>7e</b> (IC <sub>50</sub> [μM])
<i>A2780</i>	2.9 (0.8-10.7)	2.0 (1.4-2.8)
<i>LCLC-103H</i>	3.2 (2.5-4.1)	6.2 (4.4-8.8)
<i>SiSo</i>	n.d.	6.3 (4.3-9.3)
<i>5637</i>	n.d.	7.5 (4.7-11.9)

***Cell viability of pentathiepins in various adherent cell lines using the MTT assay***

Due to the relatively poor water solubility of the pentathiepins, only those were tested which were sufficiently soluble or where there was no precipitation observed in the cell culture medium. For **7c**, **7e** and **7f** we were able to obtain IC<sub>50</sub> values for viability inhibition in various cell lines of different entities using the MTT assay (Table 1.6).

**Table 1.6:** IC<sub>50</sub> values [μM] of the viability inhibition by **7c**, **7e** and **7f** in different cell lines after an incubation period of 48 h; n> 3; n.d. = not determined. For values with a relation sign (>), this means that although the relative viability was reduced at the specified concentration, this was less than 50%.

Cancer cell line	<b>7c</b> (IC <sub>50</sub> [μM])	<b>7e</b> (IC <sub>50</sub> [μM])	<b>7f</b> (IC <sub>50</sub> [μM])
<i>HAP-1</i>	2,0 (1,8-2,2)	2,5 (1,9-3,4)	>30
<i>KO.HAP-1.GPx1</i>	1,7 (1,5-2,0)	2,4 (1,7-3,3)	>30
<i>A2780</i>	0,9 (0,7-1,0)	1,3 (1,1-1,5)	5,7 (4,9-6,7)
<i>A2780cis</i>	1,2 (1,0-1,3)	1,4 (1,3-1,5)	9,0 (7,0-11,5)
<i>A427</i>	1,4 (1,1-1,9)	1,5 (1,3-1,7)	9,9 (6,4-15,1)
<i>BHY</i>	4,0 (3,8-4,2)	2,2 (2,1-2,4)	>50

## Chapter 1: Pentathiepins & Biological investigation

<i>DanG</i>	2,4 (2,1-2,7)	2,8 (2,5-3,1)	n.d.
<i>Kyse-70</i>	3,4 (3,1-3,8)	3,6 (3,3-4,0)	>50
<i>LCLC-103H</i>	2,4 (2,3-2,6)	2,3 (2,2-2,5)	>50
<i>RT-4</i>	3,4 (2,9-4,0)	8,3 (6,8-10,1)	>50
<i>SiSo</i>	1,9 (1,7-2,1)	2,2 (1,8-2,5)	9,3 (8,3-10,4)
<i>5637</i>	2,0 (1,7-2,4)	2,2 (1,9-2,6)	n.d.
<i>U87mg</i>	~25	9,6 (7,6-12,0)	n.d.
<i>LN18</i>	15,6 (12,8-18,9)	14,9 (13,3-16,6)	n.d.
<i>GL261</i>	22,2 (18,2-27,1)	~25	n.d.

Interestingly, the determined IC<sub>50</sub> values for the pentathiepins (**7c**, **7e** and **7f**) in most cell lines are in the lower  $\mu\text{M}$  range between 1–4  $\mu\text{M}$ . It is worth to mention, that relatively low IC<sub>50</sub> values were found for the A2780 (ovarian carcinoma) and its cisplatin-resistant variant A2780cis. In contrast, the esophageal squamous *Kyse-70* and the bladder *RT-4* carcinoma cell lines showed consistently less sensitivity towards the pentathiepins compared to the other cell lines. The GPx1 knockout cells (KO.HAP-1.GPx1) showed no significant differences relative to their native tumor cell line of human, chronic, myelitic leukemia (HAP-1). The lowest sensitivity towards pentathiepins was noticed for the brain tumor cell lines *U87mg*, *LN18* and *GL261*. The trifluoro substituted derivative **7f** has shown no significant toxicity effect in the viability assay. Reliable IC<sub>50</sub> concentrations could only be determined for A2780 and A2780cis, A427 and *SiSo* cell lines. However, the IC<sub>50</sub> concentrations determined here are much higher compared to literature known pentathiepins.<sup>23</sup>

Pentathiepins are described as ROS generators in many reports in the literature. Pentathiepins believed to initiate plasmid DNA cleavage via ROS formation, where the triggered hydroxyl radical is supposedly the key. However, the enrichment of ROS by pentathiepins in the cellular system was unprecedented. It would also be conceivable that the formation of ROS can be promoted after inhibition of the GPx1 enzyme. For clarification, Prof. Dr Bednarski and co-workers investigated further the pentathiepin **7e** by incubation with Gumbus and HL60 cells with a fixed concentration of 25  $\mu\text{M}$ . In preliminary experiments, it was determined that there is a significant increase in ROS in both cell lines. Moreover, the ROS production was enhanced after incubating the cells in the combination of pentathiepins and GSH. However, a fourfold

increase in the concentration of GSH in the incubation medium with respect to **7e** significantly reduced the ROS production in the cells. More detailed explanations can be found in Steven Behnisch's PhD thesis.

### 1.8.3 Pyrazine fused pentathiepins' biological activity

The Gpx1 enzyme inhibition properties of pyrazine fused pentathiepins **10a** and **10b** were investigated by using Bovine erythrocytes. Notably, the smaller size derivative **10a** has proven even more effective inhibition compared to its quinoxaline congeners and is twelve-fold more effective than the standard mercaptosuccinic acid (Table 1.7).

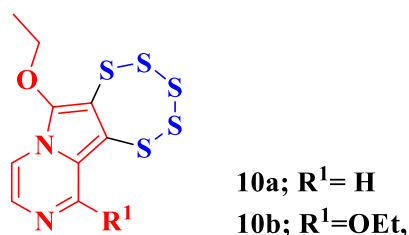


**Table 1.7:** IC<sub>50</sub> values for GPx1 inhibition and cell cytotoxicity of pentathiepins **10a** and **10b**. The IC<sub>50</sub> is defined as the median concentration of a substance that causes 50% inhibition of a given system; CI = confidence interval; n.e. = not examined, standard deviations are given in brackets.<sup>124</sup>

GPx-1 inhibition (IC <sub>50</sub> μM) (CI 95%)		
MS	5.86 (4.21-8.14)	
<b>10a</b>	0.43 (0.40-0.46)	
IC <sub>50</sub> μM (crystal violet assay)		
Cell line	<b>10a</b>	<b>10b</b>
<i>HAP1</i>	n.e.	1.6 (±0.17)
<i>KO.HAP-1.GPx1</i>	n.e.	1.77 (±0.36)
<i>A2780</i>	7.6 (5.5-10.5)	0.89 (± 0.31)
<i>SiSo</i>	16.9 (12.5-22.9)	2.4 (± 0.79)
<i>LCLC-103H</i>	9.4 (7.0-12.7)	n.e.
<i>5637</i>	24.1 (4.3-33.9)	n.e.

Compounds **10a** and **10b** have shown significant cytotoxicity in all tested cancer cell lines (Table 1.7). Although **10a** has shown an excellent Gpx1 inhibition property, the cell proliferation studies derived IC<sub>50</sub> concentrations were in a somehow higher range (7.6-24.1 μM) than those of the quinoxaline derivatives. However, **10b** which differs only by the methoxy group has shown good cytotoxicity in HAP1, KO.HAP-1.GPx1 and A2780 cells, while it appeared to be weaker in SiSo cells. Among the two tested pentathiepins, the lowest IC<sub>50</sub> values (corresponding to highest cytotoxicity) were observed at 0.89 μM for compound **10b** against A2780 cell lines.

#### 1.8.4 Pyridine fused pentathiepins' biological activity

Interestingly, <1 μM concentrations of **17a** or **17b** are effectively inhibiting 50% of the Gpx1 enzyme of Bovine erythrocytes. The pyridine fused pentathiepins exhibited 9-fold higher potency than mercaptosuccinate in Gpx1-inhibition (Table 1.8). Among these two compounds, the good solubility of compound **17b** allowed to investigate the inhibition of proliferation by using the crystal violet assay and thus to test the cytotoxicity.

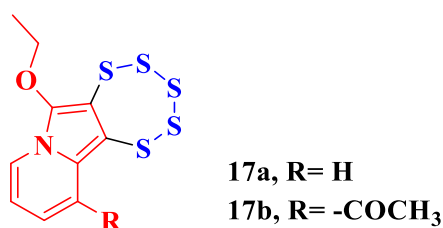
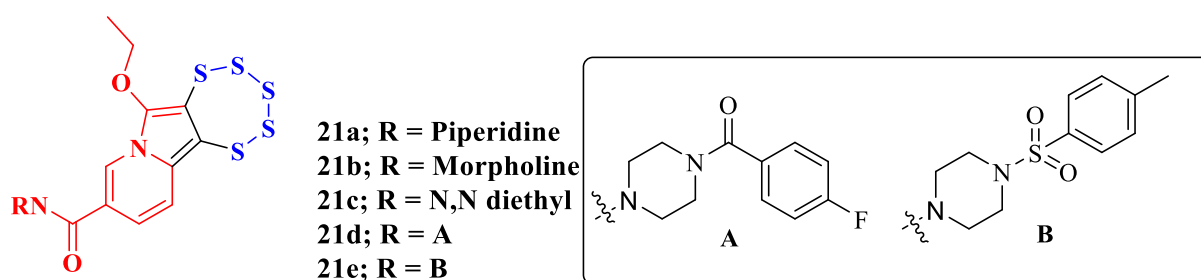


**Table 1.8:** IC<sub>50</sub> values for GPx1 inhibition and cell cytotoxicity of pentathiepins **17a** and **17b**. IC<sub>50</sub> values of **17b** in HAP-1, Ko.HAP-1.GPx1, A2780 and SiSo cell culture lines.

GPx-1 inhibition (IC <sub>50</sub> μM)		
MS		5.86
<b>17a</b>		0.66
<b>17b</b>		0.708
IC <sub>50</sub> μM (crystal violet assay)		
Cell line	<b>17a</b>	<b>17b</b>
<i>HAP1</i>	n.d.	0.664
<i>KO.HAP-1.GPx1</i>	n.d.	0.623
<i>A2780</i>	n.d.	0.448

It was possible to determine  $IC_{50}$  values in the four investigated cell culture lines for pentathiepin **17b**. From the  $IC_{50}$  values, it can be seen that **17b** has the strongest proliferation inhibition in the cell line A2780 with approximately 0.5  $\mu$ M, followed by HAP-1 and KO.HAP-1.GPx with  $IC_{50}$  values between 0.6 and 0.7  $\mu$ M. The lowest inhibition was observed in the SiSo cell line with an  $IC_{50}$  value of approx. 1.2  $\mu$ M. Notably, the pentathiepin **17b** has shown  $IC_{50}$  values in the range between 0.44 to 1.18  $\mu$ M in HAP1, KO.HAP-1.GPx1, A2780 and SiSo cells, which are much lower (i.e. highly potent cytotoxic) concentrations compared to pyrazine or quinoxaline pentathiepins (Table 1.6, 1.7, 1.8). Interestingly, **17b** has shown no significant difference in inhibition of proliferation between the HAP-1 cell line and its knockout variant without GPx1. In general, the knockout cell line lacks an important enzyme (GPx1) for the degradation of ROS. It suggests that the mechanism of action of the pentathiepins is probably not solely due to the formation of ROS. However, it is important to note that there are other GPx isoenzymes besides GPx1 that are also able to neutralize ROS. Thus, pentathiepins' fused to pyridine or substituted pyridine scaffolds would be promising leads for both GPx1 inhibition and in combination with high cytotoxicity. It would be pivotal to determine the inhibitory mechanism of the pentathiepin and establishing out the binding mode of the substance in the enzyme's active site.

### 1.8.5 Nicotinamide fused pentathiepins' biological activity



Nicotinic acid is a pyridine substituted carboxylic acid and well established in medicinal chemistry as an active biological scaffold. Five nicotinamide derivatives were synthesized, and the analytically pure samples were examined for GPx1 enzyme inhibition and anticancer properties.

**Table 1.9:** IC<sub>50</sub> values [ $\mu$ M] for GPx-1 enzyme inhibition activity

Compound	21a	21b	21c	21d	21e
Mean ( $\mu$ M)	3.246	0.914	0.749	1.174	>12.5
Std. Deviation ( $\mu$ M)	0.946	0.335	0.271	0.199	n.a.

The enzyme activity assay revealed a potent inhibition of the bovine GPx1 mediated by pentathiepins **21a-d** (IC<sub>50</sub> from 0.75-3.25  $\mu$ M), whereas the IC<sub>50</sub> of **21e** was >12.5  $\mu$ M (the residual enzymatic activity at 12.5  $\mu$ M was around 55 %). The most potent GPx1 inhibitor is **21c** with an IC<sub>50</sub> of 0.75  $\mu$ M (Table 1.9). It has to be considered that also for the active compounds **21a-d** the residual activity of the GPx1 remains between 16-29% at the highest tested concentration of 12.5  $\mu$ M.

#### *Effect on cell viability (MTT)*

The compounds **21a-e** were tested in various cell lines using the MTT assay. Cell lines of distinct origin responded differently towards the 48 h treatment in the MTT viability assay (Table 1.10).

**Table 1.10:** Cell viability studies (MTT), incubation time 48 h; most sensitive cell lines HAP-1, HAP-1.KO.GPx-1, A2780, and A2780 Cis.

Cancer cell line	21a (IC <sub>50</sub> [ $\mu$ M])	21b (IC <sub>50</sub> [ $\mu$ M])	21c (IC <sub>50</sub> [ $\mu$ M])	21d (IC <sub>50</sub> [ $\mu$ M])	21e (IC <sub>50</sub> [ $\mu$ M])
<i>HAP-1</i>	0.600 (0.154)	0.263 (0.059)	0.263 (0.049)	0.270 (0.031)	0.722 (0.292)
<i>HAP.1.KO.GPx1</i>	0.644 (0.077)	0.368(0.037)	0.322 (0.017)	0.413 (0.052)	0.778 (0.233)
<i>DanG</i>	1.990 (0.440)	1.447 (0.208)	1.648 (0.276)	1.177 (0.211)	2.179 (0.268)
<i>SiSo</i>	1.376 (0.181)	0.573 (0.059)	0.934 (0.070)	0.794 (0.091)	3.259 (0.825)
<i>Kyse-70</i>	1.582 (0.393)	0.824 (0.166)	0.976 (0.174)	0.826 (0.254)	1.950 (0.573)
<i>A2780</i>	0.430(0.129)	0.135 (0.032)	0.213 (0.078)	0.259 (0.063)	0.891 (0.025)
<i>A2780cis</i>	0.652 (0.015)	0.206 (0.040)	0.399 (0.056)	0.308 (0.046)	1.507 (0.453)
<i>RT-4</i>	1.595 (0.433)	0.878 (0.087)	1.306 (0.340)	0.716 (0.193)	1.548 (0.462)
<i>MCF-7</i>	3.040(0.452)	1.681 (0.273)	3.210 (0.470)	1.640 (0.057)	3.986 (1.371)

<i>PATU</i>	1.715 (0.597)	1.047 (0.111)	0.823 (0.292)	1.203 (0.036)	2.979 (1.394)
<i>YAPC</i>	1.551 (0.170)	1.225 (0.209)	1.150 (0.262)	1.360 (0.086)	5.166 (0.304)
<i>LCLC</i>	1.357 (0.612)	0.571 (0.175)	0.674 (0.053)	0.800 (0.293)	2.816 (1.292)
<i>RT-112</i>	1.341 (0.700)	1.047 (0.136)	1.197 (0.063)	1.079 (0.150)	3.408 (0.635)
<i>A-427</i>	1.461 (0.189)	0.785 (0.072)	1.094 (0.096)	0.906 (0.058)	1.788 (0.253)

Cells from chronic leukemia (HAP-1, HAP-1.KO.GPx1; note: there were no vast differences when comparing these two cell lines although one does not express the GPx1) and ovarian carcinoma (A2780, A2780cis) were most sensitive, whereas cells from the breast (MCF-7) or pancreas carcinoma (DanG, PA-TU-8902, YAPC) were least affected. In most cell lines the least active GPx1-inhibitor **21e** (tosyl substituted) had the weakest effect on cellular viability with a mean IC<sub>50</sub> of 2.4 μM. Throughout all the tested cell lines, the **21b** (morpholine) and **21d** (fluoro substituted) seemed to be the most toxic compounds with mean IC<sub>50</sub> values of 0.72 and 0.79 μM, respectively.

#### *Effect on cell proliferation (crystal violet)*

The crystal violet cell proliferation assay showed that all tested pentathiepins **21a-e** inhibit cellular growth after a 96 h treatment at minimal micro molar concentrations (Table 1.11)

**Table 1.11:** Cell proliferation study by crystal violet assay incubation 96 h

<b>Cancer cell line</b>	<b>21a</b> <b>(IC<sub>50</sub> [μM])</b>	<b>21b</b> <b>(IC<sub>50</sub> [μM])</b>	<b>21c</b> <b>(IC<sub>50</sub> [μM])</b>	<b>21d</b> <b>(IC<sub>50</sub> [μM])</b>	<b>21e</b> <b>(IC<sub>50</sub> [μM])</b>
<i>HAP-1</i>	0.161 (0.030)	0.064 (0.013)	0.084 (0.010)	0.120 (0.048)	0.507 (0.115)
<i>HAP.1.KO.GPx1</i>	0.173 (0.035)	0.068 (0.009)	0.116 (0.027)	0.144 (0.025)	0.524 (0.080)
<i>DanG</i>	0.644 (0.113)	0.382 (0.091)	0.459 (0.028)	0.398 (0.033)	0.711 (0.163)
<i>SiSo</i>	0.423 (0.057)	0.166 (0.054)	0.381 (0.037)	0.369 (0.019)	0.597 (0.151)
<i>Kyse-70</i>	0.409 (0.083)	0.142 (0.009)	0.284 (0.036)	0.181 (0.053)	0.481 (0.076)
<i>A2780</i>	0.164 (0.032)	0.055 (0.018)	0.106 (0.019)	0.092 (0.026)	0.538 (0.144)
<i>A2780cis</i>	0.234 (0.023)	0.088 (0.036)	0.173 (0.022)	0.142 (0.035)	0.512 (0.081)
<i>RT-4</i>	1.515 (0.471)	0.193 (0.042)	0.445 (0.111)	0.358 (0.158)	0.835 (0.364)



<i>MCF-7</i>	0.384 (0.070)	0.153 (0.050)	0.293 (0.053)	0.248 (0.083)	0.458 (0.091)
<i>PATU</i>	0.659 (0.283)	0.257 (0.039)	0.471 (0.034)	0.340 (0.048)	0.952 (0.091)
<i>YAPC</i>	0.628 (0.053)	0.350 (0.166)	0.608 (0.217)	0.411 (0.185)	1.170 (0.634)
<i>LCLC</i>	0.552 (0.202)	0.128 (0.027)	0.306 (0.079)	0.232 (0.079)	0.646 (0.372)
<i>RT-112</i>	0.599 (0.085)	0.246 (0.041)	0.469 (0.064)	0.383 (0.021)	1.104 (0.122)
<i>A-427</i>	0.401 (0.150)	0.142 (0.047)	0.310 (0.004)	0.320 (0.014)	0.352 (0.336)

The IC<sub>50</sub> values are primarily similar in most of the tested cell lines (0.06-0.6 μM), except for cell lines of pancreatic carcinoma (PA-TU-8902, YAPC), lung carcinoma (LCLC-103H) and urinary bladder carcinoma (RT-4), where values range from 0.4-1.5 μM. Pentathiepin **21b** presented the most substantial impact on proliferation with a mean IC<sub>50</sub> of 0.17 μM throughout all cell lines. The least potent GPx1 inhibitor pentathiepin **21e** had the weakest influence on cellular proliferation with IC<sub>50</sub> values > 0.5 μM (mean 0.67 μM).

In short, the pentathiepins **21a-e** followed the GPx1 enzyme inhibition potency in the order of **21c > 21b > 21d > 21a > 21e**, cell viability in the order of **21b > 21d > 21c > 21a > 21e** and lastly cell proliferation in the order of **21b > 21d > 21c > 21a > 21e**.

### 1.8.6 Biological activity of 25, 28, and 33

Heterocyclic fused pentathiepins **25** (pyrrolo-pyrazine), **28** (quinoline) and **33** (purine) were investigated for their GPx1 enzyme inhibition. The compound **28** seems to be a highly potent GPx1 inhibitor with an IC<sub>50</sub> value at 0.277 μM (Table 1.12).

The cytotoxic investigations of **25**, **28**, and **33** in HAP1, KO.HAP-1.GPx1, A2780 and SiSo cells by using crystal violet assay show that the pentathiepins **25** and **33** are more potent than **28** (Table 1.12). Compound **28** exhibits comparably high IC<sub>50</sub> concentrations (low cytotoxicity) ranging between 1.05 to 8.5 μM, whereas, **25** and **33** have shown a high potency towards inhibition of proliferation at IC<sub>50</sub> values ranging between 0.23-0.36 μM.

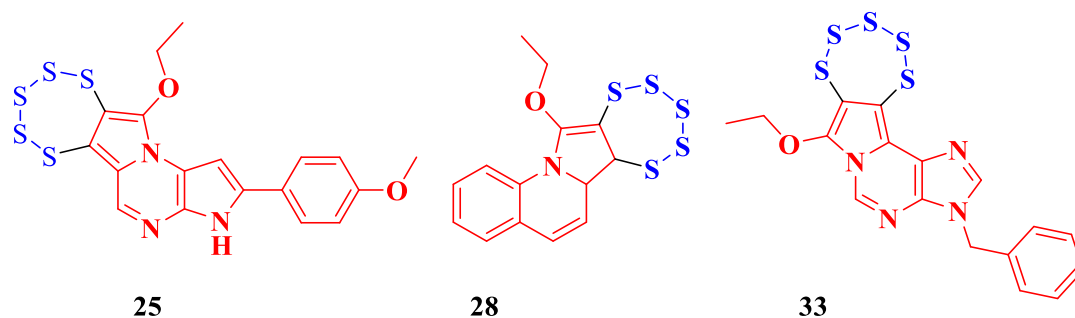


**Table 1.12:** IC<sub>50</sub> [μM] values for GPx1 inhibition and cell cytotoxicity of pentathiepins **25**, **28** and **33**. IC<sub>50</sub> values were given in HAP-1, Ko.HAP-1.GPx1, A2780 and SiSo cell culture lines.

<b>GPx1 inhibition</b>			
<b>Compound</b>	<b>IC<sub>50</sub> μM</b>		
<b>25</b>	1.485 (0.764)		
<b>28</b>	0.277 (0.044)		
<b>33</b>	n.d.		
<b>IC<sub>50</sub> μM (crystal violet assay)</b>			
<b>Cell line</b>	<b>25</b>	<b>28</b>	<b>33</b>
<i>HAP1</i>	0.339 (0.039)	8,070	0.31 (± 0.03)
<i>KO.HAP-1.GPx1</i>	0.313 (0.045)	8,584	0.33(± 0.03)
<i>A2780</i>	0.236 (0.056)	1.050	0.36 (± 0.15)
<i>SiSo</i>	0.256 (0.054)	5.105	0.72 (± 0.01)

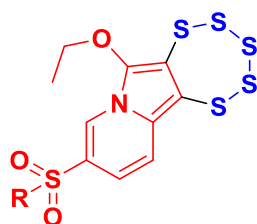
Compound **25** was further tested in various cell lines by using both MTT and crystal violet assays (Table 1.13). Interestingly, it has shown high cytotoxicity in all tested fourteen cell lines with IC<sub>50</sub> concentrations ranging between 0.39 to 1.92 μM (cell viability) and 0.20 to 0.48 μM (cell proliferation) in MTT and crystal violet assays, respectively. The breast carcinoma cells appeared to be insensitive to compound **25** in the MTT assay; however, surprisingly, the minimal IC<sub>50</sub> value at 0.209 μM was observed for the same line in the crystal violet assay. The low sensitivity of SiSo cancer cells against radiation and chemotherapy, led to the proposition of combination drug therapy.<sup>125</sup> However, compound **25** has shown significant cytotoxicity

towards SiSo cell lines and the recorded IC<sub>50</sub> value at 0.256 μM (cell proliferation) from crystal violet assay is in the same range as that of nicotinamide morpholine pentathiepin derivative **21b** (IC<sub>50</sub> 0.166 μM).

Table 1.13: IC<sub>50</sub> [μM] values of 25 for cell viability using MTT assay and cell proliferation by using crystal violet assay.

Cell line	25 (MTT assay) IC <sub>50</sub> μM Cell viability 48 h incubation	25 (CV assay) IC <sub>50</sub> μM Cell proliferation 96 h incubation
<i>HAP1</i>	0.398 (0.086)	0.339 (0.039)
<i>KO.HAP-1.GPx1</i>	0.358 (0.026)	0.313 (0.045)
<i>A2780</i>	0.692 (0.333)	0.236 (0.056)
<i>SiSo</i>	0.414 (0.493)	0.256 (0.054)
<i>Kyse-70</i>	0.477 (0.106)	0.264 (0.061)
<i>DanG</i>	1.114 (0.493)	0.340 (0.085)
<i>A2780cis</i>	0.410 (0.094)	0.228 (0.030)
<i>RT-4</i>	1.926 (1.102)	0.373 (0.041)
<i>MCF-7</i>	>10	0.209 (0.013)
<i>PATU</i>	0.579 (0.225)	0.480 (0.021)
<i>YAPC</i>	0.780 (0.091)	0.405 (0.134)
<i>LCLC</i>	1.416 (0.174)	0.441 (0.117)
<i>RT-112</i>	0.399 (0.074)	0.465 (0.096)
<i>A-427</i>	0.349 (0.057)	0.306 (0.008)

## 1.8.7 Pyridine sulfonamide pentathiepins and their biological activity



- 38a**; R = Piperidine  
**38b**; R = Morpholine  
**38c**; R = (S)-3-methylbutan-2-amine  
**38d**; R = Adamantylamine  
**38e**; R = Piperonylamine  
**38f**; R = Benzylamine

Half-maximal inhibition concentrations ( $IC_{50}$ ) were determined for pyridine sulfonamide bearing pentathiepins **38a-f** in HAP1, KO.HAP-1.GPx1, A2780 and SiSo cells by using the crystal violet assay. Noticeably, these families of compounds are exhibiting potent cytotoxicity, and the corresponding  $IC_{50}$  values are summarized in Table 1.14. In general,  $<1 \mu\text{M}$  concentrations of pentathiepins **38-f** are significantly inhibiting 50% of cell growth under experimental conditions. As evident from Table 1.14, the compounds **38a**, **38b** and **38d** exhibited more potent cytotoxicity in A2780 cells than in HAP-1 or KO.HAP-1.GPx1 cells, while **38c** and **38f** were more active in the HAP-1 and GPx1 knockout cells KO.HAP-1.GPx1. Overall **38b**, **38c** and **38f** exhibited promising cytotoxic activity with  $IC_{50}$  values of approximately  $0.5\text{-}0.6 \mu\text{M}$  in SiSo cells and for the three other cell lines these values are around  $0.3\text{-}0.4 \mu\text{M}$ . Compound **38b** is highly cytotoxic against A2780 cells, and the lowest  $IC_{50}$  values were detected at  $0.15 \mu\text{M}$ . Notably, the piperidine derivative **38a**, not bearing an oxygen functionality on its backbone has the lowest cytotoxicity. Nevertheless, **38a** is still more potent than the activity of the natural product varacin ( $IC_{50}$ :  $14.7 \mu\text{M}$ ) determined against human colon cancer HCT 116.<sup>126</sup> The activity of sulfonamide derivatives is similar to the purine-pentathiepin **33**, pyrrolo-pyrazine-pentathiepin **25**, and nicotinamide-pentathiepin **21a-e**. It is supporting the importance of the five-membered sulfur fused to various heterocyclic scaffolds for the intense cytotoxic activity.

**Table 1.14:** The results of the  $IC_{50}$  determination indicate potent cytotoxicity below  $1 \mu\text{M}$  for most compounds. The  $IC_{50}$  is defined as the median concentration of a substance that causes 50 % inhibition of a given system.<sup>124</sup> HAP-1, KO.HAP-1.GPx1 and A2780 cells generally reacted more sensitively to treatment with pentathiepins compared to SiSo cells. Standard deviations are given in brackets.

Compound	$IC_{50}$ [ $\mu\text{M}$ ] CV			
	HAP1	KO.HAP-1.GPx1	A2780	SiSo
<b>38a</b>	0.63 ( $\pm 0.15$ )	0.62 ( $\pm 0.22$ )	0.51 ( $\pm 0.07$ )	1.15 ( $\pm 0.34$ )
<b>38b</b>	0.27 ( $\pm 0.06$ )	0.3 ( $\pm 0.03$ )	0.15 ( $\pm 0.06$ )	0.57 ( $\pm 0.19$ )

<b>38c</b>	0.3 ( $\pm$ 0.04)	0.31 ( $\pm$ 0.04)	0.33 ( $\pm$ 0.09)	0.53 ( $\pm$ 0.03)
<b>38d</b>	0.52 ( $\pm$ 0.15)	0.52 ( $\pm$ 0.01)	0.43 ( $\pm$ 0.04)	0.74 ( $\pm$ 0.22)
<b>38e</b>	0.51 ( $\pm$ 0.36)	0.52 ( $\pm$ 0.06)	0.5 ( $\pm$ 0.07)	0.73 ( $\pm$ 0.23)
<b>38f</b>	0.31 ( $\pm$ 0.24)	0.36 ( $\pm$ 0.09)	0.47 ( $\pm$ 0.02)	0.54 ( $\pm$ 0.35)

### 1.8.8 Investigation of anti-microbial activity of novel pentathiepins in various pathogens.

Pentathiepins are well-established antibiotics, and many such conclusions are reported in the literature. For example, recently, Khomenko and co-workers reported the antibiotic potency of benzopentathiepin-6-amines against *S.aureus* in ranges between 4-32  $\mu\text{g/mL}$ .<sup>41</sup> The efficacy of natural pentathiepin Lissoclinotoxin A towards *Staphylococcus aureus* and many other strains was reported by Litaudon et al., where the MIC values were observed around 0.05 to 0.15  $\mu\text{g/mL}$ .<sup>24</sup> This promising data inspired the antimicrobial activity investigations for the synthesized novel pentathiepins, where the minimum inhibitory concentrations (MIC) of each compound against different microorganisms were determined. The MIC denotes the concentration at which visible growth of the investigated microorganism freezes and it should be observed by the naked eye.<sup>127</sup> As an initial screening, pentathiepins **7e** (quinoxaline), **10a** (pyrazine) and **17a** (pyridine) were selected, which differ only by their heterocyclic backbone. These pentathiepins were incubated with the different gram-positive and gram-negative bacterial cells overnight. Interestingly, pentathiepins **7e**, **10a**, and **17a** have shown MIC concentrations between 2 to 100  $\mu\text{g/mL}$  only in gram-positive strains, whereas, the gram-negative *E.coli* bacterial growth was unhindered even at higher concentrations (Table 1.15). The pyrazine-pentathiepin **10a** exhibited the highest bacterial growth inhibition with a MIC at 2  $\mu\text{g/mL}$  for gram-positive *Staphylococcus aureus* (*SA1199*) and the related *methicillin-resistant SA1199B* strains.

**Table 1.15:** Antimicrobial activity of pentathiepins **7e**, **10a**, and **17a** in bacterial cell lines and MIC given in  $\mu\text{g/mL}$ .

Compound	MIC $\mu\text{g/mL}$			
	<i>S. aureus</i> <sup>a</sup>	<i>S. aureus</i> <sup>b</sup>	<i>E. coli</i> <sup>c</sup>	<i>E. coli</i> <sup>d</sup>
<b>7e</b>	100	100	–	–
<b>10a</b>	2	2	–	–

**17a**                      80.5                      80.5                      –                      –

<sup>a</sup>*S.aureus*1199, <sup>b</sup>methicillin-resistant 1199B

<sup>c</sup>*E. coli* AG100, <sup>d</sup>resistant AG100Δ

The inactivity of the tested pentathiepins in gram-negative bacteria could be attributed to their complex membrane superstructure. In general, they possess outer and inner membranes; most importantly, the outer membrane behaves like a selective hydrophobic and size-exclusion filter with pore-forming proteins. Moreover, the active drug efflux pump mechanism prevents drug penetration, thus hampering the physiological activity of a drug.<sup>128,129</sup> Varacin's selective antimicrobial activity towards various gram-positive *B.subtilis* and *S.aureus* was well established. However, Lissoclinotoxin A has exhibited selective antimicrobial activity even against various gram-negative strains like *E.coli* and *P.aeruginosa*.<sup>130</sup>

**Table 1.16:** Results of the antimicrobial assay; MIC is given in µg/mL. The maximal tested concentrations ranged between 128-256 µg/mL.

Compound	MIC µg/mL			
	<i>S. aureus</i> <sup>a</sup>	<i>E. coli</i> <sup>b</sup>	<i>C. albicans</i>	<i>C. glabrata</i>
<b>33</b>	–	–	–	–
<b>38a</b>	–	–	–	–
<b>38b</b>	>256	>256	>256	>256
<b>38c</b>	>256	>256	>256	>256
<b>38d</b>	>128	>128	>128	>128
<b>38e</b>	>256	>256	>256	>256
<b>38f</b>	>256	>256	>256	>256
<b>10b</b>	>256	>256	>256	>256
<b>7f</b>	>128	>128	>128	>128
<b>21d</b>	>256	>256	>256	>256
<b>21e</b>	>256	>256	>256	>256

<sup>a</sup>*S.aureus*1199 and methicillin-resistant 1199B

<sup>b</sup>*E. coli* AG100

Inspired by the antimicrobial activity of novel pentathiepin **10a**, full screening studies with a wide range of pentathiepins in both *Staphylococcus aureus* (gram-positive) and *E. Coli* (gram-negative) pathogens were performed. Accordingly, the MIC concentrations were measured for **33**, **38a-f**, **10b**, **7f**, and **21d-e**, and the values are given in Table 1.16. Interestingly, not a single pentathiepin from other families has shown competitive bacterial growth inhibition potency in a tested range of concentrations (128-256 µg/mL). Compounds **38d** and **21d** are poorly soluble in DMSO, thus the targeted final concentrations in the stock solutions are hardly reachable, and in consequence, the low efficacy could have resulted. The MIC values could not be determined for **33** and **38a**, as the compounds were precipitated out upon addition of the aqueous medium to DMSO stock solution.

It is worth to mention, that the observed antimicrobial efficacy of pyrazine-pentathiepin **10a** was completely removed upon substitution with a methoxy group at position-6 as in **10b**. This result emphasizes the importance of a structure-activity relationship study with these compounds. Similarly, further well-designed experiments are needed to conclude whether the substitution at position-6 or this type of substitution (methoxy) controls the efficacy profile. In future quantitative structure activity relationship (QSAR) studies and computational binding analysis could be advantageous in obtaining supporting results. Although sulfonamide based heterocyclic moieties are popular antibiotics (sulfasalazine),<sup>131</sup> the pentathiepins derived from pyridine sulfonamides were unfortunately inactive at relevantly low concentrations.

Finally, the antifungal activities of pentathiepins were investigated against two *Candida stems*, namely, *C. albicans* and *C. glabrata*, which are eukaryotic organisms. The susceptibility towards *C. albicans* in immune-deficient cases and its resistance against fungicides gained significant importance.<sup>132-133</sup> Unfortunately, there was no antifungal activity detected with the highly cytotoxic pentathiepins. Presumably, *Candida stems* reduce the cell uptake of the toxic materials into cells via several physiological mechanisms (efflux pumps).<sup>129</sup> Alternatively, *C. albicans* and *C. glabrata* could express DNA repair/protection proteins such as GSH, glutaredoxin, thioredoxin, catalase CAT1, the superoxide dismutase (SOD) or glutathione peroxidase (GPx) against increased oxidative stress by pentathiepins.<sup>133</sup> Thus, these cells could break down the ROS and consequently protect the DNA from damage. In comparison to human cancer cells, the fungi operate differently and deal with the toxic drug-induced oxidative stress either via drug efflux pumps or developing ROS resistance.<sup>129</sup> The GPx1 enzyme inhibition properties of pentathiepins for the fungi GPx were not examined, and such investigations in this regard would possibly help understand the observed inactivity.

## 1.9 Summary of biological activity of all investigated/novel pentathiepins

The natural pentathiepins and their comparably simple synthetic mimics reported so far are known for anticancer, antimicrobial, and antifungal properties. Researchers speculated that the pentathiepin units induce DNA damage via increased ROS production. For the first time, we have investigated GPx1 enzyme inhibition properties of novel heterocycle fused pentathiepins. Fortuitously, we have realized the high potency of these polysulfur moieties over traditional mercaptosuccinic acid.

It can be seen from figure 1.17, that all investigated novel heterocyclic pentathiepins were >9 fold more efficacious than mercaptosuccinic acid. Specifically, quinolone, quinoxaline and pyrazine fused pentathiepins exhibited the GPx1 inhibition  $IC_{50}$  values at  $<1 \mu M$ . Moreover, quinoxaline fused pentathiepins offered a high level of selectivity towards GPx1 enzyme inhibition over thioredoxin reductase and catalase enzymes. Therefore, the concomitant employment of pentathiepins in combination with other anticancer drugs would be beneficial for sensitizing drug-resistant cells. Further investigations in these directions will be targeted in the future.

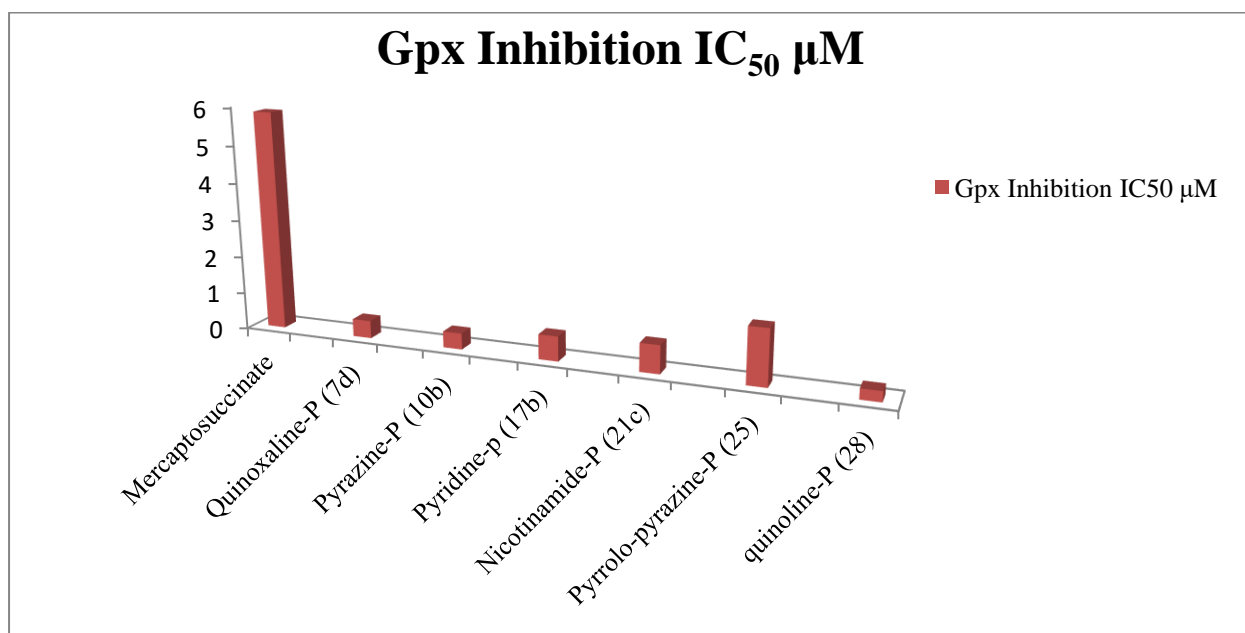


**Figure 1.17:** The GPx1 enzyme inhibition ( $IC_{50}$   $\mu M$ ) profile of various families of heterocyclic pentathiepins.

Additionally, the cytotoxic potency of all novel heterocyclic pentathiepins was investigated in various cell lines by using the crystal violet assay or the MTT assay. Notably, all tested pentathiepins exhibited high cytotoxicity even at very low concentrations ( $<0.5 \mu M$ ), and the poorly cytotoxic pentathiepins (quinolone-pentathiepin) also showed higher potency than the natural pentathiepin varacin. The cytotoxic efficacy of all pentathiepins was investigated



commonly with HAP-1, K.O-HAP-1.GPx1 (GPx1 knock out), A2780 and SiSo cell lines (Figure 1.18). HAP-1 and K.O.HAP-1.GPx1 are chronic myeloid leukemia cells where K.O.HAP-1.GPx1 are GPx1-Knockout cells. The A2780 and SiSo originated from ovarian cancer and cervix carcinoma cells, respectively.

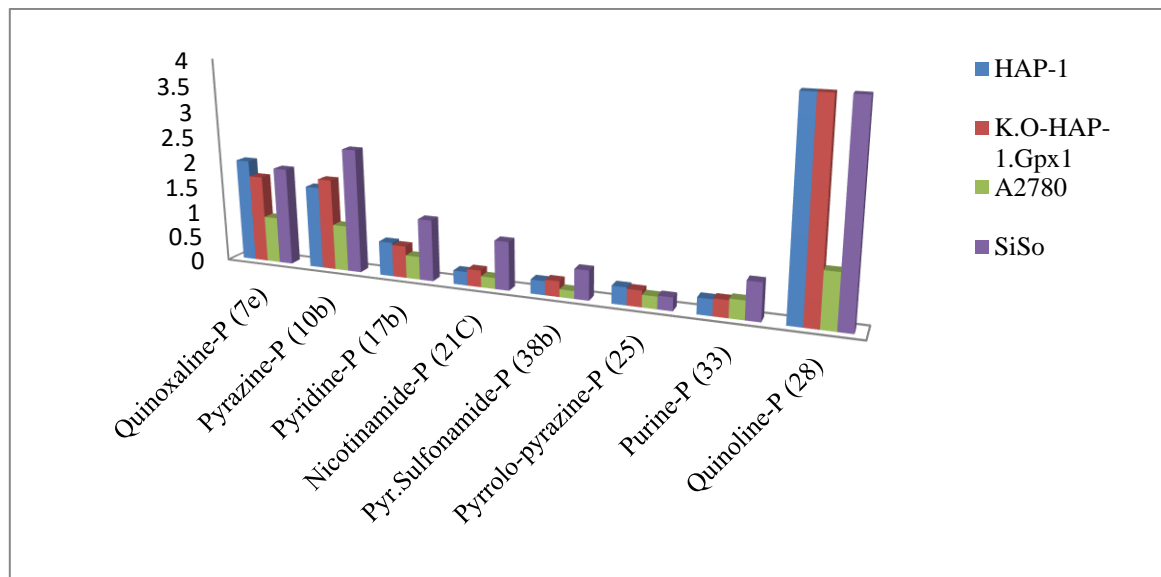


**Figure 1.18:** Cytotoxicity profile ( $IC_{50}$   $\mu$ M) of different heterocyclic pentathiepins towards HAP-1, K.O-HAP-1.GPx1, A2780 and SiSo cell lines.

Figure 1.18 shows that all novel pentathiepin families are highly potent towards the tested cell lines. Especially, pyridine and its congeners (nicotinamide and pyridine sulfonamide), as well as six and five-membered fused pyrrolo-pyrazine-pentathiepins and purine-pentathiepin, are highly potent with  $IC_{50}$  values at  $<1$   $\mu$ M. Among these four cell lines; SiSo cells have consistently shown comparably low sensitivity towards pentathiepins. SiSo cells are also known for their lower sensitivity to radiation and chemotherapy. However, further investigations into SiSo cells and their drug resistant behavior would be worth to perform. The cytotoxicity of pentathiepins in HAP-1 and its GPx1 knockout congener was not much varied, and this suggests that the role of pentathiepins is not limited to GPx1 inhibition/ROS production. Investigations in this regards will also be targeted in future projects.

## 1.10 Conclusion

The unexpected discovery of novel heterocyclic pentathiepin synthesis via a Mo(IV) mediated process has proven to become very useful. In total twenty five novel heterocyclic appended pentathiepin molecules were successfully synthesized under milder conditions in moderate to excellent yields. The biologically relevant heterocyclic scaffolds were selected with the hope

of having homologous medicinal effects. Quinoxaline, pyrazine, pyridine, nicotinamide, quinoline, imdazo-pyrazine, pyrrolo-pyrazine, purine, and pyridine sulfonamide scaffolds were functionalized with polysulfur moieties (pentathiepin). The multi-step organic synthetic approach was applied to attaining these heterocyclic scaffolds, where the sequence of Sonogashira coupling and  $(\text{Et}_4\text{N})_2[\text{MoO}(\text{S}_4)_2]$  mediated ring-closing steps were commonly employed in all pentathiepin syntheses. The analytically pure pentathiepin products were isolated after column chromatography in 10-20% ethyl acetate/hexane.  $^1\text{H}$ ,  $^{13}\text{C}$ ,  $^{19}\text{F}$ -NMR, APCI-MS, CHNS and single crystal X-ray diffraction structural analysis methods were used to confirm the final formation of the pentathiepins. Notably, all pentathiepins exhibited an AA'BB' multiplet pattern between  $\delta$ : 4.2-4.5 ppm with the integration of 2H for the methylene protons of the ethoxy functional group substituted on the five-membered ring. A total of twelve pentathiepin molecular structures were confirmed by single-crystal X-ray diffraction structural analysis. Interestingly, the polysulfur pentathiepin ring adapts the chair confirmation in all molecules with S-S and S-C bond distances and angles in agreement with reported literature data. The mechanistic investigations via control experiments suggest, that the tetra sulfur ring Mo(IV) precursor  $(\text{Et}_4\text{N})_2[\text{MoO}(\text{S}_4)_2]$  is vital along with elemental sulfur for the pentathiepin formation and the Mo(IV) complex regenerates in the reaction. Notably, the  $(\text{PPh}_4)_2[\text{Cu}(\text{S}_4)_2]$  complex also efficiently formed pentathiepin in the presence of elemental sulfur within a short time (2-5 hrs). Alternative copper(II) mediated pentathiepin synthesis would help access new classes of fused heterocyclic pentathiepin scaffolds, which were otherwise challenging with the Mo(IV) methodology due to catalyst-substrate complex formation with wrong donor atoms. The purified and fully characterized pentathiepin samples with sufficient to good solubility were further investigated for their biological relevance. For the first time, the GPx1 enzyme inhibitor properties of novel fused heterocyclic pentathiepins were established, where these probes exhibited 9-12 folds higher potency compared to traditionally employed mercaptosuccinic acid. Notably,  $<1 \mu\text{M}$  concentration of quinoxaline, pyrazine and quinoline fused pentathiepins were potent enough to inhibit 50% of GPx1 enzyme activity. Additionally, cytotoxicity, antimicrobial and antifungal studies were conducted for all pentathiepins.

The cytotoxicity profile of pentathiepins was similar to that of natural derivatives varacin and lissoclinotoxin A and exhibited  $\text{IC}_{50}$  values lie in the  $\mu\text{M}$  range. In general, the induced oxidative stress in cells by pentathiepins causes DNA damage and consequently cytotoxicity. All novel pentathiepins with  $<5\mu\text{M}$  concentrations were proven toxic to the cells in cell proliferation and cell viability studies. In cytotoxic investigations, the  $\text{IC}_{50}$  concentrations for

all pentathiepins were ranging between 0.22 to 4.7  $\mu\text{M}$ . Surprisingly, there was no correlation found between GPx1 inhibition activity and the cytotoxicity profile of the pentathiepins. For example, quinoline has shown high potency in GPx1 enzyme inhibition with reduced cytotoxic activity in tested cancer cells. Additionally, no significant activity difference was noticed for pentathiepins between HAP-1 and GPx1 free K.O.HAP-1.GPx1 cell lines. Thus, pentathiepins' multi-functionality going beyond ROS production is presumed.

Moreover, the nicotinamide fused pentathiepin **21c** has shown high cytotoxicity both in A2780 and cis-platin resistant A2780 cis cells with  $\text{IC}_{50}$  at 0.106 and 0.173  $\mu\text{M}$ , respectively. Therefore, the employment of pentathiepins in resistant cell lines, and understanding their efficacy and mechanism of actions might widen the scope and would be beneficial in target-based drug design. Although varieties of heterocyclic fused pentathiepins were synthesized, the poor solubility of all these probes in aqueous medium has been a challenge. Increased hydrophilicity certainly enhances the bioavailability of the drug moiety as well as it is vital for cell penetration. Thus, developing water-soluble pentathiepin derivatives is highly desirable, and much emphasis should be on this feature in order to improve biological efficiency.

To our surprise, the highly cytotoxic pentathiepin derivatives have shown no antimicrobial or antifungal activity. Among all tested compounds, only pyrazine pentathiepin **10a** has exhibited potent antimicrobial activity against *S.aureus*. However, the structural analogue **10b**, differing only by the ethoxy substitute at position-3 is entirely inactive. Such type of intense structure based activity is exciting to study via computational drug design methods. Presumably, the activity of **10a** could be derived from its selective binding to an enzyme or protein. At the same time, it is also essential to understand the defense mechanism of microorganisms against oxidative stress. It will be worth to develop derivatives out of **10a** without perturbing the active binding units and investigating them in microorganisms would provide valuable information concerning structure and activity. There is an excellent scope to explore the antibacterial activity of pentathiepins, and careful design and analysis would presumably result in powerful novel antibiotics.

In summary, we have identified the potent GPx1 inhibition activity of novel heterocyclic fused pentathiepins. Similarly, the obtained cytotoxicity profile of these compounds is much higher than that of the natural pentathiepin varacin. Although the antimicrobial and antifungal activities were almost entirely absent, still much work can be done in the future by developing derivatives of **10a**. Computational binding studies for the pentathiepin moiety are highly recommended for exploring structure-activity relationship within microorganisms.

## 1.11 Experimental

### *General*

All reactions were performed under a nitrogen atmosphere using oven-dried standard Schlenk glassware. The completely dried *N, N'*-dimethylformamide (DMF, 99.8%, extra dry, stored over molecular sieves) and acetonitrile (ACN, 99%, extra dry, stored over molecular sieves) purchased from Acros organics were used as received for all air or moisture-sensitive reactions. <sup>1</sup>H NMR (300 MHz) and <sup>13</sup>C NMR (75 MHz) spectra were recorded on a Bruker Avance II-300 spectrometer. Chemical shifts  $\delta$  are given in ppm, and the solvent residual peak (CDCl<sub>3</sub>: <sup>1</sup>H,  $\delta$  = 7.27; <sup>13</sup>C,  $\delta$  = 77.0) was used as an internal standard. Peak multiplicities are specified as followed: s, singlet; d, doublet; t, triplet; q, quartet; m, multiplet; br, broad. APCI-MS (m/z) spectra were recorded on an Advion MS. Mechenary-Nagel silica gel 60 F254 plates were used for thin-layer chromatography (TLC), and detection was achieved by UV light. Column chromatography was performed on Acros organics silica gel 60 (35-70  $\mu$ m). The single X-ray crystal structure experiments were conducted by using a STOE IPDS2T and a diffraction source with a fine focus sealed molybdenum tube. The ElementarVario MICRO cube was used for the experimental determination of elemental configurations of final pure products.

#### 1.11.1 Synthesis of precursors **3a-f**, **4a-f**, **12**, **A**, **B**, **19a-e**, **23**, **31**, **35** and **36a-e**

*General procedure:* The compounds **3b-f** were synthesized according to the literature procedure.<sup>134</sup> A 100 mL oven-dried round-bottomed flask was charged with the corresponding *ortho*-phenylenediamine and dissolved in 20 mL of ethanol. 1.5 equivalents of ethylene glyoxylate (50% in toluene) or trifluoromethyl substituted ethylene glyoxylate were added slowly for about 10 minutes at room temperature. The resultant mixture was refluxed for 2 h and after cooling to room temperature allowed to stir further for 1 h. The desired product precipitated out of the solution was filtered off and washed with cold ethanol and dried under vacuum. The crude product was further purified by recrystallization from ethanol.

The compound 2-chloroquinoxaline (**4a**) of >98% purity was purchased from Acros organic, Germany. Thus, the experimental procedure for compound **3a** is not given.

##### *1.11.1.1. Synthesis of 7-methylquinoxalin-2(1H)-one (3b) and 6-methylquinoxalin-2(1H)-one (3c)*

The compounds showed <sup>1</sup>H-NMR and <sup>13</sup>C-NMR data concurring with the reported spectrum.<sup>57</sup> General procedure was followed by using 4-methyl-*ortho*-phenylenediamine (3 g, 24.5 mmol) and ethylene glyoxylate (3.75 g, 56.35 mmol) yielding a white solid. The product is having 1:1

ratio of regio-isomers 7-methylquinoxaline-2(1*H*)-one (**3b**) and 6-methylquinoxalin-2(1*H*)-one (**3c**). The two isomers were separated by column chromatography in 10-15% EtOAc/hexane mobile phase. The compounds **3b** and **3c** were isolated as white solids in 41% and 45% yields, respectively.

**3b**: <sup>1</sup>H NMR (300 MHz, DMSO-*d*<sub>6</sub>) δ: 2.30 (s, 3 H), 7.07 (s, 1 H), 7.54 (s, 2 H), 8.06 (s, 1 H), 12.28 (br. s., 1 H); <sup>13</sup>C NMR (75 MHz, DMSO-*d*<sub>6</sub>) δ: 19.8 (s, 1 C), 124.5 (s, 1 C), 128.6 (s, 1 C), 129.8 (s, 1 C), 130.6 (s, 1 C), 131.1 (s, 1 C), 140.4 (s, 1 C), 150.2 (s, 1 C), 155.0 (s, 1 C).

**3c**: <sup>1</sup>H NMR (300 MHz, DMSO-*d*<sub>6</sub>) δ: 2.28 (s, 3 H), 7.20 (s, 2 H), 7.60 (s, 1 H), 8.09 (s, 1 H), 12.3 (br. s., 1 H); <sup>13</sup>C NMR (75 MHz, DMSO-*d*<sub>6</sub>) δ: 18.8 (s, 1 C), 115.7 (s, 1 C) 128.6 (s, 1 C) 129.8 (s, 1 C) 130.6 (s, 1 C) 131.1 (s, 1 C) 140.4 (s, 1 C) 150.2 (s, 1 C) 155 (s, 1 C).

#### 1.11.1.2. Synthesis of 6-methyl-3-(trifluoromethyl)quinoxaline-2(1*H*)-one (**3d**)

The compound showed a <sup>1</sup>H-NMR spectrum concurring with the reported data.<sup>135</sup> The general procedure was followed by using 4-methyl *ortho*-phenylenediamine (3.35 g, 27.42 mmol) and ethyl 3,3,3-trifluoro-2-oxopropanoate (4 mL, 30.16 mmol) yielding the crude product as 1:1 ratio of regio-isomers. The analytically pure 6-methyl-3-(trifluoromethyl)quinoxaline-2(1*H*)-one (**3d**) was isolated in 39% yield after column chromatography in 20% EtOAc/hexane solvent system. <sup>1</sup>H NMR (300 MHz, DMSO-*d*<sub>6</sub>) δ: 2.45 (s, 3 H), 7.17 (s, 1 H), 7.21 - 7.33 (m, 2 H), 13.00 (br. s., 1 H).

#### 1.11.1.3. Synthesis of 6, 7-dimethylquinoxalin-2(1*H*)-one (**3e**)

The compound showed <sup>1</sup>H-NMR and <sup>13</sup>C-NMR spectrum concurring with the reported data.<sup>57</sup> General procedure was followed by using 4,5-dimethyl-*ortho*-phenylenediamine (1 g, 7.34 mmol) and 2.24 mL of ethylene glyoxylate yielding the product **3e** in 80% isolated yield. <sup>1</sup>H NMR (300 MHz, DMSO-*d*<sub>6</sub>) δ: 2.29 (s, 6 H), 7.07 (s, 2 H), 7.54 (s, 1 H), 8.06 (s, 1 H); <sup>13</sup>C NMR (75 MHz, DMSO-*d*<sub>6</sub>) δ: 18.8 (s, 1 C), 19.8 (s, 1 C), 115.7 (s, 1 C), 128.6 (s, 1 C), 129.8 (s, 1 C), 130.6 (s, 1 C), 131.1 (s, 1 C), 140.4 (s, 1 C), 150.2 (s, 1 C), 155 (s, 1 C).

#### 1.11.1.4. Synthesis of 6, 7-dimethyl-3-(trifluoromethyl)quinoxaline-2(1*H*)-one (**3f**)

The compound showed a <sup>1</sup>H-NMR spectrum concurring with the reported data.<sup>135</sup> General procedure 1.9 was followed by using 4, 5-dimethyl-*ortho*-phenylenediamine (2 g, 14.7 mmol) and ethyl 3,3,3-trifluoro-2-oxopropanoate (1.94 mL, 15.1 mmol) yielding the product **3f** as pale yellow solid in 82% isolated yield. <sup>1</sup>H NMR (300 MHz, DMSO-*d*<sub>6</sub>) δ: 2.35 (s, 3 H), 2.30 (s, 3 H), 7.15 (s, 1 H), 7.68 (s, 1 H), 12.94 (br. s., 1 H).

Synthesis of compounds **4a-f**

The compound 2-chloroquinoxaline (**4a**) of >98% purity was purchased from Acros organic, Germany.

*General procedure:* The compounds **3b-f** were heated under reflux in neat POCl<sub>3</sub> for 2 h under nitrogen atmosphere. After completion of the reaction and cooling to room temperature the resultant mixture was evaporated to dryness under reduced pressure. Ice was added to the crude black oily material and neutralized slowly with a saturated solution of NaHCO<sub>3</sub>. The aqueous layer was filtered and extracted with ethyl acetate. The organic layers were collected, dried over Na<sub>2</sub>SO<sub>4</sub> and concentrated with a roti evaporator resulting in corresponding chlorinated quinoxaline derivatives (**4b-f**).

#### *1.11.1.5. Synthesis of 2-chloro-7-methylquinoxaline (4b)*

The compound showed <sup>1</sup>H-NMR and <sup>13</sup>C-NMR spectrum concurring with the reported data<sup>57</sup> General procedure was followed by using **3b** yielding the product **4b** as brown solid in 95% isolated yield. <sup>1</sup>H NMR (300 MHz, DMSO-*d*<sub>6</sub>) δ: 2.56 (s, 3 H), 7.71 - 7.79 (m, 2 H), 7.81 (s, 1 H), 8.93 (s, 1 H); <sup>13</sup>C NMR (75 MHz, DMSO-*d*<sub>6</sub>) δ: 21.4 (s, 1 C), 127.1 (s, 1 C), 127.9 (s, 1 C), 128 (s, 1 C), 128.8 (s, 1 C), 133 (s, 1 C), 133.1 (s, 1 C), 145.5 (s, 1 C), 170.6 (s, 1 C).

#### *1.11.1.6. Synthesis of 2-chloro-6-methylquinoxaline (4c)*

The compound showed <sup>1</sup>H-NMR and <sup>13</sup>C-NMR spectrum concurring with the reported data.<sup>57</sup> General procedure was followed by using **3c** yielding the product **4c** as brown solid in 82% isolated yield. <sup>1</sup>H NMR (300 MHz, DMSO-*d*<sub>6</sub>) δ: 2.56 (s, 3 H), 7.90 - 7.93 (m, 2 H), 8.02 (d, *J*=8.69 Hz, 1 H), 8.90 (s, 1 H); <sup>13</sup>C NMR (75 MHz, DMSO-*d*<sub>6</sub>) δ: 21 (s, 1 C), 139.3 (s, 1 C), 139.9 (s, 1 C), 140.8 (s, 1 C), 141. (s, 1 C), 141.6 (s, 1 C), 142.5 (s, 1 C), 144.6 (s, 1 C), 170.6 (s, 1 C).

#### *1.11.1.7. Synthesis of 2-chloro-6-methyl-3-(trifluoromethyl)quinoxaline (4d)*

The compound showed <sup>1</sup>H-NMR and <sup>13</sup>C-NMR spectrum concurring with the reported data.<sup>135</sup> General procedure was followed by using **3d** yielding the product **4d** as brownish yellow solid in 79% isolated yield. <sup>1</sup>H NMR (300 MHz, CHLOROFORM-*d*) δ: 2.66 (s, 3 H), 7.71 - 7.83 (m, 2 H), 7.88 (s, 1 H); <sup>13</sup>C NMR (75 MHz, CHLOROFORM-*d*) δ: 22.17 (s, 1 C), 118.64 (s, 1 C), 127.12 (s, 1 C), 127.75 (s, 1 C), 128.61 (s, 1 C), 129.33 (s, 1 C), 133.89 (s, 1 C), 135.91 (s, 1 C), 137.31 (s, 1 C), 145.01 (s, 1 C).

#### *1.11.1.8. Synthesis of 2-chloro-6, 7-dimethylquinoxaline (4e)*

The compound showed <sup>1</sup>H-NMR and <sup>13</sup>C-NMR spectrum concurring with the reported data.<sup>57</sup> General procedure was followed by using **3e** yielding the product **4e** as dark brown solid in

92% isolated yield.  $^1\text{H}$  NMR (300 MHz,  $\text{DMSO-}d_6$ )  $\delta$ : 2.5 (s, 6 H), 7.83 (s, 1 H), 7.93 (s, 1 H), 8.89 (s, 1 H);  $^{13}\text{C}$  NMR (75 MHz,  $\text{DMSO-}d_6$ )  $\delta$ : 19.8 (s, 1 C), 126.1 (s, 1 C), 127.8 (s, 2 C), 139.4 (s, 2 C), 141.2 (s, 1 C), 142.3 (s, 1 C), 144.1 (s, 1 C), 145.9 (s, 1 C).

*1.11.1.9. Synthesis of 2-chloro-6, 7-dimethyl-3-(trifluoromethyl)quinoxaline (4f)*

The compound showed a  $^1\text{H}$ -NMR spectrum concurring with the reported data.<sup>135</sup> General procedure was followed by using **3f** yielding the product **4f** as off white solid in 90% isolated yield.  $^1\text{H}$  NMR (300 MHz,  $\text{CHLOROFORM-}d$ )  $\delta$ : 2.55 (s, 6 H), 7.85 (s, 1 H), 7.97 (s, 1 H).

*1.11.1.10. Synthesis of 6,8-dibromoimidazo[1,2-a]pyrazine (12)*

The compound showed  $^1\text{H}$ -NMR and  $^{13}\text{C}$ -NMR spectrum concurring with the reported data.<sup>60</sup> To a stirred suspension of 2-amino-3,5-dibromopyrazine (2 g, 7.90 mmol) in  $\text{H}_2\text{O/THF}$  (30:2.5 mL), was added bromoacetaldehyde-diethyl acetal (3.61 mL, 23.73 mmol, 3 equiv.) in one portion. The resultant mixture was refluxed for 4 h followed by continued stirring for additional 15 h at room temperature. The suspension was filtered, and the solid was washed with methanol (5 mL) and dried at 60 °C under vacuum yielding 6,8-dibromo-imidazo[1,2-a]pyrazine (**12**) as off-white solid in 98% isolated yield.  $^1\text{H}$  NMR (300 MHz,  $\text{DMSO-}d_6$ )  $\delta$ : 7.91 (s, 1 H), 8.25 (s, 1 H), 9.04 (s, 1 H).

*1.11.1.11. Synthesis of (4-fluorophenyl)(piperazin-1-yl)methanone (A) and 1-tosylpiperazine (B)*

*Compound 'A'*: The compound showed  $^1\text{H}$ -NMR and  $^{13}\text{C}$ -NMR spectrum concurring with the reported data.<sup>136</sup> Piperazine (8.13 g, 0.94 mol) is dissolved in 1N HCl in a 250 mL oven-dried round-bottomed flask. The solution of 4-fluoro benzoyl chloride (3 g, 18.9 mmol) in 15 mL acetonitrile was added to the above solution resulting in a suspension. The resultant reaction mixture was allowed to stir for 3.5 to 4 h at room temperature. Then the mixture was added to 500 mL of 1N HCl. The crude mixture was extracted two times with 100 mL ethyl acetate. The acidified aqueous layer was neutralized with 1N KOH and extracted with two volumes of 100 mL of dichloromethane. The organic layers were combined, dried over  $\text{Na}_2\text{SO}_4$  and evaporated to dryness yielding the desired product as white crystalline solid in 96% isolated yield.  $^1\text{H}$  NMR (300 MHz,  $\text{DMSO-}d_6$ )  $\delta$ : 2.67 (br. s., 4 H), 3.18 (br. s., 4 H), 3.50 (br. s., 1 H), 7.26 (t,  $J=9.06$  Hz, 2 H), 7.44 (dd,  $J=8.88, 5.48$  Hz, 2 H);  $^{13}\text{C}$  NMR (75 MHz,  $\text{DMSO-}d_6$ )  $\delta$ : 45.6 (s, 4 C), 115.2 (s, 1 C), 129.4 (s, 1 C), 129.5 (s, 1 C), 132.5 (s, 1 C), 160.8 (s, 1 C), 164 (s, 1 C), 168 (s, 1 C).

*Compound 'B'*: Compound **B** was synthesized in a similar procedure as compound **A**.<sup>136</sup> The crude product was employed further in the next reactions without any intermediate purification.

1.11.1.12. *Synthesis of compounds 19a-e*

*General procedure:* The compounds **19a-e** were synthesized according to the literature procedure.<sup>137</sup> To a solution of 6-bromonicotinic acid in dichloromethane was added DIPEA and a corresponding secondary amine. The resultant reaction mixture was cooled to 0 °C and small portions of HBTU reagent were added. The mixture was allowed to stir at room temperature for 18 h, while the completion of the reaction was monitored by TLC. After completion of the reaction, the crude mixture was diluted with dichloromethane and washed with water 3 times. The organic layer was separated, dried over Na<sub>2</sub>SO<sub>4</sub> and concentrated with a roti evaporator yielding the crude product. Further purification by column chromatography in 3:1 mixture of EtOAc/hexane furnished the desired product in moderate to good yields.

**(6-bromopyridin-3-yl)(piperidin-1-yl)methanone (19a):** The compound showed a <sup>1</sup>H-NMR and <sup>13</sup>C-NMR spectrum concurring with the reported data.<sup>137</sup> <sup>1</sup>H NMR (300 MHz, DMSO-*d*<sub>6</sub>) δ: 1.48 (br. s., 2 H), 1.60 (br. s., 4 H), 3.26 (br. s., 2 H), 3.58 (br. s., 2 H), 7.70 - 7.80 (m, 2 H), 8.42 (d, *J*=2.27 Hz, 1 H); <sup>13</sup>C NMR (75 MHz, DMSO-*d*<sub>6</sub>) δ: 23.9 (s, 1 C), 24.7 (s, 1 C), 25.4 (s, 1 C), 48.1 (s, 1 C), 48.8 (s, 1 C), 127.1 (s, 1 C), 131.9 (s, 1 C), 137.8 (s, 1 C), 141.8 (s, 1 C), 148.2 (s, 1 C), 165.5 (s, 1 C).

**(6-bromopyridin-3-yl)(morpholino)methanone (19b)**<sup>137</sup>: colorless tan liquid; APCI(+ve)-MS for C<sub>10</sub>H<sub>11</sub>BrN<sub>2</sub>O<sub>2</sub> calc.: 270 m/z, found: 271.12 [M+H]. Crude product used further without purification.

**6-bromo-*N,N*-diethylnicotinamide (19c)**<sup>137</sup> : Brown oil; APCI(+ve)-MS for C<sub>10</sub>H<sub>13</sub>BrN<sub>2</sub>O calc.: 256.02 m/z, found: 257.14 [M+H]. Crude product used further without purification.

**(4-(6-bromonicotinoyl)piperazin-1-yl)(4-fluorophenyl)methanone (19d):** The compound showed <sup>1</sup>H-NMR and <sup>13</sup>C-NMR spectrum concurring with the reported data.<sup>137</sup> <sup>1</sup>H NMR (300 MHz, CHLOROFORM-*d*) δ: 3.50 - 3.82 (m, 8 H), 7.08 - 7.16 (m, 2 H), 7.40 - 7.46 (m, 2 H), 7.55 - 7.66 (m, 2 H), 8.43 (d, *J*=2.27 Hz, 1 H); <sup>13</sup>C NMR (75 MHz, CHLOROFORM-*d*) δ: 38.6 (s, 2 C), 115.7 (s, 2 C), 115.1 (s, 1 C), 128.3 (s, 1 C), 129.4 (s, 1 C), 129.5 (s, 1 C), 129.1 (s, 1 C), 130.8 (s, 1 C), 137.5 (s, 1 C), 143.8 (s, 1 C), 148.4 (s, 1 C), 165.3 (s, 1 C), 165.7 (s, 1 C), 167 (s, 1 C), 169.7 (s, 1 C).

**(6-bromopyridin-3-yl)(4-tosylpiperazin-1-yl)methanone (19e):** The compound showed <sup>1</sup>H-NMR and <sup>13</sup>C-NMR spectrum concurring with the reported data.<sup>137</sup> <sup>1</sup>H NMR (300 MHz, CHLOROFORM-*d*) δ: 2.42 - 2.47 (m, 3 H), 2.93 - 3.09 (m, 4 H), 3.50 - 3.90 (m, 4 H), 7.35 (m, *J*=7.93 Hz, 2 H), 7.51 - 7.58 (m, 2 H), 7.58 - 7.66 (m, 2 H), 8.32 (t, *J*=1.70 Hz, 1 H); <sup>13</sup>C NMR (75 MHz, CHLOROFORM-*d*) δ: 21.5 (s, 1 C), 38.6 (s, 2 C), 45.9 (s, 2 C), 127.8 (s, 2



C), 128.2 (s, 2 C), 129.8 (s, 1 C), 129.9 (s, 1 C), 132 (s, 1 C), 137.5 (s, 1 C), 143.8 (s, 1 C), 144.3 (s, 1 C), 148.3 (s, 1 C), 166.7 (s, 1 C).

*1.11.1.13. Synthesis of 2-bromo-6-(4-methoxyphenyl)-5H-pyrrolo[2,3-b]pyrazine (23)*

The compound showed a <sup>1</sup>H-NMR spectrum concurring with the reported data.<sup>138</sup> In an oven-dried 100 mL round-bottom flask 3,5-dibromopyrazin-2-amine (2 g, 7.908 mmol), ethynylanisol (1.04 g, 7.908 mmol) and bis(triphenylphosphine)palladium(II) chloride (0.222 g, 0.04 mmol) were mixed with 11 mL of triethylamine and degassed THF (10 mL) under nitrogen. The resulting mixture was stirred at 60°C for 3 hours. The reaction mixture was then evaporated to dryness, and the crude product was used further without purification. The crude product (1.5 g, 4.93 mmol) was transferred to a 50 mL Schlenk tube, charged with 1.5 equiv. of NaH (0.178 g, 7.4 mmol), and suspended in dry THF. The resultant mixture was stirred at 60 °C for 18 h and completion of the reaction was monitored by TLC. After completion, THF was evaporated, and the crude mixture extracted with EtOAc and washed with 100 mL of water. The organic layer was dried over Na<sub>2</sub>SO<sub>4</sub> and upon concentrating with a roti evaporator the desired product **23** resulted as a yellow powder ( 1.49 g, 62%). <sup>1</sup>H NMR (300 MHz, DMSO-*d*<sub>6</sub>) δ: 3.84 (s, 3 H), 7.03 (s, 1 H), 7.09 (m, *J*=9.06 Hz, 2 H), 7.98 (m, *J*=9.06 Hz, 2 H), 8.26 (s, 1 H), 12.66 (s, 1 H); APCI(+ve)-MS for C<sub>13</sub>H<sub>10</sub>BrN<sub>3</sub>O calc.: 304.1 m/z, found: 305.3 [M+H].

*1.11.1.14. Synthesis of 9-benzyl-6-chloropurine (31)*

The compound showed <sup>1</sup>H-NMR and <sup>13</sup>C-NMR spectrum concurring with the reported data.<sup>139</sup> In a 25 mL oven-dried Schlenk tube 1.24 g (8 mmol) of 6-chloropurine was dissolved in 10mL of acetonitrile. To this 2 equiv. K<sub>2</sub>CO<sub>3</sub> (2.21 g) and 1.5 equiv. of benzyl bromide (2.05 mg) were added slowly to the reaction mixture. The resultant reaction mixture was stirred for 2 h at room temperature. After total consumption of starting material (monitored by TLC / TLC-MS), the crude product was extracted with ethyl acetate (3x50 mL) and washed with water (3x100 mL). The collected organic phase was concentrated under reduced pressure, and the resultant residue was purified by column chromatography with hexane/ethyl acetate (20% to 30%) mobile phase. The purified product 9-benzyl-6-chloropurine (**31**) was yielded as a white powder (708mg, 36%). <sup>1</sup>H NMR (300 MHz, CHLOROFORM-*d*) δ: 5.47 (s, 2 H), 7.25 - 7.42 (m, 5 H), 8.17 (s, 1 H), 8.75 (s, 1 H); <sup>13</sup>C NMR (75 MHz, CHLOROFORM-*d*) δ: 47.5 (s, 1 C), 76.6 (s, 1 C), 77.4 (s, 1 C), 127.6 (s, 1 C), 128.5 (s, 1 C), 128.9 (s, 1 C), 131.2 (s, 1 C), 134.3 (s, 1 C), 144.9 (s, 1 C), 150.6 (s, 1 C), 151.6 (s, 1 C), 151.8 (s, 1 C); APCI (+ve) TLC-MS = 244.68 m/z calc. for C<sub>12</sub>H<sub>9</sub>ClN<sub>4</sub> [M]; found: 245.4 m/z [M+H].

*1.11.1.15. Synthesis of 6-chloropyridine-3-sulfonyl chloride (35)*

The compound was synthesized according to literature procedures.<sup>140</sup> A saturated solution of SO<sub>2</sub> was prepared from thionyl chloride (24.2 mL) and CuCl by stirring the mixture for overnight. The 5-amino-2-chloropyridine (10g, 77.8 mmol) was dissolved in concentrated HCl (80 mL) by slow portion-wise addition. The resultant saturated solution was cooled to 0 °C, and an aqueous solution of NaNO<sub>2</sub> (5.9 g, 85.5 mmol) was added drop-wise under stirring. After stirring the mixture for 30 minutes, the solution of SO<sub>2</sub> was added drop-wise at 0 °C and allowed to stir further for about 1 h. The crude product was extracted with water and chloroform. After evaporation of the organic phase under reduced pressure, 6-chloropyridine-3-sulfonyl chloride was obtained as violet solid (6.4 g, 30.2 mmol, 74%).<sup>1</sup>H NMR (300 MHz, CHLOROFORM-*d*): δ 9.04 (1H, d, *J*= 2.4 Hz), 8.32 (1H, dd, *J*= 8.5 Hz), 7.57 (1H, dd, *J*= 8.5 Hz).

*Synthesis of Sulfonamides (36a-e)*

*General procedure:* In an oven-dried 50 ml flask, 3 mmol of 6-chloropyridine-2-sulfonylchloride were dissolved in 30 ml of dichloromethane (DCM). The solution was cooled to 0 °C using ice, and 1.2 equiv. of the corresponding amine was added. The reaction was started by drop wise addition of 1.5 equiv. diisopropylethylamine (DIPEA) and was then stirred for 2 h. After consumption of starting material (monitored by TLC / TLC-MS), the solvent was removed in vacuum and the resultant residue obtained was purified by extraction with ethyl acetate or DCM and water. Few of resulting sulfonamides were used for the Sonogashira reaction without any further purification.

*1.11.1.16. 2-chloro-5-(piperidin-1-ylsulfonyl)pyridine (36a)*

The compound showed <sup>1</sup>H-NMR and <sup>13</sup>C-NMR spectrum concurring with the reported data.<sup>141</sup> General procedure for sulfonamide preparation was followed by using 6-chloropyridine-3-sulfonyl chloride (636 mg, 3 mmol) and piperidin (3.6 mmol, 1.2 equiv.) yielding 2-chloro-5-(piperidin-1-ylsulfonyl)pyridine (**36a**) (270 mg, 1 mmol 34%) as pink fluffy solid.<sup>1</sup>H NMR (300 MHz, CHLOROFORM-*d*) δ: 1.43 - 1.54 (m, 2 H), 1.68 (quin, *J*=5.66 Hz, 4 H), 2.98 - 3.14 (m, 4 H), 7.50 (dd, *J*=8.34, 0.64 Hz, 1 H), 7.99 (dd, *J*=8.34, 2.57 Hz, 1 H), 8.76 (dd, *J*=2.48, 0.64 Hz, 1 H); <sup>13</sup>C NMR (75 MHz, CHLOROFORM-*d*) δ: 23.4 (s, 1 C) 25.1 (s, 2 C) 46.8 (s, 2 C) 124.6 (s, 1 C) 132.4 (s, 1 C) 137.7 (s, 1 C) 148.7 (s, 1 C) 155.5 (s, 1 C); APCI(+ve) TLC-MS = 260.74 m/z calc. for C<sub>10</sub>H<sub>13</sub>ClN<sub>2</sub>O<sub>2</sub>S [M], found : 261.3 m/z [M+H]

1.11.1.17. 4-((6-chloropyridin-3-yl)sulfonyl)morpholine (**36b**)

The compound showed a <sup>1</sup>H-NMR and <sup>13</sup>C-NMR spectrum concurring with the reported data.<sup>142</sup>General procedure for sulfonamide preparation was followed by using 6-chloropyridine-3-sulfonyl chloride (636 mg, 3 mmol) and morpholine (3 mmol, 1 equiv.) yielding 4-((6-chloropyridin-3-yl)sulfonyl)morpholine (**36b**) (450 mg, 1.7mmol, 56%) as white fluffy solid. <sup>1</sup>H NMR (300 MHz, CHLOROFORM-*d*) δ: 3.01 - 3.14 (m, 4 H) 3.74 - 3.85 (m, 4 H) 7.54 (dd, *J*=8.34, 0.73 Hz, 1 H) 7.99 (dd, *J*=8.34, 2.57 Hz, 1 H) 8.76 (dd, *J*=2.48, 0.64 Hz, 1 H); <sup>13</sup>C NMR (75 MHz, CHLOROFORM-*d*) δ: 45.8 (s, 2 C), 65.9 (s, 2 C), 124.8 (s, 1 C), 131.2 (s, 1 C), 137.8 (s, 1 C), 148.8 (s, 1 C), 156.0 (s, 1 C); (+ve) APCI-MS = 262.71 m/z calc. for C<sub>9</sub>H<sub>11</sub>ClN<sub>2</sub>O<sub>3</sub>S [M], found: 263 m/z [M+H]

1.11.1.18. 6-chloro-*N*-[(2*S*)-3-methylbutan-2-yl]pyridine-3-sulfonamide (**36c**)

General procedure for sulfonamide preparation was followed by using 6-chloropyridine-3-sulfonyl chloride (636 mg, 3 mmol) and (2*S*)-3-methylbutan-2-amine (3.6 mmol, 1.2 equiv.) yielding 6-chloro-*N*-[(2*S*)-3-methylbutan-2-yl]pyridine-3-sulfonamide (**36c**) (687 mg, 2.6 mmol, 87%) as light-pink solid. <sup>1</sup>H NMR (300 MHz, CHLOROFORM-*d*) δ: 0.83 (dd, *J*=6.79, 1.10 Hz, 6 H), 1.02 (d, *J*=6.69 Hz, 3 H), 1.21 (t, *J*=7.02 Hz, 1 H), 1.67 (qd, *J*=6.82, 1.65 Hz, 1 H), 4.74 (br. s., 1 H), 7.48 (dd, *J*=8.39, 0.69 Hz, 1 H), 8.10 (dd, *J*=8.34, 2.57 Hz, 1 H), 8.87 (dd, *J*=2.57, 0.64 Hz, 1 H); <sup>13</sup>C NMR (75 MHz, CHLOROFORM-*d*) δ: 18.0 (s, 1 C), 18.1 (s, 1 C), 18.3 (s, 1 C), 33.4 (s, 1 C), 55.4 (s, 1 C), 124.6 (s, 1 C), 137 (s, 1 C), 137.1 (s, 1 C), 148.3 (s, 1 C), 155.1 (s, 1 C); (+ve) APCI-MS = 262.76 m/z calc. for C<sub>10</sub>H<sub>15</sub>ClN<sub>2</sub>O<sub>2</sub>S [M], found: 263.1 m/z [M+H]

1.11.1.19. *N*-((3*s*,5*s*,7*s*)-adamantan-1-yl)-6-chloropyridine-3-sulfonamide (**36d**)

General procedure for sulfonamide preparation was followed by using 6-chloropyridine-3-sulfonyl chloride (636 mg, 3 mmol) and adamantylamine (3.6 mmol, 1.2 equiv.) yielding *N*-((3*s*,5*s*,7*s*)-adamantan-1-yl)-6-chloropyridine-3-sulfonamide (**36d**) (862 mg, 2.6mmol, 88%) as violet colored solid. <sup>1</sup>H NMR (300 MHz, CHLOROFORM-*d*) δ: 1.60 (br. s., 6 H), 1.81 (d, *J*=2.75 Hz, 6 H), 2.05 (br. s., 4 H), 7.46 (dd, *J*=8.39, 0.60 Hz, 1 H), 8.12 (dd, *J*=8.44, 2.57 Hz, 1 H), 8.89 (dd, *J*=2.48, 0.55 Hz, 1 H); <sup>13</sup>C NMR (75 MHz, CHLOROFORM-*d*) δ: 29.4 (s, 2 C) 29.7 (s, 2 C) 35.7 (s, 2 C) 36.2 (s, 1 C) 43.1 (s, 1 C) 46.1 (s, 1 C) 56 (s, 1 C) 124.4 (s, 1 C) 137.1 (s, 1 C) 139.5 (s, 1 C) 148.4 (s, 1 C) 154.8 (s, 1 C); (+ve)APCI-MS m/z = 326.09 m/z calc. for C<sub>15</sub>H<sub>19</sub>ClN<sub>2</sub>O<sub>2</sub>S [M], found: 327.2 m/z [M+H]

1.11.1.20. *N*-(benzo[d][1,3]dioxol-5-ylmethyl)-6-chloropyridine-3-sulfonamide (**36e**)

General procedure for sulfonamide preparation was followed by using 6-chloropyridine-3-sulfonyl chloride (636 mg, 3 mmol) and piperonylamine (3 mmol, 1 equiv.) yielding *N*-(benzo[d][1,3]dioxol-5-ylmethyl)-6-chloropyridine-3-sulfonamide (**36e**) as violet solid. (+ve) APCI-MS = 326.75 m/z calc. for C<sub>13</sub>H<sub>11</sub>ClN<sub>2</sub>O<sub>4</sub>S [M], found: 327.3 m/z [M+H]. The product was directly used for the next step without isolation.

1.11.1.21. *N*-benzyl-6-chloropyridine-3-sulfonamide (**36f**)

General procedure for sulfonamide preparation was followed by using 6-chloropyridine-3-sulfonyl chloride (636 mg, 3 mmol) and benzylamine (3 mmol, 1 equiv.) yielding *N*-benzyl-6-chloropyridine-3-sulfonamide (**36f**) (760 mg, 2.7 mmol, 90%) as lilac solid. <sup>1</sup>H NMR (300 MHz, CHLOROFORM-*d*) δ: 4.23 (s, 2 H), 7.16 - 7.22 (m, 2 H), 7.25 - 7.30 (m, 4 H), 7.39 (dd, *J*=8.39, 0.69 Hz, 1 H) 7.98 (dd, *J*=8.39, 2.52 Hz, 1 H) 8.80 (dd, *J*=2.57, 0.64 Hz, 1 H); <sup>13</sup>C NMR (75 MHz, CHLOROFORM-*d*) δ: 47.3 (s, 1 C), 124.5 (s, 1 C), 127.9 (s, 1 C), 128.3 (s, 2 C), 128.9 (s, 2 C), 135.3 (s, 1 C), 135.9 (s, 1 C), 137.2 (s, 1 C), 148.4 (s, 1 C), 155.3 (s, 1 C); (+ve) APCI-MS = 282.74 m/z calc. for C<sub>12</sub>H<sub>11</sub>ClN<sub>2</sub>O<sub>2</sub>S [M], found: 283.1 m/z [M+H].

**1.11.2 General procedure for the Sonogashira cross-coupling-synthesis of 6a-f, 9a-b, 13, 16a-b, 20a-e, 24, 27, 32, 37a-f**

A 25 mL oven-dried Schlenk tube was charged with 2 mol% of palladium (II) acetate (Pd(OAc)<sub>2</sub>), 5 mol% of phosphine ligand (PPh<sub>3</sub>) or PdCl<sub>2</sub>(PPh<sub>3</sub>)<sub>2</sub> (2-3 mol%), 3 mol% copper(I) iodide (CuI) and 1-2 mmol of chloro- or bromo-heterocyclic derivative under N<sub>2</sub> atmosphere and the resultant mixture was dissolved in 5 mL of dry acetonitrile or DMF. The reaction mixture was stirred for 5 minutes and supplied with 2 equiv. of 3,3'-diethoxy propyne and 5 equiv. of TEA or DIPEA. It was followed by stirring at 60 °C for 3-4 h. After consumption of starting material (monitored by TLC / TLC-MS), the solvent was removed under vacuum, and the resultant residue obtained was purified by column chromatography in hexane/ethyl acetate (10% to 30%) solvent system to afford the desired product.

*Synthesis of quinoxaline Sonogashira products 6a-f:*

The compound **6a** was originally prepared by Zubair et al., in large scale.<sup>57</sup> The compound synthesis was not repeated.

1.11.2.1. *Synthesis of 2-(3,3-diethoxyprop-1-ynyl)-7-methylquinoxaline (6b)*

The compound showed a <sup>1</sup>H-NMR spectrum concurring with the reported data.<sup>57</sup> General procedure was followed by using 2-chloro-7-methylquinoxaline **4b** (1 g, 5.595 mmol), yielding

the product **6b** (0.956 g, 2.82 mmol, 47.8%) as dark brown oil. <sup>1</sup>H NMR (300 MHz, CHLOROFORM-*d*) δ: 1.27-1.32 (m, 6 H), 2.58 (s, 3 H), 3.67 - 3.77 (m, 2 H), 3.82 - 3.92 (m, 2 H), 5.58 (s, 1H), 7.56 (s, 1 H), 7.93 - 7.96 (d, J= 8.92, 2 H), 8.63 (s, 1 H).

*1.11.2.2.Synthesis of 2-(3,3-diethoxyprop-1-ynyl)-6-methylquinoxaline (6c)*

General procedure was followed by using 2-chloro-6-methylquinoxaline **4c** (2 g, 11.19 mmol), yielding the product **6c** (2.48 g, 9.174 mmol, 82.1%) as dark brown oil. <sup>1</sup>H NMR (300 MHz, CHLOROFORM-*d*) δ: 1.27-1.32 (m, 6 H), 2.60 (s, 3 H), 3.67 - 3.77 (m, 2 H), 3.82 - 3.92 (m, 2 H), 5.58 (s, 1H), 7.85 (s, 1 H), 7.93 - 7.96 (d, J= 8.92, 1 H), 7.96 - 8.00 (d, J= 9.1, 1 H), 8.87 (s, 1 H); <sup>13</sup>C NMR (75 MHz, CHLOROFORM-*d*) δ: 15.1 (s, 1 C), 21.8 (s, 1 C), 21.9 (s, 1 C), 61.4 (s, 1 C), 82.5 (s, 1 C), 87.9 (s, 1 C), 91.6 (s, 1 C), 128.1 (s, 1 C), 128.7 (s, 1 C), 128.8 (s, 1 C), 133.1 (s, 1 C), 133.1 (s, 1 C), 139.7 (s, 1 C), 140.6 (s, 1 C), 146.3 (s, 1 C), 147.1 (s, 1 C); (+ve)APCI-MS = 270.33 m/z [M] calcd. for C<sub>16</sub>H<sub>18</sub>N<sub>2</sub>O<sub>2</sub> [M], found: 271.42 m/z [M+H].

*1.11.2.3.Synthesis of 2-(3,3-diethoxyprop-1-ynyl)-6-methyl-3-(trifluoromethyl)quinoxaline (6d)*

General procedure was followed by using 2-chloro-6-methyl-3-(trifluoromethyl)quinoxaline (**4d**) (1.52 g, 6.163 mmol), yielding **6d** (2.26 g, 6.68 mmol, 80%) as dark brown oil. <sup>1</sup>H NMR (300 MHz, CHLOROFORM-*d*) δ: 1.27 (t, J=7.06 Hz, 6 H), 2.60 (s, 3 H), 3.66 - 3.79 (m, 2 H), 3.85 (dq, J=9.32, 7.13 Hz, 2 H), 5.58 (s, 1 H), 7.69 (ddd, J=10.57, 8.73, 1.79 Hz, 1 H), 7.89 (d, J=15.13 Hz, 1 H), 8.01 (dd, J=11.92, 8.71 Hz, 1 H); <sup>13</sup>C NMR (75 MHz, CHLOROFORM-*d*) δ: 15.4 (s, 1 C), 22.3 (s, 1 C), 22.4 (s, 1 C), 61.8 (s, 1 C), 91.9 (s, 1 C), 92.1 (s, 1 C), 119.3, 119.40, 123, 123.1 (s, 1 C), 128.1, 128.8, 128.9, 129.6 (s, 1 C), 135.2, 135.7, 137.6 (s, 1 C), 139.1 (s, 1 C), 141.5 (s, 1 C), 142.5 (s, 1 C), 142.9 (s, 1 C), 143.1 (s, 1 C), 143.2 (s, 1 C), 143.7 (s, 1 C), 144.5 (s, 1 C); <sup>19</sup>F NMR (282 MHz, CHLOROFORM-*d*) δ : -66.14 (s, 2 F), -66.00 (s, 1 F) ;(+ve)APCI-MS m/z = 338.32 [M] calcd. for C<sub>17</sub>H<sub>17</sub>F<sub>3</sub>N<sub>2</sub>O<sub>2</sub> [M], found: 339.53 [M+H].

*1.11.2.4.Synthesis of 2-(3,3-diethoxyprop-1-yn-1-yl)-6,7-dimethylquinoxaline (6e)*

The compound showed a <sup>1</sup>H-NMR spectrum concurring with the reported data.<sup>57</sup> General procedure for the Sonogashira reaction was followed by using **4e** (2 g, 10.38 mmol) yielding the desired product **6e** (3.5 g, 0.012 mol, 84%) as brown solid. <sup>1</sup>H NMR (300 MHz, CHLOROFORM-*d*) δ: 1.31 (t, J=6.99 Hz, 6 H), 2.51 (d, J=2.27 Hz, 6 H), 3.73 (dq, J=9.44, 7.05 Hz, 2 H), 3.88 (dq, J=9.44, 7.05 Hz, 2 H), 5.58 (s, 1 H), 7.83 (br. s., 2 H), 8.82 (s, 1 H).

*1.11.2.5.Synthesis of 2-(3,3-diethoxyprop-1-ynyl)-6,7-dimethyl-3-(trifluoromethyl)quinoxaline (6f)*

General procedure was followed by using 2-chloro-6,7-dimethyl-3-(trifluoromethyl)quinoxaline (2 g, 7.673 mmol), Pd(OAc)<sub>2</sub> (1 mol%, 17.2 mg, 0.07673 mmol), triphenylphosphine (5 mol%, 100.6 mg, 0.383 mmol), copper(I)iodide (5 mol%, 73 mg, 0.38365 mmol) and 3,3-diethoxypropyne (1.2 equiv., 1.65 mL, 11.50 mmol) and Et<sub>3</sub>N (3 equiv., 3.2 mL, 23.019 mmol). The reaction mixture was stirred in anhydrous CH<sub>3</sub>CN (20 mL) at reflux temperature for 6 h and the crude product was purified by column chromatography and eluting solvents 20% EtOAc/Hexane yielding a dark brown oil of 2.62 g, (97 %). <sup>1</sup>H NMR (300 MHz, CHLOROFORM-*d*) δ: 1.27 - 1.33 (m, 6 H), 2.54 (s, 6 H), 3.70 - 3.77 (m, 2 H), 3.87 (dd, *J*=9.44, 7.18 Hz, 2 H), 5.60 (s, 1 H), 7.89 (s, 1 H), 7.95 (s, 1 H); <sup>13</sup>C NMR (75 MHz, CHLOROFORM-*d*) δ: 15.1 (s, 2 C), 20.5 (s, 2 C), 20.6 (s, 2 C), 61.4 (s, 2 C), 79.7 (s, 1 C), 89.7 (s, 1 C), 91.6 (s, 1 C), 127.9 (s, 1 C), 128.7 (s, 1 C), 137.7 (s, 1 C), 143.4 (s, 1 C), 144.2 (s, 1 C); (+ve)APCI-MS *m/z* = 352.35 [M] calcd. for C<sub>18</sub>H<sub>19</sub>F<sub>3</sub>N<sub>2</sub>O<sub>2</sub> [M], found : 353.51[M+H].

*Synthesis of pyrazine Sonogashira products 9a-b:*

*1.11.2.6.2-(3, 3-diethoxyprop-1-yn-1-yl)pyrazine (9a):*

The spectral data of compound **9a** are in agreement with the literature.<sup>57</sup> General procedure for the Sonogashira reaction was followed by using 2-chloropyrazine (1.56 g, 1.248 mmol) yielding the desired product as pale orange oil in 73 % (0.188 g, 0.912 mmol) yield. <sup>1</sup>H NMR (300 MHz, CHLOROFORM-*d*) δ: 1.24 (t, *J*=6.99 Hz, 6 H), 3.60 - 3.71 (m, 2 H), 3.74 - 3.88 (m, 2 H), 5.49 (s, 1 H), 8.53 (s, 1 H), 8.48 (s, 1 H), 8.67 (s, 1 H).

*1.11.2.7.2-(3, 3'-diethoxyprop-1-yn-1-yl)-3-ethoxypyrazine (9b):*

General Procedure for Sonogashira reactions was followed by using 2-ethoxy-3-iodopyrazine (500 mg, 2 mmol) yielding 2-(3,3-diethoxyprop-1-yn-1-yl)-3-ethoxypyrazine as a brown oil. The product was further used directly without additional purifications.

*1.11.2.8.Synthesis of 6-bromo-8-(3,3-diethoxyprop-1-yn-1-yl)imidazo[1,2-*a*]pyrazine (13)*

The spectral data of compound **13** are in agreement with the literature.<sup>143</sup> General procedure of the Sonogashira reaction was followed by using compound **12** (2.08 g, 7.51 mmol) yielding the product as brown solid in 43% (1.05 g, 3.23 mmol) isolated yields. <sup>1</sup>H NMR (300 MHz, CHLOROFORM-*d*) δ: 1.26 - 1.30 (m, 6 H), 3.65 - 3.80 (m, 2 H), 3.80 - 3.95 (m, 2 H), 5.62 (s, 1 H), 7.72 (d, *J*=1.13 Hz, 1 H), 7.87 (d, *J*=1.13 Hz, 1 H), 8.26 - 8.32 (m, 1 H).

*1.11.2.9. Synthesis of 2-(3, 3-diethoxyprop-1-yn-1-yl)pyridine (16a):*

The spectral data of compound **16a** are in agreement with the literature.<sup>144</sup> General procedure for the Sonogashira reaction was followed by using 2-bromopyridine (5 g, 31.6 mmol) yielding the product **16a** as a dark brown oil in 88% (5.7 g, 27.8 mmol) isolated yield. <sup>1</sup>H NMR (300 MHz, DMSO-*d*<sub>6</sub>) δ: 1.18 (t, *J*=7.18 Hz, 6 H), 3.55 - 3.64 (m, 2 H), 3.65 - 3.77 (m, 2 H), 5.56 (s, 1 H), 7.39 - 7.46 (m, 1 H), 7.56 (d, *J*=7.93 Hz, 1 H), 7.79 - 7.87 (m, 1 H), 8.59 (s., 1 H); <sup>13</sup>C NMR (75 MHz, DMSO-*d*<sub>6</sub>) δ: 14.9 (s, 1 C), 15 (s, 1 C), 60.4 (s, 1 C), 64.9 (s, 1 C), 83.8 (s, 1 C), 84 (s, 1 C), 90.9 (s, 1 C), 123.9 (s, 1 C), 127.3 (s, 1 C), 136.7 (s, 1 C), 141.3 (s, 1 C), 150.1 (s, 1 C).

*1.11.2.10. Synthesis of 1-(2-(3,3-diethoxyprop-1-yn-1-yl)pyridin-3-yl)ethan-1-one (16b):*

The spectral data of compound **16b** are in agreement with the literature.<sup>144</sup> General procedure for Sonogashira reaction was followed by using 1-(2-bromopyridin-3-yl)ethan-1-one (0.467 g, 3 mmol) yielding the product **16b** as brown solid. The product was confirmed by (+ve) APCI-MS *m/z* = 247.12 [M] calcd. for C<sub>14</sub>H<sub>17</sub>NO<sub>3</sub> [M], found: 248 *m/z* [M+H]. The resultant product was used without further purification.

*Synthesis of nicotinamide Sonogashira products 20a-e:*

*1.11.2.11. Synthesis of (6-(3, 3-diethoxyprop-1-yn-1-yl)pyridin-3-yl)(piperidine-1-yl)methanone (20a)*

General procedure for the Sonogashira reaction was followed by using **19a** (1.94 g, 7.16 mmol) yielding the product as reddish-brown oil. The product was confirmed by (+ve) APCI-MS *m/z* = 316.18 [M] calcd. for C<sub>18</sub>H<sub>24</sub>N<sub>2</sub>O<sub>3</sub> [M], found: 317.22 *m/z* [M+H]. Without further purification, compound **20a** was used in the next reactions.

*1.11.2.12. Synthesis of (6-(3,3-diethoxyprop-1-yn-1-yl)pyridin-3-yl)(morpholino)methanone (20b)*

Spectral data of the compound are in agreement with previous reports.<sup>145</sup> General procedure for the Sonogashira reaction was followed by using **19b** (1 g, 3.68 mmol) yielding the product as dark red liquid in 73% (0.85 g, 2.68 mmol) yield. <sup>1</sup>H NMR (300 MHz, CHLOROFORM-*d*) δ: 0.97 - 1.29 (m, 6 H), 2.67 - 2.71 (m, 2 H), 3.51 - 3.77 (m, 10 H), 5.40 (s, 1 H), 7.44 (d, *J*=8.31 Hz, 1 H), 7.65 (dd, *J*=7.74, 2.08 Hz, 1 H), 7.89 (s, 1 H); <sup>13</sup>C NMR (75 MHz, CHLOROFORM-*d*) δ: 14.4 (s, 1 C), 20.3 (s, 1 C), 30.7 (s, 1 C), 35.7 (s, 1 C), 37.9 (s, 1 C), 60.6 (s, 1 C), 66 (s, 1 C), 82.8 (s, 1 C), 85.1 (s, 1 C), 90.8 (s, 1 C), 126.4 (s, 1 C), 129.8 (s, 1 C), 134.7 (s, 1 C), 142.7 (s, 1 C), 147.6 (s, 1 C), 161.8 (s, 1 C), 166.4 (s, 1 C); (+ve) APCI-MS *m/z* = 318.16 [M] calcd. for C<sub>17</sub>H<sub>22</sub>N<sub>2</sub>O<sub>4</sub> [M], found: 319.16 *m/z* [M+H].

*1.11.2.13. Synthesis of 6-(3,3-diethoxyprop-1-yn-1-yl)-N, N-diethylnicotinamide (20c)*

The spectral data of compound **20c** are in agreement with the literature.<sup>145</sup> General procedure for Sonogashira reaction was followed by using **19c** (1 g, 3.89 mmol) yielding the product as reddish oil in 78% (0.923 g, 3.03 mmol) yield. <sup>1</sup>H NMR (300 MHz, CHLOROFORM-*d*)  $\delta$ : 1.14 (t, *J*=6.99 Hz, 12 H), 3.13 (br. s., 2 H), 3.43 (br. s., 2 H), 3.49 - 3.61 (m, 2 H), 3.64 - 3.76 (m, 2 H), 5.38 (s, 1 H), 7.38 - 7.43 (m, 1 H), 7.58 (dd, *J*=8.12, 2.08 Hz, 1 H), 8.47 (s, 1 H); <sup>13</sup>C NMR (75 MHz, CHLOROFORM-*d*)  $\delta$ : 14.7 (s, 1 C), 20.6 (s, 1 C), 31 (s, 1 C), 36.1 (s, 1 C), 39.3 (s, 1 C), 43.1 (s, 1 C), 60.9 (s, 1 C), 83.3 (s, 1 C), 85 (s, 1 C), 91.2 (s, 1 C), 126.7 (s, 1 C), 132 (s, 1 C), 134.2 (s, 1 C), 142.4 (s, 1 C), 147.2 (s, 1 C), 162.1 (s, 1 C), 167.5 (s, 1 C); (+ve) APCI-MS *m/z* = 304.18 [M] calcd. for C<sub>17</sub>H<sub>24</sub>N<sub>2</sub>O<sub>3</sub> [M], found: 305 *m/z* [M+H].

*1.11.2.14. Synthesis of (4-(6-(3,3-diethoxyprop-1-yn-1-yl)nicotinoyl)piperazine-1-yl)(4-fluorophenyl)methanone (20d)*

General procedure for the Sonogashira coupling was followed by using **19d** (0.393 g, 1 mmol) yielding the product as a red oil. The product was confirmed by (+ve) APCI-MS *m/z* = 439.48 *m/z* [M] calcd. for C<sub>24</sub>H<sub>26</sub>FN<sub>3</sub>O<sub>4</sub> [M], found: 440.1 *m/z* [M+H]. The product was used further without additional purifications.

*1.11.2.15. Synthesis of (6-(3,3-diethoxyprop-1-yn-1-yl)pyridin-3-yl)(4-tosylpiperazin-1-yl)methanone (20e)*

General procedure for the Sonogashira reaction was followed by using **19e** (0.425 g, 1 mmol) yielding the product as red liquid. The product was confirmed by (+ve) APCI-MS *m/z* = 471.18 *m/z* [M] calcd. for C<sub>24</sub>H<sub>29</sub>N<sub>3</sub>O<sub>5</sub>S [M], found: 472.1 *m/z* [M+H]. The product was used further without additional purifications.

*1.11.2.16. Synthesis of 2-(3,3-diethoxyprop-1-yn-1-yl)-6-(4-methoxyphenyl)-5H-pyrrolo[2,3-*b*]pyrazine (24)*

General procedure for the Sonogashira coupling was followed by using **23** (0.5 g, 1.64 mmol) yielding **24** as red oil in 62% (0.357 g, 1.017 mmol) yield. <sup>1</sup>H NMR (300 MHz, DMSO-*d*<sub>6</sub>)  $\delta$ : 1.20 (t, *J*=7.18 Hz, 6 H), 3.56 - 3.66 (m, 2 H), 3.66 - 3.79 (m, 2 H), 3.84 (s, 3 H), 5.60 (s, 1 H), 7.00 - 7.13 (m, 3 H), 7.99 (d, *J*=8.69 Hz, 2 H), 8.33 (s, 1 H), 12.63 (br. s., 1 H).

*1.11.2.17. Synthesis of 2-(3,3-diethoxyprop-1-yn-1-yl)quinolone (27)*

General procedure for the Sonogashira reaction was followed by using 2-bromoquinolone (0.416 g, 2 mmol) yielding the product as brown solid. The product was confirmed by (+ve) APCI-MS *m/z* = 255.13 *m/z* [M] calcd. for C<sub>16</sub>H<sub>17</sub>NO<sub>2</sub> [M], found: 256.2 *m/z* [M+H]. The product was used further without additional purifications.



*1.11.2.18. Synthesis of 9-benzyl-6-(3,3-diethoxyprop-1-yn-1-yl)-9H-purine (32):*

General procedure for the Sonogashira reaction was followed by using 6-chlorophenylpurine (367 mg, 1.5 mmol) and PTABS (8.82 mg 2 mol%) instead of XPhos, yielding 9-benzyl-6-(3,3-diethoxyprop-1-yn-1-yl)-9H-purine as brown oil. NMR; (+ve) APCI-MS  $m/z = 336.39$  calcd. for  $C_{19}H_{20}N_4O_2$  [M], found 337.0 [M+H]. The product was used directly in subsequent reactions without additional purifications.

*Synthesis of pyridine sulfonamide Sonogashira products (37a-f):*

*1.11.2.19. 2-(3,3-diethoxyprop-1-yn-1-yl)-5-(piperidin-1-ylsulfonyl)pyridine (37a):*

General procedure for the Sonogashira reactions was followed by using 2-chloro-5-(piperidin-1-ylsulfonyl)pyridine (0.260 g, 1 mmol) and  $PdCl_2(PPh_3)_2$  (0.021 g 3 mol%), yielding 2-(3,3-diethoxyprop-1-yn-1-yl)-5-(piperidin-1-ylsulfonyl)pyridine (0.320 g, 0.9 mmol, 90%) as brown oil.  $^1H$  NMR (300 MHz, CHLOROFORM-*d*)  $\delta$ : 1.28 (t,  $J=7.06$  Hz, 6 H) 1.40 - 1.55 (m, 2 H) 1.57 - 1.75 (m, 4 H) 2.97 - 3.11 (m, 4 H) 3.61 - 3.77 (m, 2 H) 3.79 - 3.93 (m, 2 H) 5.52 (s, 1 H) 7.61 (dd,  $J=8.16$ , 0.83 Hz, 1 H) 8.00 (dd,  $J=8.21$ , 2.34 Hz, 1 H) 8.92 (dd,  $J=2.29$ , 0.83 Hz, 1 H);  $^{13}C$  NMR (75 MHz, CHLOROFORM-*d*)  $\delta$ : 15.1 (s, 1 C), 23.4 (s, 1 C), 25.1 (s, 1 C), 46.8 (s, 2 C), 53.4 (s, 2 C), 61.4 (s, 2 C), 83.1 (s, 1 C), 87.6 (s, 1 C), 91.5 (s, 1 C), 127.1 (s, 1 C), 132.5 (s, 1 C), 135.4 (s, 1 C), 145.7 (s, 1 C), 148.5 (s, 1 C); (+ve) APCI-MS  $m/z = 352.45$  calcd. for  $C_{17}H_{24}N_2O_4S$  [M], found 353.3 [M+H]

*1.11.2.20. 4-((6-(3,3-diethoxyprop-1-yn-1-yl)pyridin-3-yl)sulfonyl)morpholine (37b):*

General procedure for the Sonogashira reaction was followed by using 4-((6-chloropyridin-3-yl)sulfonyl)morpholine (0.396 g, 1.5 mmol) and  $PdCl_2(PPh_3)_2$  (0.0316 g 3 mol%) yielding 4-((6-(3,3-diethoxyprop-1-yn-1-yl)pyridin-3-yl)sulfonyl)morpholine as dark-brown oil.; (+ve) APCI-MS  $m/z = 354.42$  calcd. for  $C_{16}H_{22}N_2O_5S$  [M], found 355.2 [M+H]]. The product was further used directly without additional purifications.

*1.11.2.21. 6-(3,3-diethoxyprop-1-yn-1-yl)-N-[(2S)-3-methylbutan-2-yl]pyridine-3-sulfonamide (37c):*

General procedure for the Sonogashira reaction was followed by using 6-chloro-*N*-[(2S)-3-methylbutan-2-yl]pyridine-3-sulfonamide (0.650 g, 2.5 mmol) yielding 6-(3,3-diethoxyprop-1-yn-1-yl)-*N*-[(2S)-3-methylbutan-2-yl]pyridine-3-sulfonamide as green-brown oil.; (+ve) APCI-MS  $m/z = 354.46$  calcd. for  $C_{17}H_{26}N_2O_4S$  [M], found 355.5 [M+H] The product was used directly in subsequent reactions without additional purification.

1.11.2.22. *N-((3s,5s,7s)-adamantan-1-yl)-6-(3,3-diethoxyprop-1-yn-1-yl)pyridine-3-sulfonamide (37d):*

General procedure for the Sonogashira reaction was followed by using *N-((3s,5s,7s)-adamantan-1-yl)-6-chloropyridine-3-sulfonamide* (0.652 g, 2 mmol) yielding *N-((3s,5s,7s)-adamantan-1-yl)-6-(3,3-diethoxyprop-1-yn-1-yl)pyridine-3-sulfonamide* as light-brown oil.; (+ve) APCI-MS  $m/z = 418.55$  calcd. for  $C_{22}H_{30}N_2O_4S$  [M], found 419.6 [M+H]. The product was used directly in subsequent reactions without additional purification.

1.11.2.23. *N-(benzo[d][1,3]dioxol-5-ylmethyl)-6-(3,3-diethoxyprop-1-yn-1-yl)pyridine-3-sulfonamide (37e):*

General procedure for sonogashira reaction was followed by using *N-(benzo[d][1,3]dioxol-5-ylmethyl)-6-chloropyridine-3-sulfonamide* (0.654 g, 2 mmol) yielding *N-(benzo[d][1,3]dioxol-5-ylmethyl)-6-(3,3-diethoxyprop-1-yn-1-yl)pyridine-3-sulfonamide* as dark-brown oil. (+ve) APCI-MS  $m/z = 418.46$  calcd. for  $C_{20}H_{22}N_2O_6S$  [M], found 419.2 [M+H]. The product was further used directly without additional purifications.

1.11.2.24. *N-benzyl-6-(3,3-diethoxyprop-1-yn-1-yl)pyridine-3-sulfonamide (37f):*

General procedure for the Sonogashira reaction was followed by using *N-benzyl-6-chloropyridine-3-sulfonamide* (0.423 g, 1.5 mmol) yielding *N-benzyl-6-(3,3-diethoxyprop-1-yn-1-yl)pyridine-3-sulfonamide* as dark-brown oil.; (+ve) APCI-MS  $m/z = 374.45$  calcd. for  $C_{19}H_{22}N_2O_4S$  [M], found 375.2 [M+H]. The product was further used directly without additional purifications.

### 1.11.3 Synthesis of pentathiepin derivatives 7a-f, 10a-b, 14, 21a-e, 25, 28, 38a-f

General procedure: An oven-dried 25 ml Schlenk flask was charged with the alkyne precursor, 0.5 equiv. of  $(Et_4N)_2[MoO(S_4)_2]$  and 1 equiv. of elemental sulfur under inert gas atmosphere ( $N_2$ ). The mixture was dissolved in a dry polar non-protonating organic solvent (DMF or  $CH_3CN$ ) and allowed to react while stirring at 50 °C. The reaction progress was monitored by TLC. After the reaction was completed, the crude product mixture was concentrated under reduced pressure and purified through silica gel column chromatography with EtOAc/Hexane (5 to 20%) as the mobile phase.

#### *Synthesis of quinoxaline pentathiepins (7a-f)*

The compound **7a** was originally prepared by Zubair et al., in large scale.<sup>57</sup> The synthesis was not repeated.

*1.11.3.1.Synthesis of 12-ethoxy-2-methyl-[1,2,3,4,5]pentathiepino[6',7':3,4]pyrrolo[1,2-a]quinoxaline (7b):*

The spectral data of compound **7b** are in agreement with previously reported literature data.<sup>57</sup> General procedure was followed by using **6b** (0.3 g, 1.11 mmol) yielding the pentathiepin **7b** as yellow amorphous solid in 42% (0.179 g, 0.46 mmol). <sup>1</sup>H-NMR (d<sub>6</sub>-DMSO) δ: 8.87 (s, 1H), 8.44 (d, *J* = 7.6 Hz, 1 H), 7.80 (d, *J* = 7.9 Hz, 1 H), 7.47 (d, *J* = 7.8 Hz, 1 H), 4.62-4.56 (m, 2H), 2.46 (s, *J* = 7.3 Hz, 3 H), 1.50 (t, *J* = 7.1 Hz, 3 H); <sup>13</sup>C NMR (d<sub>6</sub>-DMSO) δ: 144.1 (s, 1 C), 143.1 (s, 1 C), 138.8 (s, 1 C), 136.2 (s, 1 C), 134.3 (s, 1 C), 129.8 (s, 1 C), 129.4 (s, 1 C), 125.9 (s, 1 C), 117.3 (s, 1 C), 116.4 (s, 1 C), 114.3 (s, 1 C), 51.4 (s, 1 C), 20.5 s, 1 C), 15.4 (s, 1 C).

*1.11.3.2.Synthesis of 6-methyl 10-ethoxy-pentathiepino-pyrrolo [1,2-a]quinoxaline (7c)*

The general procedure was followed by using **6c** (600 mg, 2.25 mmol) yielding 6-methyl-10-ethoxy-pentathiepino-pyrrolo [1,2-a]quinoxaline (432 mg, 1.125 mmol, 50%, mp: 246-248 °C) as a yellow solid. <sup>1</sup>H NMR (300 MHz, CDCl<sub>3</sub>) δ: 1.57 - 1.66 (m, 3 H,), 2.51 (s, 3 H,) 4.63 - 4.71 (m, 2 H, ), 7.34 (dd, *J*=8.50, 2.08 Hz, 1H,), 7.74 (s, 1 H,), 8.47 (d, *J*=8.31 Hz, 1 H,), 8.86 (s, 1 H,); <sup>13</sup>C NMR (75 MHz, CDCl<sub>3</sub>) δ: 15.5 (s,1C), 21.1 (s,1C), 73.1 (s, 1C), 113.9 (s,1C), 116.3 (s, 1C), 117.1 (s, 1C), 125.4 (s, 1C), 129.8 (s, 1C), 130 (s, 1C), 134.5 (s, 1C), 136.9 (s, 1C), 137.5 (s, 1C), 143.7 (s, 1C), 144.5 (s, 1C);(+ve) APCI-MS *m/z* = 384,58 [M<sup>+</sup>] calcd. for C<sub>14</sub>H<sub>12</sub>N<sub>2</sub>OS<sub>5</sub>, found : 385.44 [M+H]<sup>+</sup>. CHNS calcd.: C 43.72; H 3.15; N 7.28; S 41.69; found C 43.83; H 3.05; N 7.08; S 42.09.

*1.11.3.3.Synthesis of 6-methyl 10-ethoxy-3-(Trifluoromethyl)-pentathiepino-pyrrolo [1,2-a]quinoxaline (7d)*

General procedure was followed by using 2-(3, 3-diethoxyprop-1-ynyl)-6-methyl-3-(trifluoromethyl)-quinoxaline (500 mg, 1.478 mmol) yielding 6-methyl-10-ethoxy-3-(trifluoromethyl)-pentathiepino-pyrrolo [1,2-a]quinoxaline (421 mg, 0.932 mmol, 63%), mp: 305-306 °C) as a bright yellow solid. <sup>1</sup>H NMR (300 MHz, CDCl<sub>3</sub>) δ: 1.62 (m, *J*=5.96 Hz, 3H,), 2.57 (s, 3 H,), 4.60 - 4.68 (m, 2 H,), 7.89 (d, *J*=8.25 Hz, 1 H,), 8.50 - 8.64 (m, 2 H,); <sup>13</sup>C NMR (75 MHz, CDCl<sub>3</sub>) δ: 15.1 (s, 1C), 20.5 (s, 1C), 73 (s, 1C), 115.9 (s, 1C), 116.9 (s, 1C), 117.2 (s, 1C), 118.1, 119, 124.5 (t, 1C), 126.6 (s, 1C), 130.2 (s, 1C), 130.3 (s, 1C), 131.8 (s, 1C), 133.7 (s, 1C), 136.7 (s, 1C), 141.1 (s, 1C), 147 (s, 1C); <sup>19</sup>F NMR (282 MHz, CDCl<sub>3</sub>) δ: -63.3 (s, 2 F) -63.3 (s, 1 F); (+ve) APCI-MS *m/z* = 452.58 [M<sup>+</sup>] calcd. for C<sub>15</sub>H<sub>11</sub>F<sub>3</sub>N<sub>2</sub>OS<sub>5</sub>, found: 453.34 [M+H]<sup>+</sup>. CHNS calcd. C 39.81; H 2.45; N 6.19; S 35.42; found C 39.74; H 2.62; N 5.90; S 35.98.

*1.11.3.4. Synthesis of 12-ethoxy-2,3-dimethyl-[1,2,3,4,5]pentathiepino[6',7':3,4]pyrrolo[1,2-a]quinoxaline (7e)*

The spectral data of compound **7e** are in agreement with previously reported literature data.<sup>57</sup> General procedure was followed by using **6e** (0.228 g, 0.8 mmol) yielding the desired pentathiepin **7e** as fine yellow powder in 45% (0.143 g, 0.36 mmol) yield. <sup>1</sup>H NMR (300 MHz, CHLOROFORM-*d*)  $\delta$ : 1.62 (t, *J*=7.18 Hz, 3 H), 2.40 (s, 3 H), 2.45 (s, 3 H), 4.51 - 4.73 (m, 2 H), 7.70 (s, 1 H), 8.38 (s, 1 H), 8.83 (s, 1 H); <sup>13</sup>C NMR (75 MHz, CHLOROFORM-*d*)  $\delta$ : 15.5 (s, 1 C), 19.6 (s, 1 C), 20.6 (s, 1 C), 73.2 (s, 1 C), 106.6 (s, 1 C), 110.9 (s, 1 C), 117.1 (s, 1 C), 122.3 (s, 1 C), 130.2 (s, 1 C), 135.2 (s, 1 C), 135.6 (s, 1 C), 137.8 (s, 1 C), 143.6 (s, 1 C), 146.3 (s, 1 C); (+ve) APCI-MS *m/z* = 397.97 [*M*<sup>+</sup>] calcd. for C<sub>15</sub>H<sub>14</sub>N<sub>2</sub>OS<sub>5</sub>, found: 399.7 [*M*+H]<sup>+</sup>; CHNS calcd. C 45.20; H 3.54; N 7.03; S 40.22 found: C 45.12; H 3.62; N 7.90; S 39.98.

*1.11.3.5. Synthesis of 6, 7-dimethyl 10-ethoxy- 3-(trifluoromethyl)pentathiepino-pyrrolo [1,2-a]quinoxaline (7f)*

General procedure was followed by using 2-(3,3-diethoxyprop-1-ynyl)-6,7-dimethyl-3-(trifluoromethyl)quinoxaline (500 mg, 1.42 mmol) yielding 6,7-dimethyl 10-ethoxy- 3-(trifluoromethyl)pentathiepino-pyrrolo [1,2-*a*]quinoxaline (364 mg, 0.78 mmol, 55%, mp: 322-325 °C) as (micro-) crystalline yellow needles. <sup>1</sup>H NMR (300 MHz, CHLOROFORM-*d*)  $\delta$ : 1.63 (t, *J*=7.18 Hz, 4 H), 2.41 (s, 3 H), 2.48 (s, 3 H), 4.51 - 4.75 (m, 2 H), 7.79 (s, 1 H) 8.51 (s, 1 H); <sup>13</sup>C NMR (75 MHz, CHLOROFORM-*d*)  $\delta$ : 15.4 (s, 1C), 19.5 (s, 1C), 20.9 (s, 1C), 73.5 (s, 1C), 110.7 (s, 1C), 117 (s, 1C), 118.6 (s, 1C), 125.1, 126 (s, 1C), 131 (s, 2C) 132.5 (s, 1C), 136.3 (s, 1C), 140.6 (s, 1C), 157.9 (s, 1C), <sup>19</sup>F NMR (282 MHz, CHLOROFORM-*d*)  $\delta$  : - 63.3 (s, 3 F);(+ve)APCI-MS *m/z* = 466.61 [*M*<sup>+</sup>] calcd. for C<sub>16</sub>H<sub>13</sub>F<sub>3</sub>N<sub>2</sub>OS<sub>5</sub>, found: 467.16 [*M*+H]<sup>+</sup>. CHNS calcd. C 41.18; H 2.81; N 6.00; S 34.36; found: C 41.05; H 2.66; N 5.93; S 34.69.

*Synthesis of pyrazine pentathiepins (10a-b)*

*1.11.3.6.11-ethoxy-[1,2,3,4,5]pentathiepino[6',7':3,4]pyrrolo[1,2-a]pyrazine (10a)*

The spectral data of compound **10a** are in agreement with previous reports.<sup>57</sup> General procedure for pentathiepin was followed by using **9a** (1g, 4.85 mmol) yielding the desired pentathiepin **10a** (0.838 g, 2.619 mmol, 54%). <sup>1</sup>H NMR (300 MHz, CHLOROFORM-*d*)  $\delta$ : 1.44 - 1.56 (m, 3 H), 4.46 - 4.66 (m, 2 H), 7.54 - 7.66 (m, 2 H), 8.89 (d, *J*=1.13 Hz, 1 H); <sup>13</sup>C NMR (75 MHz, CHLOROFORM-*d*)  $\delta$ : 15.6 (s, 1 C), 72.2 (s, 1 C), 113 (s, 1 C), 114.9 (s, 1 C), 115.4 (s, 1 C), 123.8 (s, 1 C), 128.7 (s, 1 C), 140.8 (s, 1 C), 145.2 (s, 1 C); ); (+ve)APCI-MS *m/z* =

319.92 [M<sup>+</sup>] calcd. for C<sub>9</sub>H<sub>8</sub>N<sub>2</sub>OS<sub>5</sub>, found: 321.01 [M+H]; CHNS calcd. C 33.73, H 2.52, N 8.74, S 50.02; found: C 33.05, H 2.55, N 8.93, S 51.09.

*1.11.3.7.6,11-diethoxy-[1,2,3,4,5]pentathiepine[6',7':3,4]pyrrolo[1,2-a]pyrazine (10b)*

General procedure for pentathiepins was followed by using 2-(3,3-diethoxyprop-1-yn-1-yl)-3-ethoxypyrazine (**9b**) (500 mg, 2 mmol) yielding the desired 6,11-diethoxy-[1,2,3,4,5]pentathiepine[6',7':3,4]pyrrolo[1,2-a]pyrazine (**10b**) (228 mg, 0.62 mmol, 31%) as a yellow amorphous powder. Fine yellow needles were obtained through recrystallization with hexane and ethyl acetate (80:20). <sup>1</sup>H NMR (300 MHz, CHLOROFORM-*d*) δ: 1.47 (t, *J*=7.06 Hz, 6 H), 4.43 - 4.59 (m, 4 H), 7.14 (d, *J*=4.86 Hz, 1 H), 7.30 (d, *J*=4.86 Hz, 1 H); <sup>13</sup>C NMR (75 MHz, CHLOROFORM-*d*) δ: 14.4 (s, 1 C), 15.5 (s, 1 C), 62.5 (s, 1 C), 72.2 (s, 1 C), 108.8 (s, 1 C), 114.7 (s, 1 C), 115.4 (s, 1 C), 115.7 (s, 1 C), 126.2 (s, 1 C), 141.8 (s, 1 C), 156.2 (s, 1 C); (+ve) APCI-MS *m/z* = 364.55 calcd. for C<sub>11</sub>H<sub>12</sub>N<sub>2</sub>O<sub>2</sub>S<sub>5</sub> [M], found 365.1 [M+H]. CHNS calcd. for C<sub>11</sub>H<sub>12</sub>N<sub>2</sub>O<sub>2</sub>S<sub>5</sub>: C 36.24, H 3.32, N 7.68, S 43.98, found: C 36.41, H 3.33, N 7.72, S 43.93.

*1.11.3.8.Synthesis of 6-bromo-8-ethoxy-[1,2,3,4,5]pentathiepine[6',7':3,4]pyrrolo[1,2-a]imidazo[2,1-c]pyrazine (14)*

General procedure for pentathiepins was followed by using **13** (0.832 g, 2.56 mmol) yielding the desired pentathiepin **14** (0.25 g, 0.588 mmol, 23%) as a yellow solid. <sup>1</sup>H NMR (300 MHz, CHLOROFORM-*d*) δ: 1.54 (t, *J*=6.99 Hz, 3 H), 4.31 - 4.57 (m, 2 H), 7.25 (s, 1 H), 7.41 (s, 1 H), 7.48 (s, 1 H); <sup>13</sup>C NMR (75 MHz, CHLOROFORM-*d*) δ: 15.1 (s, 1 C), 75 (s, 1 C), 99.3 (s, 1 C), 113.7 (s, 1 C), 114.6 (s, 1 C), 115.8 (s, 1 C), 116.4 (s, 1 C), 120.1 (s, 1 C), 132.5 (s, 1 C), 135.7 (s, 1 C), 145.4 (s, 1 C); (+ve) APCI-MS = 436.85 *m/z* calcd. for C<sub>11</sub>H<sub>8</sub>BrN<sub>3</sub>OS<sub>5</sub> [M], found 437.9 *m/z* [M+H]. CHNS calcd. for C<sub>11</sub>H<sub>8</sub>BrN<sub>3</sub>OS<sub>5</sub>: C 30.14; H 1.84; N 9.58; S 36.56, found: C 29.99, H 1.73, N 9.42, S 36.63.

*Synthesis of pyridine pentathiepins (17a-b)*

*1.11.3.9.6-ethoxy-[1,2,3,4,5]pentathiepine[6,7-a]indolizine (17a)*

General procedure for pentathiepins was followed by using compound **16a** (1 g, 4.87 mmol) yielding the desired pentathiepin **17a** (0.388 g, 1.212 mmol, 25%) as a yellow crystalline solid. <sup>1</sup>H NMR (300 MHz, CHLOROFORM-*d*) δ 1.49 (t, *J*=6.99 Hz, 3 H), 4.43 - 4.60 (m, 2 H), 6.57 - 6.66 (m, 1 H), 6.81 - 6.90 (m, 1 H), 7.50 (d, *J*=9.06 Hz, 1 H), 7.75 (d, *J*=7.18 Hz, 1 H); <sup>13</sup>C NMR (75 MHz, CHLOROFORM-*d*) δ: 15.6 (s, 1 C), 22.1 (s, 1 C), 112.2 (s, 2 C), 118.4 (s, 2 C), 120.9 (s, 2 C), 121 (s, 2 C); (+ve) APCI-MS = 318.93 *m/z* calcd. for C<sub>10</sub>H<sub>9</sub>NOS<sub>5</sub> [M], found

320.1 m/z [M+H]; CHNS calcd. for C<sub>10</sub>H<sub>9</sub>NOS<sub>5</sub>: C 37.59, H 2.84, N 4.38, S 50.17; found: C 37.41, H 2.33, N 4.32, S 49.93.

*1.11.3.10. 1-(6-ethoxy-[1,2,3,4,5]pentathiepin[6,7-a]indolizin-11-yl)ethan-1-one (17b)*

General procedure for pentathiepins was followed by using compound **16b** (0.741 g, 3 mmol) yielding the desired pentathiepin **17b** (0.138 g, 0.38 mmol, 12.6 %) as bright yellow crystalline solid. <sup>1</sup>H NMR (300 MHz, CHLOROFORM-*d*) δ: 1.48 (t, *J*=7.01 Hz, 3 H), 2.62 (s, 3 H), 4.52 (qd, *J*=7.05, 3.81 Hz, 2 H), 6.64 (t, *J*=6.92 Hz, 1 H), 6.80 (dd, *J*=6.74, 1.05 Hz, 1 H), 7.82 (dd, *J*=7.06, 1.01 Hz, 1 H), <sup>13</sup>C NMR (75 MHz, CHLOROFORM-*d*) δ: 15.6 (s, 1 C), 31.5 (s, 1 C), 72.2 (s, 1 C), 110.2 (s, 1 C), 111.3 (s, 1 C), 114.2 (s, 1 C), 120 (s, 1 C), 122.6 (s, 1 C), 125.8 (s, 1 C), 133.6 (s, 1 C), 141.1 (s, 1 C), 200.6 (s, 1 C); (+ve) APCI-MS m/z = 360.94 m/z calcd. for C<sub>12</sub>H<sub>11</sub>NO<sub>2</sub>S<sub>5</sub> found: 362 [M+H]; CHNS calcd. for C<sub>12</sub>H<sub>11</sub>NO<sub>2</sub>S<sub>5</sub>: C 39.87; H 3.07; N 3.87; S 44.34; found: C 39.89, H 3.09, N 3.86, S 46.08%.

*Synthesis of nicotinamide pentathiepins (21a-e)*

*1.11.3.11. (6-ethoxy-[1,2,3,4,5]pentathiepin[6,7-a]indolizin-9-yl)(piperidin-1-yl)methanone (21a)*

General procedure for pentathiepins was followed by using compound **20a** (0.5 g, 1.58 mmol) yielding the product **21a** (0.421 g, 0.97 mmol, 62%) as a yellow amorphous solid. <sup>1</sup>H NMR (300 MHz, CHLOROFORM-*d*) δ: 0.87 (d, *J*=6.80 Hz, 2 H), 1.27 (br. s., 2 H), 1.48 (t, *J*=6.99 Hz, 3 H), 1.69 (br. s., 2 H), 3.56 (br. s., 4 H), 4.45 - 4.60 (m, 2 H), 6.80 - 6.87 (m, 1 H), 7.50 (dd, *J*=9.25, 0.94 Hz, 1 H), 7.95 (s, 1 H); <sup>13</sup>C NMR (75 MHz, CHLOROFORM-*d*) δ: 15.6 (s, 1 C), 24.4 (s, 2 C), 72.3 (s, 2 C), 74.7 (s, 1 C), 92.3 (s, 1 C), 110.9 (s, 1 C), 113.8 (s, 1 C), 118 (s, 1 C), 119.8 (s, 1 C), 121.2 (s, 1 C), 121.7 (s, 1 C), 129.6 (s, 1 C), 141.1 (s, 1 C), 167.1 (s, 1 C); (+ve) APCI-MS m/z = 430 calcd. for C<sub>16</sub>H<sub>18</sub>N<sub>2</sub>O<sub>2</sub>S<sub>5</sub> [M], found: 431.1 m/z [M+H]; CHNS calcd. for C<sub>16</sub>H<sub>18</sub>N<sub>2</sub>O<sub>2</sub>S<sub>5</sub>: C 44.63; H 4.21; N 6.51; S 37.22; found: C 44.55, H 4.09, N 6.97, S 37.66.

*1.11.3.12. (6-ethoxy-[1,2,3,4,5]pentathiepin[6,7-a]indolizin-9-yl)(morpholino)methanone (21b)*

General procedure for pentathiepins was followed by using compound **20b** (0.5 g, 1.57 mmol) yielding the desired pentathiepin **21b** (0.373 g, 0.8635 mmol, 55%) as an orange red crystalline solid. <sup>1</sup>H NMR (300 MHz, CHLOROFORM-*d*) δ: 1.49 (t, *J*=6.99 Hz, 3 H), 3.50 - 3.84 (m, 8 H), 4.47 - 4.62 (m, 2 H), 6.81 (dd, *J*=9.25, 1.32 Hz, 1 H), 7.51 (dd, *J*=9.25, 0.94 Hz, 1 H), 7.98 (t, *J*=1.32 Hz, 1 H); <sup>13</sup>C NMR (75 MHz, CHLOROFORM-*d*) δ: 15.5 (s, 1 C), 66.8 (s, 2 C), 72.3 (s, 2 C), 110.9 (s, 1 C), 113.8 (s, 1 C), 118.2 (s, 1 C), 119.3 (s, 1 C), 120.6 (s, 2 C), 121.9

(s, 1 C), 129.5 (s, 1 C), 141.1 (s, 1 C), 167.3 (s, 1 C); (+ve) APCI-MS  $m/z = 431.98$  calcd. for  $C_{15}H_{16}N_2O_3S_5$  [M], found: 433.1  $m/z$  [M+H]; CHNS calcd. for  $C_{15}H_{16}N_2O_3S_5$ : C 41.65, H 3.73, N 6.48, S 37.05; found: C 41.55, H 3.19, N 6.17, S 37.66.

1.11.3.13. *6-ethoxy-N, N-diethyl-[1,2,3,4,5]pentathiepino[6,7-a]indolizine-9-carboxamide (21c)*

General procedure for pentathiepins was followed by using compound **20c** (0.5 g, 1.643 mmol) yielding the desired product **21c** (0.316 g, 0.755 mmol, 46%) as bright yellow crystalline solid.  $^1H$  NMR (300 MHz, CHLOROFORM-*d*)  $\delta$ : 1.22 (t,  $J=7.18$  Hz, 6 H), 1.48 (t,  $J=6.99$  Hz, 3 H), 3.45 (br. s., 4 H), 4.52 (dd,  $J=7.18, 2.27$  Hz, 2 H), 6.83 (dd,  $J=9.06, 1.51$  Hz, 1 H), 7.51 (dd,  $J=9.06, 1.13$  Hz, 1 H), 7.86 - 7.92 (m, 1 H);  $^{13}C$  NMR (75 MHz, CHLOROFORM-*d*)  $\delta$ : 15.1 (s, 1 C), 71.9 (s, 1 C), 110 (s, 1 C), 113.2 (s, 1 C), 117.8 (s, 1 C), 119.1 (s, 1 C), 119.7 (s, 1 C), 122 (s, 1 C), 125.5 (s, 1 C), 129.2 (s, 1 C), 135 (s, 1 C), 135.9 (s, 1 C), 140.6 (s, 1 C), 145 (s, 1 C), 167.5 (s, 1 C); (+ve) APCI-MS  $m/z = 418.00$  calcd. for  $C_{15}H_{18}N_2O_2S_5$  [M], found: 419.1  $m/z$  [M+H]; CHNS calcd. for  $C_{15}H_{18}N_2O_2S_5$ : C 43.04, H 4.33, N 6.69, S 38.29; found: C 43.15, H 4.19, N 6.28, S 38.66.

1.11.3.14. *(6-ethoxy-[1,2,3,4,5]pentathiepino[6,7-a]indolizin-9-yl)(4-(4-fluorobenzoyl)piperazin-1-yl)methanone (21d)*

General procedure for pentathiepins was followed by using compound **20d** (0.410 g, 0.932 mmol) yielding the desired pentathiepin **21d** (0.298 g, 0.540 mmol, 57%) as yellow amorphous solid.  $^1H$  NMR (300 MHz, CHLOROFORM-*d*)  $\delta$ : 1.49 (t,  $J=6.99$  Hz, 3 H), 3.67 (br. s., 8 H), 4.55 (qd,  $J=7.05, 2.27$  Hz, 2 H), 6.78 - 6.84 (m, 1 H), 7.09 - 7.18 (m, 2 H), 7.41 - 7.48 (m, 2 H), 7.51 (dd,  $J=9.25, 0.94$  Hz, 1 H), 8.00 (t,  $J=1.32$  Hz, 1 H);  $^{13}C$  NMR (75 MHz, CHLOROFORM-*d*)  $\delta$ : 16 (s, 1 C), 72.7 (s, 5 C), 111.6 (s, 1 C), 114.3 (s, 1 C), 116.1 (s, 1 C), 116.4 (s, 1 C), 118.8 (s, 1 C), 119.5 (s, 1 C), 120.8 (s, 1 C), 122.5 (s, 1 C), 129.8 (s, 1 C), 129.9 (s, 1 C), 131.3 (s, 1 C), 141.6 (s, 1 C), 165.7 (s, 1 C), 167.6 (s, 1 C), 168.1 (s, 1 C), 170.2 (s, 1 C); (+ve) APCI-MS = 553.01  $m/z$  calcd. for  $C_{22}H_{20}FN_3O_3S_5$  [M], found: 554  $m/z$  [M+H]; CHNS calcd. for  $C_{22}H_{20}FN_3O_3S_5$ : C 47.72, H 3.64, N 7.59, S 28.95; found: C 47.55, H 3.49, N 7.28, S 27.66.

1.11.3.15. *(6-ethoxy-[1,2,3,4,5]pentathiepino[6,7-a]indolizin-9-yl)(4-tosylpiperazin-1-yl)methanone (21e)*

General procedure for pentathiepins was followed by using compound **20e** (.440 g, 0.933 mmol) yielding the desired pentathiepin **21e** (0.393 g, 0.671 mmol, 72%) as fine yellow amorphous solid.  $^1H$  NMR (300 MHz, CHLOROFORM-*d*)  $\delta$ : 1.46 (t,  $J=6.99$  Hz, 3 H) 2.46 (s,

3 H) 3.04 (br. s., 4 H) 3.72 (br. s., 4 H) 4.44 - 4.59 (m, 2 H) 6.71 (dd,  $J=9.44$ , 1.51 Hz, 1 H) 7.36 (m,  $J=7.93$  Hz, 2 H) 7.47 (dd,  $J=9.25$ , 0.94 Hz, 1 H) 7.60 - 7.67 (m, 2 H) 7.91 (t,  $J=1.13$  Hz, 1 H);  $^{13}\text{C}$  NMR (75 MHz, CHLOROFORM-*d*)  $\delta$ : 15.5 (s, 1 C), 21.5 (s, 1 C), 45.9 (s, 4 C), 72.2 (s, 1 C), 111.1 (s, 1 C), 113.8 (s, 1 C), 118.2 (s, 1 C), 119.1 (s, 1 C), 120.1 (s, 1 C), 122.2 (s, 1 C), 127.7 (s, 1 C), 129.4 (s, 2 C), 129.9 (s, 2 C), 132.2 (s, 1 C), 141.1 (s, 1 C), 144.2 (s, 1 C), 167.4 (s, 1 C); (+ve) APCI-MS = 585 m/z calcd. for  $\text{C}_{22}\text{H}_{23}\text{N}_3\text{O}_4\text{S}_6$  [M], found: 586.1 m/z [M+H]; CHNS calcd. for  $\text{C}_{22}\text{H}_{23}\text{N}_3\text{O}_4\text{S}_6$ : C 45.11, H 3.96, N 7.17, S 32.84; found: C 45.55, H 3.39, N 7.68, S 31.56.

*1.11.3.16. Synthesis of 11-ethoxy-2-(4-methoxyphenyl)-3H-[1,2,3,4,5]pentathiepino[6',7':3,4]pyrrolo[1,2-a]pyrrolo[2,3-e]pyrazine (25)*

General procedure for pentathiepins was followed by using **24** (0.355 g, 1.01 mmol) yielding the desired pentathiepin **25** (0.0845 g, 0.181 mmol, 18%) as red amorphous solid;  $^1\text{H}$  NMR (300 MHz, DMSO-*d*<sub>6</sub>)  $\delta$ : 1.44 - 1.57 (m, 3 H), 1.99 (s, 3 H), 4.56 (q,  $J=6.92$  Hz, 2 H), 6.98 - 7.09 (m, 4 H), 7.87 (d,  $J=8.69$  Hz, 1 H), 8.48 (s, 1 H), 12.59 (s, 1 H); (-ve) APCI-MS = 464.98 m/z calcd. for  $\text{C}_{18}\text{H}_{15}\text{N}_3\text{O}_2\text{S}_5$  [M], found: 464.1 m/z [M-H]; CHNS calcd. for  $\text{C}_{18}\text{H}_{15}\text{N}_3\text{O}_2\text{S}_5$ : C 46.43, H 3.25, N 9.02, S 34.43; found: C 46.55, H 3.19, N 8.98, S 35.36.

*1.11.3.17. Synthesis of quinoline pentathiepin (28)*

General procedure for pentathiepins was followed by using **27** (0.5 g, 1.96 mmol) yielding the desired pentathiepin **28** (0.37 g, 52%) as a yellow solid  $^1\text{H}$  NMR (300 MHz, CHLOROFORM-*d*)  $\delta$ : 1.53 - 1.63 (m, 3 H), 4.43 - 4.66 (m, 2 H), 7.13 (d,  $J=9.35$  Hz, 1 H), 7.36 - 7.57 (m, 3 H), 7.63 (dd,  $J=7.70$ , 1.56 Hz, 1 H), 8.74 (d,  $J=8.62$  Hz, 1 H),  $^{13}\text{C}$  NMR (75 MHz, CHLOROFORM-*d*)  $\delta$ : 15.5 (s, 1 C), 73.2 (s, 1 C), 76.6 (s, 1 C), 77.4 (s, 1 C), 113.4 (s, 1 C), 117 (s, 1 C), 117.1 (s, 1 C), 122.9 (s, 1 C), 124.9 (s, 1 C), 125.1 (s, 1 C), 128.3 (s, 1 C), 128.6 (s, 1 C), 129.6 (s, 1 C), 133.3 (s, 1 C); (+ve) APCI-MS m/z = 368.94 calcd. for  $\text{C}_{14}\text{H}_{11}\text{NOS}_5$ , found: 370,2 [M+H]; CHNS calcd. for  $\text{C}_{14}\text{H}_{11}\text{NOS}_5$ : C 45.50, H 3.00, N 3.79, S 43.38; found: C 47.09, H 3.68, N 3.48, S 42.45.

*1.11.3.18. Synthesis of 3-benzyl-12-ethoxy-3H-[1,2,3,4,5]pentathiepino[6',7':4,5]pyrrolo[2,1-i]purine (33)*

General procedure for pentathiepin formation was followed by using 9-benzyl-6-(3,3-diethoxyprop-1-yn-1-yl)-9H-purine (530 mg, 1.57 mmol) providing desired 3-benzyl-12-ethoxy-3H-[1,2,3,4,5]pentathiepino[6',7':4,5]pyrrolo[2,1-i]purine (100 mg, 0.22 mmol, 14%) as yellow-brown amorphous powder. Fine yellow needles were obtained through recrystallization with hot isopropanol.  $^1\text{H}$  NMR (300 MHz, CHLOROFORM-*d*)  $\delta$ : 1.52 (t,



$J=7.06$  Hz, 3 H), 4.62 (q,  $J=7.10$ , 2.71 Hz, 2 H), 5.42 (d,  $J=2.02$  Hz, 2 H), 7.24 - 7.29 (m, 3 H), 7.31 - 7.37 (m, 2 H), 7.88 (s, 1 H), 8.47 (s, 1 H);  $^{13}\text{C}$  NMR (75 MHz, CHLOROFORM-*d*)  $\delta$ : 15.5 (s, 1 C), 47.7 (s, 1 C), 72.4 (s, 1 C), 108 (s, 1 C), 112.9 (s, 1 C), 123.7 (s, 1 C), 125.7 (s, 1 C), 127.5 (s, 1 C), 128.4 (s, 1 C), 129 (s, 1 C), 132.5 (s, 1 C), 135.5 (s, 1 C), 136.5 (s, 1 C), 139.8 (s, 1 C), 140.7 (s, 1 C); (+ve) APCI-MS  $m/z = 450.64$  calcd. for  $\text{C}_{17}\text{H}_{14}\text{N}_4\text{OS}_5$  [M], found 451.0 [M+H]; CHNS calcd. for  $\text{C}_{17}\text{H}_{14}\text{N}_4\text{OS}_5$ : C 45.31, H 3.13, N 12.43, S 35.58; found C 44.23, H 3.09, N 11.97, S 35.66.

*Synthesis of pyridine sulfonamide pentathiepin (38a-f)*

*1.11.3.19. 6-ethoxy-9-(piperidin-1-ylsulfonyl)-[1,2,3,4,5]pentathiepino[6,7-a]indolizine (38a)*

General procedure for pentathiepin formation was followed by using 2-(3,3-diethoxyprop-1-yn-1-yl)-5-(piperidin-1-ylsulfonyl)pyridine (290 mg, 0.82 mmol) providing desired 6-ethoxy-9-(piperidin-1-ylsulfonyl)-[1,2,3,4,5]pentathiepino[6,7-a]indolizine (50 mg, 0.1 mmol, 13 %) as a yellow-orange amorphous powder. Fine yellow needles were obtained through recrystallization with hot isopropanol.  $^1\text{H}$  NMR (300 MHz, CHLOROFORM-*d*)  $\delta$ : 1.26 (s, 3 H), 1.45 - 1.55 (m, 6 H), 1.68 (q,  $J=5.59$  Hz, 5 H), 3.06 - 3.18 (m, 4 H), 6.99 (dd,  $J=9.54$ , 1.56 Hz, 1 H), 7.56 (dd,  $J=9.54$ , 0.92 Hz, 1 H), 8.25 - 8.29 (m, 1 H);  $^{13}\text{C}$  NMR (75 MHz, CHLOROFORM-*d*)  $\delta$ : 14.10 (s, 1 C) 15.56 (s, 1 C) 23.46 (s, 1 C) 25.23 (s, 1 C) 29.68 (s, 1 C) 46.87 (s, 1 C) 72.41 (s, 1 C) 112.29 (s, 1 C) 114.34 (s, 1 C) 117.32 (s, 1 C) 118.98 (s, 1 C) 123.44 (s, 1 C) 123.66 (s, 1 C) 128.41 (s, 1 C) 128.57 (s, 1 C) 129.18 (s, 1 C) 132.18 (s, 1 C) 132.32 (s, 1 C) 141.51 (s, 1 C); (+ve) APCI-MS  $m/z = 466.7$  calcd. for  $\text{C}_{15}\text{H}_{18}\text{N}_2\text{O}_3\text{S}_6$  [M], found 467.2 [M+H]. CHNS calcd. for  $\text{C}_{15}\text{H}_{18}\text{N}_2\text{O}_3\text{S}_6$ : C 38.61, H 3.89, N 6.00, S 41.22; found: C 38.95, H 3.85, N 5.68, S 41.46.

*1.11.3.20. 4-((6-ethoxy-[1,2,3,4,5]pentathiepino[6,7-a]indolizin-9-yl)sulfonyl)morpholine (38b)*

General procedure for pentathiepin formation was followed by using 4-((6-(3,3-diethoxyprop-1-yn-1-yl)pyridin-3-yl)sulfonyl)morpholine (354 mg, 1 mmol) providing desired 4-((6-ethoxy-[1,2,3,4,5]pentathiepino[6,7-a]indolizin-9-yl)sulfonyl)morpholine (164 mg, 0.35 mmol, 35%) as a yellow-brown amorphous powder.  $^1\text{H}$  NMR (300 MHz, CHLOROFORM-*d*)  $\delta$ : 1.47 - 1.61 (m, 3 H), 3.05 - 3.22 (m, 4 H), 3.72 - 3.84 (m, 4 H), 4.62 (dd,  $J=7.01$ , 1.42 Hz, 2 H), 6.97 (dd,  $J=9.49$ , 1.60 Hz, 1 H), 7.59 (dd,  $J=9.49$ , 0.96 Hz, 1 H), 8.23 - 8.32 (m, 1 H);  $^{13}\text{C}$  NMR (75 MHz, CHLOROFORM-*d*)  $\delta$ : 15.6 (s, 1 C), 45.91 (s, 2 C), 66.11 (s, 2 C), 72.39 (s, 1 C), 112.76 (s, 1 C), 114.48 (s, 1 C), 116.91 (s, 1 C), 119.27 (s, 1 C), 122.58 (s, 1 C), 123.89 (s, 1 C), 129.03

(s, 1 C), 141.53 (s, 1 C); (+ve) APCI-MS  $m/z = 468.68$  calcd. for  $C_{14}H_{16}N_2O_4S_6$  [M], found 469.2 [M+H]. CHNS calcd. for  $C_{14}H_{16}N_2O_4S_6$ : C 35.88, H 3.44, N 5.98, S 41.05; found C 35.75, H 3.52, N 5.89, S 41.48.

*1.11.3.21. 6-ethoxy-N-[(2S)3-methylbutan-2-yl]-[1,2,3,4,5]pentathiepino[6,7-a]indolizine-9-sulfonamide (38c)*

General procedure for pentathiepin formation was followed by using (R)-6-(3,3-diethoxyprop-1-yn-1-yl)-N-(3-methylbutan-2-yl)pyridine-3-sulfonamide (650 mg, 1.85 mmol) providing desired (R)-6-ethoxy-N-(3-methylbutan-2-yl)[1,2,3,4,5]pentathiepino-[6,7-a]indolizine-9-sulfonamide (200 mg, 0.42 mmol, 23%) as a bright yellow amorphous powder.  $^1H$  NMR (300 MHz, CHLOROFORM-*d*)  $\delta$ : 0.81 - 0.93 (m, 6 H), 1.06 (dd,  $J=7.84, 6.74$  Hz, 3 H), 1.51 (t,  $J=7.02$  Hz, 3 H), 1.63 - 1.78 (m, 1 H), 3.22 (dddd,  $J=8.70, 6.82, 5.07, 1.60$  Hz, 1 H), 4.42 - 4.52 (m, 1 H), 4.54 - 4.68 (m, 2 H), 6.98 - 7.11 (m, 1 H), 7.56 (dd,  $J=9.54, 0.92$  Hz, 1 H), 8.32 - 8.43 (m, 1 H);  $^{13}C$  NMR (75 MHz, CHLOROFORM-*d*)  $\delta$ : 15.5 (s, 1 C), 18 (s, 1 C), 18.2 (s, 1 C), 18.4 (s, 1 C), 30.9 (s, 1 C), 33.4 (s, 1 C), 55.3 (s, 1 C), 72.3 (s, 1 C), 72.4 (s, 1 C), 116.8 (s, 1 C), 119.3 (s, 1 C), 123.2 (s, 1 C), 127.2 (s, 1 C), 129 (s, 1 C), 141.7 (s, 1 C) (+ve) APCI-MS  $m/z = 468.72$  calcd. for  $C_{15}H_{20}N_2O_3S_6$ [M], found 469.6 [M+H]. CHNS calcd. for  $C_{15}H_{20}N_2O_3S_6$ : C 38.44, H 4.30, N 5.98, S 41.05; found C 38.2, H 4.24, N 5.83, S 42.82.

*1.11.3.22. N-((3s,5s,7s)-adamantan-1-yl)-6-ethoxy-[1,2,3,4,5]pentathiepino[6,7-a]indolizine-9-sulfonamide (38d)*

General procedure for pentathiepin formation was followed by using N-((3s,5s,7s)-adamantan-1-yl)-6-(3,3-diethoxyprop-1-yn-1-yl)pyridine-3-sulfonamide (418 mg, 1 mmol) providing desired N-((3s,5s,7s)-adamantan-1-yl)-6-ethoxy-[1,2,3,4,5]pentathiepino[6,7-a]indolizine-9-sulfonamide (390 mg, 0.73 mmol, 73 %) as a bright yellow amorphous powder. Yellow needles were obtained through recrystallization with hexane and ethyl acetate (80:20).  $^1H$  NMR (300 MHz, CHLOROFORM-*d*)  $\delta$ : 0.89 (s, 2 H), 1.38 - 1.71 (m, 8 H), 1.85 (d,  $J=3.21$  Hz, 3 H), 2.00 - 2.10 (m, 3 H), 2.17 (s, 3 H), 4.48 - 4.65 (m, 2 H), 7.07 (dd,  $J=9.54, 1.65$  Hz, 1 H), 7.55 (dd,  $J=9.54, 0.92$  Hz, 2 H), 8.37 (dd,  $J=1.65, 1.01$  Hz, 1 H);  $^{13}C$  NMR (75 MHz, CHLOROFORM-*d*)  $\delta$ : 15.1 (s, 3 C), 29 (s, 3 C), 35.3 (s, 2 C), 42.7 (s, 3 C), 55.3 (s, 2 C), 72 (s, 2 C), 116.9 (s, 1 C), 118.6 (s, 1 C), 122.3 (s, 1 C), 128.6 (s, 1 C), 129.6 (s, 1 C); (+ve) APCI-MS  $m/z = 532.81$  calcd. for  $C_{20}H_{24}N_2O_3S_6$  [M], found 533.1 [M+H]. CHNS calcd. for  $C_{20}H_{24}N_2O_3S_6$ : C 45.08, H 4.54, N 5.26, S 36.11, found C 44.96, H 4.09, N 4.79, S 35.83.

1.11.3.23. *N*-(benzo[d][1,3]dioxol-5-ylmethyl)-6-ethoxy-[1,2,3,4,5]pentathiepino[6,7-a]indolizine-9-sulfonamide (**38e**)

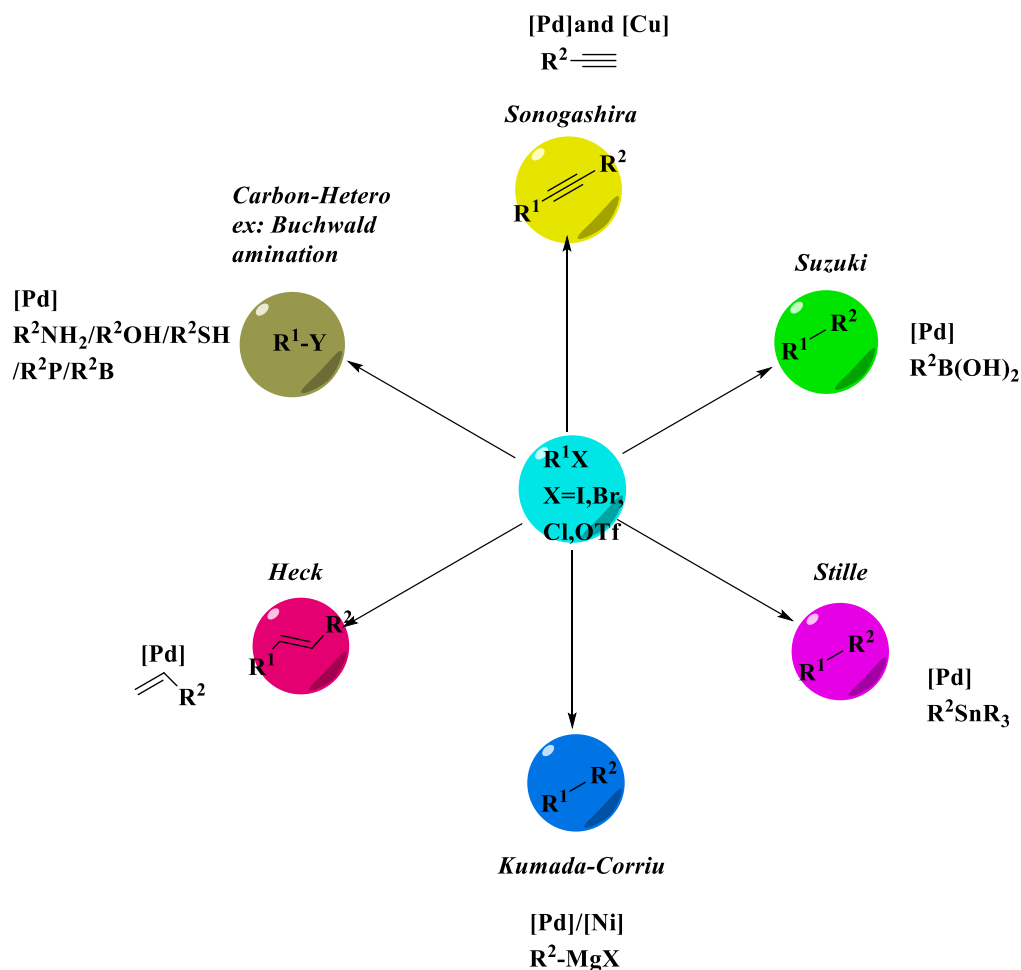
General procedure for pentathiepin formation was followed by using *N*-(benzo[d][1,3]dioxol-5-ylmethyl)-6-(3,3-diethoxyprop-1-yn-1-yl)pyridine-3-sulfonamide (520 mg, 1.2 mmol) providing desired *N*-(benzo[d][1,3]dioxol-5-ylmethyl)-6-ethoxy-[1,2,3,4,5]pentathiepino[6,7-a]indolizine-9-sulfonamide (246 mg, 0.46 mmol, 39%) as a yellow solid. Yellow platelets were obtained through recrystallization with methanol and chloroform (50:50). <sup>1</sup>H NMR (300 MHz, CHLOROFORM-*d*) δ: 1.51 (t, *J*=7.02 Hz, 3 H), 4.11 (d, *J*=5.87 Hz, 2 H), 4.50 - 4.68 (m, 2 H), 4.97 (t, *J*=5.91 Hz, 1 H), 5.88 (dd, *J*=6.14, 1.38 Hz, 2 H), 6.63 - 6.74 (m, 3 H), 7.00 (dd, *J*=9.54, 1.65 Hz, 1 H), 7.53 (dd, *J*=9.54, 1.01 Hz, 1 H), 8.20 - 8.28 (m, 1 H); <sup>13</sup>C NMR (75 MHz, CHLOROFORM-*d*) δ: 15.5 (s, 2 C), 47.25 (s, 1 C), 72.30 (s, 1 C), 101.26 (s, 1 C), 108.14 (s, 1 C), 108.37 (s, 1 C), 114.20 (s, 1 C), 116.55 (s, 1 C), 119.30 (s, 1 C), 121.60 (s, 1 C), 123.70 (s, 1 C), 126.23 (s, 1 C), 128.91 (s, 1 C), 129.12 (s, 1 C), 141.63 (s, 1 C), 147.40 (s, 1 C), 147.93 (s, 1 C); (+ve) APCI-MS *m/z* = 532.72 calcd. for C<sub>18</sub>H<sub>16</sub>N<sub>2</sub>O<sub>5</sub>S<sub>6</sub> [M], found 533,7 [M+H]. CHNS calcd. for C<sub>18</sub>H<sub>16</sub>N<sub>2</sub>O<sub>5</sub>S<sub>6</sub>: C 40.58, H 3.03, N 5.26, S 36.11, found C 39.02, H 2.88, N 5.28, S 35.96.

1.11.3.24. *N*-benzyl-6-ethoxy-[1,2,3,4,5]pentathiepino[6,7-a]indolizine-9-sulfonamide (**38f**)

General procedure for pentathiepin formation was followed by using *N*-benzyl-6-(3,3-diethoxyprop-1-yn-1-yl)pyridine-3-sulfonamide (140 mg, 0.375 mmol) providing desired *N*-benzyl-6-ethoxy-[1,2,3,4,5]pentathiepino[6,7-a]indolizine-9-sulfonamide (120 mg, 0.25 mmol, 65%) as a yellow amorphous powder. Fine yellow platelets were obtained through recrystallization with methanol and chloroform (50:50). <sup>1</sup>H NMR (300 MHz, CHLOROFORM-*d*) δ: 1.51 (t, *J*=7.06 Hz, 3 H), 4.21 (d, *J*=6.05 Hz, 2 H), 4.59 (qd, *J*=7.05, 1.79 Hz, 2 H), 4.84 (t, *J*=6.01 Hz, 1 H), 7.01 (dd, *J*=9.49, 1.60 Hz, 1 H) 7.19 - 7.27 (m, 5 H), 7.54 (dd, *J*=9.54, 0.92 Hz, 1 H), 8.28 (dd, *J*=1.56, 1.01 Hz, 1 H); <sup>13</sup>C NMR (75 MHz, CHLOROFORM-*d*) δ: 15.5 (s, 2 C), 47.3 (s, 2 C), 72.4 (s, 1 C), 116.5 (s, 1 C), 119.4 (s, 1 C), 123.8 (s, 1 C), 126.1 (s, 1 C), 127.9 (s, 1 C), 128.1 (s, 1 C), 128.7 (s, 2 C), 129 (s, 2 C), 135.5 (s, 1 C), 141.7 (s, 1 C); (+ve) APCI-MS *m/z* = 488.71 calcd. for C<sub>17</sub>H<sub>16</sub>N<sub>2</sub>O<sub>3</sub>S<sub>6</sub> [M], found 489.3 [M+H]. CHNS calcd. for C<sub>17</sub>H<sub>16</sub>N<sub>2</sub>O<sub>3</sub>S<sub>6</sub>: C 41.78, H 3.30, N 5.73, S 39.37, found: C 41.88, H, 3.34, N 5.69, S 39.55.



## Chapter 2: Pd-catalyzed cross-coupling reactions in the synthesis of biologically relevant organic molecules – State of the art

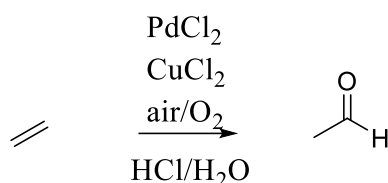


### 2.1. Background: Pd-catalyzed cross-coupling reactions

Transition metal catalyzed cross-coupling reactions and related processes comprise a dominant tool kit in modern organic synthesis and seized the highest ranking in academic and industrial research. The concept of cross-coupling was established as an advanced technology, the roots of which were set by the pioneering work of several scientists long ago. The assembly of appropriate *sp*, *sp*<sup>2</sup> and *sp*<sup>3</sup> centers to new functional C–C bonds through metal catalysis has been developed and applied for at least the last 150 years. The field started with the stoichiometric scale employment of transition metal compounds in C–C homo-coupling reactions.<sup>146</sup> Copper and alkaline earth metal-mediated cross-coupling reactions were the most popular initial discoveries. In the second half of the 20<sup>th</sup> century, transition metals (Cu, Ni, Zn, Pd) as catalysts took the most prominent place in the construction of new C–C bonds between

suitably functionalized substrates.<sup>147-149</sup> Although the unique activation profile of all transition metals is advantageous in the C–C bond formation, palladium has been outstanding in catalytic performance even at low concentrations. For example, palladium chloride (PdCl<sub>2</sub>) was successfully employed in the oxidation of ethylene to acetaldehyde in air, which is the industrially relevant Wacker's process (Scheme 2.1).<sup>150</sup> Later, Hafner developed the first Pd  $\pi$ -allyl complex<sup>151</sup> and subsequently Tsuji in 1965 demonstrated the reactions between carbon nucleophiles and Pd  $\pi$ -allyl complexes.<sup>152-153</sup> Palladium catalysis has been employed frequently in accessing complex biologically relevant organic molecules, which otherwise either involved multi-step organic synthesis or were impossible to synthesize. The cross-coupling strategy and the dominant role of palladium revolutionized the approaches in synthetic organic chemistry and widened applications in material science, polymer chemistry, agrochemicals, fine chemicals, and pharmaceutical research.<sup>154-158</sup>

These extended applications of Pd-catalysis in generating new C–C single bonds resulted in the Nobel Prize in 2010 being awarded to Richard F. Heck, Ei-ichi Negishi<sup>159</sup> and Akira Suzuki<sup>160</sup> for developing the respective reactions named after them. However, it is worth mentioning the dedicated contributions of Kumada, Kochi, Corriu and Murahasi, with which they introduced a range of organometallic reagents, such as organotin, organosilicon, organoboron, and organozinc being efficient in cross-coupling reactions.



**Scheme 2.1:** Wacker's Process 1959.

Palladium cross-coupling chemistry inspired many researchers and motivated them to introduce new variations to it, e.g. cross-coupling for carbon-heteroatom bond formation, decarboxylative coupling,  $\alpha$ -arylation, direct activation of C–H bonds. In figure 2.1, the trends in publication numbers and patent applications in the last decades are visualized. Furthermore, efforts in this research are continuing further with an ever accelerated pace. In academia and industry, the Suzuki-Miyaura cross-coupling gained the highest popularity, followed by the Heck and Sonogashira coupling reactions.

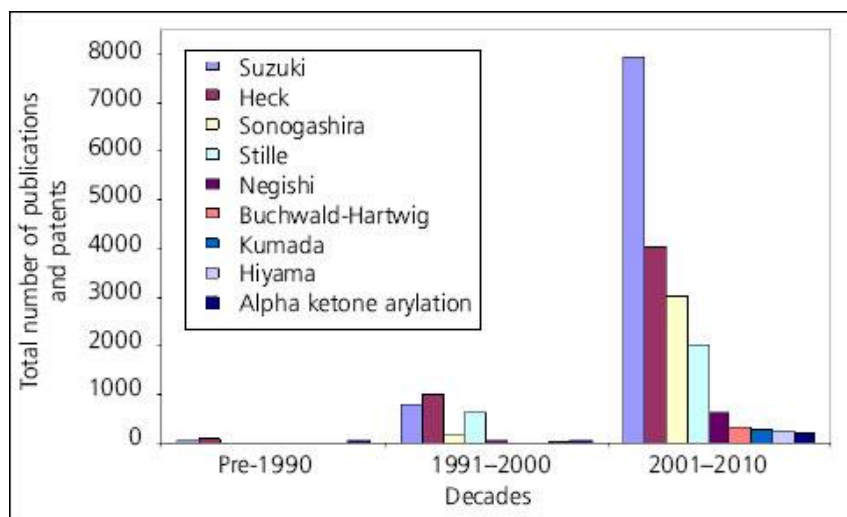


Figure 2.1: Total number of publications in transition metal catalysis over the last decades.<sup>161</sup>

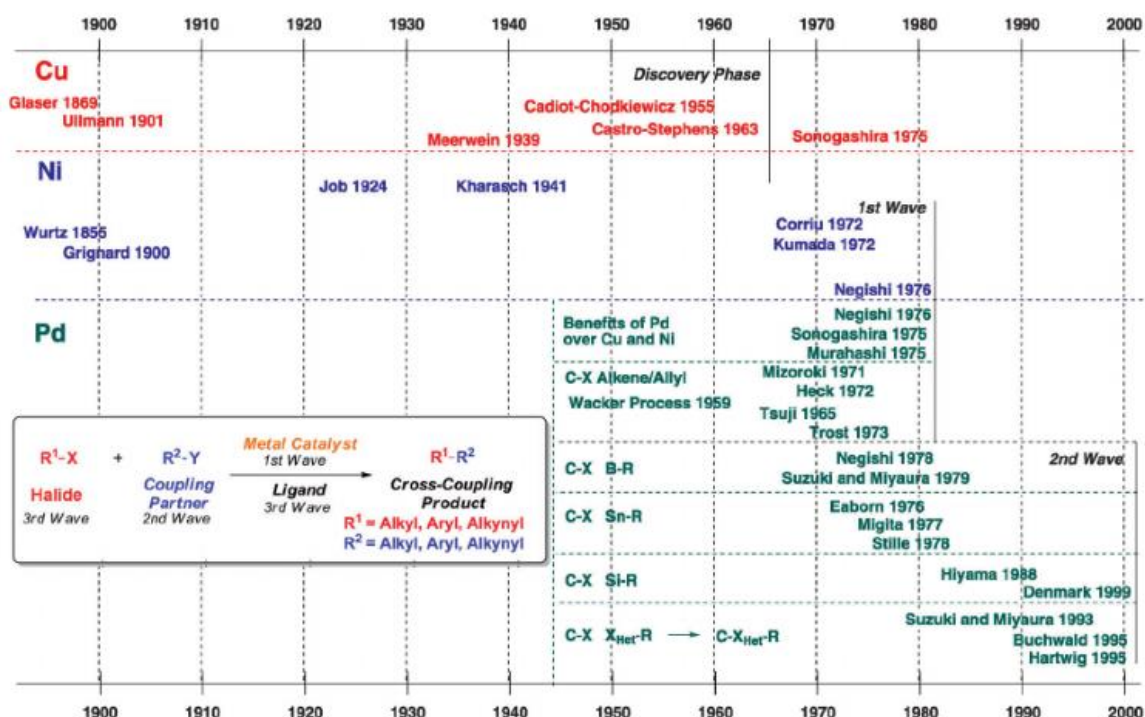
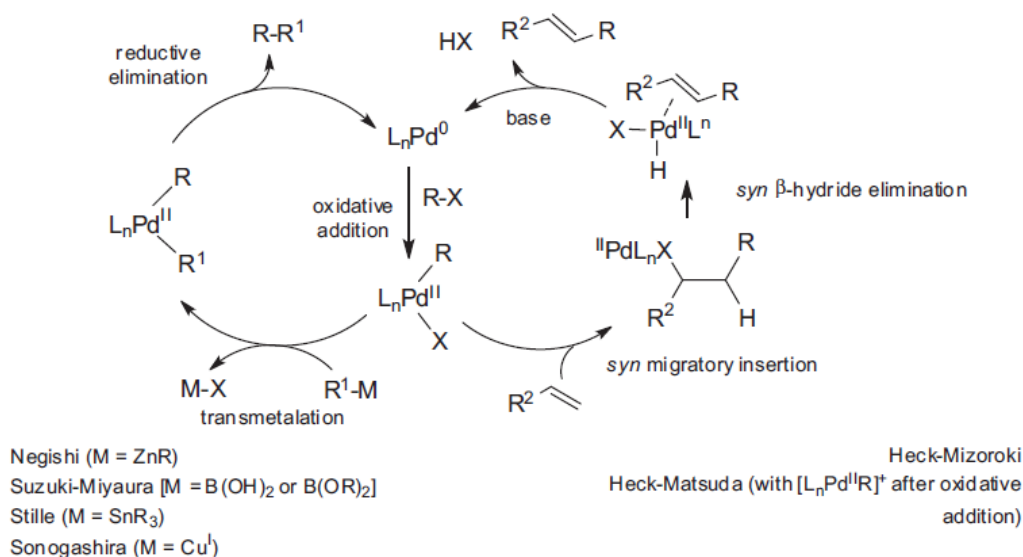


Figure 2.2: Inventions in various named reactions involving transition metals.<sup>161</sup>

The progress of the discovery of transition metal catalyzed cross coupling chemistry can be divided mainly into three phases or three waves as are: 1<sup>st</sup> phase – the identification and investigation of various metal catalysts, facilitating the desired C–C bond formations selectively. During this the addition of Cu, Ni and Pd to the arsenal of catalysis was encouraging. 2<sup>nd</sup> phase -the research was mainly focused on developing the coupling partner's capacity or functionalization of substrates. 3<sup>rd</sup> phase - continuation of an ongoing trend in the incorporation of new active ligand systems with optimized reaction conditions to increase the

applicability over a broader range of substrate scope. Figure 2.2 is depicting the development of various named reactions along the time axis; it gives a taste of a broad spectrum of the scientific thought process of researchers in transition metal catalysis.<sup>161</sup>

## 2.2. General mechanism for palladium catalysed cross-coupling reactions



**Scheme 2.2:** General Pd-mediated cross-coupling mechanistic representation.<sup>162</sup>

In general, the reaction mechanism of cross-coupling chemistry proceeds through the oxidative addition, trans-metalation and reductive elimination steps. The catalytic performance depends on the metal catalyst and electrophilic coupling partner as well as the reaction conditions. The Pd(II) complexes are chosen as a stable source of palladium, which is reduced *in situ* to catalytically active Pd(0) species. The preformed or *in situ* derived Pd(0) initiates the catalytic cycle with the oxidative addition step between C(sp<sup>2</sup>) hybridized aryl halides (pseudo halides) and forms a Pd(II) intermediate R-Pd(II)-X. The strength of carbon and halogen (pseudo halogen) bonds determines the rate of the reaction, while the oxidative addition step is considered as the rate-limiting step in the catalytic cycle. The bond strength of C–Y (where, Y= halogen) is in the order of I>OTf>Br>>Cl.<sup>147</sup> Organoborane, organozinc and organotin metal reagents participate in the trans-metalation steps in Suzuki, Negishi and Stille cross couplings, respectively. The new C–C cross-coupled product is then derived from reductive elimination and the active Pd(0) species regenerated. Scheme 2.2 represents the general mechanistic cycle.

In the Sonogashira reaction, an aryl halide reacts with an alkyne substrate in the presence of copper as co-catalyst. The *in situ* formed copper acetylide derivative undergoes the trans-



metalation step. In Heck-Mizoroki reactions, alkenes react via different catalytic intermediates in the mechanistic cycle, while the activated intermediate complex R-Pd(II)-X undergoes *syn*-migratory insertion into the double bond followed by *syn*- $\beta$ -hydride elimination in the presence of base resulting in the Pd(0) catalyst regeneration and the cross-coupled alkene derivative.<sup>162-</sup>

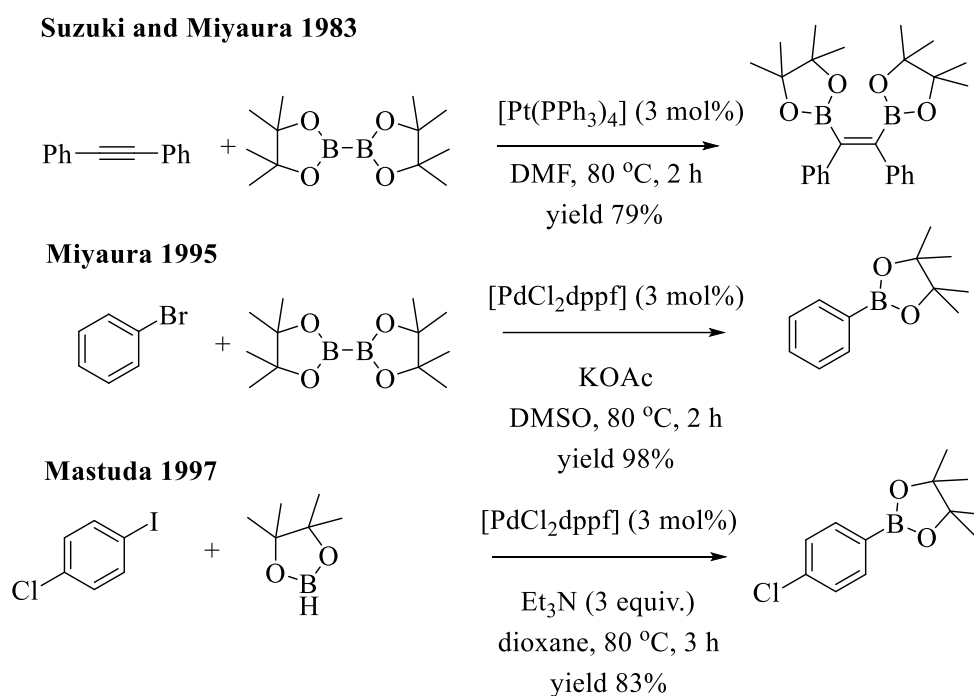
<sup>163</sup> The small mechanistic differentiation can be seen in the case of Heck-Matsuda reactions where aryl-diazonium salts were used instead of aryl halides and oxidative addition on this substrate leads to the highly reactive cationic [R-Pd]<sup>+</sup> intermediate.<sup>164-166</sup>

Certain aspects in these catalytic cycles are still unclear. For example, the precise role of the base in Suzuki-Miyaura cross-couplings, or the regioselective influences of surrounding ligand systems of central metal catalyst<sup>167</sup> required elucidation. There is a significant influence of the metal electrons on the catalytic activity. Fully understanding this concept affords eventually the development of more efficient catalysts. For this, the investigation of a more extensive variety of potent  $\sigma$ -donating ligands coordinating the central metal to allow for low catalytic loadings and milder reaction conditions is one of the keys. Such new useful ligands played a vital role in the discovery of new hetero-nuclear cross-coupling protocols (e.g. C–N, C–O, C–S, C–B, and C–P), which became an advanced tool kit for synthetic organic chemists and are important for the natural product research community. The mechanistic cycle of these carbon-heteroatom cross-coupling reactions is similar to that of previously discussed C–C bond formation process, except for the trans-metalation step; this is replaced by nucleophile coordination on the central metal.

### **2.3. Pd-catalyzed carbon-heteroatom cross-coupling reactions - mechanisms**

In nature, biologically active compounds are composed of complex organic C–C backbones along with a high ubiquity of heteroatoms such as nitrogen, oxygen, sulfur, and phosphorus. Also, derivatization of the biological activity occurs mostly at heteroatom sites where they appear as carbon-heteroatom linkages. For instance, in active pharmaceutical ingredients or conductive polymers, the C–N bond is very common, and in many natural products amine, amides, ethers, esters, thiol, thioesters, ketones, sulfonyl derivatives are essential functional moieties. In heterocyclic chemistry, C–N, C–O, C–S and C–P linkages are predominant and have been shown importance in various chemical compositions. Furthermore, conversion of synthetic intermediates often consists of C–B (or C–Si) bonds being transformed to C–C, C–N, C–O, C–S and C–P bonds.

In the classical C–C cross-coupling chemistry, so far, most often stoichiometric quantities of organometallic coupling partners are employed with the only exception being the Mizoroki-Heck reaction. At the beginning, the functionalization of organic substrates with non-carbon containing nucleophiles was a challenging task. However, in 1990, a new dimension of Pd catalysis was revealed which is efficient in catalyzing C-heteroatom coupling. Although the application of organometalloids hexamethyldisilane<sup>168</sup> and hexamethyldistannes<sup>169</sup> as coupling partners was known, at the time reports on bimetallic B–B boron compounds were very rare.



**Scheme 2.3:** C–B coupling reactions.

In 1993, Miyaura and Suzuki reported the activation of the triple bond with Pt catalyst and diborane derivative substrates (e.g. B<sub>2</sub>(pin)<sub>2</sub>) to form corresponding addition products. In the continuous development of the process, Miyaura applied such diborane species as coupling partners with aryl halides and Pd(II) catalytic systems for preparing aryl boronic acids (Scheme 2.3).<sup>171</sup> Strong bases (e.g. KOAc) would control product stability by inhibiting the competitive decomposition of formed boronic acid species from Suzuki-Miyaura coupling. In 1997, Mastuda introduced a milder version of this reaction by using reactive coupling partner HB(pin)/triethylamine to form C–B bonds; This protocol reduced not only waste generation but also established a platform for the evolution of new carbon-heteroatom (boron) cross-coupling chemistry.<sup>172</sup>

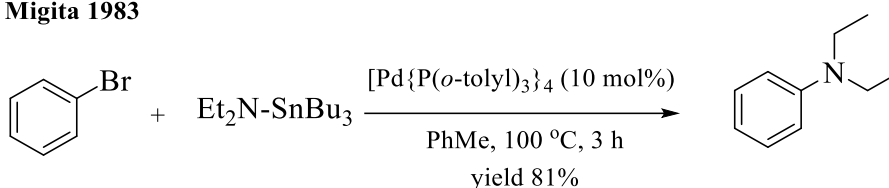
In general, amine, phenolates and thiolates are good nucleophiles to undergo a variety of organic reactions without any catalyst. However, these nucleophiles are unreactive with weak electrophiles like aryl halides and also do not react with electron-rich alkenes. Thus, expanding the expertise in conducting catalytic experiments in carbon-heteroatom coupling chemistry would extensively increase the discovery of new functional molecules.

### 2.3.1. Palladium catalyzed C–N bond formation

The palladium-catalyzed coupling of aryl halides (pseudo-halides) and amine nucleophiles is very well established and practiced synthetic methodology of recent days in both academia and industry. The critical functional nature and ubiquity of aryl amines in pharmaceuticals, natural products, organic materials, and ligands of catalysts inspired chemists to advance research into the innovation of reliable and general protocols.<sup>155, 157, 173</sup> Moreover, continuous progress in ligand design and pre-catalyst improvement steered the research in application chemistry.<sup>170, 174-176</sup>

The initiation of C–N cross-coupling procedures was provided by Ullmann and Goldberg, over a hundred years ago.<sup>177</sup> Subsequently, again in 1983, Migita and co-workers have demonstrated the C–N cross-coupling with aryl halides, albeit, in both cases, stoichiometric quantities of coupling partners were adopted. Ullmann and Goldberg applied the copper salts of amine nucleophiles, and Migita employed very high moisture sensitive tributyltinamides (Scheme 2.4) under very harsh conditions. These invented protocols come with high costs, toxicity, high waste production. Thus, the inefficiency of the processes prompted researchers to develop milder conditions and use amines as direct nucleophiles.

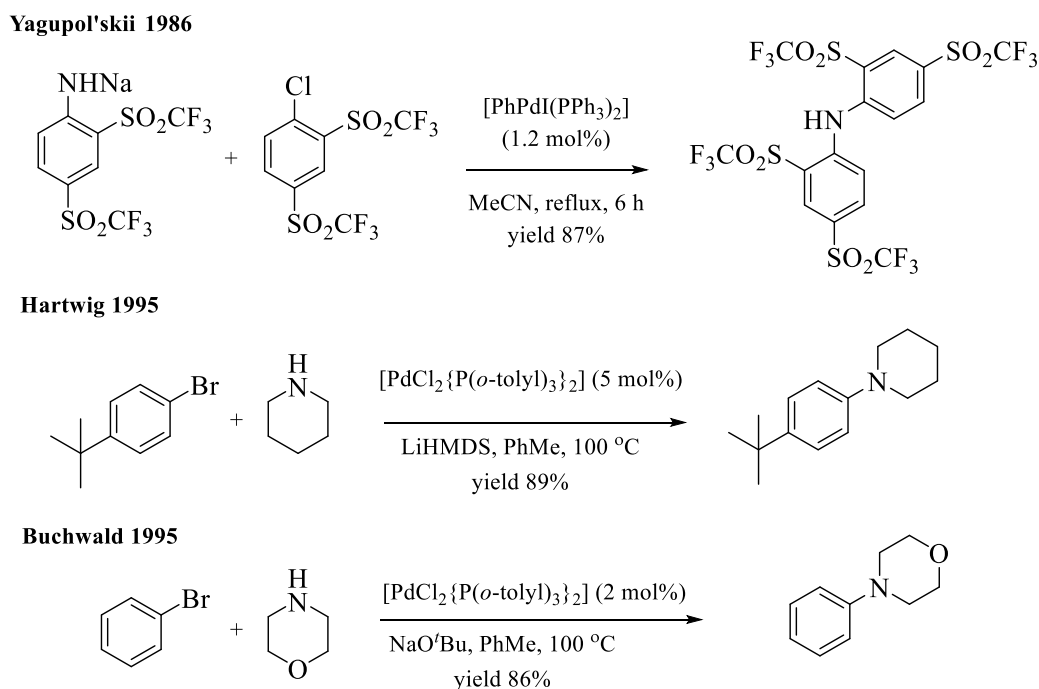
**Migita 1983**



**Scheme 2.4:** Migita amination: employment of tributylstannylamides.

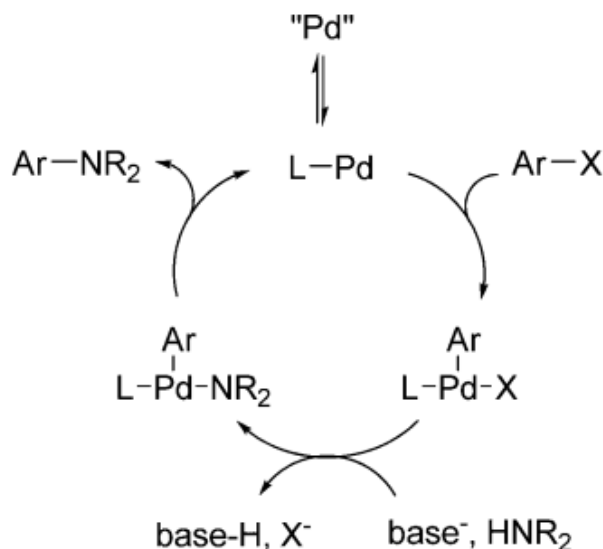
Yagupol'skii reported for the first time the usage of free amines as a nucleophile in Pd-catalysed cross-coupling with aryl halides (Scheme 2.5).<sup>178</sup> However, this study was largely neglected for the lack of experimental evidence in support of Pd-catalysis and no valid rationale to exclude the possibility of  $S_NAr$ -type of reactions. In the process of continuous development, in 1995 Buchwald<sup>179</sup> and Hartwig<sup>180</sup> individually came up with a mild alternative to Migita coupling by using free amines (R-NH<sub>2</sub>) and performing the coupling in high efficiency with

Cu or Pd-catalysts and diamines or phosphine ligands in presence of strong bases like NaO<sup>t</sup>Bu, or LiHMDS (1,1,1,3,3,3-hexamethyldisilazane) (Scheme 2.5).<sup>181</sup>



**Scheme 2.5:** Buchwald-Hartwig Pd catalysed C-N cross-coupling reactions.

Scheme 2.6 depicts the simplified catalytic cycle that explains the major findings in the Buchwald amination process. The initial Pd(0) pre-catalyst oxidative addition with the aryl halide electrophile is common in all Pd-catalyzed coupling mechanisms. The subsequent amine nucleophile coordination with the Pd-intermediate and deprotonation by the base is followed by reductive elimination resulting in the targeted amination product and regenerate the palladium catalyst.<sup>182</sup> Electron-rich monophosphine Buchwald family ligands were most widely used for this type of conversions. The nucleophilicity or relative pK<sub>a</sub> value of amine coupling partners determines the strength of the base employed. However, it is yet unclear whether base coordination to metal center is first or whether proton abstraction of base from amine occurs first.



**Scheme 2.6:** Buchwald-Hartwig amination mechanistic cycle.<sup>182</sup>

The evolution of different families of coordinating ligands like phosphines, *N*-coordinating ligands, NHC (N-heterocyclic carbenes) furthered innovation in Pd-catalyzed *N*-arylation chemistry. Among all, phosphine ligands containing alkyl or aryl substituents or both as functionalities have demonstrated high efficacy and selectivity in C–N cross-couplings.<sup>183-184</sup> Bulky electron-rich phosphines 2,2'-bis(diphenylphosphino)-1,1'-binaphthyl (BINAP) and 4,5-Bis(diphenylphosphino)-9,9-dimethylxanthene (Xanthphos)<sup>185-186</sup> have been used rather frequently in C–N cross-coupling chemistry. Also, bidentate ligands such as Bis[(2-diphenylphosphino)phenyl] ether (DPEPhos), 1,1'-Bis(diphenylphosphino)ferrocene (dppf)<sup>184, 187</sup> and (R)-1-[(SP)-2-(Dicyclohexylphosphino)ferrocenyl]ethyldi-tert-butylphosphine (CyPf-t-Bu)<sup>181</sup> have exhibited high efficiency in Pd-catalyzed *N*-arylation. Occasionally, in C–N cross-coupling the employment of 5-(Di-tert-butylphosphino)-1', 3', 5'-triphenyl-1'H-[1,4']bipyrazole (BippyPhos)<sup>188</sup> and MorDalPhos<sup>189</sup> and NHC<sup>190</sup> is reported. Figure 2.3 depicts examples for commonly applied ligands in amination protocols.

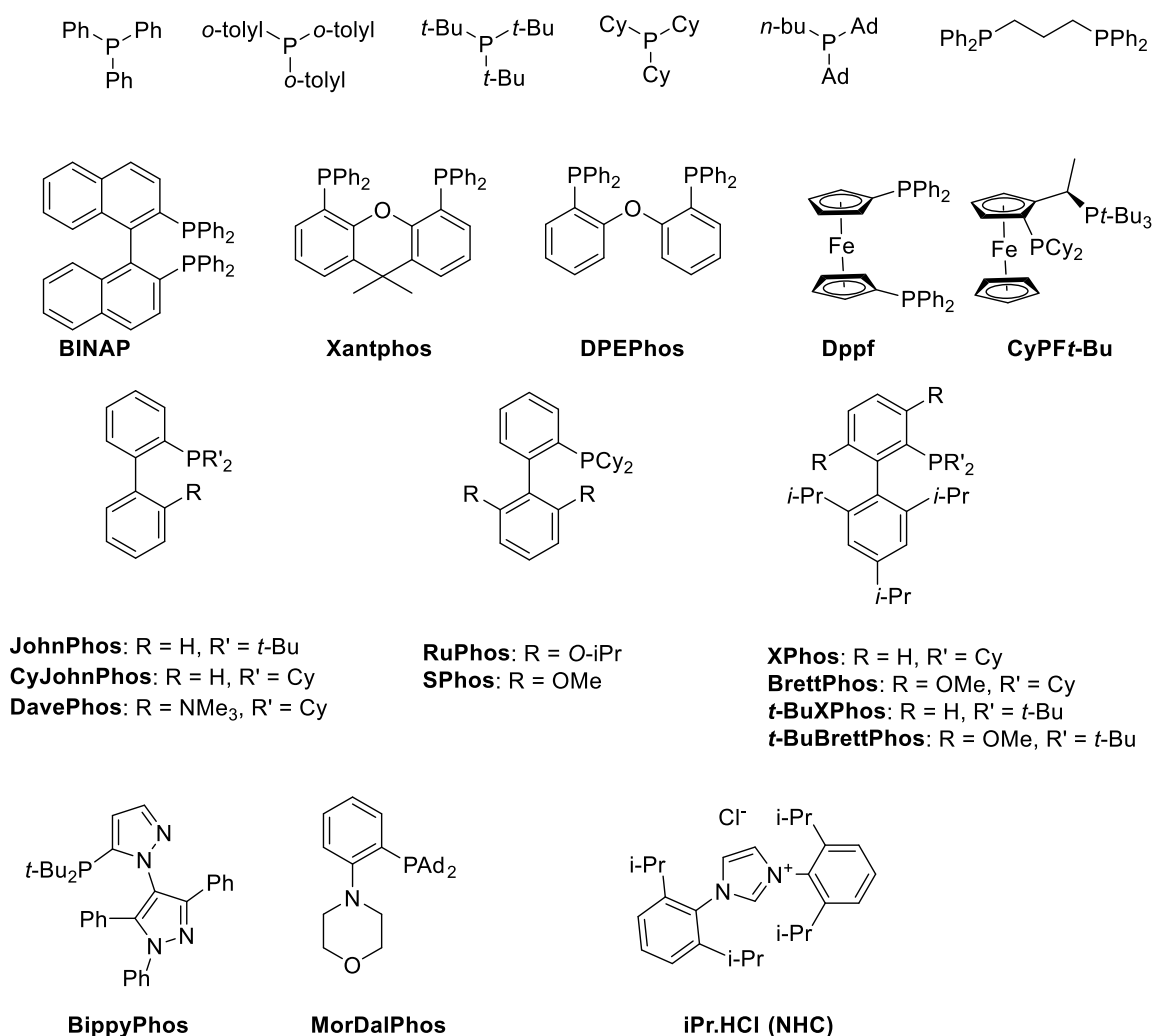


**Figure 2.3:** Examples of supporting ligands.

Similarly, introducing the concept of pre-catalytic systems which *in situ* rapidly convert into active catalyst species has shown a significant effect on the development of C–N coupling.<sup>191-192</sup> Researchers developed and applied palladium/ligand complexes bearing phosphines or NHC<sup>193-194</sup> and also various palladocycles,<sup>195-196</sup> pyridine ligated complexes,<sup>197</sup> alkenes  $\pi$ -allyl complexes in normal reaction conditions.<sup>198-199</sup> Figure 2.4 depicts few examples for Pd/pre-catalysts employed in amination reactions. These pre-catalysts significantly minimized the catalytic loadings and also facilitated the C–N cross coupling reactions at room temperature.

**Pre-catalysts**

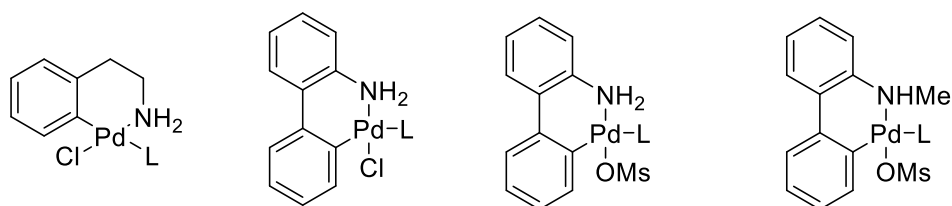


**Figure 2.4:** Palladium pre-catalysts employed in C–N cross coupling.

The application of palladium catalyzed C–N cross-coupling chemistry is rapidly growing, and the arylamines prepared by Buchwald-Hartwig amination are key building blocks in many branches of synthetic chemistry. Figure 2.5 represents the amination reaction and its applications in different fields of chemical sciences.

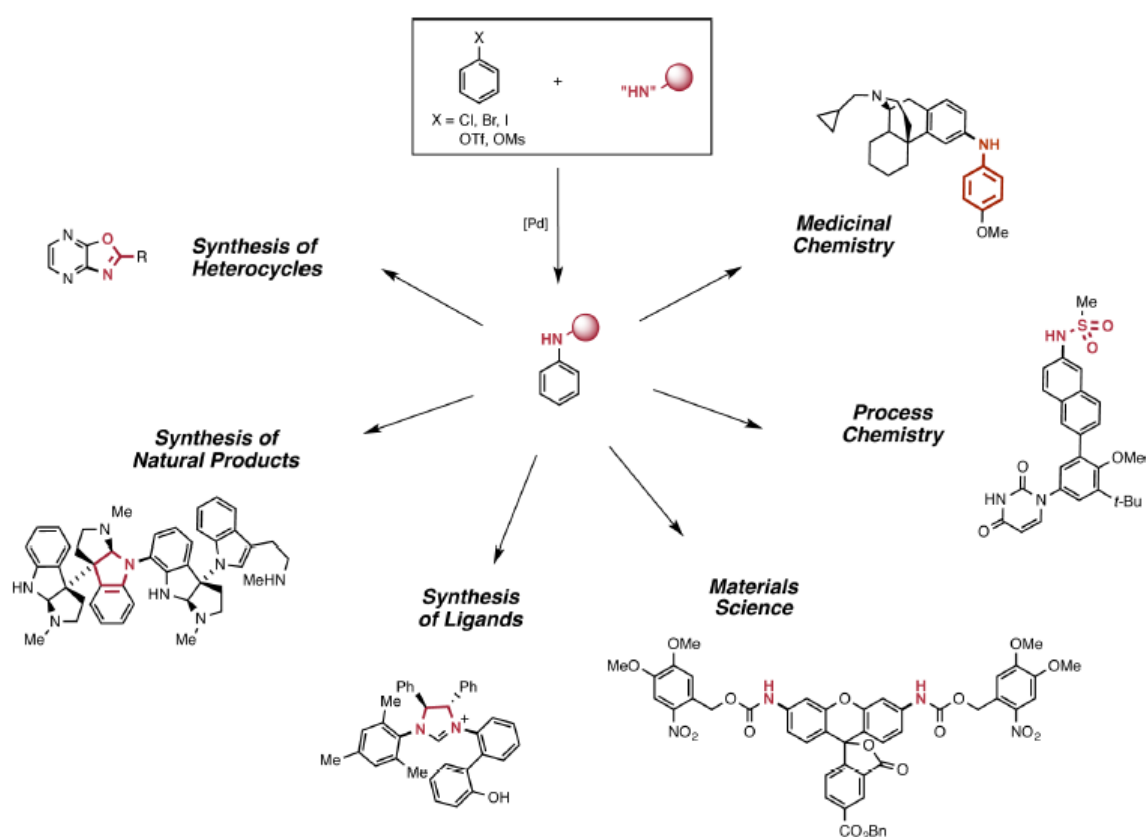
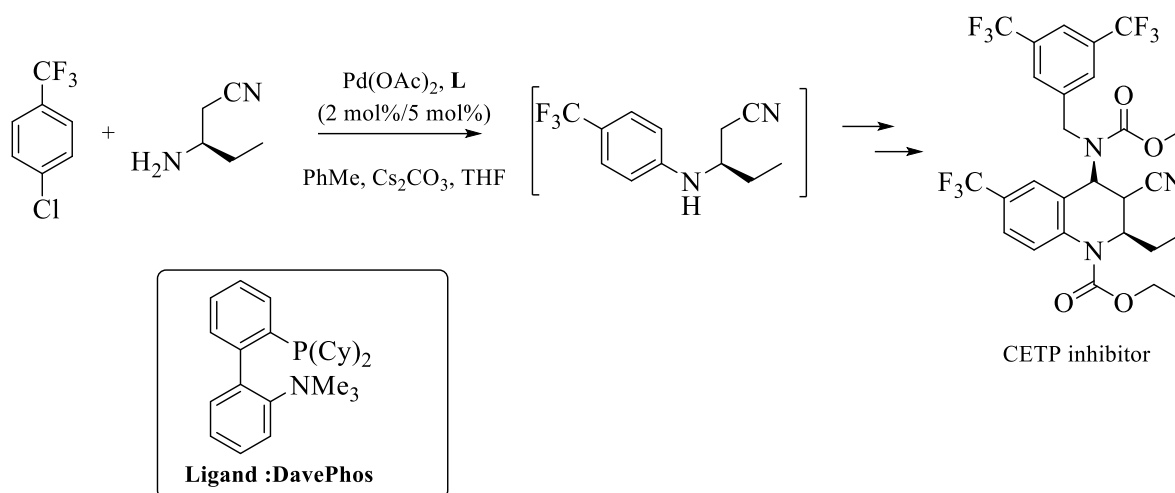


**Figure 2.5:** Wider applications of amination protocol in different branches of chemical sciences.<sup>199</sup>

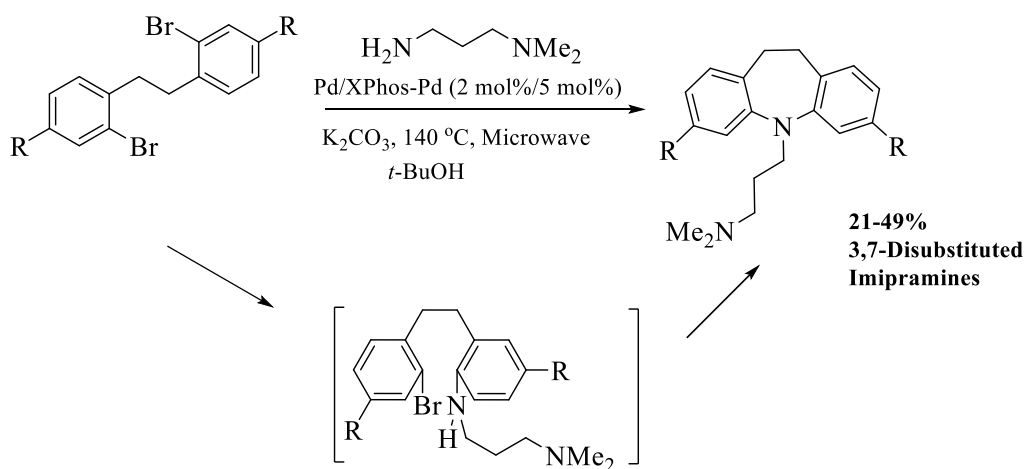
*Applications in medicinal chemistry*

Easily implementable palladium catalysis in C–N cross-coupling chemistry has inspired medicinal chemists to design novel drug candidates for specific targets with high precision.



**Scheme 2.7:** Synthesis of CETP inhibitor and application of Buchwald-Hartwig amination.

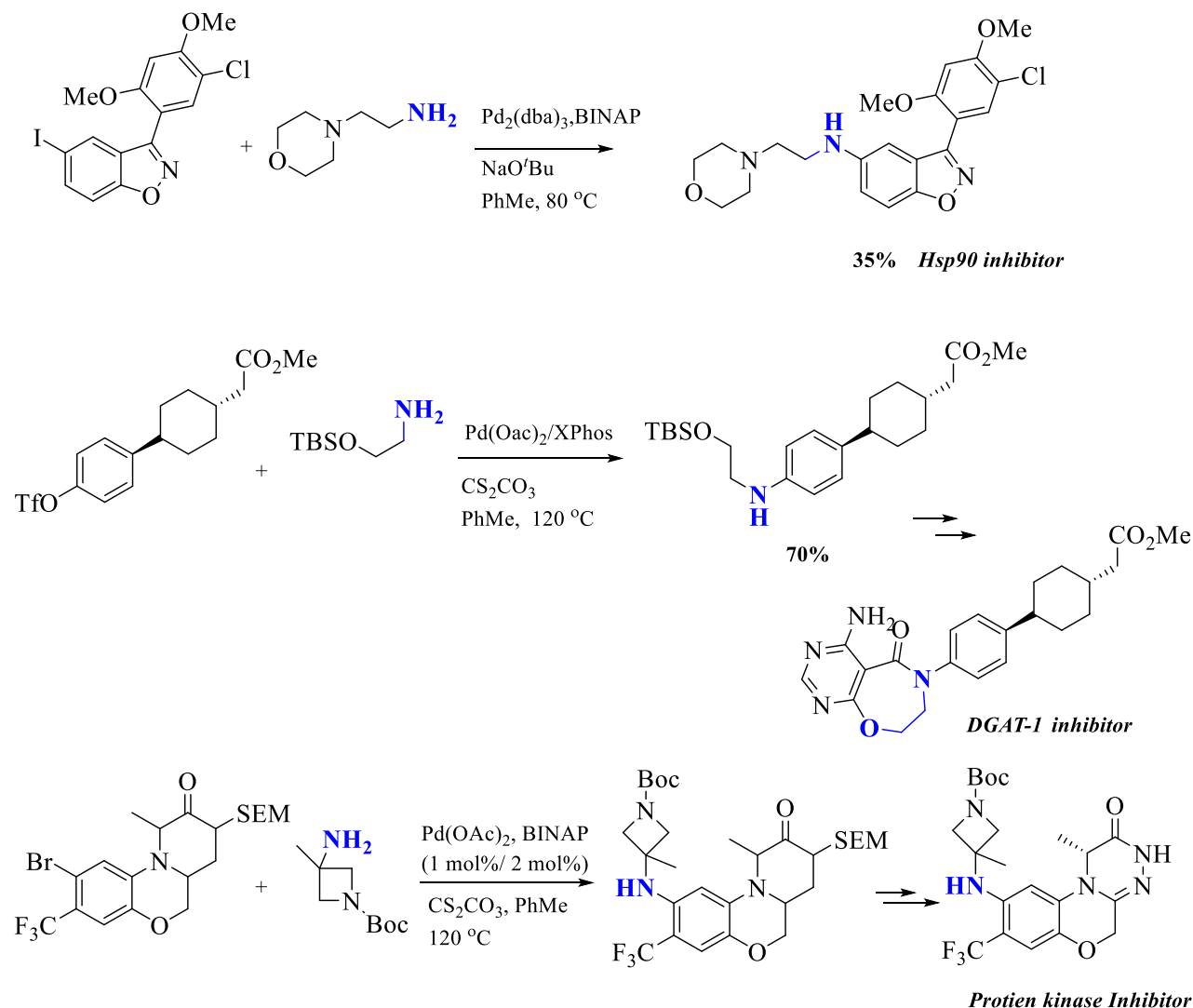
One example is the synthesis of a cholesterylester transfer protein (CETP) inhibitor, in which the Buchwald-Hartwig amination is one of the critical steps towards the final drug molecule. The reaction takes place between an aryl halide and an amine in the presence of  $\text{Pd}(\text{OAc})_2$  as catalyst and 2-Dicyclohexylphosphino-2'-(N,N-dimethylamino)biphenyl (DavePhos) as auxiliary ligand (Scheme 2.7).<sup>200</sup>



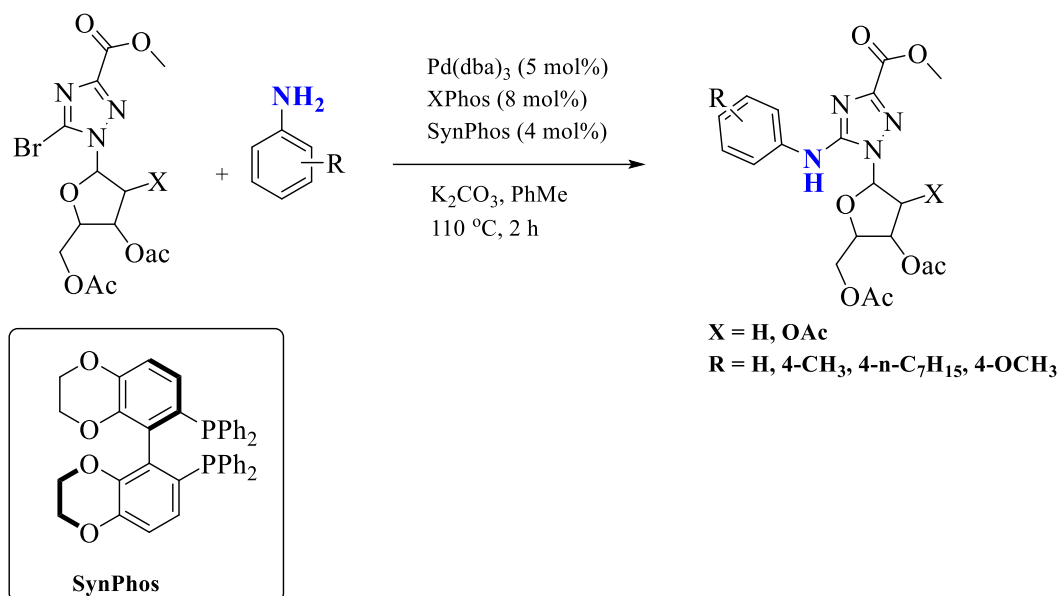
**Scheme 2.8:** Buchwald-Hartwig amination application in the synthesis of Imipramine.

Similarly, the anti-depressant drug *Imipramine* and its 3,7-disubstituted derivatives were prepared in single-pot reaction by Buchwald-Hartwig amination using 2-Dicyclohexylphosphino-2',4',6'-triisopropylbiphenyl (XPhos) and Pd-precatalyst with weak base  $\text{K}_2\text{CO}_3$  in *t*-BuOH solvent. The two N-arylation steps were performed on a bis-aryl bromide derivative to produce dibenzazapines (Scheme 2.8).<sup>201</sup>



Scheme 2.9: *N*-arylation on linear alkylamine.

Scheme 2.9 shows additional examples of *N*-arylation in drug preparation. The potential antitumor agent Hsp90 inhibitor was synthesized by selectively coupling 1-(2-aminoethyl) piperidine with aryl iodide in moderate yields.<sup>202</sup> Employing a catalytic system composed of Pd(OAc)<sub>2</sub>/XPhos was successful in the synthesis of DGAT-1 inhibitor from an enantioenriched triflate derivative and O-protected amine. These organic compounds were tested for the treatment of obesity or type II diabetes.<sup>203</sup> Likewise, the aminocycloalkanes are prevalent entities in pharmaceuticals. For example, a promising protein kinase C $\theta$  inhibitor for autoimmune therapy was synthesized by directly coupling the corresponding aryl bromide with aminoazetidine in excellent yields (Scheme 2.9).<sup>204</sup>



**Scheme 2.10:** Amination on nucleoside derivative.

Nucleosides are challenging substrates in metal catalyzed cross-coupling reactions because of their low reactivity, having multiple ligating N and O centers and highly sensitive glycoside bonds. However, modern ligands and palladium pre-catalysts efficiently access these coupling products with high selectivity under mild conditions. For example, triazole nucleosides are very low in reactivity, but the employment of Pd-catalysis with the combination of two phosphine ligands SynPhos and XPhos (2:1) in toluene for the cross-coupling of 5-bromo triazole nucleoside and substituted anilines yielded target *N*-arylamino triazole nucleoside quantitatively (Scheme 2.10). The developed catalytic system is highly efficient in all cases of electron donating, electron withdrawing or highly sterically hindered amines. Moreover, it proceeds very smoothly with bulky pyrenylamine in excellent yields. The C–N cross-coupling reaction with either of the ligands SynPhos or XPhos performed without the other was less efficient than the combination.<sup>205</sup>

All these aforementioned examples confirm the high utility power of palladium catalyzed C–N cross-coupling in medicinal chemistry. Although various electron-rich and bulky auxiliary ligand systems were developed and employed, there is still a scarcity for air stable and aqueous media soluble supportive ligands, which possibly allow reactions to proceed in aqueous phase. Such type of catalytic systems would be highly advantageous according to the green chemistry prospective.

### 2.3.2. Palladium catalyzed C–O bond formation

Alkyl aryl ethers and diaryl ethers are fundamental structural entities with high abundance in many biologically active natural products,<sup>206</sup> pharmaceuticals<sup>158</sup> and agrochemicals.<sup>207</sup> Predominantly, in 2017, the top 20% of 200 pharmaceuticals contains the alkyl aryl ether as a critical feature. In figure 2.6 few examples of biologically active alkyl aryl ether derivatives are shown.

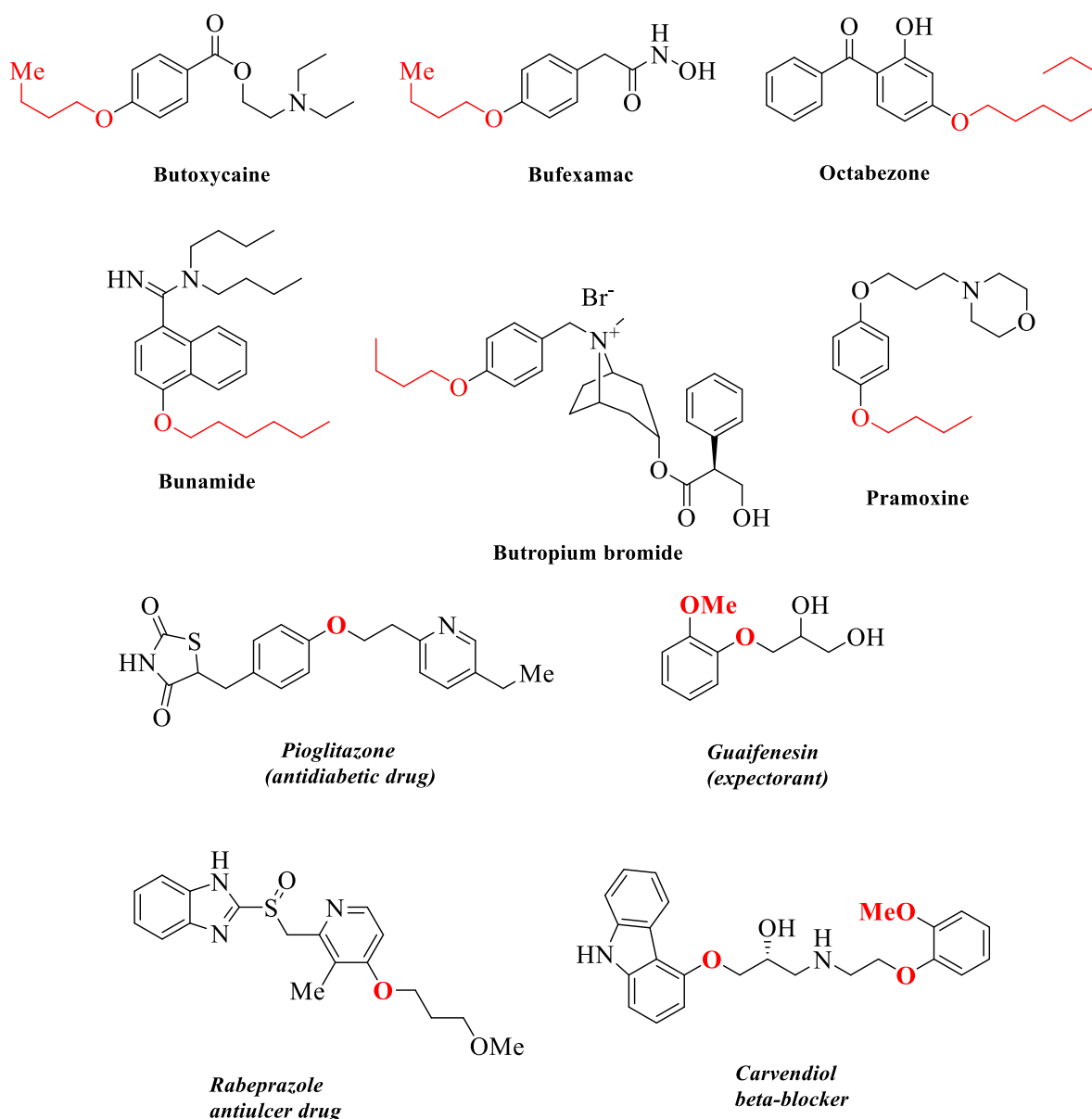
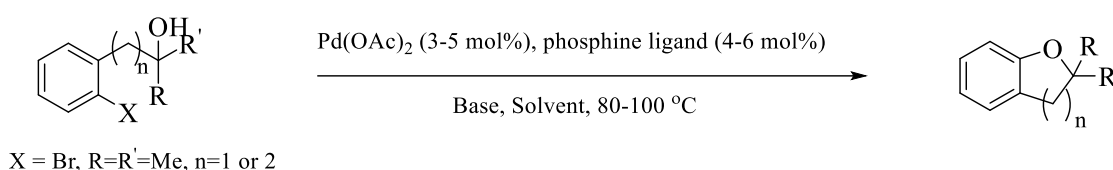


**Figure 2.6:** Examples for biologically active aryl and alkyl ethers.

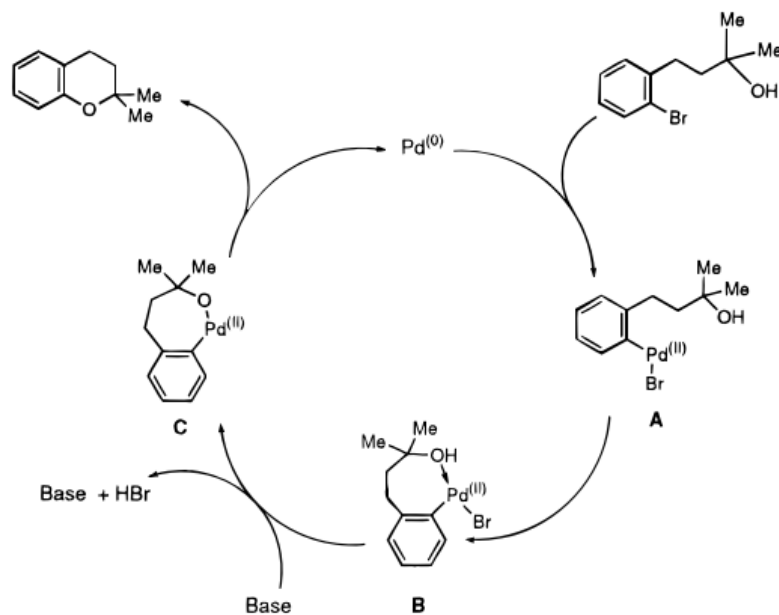
In 1850, Williamson's ether synthesis was introduced to prepare alkyl aryl ethers from organohalides and alkoxides. It involves the nucleophilic substitution of an alkoxide ion at an organohalide in  $S_N2$  fashion.<sup>208</sup> Further, the Mitsunobu reaction,<sup>209</sup> aromatic nucleophilic substitution,<sup>210</sup> Cu(I) catalyzed cross-coupling of alkoxides with aryl halides were also

traditional approaches. However, all these protocols suffer from a limited substrate scope, use of alkoxides in high excess, elevated temperatures, and stoichiometric quantities of copper catalyst.<sup>211-212</sup> Encouragingly, palladium catalyzed C–O bond formations have proven to be efficient in overcoming these limitations. In 1996, during the synthesis of oxygen heterocycles, Buchwald realized the Pd-catalyzed C–O bond formation to his surprise. Later they prepared five, six and seven-membered oxygen heterocycles via a Pd-catalyzed intramolecular *ipso*-substitution mechanism (Scheme 2.11). The catalytic systems consisting of Pd(II)/dppf or Tol-BINAP, were employed in the C–O bond formation between alcohols and aryl halides to furnish moderate to good yields of etherified products.<sup>213</sup>



**Scheme 2.11:** Buchwald intramolecular C–O bond formation.

The mechanism of Pd-catalyzed etherification proceeds similarly as in the C–N cross-coupling chemistry.<sup>179</sup> As shown in Scheme 2.12, Pd(0)L<sub>n</sub> undergoes an oxidative addition with aryl halides to form Pd(II) organometallic intermediate **A**. In the presence of a base, this proceeds through chelation (**B**)/deprotonation yielding palladacycle **C**, which undergoes reductive elimination giving the desired cyclic ether. It is not clear whether the deprotonation of alcohol occurred before chelation or after chelation to form intermediate **C**. However, application of this protocol with secondary and primary alcohols was mostly limited, because of the competing step of β-hydride elimination versus reductive elimination, which prompts the production of aldehydes or ketones. For example, the reaction of 2-bromophenethylalcohol under the given catalytic condition, produces phenylacetaldehyde. The β-hydride elimination has a high dependence on the ring size of the metallocycle intermediate in the mechanism. For larger rings the energy to adopt required confirmation of the β-hydride elimination intermediate is substantially higher. Thus, the utilisation of electron rich, bulky *o*-biphenyl phosphine (Figure 2.7) ligands (**L1-L4**) could favour the reductive elimination. As hypothesised, researchers found steric ligands to be superior and these successfully delivered the desired cyclic ethers with primary and secondary alcohols.



**Scheme 2.12:** Mechanistic representation of Pd-catalysed intramolecular C–O coupling.<sup>179</sup>

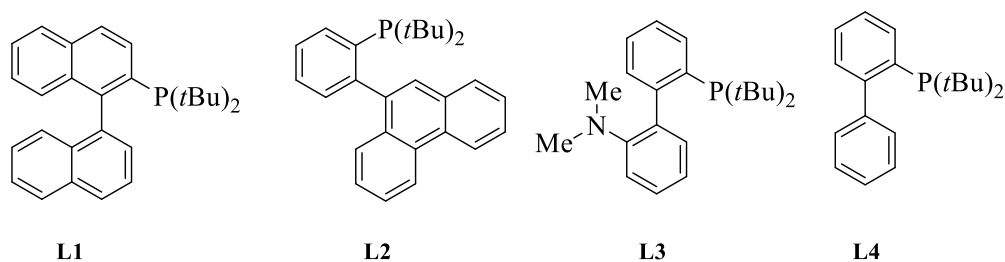
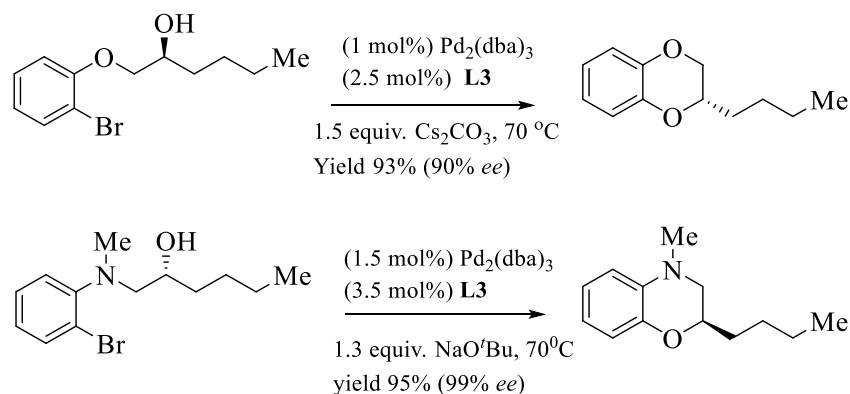


**Figure 2.7:** Examples for *ortho*-biphenyl phosphines.

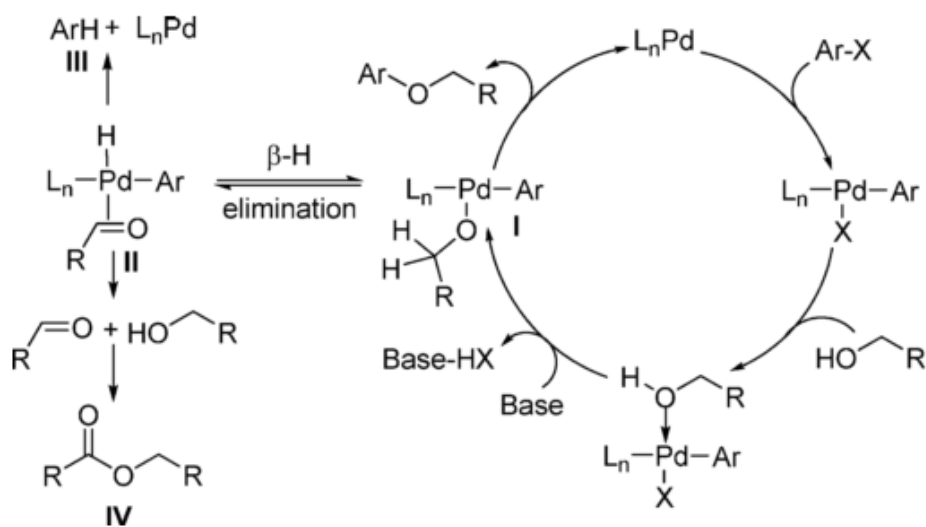
Significant advantages of this approach comprise the synthesis of versatile heterocycles containing two different heteroatoms in the ring (Scheme 2.13) and the process of highly enantioselective cyclisation of enantiopure alcohols to optically active ethers.<sup>214</sup>

Although the employment of bulky ligands in catalysis for C–O cross-coupling avoids significant limitations, it is still challenging to functionalize on un-activated aryl chlorides. Nevertheless, slight modulations in ligand electronics with alkyl functional groups on biphenyl moieties of phosphines were proven beneficial. The electron rich aryl bromides and chlorides were successfully reacted with tertiary alcohols in Pd-catalyzed C–O coupling procedures by using alkyl substituted biphenylphosphines.<sup>215</sup>



**Scheme 2.13:** Application of Pd-catalysed C–O coupling for novel fused heterocycles.

After successful intramolecular C–O coupling, the next challenge was to deliver intermolecular C–O couplings between aliphatic primary or secondary alcohols and aryl halides. The critical problem in the formation of these aryl ethers is again the competition between the formation of the desired reductive elimination product and the undesired  $\beta$ -hydride elimination intermediate Ar-Pd-OCH<sub>2</sub>R (I) (Scheme 2.14).

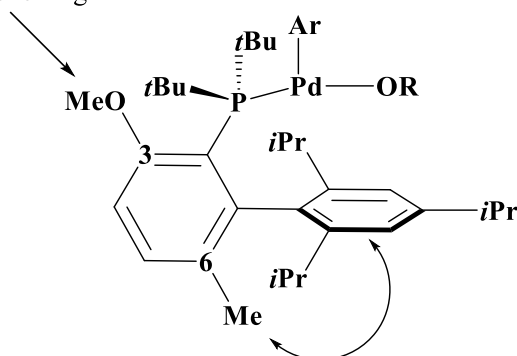


**Scheme 2.14:** Mechanistic cycle of Pd catalysed intermolecular C–O coupling reaction.<sup>215</sup>

The chemoselectivity of the reaction depends on the C–O bond formation, reductive elimination and  $\beta$ -hydride elimination steps. Moreover, in the Pd-alkoxide complexes (I), the rate of the  $\beta$ -hydride elimination step is typically higher than for the reductive elimination, while alkoxides are substantial hydrogen donors to reduce aryl halides (Scheme 2.14).<sup>216</sup> At the same time, it is well known that bulky phosphine ligands favor the reductive elimination over the  $\beta$ -hydride elimination process.<sup>217</sup> By these principles, Buchwald reported the first intermolecular C–O cross-coupling protocol with a sterically highly bulky and electron

abundant biphenyl phosphine ligand (*N,N*-dimethylamino)-2'-di-tert-butylphosphinobinaphthyl. Further optimization of phosphine ligands through the decoration with alkyl substituents enhanced the efficiency of the catalytic system even with un-activated aryl halide substrates.<sup>218-220</sup> The selective effects of the substituents on the biaryl phosphine ligands and their increased reactivity profile in Pd-catalyzed C–O bond formation with aliphatic primary alcohols was studied in detail.<sup>220</sup> For example, there is a significant influence of the substitution at the 6-position with a methyl group (rather than methoxy) of the biaryl phosphine ligand system in enhancing the reductive elimination kinetics while inhibiting the  $\beta$ -hydride elimination. Among all biaryl phosphines, RockPhos (figure 2.8) enhances the rate of desired C–O cross-coupling of (hetero)aryl halides to primary or secondary alcohols with [(allyl)PdCl]<sub>2</sub> in 0.5-2.5 mol%, Cs<sub>2</sub>CO<sub>3</sub> at 90 °C and offered moderate to good yields of aryl alkyl ethers with great regioselectivity.<sup>221</sup>

The 3-substituent fixes the Pd<sup>II</sup> over the triisopropylbenzene ring



The combination of steric effects from 3-OMe and 6-Me groups enhances the rate of reductive elimination

The 6-substituent interacts with the triisopropylbenzene ring and provides conformational rigidity

**Figure 2.8:** Various parameters in RockPhos ligand design.

#### *Biologically relevant alkylarylethers-Pd-catalysis:*

Methylarylethers are a class of organic building blocks widely found in pharmaceuticals and natural products. Figure 2.9 depicts some respective approved biologically active molecules.

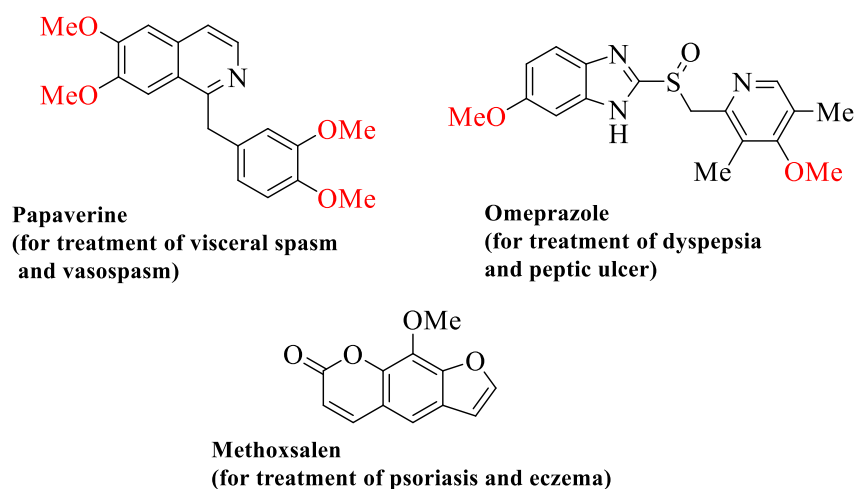
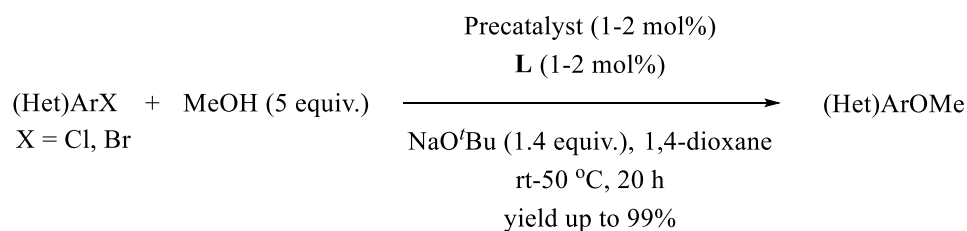
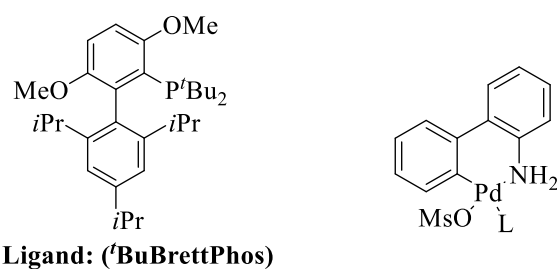


**Figure 2.9:** Examples of methoxy (aryl ethers)-containing pharmaceutical drugs.

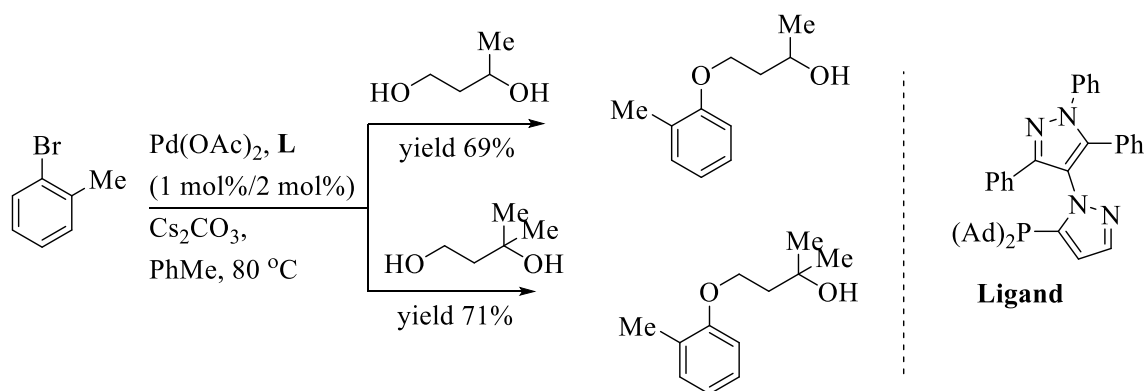
So far, the application of methanol surrogates like methoxy-substituted silanes [Si(OMe)<sub>3</sub>H, or Si(OMe)<sub>4</sub>] in Pd-catalyzed and copper-catalyzed decarboxylative cross-coupling is typical.<sup>222-223</sup> However, the methodology is limited to electron deficient aryl halides such as *ortho* substituted -NO<sub>2</sub>, -SO<sub>2</sub>Me, or -CF<sub>3</sub> aryl halides. In the process of developing a more simple direct approach towards methylarylethers, in 2012 Beller<sup>224</sup> and Peruncheralathan<sup>225</sup> and co-workers developed Pd-catalyzed C–O cross-coupling processes. They used aryl halides or halo pyridines and methanol or methanol-*d*<sub>4</sub> in the presence of palladium and sterically demanding BippyPhos-based phosphine and tertiarybutyl XPhos ligands. A few more reports of Cu-catalyzed processes in the direct synthesis of anisole and aryl methoxy ethers are available.<sup>226-228</sup>



**Scheme 2.15:** Synthesis of methylarylethers with an excess of MeOH and bulky phosphine ligands.



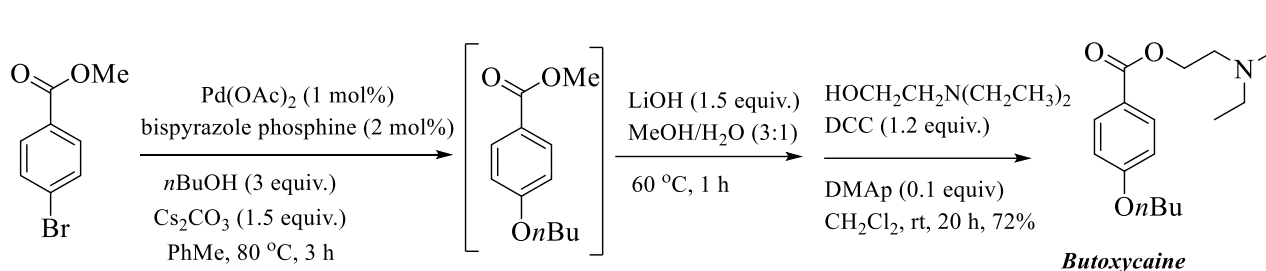
Despite many available optimized protocols, these reactions need high temperatures (>80 °C) to complete the catalytic cycle. A very mild and general approach in simple C–O cross-coupling with (hetero)aryl halides and an excess of MeOH (Scheme 2.18) was realized in the presence of bulky biaryl phosphine ligand (<sup>t</sup>BuBrettPhos) and palladacycle pre-catalyst. This developed protocol provided good yields and was found flexible in synthetic approaches towards the biologically active molecules shown in figure 2.9. Employing the bulkier functionalized biaryl phosphine <sup>t</sup>BuBrettPhos in a combination with the palladacycle enhances the substrates scope and allows the coupling of highly electron deficient or inactivated (hetero)aryl halides and biologically relevant aliphatic or heterocyclic alcohols under milder conditions with good yields.<sup>207</sup> However, these bulky ligands were highly moisture sensitive and a multi-step synthesis is involved in their preparation giving only moderate yields. Nevertheless, it is interesting to note that the palladium catalysis for cross-coupling of arylhalides with tertiary alcohols and phenols was well established.<sup>229</sup> However, application of these catalytic systems for the cross-coupling of arylhalides with primary and secondary alcohols was unsuccessful or limited to few substrates with additives. Hartwig and his co-workers proposed bulky nucleophilic phosphine ligands with Pd-catalysts for C–O cross-coupling to facilitate the reductive elimination at the expense of β-hydride elimination.<sup>217</sup>



**Scheme 2.16:** Regioselective synthesis of alkylaryl ethers by using Beller's bi-heterocyclic phosphine ligand.

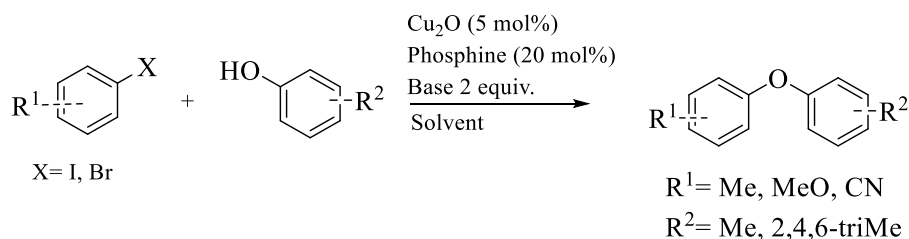
Later, Beller<sup>230</sup> and co-workers reported not only easily accessible and air-stable bispyrazole phosphine ligands but also bulky ligands sterically demanding enough to favor the reductive elimination step other than undesired β-hydride elimination. Scheme 2.16 shows the synthesis of the bispyrazole phosphine ligand. These catalysts of bi-heterocyclic phosphine ligands and palladium, delivered high regio-selectivity for primary alcohols even in presence of secondary and tertiary alcohols.<sup>231</sup> For example, in the case of 1,3-butane diol, where it has both a primary and a secondary hydroxyl group, the etherification proceeded with high regio-selectivity

towards primary alcohols (69%) under the optimized reaction conditions. Similar results were observed in the case of 3-methylbutane-1,3-diol containing primary and tertiary hydroxyl, where the etherification selectively proceeds at the primary alcohols with 71% isolated yields (Scheme 2.16).<sup>230</sup> The developed protocol was implemented successfully in the synthesis of known local anesthetic drug Butoxycaine.<sup>230</sup> This reaction was elegantly carried out with 4-bromoethoxybenzoate and proceeded in the presence of 1 mol% Pd(OAc)<sub>2</sub>, 2 mol% of ligand, 1.5 equiv. Cs<sub>2</sub>CO<sub>3</sub>, *n*-BuOH at 80 °C for 3 h to produce the etherified intermediate which consecutively was taken to hydrolysis and DCC coupling with 2-(diethylamino)ethanol resulting in Butoxycaine in overall 72% yield (Scheme 2.17).

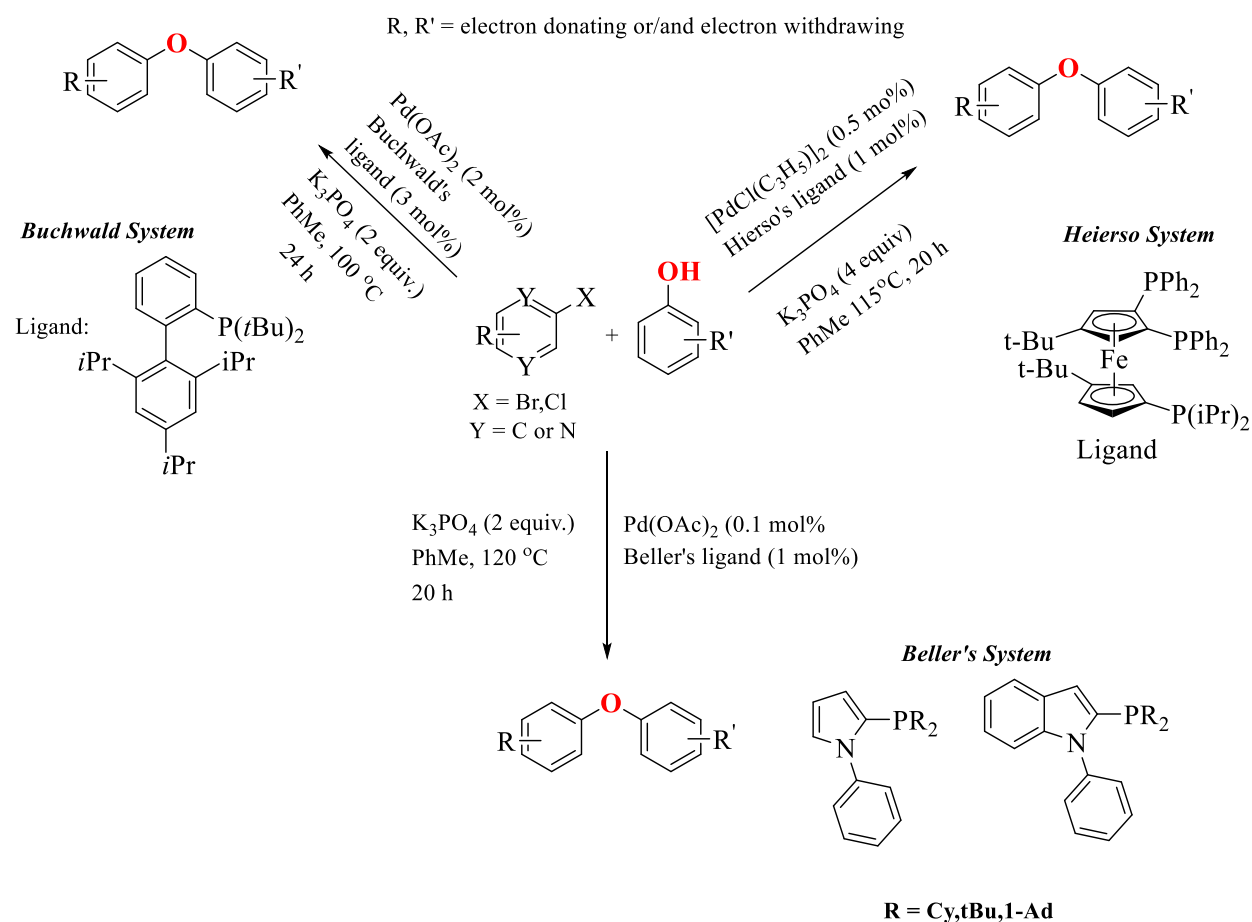


**Scheme 2.17:** Synthesis of Butoxycaine and application of C–O bond formation.

Biaryl ethers are also biologically essential structural features frequently found in many natural products and pharmaceuticals.<sup>232</sup> These ethers were prepared generally from the aryl chlorides and corresponding sodium or potassium phenoxides in the presence of Cu salts (Ullmann type reactions) (Scheme 2.18).<sup>212</sup> Despite broad substrate scope applicability, these methodologies suffer from elevated temperature requirements and the stoichiometric scale of Cu salts, which usually reduces product yields and involves laborious purification.



**Scheme 2.18:** Copper catalysed Ullmann type biarylether synthesis.



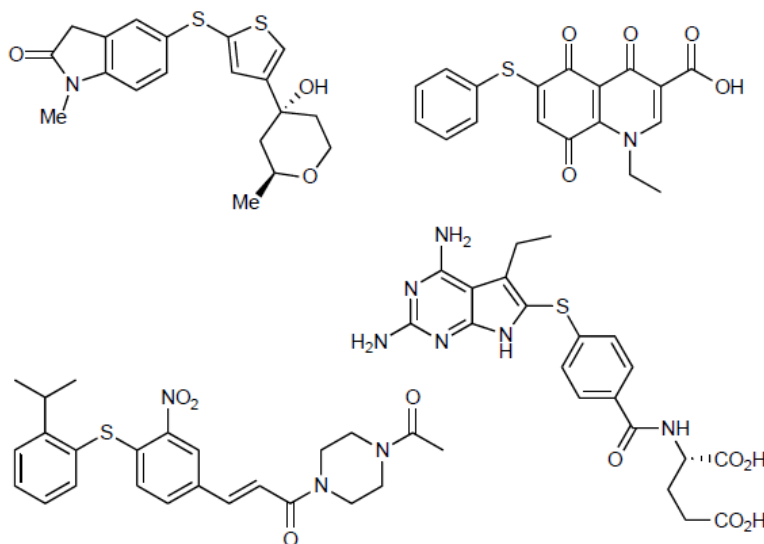
**Scheme 2.19:** Representation of Beller, Buchwald, and Hierso Pd catalyst systems for C–O coupling.

The intermolecular C–O bond formation between aryl halides ArX ( where, X = I, Br, Cl) and phenols via palladium catalysis has been explored broadly by researchers including Buchwald<sup>207</sup>, Hierso<sup>233</sup>, Olofsson<sup>234</sup> and Beller<sup>230</sup>. High reactivity and extensive substrate scope were evidenced with the use of bulky ligands (Buchwald ligands), electron-rich phosphines (Beller ligands) in combination with well pre-activated palladacycles or palladium precursors. The organic diaryl ethers synthesised through these protocols were highly versatile, and in many cases, low catalytic loadings were practiced. Scheme 2.19 shows the exact reaction conditions of the most extensively applied three intermolecular C–O coupling protocols named after their developers, the Buchwald, Hierso and Beller systems.

### 2.3.3. Palladium catalyzed C–S bond formation

In recent days, we observe a substantial improvement in Pd-catalyzed carbon-sulfur cross-coupling chemistry. However, the development of metal catalyzed carbon-sulfur bond formation processes was less intense than for C–N, and C–O cross-coupling reactions. The high prevalence of C–S bond moieties in many natural and unnatural products and their

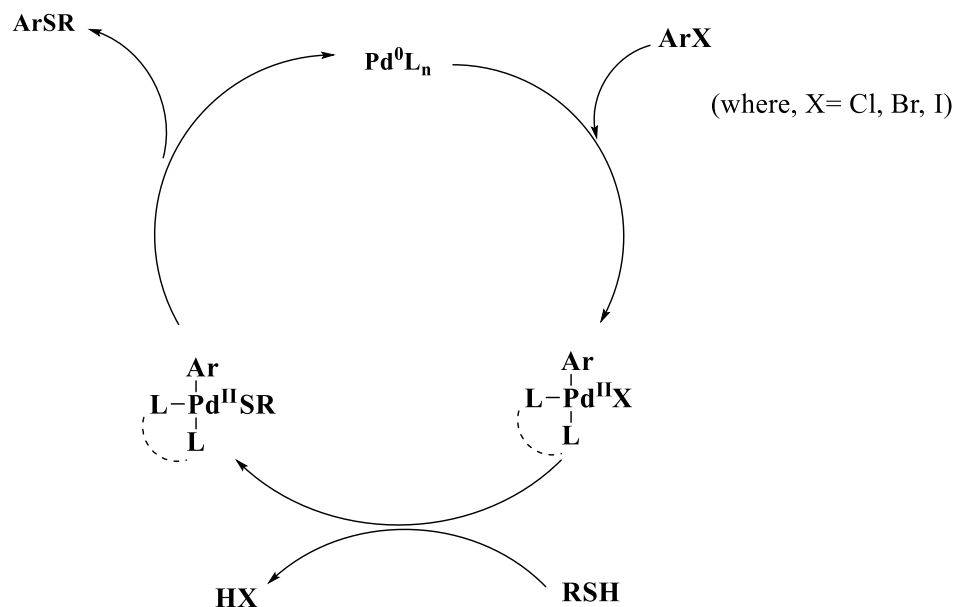
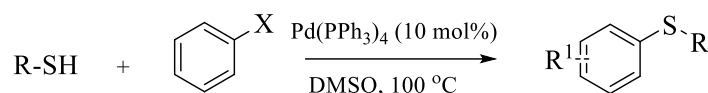
significant therapeutic activity against cancer, HIV, Alzheimer's, inflammation, and asthma diseases necessitates researchers to advance the diaryl sulfide forming chemical processes. In figure 2.10, few examples of biologically active molecules bearing biarylsulfides are presented.<sup>235-237</sup>



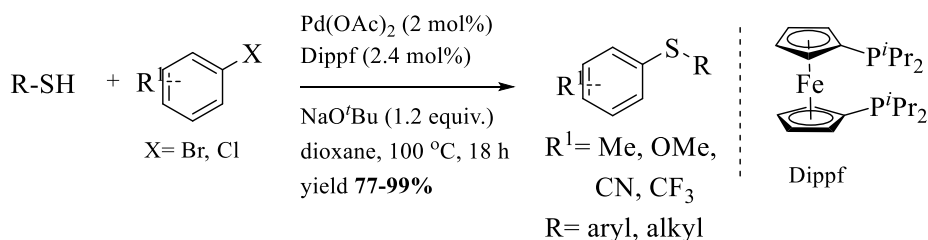
**Figure 2.10:** Biologically relevant C–S bond containing organic molecules.<sup>235</sup>

The traditional methods to synthesise diaryl sulfides comprise very harsh impractical reaction conditions and always have limited substrate scope.<sup>238</sup> Few of these approaches were through metal-disulfide reduction, nucleophilic reactions on disulfides and aromatic substitution reactions. Transition metal-catalyzed synthesis of aryl sulfides was recognised as a very mild and efficient approach towards new biologically active probes. However, metal-dithiolate complexes were known to be very stable; catalyst and substrate might interact and inhibit the catalytic activity of the process. Despite this assumption, thiols performed well as coupling partners in metal-catalyzed cross-coupling with aryl halides, and *in situ* formed metal-thiolate complexes underwent reductive elimination to favour C–S bonds.

Migita C-S coupling with Pd(tetrakis)

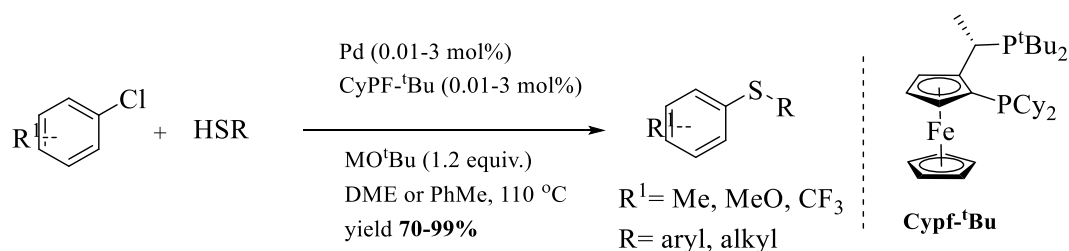
**Scheme 2.20:** Buchwald Pd/bidentate phosphine derived catalytic cycle.

Migita was first successful in arylthiolation reactions by employing Pd(PPh<sub>3</sub>)<sub>4</sub> as a catalyst (Scheme 2.20).<sup>239-240</sup> Although the protocol yields the aryl sulfides in good yields, it required high temperature and long durations to complete the reaction, which causes the partial decomposition of thiol precursors. Later, the Pd-catalyzed protocols started applying bisphosphine ligands in catalysis. The bis-phosphine ligands are expected to be in coordination during the thiolate attack on the Ar-Pd(II)-X-L<sub>n</sub> intermediate (Scheme 2.20). These reactions are considered to proceed through the typical Pd-catalyzed carbon-heteroatom cross-coupling chemistry.

**Scheme 2.21:** Buchwald Pd-catalysed C-S coupling with Dippf.

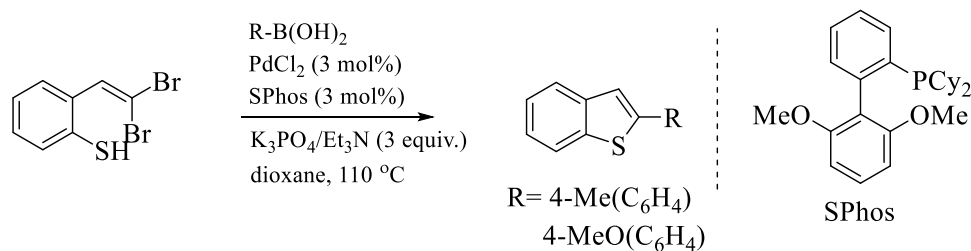
Buchwald reported the most efficient C–S cross-coupling protocol using the Pd-catalyst and bidentate ligand 1,1'-Bis(diisopropylphosphino)ferrocene (dippf) for activating electron rich

arylchlorides (Scheme 2.21).<sup>241</sup> A series of monodentate and bidentate ligands were investigated for their efficiency in C–S bond formation, where, bidentate ligands proved to stay intact under thiolate nucleophilic complexation reactions with the Pd(II) oxidative intermediate. Hartwig reported the most significant catalytic system for the thiolation in 2006 with Pd/JosiPhos.<sup>242-243</sup> This system not only exhibited the capability of selective C–S coupling with alcohol, aldehyde, amine, and amide containing substrates but also to catalyze the complete cycle at lower ppm levels of palladium (Scheme 2.22).



**Scheme 2.22:** Hartwig low catalytic loading C–S bond formation reaction.

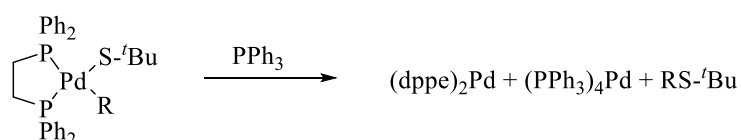
The monodentate phosphine ligand 2-Dicyclohexylphosphino-2',6'-dimethoxybiphenyl (SPhos) performed decently in tandem intramolecular C–S coupling/Suzuki/Miyaura reactions to obtain biologically significant functionalized benzothiophenes in high yields (Scheme 2.23). Albeit, SPhos demonstrated no reactivity in Pd-catalyzed intermolecular C–S coupling.<sup>244</sup> In addition, the innovative ligand-free Pd/C catalytic system for C–S bond formation is efficient. However, the catalytic system can activate only aryl iodide.<sup>245</sup>



**Scheme 2.23:** Intramolecular C–S coupling driven by monodentate SPhos ligand.

*Key mechanistic features of Pd-catalyzed C–S bond formation:*

The mechanistic investigations of the Pd-catalyzed C–S cross-coupling provided a detailed insight into the importance of the reductive elimination step in the complete catalytic cycle.

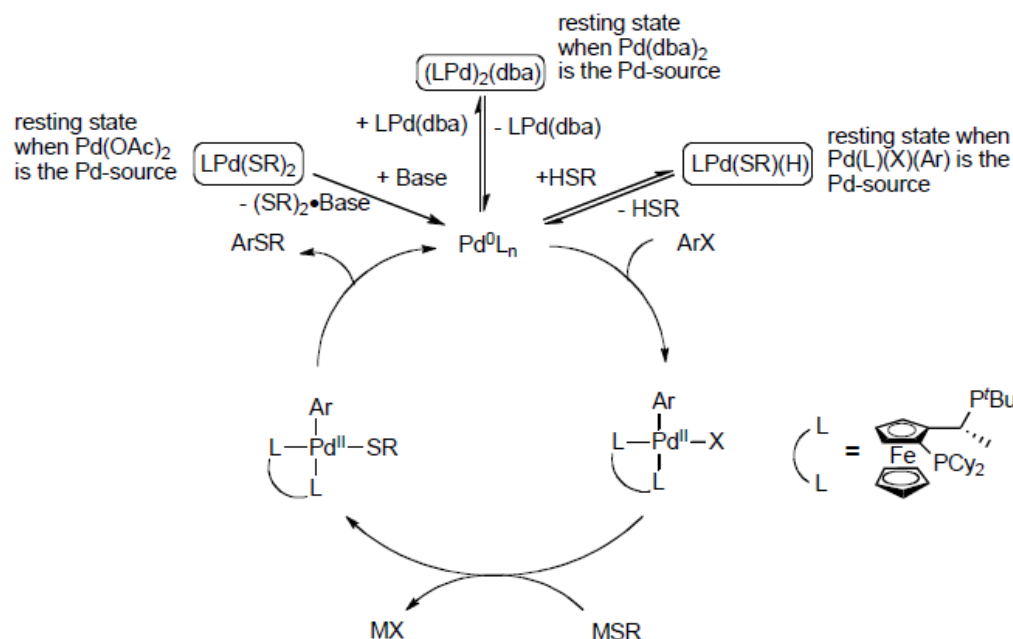


R	Temp °C	t <sub>1/2</sub> min
CH <sub>3</sub>	95	580
CHCH <sub>3</sub>	50	17
C <sub>6</sub> H <sub>5</sub>	50	48
CC(CH <sub>2</sub> ) <sub>3</sub>	95	87
CCPh	95	15

**Scheme 2.24:** The stability of the Pd thiolate complex in the presence of different moieties.

The reductive elimination step was identified as the rate-limiting step, and bidentate ligands have a significant influence on the process. The rate of formation of sulfide from thiolate-Pd-vinyl, aryl, alkynyl and alkyl complexes mainly depends on the  $\pi$ -coordination ability of these groups (Scheme 2.24). Hence, the rate order will be vinyl>aryl>alkynyl>alkyl. In terms of thermodynamic factors,  $\Delta G$  is much smaller for the alkynyl intermediate than in vinyl or aryl derivatives. The substitution at the thiol precursor can minimise the coordinative access to the Pd metal centre simply for steric reasons. The complete mechanistic cycle involves different reductive elimination electronics, comparative to classical C–C or C–H bond formation.

Cysteine-thiol derivatives were investigated in the Pd-catalyzed C–S coupling to understand the mechanistic aspects by monitoring every catalytic step through NMR and electrochemical methods and the rates of intermediate formation were measured for all.<sup>246</sup> The <sup>31</sup>P-NMR analysis suggested that the Pd-thiol complex is formed prior to the deprotonation step and addition of base results in an Ar-Pd(L<sub>n</sub>)-SR complex. The employment of electron rich bulky bisphosphine ligands increases the rate of the reaction. The oxidative addition, trans-metalation and reductive elimination steps proceed at higher rates even at ambient temperatures. However, the high temperature required to complete the overall catalytic cycle was still disadvantageous. The resting state of the reaction lies outside the catalytic cycle and is more dependent on the Pd sources used in the reaction (Scheme 2.25).<sup>247</sup>



**Scheme 2.25:** Catalytic cycle of C-S bond formation and influence of various Pd sources on Pd(0) species.<sup>247</sup>

### 2.3.4. Palladium catalyzed C–P cross-coupling

In recent years, the interest in obtaining novel organophosphorus compounds is increasing in biological and medicinal chemistry fields. Aryl phosphonates, vinyl phosphonates and allenylphosphonates are present in many biologically active anti-herpes, antiviral and anti-HIV agents, respectively (Figure 2.11).<sup>248-250</sup>

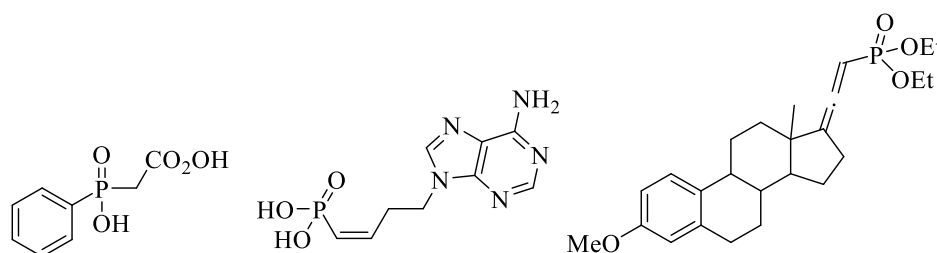
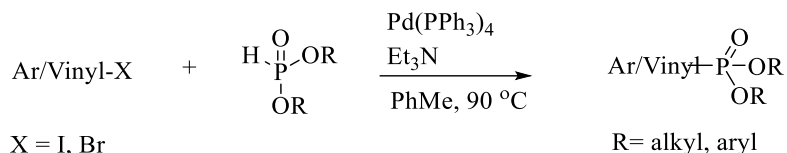


**Figure 2.4:** Biologically active molecules bearing phosphonate moieties.

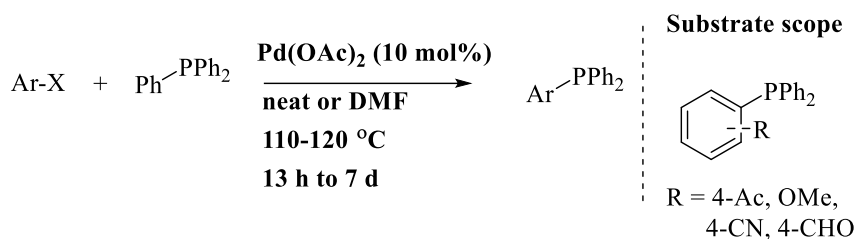
The traditional procedure to develop a carbon-phosphorus bond in organic chemistry is the Michaelis-Arbuzov reaction. However, for the low reactivity of Csp<sup>2</sup> carbon to nucleophilic substitution reactions, this methodology cannot be adopted to synthesise vinyl, aryl, or allenyl phosphorous compounds.<sup>251</sup> In general, for a long-time aryl phosphonates were accessed only through harsh conditions such as elevated temperature phosphorylation with P<sub>2</sub>O<sub>5</sub> or the Friedel-Craft reaction with POCl<sub>3</sub>. Also, the synthesis of few vinyl phosphonates or phosphinates by organometallic reagents (organolithium) reacting with phosphochloridates is a traditional method.<sup>252</sup>





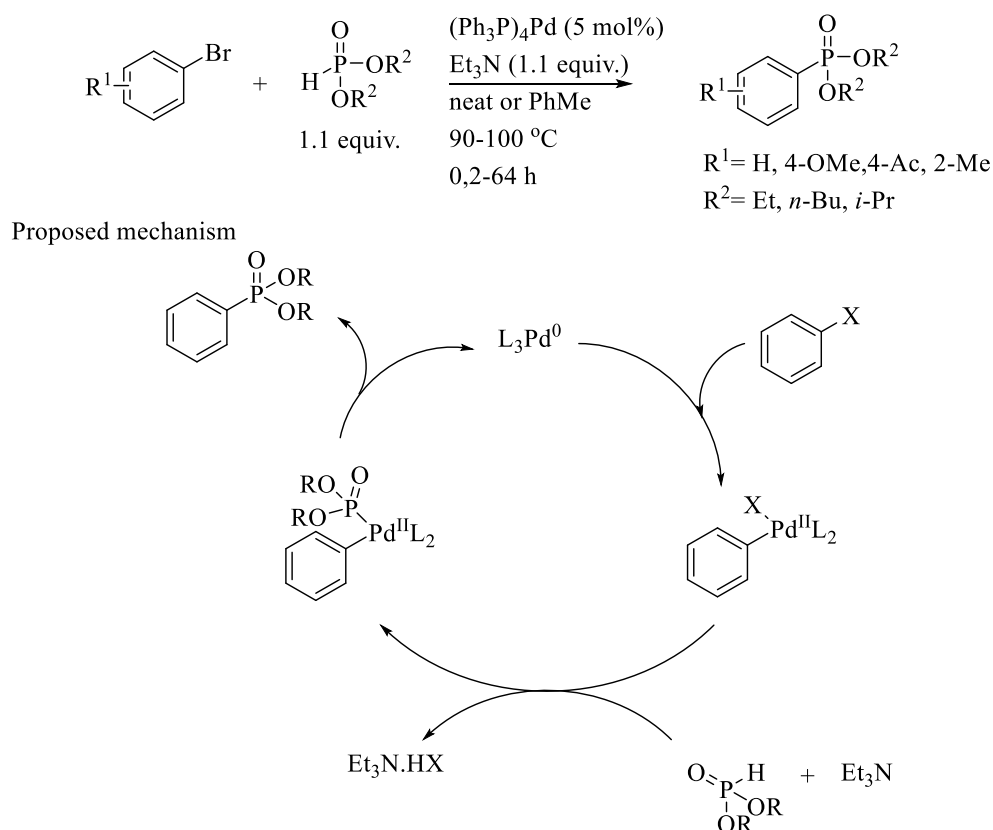
**Scheme 2.26:** Pd-catalysed phosphorylation of aryl or vinyl halides.

According to the literature, among all reported Pd-catalyzed C–heteroatom cross-coupling reactions, C–P coupling is actually the earliest discovery provided by Hiaro.<sup>253-254</sup> The C–P cross-coupling was performed successfully between aryl- and vinyl-halides and dialkyl H-phosphonate diesters in the presence of Pd(PPh<sub>3</sub>)<sub>4</sub> as a catalyst (Scheme 2.26). The advanced research in this kind of cross-coupling facilitated the reactive partner's variations. Aryl and vinyl triflates<sup>255</sup> (pseudo halides) were incorporated as electrophilic coupling partner and on the nucleophile side different phosphorous sources like phosphinates<sup>256</sup>, phosphineoxides<sup>257</sup>, HH-phosphonates<sup>258</sup>, phosphines<sup>259</sup> and boronophosphines<sup>260</sup> were successfully employed. For the more detailed discussion on the reactivity and functionalization of molecules, please refer to the respective reviews.<sup>261-263</sup> Migita reported the reaction with aryl-vinyl halides or triflates and triphenylphosphine with Pd(OAc)<sub>2</sub> as a catalyst in DMF to result in aryl phosphonium salts (Scheme 2.27). These phosphonium salts can undergo aryl exchange to form novel aryl phosphines. In the reaction mechanism of the formation of the phosphonium salt the substrate undergoes oxidative addition to the palladium complex and finally, ligand substitution leads to the C–P coupled product.<sup>240, 264</sup>



**Scheme 2.27:** Migita aryl phosphorylation using Pd(OAc)<sub>2</sub> via phosphonium salt intermediates.

In most of the C–P cross-coupling methodologies Pd(PPh<sub>3</sub>)<sub>4</sub> was utilized very frequently after Hiaro's discovery, but for some reactions, different sources of palladium were employed such as Pd(OAc)<sub>2</sub><sup>265-266</sup> and PdCl<sub>2</sub>(PPh<sub>3</sub>)<sub>2</sub><sup>267</sup> in combination with ligands 1,3-Bis(diphenylphosphino)propan (dppp)<sup>268</sup>, Butane-1,4-diylbis(diphenylphosphane) (dppb)<sup>269</sup>, dppf.<sup>270</sup>



**Scheme 2.28:** The C–P cross-coupling of dialkylphosphites according to Hiaro’s method. Proposed mechanism for the palladium-catalyzed cross-coupling of dialkyl phosphites with aryl and vinyl halides.

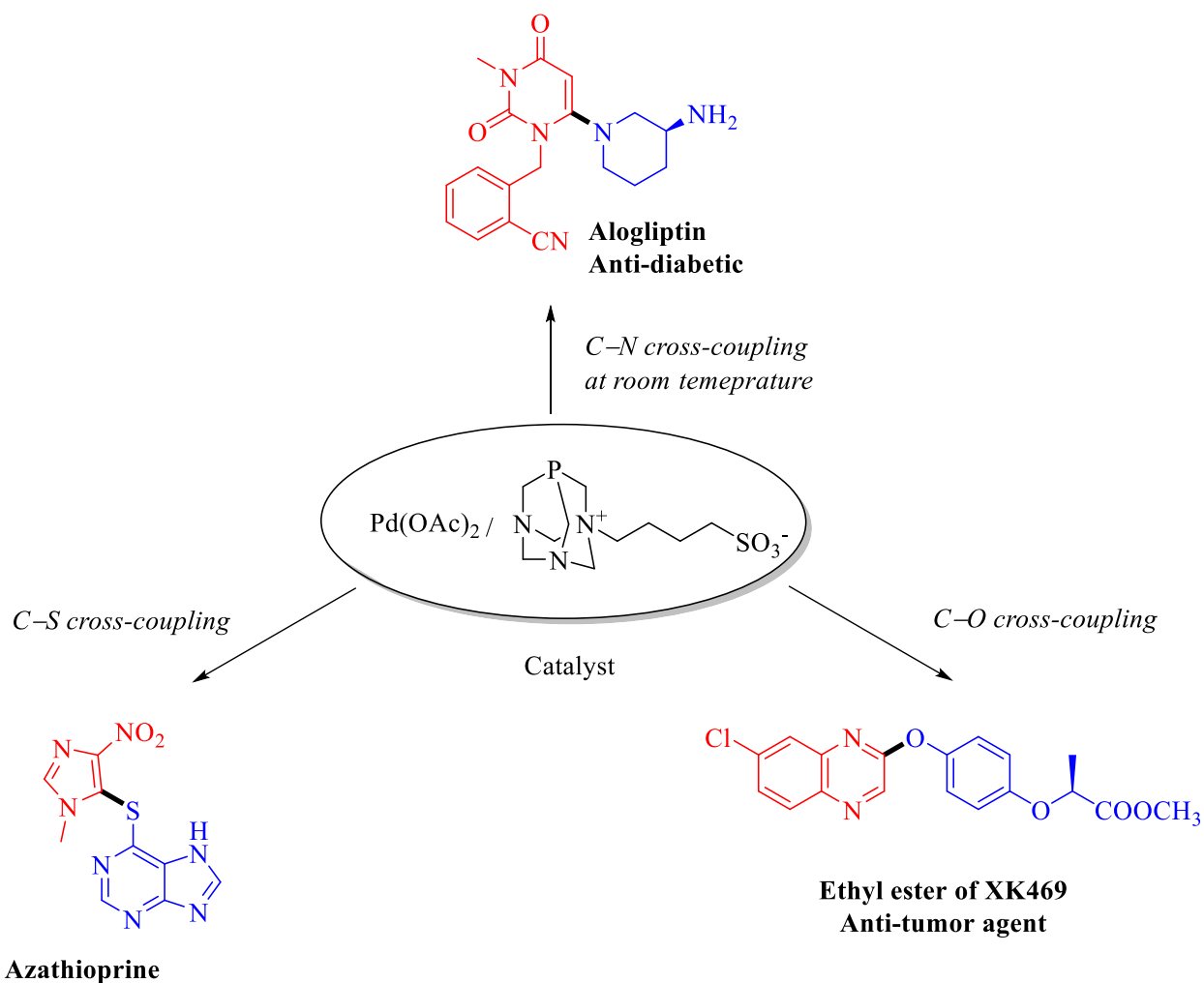
Scheme 2.28 depicts the palladium-catalyzed cross-coupling reaction of dialkyl phosphites with aryl bromides, affording dialkyl arylphosphonates.<sup>271</sup> The oxidative addition of the catalytically active palladium (0) complex to the aryl halide forms the palladium (II) complex, subsequent ligand displacement by the previously deprotonated dialkyl phosphite provides the adduct. Finally, reductive elimination generates the product with regeneration of the palladium (0) catalyst. The catalytic system depends on the palladium source, base and solvent to enhance its reactivity. In particular, Stawinski and co-workers reported a detailed mechanistic and synthetic study on the role of the palladium source and anionic additives.<sup>271-272</sup> During these investigations, they found that the reaction could be efficiently accelerated in the presence of anionic additives, e.g., halides or acetate. Presumably, these additives strongly influence the ligand substitution step in the catalytic cycle.<sup>273</sup> Such additives increased the scope of C–P cross-coupling and are applicable to a wide range of different phosphites as well as aryl halides and triflates. Additionally, mechanistic studies on the role of bidentate phosphine ligands in the cross-coupling reaction and the rates of the reductive elimination step were performed by Stockland, Jr. et al.<sup>274</sup>

## 2.4. Summary and prospective

The palladium catalyzed C–C or C–X (X= N, O, S, P etc.) cross-coupling strategies for the synthesis of medicinal-chemically relevant drug components or candidates was highlighted in the above discussions. Additionally, the mechanistic importance of pre-catalysts, ligands, additives, base, and/or solvents was highlighted via schematic representations. Among the C–C cross-coupling methodologies Suzuki-Miyaura coupling is extensively employed for the creation of bi-aryl derivatives. The key advantage with this strategy is the employment of the boronic acids as coupling partners which are known for their air stability, water-solubility, and ease of derivatization. The Heck reaction is also highly popular for its inter and intra molecular C–C bond formations involving  $Csp^2$  double bonds. Similarly, the Sonogashira coupling reactions facilitate  $Csp^2$ - $Csp$  cross-coupling under mild conditions. Besides, the palladium catalyzed carbon-heteroatom cross-coupling methods extended the applications into various fields, most notably, these strategies have proven highly efficient in developing new libraries of biologically active molecules.

Despite the success in coupling reactions, several challenges are yet to be addressed to make these methods economically realistic. For example, in medicinal chemistry scale-up synthesis generally requires high quantities of precious noble metals such as palladium as well as expensive ligands; this could be a problem. Although, several palladium pre-catalysts were well established for C–C or C–X (where, X= N, O, S, P) cross-coupling, for the large scale synthesis simple catalytic precursors such as  $Pd(OAc)_2$ ,  $Pd(dab)_3$ ,  $PdCl_2(PPh_3)_2$  and others were generally used. The ligand free palladium protocols are known as efficient alternatives for aryl iodides or highly active aryl bromides. Bis-phosphine ligands such as dppf, dppe and many others were employed when they are necessary for coupling. Noticeably, electron-rich phosphine ligand systems were employed for the activation of economically attractive aryl chlorides. However, the research towards developing highly active catalytic precursor and ligand system to achieve high turnover numbers (TON) and turnover frequencies (TOF) is as of yet challenging. Such type of catalysts or pre-catalysts would be economically attractive. Moreover, developing a catalytic system which has high water solubility and catalytic activity would be advantageous in avoiding the post synthetic organic waste (solvents). Additionally, such aqueous phase systems would be beneficial in extracting the metal impurities from the product, which reduces the contaminations. Therefore, a practical and feasible catalytic system with high reactivity and easy extraction procedure is highly desired.

### Chapter 3: The serendipitous discovery of the potent catalyst Pd/PTABS and application in C-X (X= N, O, S) cross-coupling of chloroheteroarenes under milder conditions.

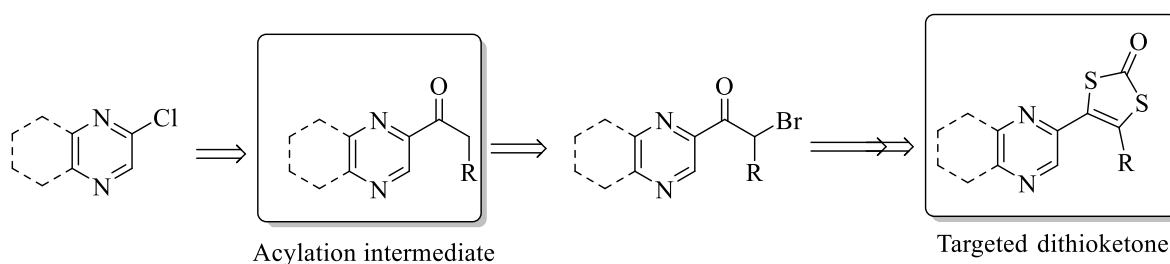


#### 3.1. The unexpected finding: acylation of chloroheteroarene and discovery of Pd/PTABS catalyst.

The history of science is full of numerous examples of serendipitous discoveries and chemistry is not an exception.<sup>275</sup> Like many other discoveries in the chemical sciences (e.g., ferrocene discovery,<sup>276</sup> Birch reduction, Wittig reaction,<sup>277</sup> hetero-Diels-Alder reaction [4+2] cycloaddition (1943),<sup>278</sup> and many others) the results described in this chapter also came as a total surprise. The actual synthetic target was an acylated pyrazine addressed by palladium

catalyzed Heck type transformation of 2-chloropyrazine. Most surprisingly, a 2-aminated pyrazine was obtained as the exclusive product and further analysis by NMR, MS and X-ray diffraction confirms the chemical structure. The zwitterionic water-soluble ligand 1,3,5-triaza-7-phosphaadamantane butylsulfonate (PTABS) was applied in combination with palladium as a catalyst in the reaction. The PTABS derived palladium catalyst had been reported as efficient system for various C–C bond formation procedures involving halonucleosides, namely, Suzuki-Miyaura, Sonogashira, and Heck cross-coupling reactions<sup>279-281</sup> but not for the “C-heteroatom coupling”.

The synthesis of acylation intermediates of heterocycles (pyrazine, quinoxaline, pterin) is one of the critical synthetic steps in the preparation of heterocycles bearing dithiolene moieties (Scheme 3.1). These species are essential targets for the working group. Therefore, the development of strategies and optimizations constitute focal issues for all team members towards ketone intermediates. In the account of this research, initially, a variety of non-transition metal approaches were investigated.



**Scheme 3.1:** Formal synthetic procedure for the synthesis of the dithioketone system. The acylation intermediate is highlighted in the left inbox.

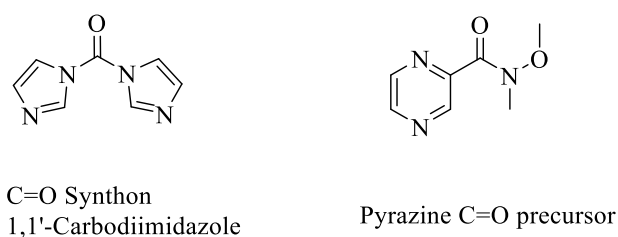
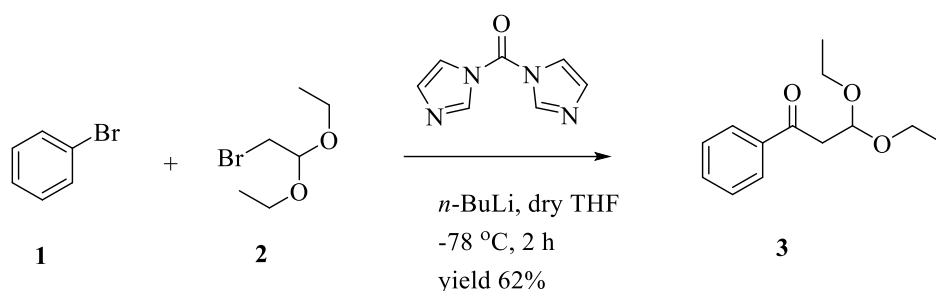


**Figure 3.1**

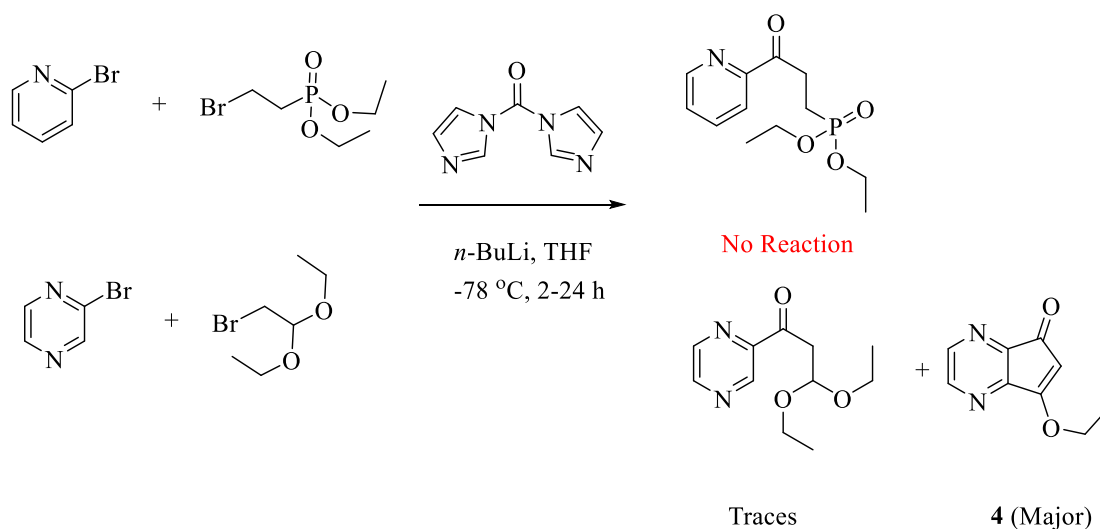
The 1,1'-carbodiimidazole (CDI) and pyrazine C=O precursors (Figure 3.1) were selected as carbon monoxide synthons in the acylation of aryl(hetero)halides. As depicted in scheme 3.2, initially, the *in situ* prepared phenyl lithium of test compound **1** reacted with CDI for one hour at lower temperatures; sequentially, a freshly prepared lithiated derivative of **2** was added at -78 °C under inert conditions in dry THF. The desired acylated phenyl derivative **3** was obtained

in moderate yields (62%). The product was isolated and characterized by <sup>1</sup>H-NMR spectroscopy.

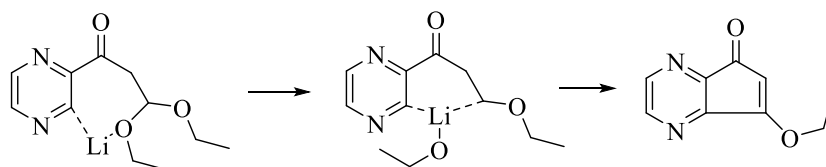


**Scheme 3.2:** CDI used as C=O synthon for preparing un-symmetrical ketones.

However, the application of a similar sequential addition strategy with nitrogen-heterocycles such as 2-bromopyridine and 2-chloropyrazine failed (Scheme 3.3). Notably, the highly reactive lithiation conditions and the sequential additions derived the cyclized product **4** as a major product with 2-bromopyrazine. The formation of cyclized product **4** was attributed to the lithium mediated C–H activation followed by aromatization (Scheme 3.3).<sup>282</sup>



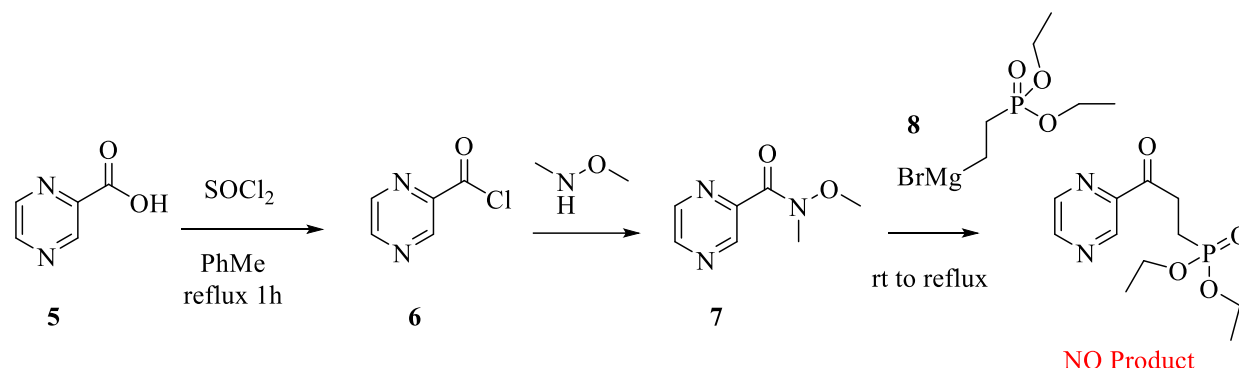
Plausible lithium mediated C-H activation and cyclization



**Scheme 3.3:** Application of the C=O synthon procedure on heterocyclic aryl halides and the proposed reaction mechanism to yield **4**.

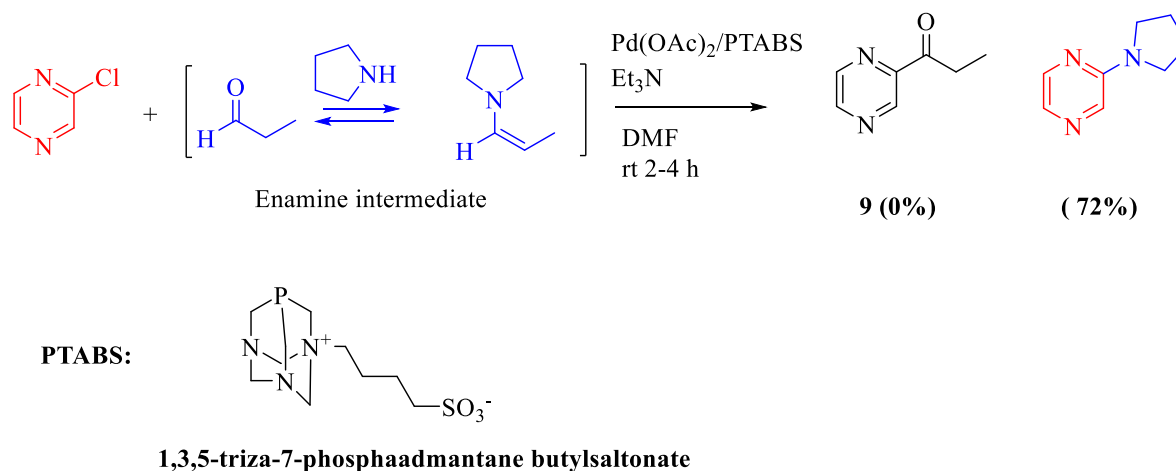
The second C=O synthon (Figure 3.1; pyrazine C=O synthon) was obtained simply from pyrazine 2-carboxylic acid (**5**) in a couple of reaction steps (Scheme 3.4). Subsequently, it was reacted with *in situ* prepared Grignard intermediate **8**. The desired product was not observed

either at room temperature or under reflux conditions. Moreover, the APCI-MS analysis of the crude reaction mixture suggested the ready decomposition of the Grignard intermediate to the corresponding de-brominated (de-halogenation) derivative under applied conditions.



**Scheme 3.4:** Employing a pyrazine amide ester precursor in acylation.

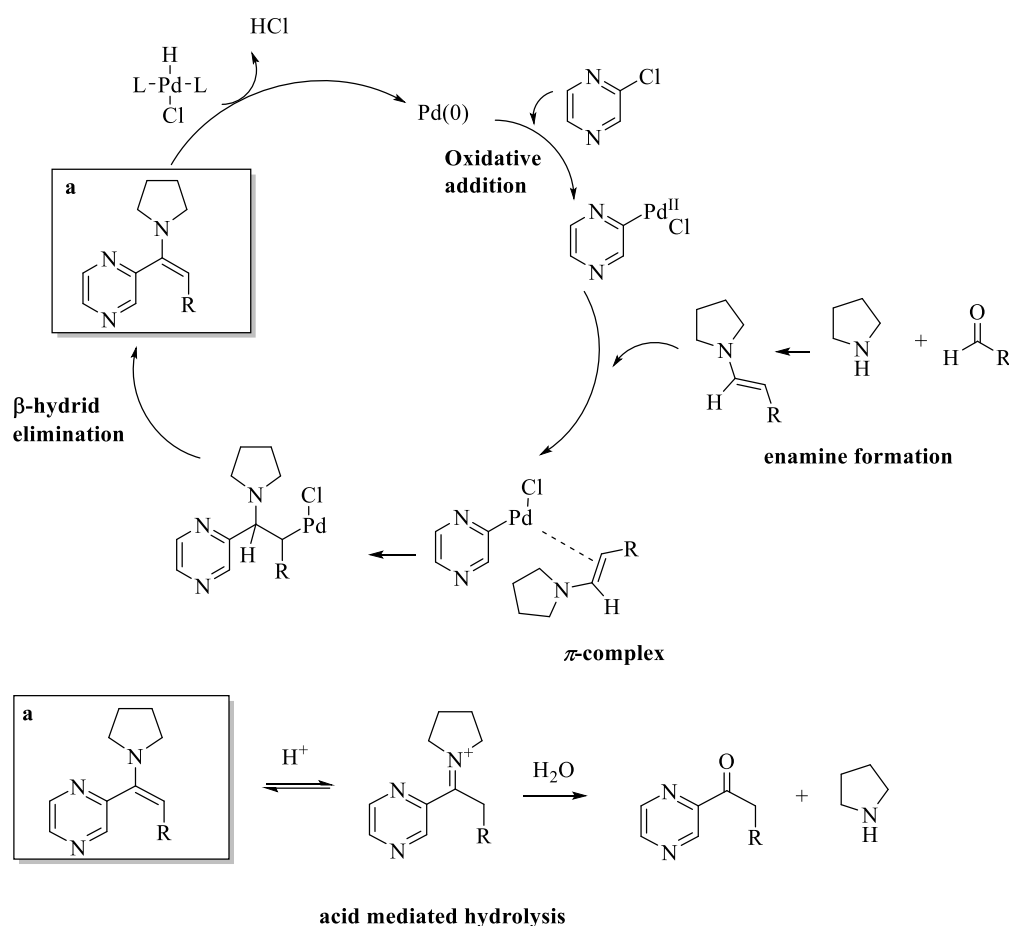
These failures with transition metal free approaches prompted us to choose a transition metal-catalyzed approach for further investigations. Accordingly, the Mizoroki-Heck type of cross-coupling of 2-chloropyrazine with an enamine intermediate of acetaldehyde (prepared *in situ* by a secondary amine) in the presence of (PTABS) derived palladium catalyst in DMF was envisaged (Scheme 3.5).



**Scheme 3.5:** Pd-PTABS catalyzed acylation trial on 2-chloropyrazine with an aldehyde (enamine). Synthesis of un-expected 2-(pyrrolin-1-yl)pyrazine).

The plausible reaction mechanism for such a reaction is depicted in scheme 3.6. The mechanism proceeds via the oxidative addition of palladium (0) on 2-chloropyrazine forming the Pyz-Pd-Cl complex which undergoes a  $\pi$ -complexation with the *in situ* prepared enamine intermediate (aldehyde and secondary amine) resulting in Pyz-Pd-Cl *syn*-insertion adduct. The subsequent  $\beta$ -hydride elimination leads to the corresponding enamine “a”. The resultant enamine, “a”, undergoes acid-mediated hydrolysis during the acidic workup and was expected

to furnish the desired acylated pyrazine product. However, the expected acylated derivative was never observed under these reaction conditions. To our surprise, the unexpected C-N cross-coupled product 2-(pyrrolidine-1-yl)pyrazine was identified as the major product. The obtained results were confirmed with another secondary amine (morpholine) under identical conditions, resulting in the formation of 2-(morpholine-1-yl)pyrazine as the only product observed. Therefore, the protocol was found to be reproducible.



**Scheme 3.6:** Plausible mechanism for Pd-catalyzed acylation.

X-ray structural analysis unambiguously confirmed the final structures. The exclusive formation of the C-N cross-coupled product is tentatively attributed to the low availability of the enamine intermediate at the time of the  $\pi$ -complexation event or the presence of excess amounts of the secondary amine might have created a competitive nucleophilic coupling partner (amine), consequently favouring C-N cross-coupling.<sup>170</sup> These findings were from a synthetic point of view relevant enough to warrant a wide classified investigation into the “C-heteroatom” cross-coupling abilities of the Pd/PTABS catalyst.



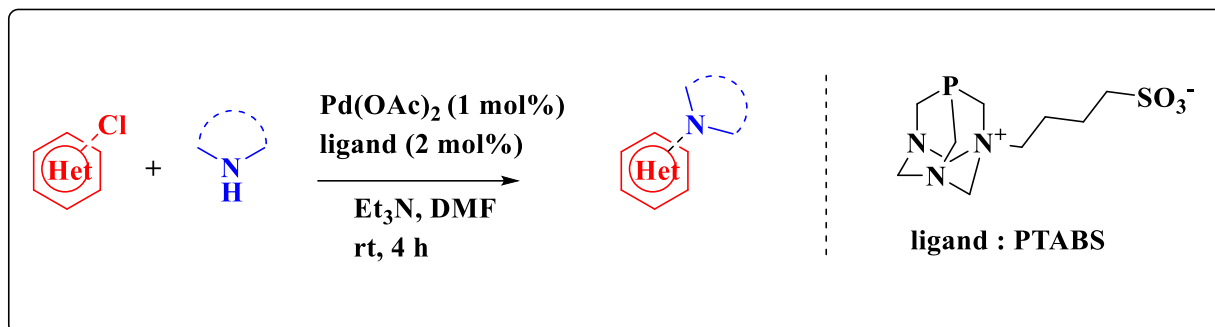
### 3.2. Pd/PTABS: Carbon-heteroatom (C-X, where X= N, O, and S) cross-coupling of *chloroheteroarenes*.

#### Overview

The serendipitously discovered Pd/PTABS catalyst was investigated thoroughly in C-heteroatom cross-coupling reactions including C-N, C-O, and C-S bond formation. The exceptional Pd/PTABS catalyst offered excellent conversion in all tested carbon-heteroatom couplings and tolerated well a wide variety of *chloroheteroarenes* and *chloronucleosides* such as pyrazine, pyrimidine, quinoxaline, pterin, uracil, purine, uridine and others. Under Pd/PTABS catalytic conditions, the C-N cross-coupling could be performed at room temperature and quantitative conversions were achieved within two hours (except for nucleosides). The important anti-diabetic DPP4-inhibitor drug “Alogliptin”, was synthesized in quantitative yields with this method. The C-O cross-coupling of *chloroheteroarenes* with a variety of phenols was efficiently catalyzed by the PTABS derived palladium catalyst under much milder than typical conditions. The anticancer agent “XRK-469” was successfully synthesized with the help of the current protocol. Interestingly, the high regio- and chemo-selectivity of the catalyst was manifested in various examples. Additionally, the employment of Pd/PTABS catalyst for the C-S cross-coupling of *chloroheteroarenes* with thiophenols and alkylthiols resulted in aryl/alkyl thioethers in excellent yields at 50°C in 4 h. Furthermore, novel sulfones and sulfoximines were also prepared from the resultant thioethers via mild oxidation procedures. The immunosuppressive drug *Imuran* (azathioprine) was synthesized in competitive yields via Pd/PTABS catalysis.

DFT studies were carried out in order to understand the detailed electronic effects of 1,3,5-triaza-7-phosphadmantane (PTA) and PTA quaternized derivatives (PTABS, PTAPS, PTABBr, PTABI, PTABCl, and PTABn) in comparison to known commercial phosphine ligands XPhos and SPhos in the catalytic thioetherification process. Each coupling reaction type is discussed in detail in the following individual sub-chapters, 3.3, 3.4 and 3.5 in which the results and discussions for C-N, C-O and C-S cross-coupling are described, respectively. More than 30 examples of cross-coupled products were prepared in each protocol partly with the help of cooperation partner Prof. Dr. Anant R. Kapdi and his co-workers. Results of the C-N, C-O, and C-S cross-coupling reactions as catalyzed by Pd/PTABS were already published by us in peer-reviewed scientific journals.<sup>283-286</sup> Comprehensive experimental detail in the respective chapter section is given only for the molecules which were prepared at the University of Greifswald.

### 3.3. Pd/PTABS: The C–N cross-coupling of *chloroheteroarenes* with secondary amines at room temperature.



#### 3.3.1. Background

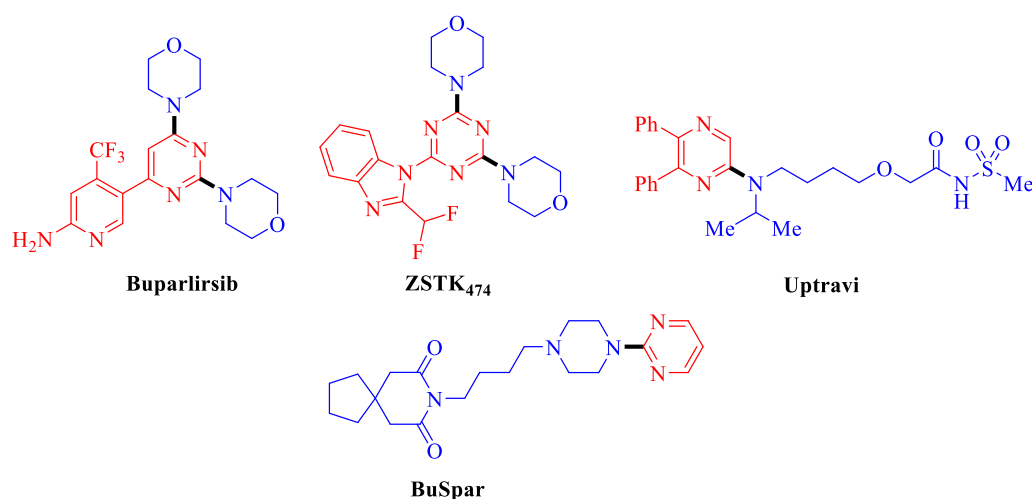


**Figure 3.2:** Secondary amine-functionalized biologically active heterocycles.

Amine substituted heteroaromatic compounds are known as critical functional and structural moieties in various biologically and pharmaceutically active compounds.<sup>287</sup> The amine functionality is prevalent in commercially available active pharmaceutical ingredients (Figure 3.2), for example, ZSTK<sub>474</sub>, buparlirib (anticancer),<sup>288-289,290</sup> uptravi (hypertension),<sup>291</sup> and BuSpar (antidepressant).<sup>292</sup> Thus, developing efficient synthetic methodologies to carry out the C–N cross-coupling reactions has become a fundamental area of research in organic synthesis.

The amination of halo(hetero)arenes via efficient C–X bond activation (where, X = I, Br and Cl) by Pd-catalyzed Buchwald-Hartwig amination is a widely accepted protocol in the scientific community.<sup>181, 184</sup> Especially, the commercial availability of the Buchwald series of ligands offered an opportunity for accelerated growth in Pd-catalyzed C–N cross-coupling research.<sup>174</sup> In recent years, several other catalytic systems were introduced for the amination

of bromo- or iodo (hetero) arenes and reactions were efficiently operated at ambient temperature.<sup>293</sup> However, there is a scarcity of an efficient catalytic protocol for the amination of commercially available and inexpensive *chloroheteroarenes*.

The combination of simple Pd precursors and different ligands was proven beneficial in the amination of *chloroheteroarenes*. For example, Beller investigated the amination of *chloroheteroarenes* in the presence of the sterically bulky diadamantylphosphine ligand<sup>294-296</sup> and Buchwald employed a few active phosphine ligands from their developed ligand library.<sup>183</sup> Phosphoramidite ligands were applied by Plenio<sup>297</sup> and Reetz<sup>298</sup>, and Organ's Pd-PEPPSI catalysts was similarly successful in C-N cross-coupling.<sup>299-300</sup> Although, the C-Cl activation was accomplished with all above mentioned active ligands, they do suffer from limited synthetic utility. Most of these synthetic protocols resulted in competitive yields at higher temperatures ranging between 80-130 °C, under strong alkaline conditions and most often at higher catalyst concentrations. Although a few aminations of *chloroheteroarenes* at ambient temperature were reported by Buchwald<sup>301</sup>, Hartwig<sup>302</sup>, Stradiotto<sup>303</sup>, and Nolan, the complexity of ligands and their moisture sensitivity limits their practical applications.<sup>304</sup> Thus, there is a need for better synthetic protocols for the amine functionalization of *chloroheteroarenes* at milder reaction conditions with high selectivity and broad applicability.

As an alternative solution to these challenges, the Pd/PTABS catalytic system was discovered and comprehensively investigated for the amination of *chloroheteroarenes*. Furthermore, to establish its catalytic superiority, a comparative study (optimization) with known active phosphine ligands was conducted. Additionally, the tolerability of the developed optimised synthetic protocol to an enormous substrate scope and subsequent synthesis of biologically active heterocyclic scaffolds was investigated.

### 3.3.2. Results and Discussion

*Synthesis of 1,3,5-triaza-7-phosphaadamantane butylsulfonate (PTABS) and 1,3,5-triaza-7-phosphaadamantane propylsulfonate (PTAPS):*

Two water-soluble zwitterionic phosphotriazine ligands **PTABS** and **PTAPS** were synthesized in quantitative yields according to the procedure of Bergamini et al.<sup>305</sup> Both zwitterionic phosphines were obtained through 1,3,5-triaza-7-phosphaadamantane (PTA) N-alkylation with 1,3-propane sulfone or 1,4-butanediol sulfone (Figure 3.3a). The N-alkylation takes place only on a single nitrogen atom with high regioselectivity, without perturbing the vacant P-site of the ligand, which is critical for the coordination with soft metals during catalysis. The purified

fractions of PTABS and PTAPS were isolated after recrystallization from hot acetone and characterized by  $^1\text{H}$ ,  $^{13}\text{C}$  and  $^{31}\text{P}$ -NMR. In the  $^{31}\text{P}$  NMR, the phosphorous signal was shifted down field in **PTABS** ( $\delta$  ppm: -84.43) and **PTAPS** ( $\delta$  ppm: -83.7) in comparison to starting material **PTA** ( $\delta$  ppm: -100.2). Also, the X-ray crystal structure analysis of **PTAPS** confirms the formation of the quaternized ionic ligand (Figure 3.3b).

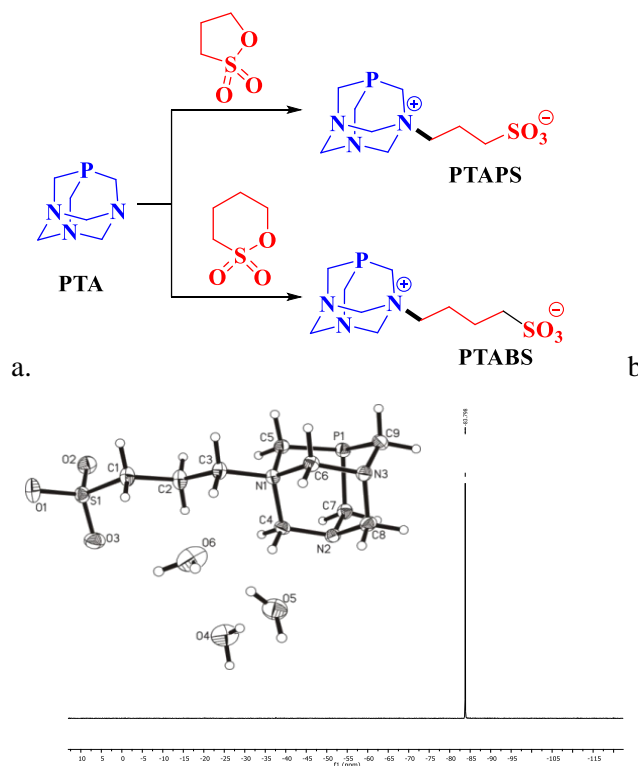


**Figure 3.3:** a) Synthesis of PTABS and PTAPS ligands. b) The  $^{31}\text{P}$  NMR and ORTEP view of compound PTAPS, thermal ellipsoids are drawn at 50% probability level.

The coordination of these ligands with metals like Pt, Ru, and Pd results in the formation of water-soluble complexes.<sup>307</sup> Due to their high water solubility, the Pt(II) and Ru(II) complexes of PTABS and PTAPS were thoroughly investigated as anti-proliferative agents in human cancer cell lines and found efficacious.<sup>307</sup> Most importantly, PTABS and PTAPS in combination with  $\text{Pd}(\text{OAc})_2$ , resulted in a powerful catalytic system for the Suzuki coupling, Heck coupling and copper-free Sonogashira coupling in halonucleosides under milder conditions in the aqueous phase.<sup>304</sup>

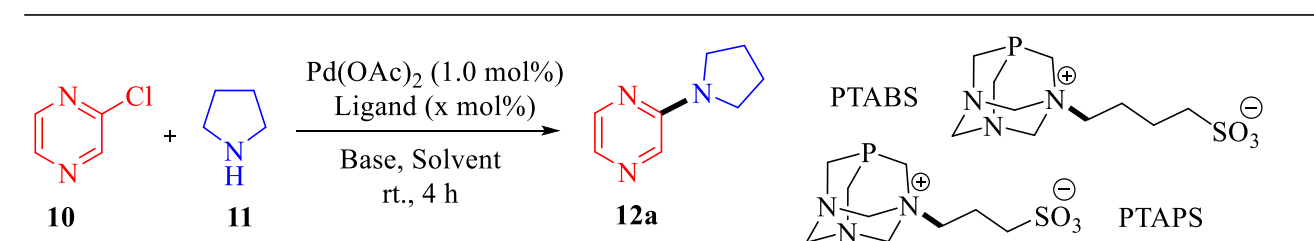
### 3.3.3. C–N cross-coupling reaction optimization

In the optimization study, different activating phosphine ligands were screened in combination with the  $\text{Pd}(\text{OAc})_2$  precursor (Table 3.1). It is worth to mention that the transition metal-free  $S_NAr$  type amination reactions are also possible at ambient temperatures. Recently, Moody and

co-workers developed a transition-metal free *chloroheteroarene* amination procedure.<sup>303</sup> These results required verification whether the reaction, under metal-free conditions, with two equivalents of pyrrolidine (acts as both starting material and base), in DMF as solvent, at room temperature, was possible. The product formation was not observed even after 24 hours of stirring; thus, a  $S_NAr$  type reaction mechanism under these conditions could be excluded. Notably, the formation of the product was identified only in lower yields in ligand-free conditions in the presence of 0.5-1.0 mol% of Pd(OAc)<sub>2</sub>, (up to 20% isolated). This proves the involvement of the Pd-catalytic cycle in product formation.

In the next step, the role of the activated ligand was investigated. The addition of triphenylphosphine to the reaction system has very little influence on the improvement of reaction yields, whereas electron-rich monophosphines SPhos or XPhos ligands enhanced the yields of the amination product up to 73%. Further, the employment of high electron-rich and sterically demanding *tert*-Bu<sub>3</sub>P.HBF<sub>4</sub> and of Beller's ligand (Ad)<sub>2</sub>BuP provided competitive yields, while the commercially available Pd-PEPPSI-Ipr catalyst resulted in the highest yield of 75% among all tested ligands. Lastly, the water-soluble PTABS and PTAPS ligands were employed in combination with the Pd precursor, and the best results were evidenced with 2 mol% PTABS and 1 mol% Pd(OAc)<sub>2</sub> in DMF when pyrrolidine was used in excess (**entry 13**, 79%). It is evident from **entry 14** that the absence of a Pd source in the reaction completely quenched the product formation. Notably, reducing the concentration of either Pd or ligand (PTABS) has shown a detrimental effect and minimized product formation (**entry 15, 16**).

**Table 3.1:** Screening of the amination of *chloroheteroarene* at room temperature.



Entry	<b>11</b> (Equiv.)	Ligands	Ligand (mol%)	Base (Equiv.)	Solvent	Yield <sup>a</sup> (%)
1. <sup>b</sup>	2.0	--	--	--	DMF	0
2. <sup>c</sup>	2.0	--	--	--	DMF	20
3.	2.0	PPh <sub>3</sub>	1.0	--	DMF	30
4.	2.0	SPhos	1.0	--	DMF	63
5.	2.0	XPhos	1.0	--	DMF	70

6.	2.0	XPhos	2.0	--	DMF	73
7.	2.0	<sup>t</sup> Bu <sub>3</sub> P	1.0	--	DMF	54
8.	2.0	<sup>t</sup> Bu <sub>3</sub> P.HBF <sub>4</sub>	1.0	--	DMF	62
9.	2.0	(Ad) <sub>2</sub> BuP	2.0	--	DMF	69
10.	2.0	PEPPSI	1.0	--	DMF	75
11.	2.0	PTABS	1.0	--	DMF	60
12.	2.0	PTApS	1.0	--	DMF	55
13.	2.0	PTAPS	2.0	--	DMF	79
14. <sup>d</sup>	2.0	PTABS	2.0	--	DMF	0
15. <sup>e</sup>	2.0	PTABS	1.0	--	DMF	58
16. <sup>f</sup>	2.0	PTABS	0.2	--	DMF	50
17.	1.2	PTABS	2.0	K <sub>2</sub> CO <sub>3</sub> (1.0)	DMF	72
18.	1.2	PTABS	2.0	<sup>t</sup> BuOK (1.0)	DMF	74
19.	1.2	PTABS	2.0	NEt <sub>3</sub> (1.0)	DMF	83
<b>20.</b>	<b>1.2</b>	<b>PTABS</b>	<b>2.0</b>	<b>NEt<sub>3</sub>(1.5)</b>	<b>DMF</b>	<b>88</b>
21.	1.2	PTABS	2.0	NEt <sub>3</sub> (1.5)	ACN	72
22.	1.2	PTABS	2.0	NEt <sub>3</sub> (1.5)	H <sub>2</sub> O	69
23.	1.2	PTABS	2.0	NEt <sub>3</sub> (1.5)	H <sub>2</sub> O:ACN	75

**Reaction conditions:** 1.0 mmol of **10**, 1.0 mol% of Pd(OAc)<sub>2</sub>, 3 mL of solvent, H<sub>2</sub>O: ACN (1:1), stirring at room temperature for 2-4 hours, <sup>a</sup> isolated yields, <sup>b</sup> without added Pd(OAc)<sub>2</sub> and ligand, <sup>c</sup> without added ligand, <sup>d</sup> without added Pd(OAc)<sub>2</sub>, <sup>e</sup> 0.5 mol% of Pd(OAc)<sub>2</sub>, <sup>f</sup> 0.1 mol% of Pd(OAc)<sub>2</sub>.

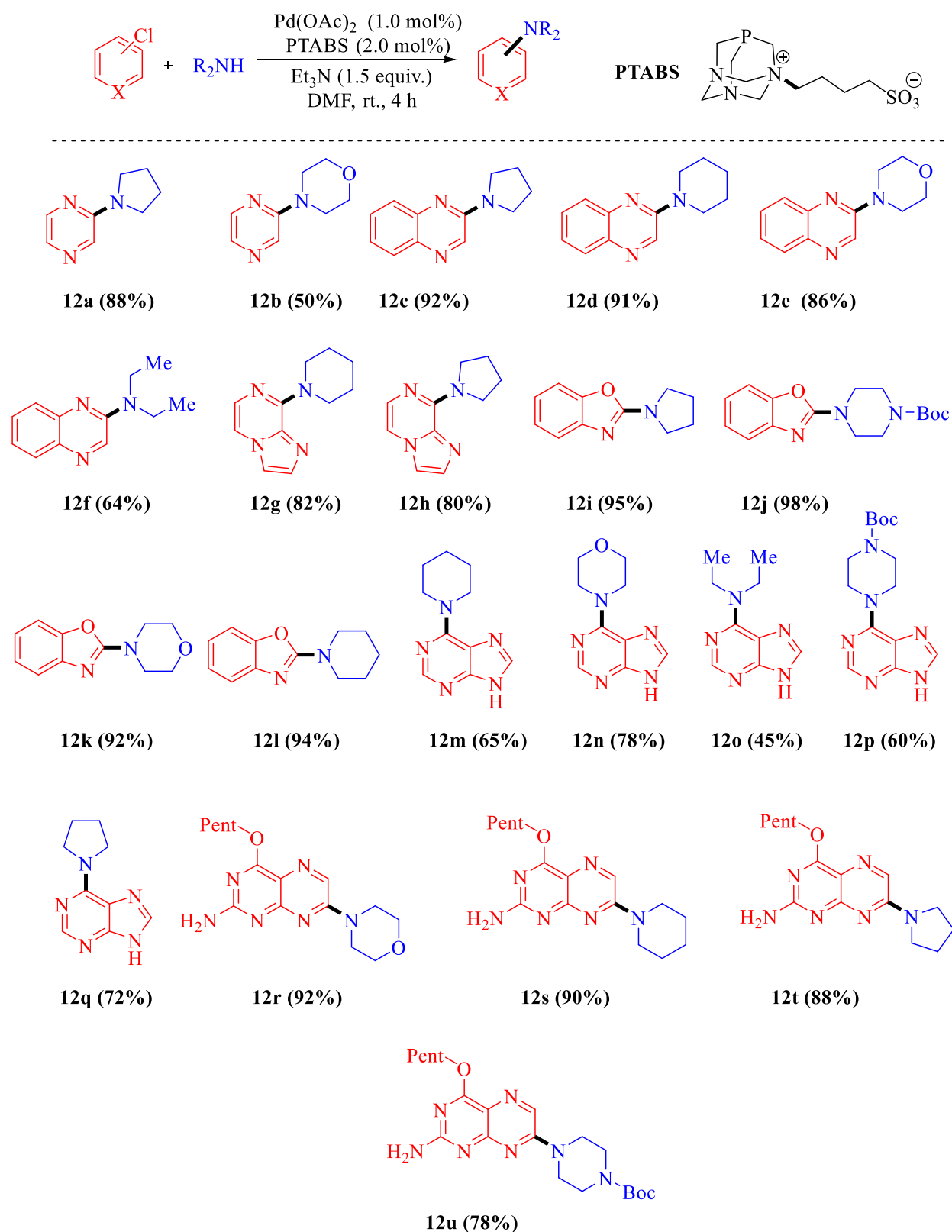
In the next phase, the dependence of the catalytic cycle on the pK<sub>a</sub> of the external inorganic or organic amine bases was investigated. Improved yields were evidenced with the employment of exogenous base triethylamine (1.5 equiv., **entry 20, 88%**), and, importantly, the yields were consistent even at lower equivalents of amine starting material (1.2 equiv.). Among all tested solvents, DMF allowed the highest catalytic conversion with Pd/PTABS, while other solvents including water or a water/ACN mixture, still resulted in appreciable product formation; however, the yields were lower. Hence, the optimized conditions for the amination of *chloroheteroarenes* at ambient temperature comprise 1 mol% Pd(OAc)<sub>2</sub>, 2 mol% of PTABS with only 1.2 equivalents of a secondary amine and 1.5 equivalents of triethylamine base in DMF.

### 3.3.4. Substrate scope development

The now optimized amination protocol at ambient temperature was then further investigated with a wide variety of *chloroheteroarenes* and cyclic or acyclic secondary amines pyrrolidine, piperidine, morpholine, NH-Boc protected piperazine, and diethylamine. Initially, 2-chloropyrazine and 2-chloroquinoxaline were coupled with these secondary amines at room temperature (Scheme 3.7, **12a-12f**). Although lower yields were observed for 2-(morpholino-

1-yl)pyrazine **12b**, all other coupled derivatives resulted in excellent yields. These promising results with simple heterocycles inspired us to also test the protocol for challenging and synthetically important heterocyclic substrates. The pyrrolo[1,2-a]pyrazines and benzofuran constitute promising bioactive scaffolds present in a variety of anticancer, antifungal and antioxidant drugs.<sup>306 307</sup> The catalytic amination of benzofuran or pyrrolo[1,2-a]pyrazine with secondary amines resulted in novel aminated products **12g-12l** in good yields.

Chapter 3: Pd/PTABS catalysis for C-N cross-coupling with *chloroheteroarenes*.



**Scheme 3.7:** Substrate scope for the amination of *chloroheteroarenes*.



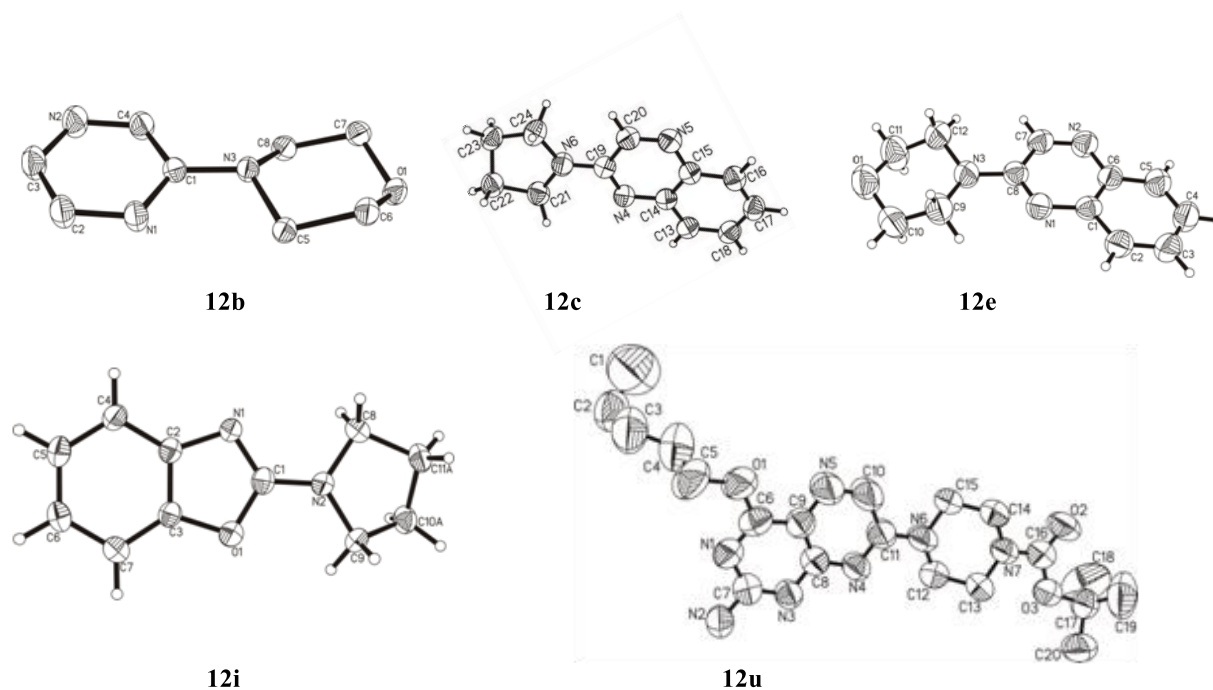


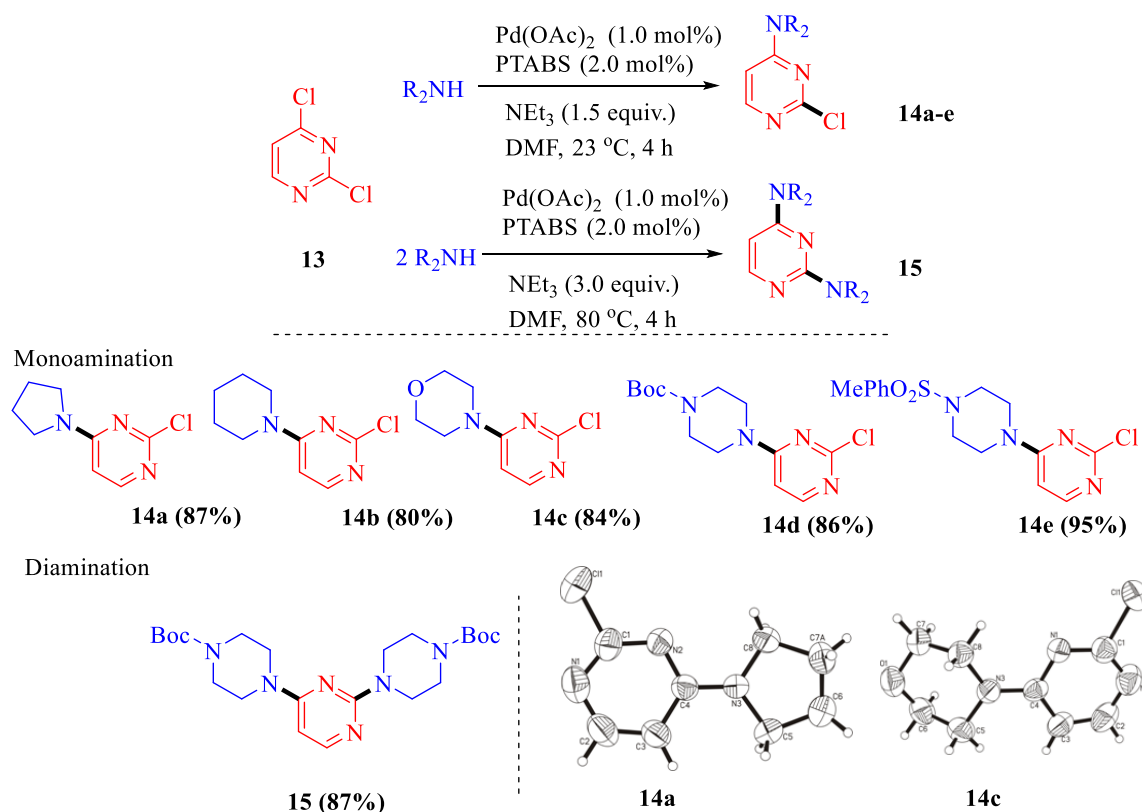
**Figure 3.4:** Molecular structures of compounds **12b**, **12c**, **12e**, **12i**, **12u** with ellipsoids at the 50% level. The hydrogen atoms in **12b** and **12u** were omitted for clarity reasons.

The Pd/PTABS catalytic amination of 6-chloropurine with various secondary amines derived the amine-functionalized purine products in good yields (Scheme 3.7, entries **12m-q**), except diethylamine for which a lower yield was evidenced. The crude reaction mixture analysis by mass spectrometry indicates more hydro-dehalogenation products in this case, while diethylamine has shown relatively low nucleophilicity under the optimized conditions.

Pteridines are vital heterocyclic units with diverse applications in medicinal chemistry. It is envisaged that further amine functionalization of pteridine derivatives would be beneficial in enhancing fluorescent properties as well as their physiological activity. Accordingly, 6-chloropteridine was used for the amination under Pd/PTABS catalytic conditions with various secondary amines at ambient temperature. In general, the protection of the free amine functionality of the pteridine is mandatory in several metal-catalyzed cross-coupling procedures.<sup>309</sup> Whereas, in the presence of Pd/PTABS, pteridines give excellent yields of amine-functionalized products **12r-12u**, without the protection of the free amine. This further confirms the milder nature, potential and extended applicability of the developed amination protocol. Furthermore, the final structures of **12b**, **12c**, **12e**, **12i** and **12u** were confirmed by X-ray single crystal diffraction analysis (Figure 3.4)

Maintaining the regioselectivity is one of the critical challenges in transition metal-catalyzed cross-coupling chemistry. The developed catalytic protocol was examined for its applicability

in substrates, in which the probability of having regioselective competition is unavoidable. Interestingly, when the substrate 2,4-dichloropyrimidine was employed in the amination reaction with a variety of secondary amines, such as pyrrolidine, piperidine, morpholine and piperazine at ambient temperatures, the selective 4-substituted amination products (Scheme 3.8, **14a-e**) were isolated in good yields. This mono-selectivity towards the 4-chloro position in 2,4-dichloropyrimidine allows further synthetic alterations on the 2-chloro position. Notably, the increase in temperature to 80 °C provided predominantly the diamination product even when only one equivalent of the secondary amine was employed in the reaction (unreactive starting material recovered). Therefore, two equivalents of secondary amines can be used at higher temperatures to furnish completely diarylated products. Hence, the desired regioselectivity is achievable through controlling the temperatures of the reaction in the developed amination protocol.

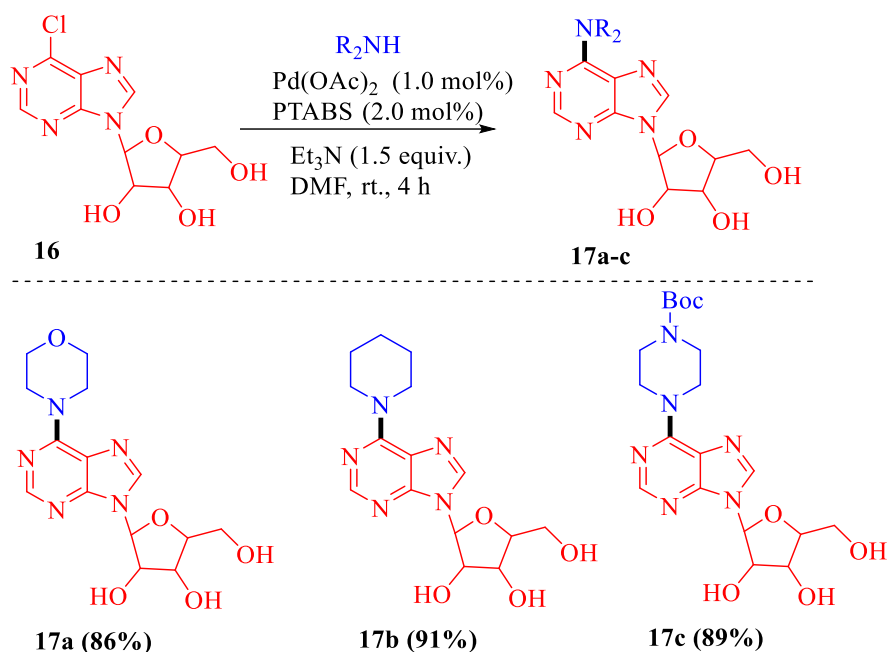


**Scheme 3.8:** Monoselective amination and diamination of 2, 4-dichloropyrimidine. Molecular structures of compounds **14a**, **14c** with ellipsoids at the 50% level.

The initial success in the amination of 6-chloropurine (Scheme 3.7, **12m-q**) and the milder operating conditions of the developed protocol were encouraging enough to investigate the catalytic amination of 6-chloro-9- $\beta$ -D-ribofuranosylpurine with various secondary amines. The amination of silyl-protected ribose nucleosides in competitive yields were previously reported

in the literature by Kooman,<sup>310</sup> Schmalz,<sup>311</sup> and Lakshman.<sup>312 313</sup> The Pd/PTABS catalyzed amination of 6-chloro-9-β-D-ribofuranosylpurine with different secondary amines resulted in respective aminated derivatives in good to excellent yields (Scheme 3.9, **17a-c**). Most importantly, the catalytic process delivered the amine-functionalized purines without any need for the protection of the hydroxyl groups on the sugar ribose backbone.

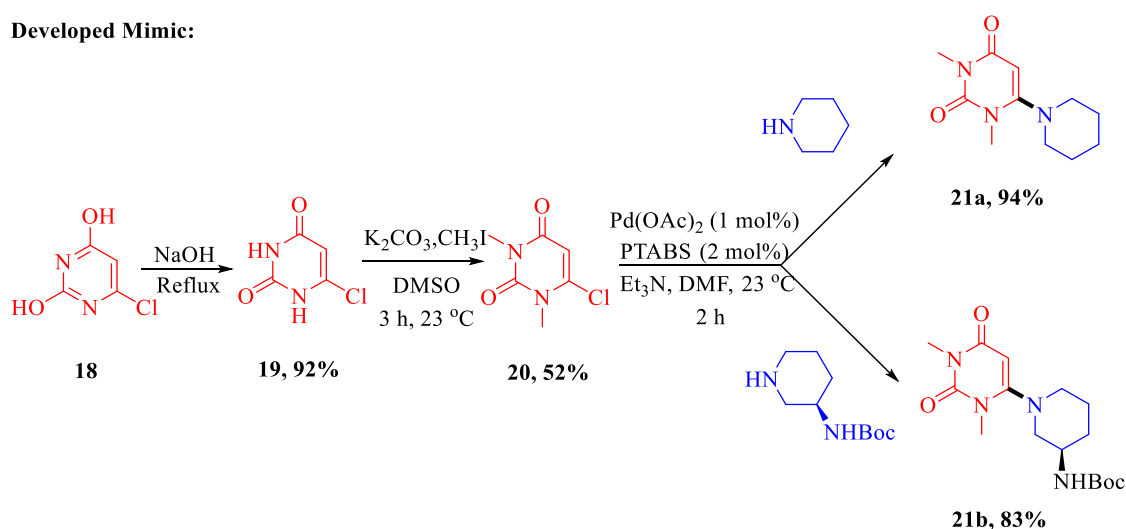
To establish the applicability of the developed catalytic amination protocol towards the synthesis of commercially available drug candidates, the formal synthesis of the anti-diabetic agent “Alogliptin” was investigated. Alogliptin is a uracil based biologically active *DPP-4* enzyme inhibitor that could be prepared by simple amidic N-H bond protections of halo-uracil followed by subsequent amination.<sup>314</sup>



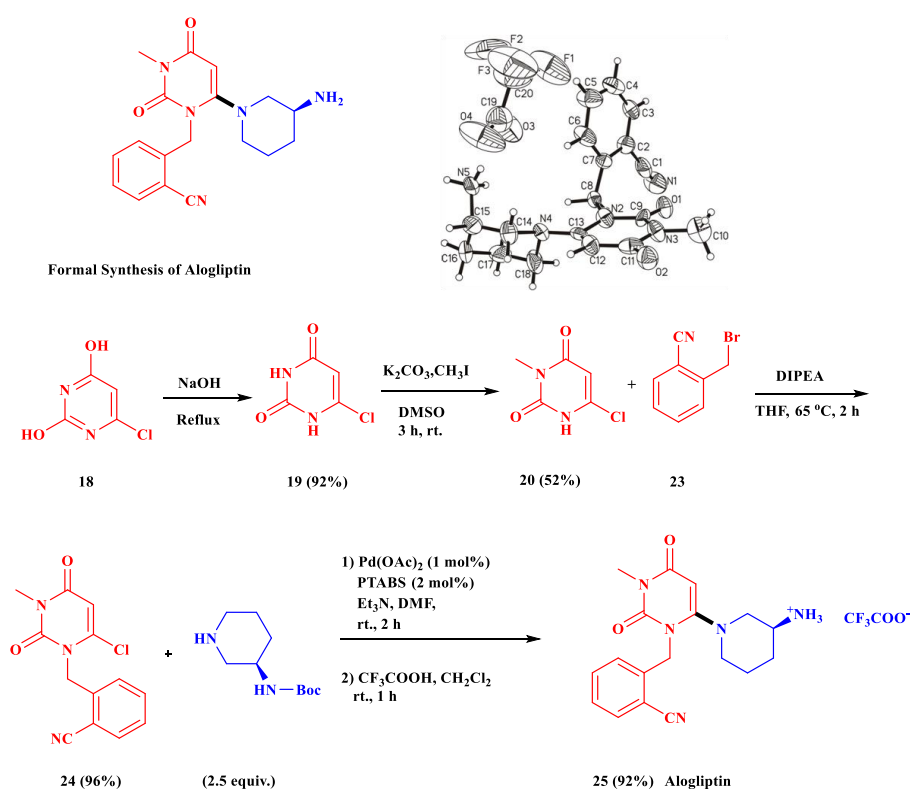
**Scheme 3.9:** Pd/PTABS catalytic amination of 6-chloropurine ribosides.

In a test reaction sequence, N-H amidic protons of 6-chloro uracil (**19**) were protected with methyl iodide under alkaline conditions, and subsequent catalytic amination of product **20** with two different secondary amines namely, piperidine and tert-butyl (*R*)-piperidine-3-ylcarbamate resulted in structural mimics of alogliptin **21a**, **21b** in excellent yields (Scheme 3.10).

Developed Mimic:



Scheme 3.10: Synthesis of structural mimics of alogliptin.

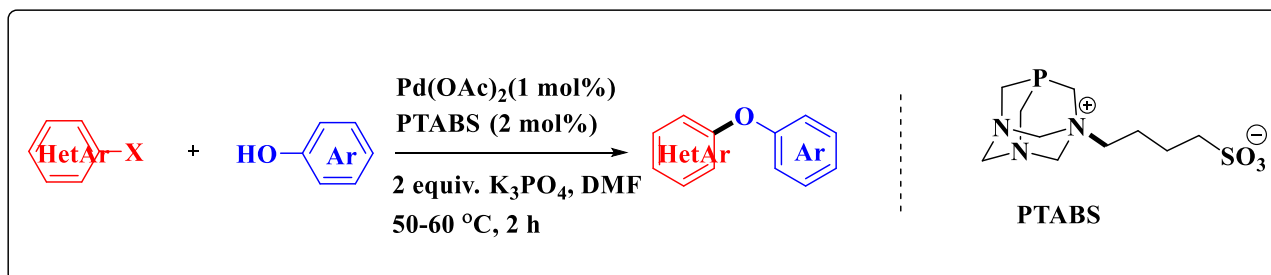


Scheme 3.11: Formal synthesis of anti-diabetic agent alogliptin. Molecular structure of alogliptin with ellipsoids at the 50% level.

Secondly, to afford “Alogliptin” itself, the 6-chlorouracil (**19**) bearing two N-H amidic protons was first sequentially protected with methyl iodide and 2-cyano benzyl bromide under alkaline conditions. These two reaction steps proceeded with quantitative conversions (Scheme 3.11, **19**, **20**) resulting in the desired protected 6-chlorouracil derivative **24** in 96% isolated yields. Consequently, in the Pd-catalyzed amination in the presence of PTABS ligand, the compound **24** reacted with the NHBoc protected 3-(R)-aminopiperidine followed by an acid-mediated

deprotection of NHBoc giving the targeted anti-diabetic drug “Alogliptin” (**25**). The catalytic process has shown higher conversions under milder reaction conditions with improved quantitative yields than previously reported procedures (Scheme 3.11).<sup>314</sup> Furthermore, the final molecular structure of the resultant Alogliptin’s ammonium salt with the trifluoroacetate counter anion was confirmed by X-ray single-crystal structural analysis.

### 3.4. Pd/PTABS: The C–O cross-coupling of *chloroheteroarenes* with substituted phenols under milder conditions.



#### 3.4.1. Background

The etherification of *chloroheteroarenes* is one of the most essential synthetic approaches practiced in organic chemistry for developing biologically active molecules such as Sorafenib,<sup>315</sup> AMG 900,<sup>316</sup> antitumor agent XK-469,<sup>317</sup> and herbicides such as bispyribac-sodium (Figure 3.4).<sup>318</sup> Given the importance of the etherification methodology for accessing novel drug moieties, researchers are always in a quest for a promising transition metal-catalyzed process. The initial reports from Ullmann and Chan-Lam-Ivan described successful Cu-catalyzed diaryl ether preparations.<sup>319-320</sup> However, these protocols were not encouraged by the industry due to the employed stoichiometric units of copper as well as highly expensive boron reagents.

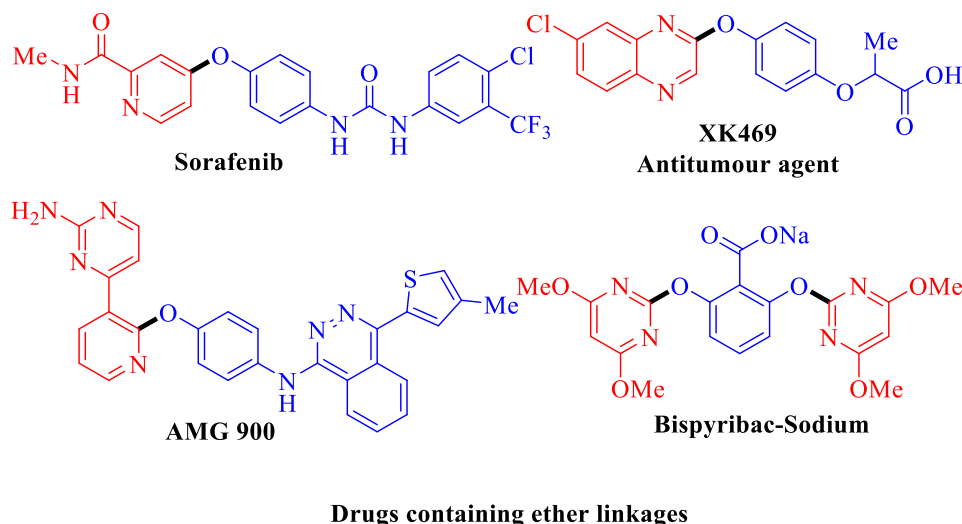


Figure 3.4: Examples of biologically active molecules with ether linkages.

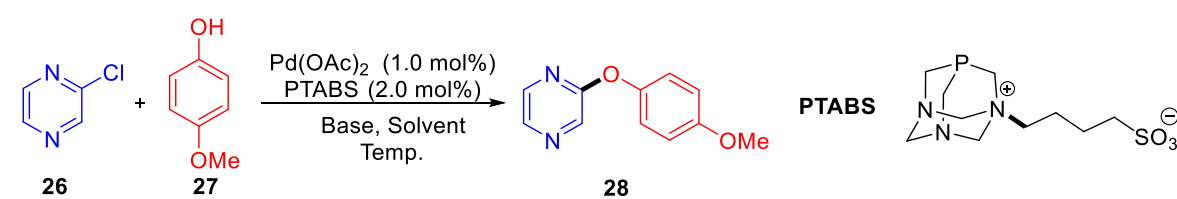
In general, most of the copper-catalyzed etherification protocols are associated with drawbacks such as low yields and limited substrate scope applicability. As an alternative, researchers used

palladium as catalyst for the etherification of aryl halides ArX (where, X= Br, I or Cl) with phenols and this gained much attention due to improved yields and a broad range of substrate tolerability. Researchers like Buchwald,<sup>207, 321, 322, 323</sup> Olofsson,<sup>234, 324</sup> Hierso,<sup>325</sup> and Beller<sup>230</sup> employed highly electron-rich bulky phosphine ligand systems in combination with palladium precursors in etherification processes.<sup>326-329</sup> Rarely, aryl silanes, and aryl stannanes were also used as coupling partners and proven effective. However, only a minimal number of protocols are known for the etherification of *chloroheteroarenes* with phenols.

The functional modification of heterocycles is an important synthetic strategy, due to their wide occurrence in many biologically active molecules and pharmaceutical drugs. Yamaguchi recently reported a Pd or Ni catalysed decarbonylative process for diaryl ether preparation in competitive yields. However, the developed protocol has a series of limitations like utilizing high-temperature conditions for long duration, restricted substrate tolerability and high Pd/Ni catalyst loadings (>5 mol%) in combination with expensive air-sensitive bulky ligands.<sup>330</sup> Such challenges in the process of preparing di(aryl)ethers were conquered employing the Pd/PTABS catalyst under substantially milder conditions. Furthermore, the catalyst's tolerability profile over a wide range of electron-rich and electron-poor phenols was investigated and the respective results are described. Finally, the practicality of the protocol was verified in drug synthesis and tandem procedures.

### 3.4.2. Results and discussion: C-O cross-coupling reaction optimization

Table 3.2: Optimization of the etherification reaction conditions <sup>a</sup>



Entry	ligand	Catalyst loading (mol%) (Pd:L)	Base ( 2 equiv.)	Solvent	Temp.(°C)	Yield <sup>b</sup> (%)
1	PTABS	1.0:2.0	NEt <sub>3</sub>	DMF	60	<5
2	PTABS	1.0:2.0	NaOH	DMF	60	<5
3	PTABS	1.0:2.0	K <sub>2</sub> CO <sub>3</sub>	DMF	60	20
4	<b>PTABS</b>	<b>1.0:2.0</b>	<b>K<sub>3</sub>PO<sub>4</sub></b>	<b>DMF</b>	<b>60</b>	<b>90</b>
5	PTABS	1.0:2.0	K <sub>3</sub> PO <sub>4</sub>	ACN	60	75
6	PTABS	1.0:2.0	K <sub>3</sub> PO <sub>4</sub>	PhMe	60	<5

7	PTABS	1.0:2.0	K <sub>3</sub> PO <sub>4</sub>	H <sub>2</sub> O	60	<5
8	PTABS	1.0:2.0	K <sub>3</sub> PO <sub>4</sub>	DMF	80	92
9	PTABS	1.0:2.0	K <sub>3</sub> PO <sub>4</sub>	DMF	30	65
10	PTABS	0.1:0.2	K <sub>3</sub> PO <sub>4</sub>	DMF	60	20
11	PTABS	0.5:1.0	K <sub>3</sub> PO <sub>4</sub>	DMF	60	45
12	PTABS	0.5:1.0	K <sub>3</sub> PO <sub>4</sub>	DMF	100	98
13	PTABS	0.2:0.4	K <sub>3</sub> PO <sub>4</sub>	DMF	100	97
14	PTABS	0.1:0.2	K <sub>3</sub> PO <sub>4</sub>	DMF	100	99
15	PTABS	0.01:0.02	K <sub>3</sub> PO <sub>4</sub>	DMF	100	72
16	PPh <sub>3</sub>	1.0:2.0	K <sub>3</sub> PO <sub>4</sub>	DMF	60	<5
17	P( <i>o</i> -Tolyl) <sub>3</sub>	1.0:2.0	K <sub>3</sub> PO <sub>4</sub>	DMF	60	25
18	XPhos	1.0:2.0	K <sub>3</sub> PO <sub>4</sub>	DMF	60	<5
19	SPhos	1.0:2.0	K <sub>3</sub> PO <sub>4</sub>	DMF	60	<5
20	IMes.HCl	1.0:2.0	K <sub>3</sub> PO <sub>4</sub>	DMF	60	38
21	IPr.HCl	1.0:2.0	K <sub>3</sub> PO <sub>4</sub>	DMF	60	42
22	PTA	1.0:2.0	K <sub>3</sub> PO <sub>4</sub>	DMF	60	66
23	PTAMeI	1.0:2.0	K <sub>3</sub> PO <sub>4</sub>	DMF	60	78

<sup>a</sup> Reaction conditions: 1.0 mmol of **26**, 1.5 mmol of **27**, 1.0 mol% of Pd(OAc)<sub>2</sub> and 2.0 mol% of PTABS, 3.0 mL of Solvent, reaction time 2 h under N<sub>2</sub> atmosphere unless stated otherwise. <sup>b</sup> isolated yields.

The previously established procedure for the Pd/PTABS catalyzed amination of *chloroheteroarenes*<sup>331</sup> was applied to the attempted cross-coupling of 2-chloropyrazine (**26**) with 4-methoxy phenol (**27**). In this reaction, employing 1 mol% of Pd(OAc)<sub>2</sub> and 2 mol% of PTABS in DMF with base triethylamine (Et<sub>3</sub>N) at 60 °C provided only <5% of the desired cross-coupling product (Table 3.2; **entry 1**). Presumably, the basicity of the triethylamine is not strong enough to abstract a proton from phenolic-OH facilitating the active catalytic nucleophile for etherification. Subsequently, several strong inorganic bases such as NaOH, K<sub>2</sub>CO<sub>3</sub>, and K<sub>3</sub>PO<sub>4</sub> were investigated. Interestingly, K<sub>3</sub>PO<sub>4</sub> provided the desired etherified derivative in excellent yields under the applied conditions (Table 3.2; **entry 4**).

In accordance with the previous protocol, aprotic polar solvents DMF or ACN were providing higher yields, while the non-polar systems (toluene) exhibited poor product conversions (Table 3.2; **entry 6**). Although the ligand PTABS is highly water-soluble, the etherification process was not efficient in H<sub>2</sub>O or a DMF/H<sub>2</sub>O mixture, yielding the desired etherified product in < 5% yield (Table 3.2; **entry 7**). This result can be attributed to the low solubility of the coupling partners in aqueous medium. The next critical parameter investigated for optimization was the temperature, which has a significant influence on the catalytic performance of any developed catalytic system.<sup>332</sup> An increase in temperature from 60°C to 80°C comes with a minimal enhancement in yields, whereas the decrease in temperature to 25 to 30°C (ambient temperatures) significantly reduces the conversion (Table 3.2; **entry 8, 9**). A catalyst's high

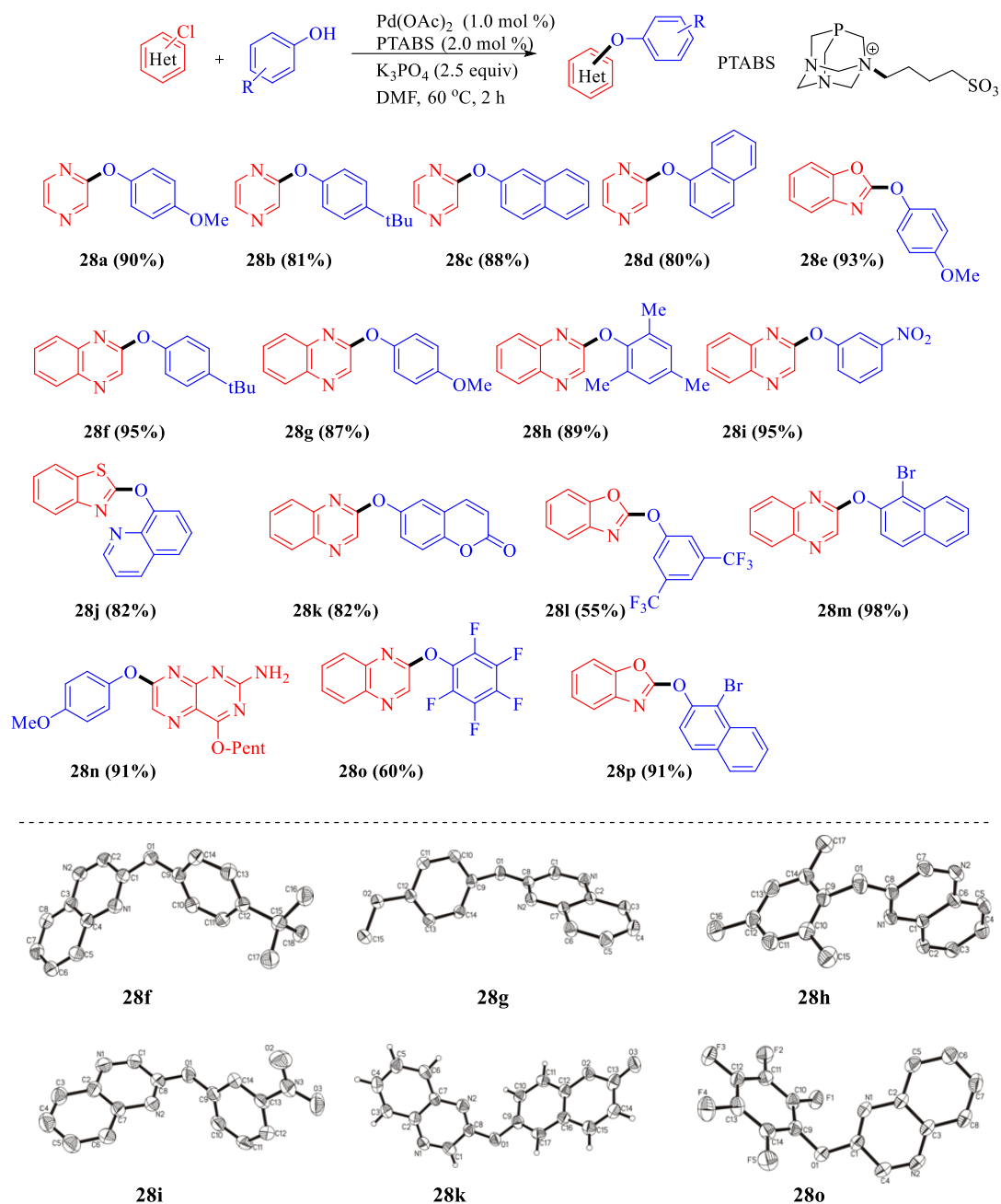


performance at lower catalytic loadings is always desirable in transition-metal catalysis. The catalytic concentration 1 mol% Pd together with 2 mol% PTABS provided maximum yields under the derived reaction conditions. Even, lower concentrations of Pd/PTABS were tested at elevated temperatures (100 °C) to compare the reactivity profile with earlier reports (Table 3.2; **entries 12-15**).<sup>325</sup> Interestingly, the catalytic system exhibited high reactivity with a reduction of catalyst concentration even down to 0.1 mol% at elevated temperatures. These results are slightly superior to the Hierso protocol, where a catalytic loading of 0.2 mol% was employed.<sup>325</sup> However, the employment of higher temperatures for any process could have detrimental impacts on temperature-sensitive coupling partners. Thus, moderate conditions (60°C) were chosen for further investigations.

Next, the efficiency of the PTABS based procedure for the etherification of *chloroheteroarenes* with phenols was compared against frequently used commercially available ligands under optimized reaction conditions. Highly active and electron-rich phosphine ligands such as PPh<sub>3</sub>, P(*o*-tolyl)<sub>3</sub>, X-Phos, and S-Phos, as well as NHC (N-heterocyclic carbene ligands) like IMes.HCl and IPr.HCl were incorporated (Table 3.2; **entries 16-21**). Notably, all of these highly electron-rich and strongly  $\sigma$ -donating phosphine and NHC ligands were inferior to PTABS under the applied conditions. In addition, the parent PTA (phosphatriazine) and methyl-substituted PTA (PTAMeI) were also investigated in comparison with PTABS giving poor conversions, though (Table 3.2; **entries 22, 23**). These results suggest that the chain length of the substituent (quaternization) on the nitrogen atom, as well as the type of counter anion, can alter the reactivity profile of the PTA based scaffolds. The quaternization of the PTA nitrogen atom presumably controls the phosphorous  $\sigma$ -donation capability towards the palladium center during coordination, which in principle governs the reactivity of the derived catalyst. Further, DFT investigations in support of this hypothesis are given and elaborated in section 3.5.4.

### 3.4.3. Substrate Scope development

Chapter 3: Pd/PTABS catalysis for C-O cross-coupling with *chloroheteroarenes*.



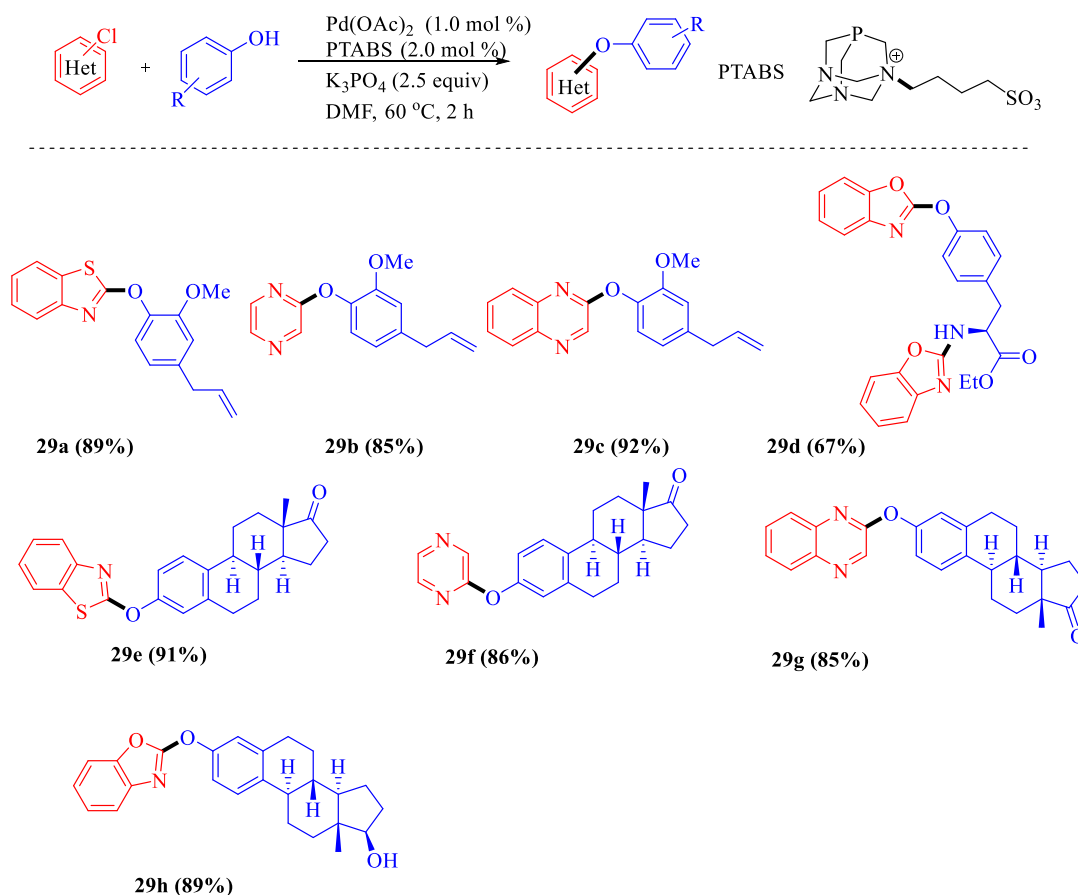
**Scheme 3.12:** Pd/PTABS catalyzed etherification of *chloroheteroarenes* with phenols. Molecular structures of **28f**, **28g**, **28h**, **28i**, **28k** and **28o** with ellipsoids at the 50% level. The hydrogen atoms of **28f**, **28g**, **28h**, **28i** and **28o** are omitted for clarity reasons.

Similar to the amination protocol, five different heterocyclic moieties were selected, namely, pyrazine, quinoxaline, benzothiazole, benzoxazole, and 7-chloro-4-(pentyloxy)pteridine-2-amine and employed as electrophilic coupling partners (Scheme 3.12). For the initial screening, 4-methoxy phenol, 4-tertiary butyl phenol and naphthol were used as nucleophilic synthons. These active (electron-rich) phenols delivered the anticipated conversions with good to excellent isolated yields of the coupled etherified products with all tested *chloroheteroarenes* (Scheme 3.12). Notably, when 2,4,6 trimethylphenol was coupled with 2-chloroquinoxaline,

the corresponding heteroaryl ether **28h** was isolated in high yields (Scheme 3.12), which demonstrated that steric factors have negligible influence on the reactivity.

Furthermore, electronically neutral or deactivated phenols (3-NO<sub>2</sub>, 3,5-CF<sub>3</sub>), which are considered to be passive in C-O cross-coupling, were well-tolerated under the developed catalytic conditions (Scheme 3.12, **28i**, **28l**). Due to the biological importance of pharmacophores, pentafluoro phenol was chosen as a coupling partner.<sup>333</sup> The highly deactivating electronics of fluoro substituents impeded reactivity and resulted in comparably lower yields of ether product (Scheme 3.12; **28o**). The molecular structures of final etherified derivatives **28f**, **28g**, **28h**, **28i**, **28k** and **28o** were further confirmed by X-ray single crystal diffraction analysis.

Notably, the Pd/PTABS catalyst also afforded good chemoselectivity with 1-bromo-2-naphthol (Scheme 3.12; **28m**, **28p**). The heterocyclic C-Cl bond was selectively activated (even in presence of an active C-Br bond) which resulted in the corresponding heteroaryl ethers in quantitative yields. This selectivity, generally, facilitates further sequential functionalization of aryl bromides in multi-step drug syntheses. The exclusive chemoselectivity observed with Pd/PTABS for C-Cl bond activation of the *N*-heteroarene is presumably due to the palladium metal center coordination to nitrogen while directed towards C-Cl oxidative addition. Interestingly, such *N*-directing coordination and subsequent C-Cl activation phenomenon was not observed in 3-chloropyridine. Consequently, the Pd/PTABS catalytic conditions ultimately failed to give the desired coupled product with 3-chloropyridine. This result from the control experiments supports the suggested hypothesis of heteroatom directed C-Cl activation by Pd/PTABS. DFT analysis also, endorsed such type of plausible mechanistic turnover (Section 3.5.4).

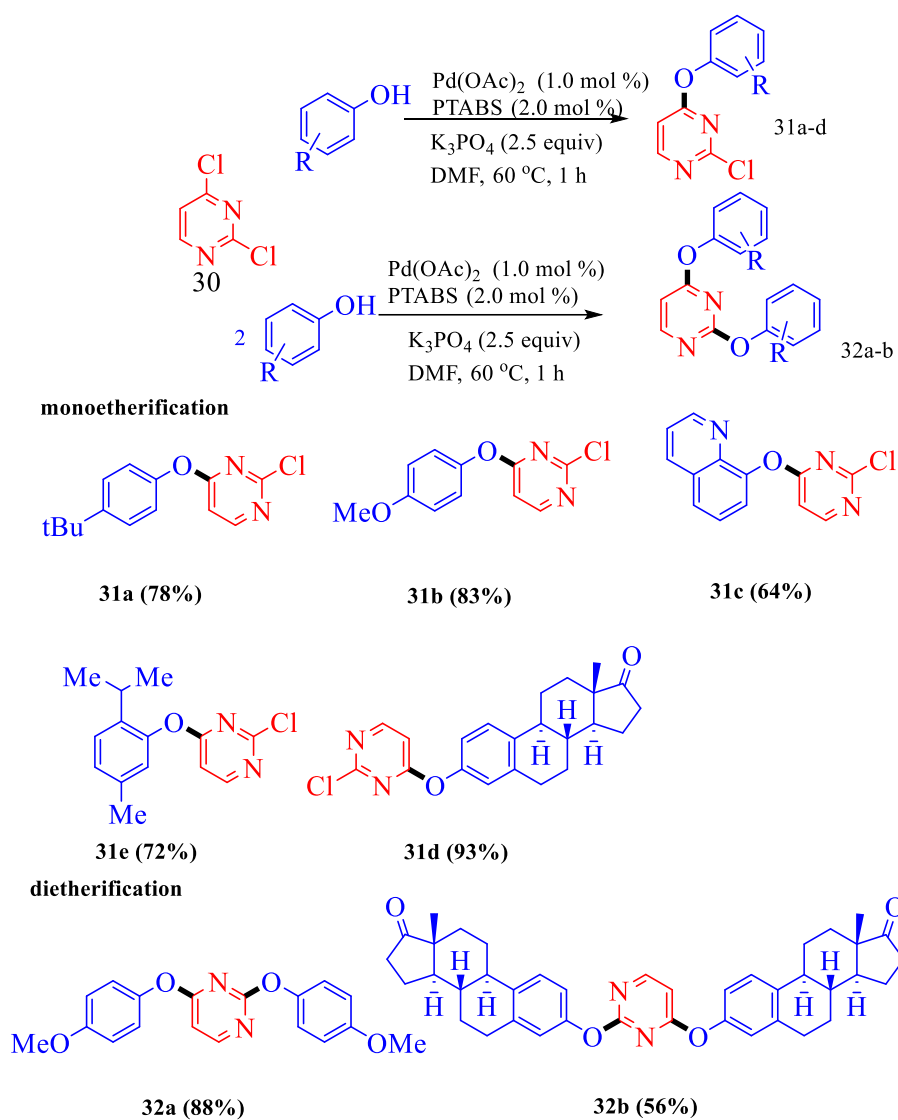


**Scheme 3.13:** Pd/PTABS mediated etherification of *chloroheteroarenes* with biologically significant phenols.

Considering the high efficiency, selectivity and milder nature of the Pd/PTABS catalytic system under the optimized conditions, encouraged further investigation of substrates bearing temperature-sensitive functional groups, which are pharmaceutically relevant. In this process, eugenol, a natural essential oil widely used for both perfume making, as well as the preparation of local anesthetics, was selected as a synthon.<sup>334</sup> Although eugenol is bearing a highly labile allyl functional group known to intervene in metal-catalyzed processes,<sup>335-337</sup> fortuitously, the etherification of three different *chloroheteroarenes* with eugenol proceeded smoothly and gave the etherified products in excellent yields (Scheme 3.13; **29a-c**). Next, the biologically relevant non-essential amino acid, tyrosine, was chosen to couple with 2-chlorobenzoxazole. Surprisingly, the di-arylated tyrosine derivative was obtained as a primary product along with minor (<5%) fractions of the mono-etherified derivative. The free -NH<sub>2</sub> of the tyrosine has similar nucleophilicity as the hydroxyl group (-OH) of the phenol, thus stimulating di-arylation (Scheme 3.13; **28d**). Next, the phenol bearing fused carbocyclic ring steroid hormones, estrone and estradiol, were selected and four different *chloroheteroarenes* were coupled independently under Pd/PTABS catalytic conditions.<sup>338</sup> It is worth mentioning, that the developed catalyst Pd/PTABS tolerated the complexity of estrone and estradiol well and provided the

corresponding ethers in high isolated yields, without perturbing their stereochemistry (Scheme 3.13; **29e-h**). It is a notable advantage that supports the developed etherification protocol at slightly lower reaction temperatures compared to previous literature reports. Such protocols would benefit late-stage modification strategies for essential pharmaceutical drugs and generate new leads in drug discovery.

Having the advantage of the regioselectivity of catalyst Pd/PTABS with poly-halogenated centers in hand, <sup>279</sup> 2,4-dichloropyrimidine was selectively coupled with various phenols namely, 4-*t*-butyl phenol, 4-methoxy phenol, 8-hydroxyquinoline, thymol and estrone (Scheme 3.14, **31a-d**). In accordance with previous observations, the 4-position etherified products were obtained when only one equivalent of phenol was employed, while di-etherification was promoted when an excess of phenol was used (Scheme 3.14, **32a-b**). However, excellent yields were obtained with 4-methoxy phenol, while the estrone coupling yielded only 56% of the respective di-etherified product, presumably, due to the steric effects of the fused system (Scheme 3.14). The molecular structures of final etherified derivatives **31b**, **31c** and **31d** are further confirmed by X-ray single crystal diffraction analysis (Figure 3.5).



**Scheme 3.14:** Regioselective mono and di etherification of 2,4-dichloropyrimidine via Pd/PTABS catalyst.

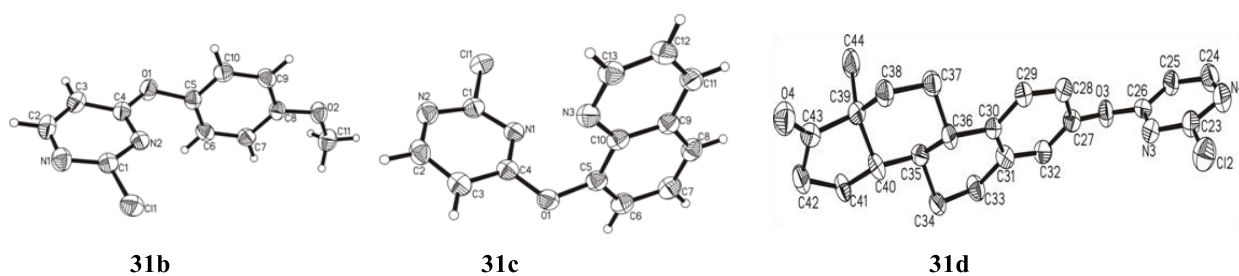
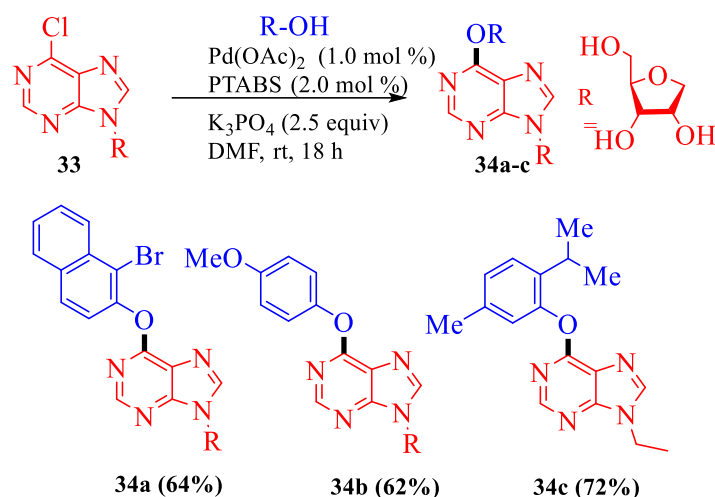


**Figure 3.5:** Molecular structures of **31b**, **31c** and **31d** with ellipsoids at the 50% level. The hydrogen atoms of **31d** are omitted for clarity reasons

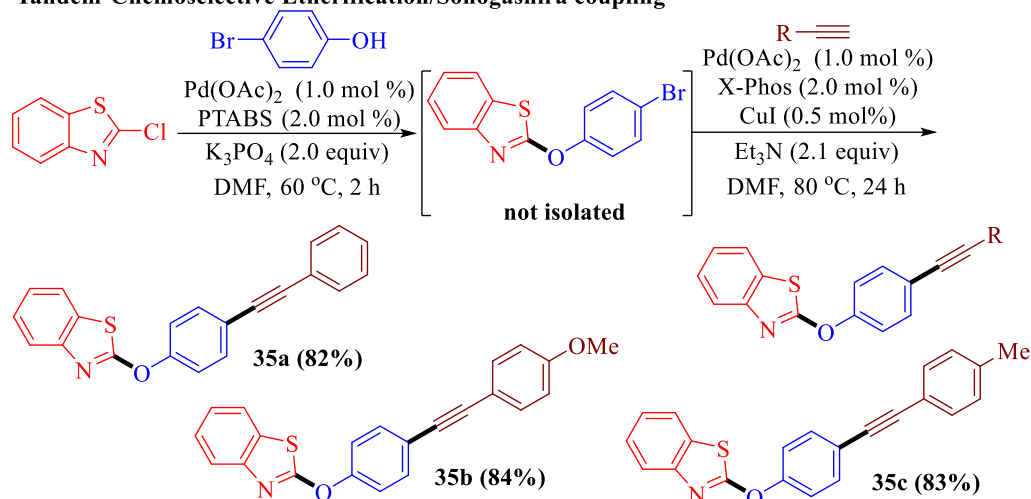


**Scheme 3.15:** Pd/PTABS mediated etherification of 6-chloropurine riboside with different phenols.

Nucleosides are another class of biologically relevant molecules, which were well tolerated by the Pd/PTABS catalyst in the earlier discussed amination procedure (section 3.3.4). In general, naturally occurring nucleobases are non-emissive. However, tagging the nucleobase to a chromophoric unit via palladium catalyzed cross-coupling is an efficient strategy towards various fluorophore bearing nucleobases. Thus, the development of a potent palladium catalyst for such type of functionalizations would be beneficial.<sup>281, 339-340, 308</sup> Accordingly, 6-chloro-9- $\beta$ -D-ribofuranosyl-purine was reacted with various phenols in the presence of Pd/PTABS at room temperature for 18 h; consequently, the ether derivatives **34a-c** were obtained in moderate yields (Scheme 3.15). Notably, the milder nature of the PTABS derived palladium catalytic protocol allowed the cross-coupling with the ribose nucleoside without introducing any bulky protecting groups on the sugar hydroxyl groups.

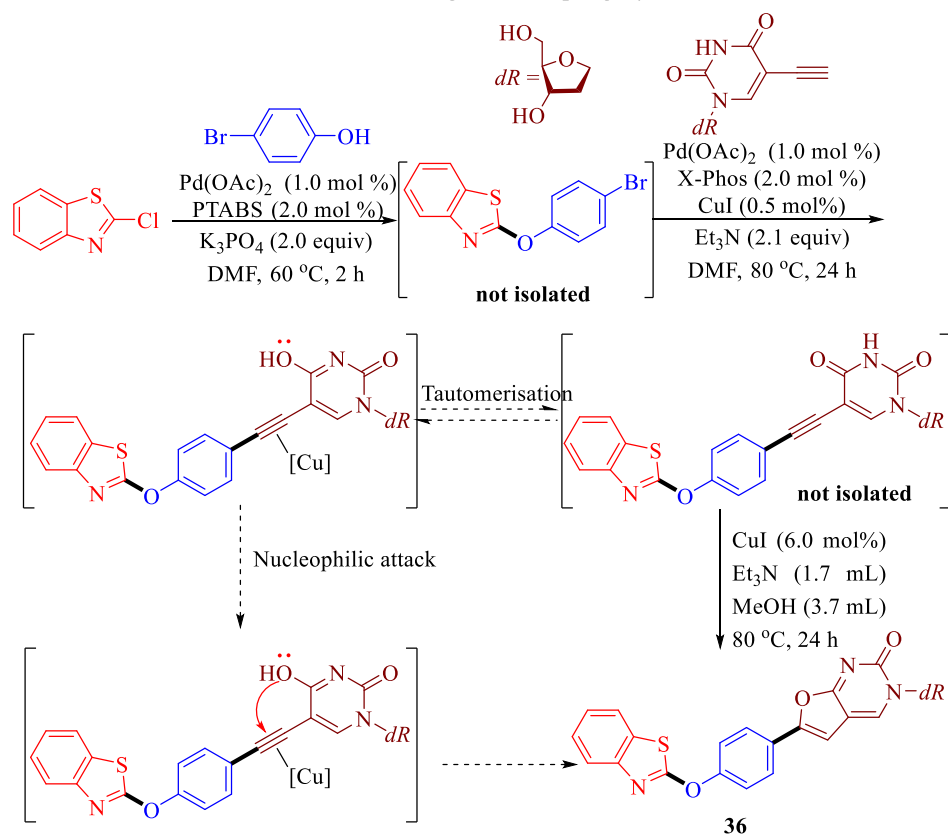
In the next step, considering the efficiency and selectivity of the derived catalyst Pd/PTABS, a sustainable chemical process was targeted. Such sustainable chemical processes can narrow the waste generation (solvent, by-products), as well as obey at least in parts green chemistry principles. Specifically, tandem catalytic processes gained importance in the scientific community due to their simple mono- or multi-metallic catalyst driven combinatorial catalytic application in a single pot. The reaction intermediates were not isolated after every step; waste accumulation of the entire process was, hence, minimized.<sup>341-343</sup> The tolerability of the Pd/PTABS catalyst for such type of sustainable tandem process was investigated by combining the etherification procedure with other catalytic reactions (Scheme 3.16, 3.17), namely, the Sonogashira cross-coupling and copper-catalyzed cyclization.

**Tandem Chemoselective Etherification/Sonogashira coupling**



**Scheme 3.16:** Pd/PTABS and Pd/X-Phos tandem reactions.

**Tandem Chemoselective Etherification/Sonogashira coupling/Cyclization**



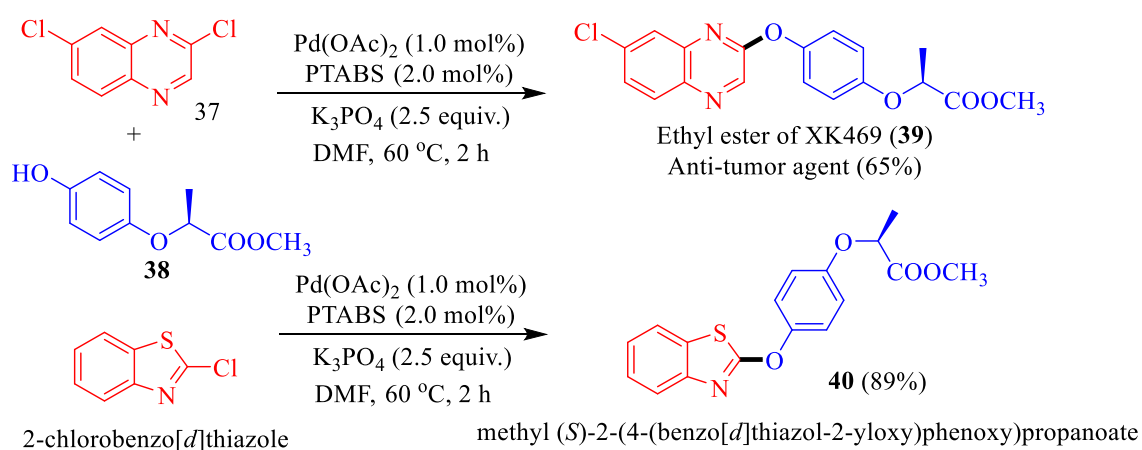
**Scheme 3.17:** Multi-metallic double tandem process via Pd/PTABS-Pd/X-phos-CuI catalysts.

As depicted in scheme 3.16, a tandem reaction was performed sequentially; i.e etherification was followed by Sonogashira cross-coupling. Initially, the 2-chlorobenzothiazole was coupled with 4-bromophenol via Pd/PTABS catalysis with high chemoselectivity towards C–Cl bond activation to result in 2-(4-bromophenoxy)benzothiazole (not isolated). Subsequently, the resultant etherified intermediate reacted with various alkynylated synthons under the



Sonogashira coupling reaction conditions in the presence of the Pd/X-Phos catalyst, providing diverse functionalized 2-(4-(arylethynyl)phenoxy)benzothiazoles (**35a-c**) in good yields.

The success in the tandem process with the developed catalyst (Pd/PTABS) again confirmed its astonishing tolerability and compatibility. Besides regular tandem processes, multi-metallic tandem catalytic processes were similarly proven superior to classical combinatorial organic synthesis.<sup>341</sup> Accordingly, the tolerability of the Pd/PTABS catalytic etherification in combination with a Cu catalyzed process was investigated. The alkyne precursor in the earlier tandem reaction was now replaced by 5-ethynyl uridine, and then the identical sequence was applied to obtain an alkynyl product. The resultant alkynylated Sonogashira intermediate undergoes a Cu-catalyzed cyclization process, in which Cu coordinates to an alkyne, at the same time the amide of uridine is tautomerized to the imino-alcohol. Finally, the nucleophilic attack of the OH of the imino alcohol on the electron-deficient alkyne (Cu-alkyne complex) provides the desired cyclized fluorescent furo-pyrimidine product **36** in good yields (Scheme 3.17).<sup>344-347</sup>



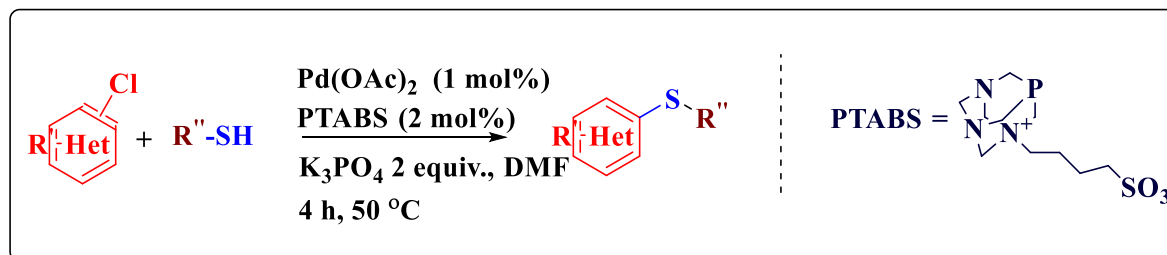
**Scheme 3.18:** Pd/PTABS catalyzed syntheses of ethyl ester of XRK469 and benzothiazole analog.

Finally, the practical applicability and the synthetic utility of the Pd/PTABS catalyst for the etherification procedure were further verified by the synthesis of the commercially important anticancer drug XRK-469. According to the literature, the *R* enantiomer of XRK-469 is known to inhibit topoisomerase-II via facilitating reversible DNA cross-linkages in mammalian cells.<sup>348</sup> The structure of XRK-469 comprises quinoxaline phenoxy propionic acid bearing one stereocenter.

In order to obtain XRK-469, the 2,7-dichloroquinoxaline (**37**) was reacted with methyl (*S*)-2-(4-hydroxyphenoxy)propanoate (**38**) in the Pd/PTABS catalyzed etherification procedure. The resultant ester derivative of the anticancer agent (Scheme 3.18; **39**) was isolated in competitive

yields. Under the similar catalytic conditions, the 2-chloro benzo[d]thiazol reacted with the phenoxy propionate ester (**38**) and resulted in the methyl (*S*)-2-(4-(benzo[d]thiazol-2-yloxy)phenoxy)propanoate in good yields (Scheme 3.18; **40**). It is worth mentioning, that the traditional base mediated procedure used for the synthesis of XRK-469 has limitations with respect to selectivity towards chlorides, thus gave poor yields.<sup>349</sup> Whereas, the Pd/PTABS catalytic procedure was offering better yields with high selectivity towards heterocyclic C-Cl activation.

### 3.5. Pd/PTABS: The C–S cross-coupling of *chloroheteroarenes* with thiophenols and access to novel thioethers, sulfones and sulfoximines.



#### 3.5.1. Background

Thioethers are prevalent structural entities in many pharmaceutical drugs,<sup>235</sup> insecticides,<sup>236</sup> and generally bioactive molecules (Figure 3.6).<sup>237</sup> The C-S bond formation, however is a synthetically onerous reaction.<sup>350</sup> Similarly, sulfones<sup>351-352</sup> and sulfoximines<sup>353-354</sup> are widely present in various cell proliferation inhibitors,<sup>355</sup> insecticides,<sup>356</sup> ATR kinase inhibitors,<sup>357</sup> prostacyclin receptor agonists (Figure 3.6).<sup>358-359</sup> In general, these can be easily prepared from thioethers in good yields by simple oxidation procedures. Although the synthetic approaches to prepare thioethers are copious,<sup>238</sup> these procedures suffer from impediments such as high temperature, long reaction duration, and mediocre reactivity of aryl thiols as nucleophiles.<sup>360-364</sup>

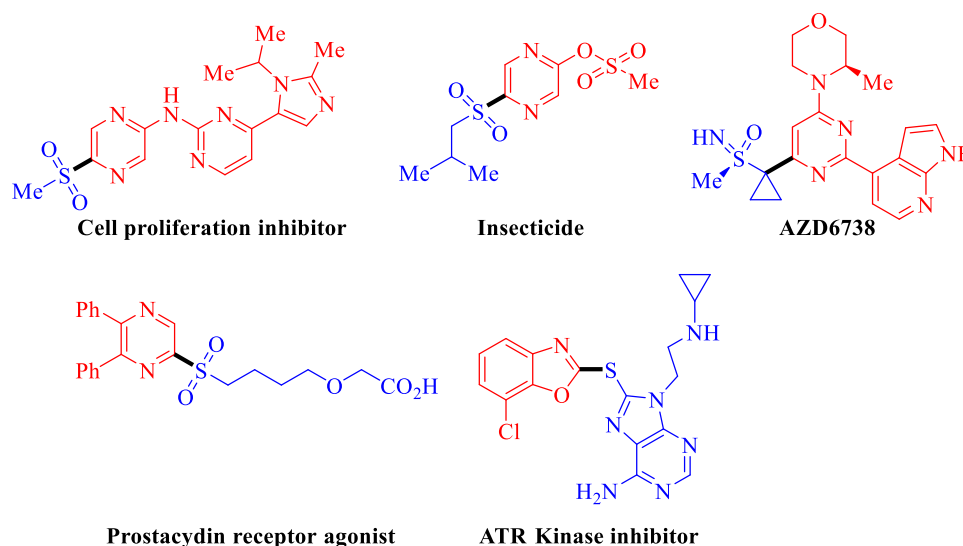


**Figure 3.6:** Bio-active molecules and commercial drugs having a C–S bond on heteroarenes.

In this context, Migita and co-workers applied rudimentary methodologies of transition-metal-catalyzed C–S cross-coupling reactions,<sup>365-366</sup> where they used  $[\text{Pd}(\text{PPh}_3)_4]$ . Migita's palladium protocol created the platform for a profusion of palladium-catalytic processes for such type of valuable transformations.<sup>367</sup> Research groups frequently employed aryl halides Ar-X (where,

X=I, Br and Cl) for coupling with arylthiols and alkyl thiols in the presence of palladium catalysts to prepare aryl or alkyl thioethers.<sup>368-370</sup> However, the C-S cross-coupling between *chloroheteroarenes* and arylthiols was not much explored due to various limitations in the reactivity of arylthiols.<sup>371-372</sup>

Thiols or any sulfur containing compounds are well-known catalyst poison agents, where they can actively form stable coordination complexes with catalytic metal centers. Despite their convenient availability, such type of unwanted ligation of thiols with a metal catalyst made them unpopular in metal-catalyzed coupling reactions.<sup>373-374</sup> Besides, the competing disulfide formation, as well as low functional group tolerability in several catalytic methodologies, further besets the development of synthetic thioether procedures.<sup>375</sup> Although, modern advanced transition-metal catalyzed processes were developed to address many of these difficulties,<sup>376</sup> thoroughly competent solutions have not yet been realized. Specifically, functional protocols for the thio-etherification of *chloroheteroarenes* with aryl thiols and alkyl thiols was not much explored, and very few reports are available so far.<sup>377-378</sup> Recently, Hierso and co-workers introduced an efficient protocol for C-S bond formation in heteroarylchlorides by using ferrocenyl polyphosphines derived palladium catalysts. Notably, the low catalytic loadings of the Pd catalyst afforded relatively good catalytic turnovers.<sup>379</sup> However, the protocol operates at very higher temperatures (115 °C) for long durations, thereby excluding temperature-sensitive substrates from this protocol. A milder and efficient methodology is hence highly desirable for palladium mediated C-S coupling with *chloroheteroarenes*. Accordingly, the thio-etherification of *chloroheteroarenes* with a variety of aryl and alkyl thiols was investigated at relatively lower temperatures by using Pd/PTABS as a potent catalyst.<sup>304</sup> The following part of the chapter describes in detail the optimization study for the developed protocol as well as the efficiency of the process with various *chloroheteroarenes* and thiols.

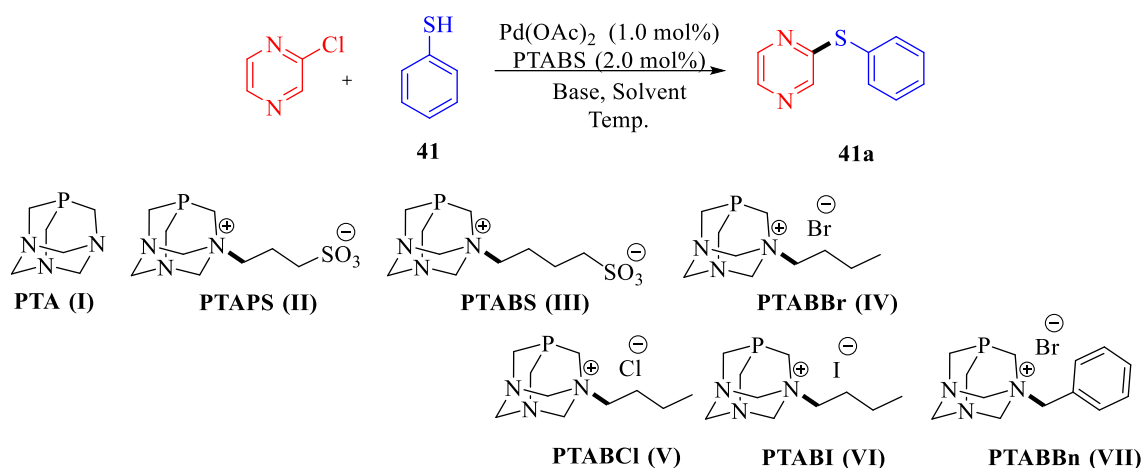
### 3.5.2. Results and discussion: C-S cross-coupling reaction optimization

Since the discovery of the Pd/PTABS catalyst a variety of synthetically challenging catalytic reactions were successfully performed.<sup>380</sup> For example, the nucleoside modification via C-C cross-coupling (Suzuki, Sonogashira, and Heck),<sup>284</sup> aminations of *chloroheteroarenes* at room temperature,<sup>331</sup> moderate temperature etherification of *chloroheteroarenes*,<sup>381</sup> and oxadiazole C-H bond activation.<sup>382</sup> Having such an active catalyst in hand was highly motivating to investigate the C-S coupling of *chloroheteroarenes* with aryl thiols or alkylthiols as well.

Table 3.3 depicts the optimization study data for the thio-etherification of 2-chloropyrazine with thiophenol in the presence of a variety of catalysts, including the Pd/PTABS system.<sup>379</sup> Most often the study was performed at relatively moderate temperatures (50 °C) in comparison to already published reports.<sup>383</sup> Initial control experiments, in the absence of either palladium or the ligand source in DMF, at 50 °C, while employing only base (K<sub>3</sub>PO<sub>4</sub>), resulted in no product formation (Table 3.3; **entry 1**). The first sample of the desired product was isolated under ligand-free conditions by using Pd(OAc)<sub>2</sub>. The isolated yield was only 38%, though (Table 3.3; **entry 2**). Next, ligand optimization was carried out, in which PTA(I), and zwitterionic PTAPS(II) and PTABS(III) were included.<sup>37-40,280, 305</sup> Interestingly, already the employment of PTA enhanced the reactivity and offered the desired thioether in 62% isolated yield (Table 3.3; **entry 3**). PTABS and PTAPS surpassed their parent PTA, however, and provided the thioether in 91% and 85% of isolated yields, respectively (Table 3.3, **entry 4-5**). Considering the high efficacy of zwitterionic PTA congeners in the C–S bond formation, a series of PTA substituted quaternized salts, namely, PTABBr(IV), PTABCl(V), PTABI(VI), PTABBn(VII) were prepared by direct alkylation of PTA.

The ionic species IV-VI, differing only by the counter anion, showed high efficacy under the applied conditions, although the highest yields were obtained with zwitterionic PTABS, (Table 3.3, and **entries 6-8**). The incorporation of the alternative benzyl unit instead of the alkyl chain on the PTA backbone resulted in minimal improvement in thioether formation (82%, Table 3.3; **entry 9**). Consistently, the PTABS derived palladium catalyst has displayed superior reactivity under the optimized reaction conditions.

Recently, Hartwig,<sup>241</sup> Itoh,<sup>368</sup>, Nolan,<sup>384</sup> and their co-workers found significant efficiency with highly electron-rich phosphine ligands<sup>242-243</sup> and N-heterocyclic carbenes<sup>385-387</sup> in the thioetherification of aryl halides. Based on this bulky phosphine ligand system such as, XPhos, SPhos and the bis-phosphine ligand Xantphos were also included in the investigations. Notably, these ligands performed incompetently under the operating reaction conditions yielding the targeted thioethers in lower yields than PTABS (Table 3.3; **entries 10-12**).

**Table 3.3:** Optimization experiments for thio-etherification of chloroheteroarenes.

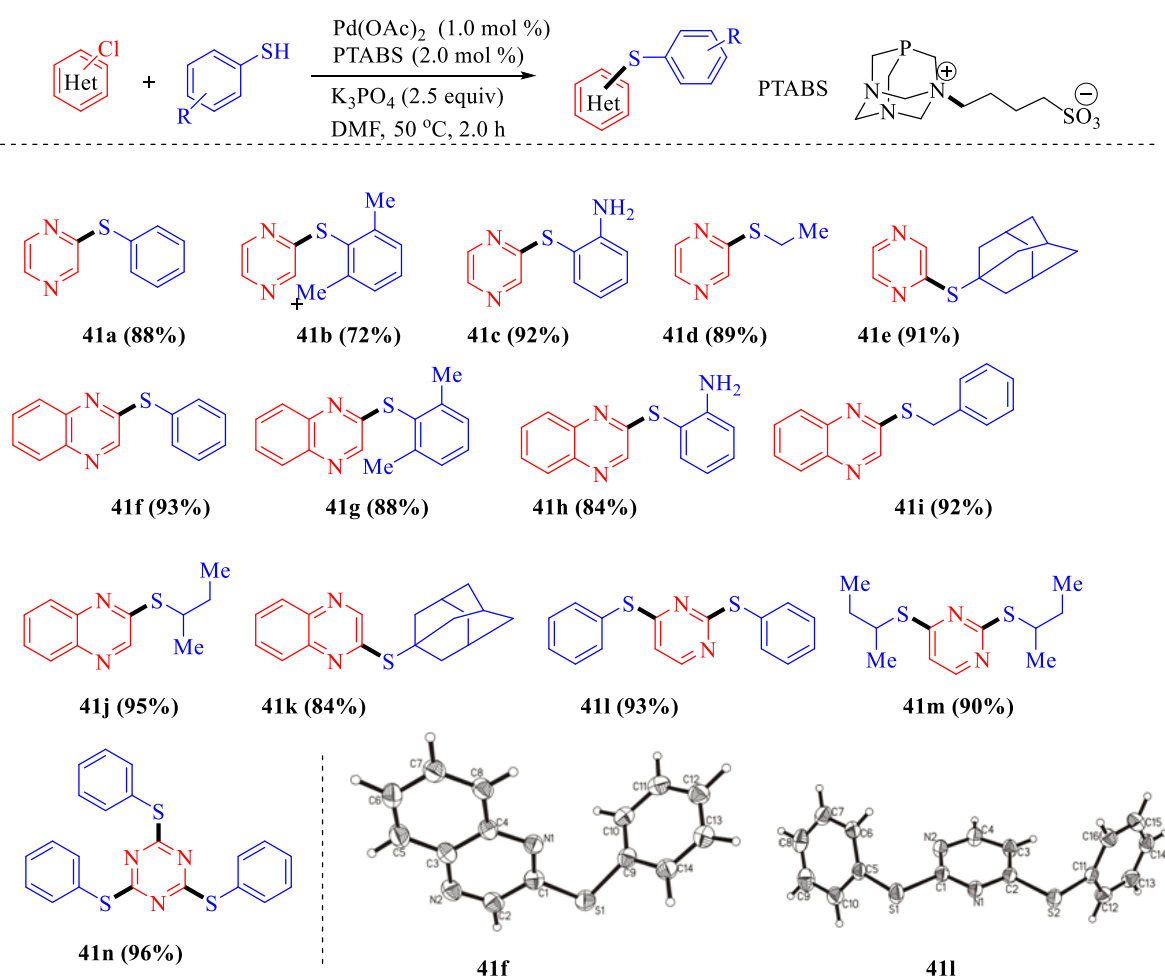
S.No.	Catalyst (1.0 mol%)	Ligand (2.0 mol%)	Base (2 equiv.)	Solvent	Temperature ( $^{\circ}\text{C}$ )	Yield <sup>a</sup> (%)
1	-	-	$\text{K}_3\text{PO}_4$	DMF	50	NR
2	$\text{Pd(OAc)}_2$	-	$\text{K}_3\text{PO}_4$	DMF	50	38
3	$\text{Pd(OAc)}_2$	PTA	$\text{K}_3\text{PO}_4$	DMF	50	62
4	<b><math>\text{Pd(OAc)}_2</math></b>	<b>PTABS</b>	<b><math>\text{K}_3\text{PO}_4</math></b>	<b>DMF</b>	<b>50</b>	<b>91</b>
5	$\text{Pd(OAc)}_2$	PTAPS	$\text{K}_3\text{PO}_4$	DMF	50	85
6	$\text{Pd(OAc)}_2$	PTABI	$\text{K}_3\text{PO}_4$	DMF	50	85
7	$\text{Pd(OAc)}_2$	PTABBr	$\text{K}_3\text{PO}_4$	DMF	50	80
8	$\text{Pd(OAc)}_2$	PTABCl	$\text{K}_3\text{PO}_4$	DMF	50	76
9	$\text{Pd(OAc)}_2$	PTABBn	$\text{K}_3\text{PO}_4$	DMF	50	82
10	$\text{Pd(OAc)}_2$	XPhos	$\text{K}_3\text{PO}_4$	DMF	50	53
11	$\text{Pd(OAc)}_2$	SPhos	$\text{K}_3\text{PO}_4$	DMF	50	62
12	$\text{Pd(OAc)}_2$	Xantphos	$\text{K}_3\text{PO}_4$	DMF	50	68
13	$\text{PdCl}_2$	PTABS	$\text{K}_3\text{PO}_4$	DMF	50	85
14	$\text{Pd(OAc)}_2$	PTABS	$\text{K}_3\text{PO}_4$	$\text{CH}_3\text{CN}$	50	42
15	$\text{Pd(OAc)}_2$	PTABS	$\text{K}_3\text{PO}_4$	Dioxane	50	68
16	$\text{Pd(OAc)}_2$	PTABS	$\text{K}_3\text{PO}_4$	THF	50	27
17	$\text{Pd(OAc)}_2$	PTABS	$\text{Na}_2\text{CO}_3$	DMF	50	22
18	$\text{Pd(OAc)}_2$	PTABS	$\text{Cs}_2\text{CO}_3$	DMF	50	68
19	$\text{Pd(OAc)}_2$	PTABS	$\text{KO}^t\text{Bu}$	DMF	50	54
20	$\text{Pd(OAc)}_2$	PTABS	$\text{K}_3\text{PO}_4$	DMF	rt ( $22^{\circ}\text{C}$ )	25
21	$\text{Pd(OAc)}_2$	PTABS	$\text{K}_3\text{PO}_4$	DMF	60	88
22	$\text{Pd(OAc)}_2$	PTABS	$\text{K}_3\text{PO}_4$	DMF	100	73

Reaction conditions: 1.0 mmol of 2-chloropyrazine, 1.5 mmol of **41**, 1.0 mol % of  $\text{Pd(OAc)}_2$  or  $\text{PdCl}_2$ , 2.0 mol% of PTABS/ligand, 3.0 mL of solvent, DMF stirring at  $50^{\circ}\text{C}$  for 2 hours, <sup>a</sup> isolated yields.

Furthermore, neither replacing  $\text{Pd(OAc)}_2$  by  $\text{PdCl}_2$  nor replacing the solvent DMF and/or base  $\text{K}_3\text{PO}_4$  by other combinations have significantly altered the reactivity (Table 3.3; **entries 13-**

16). The highest isolated yields for the thioetherification of 2-chloropyrazine with thiophenol was observed in a reaction at 50 °C for 4 h. Furthermore, either decreasing the temperature (22°C) or increasing it (100°C) has an inimical effect on the thio-etherification process (Table 3.3; **entries 21-22**). Thus, the optimal conditions for the thioetherification of *chloroheteroarenes* with aryl or alkyl thiophenol involves the employment of 1 mol% of Pd(OAc)<sub>2</sub> in combination of 2 mol% PTABS in DMF (solvent) with 2 equiv. of K<sub>3</sub>PO<sub>4</sub> base at 50°C for 4 h (Table 3.3, **entry 4**).

### 3.5.3. Substrate scope development



**Scheme 3.19:** Pd/PTABS catalyzed thioetherification of pyrimidine and purine substrates at milder reaction conditions. Molecular structures of compounds **41f** and **41i** are with ellipsoids at the 50% level.

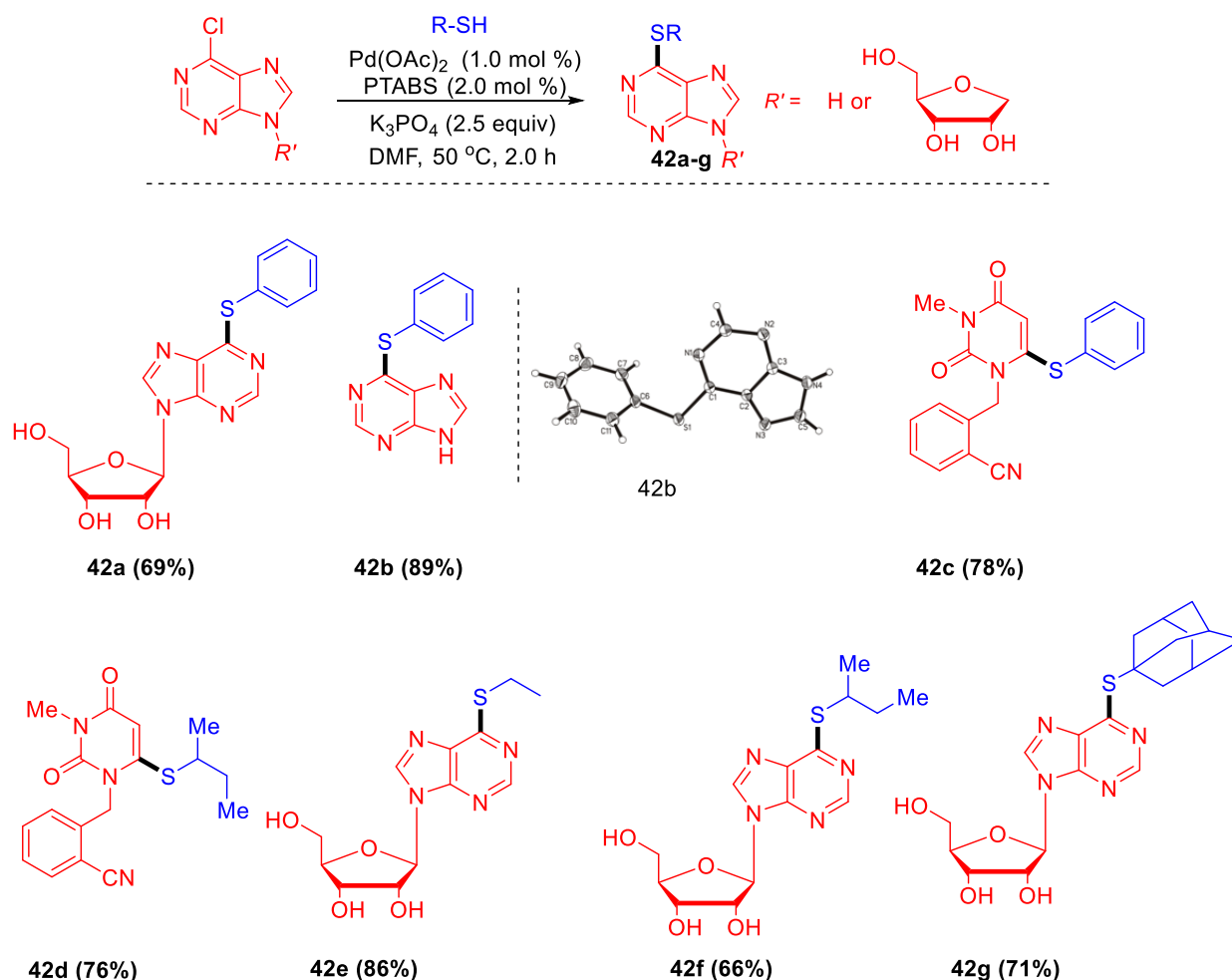
Various *chloroheteroarenes* and arylthiols were readily assimilated in the C–S coupling procedure catalyzed by Pd/PTABS with wide functional group tolerability. 2-chloroquinoxaline and 2-chloropyrazine were coupled with sterically hindered 2,6-dimethyl thiophenol and less reactive aromatic thiophenol, resulting in corresponding thioethers **41b**, **41g** in good yields (Scheme 3.19). Under Pd/PTABS catalytic conditions, the free amine group of 2-amino thiophenol was well tolerated and resulted in 92% and 84% of thioetherified

products **41c**, **41h** with 2-chloropyrazine and 2-chloroquinoxaline, respectively. Alkyl thiols possess complex reactive profiles albeit, the employment of ethanethiol, adamantane thiol, 2-butyl thiol and benzyl thiol provided well-defined products in good to excellent yields (Scheme 3.19; **41d**, **41e**, **41j** and **41k**). Surprisingly, the previously observed regioselectivity in amination and etherification procedures (3.3.5, 3.4.5) with substrate 2,4-dichloropyrimidine was not achieved. However, excellent yields of di-thioetherified derivatives were isolated with thiophenol and alkyl thiophenol substrates (Scheme 3.19; **41l**, **41m**). This observed lack of regioselectivity is attributed to the uncontrolled reactivity of the thiol nucleophiles under the operating conditions. In the investigation of triple thioetherification with 2,4,6-trichlorotriazine providing excellent yields of the corresponding tris-thioetherified product were observed (Scheme 3.19, **41n**). The molecular structures of compounds **41f** and **41l** were further confirmed by X-ray single crystal diffraction analysis (Scheme 3.19)

Considering the biological relevance of the pyrimidine motif<sup>388,389</sup>, the off-shelf halo precursor from the synthesis of anti-diabetic drug “Alogliptin”, i.e., chloro-3-methyl-2,4-dioxo-3,4-dihydro pyrimidine-1(2*H*)-yl-methyl)benzotrile, was reacted with thiophenol or 2-butylthiophenol in the presence of Pd/PTABS catalyst and novel thioetherified derivative of “Alogliptin” were isolated in good yields (Scheme 3.20; **42c,42d**).

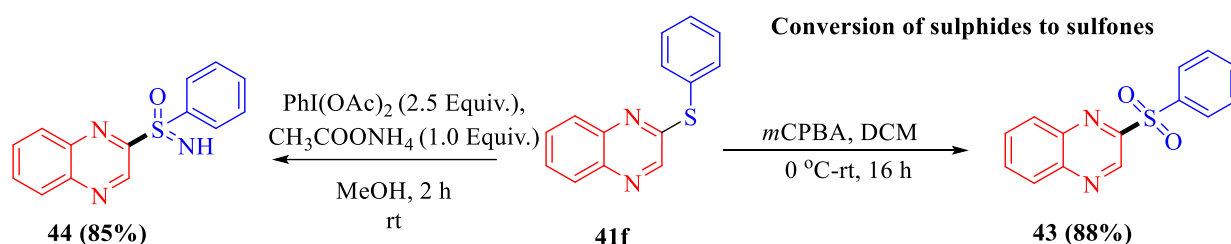
The strong reactivity of the Pd/PTABS catalyst with purines or purine ribosides was previously demonstrated (sections 3.3.4, 3.4.4). Furthermore, their presence in various fluorescent probes,<sup>390</sup> anticancer<sup>391</sup> and antiviral drug candidates<sup>392-393</sup> was encouraging to look into further functionalization. Recently, Jian and co-workers reported the thiomethylation of purines. However, the high operating temperatures of this protocol have limited the substrate scope for nucleosides.<sup>394</sup> In contrast, Pd/PTABS catalyzed the thioetherification of 6-chloroquine riboside with thiophenols or alkylthiols very efficiently at moderate temperatures and furnished moderate to good yields of thioetherified products (Scheme 3.20; **42a**, **42b**, **42e-g**).





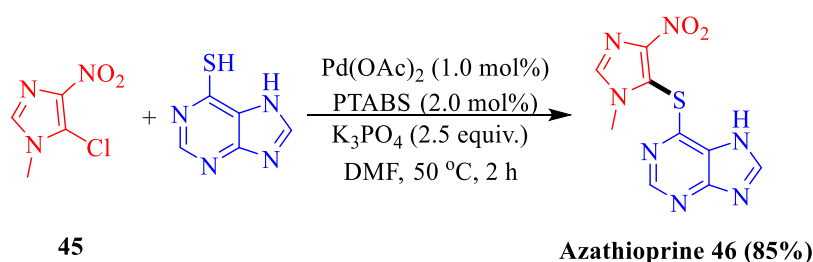
**Scheme 3.20:** Pd/PTABS catalyzed thioetherification of pyrimidine and purine substrates at milder reaction conditions. The molecular structure of **42b** is shown with ellipsoids at the 50% level.

Next, subsequent thioether transformation to sulfones and sulfoximines was targeted, as such types of entities are ubiquitous structural units in many pharmaceutically active drugs<sup>395</sup>. These molecules can be easily prepared via simple oxidations of thioethers,<sup>396-397-398</sup> while the synthesis of the later is challenging. Considering all these, the synthesized quinoxaline thioether **41f** was converted also into its respective sulfone **43** (88%) by simple oxidation in the presence of *meta*-chloroperoxybenzoic acid (*m*CPBA) in dichloromethane (DCM) (Scheme 3.21, right reaction arrow). Sulfoximines<sup>399-400</sup> are similarly common structural motifs<sup>401</sup> in pharmaceutical<sup>402</sup> and medicinal<sup>379</sup> anticancer agents such as the pan-CDK inhibitor from Bayer<sup>387</sup> and the ATR inhibitor from AstraZeneca.<sup>403-404</sup> The thioetherified product **41f** prepared with Pd/PTABS catalyzed thioetherification of 2-chloroquinoxaline was subsequently converted to its corresponding *NH*-sulfoximine via single-pot N and O transformation (scheme 3.21 left reaction arrow; **44**).<sup>401</sup>



**Scheme 3.21:** Synthesis of sulfone and sulfoximines from 2-(phenylthio)quinoxaline.

Finally, the applicability and usefulness of the Pd/PTABS thioetherification protocol was further emphasized by the synthesis of the vital immunosuppressant drug *Imuran* (**azathioprine**).<sup>405</sup> Azathioprine is a purine derived molecule bearing a thioether linkage, usually administered in patients who undergo kidney or liver transplantation. The drug decreases the body's immune responses while implanting the foreign organ into the system.<sup>406</sup> Azathioprine was synthesized in good yields (85%) via cross-coupling of 5-chloro-4-nitro-*N*-Methylimidazole and 7-*H* purine-6-thiol in the presence of the Pd/PTABS catalyst in DMF at moderate temperature (Scheme 3.22; **46**).

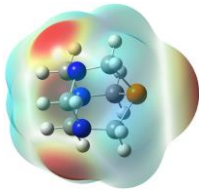
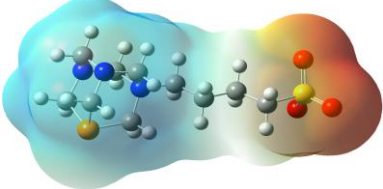
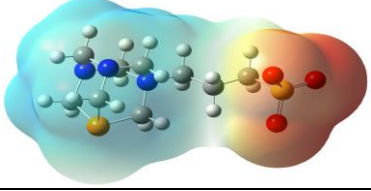
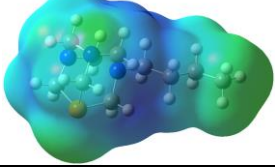
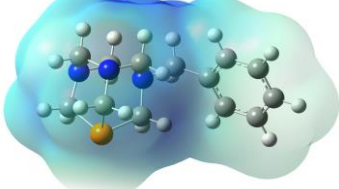
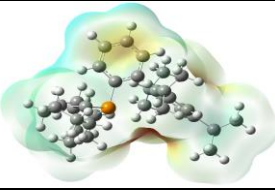
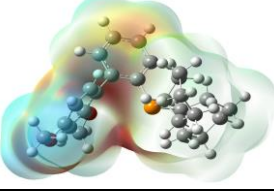


**Scheme 3.22:** Synthesis of azathioprine via Pd/PTABS catalytic system.

### 3.5.4. Mechanistic Investigation and DFT (density-functional theory) studies

Despite having a powerful catalytic system in hand, which has been shown high efficiency in various catalytic organic transformations (e.g., amination, etherification, and thioetherification), the knowledge of the mechanistic specifics of the Pd/PTABS catalyst is ambiguous.

**Table 3.4:** Analysis of the electronic structures of the phosphorous ligands: computational data from DFT study.

Sl.No	Molecule	NPA on P-center (e)	Mapped MEP <sup>a</sup>
1	PTA	0.715	
2	PTABS	0.822	
3	PTAPS	0.822	
4	PTAB <sup>+</sup>	0.838	
5	PTABn <sup>+</sup>	0.837	
6	XPhos	0.864	
7	SPhos	0.874	

<sup>a</sup>The MEP plotting ranges from -0.028 to 0.028 for PTA, XPhos, and SPhos, 0 to 0.160 for PTAB<sup>+</sup> and PTABn<sup>+</sup>, -0.128 to 0.128 for PTABS and -0.114 to 0.114 for PTAPS. In the MEP drawings, red indicates an electronegative and blue, an electropositive nature.

In order to further improve this knowledge, density-function theory (DFT) studies were carried out by cooperation partner Dr. Anant R. Kapdi and his co-workers, and relevant results are depicted in Table 3.4. The computational investigations were carried out on all PTA derived ligands PTA, PTAPS, PTABS, PTABCl, PTABBr, PTABI, and PTABnBr along with frequently used XPhos and SPhos. An attempt was made to correlate the electronic factors to

their reactivity profiles in catalysis. The influence of the halide counterion was normalized during the analysis of PTABX (where, X= Cl<sup>-</sup>, Br<sup>-</sup>, I<sup>-</sup>) and PTABnBr derivatives while these ligands were treated as cationic species. B3LYP/6-31G (d,p) level of theory was applied using the Gaussian 16 program suit to perform geometrical optimizations for all derivatives.<sup>407</sup> The structural minima on potential energy surfaces were confirmed by obtaining second-order positive energy gradients. Natural population analysis (NPA) data were generated from the optimized geometries and the resultant molecular electrostatic potentials (MEP) were mapped vs. the total electron density of the same derivatives.

According to the NPA values, the central phosphorus atom of all derivatives exhibits electro positivity, with PTA exhibiting the lowest respective charge. The net charge on the phosphorous atom in PTA is only 0.715 e, whereas this value is around 0.822 e for PTABS and PTAPS derivatives and the ionic congeners PTABX (where, X= Br, I, Cl) and PTABnBr exhibited a charge of 0.837 e on P. Though XPhos and SPhos showed substantially high charges of c.a 0.864 e and 0.874 e, respectively, they have exhibited identical efficiency in the catalytic thio-etherification experiment as with less charge bearing PTA. Thus, the catalytic efficiency is not directly related to the electropositive potential of the ligand's P-donor atom. The computational study was then extended beyond the phosphorous atom. The MEP maps of all ligands were plotted to explain the phenomenon of high performance from ionic PTA derived families in C-S cross-coupling compared to PTA, XPhos, and SPhos. Interestingly, the phosphorous atoms of PTA, XPhos, SPhos have negative potential charges (-0.028 au), while all other ionic PTA derivatives have positively charged P (0.026, 0.015, 0.0127, and 0.080 au for PTABS, PTAPS, PTAB<sup>+</sup> and PTABn<sup>+</sup>, respectively). Presumably, the partial positive charge on the P atom in the ionic ligands is due to the alkyl substitution (quaternization) on one of the nitrogen atoms. This significant charge difference suggests better  $\pi$ -accepting and weaker  $\sigma$ -donating abilities of the P atom in PTA ionic salts. Such an intensive variation in electron density around a phosphorous atom is surmised to have a significant influence on the coordination with the palladium center, which controls the catalytic activity.

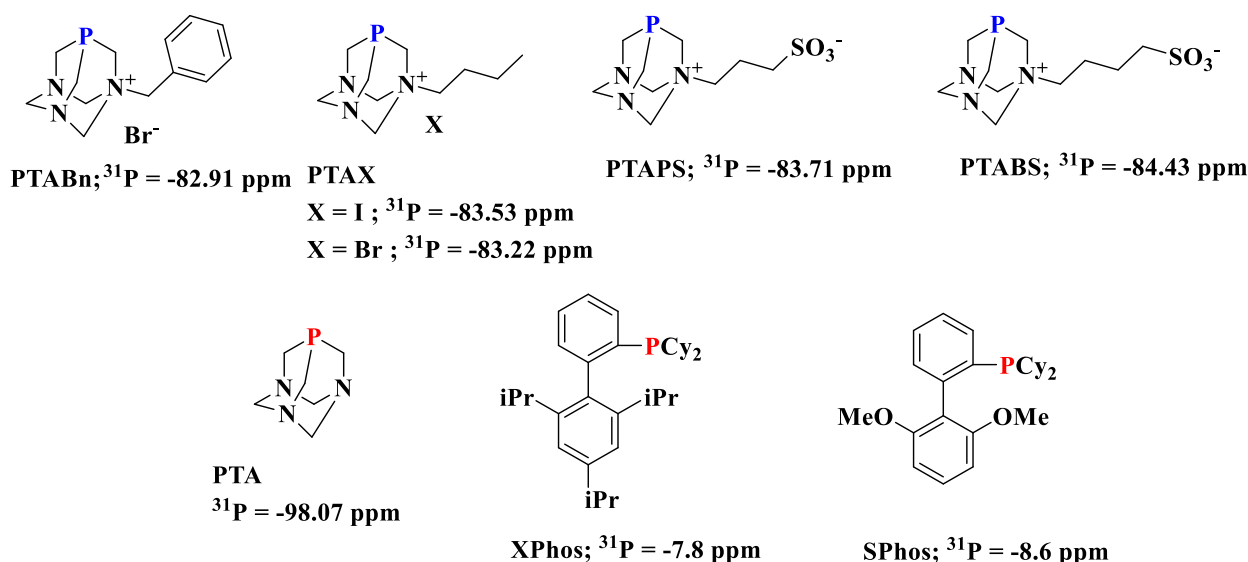


**Figure 3.7:**  $^{31}\text{P}$  NMR values of PTA and its quaternary salts, SPhos, XPhos ligands.

The negative electrostatic potentials were also evidenced in XPhos and SPhos (i.e., -0.035 au) similar to PTA, which was in agreement with their lower efficacy in C–S cross-coupling. Hence, it must be stated that not only the charge on the central P atom of the ligand is essential but also the electrostatic potentials around the P-ligands, which eventually control metal-ligand interactions (Figure 3.7). Additionally,  $^{31}\text{P}$  NMR experiments were performed for PTA and PTA ionic derivatives. A significant down field shift of 13-15 ppm was observed in PTA ionic salts compared to PTA. Such deshielding effect on the P atom of PTA could have originated from the quaternization of the  $\beta$ -nitrogen atom. The exchange of the counter anion species in PTA ionic salt derivatives has a negligible effect on  $^{31}\text{P}$  NMR values (Figure 3.7).

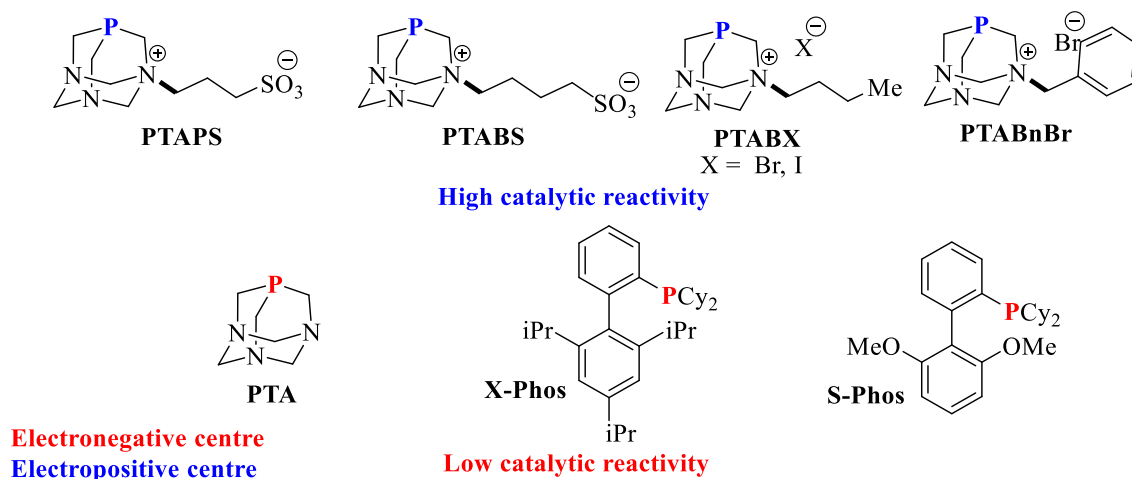


**Figure 3.8:** The correlation between the charge on the P atom and their reactivity in C–S cross-coupling.

The plausible coordination modes of the PTA and PTABX (where, X= Br, I, Cl) ligands with the palladium center in the presence of 2-chloroquinoxaline are depicted in figure 3.8.<sup>408-409</sup> It

is assumed that when highly electron-rich ligands such as PTA, XPhos, and SPhos coordinate to Pd, this enhances the nucleophilicity of the central metal atom. Thus, the nucleophilic Pd center forms stable complexes with a heteroatom (nitrogen) of electron-deficient *chloroheteroarene* (pyrazine, pyrimidine and others), consequently limiting the rate of oxidative addition to the C–Cl bond. Accordingly, the relative reactivity of electron-rich ligands in the C–S cross-coupling experiments was impaired. In contrast, the positively charged electron-poor phosphines PTAPS, PTABS, PTABX (where, X= Br, I, Cl) and PTABnBr were highly reactive. The  $\pi$ -accepting nature of these ligands reduces the nucleophilicity of the palladium center, therefore Pd and heteroatom are coordinated weakly and create a possibility for heteroatom directed oxidative addition of Pd to the C–Cl bond.

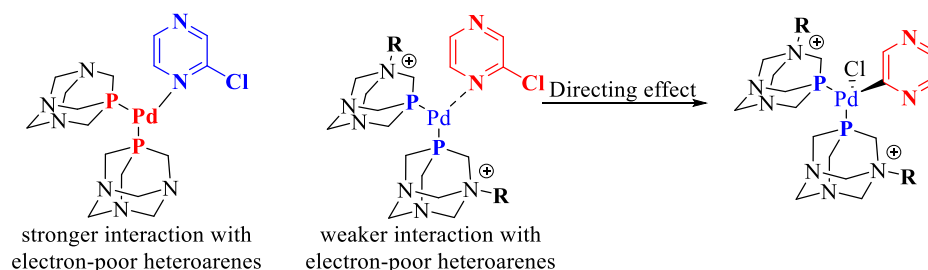


**Figure 3.8:** Plausible mechanistic coordination of ligand bearing Pd centers and its directing effect for C-Cl activation.

In short, the plausible heteroatom directed C–Cl activation in the presence of the Pd/PTABS catalyst convincingly explains the observed reactivity. In control experiments with 3-chloropyridine without such type of directing group, activation is not observed, which further supports the aforementioned mechanism. Notably, the Pd/PTABS catalyst is ineffective with 2-chloropyridine in all types of C–heteroatom bond formation reactions. The unreactivity is attributed to the high nucleophilic nature of the pyridine nitrogen which can form stable complexes with the active Pd center, consequently hindering the catalytic cycle. Additional mechanistic experiments and more elaborated computational analysis are under process and the comprehensive results are yet to be obtained, which are expected to conclusively explain the observed reactivity differences.

### 3.6. Conclusion

In summary, the serendipitous discovery of a novel, mild and efficient Pd/PTABS catalytic system was successfully employed at low catalytic loadings (1 mol %) for the amination (C–N), etherification (C–O) and thioetherification (C–S) of *chloroheteroarenes* at ambient to moderate temperatures. The Pd/PTABS catalyst is well-tolerating a variety of heterocyclic

scaffolds including, pyrazine, pyrimidine, purines/purine-nucleosides, uridine, pterin and others. Moreover, under the optimized catalytic conditions, various secondary amines, electron-rich or electron-poor phenols, thiophenols, and alkylthiols, were efficiently employed as nucleophilic coupling partners. Importantly, the catalyst offered in combination with simple starting materials tremendous regio and chemoselectivity which can be easily controlled by temperature. The milder nature of the protocols facilitated the synthesis of significantly diverse product libraries with minimum efforts in excellent isolated yields. More than fifteen molecular structures of products were characterized by X-ray single crystal diffraction analysis. Novel sulfones and sulfoximines were prepared from the thioethers obtained via Pd/PTABS. In total fifty five novel C–N, C–O and C–S cross-coupled derivatives were developed by using the Pd/PTABS catalytic system. It is planned to submit some of them to biological investigations in the near future. Furthermore, the practical applicability of the catalyst was demonstrated by synthesizing biologically significant known drugs or drug candidates such as alogliptin (anti-diabetic agent), XRK 469 (antitumor agent) and *Imuran*-Azathioprine (immunosuppressive) in competitive yields. The extraordinary tolerability of the Pd/PTABS catalyst was also utilized for various industrially relevant single-pot mono- and multi-metallic tandem procedures. Additional ionic derivatives of PTA, such as PTAPS, PTABX (X=Cl, Br, I) and PTABnBr ligands were prepared to investigate the effect of the counter ion on the total reactivity of the catalyst. Finally, an attempt was made to draw mechanistic conclusions and in rationalizing the unprecedented activity of Pd/PTABS in C-heteroatom cross-coupling. Preliminary DFT investigations were performed on PTA and its ionic congeners along with XPhos, and SPhos ligands, where the later were considered as reference standards. Based on the DFT analysis, the low reactivity of PTA, XPhos and SPhos was attributed to the electronegative nature of the P donor atom in these ligands. In contrast, the electropositive character of the phosphorous atom in quaternary ammonium salts of PTABS, PTAPS, PTABX (X=Cl, Br, I) and PTABnBr induces and supports the heteroatom directed C–Cl activation. Additional theoretical and NMR, ESI-MS spectroscopic experiments are planned to generate even more conclusive evidence for involved mechanistic intermediates, but could not be included in this thesis for reasons of duration and scope.

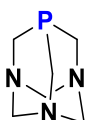
### 3.7. Experimental

#### General

All reactions were performed under a nitrogen atmosphere using oven-dried standard Schlenk glassware. The completely dried N, N-Dimethylformamide (DMF, 99.8%, extra dry, stored over molecular sieves) was purchased from Acros organics and used as received for all air or moisture-sensitive reactions.  $^1\text{H}$  NMR (300 MHz) and  $^{13}\text{C}$  NMR (75 MHz) spectra were recorded on the NMR EMAU Advance II-300 spectrometer. Chemical shifts  $\delta$  are given in ppm and the solvent residual peak ( $\text{CDCl}_3$ :  $^1\text{H}$ ,  $\delta = 7.27$ ;  $^{13}\text{C}$ ,  $\delta = 77.0$  and  $\text{DMSO-d}_6$ :  $^1\text{H}$ ,  $\delta = 2.50$ ;  $^{13}\text{C}$ ,  $\delta = 40$ ) was used as an internal standard. Peak multiplicities are specified as follows: s, singlet; d, doublet; t, triplet; q, quartet; m, multiplet; br, broad. APCI-MS ( $m/z$ ) spectra were recorded on Advion MS. Mechenary-Nagel silica gel 60 F254 plates were used for thin-layer chromatography (TLC), and detection was achieved by UV light. Column chromatography was performed on silica gel 60 (40-63  $\mu\text{m}$ ) or Acros organics silica gel 60 (35-70  $\mu\text{m}$ ). The single X-ray crystal structure analysis was conducted by using “STOE IPDS2T” and diffraction source with fine-focus sealed molybdenum tube. “Elementar Vario MICRO cube” was used for the experimental determination of elemental configurations of final pure products.

#### 3.7.1. Synthesis of PTA, PTABS, PTAPS, PTABX (X= Cl, Br, I) and PTABBn

##### *Synthesis of (1s,3s,5s)-1,3,5-triaza-7-phosphaadamantane (PTA)<sup>410</sup>*



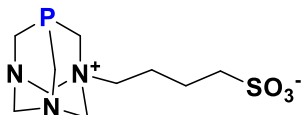
**PTA**

The  $^1\text{H}$ ,  $^{13}\text{C}$ , and  $^{31}\text{P}$ -NMR data of the product agree with the reported literature data.<sup>411</sup> To a 500 mL beaker containing 50 g of ice was added 50 mL of tetrakis(hydroxymethyl)phosphonium chloride (THPC). A saturated solution of sodium hydroxide of 18 g (50 % w/w  $\text{H}_2\text{O}$ ) was added to the cold THPC solution. The resultant mixture was warmed slowly to room temperature then supplied with 127 g (118 mL) of formaldehyde (37%) solution and 39 g of hexamethylenetetramine (HMTA) under continuous stirring. The reaction mixture was stirred for 20 h, transferred to an evaporating dish, and allowed to concentrate for 5 to 7 days until a white crystalline solid was observed. The crude product was recrystallized from acetone to give a transparent crystalline material in 90% isolated yield.



$^1\text{H}$  NMR (300 MHz, DEUTERIUM OXIDE)  $\delta$ : 3.95 (s, 3 H), 3.92 (s, 3 H), 4.42 - 4.56 (m, 6 H);  $^{13}\text{C}$  NMR (75 MHz, DEUTERIUM OXIDE)  $\delta$ : 49.23 (s, 2 C), 49.50 (s, 2 C), 72.49 (s, 1 C), 73.41 (s, 1 C);  $^{31}\text{P}$  NMR (121 MHz, DEUTERIUM OXIDE)  $\delta$ : -98.07 (s, 1 P).

***Synthesis of 4-((1*s*,3*R*,5*S*,7*r*)-1,3,5-triaza-7-phosphaadamantane-1-ium-1-yl)butane-1-sulfonate(PTABS)***<sup>305</sup>

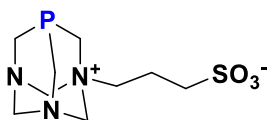


**PTABS**

The  $^1\text{H}$ ,  $^{13}\text{C}$ , and  $^{31}\text{P}$ -NMR data of the product are in agreement with the literature data.<sup>305</sup> To the suspension of PTA (0.1 g, 0.64 mmol) in acetone (12 mL) 4 equiv. of 1,4-butanediol (0.78 mL, 7.6 mmol) were added, and the resultant mixture stirred at room temperature for 20 h. After completion of reaction 5 mL of diethyl ether were added and the obtained white precipitate was filtered and washed with excess diethyl ether to isolate the pure product in 86% (0.483 g, 1.65 mmol) yield.

$^1\text{H}$  NMR (300 MHz, DEUTERIUM OXIDE)  $\delta$ : 1.70 - 1.85 (m, 2 H), 1.85 - 1.99 (m, 2 H), 2.87 - 3.08 (m, 4 H), 3.78 - 4.05 (m, 4 H), 4.34 (d, J=6.24 Hz, 2 H), 4.45 (d, J=13.75 Hz, 1 H), 4.62 (d, J=13.75 Hz, 1 H), 4.81 (d, J=11.74 Hz, 2 H), 4.99 (d, J=11.00 Hz, 2 H);  $^{13}\text{C}$  NMR (75 MHz, DEUTERIUM OXIDE)  $\delta$ : 19.5 (s, 1 C), 22.6 (s, 1 C), 46.7 (s, 1 C), 47.2 (s, 1 C), 51.2 (s, 1 C), 54.1 (s, 1 C), 54.5 (s, 1 C), 63.6 (s, 1 C), 70.8 (s, 1 C), 80.3 (s, 1 C);  $^{31}\text{P}$  NMR (121 MHz, DEUTERIUM OXIDE)  $\delta$ : -84.43 (s, 1 P).

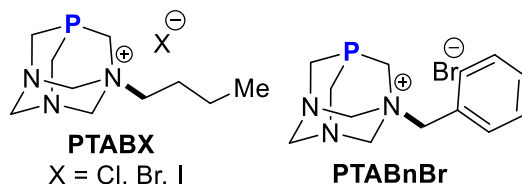
***3-((1*s*,3*R*,5*S*,7*r*)-1,3,5-triaza-7-phosphaadamantane-1-ium-1-yl)propane-1-sulfonate (PTAPS)***<sup>305</sup>



**PTAPS**

**PTAPS** was synthesized by cooperation partner Dr. Anant Kapdi and group.  $^{31}\text{P}$  NMR (121 MHz, DEUTERIUM OXIDE)  $\delta$  ppm: -83.71 (s, 1 P)

***Synthesis of PTA quaternized ionic salts PTABBr, PTABCl, PTABI and PTABnBr***



General procedure for PTABX (Where, X= Cl, Br, I) and PTABnBr: The PTA substitution was performed according to the procedure from Sascha et al.<sup>412</sup> To an oven-dried 100 mL round bottom flask was added 1,3,5-triaza-7-phosphadamantane (PTA) and was dissolved in acetone (50 mL) under N<sub>2</sub> atmosphere. To this resultant mixture, a saturated solution of a respective alkyl halide in acetone (10 mL) was added slowly and dropwise at room temperature under inert conditions over 15 minutes. After completion of the addition, the resultant reaction mixture was refluxed for 2 h until a white precipitate was obtained. More product precipitated upon cooling to room temperature. The white powder was filtered and washed with acetone and diethyl ether and dried under vacuum.

**PTABBr:** General procedure was followed with 1-butyl bromide <sup>1</sup>H NMR (300 MHz, DEUTERIUM OXIDE) δ: 0.90 (t, *J*=7.34 Hz, 3 H), 1.23 - 1.41 (m, 2 H), 1.61 - 1.77 (m, 2 H), 2.85 - 2.98 (m, 2 H), 3.75 - 4.03 (m, 4 H), 4.30 (d, *J*=6.24 Hz, 2 H), 4.42 (d, *J*=13.66 Hz, 1 H), 4.59 (d, *J*=13.75 Hz, 1 H), 4.77 (d, *J*=12.01 Hz, 2 H), 4.90 - 4.99 (m, 2 H); <sup>13</sup>C NMR (75 MHz, DEUTERIUM OXIDE) δ: 14.3 (s, 1 C), 20.9 (s, 1 C), 22.7 (s, 1 C), 47.5 (s, 1 C), 54.3 (s, 1 C), 54.8 (s, 1 C), 64.6 (s, 1 C), 71.1 (s, 1 C), 79.7 (s, 1 C), 80.4 (s, 1 C); <sup>31</sup>P NMR (121 MHz, DEUTERIUM OXIDE) δ: -84.6 (s, 1 P).

**PTABCl:** General procedure was followed with 1-butyl chloride. <sup>31</sup>P NMR (121 MHz, DEUTERIUM OXIDE) δ: -84.7 (s, 1 P)

**PTABI:** General procedure was followed with 1-butyl iodide. <sup>31</sup>P NMR (121 MHz, METHANOL-*d*<sub>4</sub>) δ: -83.5 (s, 1 P)

**PTABnBr:** General procedure was followed with benzyl bromide. <sup>1</sup>H NMR (300 MHz, DEUTERIUM OXIDE) δ: 3.65 - 3.79 (m, 2 H), 3.83 - 3.98 (m, 2 H), 4.13 (s, 2 H), 4.22 (d, *J*=6.33 Hz, 2 H), 4.41 (d, *J*=13.76 Hz, 1 H), 4.57 (d, *J*=13.75 Hz, 1 H), 4.83 - 5.01 (m, 4 H), 7.43 - 7.62 (m, 5 H); <sup>13</sup>C NMR (75 MHz, DEUTERIUM OXIDE) δ : 47.1 (s, 1 C), 47.3 (s, 1 C), 54.2 (s, 1 C), 54.6 (s, 1 C), 68.4 (s, 1 C), 71 (s, 1 C), 80.3 (s, 1 C), 126.1 (s, 2 C), 130.9 (s, 2 C), 132.5 (s, 1 C), 134.5 (s, 1 C); <sup>31</sup>P NMR (121 MHz, DEUTERIUM OXIDE) δ : -82.9 (s, 1 P).

### 3.7.2. Pd/PTABS catalytic amination of *chloroheteroarenes* at ambient temperature.

#### *General procedure (GP)*

A 25 mL oven-dried Schlenk tube was charged with 1 mol% of Pd(OAc)<sub>2</sub>, 2 mol% of PTABS (ligand, phosphoadamantinebutylsaltonate) and 1 mmol of chloroheterocyclic derivative under N<sub>2</sub> atmosphere and the resultant mixture dissolved in 3 mL of dry DMF. The reaction mixture was stirred for 5 minutes and 1.1 equiv. of corresponding secondary amine were added plus, 1.5 equiv. of triethylamine followed by stirring at room temperature for 4 to 18 h. After consumption of starting material (monitored by TLC-MS), the solvent was removed under vacuum, and the resultant residue was purified by column chromatography in EtOAc/hexane (10% to 50%) solvent system to afford the desired product.

#### 3.7.2.1. 2-(pyrrolidine-1-yl)pyrazine (**12a**)

The compound exhibited identical <sup>1</sup>H and <sup>13</sup>C NMR data as in previous reports.<sup>303</sup> General procedure (GP) was followed with 2-chloropyrazine (114.5 mg, 1 mmol) and pyrrolidine (0.092 mL, 1.1 mmol, 1.1 equiv.) yielding the desired 2-(pyrrolidine-1-yl)pyrazine (118 mg, 0.79 mmol, 88%) as white crystals. <sup>1</sup>H NMR (300 MHz, CHLOROFORM-*d*) δ: 2.00 (dt, *J*=6.61, 3.49 Hz, 4 H), 3.35 - 3.57 (m, 4 H), 7.72 (d, *J*=2.64 Hz, 1 H), 7.83 (d, *J*=1.51 Hz, 1 H), 7.98 (dd, *J*=2.64, 1.51 Hz, 1 H); <sup>13</sup>C NMR (75 MHz, CHLOROFORM-*d*) δ: 25.7 (s, 1 C), 46.6 (s, 1 C), 77.4 (s, 1 C), 77.8 (s, 1 C), 131.1 (s, 1 C), 131.6 (s, 1 C), 142.4 (s, 1 C), 153.4 (s, 1 C); (+ve)APCI-MS *m/z* = 149.19 calcd. for C<sub>8</sub>H<sub>11</sub>N<sub>3</sub> [M], found: 150.12 [M+H].

#### 3.7.2.2. 2-morpholinopyrazine (**12b**)

The compound exhibited identical <sup>1</sup>H and <sup>13</sup>C NMR data as in previous reports.<sup>413</sup> General procedure (GP) was followed with 2-chloropyrazine (114.5 mg, 1 mmol) and morpholine (0.10 mL, 1.1 mmol, 1.1 equiv.) providing the desired 2-morpholinopyrazine (83 mg, 0.51 mmol, 50%) as colorless crystals. X-ray single crystal structure determined. <sup>1</sup>H NMR (300 MHz, CHLOROFORM-*d*) δ: 3.51 - 3.63 (m, 4 H), 3.79 - 3.90 (m, 4 H), 7.90 (d, *J*=2.64 Hz, 1 H), 8.14 (d, *J*=7.6 Hz, 1 H), 9.61 (d, *J*=7.8 Hz, 1 H); <sup>13</sup>C NMR (75 MHz, CHLOROFORM-*d*) δ: 45.2 (s, 2 C), 66.9 (s, 2 C), 131.3 (s, 1 C), 134 (s, 1 C), 142.2 (s, 1 C) 155.5 (s, 1 C); (+ve)APCI-MS *m/z* = 165.19 calcd. for C<sub>8</sub>H<sub>11</sub>N<sub>3</sub>O [M], found: 166.22 [M+H].

#### 3.7.2.3. 2-(pyrrolidin-1-yl)quinoxaline (**12c**)

The compound exhibited identical <sup>1</sup>H and <sup>13</sup>C NMR data as in previous reports.<sup>303</sup> General procedure (GP) was followed with 2-chloroquinoxaline (164 mg, 1 mmol) and pyrrolidine (0.092 mL, 1.1 mmol, 1.1 equiv.) providing the desired 2-(pyrrolidin-1-yl)quinoxaline (176

mg, 0.928 mmol, 92%) as pale yellow crystals.  $^1\text{H}$  NMR (300 MHz, CHLOROFORM-*d*)  $\delta$ : 2.00 - 2.17 (m, 4 H), 3.60 - 3.75 (m, 4 H), 7.33 (ddd,  $J=8.21, 6.89, 1.51$  Hz, 1 H), 7.55 (ddd,  $J=8.50, 6.99, 1.51$  Hz, 1 H), 7.69 (dd,  $J=8.50, 1.32$  Hz, 1 H), 7.87 (dd,  $J=8.31, 1.51$  Hz, 1 H), 8.34 (s, 1 H);  $^{13}\text{C}$  NMR (75 MHz, CHLOROFORM-*d*)  $\delta$ : 25 (s, 2 C), 46.2 (s, 2 C), 123.2 (s, 1 C), 125.7 (s, 1 C), 128.4 (s, 1 C), 129.5 (s, 1 C), 135.9 (s, 1 C), 136.1 (s, 1 C), 142.1 (s, 1 C), 150.2 (s, 1 C); (+ve)APCI-MS  $m/z = 199.115$  calcd. for  $\text{C}_{12}\text{H}_{13}\text{N}_3$  [M]; found: 200.69 [M+H].

#### 3.7.2.4. 2-(piperidin-1-yl)quinoxaline (**12d**)

The compound exhibited identical  $^1\text{H}$  and  $^{13}\text{C}$  NMR data as in previous reports.<sup>414</sup> General procedure (GP) was followed with 2-chloroquinoxaline (164 mg, 1 mmol) and piperidine (0.11 mL, 1.1 mmol, 1.1 equiv.) providing the desired 2-(piperidin-1-yl)quinoxaline (196 mg, 0.912 mmol, 91%) as pale yellow crystals.  $^1\text{H}$  NMR (300 MHz, CHLOROFORM-*d*)  $\delta$ : 1.67 - 1.76 (m, 6 H), 3.71 - 3.83 (m, 4 H), 7.33 - 7.40 (m, 1 H), 7.52 - 7.59 (m, 1 H), 7.64 - 7.72 (m, 1 H), 7.86 (dd,  $J=8.31, 1.51$  Hz, 1 H), 8.58 (s, 1 H);  $^{13}\text{C}$  NMR (75 MHz, CHLOROFORM-*d*)  $\delta$ : 24.6 (s, 2 C), 25.6 (s, 2 C), 45.8 (s, 1 C), 124.3 (s, 1 C), 126.3 (s, 1 C), 128.5 (s, 1 C), 129.9 (s, 1 C), 136 (s, 1 C), 136.4 (s, 1 C), 141.9 (s, 1 C), 152.4 (s, 1 C); APCI-MS  $m/z = 213.13$  calcd. for  $\text{C}_{13}\text{H}_{15}\text{N}_3$  [M]; found: 214,72 [M+H].

#### 3.7.2.5. 2-morpholinoquinoxaline (**12e**)

The compound exhibited identical  $^1\text{H}$  and  $^{13}\text{C}$  NMR data to previous reports.<sup>414</sup> General procedure (GP) was followed with 2-chloroquinoxaline (164 mg, 1 mmol) and morpholine (0.10 mL, 1.1 mmol, 1.1 equiv.) providing the desired 2-morpholinoquinoxaline (192 mg, 0.89 mmol, 89%) as pale yellow crystals.  $^1\text{H}$  NMR (300 MHz, CHLOROFORM-*d*)  $\delta$ : 3.73 - 3.80 (m, 4 H), 3.83 - 3.91 (m, 4 H), 7.38 - 7.46 (m, 1 H), 7.59 (td,  $J=7.74, 1.51$  Hz, 1 H), 7.68 - 7.74 (m, 1 H), 7.90 (dd,  $J=8.12, 1.32$  Hz, 1 H), 8.56 (s, 1 H);  $^{13}\text{C}$  NMR (75 MHz, CHLOROFORM-*d*)  $\delta$ : 44.6 (s, 2 C), 66.1 (s, 1 C), 66.5 (s, 1 C), 124.6 (s, 1 C), 126.1 (s, 1 C), 128.2 (s, 1 C), 129.7 (s, 1 C), 135 (s, 1 C), 136.6 (s, 1 C), 141 (s, 1 C), 151.8 (s, 1 C); (+ve)APCI-MS  $m/z = 215.11$  calcd. for  $\text{C}_{12}\text{H}_{13}\text{N}_3\text{O}$  [M]; found: 216.31[M+H].

#### 3.7.2.6. *N,N*-diethylquinoxalin-2-amine (**12f**)

The compound exhibited identical  $^1\text{H}$  and  $^{13}\text{C}$  NMR data as in previous reports.<sup>414</sup> General procedure (GP) was followed with 2-chloroquinoxaline (164 mg, 1 mmol) and *N,N'*-diethylamine (0.12 mL, 1.1 mmol, 1.1 equiv.) providing the desired *N,N'*-diethylquinoxalin-2-amine (129 mg, 0.646 mmol, 64%) as colorless crystals.  $^1\text{H}$  NMR (300 MHz, CHLOROFORM-*d*)  $\delta$ : 1.29 (t,  $J=7.18$  Hz, 6 H), 3.70 (q,  $J=7.18$  Hz, 4 H), 7.30-7.36 (m, 1 H),

7.51-7.58 (m, 1 H), 7.64-7.68 (m, 1 H), 7.85 (dd,  $J=7.93, 1.51$  Hz, 1 H), 8.44 (s, 1 H);  $^{13}\text{C}$  NMR (75 MHz, CHLOROFORM-*d*)  $\delta$ : 13.2 (s, 2 C), 42.4 (s, 2 C), 123.6 (s, 1 C), 126.2 (s, 1 C), 128.6 (s, 1 C), 129.8 (s, 1 C), 135.1 (s, 1 C), 136.2 (s, 1 C), 142.4 (s, 1 C) 150.9 (s, 1 C); (+ve)APCI-MS  $m/z = 201.27$  calcd. for  $\text{C}_{12}\text{H}_{15}\text{N}_3$  [M], found: 202.29 [M+H].

#### 3.7.2.7. 8-(piperidin-1-yl)imidazo[1,2-*a*]pyrazine (**12g**)

General procedure (GP) was followed with 8-chloroimidazo[1,2-*a*]pyrazine (154 mg, 1mmol) and piperidine (0.11 mL, 1.1 mmol, 1.1 equiv.) providing the desired 8-(piperidin-1-yl)imidazo[1,2-*a*]pyrazine (166 mg, 0.823 mmol, 82%) as dark violet liquid.  $^1\text{H}$  NMR (300 MHz, CHLOROFORM-*d*)  $\delta$ : 1.70 (s, 6 H), 4.15 (br. s., 4 H), 7.28-7.32 (m, 1 H), 7.44-7.47 (m, 2 H), 7.51 (d,  $J=1.13$ Hz, 1 H);  $^{13}\text{C}$  NMR (75 MHz, CHLOROFORM-*d*)  $\delta$ : 25.2 (s,4 C), 48 (s,1 C), 110.7 (s,1 C), 114.4 (s,1 C), 128.2 (s,1 C), 131.3 (s,1 C), 134.6 (s,1 C), 150.3 (s,1 C); (+ve)APCI-MS  $m/z = 202.26$  calcd. for  $\text{C}_{11}\text{H}_{14}\text{N}_4$  [M], found: 203.32 [M+H].

#### 3.7.2.8. 8-(pyrrolidin-1-yl)imidazo[1,2-*a*]pyrazine (**12h**)

General procedure (GP) was followed with 8-chloroimidazo[1,2-*a*]pyrazine (154 mg, 1mmol) and pyrrolidine (0.092 mL, 1.1 mmol, 1.1 equiv.) providing the desired 8-(pyrrolidin-1-yl)imidazo[1,2-*a*]pyrazine (151 mg, 0.805 mmol, 80%) as violet colored viscous liquid.  $^1\text{H}$  NMR (300 MHz, DMSO-*d*<sub>6</sub>)  $\delta$ : 1.87-1.99 (m, 4 H), 3.91 (br. s., 4 H), 7.24 (d,  $J=4.53$  Hz, 1 H), 7.50 (d,  $J=1.13$  Hz, 1 H), 7.72 (d,  $J=4.53$  Hz, 1 H), 7.86 (d,  $J=1.13$  Hz, 1 H);  $^{13}\text{C}$  NMR (75 MHz, DMSO-*d*<sub>6</sub>)  $\delta$ : 24.6 (s, 2 C), 48.2 (s, 2 C), 109.5 (s, 1 C), 114.6 (s, 1 C), 127.9 (s, 1 C), 131.1 (s, 1 C), 133.3 (s, 1 C), 147.7 (s, 1 C); (+ve)APCI-MS  $m/z = 188.23$  calcd. for  $\text{C}_{10}\text{H}_{12}\text{N}_4$  [M], found: 189.28 [M+H].

#### 3.7.2.9. 2-(pyrrolidin-1-yl)benzo[*d*]oxazole (**12i**)

The compound exhibited identical  $^1\text{H}$  and  $^{13}\text{C}$  NMR data as in previous reports.<sup>415</sup> General procedure (GP) was followed with 2-chlorobenzo[*d*]oxazole (0.12 mL, 1 mmol) and pyrrolidine (0.092 mL, 1.1 mmol, 1.1 equiv.) providing 2-(pyrrolidin-1-yl)benzo[*d*]oxazole (179 mg, 0.954 mmol, 95%) as colorless shiny crystals.  $^1\text{H}$  NMR (300 MHz, CHLOROFORM-*d*)  $\delta$ : 2.00 - 2.07 (m, 4 H), 3.60 - 3.69 (m, 4 H), 6.95 - 7.01 (m, 1 H), 7.14 (td,  $J=7.74, 1.13$  Hz, 1 H), 7.23 - 7.27 (m, 1 H), 7.33 - 7.39 (m, 1 H);  $^{13}\text{C}$  NMR (75 MHz, CHLOROFORM-*d*)  $\delta$ : 26 (s, 2 C), 47.8 (s, 2 C), 108.9 (s, 1 C), 116.3 (s, 1 C), 120.4 (s, 1 C), 124.2 (s, 1 C), 144 (s, 1 C), 149.4 (s, 1 C), 161.4 (s, 1 C); APCI-MS  $m/z = 188.23$  calcd. for  $\text{C}_{11}\text{H}_{12}\text{N}_2\text{O}$  [M]; found: 189.34 [M+H].

3.7.2.10. *tert-butyl 4-(benzo[d]oxazol-2-yl)piperazine-1-carboxylate (12j)*

The compound exhibited identical <sup>1</sup>H and <sup>13</sup>C NMR data as in previous reports.<sup>416</sup> General procedure (GP) was followed with 2-chlorobenzo[d]oxazole (0.12 mL, 1 mmol) and NHBoc piperazine (370 mg, 1.1 mmol, 1.1 equiv.) providing *tert-butyl 4-(benzo[d]oxazol-2-yl)piperazine-1-carboxylate* (298 mg, 0.985 mmol, 98%) as white crystals. <sup>1</sup>H NMR (300 MHz, CHLOROFORM-d) δ: 1.49 (s, 9 H), 3.52 - 3.63 (m, 4 H), 3.63 - 3.74 (m, 4 H), 6.99 - 7.09 (m, 1 H), 7.17 (td, J=7.74, 1.13 Hz, 1 H), 7.24 - 7.30 (m, 1 H), 7.33 - 7.41 (m, 1 H); <sup>13</sup>C NMR (75 MHz, CHLOROFORM-d) δ: 28.3 (s, 2 C), 45.4 (s, 2 C), 76.6 (s, 1 C), 77.4 (s, 2 C), 80.4 (s, 1 C), 108.8 (s, 1 C), 116.4 (s, 1 C), 120.9 (s, 1 C), 124.1 (s, 1 C), 142.8 (s, 1 C), 148.7 (s, 1 C), 154.5 (s, 1 C), 161.9 (s, 1 C); APCI-MS m/z = 303.36 calcd. for C<sub>16</sub>H<sub>21</sub>N<sub>3</sub>O<sub>3</sub> [M]; found: 304.21 [M+H].

3.7.2.11. *2-morpholinobenzo[d]oxazole (12k)*

The compound exhibited identical <sup>1</sup>H and <sup>13</sup>C NMR data as in previous reports.<sup>417</sup> General procedure (GP) was followed with 2-chlorobenzo[d]oxazole (0.12 mL, 1 mmol) and morpholine (0.10 mL, 1.1 mmol, 1.1 equiv.) providing *2-morpholinobenzo[d]oxazole* (188 mg, 0.925 mmol, 92%) as white solid. <sup>1</sup>H NMR (300 MHz, CHLOROFORM-d) δ: 3.66 - 3.73 (m, 4 H), 3.79 - 3.86 (m, 4 H), 7.01 - 7.08 (m, 1 H), 7.18 (td, J=7.65, 1.32 Hz, 1 H), 7.25 - 7.30 (m, 1 H), 7.37 (dd, J=7.93, 0.76 Hz, 1 H); <sup>13</sup>C NMR (75 MHz, CHLOROFORM-d) δ: 45.7 (s, 2 C), 66.2 (s, 2 C), 108.8 (s, 1 C), 116.5 (s, 1 C), 120.9 (s, 1 C), 124.1 (s, 1 C), 142.8 (s, 1 C), 148.7 (s, 1 C), 162.1 (s, 1 C); (+ve)APCI-MS m/z = 204.09 calcd. for C<sub>11</sub>H<sub>12</sub>N<sub>2</sub>O<sub>2</sub> [M]; found: 205.12 [M+H].

3.7.2.12. *2-(piperidin-1-yl)benzo[d]oxazole (12l)*

The compound exhibited identical <sup>1</sup>H and <sup>13</sup>C NMR data as in previous reports.<sup>418</sup> General procedure (GP) was followed with 2-chlorobenzo[d]oxazole (0.12 mL, 1 mmol) and piperidine (0.11 mL, 1.1 mmol, 1.1 equiv.) providing *2-(piperidin-1-yl)benzo[d]oxazole* (191 mg, 0.946 mmol, 94%) as shiny crystals. <sup>1</sup>H NMR (300 MHz, CHLOROFORM-d) δ: 1.61 - 1.76 (m, 6 H), 3.60 - 3.71 (m, 4 H), 6.96 - 7.02 (m, 1 H), 7.14 (td, J=7.74, 1.13 Hz, 1 H), 7.23 (dt, J=7.93, 0.94 Hz, 1 H), 7.34 (dt, J=8.12, 0.85 Hz, 1 H); <sup>13</sup>C NMR (75 MHz, CHLOROFORM-d) δ: 24 (s, 2 C), 25.2 (s, 2 C), 46.6 (s, 1 C), 108.5 (s, 1 C) 116 (s, 1 C) 120.2 (s, 1 C) 123.8 (s, 1 C) 143.4 (s, 1 C) 148.7 (s, 1 C) 162.4 (s, 1 C); APCI-MS m/z = 202.11 calcd. for C<sub>12</sub>H<sub>14</sub>N<sub>2</sub>O [M]; found: 203.55 [M+H].

3.7.2.13. *6-(piperidin-1-yl)-9H-purine (12m)*

The compound exhibited identical <sup>1</sup>H and <sup>13</sup>C NMR data as in previous reports.<sup>419</sup> General procedure (GP) was followed with 6-chloropurine (154.56 mg, 1 mmol) and piperidine (0.11 mL, 1.1 mmol, 1.1 equiv.) providing the desired 6-(piperidin-1-yl)-9H-purine at 80 °C for 2 h (132 mg, 0.65 mmol, 65%) as white solid. <sup>1</sup>H NMR (300 MHz, <sup>13</sup>C NMR CHLOROFORM-*d*) δ: 1.68-1.81 (m, 6 H), 4.30 (br. s., 5 H), 7.95 (s, 1 H), 8.38 (s, 1 H), (75 MHz, CHLOROFORM-*d*) δ: 24.8 (s, 2 C), 26.2 (s, 2 C), 45.6 (s, 1 C), 119.5 (s, 1 C), 136.3 (s, 1 C), 151.1 (s, 1 C), 151.6 (s, 1 C), 153.9 (s, 1 C); (+ve)APCI-MS *m/z* = 203.24 calcd. for C<sub>10</sub>H<sub>13</sub>N<sub>5</sub> [M], found: 204.32 [M+H].

3.7.2.14. *6-morpholino-9H-purine (12n)*

The compound exhibited identical <sup>1</sup>H and <sup>13</sup>C NMR data as in previous reports.<sup>419</sup> General procedure (GP) was followed with 6-chloropurine (154.6 mg, 1 mmol) and piperidine (0.10 mL, 1.1 mmol, 1.1 equiv.) providing the desired 6-morpholino-9H-purine at 80 °C for 2 h (139 mg, 0.65 mmol, 78%) as white solid. <sup>1</sup>H NMR (300 MHz, DMSO-*d*<sub>6</sub>) δ: 3.67-3.73 (m, 4 H), 4.20 (br. s., 5 H), 8.12 (s, 1H), 8.22 (s, 1 H); <sup>13</sup>C NMR (75 MHz, DMSO-*d*<sub>6</sub>) δ: 45.4 (s, 2 C), 66.5 (s, 2 C), 119.1 (s, 1 C), 138.6 (s, 1 C), 152 (s, 2 C), 153.5 (s, 1 C); (+ve)APCI-MS *m/z* = 205.22 calcd. for C<sub>9</sub>H<sub>11</sub>N<sub>5</sub>O [M], found: 206.11 [M+H].

3.7.2.15. *N, N'-diethyl-9H-purin-6-amine (12o)*

The compound exhibited identical <sup>1</sup>H and <sup>13</sup>C NMR data as in previous reports.<sup>420</sup> General procedure (GP) was followed with 6-chloropurine (154.6 mg, 1 mmol) and *N,N'*-diethylamine (0.12 mL, 1.1 mmol, 1.1 equiv.) providing the desired *N,N'*-diethyl-9H-purin-6-amine at 80 °C for 2 h (58 mg, 0.30 mmol, 45%) as colorless solid. <sup>1</sup>H NMR (300 MHz, DMSO-*d*<sub>6</sub>) δ; 1.17-1.22 (m, 6 H), 3.78-4.10 (m, 4 H), 8.07 (s, 1 H), 8.16 (s, 1 H), 12.90 (br. s., 1 H); <sup>13</sup>C NMR (75 MHz, DMSO-*d*<sub>6</sub>) δ: 30.7 (s, 2 C), 54.9 (s, 2 C), 118.4 (s, 1 C), 137.9 (s, 1 C), 151.1 (s, 1 C), 151.9 (s, 1 C), 153 (s, 1 C); (+ve)APCI-MS *m/z* = 191.24 calcd. for C<sub>9</sub>H<sub>13</sub>N<sub>5</sub> [M]; found: 192.18 [M+H].

3.7.2.16. *tert-butyl 4-(9H-purin-6-yl)piperazine-1-carboxylate (12p)*

The compound exhibited identical <sup>1</sup>H and <sup>13</sup>C NMR data as in previous reports.<sup>421</sup> General procedure (GP) was followed with 6-chloropurine (154.6 mg, 1 mmol) and *NHBoc* piperazine (370 mg, 1.1 mmol, 1.1 equiv.) providing the desired *tert*-butyl 4-(9H-purin-6-yl)piperazine-1-carboxylate at 80 °C for 2 h (182mg, 0.60 mmol, 60%) as colorless solid. <sup>1</sup>H NMR (300 MHz, DMSO-*d*<sub>6</sub>) δ:1.43 (s, 9 H), 3.46 (d, *J*=5.29 Hz, 4 H), 4.20 (br. s., 4 H), 8.14 (s, 1 H), 8.23 (s, 1

H), 13.12 (br. s., 1 H);  $^{13}\text{C}$  NMR (75 MHz, DMSO- $d_6$ )  $\delta$ : 28 (s, 2 C), 44.3 (s, 2 C), 79.1 (s, 3 C), 118.8 (s, 1 C), 138.4 (s, 1 C), 151.4 (s, 1 C), 151.5 (s, 1 C), 151.7 (s, 1 C), 153.1 (s, 1C), 160.9 (s, 1 C); (+ve)APCI-MS  $m/z$  = 304.35 calcd. for  $\text{C}_{14}\text{H}_{20}\text{N}_6\text{O}_2$  [M], found: 305.42 [M+H].

3.7.2.17. *6-(pyrrolidin-1-yl)-9H-purine (12q)*

The compound exhibited identical  $^1\text{H}$  and  $^{13}\text{C}$  NMR data as in previous reports.<sup>419</sup> General procedure (GP) was followed with 6-chloropurine (154.6 mg, 1 mmol) and pyrrolidine (0.092 mL, 1.1 mmol, 1.1 equiv.) providing the desired 6-(pyrrolidin-1-yl)-9H-purine at 80 °C for 2 h (116 mg, 0.62 mmol, 72%) as white solid.  $^1\text{H}$  NMR (300 MHz, DMSO- $d_6$ )  $\delta$ : 1.85 - 2.07 (m, 4 H), 3.64 (br. s., 2 H), 3.88-4.20 (m, 2 H), 8.04 (s, 1 H), 8.16 (s, 1 H), 12.88 (br. s., 1 H);  $^{13}\text{C}$  NMR (75 MHz, DMSO- $d_6$ )  $\delta$ : 24.7 (s, 2 C), 46.1 (s, 2 C), 119.1 (s, 1 C), 138.1 (s, 1 C), 150.6 (s, 1 C), 152.1 (s, 1 C), 152.5 (s, 1 C); (+ve)APCI-MS  $m/z$  = 188.22 calcd. for  $\text{C}_9\text{H}_{11}\text{N}_5$ [M], found: 189.32 [M+H].

3.7.2.18. *7-morpholino-4-(pentyloxy)pteridin-2-amine (12r)*

General Procedure (GP) was followed with 7-chloro-4-(pentyloxy)pteridin-2-amine (268 mg, 1 mmol) and morpholine (0.10 mL, 1.1 mmol, 1.1 equiv.) providing 7-morpholino-4-(pentyloxy)pteridin-2-amine (293 mg, 0.92 mmol, 92%) as pale yellow solid.  $^1\text{H}$  NMR (300 MHz, CHLOROFORM- $d$ )  $\delta$ : 0.81 - 0.96 (m, 3 H), 1.31 - 1.46 (m, 4 H), 1.80 - 1.96 (m, 2 H), 3.80 (s, 8 H), 4.48 (t,  $J=6.99$  Hz, 2 H), 5.25 (br. s., 2 H), 8.12 (s, 1 H);  $^{13}\text{C}$  NMR (75 MHz, CHLOROFORM- $d$ )  $\delta$ : 13.8 (s, 1 C), 22.3 (s, 1 C), 27.9 (s, 1 C), 28.3 (s, 1 C), 44.5 (s, 1 C), 66.4 (s, 1 C), 67.6 (s, 1 C), 76.5 (s, 1 C), 77 (s, 1 C), 77.4 (s, 1 C), 129.2 (s, 1 C), 155.9 (s, 1 C), 157.1 (s, 1 C), 161.9 (s, 1 C), 162.4 (s, 1 C); APCI-MS  $m/z$  = 318.37 calcd. for  $\text{C}_{15}\text{H}_{22}\text{N}_6\text{O}_2$  [M]; found : 319.54 [M+H], CHNS calcd. C, 56.59; H, 6.96; N, 26.40; found: C, 56.71; H, 7.01; N, 26.32.

3.7.2.19. *4-(pentyloxy)-7-(piperidin-1-yl)pteridin-2-amine (12s)*

General procedure (GP) was followed with 7-chloro-4-(pentyloxy)pteridin-2-amine (268 mg, 1 mmol) and piperidine (0.11 mL, 1.1 mmol, 1.1 equiv.) providing 4-(pentyloxy)-7-(piperidin-1-yl)pteridin-2-amine (285 mg, 9.90 mmol, 90%) as pale yellow solid.  $^1\text{H}$  NMR (300 MHz, CHLOROFORM- $d$ )  $\delta$ : 0.87 - 0.95 (m, 3 H), 1.33 - 1.48 (m, 4 H), 1.62 - 1.75 (m, 6 H), 1.80 - 1.94 (m, 2 H), 3.69 - 3.91 (m, 4 H), 4.47 (t,  $J=7.18$  Hz, 2 H), 5.15 (br. s., 2 H), 8.14 (s, 1 H);  $^{13}\text{C}$  NMR (75 MHz, CHLOROFORM- $d$ )  $\delta$ : 13.9 (s, 1 C), 22.4 (s, 1 C), 24.5 (s, 1 C), 25.7 (s, 1 C), 27.9 (s, 1 C), 28.4 (s, 1 C), 45.6 (s, 1 C), 67.5 (s, 1 C), 76.6 (s, 1 C), 77 (s, 1 C), 77.4 (s, 1 C), 129.8 (s, 1 C), 155.7 (s, 1 C), 157.5 (s, 1 C), 161.8 (s, 1 C), 166.8 (s, 1 C); APCI-MS  $m/z$



= 316.4 calcd. for C<sub>16</sub>H<sub>24</sub>N<sub>6</sub>O [M]; found: 317.21 [M+H], CHNS calcd. C, 60.74; H, 7.65; N, 26.56; found: C, 60.69; H, 7.23; N, 26.01.

3.7.2.20. *4-(pentyloxy)-7-(pyrrolidin-1-yl)pteridin-2-amine (12t)*

General procedure (GP) was followed with 7-chloro-4-(pentyloxy)pteridin-2-amine (268 mg, 1 mmol) and pyrrolidine (0.092 mL, 1.1 mmol, 1.1 equiv.) providing the desired 4-(pentyloxy)-7-(pyrrolidin-1-yl)pteridin-2-amine(-) (266 mg, 0.88 mmol, 88%) as pale yellow solid. <sup>1</sup>H NMR (300 MHz, CHLOROFORM-*d*) δ: 0.76 - 1.01 (m, 3 H), 1.35 (d, *J*=3.40 Hz, 4 H), 1.72 - 1.87 (m, 2 H), 1.99 (br. s., 3 H), 2.07 (s, 1 H), 3.57 (br. s., 4 H), 4.38 (t, *J*=6.80 Hz, 2 H), 6.11 (br. s., 2 H), 7.84 (s, 1 H); <sup>13</sup>C NMR (75 MHz, CHLOROFORM-*d*) δ: 12.4 (s, 1 C), 20.6 (s, 1 C), 26.3 (s, 1 C), 26.7 (s, 2 C), 44.9 (s, 2 C), 65.1 (s, 1 C), 112.2 (s, 1 C), 128.4 (s, 1 C), 152.5 (s, 1 C), 156.1 (s, 2 C), 160.4 (s, 1 C), 164.9 (s, 1 C); APCI-MS *m/z* = 302.37 calcd. for C<sub>15</sub>H<sub>22</sub>N<sub>6</sub>O [M]; found: 303.58 [M+H], CHNS calcd. C, 58.91; H, 8.09; N, 18.74; found: C, 58.82; H, 8.01; N, 18.53.

3.7.2.21. *tert-butyl-4-(2-amino-4-(pentyloxy)pteridin-7-yl)piperazine-1-carboxylate (12u)*

General procedure (GP) was followed with 7-chloro-4-(pentyloxy)pteridin-2-amine (268 mg, 1 mmol) and NHBoc piperazine (370 mg, 1.1 mmol, 1.1 equiv.) providing tert-butyl 4-(2-amino-4-(pentyloxy)pteridin-7-yl)piperazine-1-carboxylate (326 mg, 0.781 mmol, 78%) as pale yellow crystals. <sup>1</sup>H NMR (300 MHz, CHLOROFORM-*d*) δ: 0.86 - 0.99 (m, 3 H), 1.32 - 1.57 (m, 13 H), 1.84 - 1.97 (m, 2 H), 3.52 - 3.64 (m, 4 H), 3.79 - 3.92 (m, 4 H), 4.50 (t, *J*=6.99 Hz, 2 H), 5.25 (br. s., 2 H), 8.15 (s, 1 H); <sup>13</sup>C NMR (75 MHz, CHLOROFORM-*d*) δ: 13.9 (s, 1 C), 22.3 (s, 1 C), 27.9 (s, 1 C), 28.3 (s, 1 C), 44 (s, 2 C), 67.7 (s, 2 C), 76.6 (s, 3 C), 77.4 (s, 2 C), 80.3 (s, 1 C), 129.3 (s, 1 C), 154.5 (s, 1 C), 155.7 (s, 1 C), 157.1 (s, 1 C), 161.9 (s, 1 C), 167 (s, 1 C); APCI-MS *m/z* = 417.51 calcd. for C<sub>20</sub>H<sub>31</sub>N<sub>7</sub>O<sub>3</sub> [M]; found: 418.73 [M+H], CHNS calcd. C, 57.54; H, 7.48; N, 23.48; found: C, 57.23; H, 7.32; N, 23.22.

3.7.2.22. *2-chloro-4-(pyrrolidin-1-yl)pyrimidine (14a)*

The compound exhibited identical <sup>1</sup>H and <sup>13</sup>C NMR data as in previous reports.<sup>422</sup> General procedure (GP) was followed with 2,4-dichloropyrimidine (149 mg, 1 mmol) and pyrrolidine (0.092 mL, 1.1 mmol, 1.1 equiv.) providing the desired 2-chloro-4-(pyrrolidin-1-yl)pyrimidine (159 mg, 0.87 mmol, 87%) as colorless needles. <sup>1</sup>H NMR (300 MHz, DMSO-*d*<sub>6</sub>) δ: 1.80-2.05 (m, 4 H), 3.37-3.50 (m, 4 H), 6.46 (d, *J*=6.04 Hz, 1 H), 8.00 (d, *J*=6.04 Hz, 1 H); <sup>13</sup>C NMR (75 MHz, DMSO-*d*<sub>6</sub>) δ: 24.6 (s, 1 C), 25.2 (s, 1 C), 46.7 (s, 2 C), 103.3 (s, 1 C), 156.5 (s, 1 C),

159.7 (s, 1 C), 160.8 (s, 1 C); APCI-MS  $m/z$  = 183.64 calcd. for  $C_8H_{10}ClN_3$  [M]; found: 184.72 [M+H].

3.7.2.23. *2-chloro-4-(piperidin-1-yl)pyrimidine (14b)*

The compound exhibited identical  $^1H$  and  $^{13}C$  NMR data as in previous reports.<sup>422</sup> General procedure (GP) was followed with 2,4-dichloropyrimidine (149 mg, 1 mmol) and piperidine (0.11 mL, 1.1 mmol, 1.1 equiv.) providing the desired 2-chloro-4-(piperidin-1-yl)pyrimidine (158 mg, 0.80 mmol, 80%) as colorless needles.  $^1H$  NMR (300 MHz, DMSO- $d_6$ )  $\delta$ : 1.47-1.57 (m, 4 H), 1.57-1.68 (m, 2 H), 3.52-3.67 (m, 4 H), 6.80 (d,  $J=6.42$  Hz, 1 H), 8.01 (d,  $J=6.42$  Hz, 1 H);  $^{13}C$  NMR (75 MHz, DMSO- $d_6$ )  $\delta$ : 23.9 (s, 2 C), 25.1 (s, 2 C), 44.7 (s, 1 C), 102.1 (s, 1 C), 157.2 (s, 1 C), 159.6 (s, 1 C), 162 (s, 1 C); APCI-MS  $m/z$ = 197.67 calcd. for  $C_9H_{12}ClN_3$ [M], found: 198.89 [M+H].

3.7.2.24. *2-chloro-4-morpholinopyrimidine (14c)*

The compound exhibited identical  $^1H$  and  $^{13}C$  NMR data as in previous reports.<sup>422</sup> General procedure (GP) was followed with 2,4-dichloropyrimidine (149 mg, 1 mmol) and morpholine (0.10 mL, 1.1 mmol, 1.1 equiv.) providing the desired 2-chloro-4-morpholinopyrimidine (168 mg, 0.84 mmol, 84%) as colorless needles.  $^1H$  NMR (300 MHz, CHLOROFORM- $d$ )  $\delta$ : 3.63-3.87 (m, 8 H), 6.39 (d,  $J=6.04$  Hz, 1 H), 8.07 (d,  $J=6.42$  Hz, 1 H);  $^{13}C$  NMR (75 MHz, CHLOROFORM- $d$ )  $\delta$ : 43.6 (s, 1 C), 43.7 (s, 1 C), 43.8 (s, 1 C), 65.8 (s, 2 C), 100.6 (s, 1 C), 157 (s, 1 C), 162.4 (s, 1 C); APCI-MS  $m/z$ = 199.64 calcd. for  $C_8H_{10}ClN_3O$  [M], found: 200.86 [M+H].

3.7.2.25. *tert-butyl 4-(2-chloropyrimidin-4-yl)piperazine-1-carboxylate (14d)*

The compound exhibited identical  $^1H$  and  $^{13}C$  NMR data as in previous reports.<sup>423</sup> General procedure (GP) was followed with 2,4-dichloropyrimidine (149 mg, 1 mmol) and NHBoc piperazine (370 mg, 1.1 mmol, 1.1 equiv.) providing the desired tert-butyl 4-(2-chloropyrimidin-4-yl)piperazine-1-carboxylate (257 mg, 0.86 mmol, 86%) as colorless needles.  $^1H$  NMR (300 MHz, DMSO- $d_6$ )  $\delta$ : 1.42 (s, 9 H), 3.37-3.46 (m, 4 H), 3.54-3.72 (m, 4 H), 6.83 (d,  $J=6.04$  Hz, 1 H), 8.09 (d,  $J=6.42$  Hz, 1 H);  $^{13}C$  NMR (75 MHz, DMSO- $d_6$ )  $\delta$ : 28 (s, 2 C), 43.3 (s, 2 C), 79.2 (s, 3 C), 102.5 (s, 2 C), 153.8 (s, 1 C), 157.5 (s, 1 C), 159.5 (s, 1 C), 162.4 (s, 1 C); APCI-MS  $m/z$  = 298.77 calcd. for  $C_{13}H_{19}ClN_4O_2$ [M]; found: 299.92 [M+H].

3.7.2.26. *2-chloro-4-(4-tosylpiperazin-1-yl)pyrimidine (14e)*

The compound exhibited identical  $^1H$  and  $^{13}C$  NMR data as in previous reports.<sup>424</sup> General procedure (GP) was followed with 2,4-dichloropyrimidine (149 mg, 1 mmol) and 1-

tosylpiperazine (264 mg, 1.1 mmol, 1.1 equiv.) providing the desired 2-chloro-4-(4-tosylpiperazin-1-yl)pyrimidine (229 mg, 0.95 mmol, 95%) as white shiny crystalline solid. <sup>1</sup>H NMR (300 MHz, CHLOROFORM-*d*) δ: 2.43 (s, 3 H), 3.01-3.15 (m, 4 H), 3.65-3.89 (m, 4 H), 6.34 (d, *J*=6.04 Hz, 1 H), 7.33 (dd, *J*=8.69, 0.76 Hz, 2 H), 7.60-7.67 (m, 2 H), 8.03 (d, *J*=6.04 Hz, 1 H); <sup>13</sup>C NMR (75 MHz, CHLOROFORM-*d*) δ: 21.1 (s, 2 C), 42.9 (s, 2 C), 45.1 (s, 1 C), 100.7 (s, 1 C), 127.3 (s, 1 C), 129.4 (s, 2 C), 131.6 (s, 2 C), 143.8 (s, 1 C), 157.3 (s, 1 C), 160.3 (s, 1 C), 161.8 (s, 1 C); APCI-MS *m/z*= 352.08 calcd. for C<sub>15</sub>H<sub>17</sub>ClN<sub>4</sub>O<sub>2</sub>S [M], found: 353.22 [M+H].

### 3.7.2.27. *di-tert-butyl 4,4'-(pyrimidine-2,4-diyl)bis(piperazine-1-carboxylate) (15)*

General procedure (GP) was followed with 2,4 dichloropyrimidine (149 mg, 1 mmol) and NHBoc piperazine (750 mg, 2.2 mmol, 2.2 equiv.) providing the desired *di-tert-butyl 4,4'-(pyrimidine-2,4-diyl)bis(piperazine-1-carboxylate)* (225 mg, 0.51 mmol, 87%) as white amorphous solid. <sup>1</sup>H NMR (300 MHz, CHLOROFORM-*d*) δ: 1.42-1.54 (m, 18 H), 3.42-3.77 (m, 16 H), 6.39 (d, *J*=6.04 Hz, 1 H), 8.06 (d, *J*=6.04 Hz, 1 H); <sup>13</sup>C NMR (75 MHz, CHLOROFORM-*d*) δ: 28.7 (s, 2 C), 28.8 (s, 2 C), 43.9 (s, 2 C), 44 (s, 2 C), 80.8 (s, 6 C), 101.6 (s, 2 C), 155.1 (s, 1 C), 157.9 (s, 1 C), 161.2 (s, 2 C), 163 (s, 2 C); (+ve)APCI-MS *m/z*= 448.56 calcd. for C<sub>22</sub>H<sub>36</sub>N<sub>6</sub>O<sub>4</sub>[M], found : 449. 61 [M+H]. CHNS calcd. C, 58.91; H, 8.09; N, 18.74; found: C, 58.82; H, 8.01; N, 18.53.

### 3.7.2.28. *2-(hydroxymethyl)-5-(6-morpholino-9H-purin-9-yl)-tetrahydrofuran-3,4-diol (17a)*

The compound exhibited identical <sup>1</sup>H and <sup>13</sup>C NMR data as in previous reports.<sup>425</sup> General procedure (GP) was followed with 2-(6-chloro-9H-purin-9-yl)-5-(hydroxymethyl)-tetrahydrofuran-3,4-diol (287 mg, 1 mmol) and pyrrolidine (0.092 mL, 1.1 mmol, 1.1 equiv) providing 2-(hydroxymethyl)-5-(6-morpholino-9H-purin-9-yl)-tetrahydrofuran-3,4-diol (276 mg, 0.86 mmol, 86%) as white solid. <sup>1</sup>H NMR (300 MHz, DMSO-*d*<sub>6</sub>) δ: 3.58 (dd, *J*=6.80, 3.78 Hz, 1 H), 3.63 - 3.80 (m, 5 H), 3.97 (d, *J*=3.40 Hz, 1 H), 4.09 - 4.36 (m, 5 H), 4.58 (d, *J*=4.91 Hz, 1 H), 5.19 (d, *J*=4.91 Hz, 1 H), 5.31 (dd, *J*=6.80, 4.91 Hz, 1 H), 5.46 (d, *J*=6.04 Hz, 1 H), 5.93 (d, *J*=6.04 Hz, 1 H), 8.27 (s, 1 H), 8.43 (s, 1 H); <sup>13</sup>C NMR (75 MHz, DMSO-*d*<sub>6</sub>) δ: 45.2 (s, 2 C), 61.5 (s, 2 C), 66.2 (s, 1 C), 70.4 (s, 1 C), 73.5 (s, 1 C), 85.7 (s, 1 C), 87.8 (s, 1 C), 119.6 (s, 1 C), 139 (s, 1 C), 150.3 (s, 1 C), 151.7 (s, 1 C), 153.3 (s, 1 C); APCI-MS *m/z* = 337.34 calcd. for C<sub>14</sub>H<sub>19</sub>N<sub>5</sub>O<sub>5</sub> [M]; found: 338.41 [M+H], 204.21 [M-ribose].

3.7.2.29. *2-(hydroxymethyl)-5-(6-(piperidin-1-yl)-9H-purin-9-yl)-tetrahydrofuran-3,4-diol (17b)*

The compound exhibited identical  $^1\text{H}$  and  $^{13}\text{C}$  NMR data as in previous reports.<sup>425</sup> General procedure (GP) was followed with 2-(6-chloro-9H-purin-9-yl)-5-(hydroxymethyl)-tetrahydrofuran-3,4-diol (287 mg, 1 mmol) and piperidine (0.11 mL, 1.1 mmol, 1.1 equiv.) providing 2-(hydroxymethyl)-5-(6-(piperidin-1-yl)-9H-purin-9-yl)-tetrahydrofuran-3,4-diol (295mg, 0.88 mmol, 91%) as colorless solid.  $^1\text{H}$  NMR (300 MHz, DMSO-d<sub>6</sub>)  $\delta$ : 1.58 (d, J=3.78 Hz, 4 H), 1.67 (d, J=4.53 Hz, 2 H), 3.55 (ddd, J=11.99, 7.08, 3.59 Hz, 1 H), 3.67 (dt, J=12.09, 3.97 Hz, 1 H), 3.96 (q, J=3.40 Hz, 1 H), 4.06 - 4.33 (m, 5 H), 4.58 (q, J=6.04 Hz, 1 H), 5.17 (d, J=4.53 Hz, 1 H), 5.36 (dd, J=6.80, 4.53 Hz, 1 H), 5.44 (d, J=6.04 Hz, 1 H), 5.91 (d, J=6.04 Hz, 1 H), 8.21 (s, 1 H), 8.37 (s, 1 H);  $^{13}\text{C}$  NMR (75 MHz, DMSO-d<sub>6</sub>)  $\delta$ : 24.5 (s, 2 C), 26 (s, 2 C), 45.9 (s, 1 C), 61.8 (s, 1 C), 70.8 (s, 1 C), 73.7 (s, 1 C), 86 (s, 1 C), 88.1 (s, 1 C), 119.8 (s, 1 C), 138.8 (s, 1 C), 150.4 (s, 1 C), 152.1 (s, 1 C), 153.4 (s, 1 C); APCI-MS  $m/z$  = 335.16 calcd. for C<sub>15</sub>H<sub>21</sub>N<sub>5</sub>O<sub>4</sub> [M]; found: 336.27[M+H], 202.24 [M-ribose].

3.7.2.30. *tert-butyl 4-(9-(3,4-dihydroxy-5-(hydroxymethyl)-tetrahydrofuran-2-yl)-9H-purin-6-yl)piperazine-1-carboxylate (17c)*

General procedure (GP) was followed with 2-(6-chloro-9H-purin-9-yl)-5-(hydroxymethyl)-tetrahydrofuran-3,4-diol (287 mg, 1 mmol) and NHBoc piperazine (370 mg, 1.1 mmol, 1.1 equiv.) providing tert-butyl 4-(9-(3,4-dihydroxy-5-(hydroxymethyl)-tetrahydrofuran-2-yl)-9H-purin-6-yl)piperazine-1-carboxylate (393 mg, 0.901 mmol, 89%) as colorless solid.  $^1\text{H}$  NMR (300 MHz, DMSO-d<sub>6</sub>)  $\delta$ : 1.43 (s, 9 H), 3.42 - 3.49 (m, 2 H), 3.51 - 3.61 (m, 2 H), 3.61 - 3.75 (m, 2 H), 3.96 q, (J=3.40 Hz, 2 H), 4.09 - 4.38 (m, 4 H), 4.51 - 4.64 (m, 1 H), 5.18 (d, J=4.91 Hz, 1 H), 5.30 (dd, J=6.80, 4.53 Hz, 1 H), 5.45 (d, J=6.04 Hz, 1 H), 5.93 (d, J=6.04 Hz, 1 H), 8.27 (s, 1 H) 8.44 (s, 1 H);  $^{13}\text{C}$  NMR (75 MHz, DMSO-d<sub>6</sub>)  $\delta$ : 28 (s, 2 C), 61.4 (s, 2 C), 70.4 (s, 2 C), 73.5 (s, 2 C), 79.1 (s, 2 C), 85.7 (s, 2 C), 87.7 (s, 1 C), 119.6 (s, 1 C), 139 (s, 1 C), 150.3 (s, 1 C), 151.7 (s, 1 C), 153.2 (s, 1 C), 153.9 (s, 1 C); (+ve)APCI-MS  $m/z$  = 436.21 calcd. for C<sub>19</sub>H<sub>28</sub>N<sub>6</sub>O<sub>6</sub> [M]; found: 437.55 [M+H], 303.35 [M-ribose]; CHNS calcd. C, 52.28; H, 6.47; N, 19.25; found: C, 52.76; H, 6.44; N, 19.02.

3.7.2.31. *6-chloropyrimidine-2,4(1H, 3H)-dione (19)*

The compound exhibited identical  $^1\text{H}$  and  $^{13}\text{C}$  NMR data as in previous report.<sup>426</sup> In a 100 ml round bottomed flask a saturated solution of NaOH (27.3 g, 0.68 mol) in 20 mL of water was supplied with 2,4,6 trichloropyrimidine (14 mL, 0.12 mol) under continuous stirring. The resultant reaction mixture was refluxed for 2 h. After the completion of reaction (monitored by

TLC) the pH of the solution was adjusted to pH = 2 by adding con.HCl while cooling in an ice-bath. The product was precipitated out as a white solid which was filtered, washed with hot water and dried under vacuum at 50 °C and isolated as a white solid (16 g, 0.11 mol, 92%). <sup>1</sup>H NMR (300 MHz, DMSO-d<sub>6</sub>) δ: 5.63 (s, 1 H), 11.03 (br. s., 2 H); <sup>13</sup>C NMR (75 MHz, DMSO-d<sub>6</sub>) δ: 98.7 (s, 1 C), 147.3 (s, 1 C), 151.6 (s, 1 C), 163.2 (s, 1 C); APCI-MS m/z = 145.99 calcd. for C<sub>4</sub>H<sub>3</sub>ClN<sub>2</sub>O<sub>2</sub> [M]; found: 146.12 [M+H].

### 3.7.2.32. 6-chloro-1,3-dimethylpyrimidine-2,4(1H,3H)-dione (**20**)

The compound exhibited identical <sup>1</sup>H and <sup>13</sup>C NMR data as in previous reports.<sup>426</sup> To a suspension of 6-chloropyrimidine-2,4(1H,3H)-dione (5.84 g, 40 mmol) and K<sub>2</sub>CO<sub>3</sub> (1 equiv. 5.6 g, 40 mmol) in DMSO (25 mL) was added an excess of CH<sub>3</sub>I (8 mL) and the mixture stirred at room temperature for 3 h. Then the reaction mixture was cooled to 0 °C followed by addition of water (50 mL) and stirring continued for another 3 h to obtain a white precipitate. The crude product was extracted with EtOAc (3x 150 mL), the organic layer was washed with ice-cold water 3 times (3x100 mL), brine solution (2 x 50 mL) dried over Na<sub>2</sub>SO<sub>4</sub>, filtered and evaporated on a roto-evaporator to provide a pale-yellow solid (3.63 g, 20.8 mmol, 52%). <sup>1</sup>H NMR (300 MHz, CHLOROFORM-d) δ: 3.33 (s, 3 H), 3.56 (s, 3 H), 5.94 (s, 1 H); <sup>13</sup>C NMR (75 MHz, CHLOROFORM-d) δ: 28.3 (s, 1 C), 33.6 (s, 1 C), 101.7 (s, 1 C), 146 (s, 1 C), 151.2 (s, 1 C), 160.8 (s, 1 C); APCI-MS m/z = 174.02 calcd. for C<sub>6</sub>H<sub>7</sub>ClN<sub>2</sub>O<sub>2</sub> [M]; found: 175.11 [M+H].

### 3.7.2.33. 1,3-dimethyl-6-(piperidin-1-yl)pyrimidine-2,4(1H,3H)-dione (**21a**)

The compound exhibited identical <sup>1</sup>H and <sup>13</sup>C NMR data as in previous reports.<sup>427</sup> General procedure (GP) was followed with 6-chloro-1,3-dimethylpyrimidine-2,4(1H, 3H)-dione (175 mg, 1 mmol) and piperidine (0.11 mL, 1.1 mmol, 1.1 equiv.) providing 1,3-dimethyl-6-(piperidin-1-yl)pyrimidine-2,4(1H, 3H)-dione (168 mg, 0.753 mmol, 94%) as white solid. <sup>1</sup>H NMR (300 MHz, CHLOROFORM-d) δ: 1.57 - 1.77 (m, 6 H), 2.76 - 3.02 (m, 4 H), 3.37 (s, 3 H), 3.32 (s, 3 H), 5.21 (s, 1 H); <sup>13</sup>C NMR (75 MHz, CHLOROFORM-d) δ: 23.8 (s, 2 C), 25.3 (s, 1 C), 27.7 (s, 1 C), 32.6 (s, 2 C), 51.6 (s, 1 C), 87.7 (s, 1 C), 153.2 (s, 1 C), 160.3 (s, 1 C), 163.4 (s, 1 C); APCI-MS m/z = 223.27 calcd. for C<sub>11</sub>H<sub>17</sub>N<sub>3</sub>O<sub>2</sub> [M]; found: 224.28 [M+H].

### 3.7.2.34. tert-butyl (R)-(1-(1,3-dimethyl-2,6-dioxo-1,2,3,6-tetrahydropyrimidin-4-yl)piperidin-3-yl)carbamate (**21b**)

General procedure (GP) was followed with 6-chloro-1,3-dimethylpyrimidine-2,4(1H, 3H)-dione (175 mg, 1 mmol) and tert-butyl piperidin-3-ylcarbamate (249 mg, 1.2 mmol, 1.2 equiv.) providing tert-butyl (R)-(1-(1,3-dimethyl-2,6-dioxo-1,2,3,6-tetrahydropyrimidin-4-

yl)piperidin-3-yl)carbamate (236 mg, 0.699 mmol, 69%) as colorless crystals.  $^1\text{H}$  NMR (300 MHz, CHLOROFORM- $d$ )  $\delta$ : 1.43 (s, 9 H), 1.63 - 1.89 (m, 3 H), 1.89 - 2.06 (m, 1 H), 2.49 (br. s., 1 H), 2.71 (d,  $J=9.06$  Hz, 1 H), 2.95 (br. s., 1 H), 3.30 (s, 4 H), 3.40 (s, 3 H), 3.75 (br. s., 1 H), 4.65 (br. s., 1 H), 5.20 (s, 1 H);  $^{13}\text{C}$  NMR (75 MHz, CHLOROFORM- $d$ )  $\delta$ : 23 (s, 3 C), 27.7 (s, 2 C), 28.3 (s, 1 C), 29.7 (s, 1 C), 32.4 (s, 1 C), 46.5 (s, 1 C), 50.6 (s, 1 C), 55.7 (s, 1 C), 88.3 (s, 1 C), 152.9 (s, 1 C), 154.9 (s, 1 C), 159.5 (s, 1 C), 163.2 (s, 1 C); APCI-MS  $m/z$  = 338.2 calcd. for  $\text{C}_{16}\text{H}_{26}\text{N}_4\text{O}_4$  [M]; found: 339.25 [M+H]. CHNS calcd. C, 56.79; H, 7.74; N, 16.56; found: C, 56.76; H, 7.44; N, 16.02.

3.7.2.35. *Synthetic approach to Alogliptin:2-((6-chloro-3-methyl-2,4-dioxo-3,4-dihydropyrimidin-1(2H)-yl)methyl)benzotrile (24)*

The compound exhibited identical  $^1\text{H}$  and  $^{13}\text{C}$  NMR data as in previous reports.<sup>428</sup> To a saturated solution of 6-chloro-3-methylpyrimidine-2,4(1*H*, 3*H*)-dione (1 g, 6.23 mmol) in dry THF was added DIPEA (4.2 mL, 24.92 mmol, 4 equiv.) and stirred at room temperature for 15 min then followed by the addition of 1.2 equiv. of 2(bromomethyl)benzotrile (1.465 g, 7.476 mmol). The resultant reaction mixture was stirred at 65 °C for 2 h (monitored by TLC). After the completion of the reaction, the mixture was neutralized by adding water 100 mL and extracted with  $\text{CHCl}_3$  (2x100 mL). The combined organic layers were dried over  $\text{Na}_2\text{SO}_4$ , filtered, and concentrated under reduced pressure. The crude product was washed with hexane to produce a white solid 2-((6-chloro-3-methyl-2,4-dioxo-3,4-dihydropyrimidin-1(2*H*)-yl)methyl)benzotrile (1.64 g, 5.95 mmol, 96%).  $^1\text{H}$  NMR (300 MHz, CHLOROFORM- $d$ )  $\delta$ : 3.35 - 3.45 (m, 3 H), 5.52 (s, 2 H), 6.02 (s, 1 H), 7.22 (d,  $J=7.55$  Hz, 1 H), 7.39 - 7.48 (m, 1 H), 7.61 (td,  $J=7.84$ , 1.32 Hz, 1 H), 7.68 - 7.74 (m, 1 H);  $^{13}\text{C}$  NMR (75 MHz, CHLOROFORM- $d$ )  $\delta$ : 28.1 (s, 1 C), 102.3 (s, 1 C), 110.6 (s, 1 C), 116.3 (s, 1 C), 126 (s, 1 C), 128 (s, 1 C), 132.6 (s, 1 C), 132.9 (s, 1 C), 133 (s, 1 C), 138.6 (s, 1 C), 144.7 (s, 1 C), 150.8 (s, 1 C), 160 (s, 1 C); APCI-MS  $m/z$  = 275.05 calcd. for  $\text{C}_{13}\text{H}_{10}\text{ClN}_3\text{O}_2$  [M]; found: 276.12 [M+H].

3.7.2.36. *(R)-2-((6-(3-aminopiperidin-1-yl)-3-methyl-2,4-dioxo-3,4-dihydropyrimidin-1(2H)-yl)methyl)benzotrile (25)*

The compound exhibited identical  $^1\text{H}$  and  $^{13}\text{C}$  NMR data as in previous reports.<sup>314</sup> General procedure (GP) was followed with 2-((6-chloro-3-methyl-2,4-dioxo-3,4-dihydropyrimidin-1(2*H*)-yl)methyl)benzotrile (276 mg, 1 mmol) and *tert*-butyl piperidin-3-ylcarbamate (249 mg, 1.2 mmol, 4 equiv.) providing (*R*)-2-((6-(3-aminopiperidin-1-yl)-3-methyl-2,4-dioxo-3,4-dihydropyrimidin-1(2*H*)-yl)methyl)benzotrile as white solid. The crude mixture was dissolved in  $\text{CH}_2\text{Cl}_2$  (10 mL) to which 1 mL of  $\text{CF}_3\text{COOH}$  was added slowly at room

temperature. The solution was stirred for 1 h at the same temperature and monitored by TLC. After the completion of reaction, the solvent was evaporated under reduced pressure, the crude viscous liquid mixed with a small quantity of MeOH and precipitated by diethyl ether. The white crystalline powder was filtered and dried (313 mg, 0.92 mmol, 92%). <sup>1</sup>H NMR (300 MHz, CHLOROFORM-d) δ: 1.22 (t, J=6.99 Hz, 1 H), 1.66 (br. s., 2 H), 2.13 (br. s., 1 H), 2.69 (br. s., 1 H), 2.86 - 3.05 (m, 2 H), 3.17 - 3.28 (m, 3 H), 3.38 - 3.56 (m, 2 H), 5.15 - 5.29 (m, 2 H), 5.42 (br. s., 1 H), 7.24 (d, J=7.55 Hz, 1 H), 7.32 - 7.41 (m, 1 H), 7.51 - 7.64 (m, 2 H), 8.29 (br. s., 2 H); <sup>13</sup>C NMR (75 MHz, CHLOROFORM-d) δ: 27.6 (s, 1 C), 28 (s, 1 C), 46.6 (s, 1 C), 47.3 (s, 1 C), 52 (s, 1 C), 52.8 (s, 1 C), 65.8 (s, 1 C), 90.3 (s, 1 C), 110.5 (s, 1 C), 117.4 (s, 1 C), 128 (s, 1 C), 128.2 (s, 1 C), 133.2 (s, 1 C), 133.3 (s, 1 C), 140.2 (s, 1 C), 152 (s, 1 C), 159.7 (s, 1 C), 163.9 (s, 1 C); APCI-MS m/z = 339.17 calcd. for C<sub>18</sub>H<sub>21</sub>N<sub>5</sub>O<sub>2</sub> [M]; found: 340.27 [M+H].

### 3.7.3. Pd/PTABS catalytic etherification of chloroheteroarenes at moderate temperatures.

*General procedure:* A 25 mL of oven-dried Schlenk tube was charged with 1 mol% of Pd(OAc)<sub>2</sub>, 2 mol% of PTABS (ligand, phosphoadamantinebutylsaltonate) and 1 mmol of chloroheterocyclic derivative under N<sub>2</sub> atmosphere and the resultant mixture dissolved in 3 mL of dry DMF. The reaction mixture was stirred for 5 minutes then 1.2 equiv. of corresponding phenol and a 2.0 equiv. of K<sub>3</sub>PO<sub>4</sub> were added followed by stirring at 60 °C for 1 to 2 h. After consumption of starting material (monitored by TLC/TLC-MS), the solvent was removed in vacuum, and the resultant residue obtained was purified by column chromatography in EtOAc/hexane (10% to 50%) solvent system to afford the desired product. In the case of riboside derivatives and purine substrate (**34a-c**) CHCl<sub>3</sub>/MeOH (9:1) was used as a mobile phase for column chromatography.

#### 3.7.3.1. 2-(4-Methoxyphenoxy)pyrazine (**28a**)

General procedure (GP) was followed with 2-chloropyrazine (1 mmol, 1 equiv.) and 4-methoxy phenol (1.1 mmol, 1.1 equiv.) yielding the desired product 2-(4-Methoxyphenoxy)pyrazine (182 mg, 0.902 mmol, 90%) as white solid. Mp: 78-80 °C, <sup>1</sup>H NMR (300 MHz, CHLOROFORM-d) δ: 8.38 (d, J = 1.0 Hz, 1 H), 8.21 (d, J = 2.5 Hz, 1 H), 8.09 – 8.05 (m, 1 H), 7.07 (dd, J = 6.8, 2.2 Hz, 2 H), 6.95 – 6.91 (m, 2 H), 3.80 (s, 3 H). <sup>13</sup>C NMR (75 MHz, CHLOROFORM-d) δ: 160.5 (s, 1 C), 157.0 (s, 1 C), 146.2 (s, 1 C), 141.0 (s, 1 C), 138.1 (s, 2 C), 135.6 (s, 2 C), 122.2 (s, 1 C), 114.8 (s, 1 C), 55.5 (s, 1 C), CHNS- calcd. for C<sub>11</sub>H<sub>10</sub>N<sub>2</sub>O<sub>2</sub>: C, 65.34; H, 4.98; N, 13.85, found: C, 65.23; H, 4.94; N, 13.87.

3.7.3.2. 2-(4-(*tert*-Butyl)phenoxy)pyrazine (**28b**)

General procedure (GP) was followed with 2-chloropyrazine (1 mmol, 1 equiv.) and 4-*tert* butyl phenol (1.1 mmol, 1.1 equiv.) yielding the desired product (184 mg, 0.806 mmol, 81%) as white solid. <sup>1</sup>H NMR (300 MHz, CHLOROFORM-*d*) δ: 8.33 (s, 1 H), 8.17 (d, *J* = 2.5 Hz, 1 H), 8.04 (s, 1 H), 7.36 (d, *J* = 8.7 Hz, 2 H), 7.01 (d, *J* = 8.7 Hz, 2 H), 1.27 (s, 9 H). <sup>13</sup>C NMR (75 MHz, CHLOROFORM-*d*) δ: 159.3 (s, 1 C), 149.5 (s, 1 C), 147.1 (s, 1 C), 140 (s, 1 C), 137.2 (s, 2 C), 134.8 (s, 2 C), 125.7 (s, 1 C), 119.4 (s, 1 C), 33.4 (s, 1 C), 30.4 (s, 3 C); CHNScaled. for C<sub>14</sub>H<sub>16</sub>N<sub>2</sub>O: C, 73.66; H, 7.06; N, 12.27, found: C, 74.01; H, 7.21; N, 12.21.

3.7.3.3. 2-(Naphthalen-2-yloxy)pyrazine (**28c**)

General procedure (GP) was followed with 2-chloropyrazine (1 mmol, 1 equiv.) and 2-naphthol (1.1 mmol, 1.1 equiv.) yielding the desired product (195 mg, 0.877 mmol, 88%) as white solid. Mp: 116-118 °C, <sup>1</sup>H NMR (300 MHz, CHLOROFORM-*d*) δ: 8.48 (s, 1 H), 8.28 (s, 1 H), 8.10 (s, 1 H), 7.88 (dd, *J* = 16.7, 8.2 Hz, 2 H), 7.80 (d, *J* = 7.6 Hz, 1 H), 7.61 (s, 1 H), 7.52 – 7.44 (m, 2 H), 7.29 (d, *J* = 8.8 Hz, 1 H); <sup>13</sup>C NMR (75 MHz, CHLOROFORM-*d*) δ: 160.3 (s, 1 C), 150.6 (s, 1 C), 141.1 (s, 1 C), 138.5 (s, 1 C), 135.9 (s, 1 C), 134 (s, 1 C), 131.2 (s, 1 C), 129.8 (s, 1 C), 127.8 (s, 1 C), 127.5 (s, 1 C), 126.6 (s, 1 C), 125.5 (s, 1 C), 120.9 (s, 1 C), 117.8 (s, 1 C); CHNS calcd. for C<sub>14</sub>H<sub>10</sub>N<sub>2</sub>O: C, 75.66; H, 4.54; N, 12.60, found: C, 76.56; H, 4.56; N, 12.42.

3.7.3.4. 2-(Naphthalen-1-yloxy)pyrazine (**28d**)

General procedure (GP) was followed with 2-chloropyrazine (1 mmol, 1 equiv.) and 1-naphthol (1.1 mmol, 1.1 equiv.) yielding the desired product (177 mg, 0.796 mmol, 80%) as white solid. Mp: 100-102 °C, <sup>1</sup>H NMR (300 MHz, CHLOROFORM-*d*) δ: 8.53 (d, *J* = 2.9 Hz, 1 H), 8.28 (d, *J* = 2.4 Hz, 1 H), 8.07 (d, *J* = 1.3 Hz, 1 H), 7.92 (dd, *J* = 5.2, 1.8 Hz, 2 H), 7.82 – 7.75 (m, 1 H), 7.56 – 7.44 (m, 3 H), 7.30 – 7.23 (m, 1 H); <sup>13</sup>C NMR (75 MHz, CHLOROFORM-*d*) δ: 148.9 (s, 2 C), 141.3 (s, 1 C), 138.5 (s, 1 C), 135.3 (s, 1 C), 134.9 (s, 2 C), 128.1 (s, 1 C), 127.1 (s, 2 C), 126.5 (s, 1 C), 125.68 (s, 1 C), 121.5 (s, 1 C), 117.3 (s, 1 C); CHNS calcd. for C<sub>14</sub>H<sub>10</sub>N<sub>2</sub>O: C, 75.66; H, 4.54; N, 12.60, found: C, 76.44; H, 4.70; N, 12.34.

3.7.3.5. 2-(4-Methoxyphenoxy)benzo[d]oxazole (**28e**)

General procedure (GP) was followed with 2-chlorobenzo[d]oxazole (0.116 mL, 1 mmol) and 4-methoxy phenol (149 mg, 1.2 mmol, 1.2 equiv.) providing the desired 2-(4-methoxyphenoxy)benzo[d]oxazole (224 mg, 0.93 mmol, 93%) as colorless solid. <sup>1</sup>H NMR (300 MHz, CHLOROFORM-*d*) δ: 3.82 (s, 3 H), 6.92 - 6.99 (m, 2 H), 7.18 - 7.28 (m, 2 H), 7.28



- 7.35 (m, 2 H), 7.37 - 7.43 (m, 1 H), 7.47 - 7.53 (m, 1 H);  $^{13}\text{C}$  NMR (75 MHz, CHLOROFORM-*d*)  $\delta$ : 55.6 (s, 1 C), 109.8 (s, 1 C), 114.8 (s, 1 C), 118.6 (s, 1 C), 121.2 (s, 2 C), 123.2 (s, 2 C), 124.4 (s, 1 C), 140.8 (s, 1 C), 146.3 (s, 1 C), 148.4 (s, 1 C), 157.6 (s, 1 C), 162.8 (s, 1 C); (+ve) APCI-MS  $m/z$  = 241.07  $m/z$  calcd. for  $\text{C}_{14}\text{H}_{11}\text{NO}_3$  [M]; found : 242.21[M+H], CHNS calcd. for  $\text{C}_{14}\text{H}_{11}\text{NO}_3$ : C, 69.70; H, 4.60; N, 5.81, found: C, 69.52; H, 4.44; N, 5.79.

### 3.7.3.6. 2-(4-*tert*-Butylphenoxy)quinoxaline (28f)

General procedure (GP) was followed with 2-chloroquinoxaline (164 mg, 1 mmol) and 1-*tert*-butyl-4-methoxybenzene (180 mg, 1.2 mmol, 1.2 equiv.) providing the desired 2-(4-*tert*-butylphenoxy)quinoxaline (265 mg, 0.949 mmol, 95%) as colorless crystals. Mp: 66.7-68.7 °C,  $^1\text{H}$  NMR (300 MHz, CHLOROFORM-*d*)  $\delta$ : 1.37 (s, 9 H), 7.21 - 7.27 (m, 2 H), 7.43 - 7.51 (m, 2 H), 7.57 - 7.70 (m, 2 H), 7.76 - 7.83 (m, 1 H), 8.06 (dd,  $J=8.07$ , 1.56 Hz, 1 H), 8.68 (s, 1 H);  $^{13}\text{C}$  NMR (75 MHz, CHLOROFORM-*d*)  $\delta$ : 31.8 (s, 3 C), 31.9 (s, 1 C), 34.9 (s, 1 C), 121 (s, 1 C), 126.8 (s, 1 C), 126.9 (s, 1 C), 127.7 (s, 1 C), 128.1 (s, 2 C), 129.2 (s, 1 C), 130.7 (s, 1 C), 139.6 (s, 1 C), 139.9 (s, 1 C), 148.6 (s, 1 C), 150.8 (s, 1 C), 157.4 (s, 1 C); (+ve)APCI-MS  $m/z$  = 278.35 calcd. for  $\text{C}_{18}\text{H}_{18}\text{N}_2\text{O}$ [M], found : 279.4 [M+H]. CHNS calcd. for  $\text{C}_{18}\text{H}_{18}\text{N}_2\text{O}$ : C, 77.67; H, 6.52; N, 10.06; found: C, 77.59; H, 6.48; N, 10.17.

### 3.7.3.7. 2-(4-Methoxyphenoxy)quinoxaline (28g)

General procedure (GP) was followed with 2-chloroquinoxaline (164 mg, 1 mmol) and 4-methoxy phenol (149 mg, 1.2 mmol, 1.2 equiv.) yielding the desired 2-(4-methoxyphenoxy)quinoxaline (219 mg, 0.79 mmol, 87%) as white crystals. Mp: 144.7-146.7 °C,  $^1\text{H}$  NMR (300 MHz, CHLOROFORM-*d*)  $\delta$ : 3.86 (s, 3 H), 6.96 - 7.02 (m, 2 H), 7.19 - 7.25 (m, 2 H), 7.57 - 7.70 (m, 2 H), 7.75 - 7.81 (m, 1 H), 8.07 (dd,  $J=7.98$ , 1.56 Hz, 1 H), 8.68 (s, 1 H) ;  $^{13}\text{C}$  NMR (75 MHz, CHLOROFORM-*d*)  $\delta$ : 55.6 (s, 1 C), 55.7 (s, 1 C), 114.6 (s, 1 C), 114.7 (s, 1 C), 116.0 (s, 1 C), 122.3 (s, 1 C), 127.2 (s, 1 C), 127.6 (s, 1 C), 128.8 (s, 1 C), 130.3 (s, 1 C), 139.1 (s, 1 C) 139.4 (s, 1 C), 140 (s, 1 C), 146.1 (s, 1 C), 156.9 (s, 1 C); (+ve)APCI-MS  $m/z$  = 252.27 [M] calcd. for  $\text{C}_{15}\text{H}_{12}\text{N}_2\text{O}_2$  [M], found: 253.33 [M+H]; CHNS calcd. for  $\text{C}_{15}\text{H}_{12}\text{N}_2\text{O}_2$ : C, 71.42; H, 4.79; N, 11.10; found: C, 71.09; H, 4.98; N, 11.07.

### 3.7.3.8. 2-(*Mesityloxy*)quinoxaline (28h)

General procedure (GP) was followed with 2-chloroquinoxaline (164 mg, 1 mmol) and 2,4,6-trimethylphenol (163 mg, 1.2 mmol, 1.2 equiv.) providing the desired 2-(*mesityloxy*)quinoxaline (243 mg, 0.92 mmol, 92%) as shiny white needles. Mp: 92.3-94.0 °C,

$^1\text{H}$  NMR (300 MHz, CHLOROFORM-*d*)  $\delta$ : 2.13 (s, 6 H), 2.36 (s, 3 H), 6.97 (s, 2 H), 7.62 (td,  $J=7.45, 1.79$  Hz, 2 H), 7.71 - 7.81 (m, 1 H), 8.04 - 8.12 (m, 1 H), 8.73 (s, 1 H);  $^{13}\text{C}$  NMR (75 MHz, CHLOROFORM-*d*)  $\delta$ : 16.5 (s, 2 C), 20.8 (s, 1 C), 127 (s, 1 C), 127.7 (s, 1 C), 128.8 (s, 1 C), 129.3 (s, 1 C), 130.1 (s, 1 C), 130.3 (s, 1 C), 135 (s, 2 C), 138.5 (s, 2 C), 139.4 (s, 1 C), 140.4 (s, 1 C), 147.4 (s, 1 C), 156.3 (s, 1 C); (+ve)APCI-MS  $m/z = 264.32$  calcd. for  $\text{C}_{17}\text{H}_{16}\text{N}_2\text{O}$  [M], found: 265.43 [M+H]; CHNS calcd. for  $\text{C}_{17}\text{H}_{16}\text{N}_2\text{O}$ : C, 77.25; H, 6.10; N, 10.60; found: C, 77.22; H, 6.48; N, 10.43.

### 3.7.3.9. 2-(3-Nitrophenoxy)quinoxaline (**28i**)

The compound exhibited identical  $^1\text{H}$  and  $^{13}\text{C}$  NMR data to previous reports.<sup>429</sup> General procedure (GP) was followed with 2-chloroquinoxaline (164 mg, 1 mmol) and 3-nitrophenol (208 mg, 1.5 mmol, 1.5 equiv.) providing the desired 2-(3-nitrophenoxy)quinoxaline (254 mg, 0.95 mmol, 95%) as colorless crystals.  $^1\text{H}$  NMR (300 MHz, CHLOROFORM-*d*)  $\delta$ : 7.61 - 7.72 (m, 4 H), 7.72 - 7.79 (m, 1 H), 8.07 - 8.15 (m, 1 H), 8.18 (dt,  $J=6.95, 2.21$  Hz, 1 H), 8.23 - 8.28 (m, 1 H), 8.77 (s, 1 H);  $^{13}\text{C}$  NMR (75 MHz, CHLOROFORM-*d*)  $\delta$ : 117.2 (s, 1 C), 120.3 (s, 1 C), 127.6 (s, 1 C), 127.9 (s, 1 C), 128 (s, 1 C), 129 (s, 1 C), 130.1 (s, 1 C), 130.7 (s, 1 C), 138.7 (s, 1 C), 139.4 (s, 1 C), 140 (s, 1 C), 149 (s, 1 C), 153 (s, 1 C), 155.9 (s, 1 C); (+ve) APCI-MS  $m/z = 267.24$  calcd. for  $\text{C}_{14}\text{H}_9\text{N}_3\text{O}_3$  [M], found: 268.18 [M+H].

### 3.7.3.10. 2-(Quinolin-8-yloxy)benzo[d]thiazole (**28j**)

The compound exhibited identical  $^1\text{H}$  and  $^{13}\text{C}$  NMR data as in previous reports.<sup>429</sup> General procedure (GP) was followed with 2-chlorobenzothiazole (1 mmol, 1 equiv.) and 8-hydroxyquinoline (1.1 mmol, 1.1 equiv.) yielding the desired product (228 mg, 82%) as white solid.  $^1\text{H}$  NMR (400 MHz, CHLOROFORM-*d*)  $\delta$ : 8.89 (d,  $J = 3.9$  Hz, 1H), 8.19 (d,  $J = 8.2$  Hz, 1H), 7.76 (t,  $J = 7.8$  Hz, 2H), 7.68 - 7.62 (m, 2H), 7.61 - 7.56 (m, 1H), 7.43 (dd,  $J = 7.9, 3.9$  Hz, 1H), 7.33 (t,  $J = 7.7$  Hz, 1H), 7.26 - 7.22 (m, 1H).  $^{13}\text{C}$  NMR (75 MHz, CHLOROFORM-*d*)  $\delta$ : 172.6 (s, 1 C), 150.7 (s, 1 C), 150.5 (s, 1 C), 149 (s, 1 C), 140.8 (s, 1 C), 136 (s, 1 C), 132.6 (s, 2 C), 129.9 (s, 1 C), 126.3 (s, 1 C), 126.1 (d, 1 C), 123.87 (s, 1 C), 121.9 (s, 1 C), 121.6 (s, 1 C), 121.2 (s, 1 C), 120.7 (s, 1 C).

### 3.7.3.11. 6-(Quinoxalin-2-yloxy)-2H-chromen-2-one (**28k**)

General procedure (GP) was followed with 2-chloroquinoxaline (164 mg, 1 mmol) and 6-hydroxycoumarin (194.6 mg, 1.2 mmol, 1.2 equiv.) providing the desired 6-(quinoxalin-2-yloxy)-2H-chromen-2-one (238 mg, 0.82 mmol, 82%) as white shiny feathery needles. Mp: 207.2-208.9°C,  $^1\text{H}$  NMR (300 MHz, CHLOROFORM-*d*)  $\delta$ : 6.51 (d,  $J=9.63$  Hz, 1 H), 7.42 -

7.52 (m, 3 H), 7.64 - 7.78 (m, 4 H), 8.07 - 8.13 (m, 1 H), 8.75 (s, 1 H);  $^{13}\text{C}$  NMR (75 MHz,  $\text{CDCl}_3$ )  $\delta$ : 117.4 (s, 1 C), 118.1 (s, 1 C), 119.4 (s, 1 C), 119.9 (s, 1 C), 125.6 (s, 1 C), 127.6 (s, 1 C), 127.7 (s, 1 C), 129 (s, 1 C), 130.6 (s, 1 C), 138.9 (s, 1 C), 139.6 (s, 1 C), 139.8 (s, 1 C), 142.8 (s, 1 C), 148.6 (s, 1 C), 151.3 (s, 1 C), 156.6 (s, 1 C), 160.5 (s, 1 C); (+ve) APCI-MS  $m/z$  = 290.07 calcd. for  $\text{C}_{17}\text{H}_{10}\text{N}_2\text{O}_3$  [M], found : 291.3 [M+H]; CHNS calcd. for  $\text{C}_{17}\text{H}_{10}\text{N}_2\text{O}_3$ : C, 70.34; H, 3.47; N, 9.65; found: C, 70.13; H, 3.27; N, 9.35.

### 3.7.3.12. 2-(3, 5-Bis(trifluoromethyl)phenoxy)benzo[d]oxazole (**28l**)

The compound exhibited identical  $^1\text{H}$  and  $^{13}\text{C}$  NMR data as in previous reports.<sup>171</sup> General procedure (GP) was followed with 2-chlorobenzo[d]oxazole (0.116 mL, 1 mmol) and 3,5-bis(trifluoromethyl)phenol (276 mg, 1.2 mmol, 1.2 equiv.) providing the desired 2-(3,5-bis(trifluoromethyl)phenoxy)benzo[d]oxazole (191 mg, 0.55 mmol, 55%) as viscous liquid.  $^1\text{H}$  NMR (300 MHz, CHLOROFORM-d)  $\delta$ : 7.20 - 7.34 (m, 2 H), 7.38 - 7.46 (m, 1 H), 7.48 - 7.59 (m, 1 H), 7.81 (s, 1 H), 8.00 (s, 2 H);  $^{13}\text{C}$  NMR (75 MHz, CHLOROFORM-d)  $\delta$ : 110.1 (s, 1 C), 120 (s, 1 C), 120.7 (s, 1 C), 124.2 (s, 1 C), 124.4 (s, 1 C), 124.9 (s, 1 C), 128 (s, 1 C), 132.7 (s, 1 C), 133.2 (s, 1 C), 133.7 (s, 1 C), 134.1 (s, 1 C), 140.1 (s, 1 C), 148.4 (s, 1 C), 152.9 (s, 1 C), 160.6 (s, 1 C);  $^{19}\text{F}$  NMR (282 MHz,  $\text{CDCl}_3$ )  $\delta$ : -63.0 (s, 1 F); (+ve) APCI-MS  $m/z$  = 347.04  $m/z$  calcd. for  $\text{C}_{15}\text{H}_7\text{F}_6\text{NO}_2$  [M]; found: 348.13[M+H].

### 3.7.3.13. 2-(1-Bromonaphthalen-2-yloxy)quinoxaline (**28m**)

General procedure (GP) was followed with 2-chloroquinoxaline (164 mg, 1 mmol) and 1-bromonaphthalen-2-ol (334.6 mg, 1.5 mmol, 1.5 equiv.) providing the desired 2-(1-bromonaphthalen-2-yloxy)quinoxaline (344.2 mg, 0.98 mmol, 98%) as brown Solid. Mp: 183.9-185.3 °C,  $^1\text{H}$  NMR (300 MHz, CHLOROFORM-d)  $\delta$ : 7.46 (d,  $J=8.90$  Hz, 1 H), 7.55 - 7.73 (m, 5 H), 7.94 (d,  $J=8.53$  Hz, 2 H), 8.07 - 8.15 (m, 1 H), 8.33 (d,  $J=8.44$  Hz, 1 H), 8.86 (s, 1 H);  $^{13}\text{C}$  NMR (75 MHz, CHLOROFORM-d)  $\delta$ : 115.1 (s, 1 C), 122.3 (s, 1 C), 126.3 (s, 1 C), 127 (s, 1 C), 127.5 (s, 1 C), 127.7 (s, 1 C), 127.7 (s, 1 C), 128.2 (s, 1 C), 128.8 (s, 1 C), 128.9 (s, 1 C), 130.4 (s, 1 C), 132.3 (s, 1 C), 133 (s, 1 C), 138.7 (s, 1 C), 139.8 (s, 1 C), 139.9 (s, 1 C), 148 (s, 1 C), 156.4 (s, 1 C); (+ve) APCI-MS  $m/z$  = 351.12 calcd. for  $\text{C}_{18}\text{H}_{11}\text{BrN}_2\text{O}$  [M], found: 352.2 [M+H]; CHNS calcd. for  $\text{C}_{18}\text{H}_{11}\text{BrN}_2\text{O}$ : C, 61.56; H, 3.16; N, 7.98; found: C, 61.52; H, 3.18; N, 7.93.

### 3.7.3.14. 7-(4-Methoxyphenoxy)-4-(pentyloxy)pteridin-2-amine (**28n**)

General procedure (GP) was followed with chloropterin (1 mmol, 1 equiv.) and 4-methoxyphenol (1.1 mmol, 1.1 equiv.) yielding the desired product (244 mg, 0.686 mmol, 91%) as white solid. Mp: 194-196 °C,  $^1\text{H}$  NMR (300 MHz, CHLOROFORM-d)  $\delta$ : 8.61 (d,  $J = 1.3$  Hz,

1 H), 7.21 – 7.15 (m, 2 H), 6.92 (d,  $J = 7.4$  Hz, 2 H), 5.24 (s, 2 H), 4.42 (t,  $J = 6.3$  Hz, 2 H), 3.81 (s, 3 H), 1.85 – 1.77 (m, 2 H), 1.37 (tt,  $J = 14.0, 6.9$  Hz, 4 H), 0.90 (t,  $J = 6.3$  Hz, 3 H).  $^{13}\text{C}$  NMR (75 MHz, CHLOROFORM- $d$ )  $\delta$ : 160.2 (s, 1 C), 157.7 (s, 1 C), 156.8 (s, 1 C), 155.1 (s, 1 C), 144 (s, 1 C), 121.6 (s, 2 C), 118.9 (s, 2 C), 114.6 (s, 1 C), 68 (s, 1 C), 55.5 (s, 2 C), 35.8 (s, 2 C), 28 (s, 1 C), 22.3 (s, 1 C), 13.9 (s, 1 C); CHNS calcd. for  $\text{C}_{18}\text{H}_{21}\text{N}_5\text{O}_3$ : C, 60.83; H, 5.96; N, 19.71. found: C, 60.97; H, 6.21; N, 19.80.

### 3.7.3.15. 2-(Pentafluorophenoxy)quinoxaline (**28o**)

General procedure (GP) was followed with 2-chloroquinoxaline (164 mg, 1 mmol) and 2, 3, 4, 5, 6-pentafluorophenol (276.1 mg, 1.5 mmol, 1.5 equiv.) providing the desired 2-(perfluorophenoxy)quinoxaline (187 mg, 0.598 mmol, 60%) as colorless crystals. Mp: 83.1-84.3 °C.  $^1\text{H}$  NMR (300 MHz, CHLOROFORM- $d$ )  $\delta$ : 7.61 - 7.85 (m, 3 H), 8.09 - 8.24 (m, 1 H), 8.86 (s, 1 H);  $^{13}\text{C}$  NMR (75 MHz, CHLOROFORM- $d$ )  $\delta$ : 127.6 (s, 1 C), 128.3 (s, 1 C), 129.1 (s, 1 C), 130.9 (s, 1 C), 137.3 (s, 1 C), 139.3 (s, 1 C), 139.7 (s, 1 C), 140 (s, 1 C), 140.1 (s, 1 C), 140.4 (s, 1 C), 143.4 (s, 1 C), 143.5 (s, 1 C), 143.5 (s, 1 C), 154.4 (s, 1 C);  $^{19}\text{F}$  NMR (282 MHz,  $\text{CDCl}_3$ )  $\delta$ : -162.4 (s, 1 F), -162.3 (s, 1 F), -158.5 (s, 1 F), -152.1 (s, 1 F), -152.0 (s, 1 F); (+ve)APCI-MS  $m/z = 312.19$  calcd. for  $\text{C}_{14}\text{H}_5\text{F}_5\text{N}_2\text{O}$  [M], found: 313.22 [M+H], anal for  $\text{C}_{14}\text{H}_5\text{F}_5\text{N}_2\text{O}$ : C, 53.86; H, 1.61; N, 8.97; found: C, 53.89; H, 1.58; N, 8.93.

### 3.7.3.16. 2-(8-Bromonaphthalen-1-yloxy)benzo[ $d$ ]oxazole (**28p**)

General procedure (GP) was followed with 2-chlorobenzo[ $d$ ]oxazole (0.116 mL, 1 mmol) and 1-bromo naphthol (268 mg, 1.2 mmol, 1.2 equiv.) providing the desired 2-(8-bromonaphthalen-1-yloxy)benzo[ $d$ ]oxazole (308 mg, 0.909 mmol, 91%) as white amorphous solid. Mp: 139.6-140.5 °C,  $^1\text{H}$  NMR (300 MHz, CHLOROFORM- $d$ )  $\delta$ : 7.25 (dd,  $J=7.24, 1.93$  Hz, 2 H), 7.46 - 7.53 (m, 2 H), 7.55 - 7.62 (m, 2 H), 7.67 (td,  $J=7.68, 1.24$  Hz, 1 H), 7.88 - 7.99 (m, 2 H), 8.31 (d,  $J=8.44$  Hz, 1 H);  $^{13}\text{C}$  NMR (75 MHz, CHLOROFORM- $d$ )  $\delta$ : 110 (s, 1 C), 114.3 (s, 1 C), 118.8 (s, 1 C), 120.4 (s, 1 C), 123.5 (s, 1 C), 124.6 (s, 1 C), 126.8 (s, 1 C), 127.2 (s, 1 C), 128.1 (s, 1 C), 128.3 (s, 1 C), 129.5 (s, 1 C), 132.7 (s, 1 C), 132.8 (s, 1 C), 140.7 (s, 1 C), 147.6 (s, 1 C), 148.8 (s, 1 C), 161.8 (s, 1 C); (+ve) APCI-MS  $m/z = 338.99$   $m/z$  calcd. for  $\text{C}_{17}\text{H}_{10}\text{BrNO}_2$ [M]; found: 340.11[M+H]; CHNS calcd. for  $\text{C}_{17}\text{H}_{10}\text{BrNO}_2$ : C, 60.02; H, 2.96; N, 4.12; found: C, 59.99; H, 2.66; N, 4.18.

### 3.7.3.17. 2-(4-Allyl-2-methoxyphenoxy)benzo[ $d$ ]thiazole (**29a**)

The compound exhibited identical  $^1\text{H}$  and  $^{13}\text{C}$  NMR data as in previous reports.<sup>401</sup> General procedure (GP) was followed with 2-chlorobenzothiazole (1 mmol, 1 equiv.) and eugenol (1.1 mmol, 1.1 equiv.) yielding the desired product (264 mg, 0.887 mmol, 89%) as pale yellow

liquid.  $^1\text{H}$  NMR (300 MHz, CHLOROFORM-*d*)  $\delta$ : 7.77 – 7.69 (m, 1 H), 7.62 (d,  $J = 7.9$  Hz, 1 H), 7.35 (t,  $J = 7.7$  Hz, 1 H), 7.23 (dd,  $J = 7.8, 3.0$  Hz, 2 H), 6.90 – 6.81 (m, 2 H), 6.04 – 5.93 (m, 1 H), 5.20 – 5.09 (m, 2 H), 3.79 (s, 3 H), 3.41 (d,  $J = 6.1$  Hz, 2 H).  $^{13}\text{C}$  NMR (101 MHz, CHLOROFORM-*d*)  $\delta$ : 172.9 (s, 1 C), 151 (s, 1 C), 149.3 (s, 1 C), 141.9 (s, 1 C), 139.8 (s, 1 C), 136.7 (s, 1 C), 132.4 (s, 1 C), 126 (s, 1 C), 123.6 (s, 1 C), 122.3 (s, 1 C), 121.6 (s, 1 C), 121.2 (s, 1 C), 120.9 (s, 1 C), 116.3 (s, 1 C), 113.5 (s, 1 C), 55.9 (s, 1 C), 40.1 (s, 1 C). (+ve) APCI-MS  $m/z = 297.08$  calcd. for  $\text{C}_{17}\text{H}_{15}\text{NO}_2\text{S}$  [M], found: 298.20 [M+H].

### 3.7.3.18. 2-(4-Allyl-2-methoxyphenoxy)pyrazine (**29b**)

General procedure (GP) was followed with 2-chloropyrazine (1 mmol, 1 equiv.) and eugenol (1.1 mmol, 1.1 equiv.) yielding the desired product (205 mg, 0.846 mmol, 85%) as a green liquid.  $^1\text{H}$  NMR (300 MHz, CHLOROFORM-*d*)  $\delta$ : 8.42 (s, 1 H), 8.20 (d,  $J = 2.5$  Hz, 1 H), 8.07 – 8.02 (m, 1 H), 7.11 – 7.05 (m, 1 H), 6.83 (d,  $J = 7.4$  Hz, 2 H), 6.03 – 5.94 (m, 1 H), 5.16 – 5.08 (m, 2 H), 3.73 (s, 3 H), 3.41 (d,  $J = 5.0$  Hz, 2 H).  $^{13}\text{C}$  NMR (75 MHz, CHLOROFORM-*d*)  $\delta$  160.1 (s, 1 C), 151.2 (s, 1 C), 141 (s, 1 C), 139.6 (s, 1 C), 138.7 (s, 1 C), 137.9 (s, 1 C), 136.9 (s, 1 C), 135.2 (s, 1 C), 122.6 (s, 1 C), 120.9 (s, 1 C), 116.2 (s, 1 C), 113 (s, 1 C), 55.7 (s, 1 C), 40 (s, 1 C). (+ve)APCI-MS  $m/z = 242.11$  calcd. for  $\text{C}_{14}\text{H}_{14}\text{N}_2\text{O}_2$  [M], found: 243.48 [M+H], CHNS calcd. for  $\text{C}_{14}\text{H}_{14}\text{N}_2\text{O}_2$ : C, 69.41; H, 5.82; N, 11.56; found: C, 69.69; H, 5.74; N, 11.59.

### 3.7.3.19. 2-(5-allyl-2-methoxyphenoxy)quinoxaline (**29c**)

General procedure (GP) was followed with 2-chloroquinoxaline (164 mg, 1 mmol) and eugenol (0.23 mL, 1.5 mmol, 1.5 equiv.) providing the desired 2-(5-allyl-2-methoxyphenoxy)quinoxaline (248.5 mg, 0.85 mmol, 85%) as brown oil.  $^1\text{H}$  NMR (300 MHz, CHLOROFORM-*d*)  $\delta$ : 3.42 (d,  $J=6.69$  Hz, 2 H), 3.78 (s, 3 H), 5.09 - 5.16 (m, 2 H), 5.96 - 6.03 (m, 1 H), 6.85 - 6.88 (m, 2 H), 7.19 (d,  $J=7.79$  Hz, 1 H), 7.50 - 7.63 (m, 2 H), 7.70 - 7.79 (m, 1 H), 8.04 - 8.13 (m, 1 H), 8.73 (s, 1 H);  $^{13}\text{C}$  NMR (75 MHz, CHLOROFORM-*d*)  $\delta$ : 39.7 (s, 1 C), 55.4 (s, 1 C), 115.1 (s, 1 C), 115.8 (s, 1 C), 120.7 (s, 1 C), 122.4 (s, 1 C), 127.3 (s, 1 C), 128.4 (s, 1 C), 129.8 (s, 1 C), 131.3 (s, 1 C), 136.7 (s, 1 C), 137.5 (s, 1 C), 138.3 (s, 1 C), 139.1 (s, 1 C), 139.4 (s, 1 C), 139.9 (s, 1 C), 150.9 (s, 1 C), 156.7 (s, 1 C); (+ve) APCI-MS  $m/z = 292.33$  calcd. for  $\text{C}_{18}\text{H}_{16}\text{N}_2\text{O}_2$ [M], found: 293.5 [M+H].

### 3.7.3.20. Ethyl-2-(benzo[d]oxazol-2-ylamino)-3-(4-(benzo[d]oxazol-2-yl)phenoxy)propanoate (**29d**)

General procedure (GP) was followed with 2-chlorobenzo[d]oxazole (0.116 mL, 1 mmol) and L-tyrosin ethylester (251 mg, 1.2 mmol, 1.2 equiv.) providing the desired ethyl-2-

(benzo[d]oxazol-2-ylamino)-3-(4-(benzo[d]oxazol-yloxy)phenyl)propanoate (296 mg, 0.669 mmol, 67%) as pale yellow solid. Mp: 136-138 °C, <sup>1</sup>H NMR (300 MHz, CHLOROFORM-d) δ: 1.21 - 1.31 (m, 3 H), 3.28 (d, *J*=6.14 Hz, 1 H), 3.35 (d, *J*=5.69 Hz, 1 H), 4.21 (q, *J*=7.12 Hz, 2 H), 4.89 (br. s., 1 H), 6.25 (br. s., 1 H), 7.03 (dd, *J*=7.66, 1.24 Hz, 1 H), 7.11 - 7.29 (m, 6 H), 7.29 - 7.35 (m, 2 H), 7.35 - 7.41 (m, 2 H), 7.44 - 7.51 (m, 1 H); <sup>13</sup>C NMR (75 MHz, CHLOROFORM-d) δ: 13.9 (s, 1 C), 37 (s, 1 C), 56.4 (s, 1 C), 61.7 (s, 1 C), 108.8 (s, 1 C), 109.7 (s, 1 C), 116.5 (s, 1 C), 118.5 (s, 1 C), 119.9 (s, 1 C), 121 (s, 1 C), 123.2 (s, 2 C), 123.8 (s, 2 C), 124.3 (s, 1 C), 130.7 (s, 1 C), 133.9 (s, 1 C), 140.5 (s, 1 C), 142.4 (s, 1 C), 148.2 (s, 1 C), 148.4 (s, 1 C), 151.7 (s, 1 C), 160.7 (s, 1 C), 161.8 (s, 1 C), 171.1 (s, 1 C); (+ve) APCI-MS *m/z* = 443.15 *m/z* calcd. for C<sub>25</sub>H<sub>21</sub>N<sub>3</sub>O<sub>5</sub> [M]; found: 444.72 [M+H]; CHNS calcd. for C<sub>25</sub>H<sub>21</sub>N<sub>3</sub>O<sub>5</sub>: C, 67.71; H, 4.77; N, 9.48; found: C, 67.72; H, 4.98; N, 9.44.

3.7.3.21. *3-(Benzo[d]thiazol-2-yloxy)-13-methyl-6,7,8,9,11,12,13,14,15,16-decahydro-17H-cyclopenta[a]phenanthren-17-one (29e)*

General procedure (GP) was followed with 2-chlorobenzothiazole (1 mmol, 1 equiv.) and estrone (1.1 mmol, 1.1 equiv.) yielding the desired product (367 mg, 0.909 mmol, 91%) as white solid. Mp: 166-168 °C, <sup>1</sup>H NMR (300 MHz, CHLOROFORM-d) δ: 7.72 (d, *J* = 7.9 Hz, 1 H), 7.64 (d, *J* = 7.8 Hz, 1 H), 7.35 (dd, *J* = 15.0, 7.8 Hz, 2 H), 7.24 (t, *J* = 7.1 Hz, 1 H), 7.11 (d, *J* = 8.2 Hz, 1 H), 7.06 (s, 1 H), 2.93 (d, *J* = 4.3 Hz, 2 H), 2.54 – 2.46 (m, 1 H), 2.44 – 2.39 (m, 1 H), 2.34 – 2.27 (m, 1 H), 2.20 – 1.91 (m, 5 H), 1.59 – 1.40 (m, 5 H), 0.91 (s, 3 H). <sup>13</sup>C NMR (75 MHz, CHLOROFORM-d) δ: 220.6 (s, 1 C), 172.2 (s, 1 C), 152.6 (s, 1 C), 149.1 (s, 1 C), 138.6 (s, 1 C), 137.9 (s, 1 C), 132.2 (s, 1 C), 126.1 (s, 1 C), 123.9 (s, 1 C), 121.6 (s, 1 C), 120.5 (s, 1 C), 117.8 (s, 1 C), 77 (s, 1 C), 76.6 (s, 1 C), 50.4 (s, 1 C), 47.9 (s, 1 C), 44.1 (s, 1 C), 37.9 (s, 1 C), 35.8 (s, 1 C), 31.5 (s, 1 C), 29.4 (s, 1 C), 26.2 (s, 1 C), 25.7 (s, 1 C), 21.5 (s, 1 C), 13.8 (s, 1 C); CHNS calcd. for C<sub>25</sub>H<sub>25</sub>NO<sub>2</sub>S: C, 74.41; H, 6.24; N, 3.47; S, 7.94, found: C, 74.79; H, 6.55; N, 3.38; S, 7.97.

3.7.3.22. *13-Methyl-3-(pyrazin-2-yloxy)-6,7,8,9,11,12,13,14,15,16-decahydro-17H-cyclopentaphenanthren-17-one (29f)*

General procedure (GP) was followed with 2-chloropyrazine (1 mmol, 1 equiv.) and estrone (1.1 mmol, 1.1 equiv.) yielding the desired product (300 mg, 0.882 mmol, 86%) as white solid. Mp: 136-138 °C, <sup>1</sup>H NMR (300 MHz, CHLOROFORM-d) δ: 8.39 (s, 1 H), 8.22 (d, *J* = 2.4 Hz, 1 H), 8.09 (s, 1 H), 7.32 (d, *J* = 8.4 Hz, 1 H), 6.94 – 6.89 (m, 1 H), 6.88 (s, 1 H), 2.94 – 2.88 (m, 2 H), 2.53 – 2.46 (m, 1 H), 2.43 – 2.37 (m, 1 H), 2.30 (ddd, *J* = 9.9, 6.0, 2.6 Hz, 1 H), 2.14 (ddd, *J* = 9.9, 9.3, 3.9 Hz, 1 H), 2.09 – 1.93 (m, 4 H), 1.63 (s, 2 H), 1.54 (d, *J* = 5.3 Hz, 1 H),

1.49 – 1.42 (m, 2 H), 0.90 (s, 3 H). <sup>13</sup>C NMR (75 MHz, CHLOROFORM-d) δ: 220.7 (s, 1 C), 160.3 (s, 1 C), 150.7 (s, 1 C), 141.1 (s, 1 C), 138.4 (s, 1 C), 138.2 (s, 1 C), 136.9 (s, 1 C), 135.8 (s, 1 C), 126.7 (s, 1 C), 121.2 (s, 1 C), 118.4 (s, 1 C), 50.4 (s, 1 C), 47.9 (s, 1 C), 44.1 (s, 1 C), 37.9 (s, 1 C), 35.8 (s, 1 C), 31.5 (s, 1 C), 29.4 (s, 1 C), 26.3 (s, 1 C), 25.7 (s, 1 C), 21.5 (s, 1 C), 13.8 (s, 1 C), CHNScaled. for C<sub>22</sub>H<sub>24</sub>N<sub>2</sub>O<sub>2</sub>: C, 75.83; H, 6.94; N, 8.04. found: C, 76.01; H, 6.55; N, 7.92.

3.7.3.23. (8*R*,9*S*,13*S*,14*S*)-13-methyl-3-(quinoxalin-2-yloxy)-6,7,8,9,11,12,13,14,15,16-decahydro-17*H*-cyclopenta[*a*]phenanthren-17-one (**29g**)

General procedure (GP) was followed with 2-chloroquinoxaline (1 mmol, 1 equiv.) and estrone (1.1 mmol, 1.1 equiv.) yielding the desired product (338 mg, 0.848 mmol, 85%) as white solid. Mp: 206-208 °C, <sup>1</sup>H NMR (300 MHz, CHLOROFORM-d) δ: 8.60 (s, 1 H), 8.01 – 7.96 (m, 1 H), 7.72 (dd, *J* = 7.7, 0.7 Hz, 1 H), 7.61 – 7.50 (m, 2 H), 7.29 (d, *J* = 8.3 Hz, 1 H), 7.00 (ddd, *J* = 4.9, 1.9, 0.7 Hz, 1 H), 6.94 (s, 1 H), 2.92 – 2.84 (m, 2 H), 2.49 – 2.36 (m, 2 H), 2.32 – 2.24 (m, 1 H), 2.14 – 2.06 (m, 1 H), 2.04 – 1.91 (m, 3 H), 1.58 (dd, *J* = 13.2, 8.0 Hz, 3 H), 1.50 – 1.40 (m, 3 H), 0.87 (s, 3 H). <sup>13</sup>C NMR (75 MHz, CHLOROFORM-d) δ: 220.6 (s, 1 C), 156.9 (s, 1 C), 150.6 (s, 1 C), 140 (s, 1 C), 139.5 (s, 1 C), 139.2 (s, 1 C), 138.2 (s, 1 C), 136.8 (s, 1 C), 130.2 (s, 1 C), 128.8 (s, 1 C), 127.7 (s, 1 C), 127.3 (s, 1 C), 126.5 (s, 1 C), 121.1 (s, 1 C), 118.5 (s, 1 C), 50.4 (s, 1 C), 47.9 (s, 1 C), 44.2 (s, 1 C), 38 (s, 1 C), 35.8 (s, 1 C), 31.5 (s, 1 C), 29.4 (s, 1 C), 26.3 (s, 1 C), 25.7 (s, 1 C), 21.5 (s, 1 C), 13.8 (s, 1 C). (+ve) APCI-MS *m/z* = 398.5 *m/z* calcd. for C<sub>26</sub>H<sub>26</sub>N<sub>2</sub>O<sub>2</sub>[M]; found: 399.7 [M+H]; CHNS calcd. for C<sub>26</sub>H<sub>26</sub>N<sub>2</sub>O<sub>2</sub>: C, 78.36; H, 6.58; N, 7.03, found: C, 78.09; H, 6.28; N, 7.06.

3.7.3.24. (13*S*)-3-(Benzo[*d*]oxazol-2-yloxy)-13-methyl-7,8,9,11,12,13,14,15,16,17-decahydro-6*H*-cyclopenta[*a*]phenanthren-17-ol (**29h**)

General procedure (GP) was followed with 2-chlorobenzo[*d*]oxazole (0.116 mL, 1 mmol) and estradiol (327 mg, 1.2 mmol, 1.2 equiv.) providing the desired (13*S*)-3-(benzo[*d*]oxazol-2-yloxy)-13-methyl-7,8,9,11,12,13,14,15,16,17-decahydro-6*H*-cyclopenta[*a*]phenanthren-17-ol (346 mg, 0.89 mmol, 89%) as white solid. Mp: 108.3-110 °C, <sup>1</sup>H NMR (300 MHz, CHLOROFORM-d) δ: 0.68 - 0.84 (m, 3 H), 1.08 - 1.23 (m, 1 H), 1.23 - 1.39 (m, 3 H), 1.39 - 1.60 (m, 3 H), 1.60 - 1.74 (m, 1 H), 1.83 - 2.00 (m, 2 H), 2.00 - 2.14 (m, 1 H), 2.14 - 2.36 (m, 2 H), 2.51 (br. s., 1 H), 2.87 (d, *J*=4.49 Hz, 2 H), 3.68 (t, *J*=8.48 Hz, 1 H), 7.06 (d, *J*=2.48 Hz, 1 H), 7.08 - 7.17 (m, 1 H), 7.17 - 7.26 (m, 2 H), 7.30 - 7.42 (m, 2 H), 7.46 - 7.53 (m, 1 H); <sup>13</sup>C NMR (75 MHz, CHLOROFORM-d) δ: 10.8 (s, 1 C), 22.8 (s, 1 C), 25.9 (s, 1 C), 26.7 (s, 1 C), 29.3 (s, 1 C), 30.1 (s, 1 C), 36.4 (s, 1 C), 38.1 (s, 1 C), 42.9 (s, 1 C) 43.9 (s, 1 C), 49.8 (s, 1 C), 81.2 (s, 1 C), 109.5 (s, 1 C), 116.9 (s, 1 C), 118.3 (s, 1 C), 119.8 (s, 1 C), 123.0 (s, 2 C), 124.1

(s, 1 C), 126.6 (s, 1 C), 138.5 (s, 1 C), 138.6 (s, 1 C), 140.5 (s, 1 C), 148.1 (s, 1 C), 150.2 (s, 1 C); (+ve) APCI-MS  $m/z = 389.2$   $m/z$  calcd. for  $C_{25}H_{27}NO_3$  [M]; found: 390.3 [M+H]; CHNS calcd. for  $C_{25}H_{27}NO_3$ : C, 77.09; H, 6.99; N, 3.60; found: C, 77.02; H, 6.98; N, 3.44.

3.7.3.25. *4-(4-tert-Butylphenoxy)-2-chloropyrimidine (31a)*

The compound exhibited identical  $^1H$  and  $^{13}C$  NMR data as in previous reports.<sup>431</sup> General procedure (GP) was followed with 2,4 dichloropyrimidine (149 mg, 1 mmol) and 4-tertiary butyl phenol (165 mg, 1.1 mmol, 1.1 equiv.) providing the desired 4-(4-*tert*-butylphenoxy)-2-chloropyrimidine (205 mg, 0.78 mmol, 78%) as white solid.  $^1H$  NMR (300 MHz, CHLOROFORM-*d*)  $\delta$ : 1.36 (s, 9 H), 6.75 (d,  $J=5.69$  Hz, 1 H), 7.07 - 7.11 (m, 2 H), 7.42 - 7.48 (m, 2 H), 8.42 (d,  $J=5.69$  Hz, 1 H);  $^{13}C$  NMR (75 MHz, CHLOROFORM-*d*)  $\delta$ : 31.3 (s, 2 C), 31.5 (s, 1 C), 34.5 (s, 1 C), 106.3 (s, 1 C), 120.4 (s, 1 C), 120.7 (s, 1 C), 126.2 (s, 1 C), 126.3 (s, 1 C), 126.8 (s, 1 C), 149.1 (s, 1 C), 149.4 (s, 1 C), 160.1 (s, 1 C), 170.6 (s, 1 C); (+ve) APCI-MS  $m/z = 262.73$   $m/z$  calcd. for  $C_{14}H_{15}ClN_2O$  [M]; found: 263.52 [M+H].

3.7.3.26. *2-chloro-4-(4-methoxyphenoxy)pyrimidine (31b)*

The compound exhibited identical  $^1H$  and  $^{13}C$  NMR data as in previous reports.<sup>431</sup> General procedure (GP) was followed with 2,4-dichloropyrimidine (149 mg, 1 mmol) and 4-methoxyphenol (0.092 mL, 1.1 mmol, 1.1 equiv.) providing the desired 2-chloro-4-(pyrrolidin-1-yl)pyrimidine (159, 0.87 mmol, 83%) as colorless needles.  $^1H$  NMR (300 MHz, CHLOROFORM-*d*)  $\delta$ : 3.82 (s, 3 H), 6.74 (d,  $J=5.78$  Hz, 1 H), 6.90 - 6.99 (m, 2 H), 7.03 - 7.13 (m, 2 H), 8.40 (d,  $J=5.69$  Hz, 1 H);  $^{13}C$  NMR (75 MHz, CHLOROFORM-*d*)  $\delta$ : 55.5 (s, 1 C), 106.2 (s, 1 C), 114.8 (s, 2 C), 122 (s, 2 C), 145.1 (s, 1 C), 157.5 (s, 1 C), 160.1 (s, 1 C), 160.6 (s, 1 C), 170.7 (s, 1 C); (+ve) APCI-MS  $m/z = 236.04$   $m/z$  calcd. for  $C_{11}H_9ClN_2O_2$  [M]; found: 237.1[M+H].

3.7.3.27. *8-((2-chloropyrimidin-4-yl)oxy)quinoline (31c)*

General procedure (GP) was followed with 2,4-dichloropyrimidine (149 mg, 1 mmol) and quinolin-8-ol (159.6 mg, 1.1 mmol, 1.1 equiv.) providing the desired 8-((2-chloropyrimidin-4-yl)oxy)quinoline (164 mg, 0.64 mmol, 64%) as bright yellow cubic crystals. Mp: 176.5-177.7 °C,  $^1H$  NMR (300 MHz, CHLOROFORM-*d*)  $\delta$ : 6.97 (d,  $J= 5.69$  Hz, 1 H), 7.44 (dd,  $J=8.34$ , 4.22 Hz, 1 H), 7.52 - 7.63 (m, 2 H), 7.79 (dd,  $J=7.79$ , 1.83 Hz, 1 H), 8.21 (dd,  $J=8.34$ , 1.65 Hz, 1 H), 8.45 (d,  $J=5.69$  Hz, 1 H), 8.82 (dd,  $J=4.22$ , 1.65 Hz, 1 H);  $^{13}C$  NMR (75 MHz, CHLOROFORM-*d*)  $\delta$ : 106.8 (s, 1 C), 121.3 (s, 1 C), 121.8 (s, 1 C), 126.2 (s, 1 C), 126.3 (s, 1 C), 129.8 (s, 1 C), 136.1 (s, 1 C), 140.9 (s, 1 C), 148 (s, 1 C), 150.4 (s, 1 C), 159.9 (s, 1 C),



160.3 (s, 1 C), 171 (s, 1 C); (+ve) APCI-MS  $m/z = 257.68$ ,  $m/z$  calcd. for  $C_{13}H_8ClN_3O$  [M]; found: 258.72[M+H]; CHNS calcd. for  $C_{13}H_8ClN_3O$ : C, 60.60; H, 3.13; N, 16.31; found: C, 60.82; H, 3.18; N, 16.43.

3.7.3.28. *(13S)*-2-(2-Chloropyrimidin-4-yloxy)-13-methyl-7, 8, 9, 11, 12, 13, 15, 16-octahydro-6H-cyclopenta[*a*]phenanthren-17(14H)-one (**31d**)

General procedure (GP) was followed with 2,4-dichloropyrimidine (149 mg, 1 mmol) and estrone (298 mg, 1.1 mmol, 1.1 equiv.) providing the desired (*13S*)-2-(2-chloropyrimidin-4-yloxy)-13-methyl-7,8,9,11,12,13,15,16-octahydro-6H-cyclopenta[*a*]phenanthren-17(14H)-one (368.8 mg, 0.93 mmol, 93%) as white sharp needles. Mp: 153-155 °C,  $^1H$  NMR (300 MHz, CHLOROFORM-*d*)  $\delta$ : 0.94 (s, 3 H), 1.41 - 1.74 (m, 6 H), 1.95 - 2.25 (m, 4 H), 2.27 - 2.37 (m, 1 H), 2.37 - 2.61 (m, 2 H), 2.94 (dd,  $J=8.48, 3.90$  Hz, 2 H), 6.76 (d,  $J=5.78$  Hz, 1 H), 6.85 - 6.98 (m, 2 H), 7.35 (d,  $J=8.53$  Hz, 1 H), 8.41 (d,  $J=5.69$  Hz, 1 H);  $^{13}C$  NMR (75 MHz, CHLOROFORM-*d*)  $\delta$ : 13.8 (s, 1 C), 21.5 (s, 1 C), 25.7 (s, 1 C), 26.2 (s, 1 C), 29.4 (s, 1 C), 31.5 (s, 1 C), 35.8 (s, 1 C), 37.9 (s, 1 C), 44.1 (s, 1 C), 47.9 (s, 1 C), 50.4 (s, 1 C), 106.4 (s, 1 C), 118.3 (s, 1 C), 121 (s, 2 C), 126.6 (s, 1 C), 137.8 (s, 1 C), 138.6 (s, 1 C), 149.7 (s, 1 C), 160.1 (s, 1 C), 160.6 (s, 1 C), 170.6 (s, 1 C); (+ve) APCI-MS  $m/z = 382.14$ , calcd. for  $C_{22}H_{23}ClN_2O_2$ , found: 383.23[M+H]; CHNS. calcd. for  $C_{22}H_{23}ClN_2O_2$ : C, 69.42; H, 6.59; N, 7.04; found: C, 69.22; H, 6.48; N, 7.14.

3.7.3.29. *2-Chloro-4-(2-isopropyl-4-methylphenoxy)pyrimidine* (**31e**)

General procedure (GP) was followed with 2,4-dichloropyrimidine (149 mg, 1 mmol) and thymol (151 mg, 1.0 mmol, 1.0 equiv.) providing the desired 2-chloro-4-(2-isopropyl-4-methylphenoxy)pyrimidine (165.4 mg, 0.63 mmol, 63%) as green oil.  $^1H$  NMR (300 MHz, CHLOROFORM-*d*)  $\delta$ : 1.16 (d,  $J=6.88$  Hz, 6 H), 2.32 (s, 3 H), 2.84 - 3.03 (m, 1 H), 6.68 (d,  $J=5.69$  Hz, 1 H), 7.07 (dd,  $J=7.20, 5.36$  Hz, 2 H), 7.26 (d,  $J=7.89$  Hz, 1 H), 8.38 (d,  $J=5.69$  Hz, 1 H);  $^{13}C$  NMR (75 MHz, CHLOROFORM-*d*)  $\delta$ : 20.7 (s, 1 C), 22.9 (s, 1 C), 23 (s, 1 C), 26.8 (s, 1 C), 105.7 (s, 1 C), 115.9 (s, 1 C), 127 (s, 1 C), 127.6 (s, 1 C), 137.2 (s, 1 C), 137.3 (s, 1 C), 148.9 (s, 1 C), 152.8 (s, 1 C), 160.1 (s, 1 C), 170.9 (s, 1 C); (+ve) APCI-MS  $m/z = 262.73$   $m/z$  calcd. for  $C_{14}H_{15}ClN_2O$  [M]; found: 263.52[M+H].

3.7.3.30. *2,4-bis(4-methoxyphenoxy)pyrimidine* (**32a**)

General procedure (GP) was followed with 2,4-dichloropyrimidine (149 mg, 1 mmol) and 4-methoxy phenol (273mg, 2.2 mmol, 2.2 equiv.) providing the desired 2,4-bis(4-methoxyphenoxy)pyrimidine (285 mg, 0.88 mmol, 88%) as white solid. Mp: 141.2-143.7 °C,  $^1H$  NMR (300 MHz, CHLOROFORM-*d*)  $\delta$ : 3.82 (s, 3 H), 3.81 (s, 3 H), 6.50 (d,  $J=5.69$  Hz, 1

H), 6.85 - 6.97 (m, 4 H), 7.01 - 7.13 (m, 4 H), 8.30 (d,  $J=5.69$  Hz, 1 H);  $^{13}\text{C}$  NMR (75 MHz, CHLOROFORM- $d$ )  $\delta$ : 55.5 (s, 2 C), 102.2 (s, 1 C), 114.4 (s, 2 C), 114.7 (s, 2 C), 122.3 (s, 2 C), 122.5 (s, 2 C), 145.5 (s, 1 C), 146.2 (s, 1 C), 156.8 (s, 1 C), 157.2 (s, 1 C), 160.1 (s, 1 C), 165.5 (s, 1 C), 171.8 (s, 1 C); (+ve) APCI-MS  $m/z = 324.33$ ;  $m/z$  calcd. for  $\text{C}_{18}\text{H}_{16}\text{N}_2\text{O}_4$  [M]; found: 325.47 [M+H]; CHNS calcd. for  $\text{C}_{18}\text{H}_{16}\text{N}_2\text{O}_4$ : C, 66.66; H, 4.97; N, 8.64; found: C, 66.89; H, 5.12; N, 8.41.

### 3.7.3.31. 2,4 (Di-estrogen)) pyrimidine (**32b**)

General procedure (GP) was followed with 2,4 dichloropyrimidine (149 mg, 1 mmol) and estrone (596 mg, 2.2 mmol, 2.2 equiv.) providing the desired (13*S*)-13-methyl-2-(2-((13*R*)-13-methyl-17-oxo-7,8,9,11,12,13,14,15,16,17-decahydro-6*H*-cyclopenta[*a*]phenanthren-2-yloxy)pyrimidin-4-yloxy)-7,8,9,11,12,13,15,16-octahydro-6*H*-cyclopenta[*a*]phenanthren-17(14*H*)-one (357 mg, 0.58 mmol, 58%) as white amorphous solid. Mp: 203-205 °C,  $^1\text{H}$  NMR (300 MHz, CHLOROFORM- $d$ )  $\delta$ : 0.86 - 0.93 (m, 6 H), 1.46 - 1.66 (m, 12 H), 1.94 - 2.15 (m, 8 H), 2.29 (br. s., 1 H), 2.33 - 2.56 (m, 5 H), 2.85 - 2.97 (m, 4 H), 6.52 (d,  $J=5.69$  Hz, 1 H), 6.87 - 6.97 (m, 4 H), 7.21 - 7.40 (m, 2 H), 8.29 (d,  $J=5.59$  Hz, 1 H);  $^{13}\text{C}$  NMR (75 MHz, CHLOROFORM- $d$ )  $\delta$ : 13.5 (s, 1 C), 20.9 (s, 1 C), 25 (s, 1 C), 25.7 (s, 1 C), 25.9 (s, 1 C), 28.7 (s, 1 C), 28.8 (s, 1 C), 29 (s, 1 C), 30.2 (s, 1 C), 30.9 (s, 1 C), 35.2 (s, 1 C), 37.3 (s, 1 C), 37.3 (s, 1 C), 43.3 (s, 1 C), 43.5 (s, 1 C), 47.3 (s, 1 C), 49.7 (s, 1 C), 101.9 (s, 1 C), 112.3 (s, 1 C), 114.7 (s, 1 C), 118 (s, 1 C), 118.2 (s, 1 C), 120.7 (s, 1 C), 120.9 (s, 1 C), 125.6 (s, 1 C), 125.7 (s, 1 C), 126 (s, 1 C), 130.5 (s, 1 C), 136.1 (s, 1 C), 136.7 (s, 1 C), 137 (s, 1 C), 137.3 (s, 1 C), 137.7 (s, 1 C), 149.4 (s, 1 C), 149.9 (s, 1 C), 153.8 (s, 1 C), 159.4 (s, 1 C), 164.7 (s, 1 C), 171 (s, 1 C), 206.5 (s, 1 C); (+ve)APCI-MS  $m/z = 616.79$ ;  $m/z$  calcd. for  $\text{C}_{40}\text{H}_{44}\text{N}_2\text{O}_4$  [M]; found: 617.82 [M+H]; CHNS calcd. for  $\text{C}_{40}\text{H}_{44}\text{N}_2\text{O}_4$ : C, 77.89; H, 7.19; N, 4.54; found: C, 77.92; H, 7.21; N, 4.34.

### 3.7.3.32. 2-(6-(8-Bromonaphthalen-1-yloxy)-9*H*-purin-9-yl)-5-(hydroxymethyl)-tetrahydrofuran-3,4-diol (**34a**)

General procedure (GP) was followed with 6-chloro purine riboside (287 mg, 1 mmol) and 1-bromo naphthol (268 mg, 1.2 mmol, 1.2 equiv.) providing the desired 2-(6-(8-bromonaphthalen-1-yloxy)-9*H*-purin-9-yl)-5-(hydroxymethyl)-tetrahydrofuran-3,4-diol (302 mg, 0.64 mmol, 64%) as colorless solid. Mp: >261 °C (decomposes),  $^1\text{H}$  NMR (300 MHz, DMSO- $d_6$ )  $\delta$ : 3.55 - 3.67 (m, 1 H), 3.67 - 3.79 (m, 1 H), 4.02 (q,  $J=3.67$  Hz, 1 H), 4.18 - 4.26 (m, 1 H), 4.68 (q,  $J=5.65$  Hz, 1 H), 5.15 (t,  $J=5.50$  Hz, 1 H), 5.28 (d,  $J=4.95$  Hz, 1 H), 5.58 (d,  $J=5.96$  Hz, 1 H), 6.08 (d,  $J=5.78$  Hz, 1 H), 7.58 - 7.65 (m, 1 H), 7.65 - 7.71 (m, 1 H), 7.71 - 7.79 (m, 1 H), 8.06

- 8.14 (m, 2 H), 8.20 (d,  $J=8.34$  Hz, 1 H), 8.46 (s, 1 H) 8.84 (s, 1 H);  $^{13}\text{C}$  NMR (75 MHz, DMSO- $d_6$ )  $\delta$ : 61 (s, 1 C), 73.5 (s, 1 C), 78.8 (s, 1 C), 85.5 (s, 1 C), 87.6 (s, 1 C), 114 (s, 1 C), 120.8 (s, 1 C), 122.5 (s, 1 C), 125.8 (s, 1 C), 126.4 (s, 1 C), 128.1 (s, 1 C), 128.3 (s, 1 C), 129.1 (s, 1 C), 131.7 (s, 1 C), 131.8 (s, 1 C), 143.5 (s, 1 C), 147.5 (s, 1 C), 151.1 (s, 1 C), 152.8 (s, 1 C), 158.4 (s, 1 C); (+ve) APCI-MS  $m/z = 472.04$   $m/z$  calcd. for  $\text{C}_{20}\text{H}_{17}\text{BrN}_4\text{O}_5$  [M]; found: 473.12 [M+H], CHNS calcd. for  $\text{C}_{20}\text{H}_{17}\text{BrN}_4\text{O}_5$ : C, 50.76; H, 3.62; N, 11.84; found: C, 51.02; H, 3.88; N, 11.94.

3.7.3.33. *2-(Hydroxymethyl)-5-(6-(4-methoxyphenoxy)-9H-purin-9-yl)-tetrahydrofuran-3,4-diol (34b)*

The compound exhibited identical  $^1\text{H}$  and  $^{13}\text{C}$  NMR data as in previous reports.<sup>433</sup> General procedure (GP) was followed with 6-chloro purine riboside (287 mg, 1 mmol) and 4-methoxy phenol (149 mg, 1.2 mmol, 1.2 equiv.) providing the desired 2-(hydroxymethyl)-5-(6-(4-methoxyphenoxy)-9H-purin-9-yl)-tetrahydrofuran-3,4-diol (231.9 mg, 0.62 mmol, 62%) as colorless solid. Mp:  $>253$  °C (decomposes),  $^1\text{H}$  NMR (300 MHz, CHLOROFORM- $d$ )  $\delta$ : 3.66 - 3.81 (m, 3 H), 3.86 - 3.97 (m, 2 H), 4.28 (s, 1 H), 4.40 (br. s., 1 H), 4.50 (d,  $J=4.95$  Hz, 1 H), 5.10 (br. s., 1 H), 5.87 - 6.13 (m, 3 H), 6.89 (m,  $J=9.08$  Hz, 2 H), 7.12 (m,  $J=8.99$  Hz, 2 H), 8.16 (s, 1 H), 8.32 (s, 1 H);  $^{13}\text{C}$  NMR (75 MHz, CHLOROFORM- $d$ )  $\delta$ : 55.4 (s, 1 C), 62.8 (s, 1 C), 72.2 (s, 1 C), 73.6 (s, 1 C), 87.5 (s, 1 C), 91.3 (s, 1 C), 114.6 (s, 1 C), 115.8 (s, 2 C), 121.8 (s, 1 C), 122.2 (s, 1 C), 143.4 (s, 1 C), 144.9 (s, 1 C), 150.8 (s, 1 C), 151.7 (s, 1 C), 157.2 (s, 1 C), 160.1 (s, 1 C).

3.7.3.34. *9-Ethyl-6-(2-isopropyl-5-methylphenoxy)-9H-purine (34c)*

General procedure (GP) was followed with 6-chloro-9-ethyl-9H-purine (164 mg, 1 mmol) and thymol (180 mg, 1.2 mmol, 1.2 equiv.) providing the desired 9-ethyl-6-(2-isopropyl-4-methylphenoxy)-9H-purine (213 mg, 0.719 mmol, 72%) as colorless oil;  $^1\text{H}$  NMR (300 MHz, CHLOROFORM- $d$ )  $\delta$ : 1.24 (s, 6 H), 1.66 (t,  $J=7.24$  Hz, 3 H), 2.38 (s, 3 H), 2.98 - 3.11 (m, 1 H), 4.55 (q,  $J=7.24$  Hz, 2 H), 6.95 - 7.01 (m, 1 H), 7.12 - 7.20 (m, 1 H), 7.35 (d,  $J=7.98$  Hz, 1 H), 8.24 (s, 1 H), 8.64 (s, 1 H);  $^{13}\text{C}$  NMR (75 MHz, CHLOROFORM- $d$ )  $\delta$ : 17.2 (s, 1 C), 21.1 (s, 1 C), 23 (s, 1 C), 23.3 (s, 1 C), 27.3 (s, 1 C), 43.3 (s, 1 C), 120.8 (s, 1 C), 122.8 (s, 1 C), 126.1 (s, 1 C), 127.1 (s, 1 C), 132.1 (s, 1 C), 137.3 (s, 1 C), 137.6 (s, 1 C), 149 (s, 1 C), 152.6 (s, 1 C), 154 (s, 1 C), 162.7 (s, 1 C); (+ve) APCI-MS  $m/z = 296.37$  calcd. for  $\text{C}_{17}\text{H}_{20}\text{N}_4\text{O}$  [M], found: 297.42 [M+H].

### 3.7.4. Tandem Catalytic Processes Using the Pd/PTABS System.

*General Procedure:* A 25 mL oven-dried Schlenk tube was charged with 1 mol% of Pd(OAc)<sub>2</sub>, 2 mol % of PTABS (ligand), and 0.5 mmol of 2-chlorobenzthiazole under N<sub>2</sub> atmosphere, and the resultant mixture was dissolved in 1.5 mL of dry DMF. The reaction mixture was stirred for 5 min, and 2.5 equiv. of potassium phosphate, 1.2 equiv. of 4-bromophenol, and 1.5 mL of dry DMF were added. The resultant mixture was stirred at 60 °C for 2 h. After consumption of starting material (monitored by TLC/TLC-MS), to the reaction mixture was added 1 mol % of Pd(OAc)<sub>2</sub>, 2 mol % of XPhos, 1.5 equiv of terminal alkyne, 0.5 mol % of copper iodide and lastly 2.1 equiv. of triethyl amine and continuously stirred at 80 °C for 24 h. Then, the solvent was removed in vacuum, and the resultant residue obtained was purified by column chromatography in EtOAc/hexane (10%–30%) solvent system to afford the desired product.

#### 3.7.4.1. 2-(4-(Phenylethynyl)phenoxy)benzo[d]thiazole (**35a**)

General procedure was followed with 2-chlorobenzthiazole (84.82 mg, 0.065 mL, 0.50 mmol), 4-bromo phenol (104.3 mg, 0.60 mmol, 1.2 equiv.), and phenyl acetylene (76.5 mg, 0.09 mL, 0.75 mmol, 1.5 equiv.), which yielded the desired product (134 mg, 0.41 mmol, 82%) as yellow powder. <sup>1</sup>H NMR (300 MHz, CHLOROFORM-d) δ: 7.74 (dd, J = 7.6, 0.5 Hz, 1 H), 7.68 (dd, J = 7.7, 0.4 Hz, 1 H), 7.60 (d, J = 8.6 Hz, 2 H), 7.53 (dd, J = 6.0, 2.6 Hz, 2 H), 7.42–7.31 (m, 6 H), 7.29 (d, J = 7.0 Hz, 1 H). <sup>13</sup>C NMR (75 MHz, CHLOROFORM-d) δ: 156.9 (s, 1 C), 154.2 (s, 1 C), 133.2 (s, 1 C), 131.6 (s, 1 C), 131.5 (s, 2 C), 128.3 (s, 2 C), 128.3 (s, 2 C), 126.3 (s, 2 C), 124.2 (s, 2 C), 121.8 (s, 2 C), 121.2 (s, 2 C), 120.5 (s, 1 C), 89.7 (s, 1 C), 88.7 (s, 1 C); CHNS calcd for C<sub>21</sub>H<sub>13</sub>NOS: C, 77.04; H, 4.00; N, 4.28; S, 9.79; found: C, 76.75; H, 3.97; N, 4.07; S, 9.94.

#### 3.7.4.2. 2-(4-((4-Methoxyphenyl)ethynyl)phenoxy)benzo[d]thiazole (**35b**)

General procedure was followed with 2-chlorobenzthiazole (84.82 mg, 0.065 mL, 0.50 mmol), 4-bromo phenol (104.3 mg, 0.60 mmol, 1.2 equiv.), and 4-methoxyphenyl acetylene (132.2 mg, 0.1 mL, 0.75 mmol, 1.5 equiv.), which yielded the desired product (149 mg, 0.42 mmol, 84%) as white powder. <sup>1</sup>H NMR (300 MHz, CHLOROFORM-d) δ: 7.77–7.72 (m, 1 H), 7.68 (d, J = 8.7 Hz, 1 H), 7.60–7.53 (m, 2 H), 7.47 (d, J = 8.9 Hz, 2 H), 7.41–7.31 (m, 3 H), 7.29 (d, J = 6.7 Hz, 1 H), 6.88 (d, J = 8.5 Hz, 2 H), 3.82 (s, 3 H). <sup>13</sup>C NMR (75 MHz, CHLOROFORM-d) δ: 133 (s, 2 C), 133.2 (s, 2 C), 126.2 (s, 2 C), 124.1 (s, 2 C), 121.8 (s, 2 C), 121.2 (s, 2 C), 120.5 (s, 2 C), 114 (s, 2 C), 114.3 (s, 3 C), 89.8 (s, 2 C), 55.2 (s, 1 C); CHNS calcd for C<sub>22</sub>H<sub>15</sub>NO<sub>2</sub>S: C, 73.93; H, 4.23; N, 3.92; S, 8.97; found: C, 73.67; H, 4.19; N, 3.70; S, 8.85.

3.7.4.3. 2-(4-(*p*-Tolylolethynyl)phenoxy)benzo[*d*]thiazole (**35c**)

General procedure was followed with 2-chlorobenzthiazole (84.82 mg, 0.065 mL, 0.50 mmol), 4-bromo phenol (104.3 mg, 0.60 mmol, 1.2 equiv.), and 4-tolylphenyl acetylene (87 mg, 0.09 mL, 0.75 mmol, 1.5 equiv.), which yielded the desired product (141 mg, 0.41 mmol, 83%) as white powder. <sup>1</sup>H NMR (300 MHz, CHLOROFORM-*d*) δ: 7.74 (d, *J* = 7.1 Hz, 1 H), 7.68(d, *J* = 7.6 Hz, 1 H), 7.58 (dd, *J* = 6.9, 1.8 Hz, 2 H), 7.41 (t, *J* = 7.0 Hz, 3 H), 7.35 (d, *J* = 8.8 Hz, 2 H), 7.28 (d, *J* = 8.6 Hz, 1 H), 7.15 (d, *J* = 7.5 Hz, 2 H), 2.36 (s, 3 H); <sup>13</sup>C NMR (75 MHz, CHLOROFORM-*d*) δ: 154.2 (s, 1 C), 152.9 (s, 1 C), 148.9 (s, 1 C), 138.5 (s, 1 C), 133.1 (s, 1 C), 131.4 (s, 1 C), 129.1 (s, 2 C), 126.2 (s, 2 C), 124.2 (s, 2 C), 121.8 (s, 2 C), 121.5 (s, 2 C), 121.2 (s, 2 C), 120.5 (s, 1 C), 89.9 (s, 2 C), 21.4 (s, 1 C); CHNScaled. for C<sub>22</sub>H<sub>15</sub>NOS: C, 77.39; H, 4.43; N, 4.10; S, 9.39; found: C, 77.09; H, 4.37; N, 4.04; S, 9.04.

3.7.4.4. 6-(4-(Benzo[*d*]thiazol-2-yloxy)phenyl)-3-(4-hydroxy-5-(hydroxymethyl)tetrahydrofuran-2 yl)furo[2,3-*d*]pyrimidin-2(3*H*)-one (**36**)

A 25 mL oven-dried Schlenk tube was charged with 1 mol% of Pd(OAc)<sub>2</sub>, 2 mol % of PTABS (ligand), and 2-chlorobenzthiazole (84.82 mg, 0.065 mL, 0.50 mmol) derivative under N<sub>2</sub> atmosphere, and the resultant mixture dissolved in 1.5 mL of dry DMF. The reaction mixture stirred for 5 min, and 2.5 equiv. of potassium phosphate, 4-bromo phenol (104.3 mg, 0.60 mmol, 1.2 equiv.), and 1.5 mL dry DMF were added. The resultant mixture was stirred at 60 °C for 2 h. After consumption of starting material (monitored by TLC-MS), to the reaction mixture was added 1 mol % Pd(OAc)<sub>2</sub>, 2 mol % XPhos, 5-ethynyl deoxy uridine (EDU) (113 mg, 0.49 mmol, 0.98 equiv.), 0.5 mol % of copper iodide, and lastly 2.1 equiv. of triethylamine and stirring continued at 80 °C for 24 h. This was followed by addition of 3.7 mL of methanol, 1.7 mL of triethylamine, and 6.0 mol % of copper iodide and stirring continued for another 24 h at 80 °C. Then, the solvent was removed in vacuum, and the resultant residue was purified by column chromatography in dichloromethane/methanol (3.0 to 4.0%) solvent system to afford the desired product (174 mg, 0.36 mmol, 73%) as white powder.

<sup>1</sup>H NMR (300 MHz, DMSO- *d*<sub>6</sub>) δ: 8.87 (s, 1 H), 7.99–7.85 (m, 3 H), 7.68 (d, *J* = 8.0 Hz, 1 H), 7.57 (d, *J* = 8.4 Hz, 2 H), 7.45–7.36 (m, 1 H), 7.32 (d, *J* = 10.1 Hz, 2 H), 6.16 (t, *J* = 6.0 Hz, 1 H), 5.29 (d, *J* = 3.1 Hz, 1 H), 5.17 (t, *J* = 5.0 Hz, 1 H), 4.23 (d, *J* = 4.2 Hz, 1 H), 3.92 (d, *J* = 2.6 Hz, 1 H), 3.65 (dd, *J* = 30.1, 12.8 Hz, 2 H), 2.38 (dd, *J* = 5.9, 4.4 Hz, 1 H), 2.09 (dt, *J* = 8.5, 4.7 Hz, 1 H). <sup>13</sup>C NMR (75 MHz, DMSO- *d*<sub>6</sub>) δ: 171.6 (s, 1 C), 171.4 (s, 1 C), 155 (s, 1 C), 154.1 (s, 1 C), 153.1 (s, 1 C), 148.8 (s, 1 C), 138.9 (s, 1 C), 132.3 (s, 1 C), 127 (s, 1 C), 126.8 (s, 1 C), 124.8 (s, 1 C), 122.7 (s, 2 C), 122 (s, 2 C), 121.7 (s, 2 C), 107.1 (s, 1 C), 100.5 (s, 1 C),

88.6 (s, 1 C), 88.1 (s, 1 C), 69.9 (s, 1 C), 61 (s, 1 C), 41.7 (s, 1 C); CHNS calcd. for C<sub>24</sub>H<sub>19</sub>N<sub>3</sub>O<sub>6</sub>S: C, 60.37; H, 4.01; N, 8.80; S, 6.72; found: C, 60.45; H, 4.02; N, 8.93; S, 6.50.<sup>285</sup>

### 3.7.5. Pd/PTABS catalytic thioetherification of chloroheteroarenes at moderate temperatures.

*General procedure (GP1):* A 25 mL of oven-dried Schlenk tube was charged with 1 mol% of Pd(OAc)<sub>2</sub>, 2 mol% of PTABS (phosphoadamantine butylsulfonate) and 1 mmol of a *chloroheteroarene* derivative under N<sub>2</sub> atmosphere and the resultant mixture dissolved in 3 mL of dry DMF. The reaction mixture was stirred for 5 minutes followed by addition of 1.2 to 1.5 equiv. of the corresponding thiophenol, and 2.0 to 2.5 equiv. of K<sub>3</sub>PO<sub>4</sub> then stirred at 50 °C for 1 to 2 h. After consumption of starting material (monitored by TLC/TLC-MS), the solvent was removed in vacuum, and the resultant residue was purified by column chromatography in EtOAc/hexane (10% to 50%) solvent system to afford the desired product. In the case of nucleoside derivatives of purine and pyrimidine substrates CHCl<sub>3</sub>/MeOH (9:1) was used as a mobile phase for column chromatography.

*General procedure thioether oxidation to sulfones (GP2):* In a dry Schlenk tube, the thioether (1 mmol) was dissolved in DCM (5 mL). The solution was cooled to 0 °C, and then *m*CPBA (2.5 equiv. in 3 mL of DCM) was added dropwise at 0 °C. The reaction was then stirred at room temperature until complete conversion was reached (progress monitored by TLC). The mixture was washed with a saturated aqueous solution of Na<sub>2</sub>S<sub>2</sub>O<sub>3</sub> (3 x 10 mL). After separation, the organic layers were washed with a saturated aqueous solution of sodium bicarbonate (3 x 5 mL). The organic phase was dried over Na<sub>2</sub>SO<sub>4</sub>. The organic solvent was evaporated to yield the corresponding sulfones.

*General procedure for thioethers oxidation to sulfoximine (GP3):* In a Schlenk tube, thioether (1 mmol), PhI(OAc)<sub>2</sub> (3 mmol) and ammonium acetate (2 mmol) were dissolved in MeOH (4 mL) at room temperature. The mixture was stirred until the complete conversion was reached (progress monitored by TLC). The solvent was evaporated under reduced pressure by using a roto evaporator. The residue was then purified by silica gel column chromatography to yield the corresponding sulfoximine.

#### 3.7.5.1. 2-(Phenylthio)pyrazine (**41a**)

The compound exhibited identical <sup>1</sup>H and <sup>13</sup>C NMR spectra as in previous reports.<sup>430</sup> General procedure (GP1) was followed with 2-chloropyrazine (0.89 mL, 1 mmol) and thiophenol (0.123 mL, 1.2 mmol, 1.2 equiv.) yielding the desired 2-(phenylthio)pyrazine as pale pink oil (165 mg, 0.88 mmol, 88%). Hexane/EtOAc (7:3) was used as a mobile phase for column

chromatography.  $^1\text{H}$  NMR (300 MHz, CHLOROFORM-*d*)  $\delta$ : 7.37 - 7.50 (m, 3 H), 7.56 - 7.66 (m, 2 H), 8.21 (dd,  $J=5.96, 2.02$  Hz, 2 H), 8.29 - 8.36 (m, 1 H);  $^{13}\text{C}$  NMR (75 MHz, CHLOROFORM-*d*)  $\delta$ : 129.3 (s, 1 C), 129.9 (s, 1 C), 130.1 (s, 2 C), 135.3 (s, 2 C), 140.4 (s, 1 C), 143 (s, 1 C), 144.1 (s, 1 C), 158.9 (s, 1 C); APCI-MS  $m/z = 188.04$   $m/z$  calcd. for  $\text{C}_{10}\text{H}_8\text{N}_2\text{S}$  [M]; found: 189.12[M+H].

#### 3.7.5.2. 2-(2,6-Dimethylphenylthio)pyrazine (**41b**)

The compound exhibited identical  $^1\text{H}$  and  $^{13}\text{C}$  NMR spectra as in a previous reports.<sup>431</sup> General procedure (GP1) was followed with 2-chloropyrazine (0.89 mL, 1 mmol) and 2, 6-dimethylbenzenethiol (0.2 mL, 1.5 mmol, 1.5 equiv.) yielding the desired 2-(2,6-dimethylphenylthio)pyrazine as pale yellow oil (156 mg, 0.72 mmol, 72%). Hexane/EtOAc (7:3) was used as a mobile phase for column chromatography.  $^1\text{H}$  NMR (300 MHz, CHLOROFORM-*d*)  $\delta$ : 2.44 (s, 6 H), 7.17 - 7.24 (m, 2 H), 7.24 - 7.31 (m, 1 H), 7.98 (d,  $J=1.56$  Hz, 1 H), 8.18 (d,  $J=2.57$  Hz, 1 H), 8.27 - 8.34 (m, 1 H);  $^{13}\text{C}$  NMR (75 MHz, CHLOROFORM-*d*)  $\delta$ : 21.7 (s, 2 C), 127.1 (s, 1 C), 128.6 (s, 2 C), 130 (s, 1 C), 139.5 (s, 2 C), 141.3 (s, 1 C), 143.6 (s, 1 C), 143.8 (s, 1 C), 158 (s, 1 C); (+ve) APCI-MS  $m/z = 216.07$   $m/z$  calcd. for  $\text{C}_{12}\text{H}_{12}\text{N}_2\text{S}$  [M]; found: 217.82 [M+H].

#### 3.7.5.3. 2-(Pyrazin-2-ylthio)benzenamine (**41c**)

The compound exhibited identical  $^1\text{H}$  and  $^{13}\text{C}$  NMR spectra as in a previous report.<sup>432</sup> General procedure (GP1) was followed with 2-chloropyrazine (0.89 mL, 1 mmol) and 2-aminobenzenethiol (0.160 mL, 1.5 mmol, 1.5 equiv.) yielding the desired 2-(pyrazin-2-ylthio)benzenamine as pale yellow oil (186 mg, 0.92 mmol, 92%). Hexane/EtOAc (7:3) was used as a mobile phase for column chromatography.  $^1\text{H}$  NMR (300 MHz, CHLOROFORM-*d*)  $\delta$ : 4.38 (br. s., 2 H), 6.72 - 6.90 (m, 2 H), 7.23 - 7.34 (m, 1 H), 7.49 (dd,  $J=7.70, 1.56$  Hz, 1 H), 8.08 (d,  $J=1.56$  Hz, 1 H), 8.23 (d,  $J=2.57$  Hz, 1 H), 8.34 (dd,  $J=2.57, 1.56$  Hz, 1 H);  $^{13}\text{C}$  NMR ( $^1\text{H}$ ) (75 MHz, CHLOROFORM-*d*)  $\delta$ : 115.6 (s, 1 C), 119 (s, 2 C), 132.2 (s, 2 C), 137.5 (s, 1 C), 140 (s, 1 C), 141.9 (s, 1 C), 143.7 (s, 1 C), 149.2 (s, 1 C); (+ve) APCI-MS  $m/z = 203.05$   $m/z$  calcd. for  $\text{C}_{10}\text{H}_9\text{N}_3\text{S}$  [M]; found: 204.1 [M+H].

#### 3.7.5.4. 2-(Ethylthio)pyrazine (**41d**)

The compound exhibited identical  $^1\text{H}$  and  $^{13}\text{C}$  NMR spectra as in a previous reports.<sup>433</sup> General procedure (GP1) was followed with 2-chloropyrazine (0.89 mL, 1 mmol) and ethanethiol (0.110 mL, 1.5 mmol, 1.5 equiv.) yielding the desired 2-(ethylthio)pyrazine as colorless oil (125 mg, 0.89 mmol, 89%). Hexane/EtOAc (7:3) was used as a mobile phase for column

chromatography.  $^1\text{H}$  NMR (300 MHz, CHLOROFORM-*d*)  $\delta$ : 1.33 (t,  $J=7.34$  Hz, 3 H), 3.13 (q,  $J=7.37$  Hz, 2 H), 8.13 (d,  $J=2.66$  Hz, 1 H), 8.29 (dd,  $J=2.61, 1.60$  Hz, 1 H), 8.38 (d,  $J=1.56$  Hz, 1 H);  $^{13}\text{C}$  NMR (75 MHz, CHLOROFORM-*d*)  $\delta$ : 14.31 (s, 1 C), 23.8 (s, 1 C), 139 (s, 1 C), 143.6 (s, 1 C), 143.7 (s, 1 C), 157.1 (s, 1 C); (+ve) APCI-MS  $m/z = 140.04$   $m/z$  calcd. for  $\text{C}_6\text{H}_8\text{N}_2\text{S}$  [M]; found: 141.19 [M+H].

#### 3.7.5.5. 2-Adamantanethiopyrazine (**41e**)

General procedure (GP1) was followed with 2-chloropyrazine (0.89 mL, 1 mmol) and adamantanethiol (0.202 mg, 1.2 mmol, 1.2 equiv.) yielding the desired 2-adamantanethiopyrazine as colorless solid (237 mg, 0.91 mmol, 91%). Hexane/EtOAc (7:3) was used as a mobile phase for column chromatography.  $^1\text{H}$  NMR (300 MHz, CHLOROFORM-*d*)  $\delta$ : 1.69 (t,  $J=2.98$  Hz, 6 H), 1.98 - 2.17 (m, 9 H), 8.30 (d,  $J=2.48$  Hz, 1 H), 8.43 (dd,  $J=2.57, 1.56$  Hz, 1 H), 8.51 (d,  $J=1.47$  Hz, 1 H);  $^{13}\text{C}$  NMR (75 MHz, CHLOROFORM-*d*)  $\delta$ : 30.4 (s, 1 C) 36.5 (s, 2 C) 43.7 (s, 2 C) 51.4 (s, 2 C) 77.4 (s, 2 C) 77.8 (s, 1 C) 141.5 (s, 1 C) 144.3 (s, 1 C) 148.4 (s, 1 C) 155.7 (s, 1 C); (+ve) APCI-MS  $m/z = 246.12$   $m/z$  calcd. for  $\text{C}_{14}\text{H}_{18}\text{N}_2\text{S}$  [M]; found: 247.21 [M+H]; CHNS calcd. for  $\text{C}_{14}\text{H}_{18}\text{N}_2\text{S}$ : C, 68.25; H, 7.36; N, 11.37; S, 13.01. found: C, 68.21; H, 7.32; N, 11.34; S, 12.97.

#### 3.7.5.6. 2-(Phenylthio)quinoxaline (**41f**)

The compound exhibited identical  $^1\text{H}$  and  $^{13}\text{C}$  NMR spectra as in previous reports.<sup>434</sup> General procedure (GP1) was followed with 2-chloroquinoxaline (146 mg, 1 mmol) and thiophenol (0.154 mL, 1.5 mmol, 1.5 equiv.) yielding the desired 2-(phenylthio)quinoxaline as colorless needles (222 mg, 0.93 mmol, 93%). Hexane/EtOAc (7:3) was used as a mobile phase for column chromatography.  $^1\text{H}$  NMR (300 MHz, CHLOROFORM-*d*)  $\delta$ : 7.45 - 7.51 (m, 3 H), 7.63 - 7.73 (m, 4 H), 7.88 - 7.92 (m, 1 H), 7.97 - 8.03 (m, 1 H), 8.44 (s, 1 H);  $^{13}\text{C}$  NMR (75 MHz, CHLOROFORM-*d*)  $\delta$ : 128.2 (s, 1 C), 128.7 (s, 2 C), 128.9 (s, 1 C), 129.1 (s, 1 C), 129.6 (s, 2 C), 129.7 (s, 1 C), 130.4 (s, 1 C), 134.9 (s, 1 C), 139.8 (s, 1 C), 142.1 (s, 1 C), 143.4 (s, 1 C), 157.1 (s, 1 C); (+ve) APCI-MS  $m/z = 238.06$   $m/z$  calcd. for  $\text{C}_{14}\text{H}_{10}\text{N}_2\text{S}$  [M]; found: 239.09 [M+H]. CHNS calcd. for  $\text{C}_{14}\text{H}_{10}\text{N}_2\text{S}$ : C, 70.56; H, 4.23; N, 11.76; S, 13.46; found: C, 70.51; H, 4.19; N, 11.71, S, 13.41;

#### 3.7.5.7. 2-(2,6-Dimethylphenylthio)quinoxaline (**41g**)

General procedure (GP1) was followed with 2-chloroquinoxaline (146 mg, 1 mmol) and 2,6-dimethylbenzenethiol (0.2 mL, 1.5 mmol, 1.5 equiv.) yielding the desired 2-(2,6-dimethylphenylthio)quinoxaline as colorless solid (234 mg, 0.88 mmol, 88%). Hexane/EtOAc



(7:3) was used as a mobile phase for column chromatography.  $^1\text{H}$  NMR (300 MHz, CHLOROFORM-*d*)  $\delta$ : 2.49 (s, 6 H), 7.23 - 7.28 (m, 2 H), 7.30 - 7.36 (m, 1 H), 7.68 (dd,  $J=8.21$ , 1.70 Hz, 1 H), 7.64 (dd,  $J=8.12$ , 1.60 Hz, 1 H), 7.88 - 7.92 (m, 1 H), 7.97 - 8.03 (m, 1 H), 8.26 (s, 1 H);  $^{13}\text{C}$  NMR (75 MHz, CHLOROFORM-*d*)  $\delta$ : 21.9 (s, 2 C), 127.1 (s, 1 C), 128 (s, 2 C), 128.2 (s, 1 C), 128.6 (s, 1 C), 129.0 (s, 2 C), 130.1 (s, 1 C), 130.3 (s, 1 C), 139.6 (s, 1 C), 142.2 (s, 1 C), 142.3 (s, 1 C), 143.8 (s, 1 C), 156.7 (s, 1 C); (+ve) APCI-MS  $m/z = 266.09$   $m/z$  calcd. for  $\text{C}_{16}\text{H}_{14}\text{N}_2\text{S}$  [M]; found: 267.1 [M+H]; CHNS calcd. for  $\text{C}_{16}\text{H}_{14}\text{N}_2\text{S}$ : C, 72.15; H, 5.30; N, 10.52; S, 12.04; found: C, 72.09; H, 5.26; N, 10.59; S, 12.34.

#### 3.7.5.8. 2-(Quinoxalin-2-ylthio)benzenamine (**41h**)

General procedure (GP1) was followed with 2-chloroquinoxaline (146 mg, 1 mmol) and 2-aminobenzenethiol (0.160 mL, 1.5 mmol, 1.5 equiv.) yielding the desired 2-(quinoxalin-2-ylthio)benzenamine as yellow oil (212.5 mg, 0.84 mmol, 84%). Hexane/EtOAc (7:3) was used as a mobile phase for column chromatography.  $^1\text{H}$  NMR (300 MHz, CHLOROFORM-*d*)  $\delta$ : 4.46 (s, 2 H), 6.62 - 6.71 (m, 1 H), 6.74 - 6.86 (m, 2 H), 7.18 - 7.35 (m, 1 H), 7.56 - 7.71 (m, 2 H), 7.86 - 7.93 (m, 1 H), 7.94 - 7.99 (m, 1 H), 8.27 - 8.35 (m, 1 H);  $^{13}\text{C}$  NMR (75 MHz, DMSO-*d*<sub>6</sub>)  $\delta$ : 115.5 (s, 1 C), 117.8 (s, 1 C), 118.7 (s, 1 C), 127.8 (s, 2 C), 128.4 (s, 1 C), 129 (s, 1 C), 130.2 (s, 1 C), 131.3 (s, 1 C), 132 (s, 1 C), 139.6 (s, 1 C), 142.3 (s, 1 C), 149.3 (s, 1 C), 156.3 (s, 1 C); (+ve) APCI-MS  $m/z = 253.07$   $m/z$  calcd. for  $\text{C}_{14}\text{H}_{11}\text{N}_3\text{S}$  [M]; found: 254.62 [M+H]; CHNS calcd. for  $\text{C}_{14}\text{H}_{11}\text{N}_3\text{S}$ : C, 66.38; H, 4.38; N, 16.59; S, 12.66; found: C, 66.42; H, 4.28; N, 16.45; S, 12.61.

#### 3.7.5.9. 2-(Benzylthio)quinoxaline (**41i**)

The compound exhibited identical  $^1\text{H}$  and  $^{13}\text{C}$  NMR spectra as in a previous reports.<sup>435</sup> General procedure (GP1) was followed with 2-chloroquinoxaline (164 mg, 1 mmol) and benzylthiol (150 mg, 1.2 mmol, 1.2 equiv.) yielding the desired 2-(benzylthio)quinoxaline as semi-solid sticky material (231 mg, 0.92 mmol, 92%). Hexane/EtOAc (7:3) was used as a mobile phase for column chromatography.  $^1\text{H}$  NMR (300 MHz, CHLOROFORM-*d*)  $\delta$ : 4.58 (s, 2 H), 7.20 - 7.34 (m, 3 H), 7.44 - 7.50 (m, 2 H), 7.57 - 7.65 (m, 1 H), 7.65 - 7.73 (m, 1 H), 7.93 - 8.05 (m, 2 H), 8.57 (s, 1 H);  $^{13}\text{C}$  NMR (75 MHz, CHLOROFORM-*d*)  $\delta$ : 33.6 (s, 1 C), 76.6 (s, 1 C), 127.3 (s, 1 C), 127.7 (s, 1 C), 128 (s, 1 C), 128.5 (s, 1 C), 129.1 (s, 2 C), 129.2 (s, 1 C), 130.1 (s, 1 C), 137.3 (s, 1 C), 139.9 (s, 1 C), 142.6 (s, 1 C), 144.5 (s, 1 C), 155.6 (s, 1 C); (+ve) APCI-MS  $m/z = 252.07$   $m/z$  calcd. for  $\text{C}_{15}\text{H}_{12}\text{N}_2\text{S}$  [M]; found: 253.1 [M+H].

3.7.5.10. 2-(*sec*-Butylthio)quinoxaline (**41j**)

General procedure (GP1) was followed with 2-chloroquinoxaline (82 mg, 0.5 mmol) and 2-butanethiol (0.081 mL, 0.75 mmol, 1.5 equiv.) yielding the desired 2-(*sec*-butylthio)quinoxaline as pale yellow solid (104 mg, 0.475 mmol, 95%). Hexane/EtOAc (7:3) was used as a mobile phase for column chromatography. <sup>1</sup>H NMR (300 MHz, CHLOROFORM-*d*) δ: 1.07 (t, *J*=7.43 Hz, 3 H), 1.47 (d, *J*=6.88 Hz, 3 H), 1.68 - 1.94 (m, 2 H), 4.04 - 4.20 (m, 1 H), 7.53 - 7.71 (m, 2 H), 7.86 - 7.94 (m, 1 H), 7.95 - 8.04 (m, 1 H), 8.54 (s, 1 H); <sup>13</sup>C NMR (75 MHz, CHLOROFORM-*d*) δ: 11.4 (s, 1 C), 20.4 (s, 1 C), 29.3 (s, 1 C), 41.2 (s, 1 C), 127.7 (s, 1 C), 127.8 (s, 1 C), 129.1 (s, 1 C), 129.9 (s, 1 C), 139.6 (s, 1 C), 142.7 (s, 1 C), 145 (s, 1 C), 156.7 (s, 1 C); (+ve) APCI-MS *m/z* = 218.09 *m/z* calcd. for C<sub>12</sub>H<sub>14</sub>N<sub>2</sub>S [M]; found: 219.17 [M+H], CHNS. calcd. for C<sub>12</sub>H<sub>14</sub>N<sub>2</sub>S: C, 66.02; H, 6.46; N, 12.83; S, 14.69; found: C, 65.97; H, 6.33; N, 12.96; S, 14.79.

3.7.5.11. Adamantanethio2- quinoxaline (**41k**)

General procedure (GP1) was followed with 2-chloro quinoxaline (164 mg, 1 mmol) and 2-butanethiol (0.38 mL, 2.5 mmol, 2.5 equiv.) yielding the desired 2-adamantan(-1-yl)thio)quinoxaline as white amorphous solid (266 mg, 0.90 mmol, 90%). Hexane/EtOAc (7:3) was used as a mobile phase for column chromatography. <sup>1</sup>H NMR (300 MHz, CHLOROFORM-*d*) δ: 1.71 - 1.88 (m, 6 H), 2.12 (br. s., 3 H), 2.35 (d, *J*=2.75 Hz, 6 H), 7.60 - 7.76 (m, 2 H), 7.91 - 8.06 (m, 2 H), 8.57 (s, 1 H); <sup>13</sup>C NMR (75 MHz, CHLOROFORM-*d*) δ: 30 (s, 2 C), 36.3 (s, 2 C), 42.7 (s, 2 C), 51.9 (s, 2 C), 128.3 (s, 2 C), 128.4 (s, 1 C), 129.2 (s, 2 C), 129.9 (s, 1 C), 139.7 (s, 1 C), 142.4 (s, 1 C), 146.7 (s, 1 C), 156.3 (s, 1 C); (+ve) APCI-MS *m/z* = 296,13 *m/z* calcd. for C<sub>18</sub>H<sub>20</sub>N<sub>2</sub>S [M]; found: 297.22 [M+H]; CHNS calcd. for C<sub>18</sub>H<sub>20</sub>N<sub>2</sub>S: C,72.93; H, 6.80; N, 9.45; S, 10.82; found: C, 72.89; H, 6.75; N, 9.41; S, 10.80.

3.7.5.12. 2,4-Bis(phenylthio)pyrimidine (**41l**)

The compound exhibited identical <sup>1</sup>H and <sup>13</sup>C NMR spectra as in a previous reports.<sup>436</sup> General procedure (GP1) was followed with 2,4-dichloropyrimidine (149 mg, 1 mmol) and thiophenol (0.225 mL, 2.2 mmol, 2.2 equiv.) yielding the desired 2,4-bis(phenylthio)pyrimidine as colorless cubes (275 mg, 0.93 mmol, 93%). Hexane/EtOAc (7:3) was used as a mobile phase for column chromatography. <sup>1</sup>H NMR (300 MHz, CHLOROFORM-*d*) δ: 6.45 (d, *J*=5.41 Hz, 1 H), 7.33 - 7.50 (m, 6 H), 7.50 - 7.60 (m, 4 H), 8.08 (d, *J*=5.41 Hz, 1 H); <sup>13</sup>C NMR (75 MHz, CHLOROFORM-*d*) δ:112.5 (s, 1 C), 127.2 (s, 1 C), 128.6 (s, 2 C), 128.6 (s, 2 C), 128.8 (s, 2 C), 129.3 (s, 2 C), 129.5 (s, 1 C), 134.6 (s, 1 C), 135.1 (s, 1 C), 155.5 (s, 1 C), 171.5 (s, 1 C), 172.7 (s, 1 C); (+ve) APCI-MS *m/z* = 296.04 *m/z* calcd. for C<sub>16</sub>H<sub>12</sub>N<sub>2</sub>S<sub>2</sub> [M]; found:

297.10[M+H], CHNS calcd. for C<sub>16</sub>H<sub>12</sub>N<sub>2</sub>S<sub>2</sub>: C, 64.83; H, 4.08; N, 9.45; S, 21.64: found: C, 64.78; H, 4.04; N, 9.41, S, 21.59.

3.7.5.13. *2,4-Bis(sec-butylthio)pyrimidine (41m)*

General procedure (GP1) was followed with 2,4-dichloropyrimidine (0.149 mg, 1 mmol) and 2-butanethiol (0.269.3 mL, 2.5 mmol, 2.5 equiv.) yielding the desired 2,4-bis(sec-butylthio)pyrimidine as pale yellow low melting solid (230.8 mg, 0.90 mmol, 90%). Hexane/EtOAc (7:3) was used as a mobile phase for column chromatography. <sup>1</sup>H NMR (300 MHz, CHLOROFORM-*d*) δ: 0.92 - 1.10 (m, 6 H), 1.33 - 1.45 (m, 6 H), 1.57 - 1.84 (m, 4 H), 3.77 (qd, *J*=6.79, 1.93 Hz, 1 H), 3.92 (qd, *J*=6.76, 2.11 Hz, 1 H), 6.71 (d, *J*=5.41 Hz, 1 H), 8.04 (d, *J*=5.41 Hz, 1 H); <sup>13</sup>C NMR (75 MHz, CHLOROFORM-*d*) δ: 10.9 (s, 2 C), 19.9 (s, 2C), 20.0 (s, 1 C), 28.8 (s, 1 C), 40.1 (s, 1 C), 41.3 (s, 1 C), 113.8 (s, 1 C), 153.7 (s, 1 C), 169.8 (s, 1 C), 171.4 (s, 1 C); (+ve) APCI-MS *m/z* = 256.11 *m/z* calcd. for C<sub>12</sub>H<sub>20</sub>N<sub>2</sub>S<sub>2</sub> [M]; found: 257.43[M+H]; CHNS calcd. for C<sub>12</sub>H<sub>20</sub>N<sub>2</sub>S<sub>2</sub>: C, 56.21; H, 7.86; N, 10.92; S, 25.01; found: C, 56.08; H, 7.56; N, 10.63; S, 25.21.

3.7.5.14. *2,4,6-Tris(phenylthio)-1,3,5-triazine (41n)*

General procedure (GP1) was followed with 2,4,6-trichloro-1,3,5-triazine (185 mg, 1 mmol) and thiophenol (0.310 mL, 3.2 mmol, 3.2 equiv.) yielding the desired 2,4,6-tris(phenylthio)-1,3,5-triazine as low melting solid (388 mg, 0.96 mmol, 96%). Hexane/EtOAc (7:3) was used as a mobile phase for column chromatography. <sup>1</sup>H NMR (300 MHz, CHLOROFORM-*d*) δ : 7.16 - 7.25 (m, 6 H), 7.26 - 7.40 (m, 9 H); <sup>13</sup>C NMR (75 MHz, CHLOROFORM-*d*) δ : 127 (s, 6 C), 129 (s, 6 C), 129.3 (s, 6 C), 134.8 (s, 2 C), 180.2 (s, 1 C); (+ve) APCI-MS *m/z* =405.04 *m/z* calcd. for C<sub>21</sub>H<sub>15</sub>N<sub>3</sub>S<sub>3</sub> [M]; found: 406.2 [M+H]; CHNS calcd. for C<sub>21</sub>H<sub>15</sub>N<sub>3</sub>S<sub>3</sub>: C, 62.19; H, 3.73; N, 10.36; S, 23.72; found: C, 62.14; H, 3.69; N, 10.35; S, 23.75.

3.7.5.15. *(2R, 3R, 4S, 5R)-2-(Hydroxymethyl)-5-(6-(phenylthio)-9H-purin-9-yl)-tetrahydrofuran-3,4-diol (42a)*

General procedure (GP1) was followed with 6-chloropurinriboside (287 mg, 1 mmol) and thiophenol (0.154 mL, 1.5 mmol, 1.5 equiv.) yielding the desired (2*R*,3*R*,4*S*,5*R*)-2-(hydroxymethyl)-5-(6-(phenylthio)-9*H*-purin-9-yl)-tetrahydrofuran-3,4-diol as fluffy white solid (237 mg, 0.69 mmol, 69%). CHCl<sub>3</sub>/MeOH (9:1) was used as a mobile phase for column chromatography. <sup>1</sup>H NMR (300 MHz, DMSO-*d*<sub>6</sub>) δ: 3.58 (s, 1 H), 3.67 (br. s., 1 H), 3.98 (d, *J*=3.85 Hz, 1 H), 4.18 (br. s., 1 H), 4.56 - 4.65 (m, 1 H), 5.15 (br. s., 1 H), 5.27 (br. s., 1 H), 5.55 (br. s., 1 H), 5.99 (d, *J*=5.59 Hz, 1 H), 7.46 - 7.55 (m, 3 H), 7.60 - 7.70 (m, 2 H), 8.58 (s, 1 H), 8.76 (s, 1 H); <sup>13</sup>C NMR (75 MHz, DMSO-*d*<sub>6</sub>) δ: 61 (s, 1 C), 70 (s, 1 C), 73.6 (s, 1 C),

85.5 (s, 1 C), 87.7 (s, 1 C), 126.4 (s, 2 C), 129.39 (s, 2 C), 129.5 (s, 1 C), 130.4 (s, 1 C), 135.3 (s, 1 C), 143.5 (s, 1 C), 148.4 (s, 1 C), 151.5 (s, 1 C), 158.9 (s, 1 C); (+ve) APCI-MS  $m/z = 360.09$   $m/z$  calcd. for  $C_{16}H_{16}N_4O_3S$  [M]; found: 361.19 [M+H], 227.1 [M-sugar]; CHNS calcd. for  $C_{16}H_{16}N_4O_4S$ : C, 53.32; H, 4.47; N, 15.55; S, 8.90; found: C, 53.29; H, 4.41; N, 15.59; S, 8.93.

#### 3.7.5.16. 6-(Phenylthio)-9H-purine (**42b**)

The compound exhibited identical  $^1H$  and  $^{13}C$  NMR spectra as in a previous reports.<sup>437</sup> General procedure (GP1) was followed with 6-chloropurine (155 mg, 1 mmol) and thiophenol (0.154 mL, 1.5 mmol, 1.5 equiv.) yielding the desired 6-(phenylthio)-9H-purine as white needle (203 mg, 0.89 mmol, 89%).  $CHCl_3/MeOH$  (9:1) was used as a mobile phase for column chromatography.  $^1H$  NMR (300 MHz, DMSO- $d_6$ )  $\delta$ : 7.48 - 7.55 (m, 4 H), 7.61 - 7.71 (m, 2 H), 8.50 (s, 1 H), 8.54 (s, 1 H);  $^{13}C$  NMR (75 MHz, DMSO- $d_6$ )  $\delta$ : 127.1 (s, 2 C), 129.5 (s, 2 C), 129.6 (s, 2 C), 135.5 (s, 2 C), 144 (s, 1 C), 151.7 (s, 2 C); (+ve) APCI-MS  $m/z = 228.05$   $m/z$  calcd. for  $C_{11}H_8N_4S$  [M]; found: 229.31[M+H]; CHNS calcd. for  $C_{11}H_8N_4S$ : C, 57.88; H, 3.53; N, 24.54; S, 14.05, found: C, 57.82; H, 3.49; N, 24.50; S, 14.00.

#### 3.7.5.17. 2-((3-Methyl-2,4-dioxo-6-(phenylthio)-3,4-dihydropyrimidin-1(2H)-yl)methyl)benzotrile (**42c**)

General procedure (GP1) was followed with 2-((6-chloro-3-methyl-2,4-dioxo-3,4-dihydropyrimidin-1(2H)-yl)methyl)benzotrile (137.5 mg, 0.5 mmol) and thiophenol (0.077 mL, 0.75 mmol, 1.5 equiv.) yielding the desired 2-((3-methyl-2,4-dioxo-6-(phenylthio)-3,4-dihydropyrimidin-1(2H)-yl)methyl)benzotrile as white solid (140 mg, 0.78 mmol, 78%).  $CHCl_3/MeOH$  (9:1) was used as a mobile phase for column chromatography.  $^1H$  NMR (300 MHz, CHLOROFORM- $d$ )  $\delta$ : 3.31 (s, 3 H), 5.10 (s, 1 H), 5.52 (s, 2 H), 7.19 - 7.26 (m, 1 H), 7.37 - 7.52 (m, 6 H), 7.56 - 7.64 (m, 1 H), 7.69 (dd,  $J=7.70$ , 1.01 Hz, 1 H);  $^{13}C$  NMR (75 MHz, CHLOROFORM- $d$ )  $\delta$ : 28 (s, 1 C), 47 (s, 1 C), 98.5 (s, 1 C), 110.8 (s, 1 C), 116.7 (s, 1 C), 125.6 (s, 1 C), 126 (s, 2 C), 128.1 (s, 2 C), 130.4 (s, 1 C), 131.2 (s, 1 C), 133.1 (s, 1 C), 133.2 (s, 1 C), 135.8 (s, 1 C), 139.2 (s, 1 C), 151.7 (s, 1 C), 157.1 (s, 1 C), 160.7 (s, 1 C); (+ve) APCI-MS  $m/z = 349.09$   $m/z$  calcd. for  $C_{19}H_{15}N_3O_2S$  [M]; found: 350.2 [M+H]; CHNS calcd. for  $C_{19}H_{15}N_3O_2S$ : C, 65.31; H, 4.33; N, 12.03; S, 9.18; found: C, 65.29; H, 4.28; N, 12.00; S, 9.15.

#### 3.7.5.18. 2-((6-(sec-Butylthio)-3-methyl-2,4-dioxo-3,4-dihydropyrimidin-1(2H)-yl)methyl)benzotrile (**42d**)

General procedure (GP1) was followed with 2-((6-chloro-3-methyl-2,4-dioxo-3,4-dihydropyrimidin-1(2H)-yl)methyl)benzotrile (137.5 mg, 0.5 mmol) and 2-butanethiol

(0.081 mL, 0.75 mmol, 1.5 equiv.) yielding the desired 2-((6-(*sec*-butylthio)-3-methyl-2,4-dioxo-3,4-dihydropyrimidin-1(2*H*)-yl)methyl)benzotrile as colourless solid (250 mg, 0.76 mmol, 76%). CHCl<sub>3</sub>/MeOH (9:1) was used as a mobile phase for column chromatography. <sup>1</sup>H NMR (300 MHz, CHLOROFORM-*d*) δ: 0.87 - 1.01 (m, 3 H), 1.33 (d, *J*=6.69 Hz, 3 H), 1.45 - 1.78 (m, 2 H), 3.13 - 3.26 (m, 1 H), 3.33 (s, 3 H), 5.42 (s, 2 H), 5.66 (s, 1 H), 7.11 (d, *J*=7.98 Hz, 1 H), 7.32 - 7.41 (m, 1 H), 7.49 - 7.58 (m, 1 H), 7.65 (dd, *J*=7.70, 1.01 Hz, 1 H); <sup>13</sup>C NMR (75 MHz, CHLOROFORM-*d*) δ: 11 (s, 1 C), 19.5 (s, 1 C), 28.5 (s, 1 C), 32.8 (s, 1 C), 36.3 (s, 1 C), 44.9 (s, 1 C), 97.8 (s, 1 C), 110.8 (s, 1 C), 116.7 (s, 1 C), 125.8 (s, 1 C), 127.8 (s, 1 C), 133 (s, 1 C), 133 (s, 1 C), 139.4 (s, 1 C), 151.8 (s, 1 C), 155.1 (s, 1 C), 160.7 (s, 1 C); (+ve) APCI-MS *m/z* = 329.12 *m/z* calcd. for C<sub>17</sub>H<sub>19</sub>N<sub>3</sub>O<sub>2</sub>S [M]; found: 330.19 [M+H]; CHNS calcd. for C<sub>17</sub>H<sub>19</sub>N<sub>3</sub>O<sub>2</sub>S: C, 61.98; H, 5.81; N, 12.76; S, 9.73; found: C, 61.92; H, 5.80; N, 12.80; S, 9.71.

3.7.5.19. (2*R*, 3*S*, 4*R*, 5*R*)-2-(6-(Ethylthio)-9*H*-purin-9-yl)-5-(hydroxymethyl)-tetrahydrofuran-3,4-diol (**42e**)

The compound exhibited identical <sup>1</sup>H and <sup>13</sup>C NMR spectra as in a previous reports.<sup>438</sup> General procedure (GP1) was followed with 6-chloro purine riboside (2 mmol, 1 equiv.) and ethylthiol (2.4 mmol, 1.2 equiv.) yielding the desired product as white solid (509 mg, 1.63 mmol, 86%). CHCl<sub>3</sub>/MeOH (9:1) was used as a mobile phase for column chromatography. <sup>1</sup>H NMR (500 MHz, DMSO-*d*<sub>6</sub>) δ: 8.72 (s, 1 H), 8.69 (s, 1 H), 5.97 (d, *J* = 5.6 Hz, 1 H), 5.53 (d, *J* = 6.0 Hz, 1 H), 5.24 (d, *J* = 5.0 Hz, 1 H), 5.12 (t, *J* = 5.6 Hz, 1 H), 4.58 (dd, *J* = 10.9, 5.6 Hz, 1 H), 4.16 (dd, *J* = 8.7, 4.8 Hz, 1 H), 3.95 (q, *J* = 3.8 Hz, 1 H), 3.69 – 3.64 (m, 1 H), 3.55 (ddd, *J* = 11.9, 6.0, 4.0 Hz, 1 H), 3.34 – 3.30 (m, 2 H), 1.33 (d, *J* = 7.3 Hz, 3 H). <sup>13</sup>C NMR (126 MHz, DMSO-*d*<sub>6</sub>) δ : 160.3 (s, 1 C), 151.9 (s, 1 C), 148.5 (s, 1 C), 143.6 (s, 1 C), 131.6 (s, 1 C), 88.1 (s, 1 C), 86.1 (s, 1 C), 74.1 (s, 1 C), 70.6 (s, 1 C), 61.6 (s, 1 C), 22.8 (s, 1 C), 15.3 (s, 1 C); ESI-MS *m/z* = 312.09 *m/z* calcd. for C<sub>12</sub>H<sub>16</sub>N<sub>4</sub>O<sub>4</sub>S [M]; found: 313.21[M+H].

3.7.5.20. (2*R*, 3*S*, 4*R*, 5*R*)-2-(6-(*sec*-Butylthio)-9*H*-purin-9-yl)-5-(hydroxymethyl)-tetrahydrofuran-3,4-diol (**42f**)

The compound exhibited identical <sup>1</sup>H and <sup>13</sup>C NMR as in previous reports.<sup>438</sup> General procedure (GP1) was followed with 6-chloropurinriboside (287 mg, 1 mmol) and 2-butanethiol (0.162 mL, 1.5 mmol, 1.5 equiv.) yielding the desired (2*R*, 3*S*, 4*R*, 5*R*)-2-(6-(*sec*-butylthio)-9*H*-purin-9-yl)-5-(hydroxymethyl)-tetrahydrofuran-3,4-diol as colorless oil (224 mg, 0.66 mmol, 66%). CHCl<sub>3</sub>/MeOH (9:1) was used as a mobile phase for column chromatography. <sup>1</sup>H NMR (300 MHz, CHLOROFORM-*d*) δ: 0.64 (td, *J*=7.36, 1.70 Hz, 3 H), 1.05 (d, *J*=6.79 Hz,

3 H), 1.23 - 1.50 (m, 2 H), 3.29 - 3.44 (m, 1 H), 3.46 - 3.56 (m, 1 H), 3.80 - 3.91 (m, 2 H), 3.99 - 4.09 (m, 1 H), 4.44 (t,  $J=5.78$  Hz, 2 H), 5.00 (br. s., 1 H), 5.29 (d,  $J=8.16$  Hz, 1 H), 5.62 (d,  $J=6.69$  Hz, 1 H), 7.93 (s, 1 H), 8.21 (s, 1 H);  $^{13}\text{C}$  NMR (75 MHz, CHLOROFORM-*d*)  $\delta$ : 10.3 (s, 1 C), 19.9 (s, 1 C), 28.6 (s, 1 C), 39.4 (s, 1 C), 39.4 (s, 1 C), 61.8 (s, 1 C), 70.8 (s, 1 C), 73.4 (s, 1 C), 86.4 (s, 1 C), 89.5 (s, 1 C), 131.5 (s, 1 C), 142.1 (s, 1 C), 146.6 (s, 1 C), 150.1 (s, 1 C); (+ve) APCI-MS  $m/z = 340.12$   $m/z$  calcd. for  $\text{C}_{14}\text{H}_{20}\text{N}_4\text{O}_4\text{S}$  [M]; found: 341.32[M+H], 207.19 [M-ribose].

3.7.5.21. (2*R*, 3*R*, 4*S*, 5*R*)-2-(6-(Adamantan-1-ylthio)-9*H*-purin-9-yl)-5-(hydroxymethyl)tetrahydrofuran-3,4-diol (**42g**)

General procedure (GP1) was followed with 6-chloropurineriboside (287 mg, 1 mmol) and adamantanethiol (300 mg, 1.8 mmol, 1.8 equiv.) yielding the desired purine riboside thio derivative as white solid (297 mg, 0.71 mmol, 71%).  $\text{CHCl}_3/\text{MeOH}$  (9:1) was used as a mobile phase for column chromatography.  $^1\text{H}$  NMR (300 MHz, DMSO- $d_6$ )  $\delta$ : 1.54 - 1.65 (m, 2 H), 1.65 - 2.02 (m, 10 H), 2.06 (br. s., 3 H), 3.53 - 3.63 (m, 1 H), 3.66 - 3.76 (m, 1 H), 3.93 - 4.04 (m, 1 H), 4.19 (br. s., 1 H), 4.54 - 4.67 (m, 1 H), 5.11 (t,  $J=5.46$  Hz, 1 H), 5.21 (br. s., 1 H), 5.44 - 5.59 (m, 1 H), 5.99 (d,  $J=5.50$  Hz, 1 H), 8.67 (d,  $J=4.77$  Hz, 2 H);  $^{13}\text{C}$  NMR (75 MHz, DMSO- $d_6$ )  $\delta$ : 29.4 (s, 2 C), 29.5 (s, 2 C), 35.3 (s, 1 C), 42.1 (s, 2 C), 46.9 (s, 2 C), 50.8 (s, 1 C), 61.2 (s, 1 C), 70.3 (s, 1 C), 73.8 (s, 1 C), 85.7 (s, 1 C), 87.8 (s, 1 C), 131.3 (s, 1 C), 142.9 (s, 1 C), 148.2 (s, 1 C), 150.8 (s, 1 C), 161 (s, 1 C); (+ve) APCI-MS  $m/z = 418.17$   $m/z$  calcd. for  $\text{C}_{20}\text{H}_{26}\text{N}_4\text{O}_4\text{S}$  [M]; found: 419.21[M+H], 285.21 [M-ribose]; CHNS calcd. for  $\text{C}_{20}\text{H}_{26}\text{N}_4\text{O}_4\text{S}$ : C, 57.40; H, 6.26; N, 13.39; S, 7.66; found: C, 57.35; H, 6.21; N, 13.33; S, 7.62.

3.7.5.22. 2-(Phenylsulfonyl)quinoxaline (**43**)

The compound exhibited identical  $^1\text{H}$  and  $^{13}\text{C}$  NMR as in previous reports.<sup>439</sup> General procedure (GP2) was followed with tert-butyl 2-(phenylthio)quinoxaline (0.5 mmol, 1 equiv.) and *m*CPBA (1.5 mmol, 3 equiv.) yielding the desired product as white solid (237 mg, 0.876 mmol, 88%).  $^1\text{H}$  NMR (300 MHz, CHLOROFORM-*d*)  $\delta$ : 7.42 - 7.52 (m, 3 H), 7.78 - 7.92 (m, 4 H), 8.08 - 8.19 (m, 2 H), 9.42 (s, 1 H);  $^{13}\text{C}$  NMR (75 MHz, CHLOROFORM-*d*)  $\delta$ : 129.1 (s, 2 C), 129.2 (s, 2C), 129.3 (s, 1 C), 129.4 (s, 1 C), 129.5 (s, 1 C), 131.2 (s, 1 C), 131.4 (s, 1 C), 139.8 (s, 1 C), 141.1 (s, 1 C), 142.7 (s, 1 C), 143.1 (s, 1 C), 160.1 (s, 1 C); (+ve) APCI-MS  $m/z = 270.05$   $m/z$  calcd. for  $\text{C}_{14}\text{H}_{10}\text{N}_2\text{O}_2\text{S}$  [M]; found: 271.39 [M+H]; CHNS calcd. for  $\text{C}_{14}\text{H}_{10}\text{N}_2\text{O}_2\text{S}$ : C, 62.21; H, 3.73; N, 10.36; S, 11.86; found: C, 62.19; H, 3.69; N, 10.31; S, 11.82.

3.7.5.23. *Imino(phenyl)(quinoxalin-2-yl)-sulfanone (44)*

The compound exhibited identical  $^1\text{H}$  and  $^{13}\text{C}$  NMR spectra as in a previous reports.<sup>439</sup> General procedure (GP3) was followed with 2-(phenylthio)quinoxaline (0.5 mmol, 1 equiv.) yielding the desired product as pale yellow solid (115 mg, 0.854 mmol, 85%). Hexane/EtOAc (1:1) was used as a mobile phase for column chromatography.  $^1\text{H}$  NMR (400 MHz, CHLOROFORM-d)  $\delta$ : 3.71 (br. s., 1 H), 7.52 - 7.65 (m, 3 H), 7.83 - 7.91 (m, 2 H), 8.14 - 8.27 (m, 4 H), 9.58 (s, 1 H);  $^{13}\text{C}$  NMR (75 MHz, CHLOROFORM-d)  $\delta$ : 129.6 (s, 2 C), 129.6 (s, 2 C), 130.5 (s, 2 C), 131.8 (s, 1 C), 132.9 (s, 1 C), 133.9 (s, 1 C), 140.3 (s, 1 C), 141.2 (s, 1 C), 142.5 (s, 1 C), 143.3 (s, 1 C), 154.9 (s, 1 C); (+ve) APCI-MS  $m/z = 269.32$   $m/z$  calcd. for  $\text{C}_{14}\text{H}_{11}\text{N}_3\text{OS}$  [M]; found: 270.39 [M+H].

3.7.5.24. *Azathioprin (46)*

The compound exhibited identical  $^1\text{H}$  and  $^{13}\text{C}$  NMR spectra data as in a previous report.<sup>440</sup> General procedure (GP1) was followed with 5-chloro-1-methyl-4-nitro-1H-imidazole (2 mmol, 1 equiv.) and 6-thiopurine (2.4 mmol, 1.2 equiv.) yielding the desired product as pale-yellow solid (470 mg, 1.695 mmol, 85%).  $\text{CHCl}_3/\text{MeOH}$  (9:1) was used as a mobile phase for column chromatography.  $^1\text{H}$  NMR (500 MHz,  $\text{DMSO}-d_6$ )  $\delta$ : 13.76 (s, 1 H), 8.56 (s, 1 H), 8.54 (s, 1 H), 8.23 (s, 1 H), 3.68 (s, 3 H).  $^{13}\text{C}$  NMR (75 MHz,  $\text{DMSO}-d_6$ )  $\delta$ : 152.1 (s, 1 C), 152.9 (s, 1 C), 150.1 (s, 1 C), 145.1 (s, 1 C), 144.9 (s, 1 C), 139.9 (s, 1 C), 139.7 (s, 1 C), 117.6 (s, 1 C), 33.4 (s, 1 C).<sup>440</sup>

**3.8. Molecular structures and X-ray single crystal diffraction data**

Identification code	<b>7f</b>
Empirical formula	C <sub>16</sub> H <sub>13</sub> F <sub>3</sub> N <sub>2</sub> O <sub>5</sub> S
Formula weight	466.58
Temperature	298(2) K
Wavelength	0.71073 Å
Crystal system, space group	Monoclinic, P 2 <sub>1</sub> /c
Unit cell dimensions	a = 18.941(4) Å; α = 90 deg., b = 11.048(2) Å; β = 94.92(3) deg., c = 9.2081(18) Å
Volume	1919.8(7) Å <sup>3</sup>
Z, Calculated density	4, 1.614 Mg/m <sup>3</sup>
Absorption coefficient	0.641 mm <sup>-1</sup>
F(000)	952
Crystal size	0.468 x 0.076 x 0.053 mm
Theta range for data collection	1.079 to 26.128 deg.
Limiting indices	-23 ≤ h ≤ 23, -13 ≤ k ≤ 13, -11 ≤ l ≤ 9
Reflections collected / unique	18211 / 18211 [R(int) = ?]
Completeness to theta = 25.242	100.0 %
Absorption correction	Numerical
Max. and min. transmission	0.9859 and 0.7121
Refinement method	Full-matrix least-squares on F <sup>2</sup>
Data / restraints / parameters	18211 / 0 / 248
Goodness-of-fit on F <sup>2</sup>	1.223
Final R indices [I > 2σ(I)]	R <sub>1</sub> = 0.1880, wR <sub>2</sub> = 0.3928
R indices (all data)	R <sub>1</sub> = 0.3032, wR <sub>2</sub> = 0.4632
Extinction coefficient	0.011(6)
Largest diff. peak and hole	2.909 and -0.984 e.Å <sup>-3</sup>
Identification code	<b>10a</b>
Empirical formula	C <sub>9</sub> H <sub>8</sub> N <sub>2</sub> O <sub>5</sub> S
Formula weight	320.47
Temperature	170(2) K
Wavelength	0.71073 Å
Crystal system, space group	Triclinic, P -1
Unit cell dimensions	a = 8.5770(17) Å α = 104.68(3) deg., b = 8.8818(18) Å β = 101.55(3) deg., c = 8.8886(18) Å γ = 92.98(3) deg.
Volume	638.0(2) Å <sup>3</sup>
Z, Calculated density	2, 1.668 Mg/m <sup>3</sup>
Absorption coefficient	0.890 mm <sup>-1</sup>
F(000)	328
Crystal size	0.207 x 0.203 x 0.166 mm
Theta range for data collection	3.221 to 29.171 deg.
Limiting indices	-11 ≤ h ≤ 11, -12 ≤ k ≤ 12, -12 ≤ l ≤ 11
Reflections collected / unique	5763 / 2917 [R(int) = 0.0297]
Completeness to theta = 25.000	86.7 %
Absorption correction	Numerical
Max. and min. transmission	0.8927 and 0.7861
Refinement method	Full-matrix least-squares on F <sup>2</sup>
Data / restraints / parameters	2917 / 0 / 156
Goodness-of-fit on F <sup>2</sup>	1.114
Final R indices [I > 2σ(I)]	R <sub>1</sub> = 0.0491, wR <sub>2</sub> = 0.1244
R indices (all data)	R <sub>1</sub> = 0.0720, wR <sub>2</sub> = 0.1557
Extinction coefficient	0.035(7)
Largest diff. peak and hole	0.527 and -0.518 e.Å <sup>-3</sup>



## X-ray structural data

Identification code	<b>17a</b>
Empirical formula	C10 H9 N O S5
Formula weight	319.48
Temperature	170(2) K
Wavelength	0.71073 Å
Crystal system, space group	Orthorhombic, P b c a
Unit cell dimensions	a = 8.6214(17) Å alpha = 90 deg. b = 16.866(3) Å beta = 90 deg. c = 17.750(4) Å gamma = 90 deg.
Volume	2581.1(9) Å <sup>3</sup>
Z, Calculated density	8, 1.644 Mg/m <sup>3</sup>
Absorption coefficient	0.878 mm <sup>-1</sup>
F(000)	1312
Crystal size	0.212 x 0.175 x 0.167 mm
Theta range for data collection	3.294 to 26.766 deg.
Limiting indices	-10<=h<=10, -21<=k<=21, -19<=l<=22
Reflections collected / unique	20574 / 2723 [R(int) = 0.0499]
Completeness to theta = 25.242	99.8 %
Absorption correction	Numerical
Max. and min. transmission	0.9933 and 0.8297
Refinement method	Full-matrix least-squares on F <sup>2</sup>
Data / restraints / parameters	2723 / 0 / 155
Goodness-of-fit on F <sup>2</sup>	1.032
Final R indices [I>2sigma(I)]	R1 = 0.0314, wR2 = 0.0789
R indices (all data)	R1 = 0.0430, wR2 = 0.0823
Extinction coefficient	n/a
Largest diff. peak and hole	1.027 and -0.610 e.Å <sup>-3</sup>
<hr/>	
Identification code	<b>21a</b>
Empirical formula	C16 H18 N2 O2 S5
Formula weight	430.62
Temperature	170(2) K
Wavelength	0.71073 Å
Crystal system, space group	Orthorhombic, P b c a
Unit cell dimensions	a = 11.742(2) Å alpha = 90 deg. b = 17.417(3) Å beta = 90 deg. c = 18.094(4) Å gamma = 90 deg.
Volume	3700.4(12) Å <sup>3</sup>
Z, Calculated density	8, 1.546 Mg/m <sup>3</sup>
Absorption coefficient	0.640 mm <sup>-1</sup>
F(000)	1792
Crystal size	0.192 x 0.125 x 0.037 mm
Theta range for data collection	2.251 to 26.361 deg.
Limiting indices	-14<=h<=14, -19<=k<=21, -22<=l<=22
Reflections collected / unique	30042 / 3784 [R(int) = 0.1667]
Completeness to theta = 25.242	100.0 %
Absorption correction	None
Refinement method	Full-matrix least-squares on F <sup>2</sup>
Data / restraints / parameters	3784 / 0 / 227
Goodness-of-fit on F <sup>2</sup>	0.898
Final R indices [I>2sigma(I)]	R1 = 0.0475, wR2 = 0.0860
R indices (all data)	R1 = 0.1133, wR2 = 0.1060
Extinction coefficient	n/a
Largest diff. peak and hole	0.362 and -0.337 e.Å <sup>-3</sup>

## X-ray structural data

Identification code	<b>21b</b>
Empirical formula	C <sub>15</sub> H <sub>16</sub> N <sub>2</sub> O <sub>3</sub> S <sub>5</sub>
Formula weight	432.60
Temperature	298(2) K
Wavelength	0.71073 Å
Crystal system, space group	Orthorhombic, P b c a
Unit cell dimensions	a = 11.924(2) Å    alpha = 90 deg. b = 17.249(3) Å    beta = 90 deg. c = 17.974(4) Å gamma = 90 deg.
Volume	3696.8(12) Å <sup>3</sup>
Z, Calculated density	8, 1.555 Mg/m <sup>3</sup>
Absorption coefficient	0.645 mm <sup>-1</sup>
F(000)	1792
Crystal size	0.277 x 0.158 x 0.080 mm
Theta range for data collection	3.074 to 24.718 deg.
Limiting indices	-13<=h<=14, -20<=k<=20, -20<=l<=21
Reflections collected / unique	25566 / 3148 [R(int) = 0.1140]
Completeness to theta = 24.718	99.8 %
Absorption correction	Numerical
Max. and min. transmission	0.9444 and 0.8627
Refinement method	Full-matrix least-squares on F <sup>2</sup>
Data / restraints / parameters	3148 / 115 / 248
Goodness-of-fit on F <sup>2</sup>	0.882
Final R indices [I>2sigma(I)]	R1 = 0.0408, wR2 = 0.0848
R indices (all data)	R1 = 0.0955, wR2 = 0.0994
Extinction coefficient	n/a
Largest diff. peak and hole	0.282 and -0.239 e.Å <sup>-3</sup>
<hr/>	
Identification code	<b>21c</b>
Empirical formula	C <sub>15</sub> H <sub>18</sub> N <sub>2</sub> O <sub>2</sub> S <sub>5</sub>
Formula weight	418.61
Temperature	298(2) K
Wavelength	0.71073 Å
Crystal system, space group	Triclinic, P -1
Unit cell dimensions	a = 9.3490(19) Å    alpha = 70.63(3) deg. b = 10.261(2) Å    beta = 81.12(3) deg. c = 11.274(2) Å    gamma = 66.08(3) deg.
Volume	932.4(4) Å <sup>3</sup>
Z, Calculated density	2, 1.491 Mg/m <sup>3</sup>
Absorption coefficient	0.632 mm <sup>-1</sup>
F(000)	436
Crystal size	0.495 x 0.478 x 0.438 mm
Theta range for data collection	3.383 to 29.464 deg.
Limiting indices	-12<=h<=12, -13<=k<=14, -15<=l<=15
Reflections collected / unique	10431 / 5100 [R(int) = 0.0334]
Completeness to theta = 25.242	99.5 %
Absorption correction	Numerical
Max. and min. transmission	0.8775 and 0.8084
Refinement method	Full-matrix least-squares on F <sup>2</sup>
Data / restraints / parameters	5100 / 0 / 220
Goodness-of-fit on F <sup>2</sup>	1.012
Final R indices [I>2sigma(I)]	R1 = 0.0423, wR2 = 0.1016
R indices (all data)	R1 = 0.0733, wR2 = 0.1137
Extinction coefficient	n/a
Largest diff. peak and hole	0.433 and -0.324 e.Å <sup>-3</sup>

## X-ray structural data

Identification code	<b>33</b>
Empirical formula	C17 H14 N4 O S5
Formula weight	450.62
Temperature	170(2) K
Wavelength	0.71073 Å
Crystal system, space group	Monoclinic, P 21/c
Unit cell dimensions	a = 10.018(2) Å alpha = 90 deg.
	b = 7.8214(16) Å beta = 96.92(3) deg.
	c = 24.506(5) Å gamma = 90 deg.
Volume	1906.2(7) Å <sup>3</sup>
Z, Calculated density	4, 1.570 Mg/m <sup>3</sup>
Absorption coefficient	0.624 mm <sup>-1</sup>
F(000)	928
Crystal size	0.398 x 0.184 x 0.060 mm
Theta range for data collection	3.096 to 29.834 deg.
Limiting indices	-13<=h<=13, -10<=k<=10, -33<=l<=33
Reflections collected / unique	21439 / 5299 [R(int) = 0.4580]
Completeness to theta = 25.242	99.9 %
Absorption correction	None
Refinement method	Full-matrix least-squares on F <sup>2</sup>
Data / restraints / parameters	5299 / 0 / 245
Goodness-of-fit on F <sup>2</sup>	0.861
Final R indices [I>2sigma(I)]	R1 = 0.1079, wR2 = 0.2453
R indices (all data)	R1 = 0.3639, wR2 = 0.3924
Extinction coefficient	n/a
Largest diff. peak and hole	0.522 and -0.573 e.Å <sup>-3</sup>
<hr/>	
Identification code	<b>38a</b>
Empirical formula	C15 H18 N2 O3 S6
Formula weight	466.67
Temperature	170(2) K
Wavelength	0.71073 Å
Crystal system, space group	Orthorhombic, P b c a
Unit cell dimensions	a = 11.103(2) Å alpha = 90 deg.
	b = 17.372(3) Å beta = 90 deg.
	c = 20.504(4) Å gamma = 90 deg.
Volume	3954.8(13) Å <sup>3</sup>
Z, Calculated density	8, 1.568 Mg/m <sup>3</sup>
Absorption coefficient	0.711 mm <sup>-1</sup>
F(000)	1936
Crystal size	0.142 x 0.133 x 0.084 mm
Theta range for data collection	3.074 to 26.372 deg.
Limiting indices	-13<=h<=13, -21<=k<=20, -25<=l<=25
Reflections collected / unique	32136 / 4035 [R(int) = 0.2037]
Completeness to theta = 25.242	99.8 %
Absorption correction	Numerical
Max. and min. transmission	0.8985 and 0.6430
Refinement method	Full-matrix least-squares on F <sup>2</sup>
Data / restraints / parameters	4035 / 0 / 236
Goodness-of-fit on F <sup>2</sup>	1.022
Final R indices [I>2sigma(I)]	R1 = 0.0640, wR2 = 0.1480
R indices (all data)	R1 = 0.1091, wR2 = 0.1756
Extinction coefficient	n/a
Largest diff. peak and hole	0.736 and -0.711 e.Å <sup>-3</sup>

## X-ray structural data

Identification code	<b>38d</b>
Empirical formula	C <sub>20</sub> H <sub>24</sub> N <sub>2</sub> O <sub>3</sub> S <sub>6</sub>
Formula weight	532.77
Temperature	170(2) K
Wavelength	0.71073 Å
Crystal system, space group	Monoclinic, P 21/n
Unit cell dimensions	a = 11.513(2) Å alpha = 90 deg.
	b = 13.716(3) Å beta = 102.10(3) deg.
	c = 15.487(3) Å gamma = 90 deg.
Volume	2391.2(9) Å <sup>3</sup>
Z, Calculated density	4, 1.480 Mg/m <sup>3</sup>
Absorption coefficient	0.598 mm <sup>-1</sup>
F(000)	1112
Crystal size	0.261 x 0.251 x 0.043 mm
Theta range for data collection	3.261 to 28.286 deg.
Limiting indices	-15<=h<=14, -18<=k<=18, -20<=l<=20
Reflections collected / unique	24685 / 5932 [R(int) = 0.1172]
Completeness to theta = 25.242	99.8 %
Absorption correction	Numerical
Max. and min. transmission	0.9343 and 0.0802
Refinement method	Full-matrix least-squares on F <sup>2</sup>
Data / restraints / parameters	5932 / 1 / 286
Goodness-of-fit on F <sup>2</sup>	1.071
Final R indices [I>2sigma(I)]	R1 = 0.0742, wR2 = 0.1881
R indices (all data)	R1 = 0.1116, wR2 = 0.2278
Extinction coefficient	0.0088(18)
Largest diff. peak and hole	0.853 and -0.666 e.Å <sup>-3</sup>
<hr/>	
Identification code	<b>38e</b>
Empirical formula	C <sub>18</sub> H <sub>16</sub> N <sub>2</sub> O <sub>5</sub> S <sub>6</sub>
Formula weight	532.69
Temperature	170(2) K
Wavelength	0.71073 Å
Crystal system, space group	Triclinic, P -1
Unit cell dimensions	a = 8.0376(16) Å alpha = 100.52(3) deg.
	b = 11.755(2) Å beta = 93.44(3) deg.
	c = 12.065(2) Å gamma = 106.01(3) deg.
Volume	1069.9(4) Å <sup>3</sup>
Z, Calculated density	2, 1.654 Mg/m <sup>3</sup>
Absorption coefficient	0.675 mm <sup>-1</sup>
F(000)	548
Crystal size	0.146 x 0.105 x 0.094 mm
Theta range for data collection	3.213 to 29.529 deg.
Limiting indices	-11<=h<=9, -15<=k<=16, -16<=l<=16
Reflections collected / unique	12114 / 5862 [R(int) = 0.0655]
Completeness to theta = 25.242	99.8 %
Absorption correction	Numerical
Max. and min. transmission	0.9470 and 0.8551
Refinement method	Full-matrix least-squares on F <sup>2</sup>
Data / restraints / parameters	5862 / 0 / 285
Goodness-of-fit on F <sup>2</sup>	1.011
Final R indices [I>2sigma(I)]	R1 = 0.0593, wR2 = 0.1552
R indices (all data)	R1 = 0.1226, wR2 = 0.1884
Extinction coefficient	n/a
Largest diff. peak and hole	0.747 and -0.679 e.Å <sup>-3</sup>

## X-ray structural data

Identification code	<b>38f</b>
Empirical formula	C17 H16 N2 O3 S6
Formula weight	488.68
Temperature	170(2) K
Wavelength	0.71073 Å
Crystal system, space group	Triclinic, P -1
Unit cell dimensions	a = 10.887(2) Å alpha = 86.86(3) deg.
	b = 11.075(2) Å beta = 85.12(3) deg.
	c = 18.199(4) Å gamma = 69.86(3) deg.
Volume	2051.7(8) Å <sup>3</sup>
Z, Calculated density	4, 1.582 Mg/m <sup>3</sup>
Absorption coefficient	0.689 mm <sup>-1</sup>
F(000)	1008
Crystal size	0.245 x 0.244 x 0.078 mm
Theta range for data collection	3.111 to 29.625 deg.
Limiting indices	-15<=h<=13, -15<=k<=15, -25<=l<=25
Reflections collected / unique	24853 / 11260 [R(int) = 0.0684]
Completeness to theta = 25.242	99.5 %
Absorption correction	Numerical
Max. and min. transmission	0.9900 and 0.6256
Refinement method	Full-matrix least-squares on F <sup>2</sup>
Data / restraints / parameters	11260 / 464 / 708
Goodness-of-fit on F <sup>2</sup>	1.048
Final R indices [I>2sigma(I)]	R1 = 0.0817, wR2 = 0.1743
R indices (all data)	R1 = 0.1467, wR2 = 0.1948
Extinction coefficient	0.0118(8)
Largest diff. peak and hole	0.738 and -0.627 e.Å <sup>-3</sup>
<hr/>	
Identification code	<b>12b</b>
Empirical formula	C8 H11 N3 O
Formula weight	165.20
Temperature	170(2) K
Wavelength	0.71073 Å
Crystal system, space group	Monoclinic, P 21/c
Unit cell dimensions	a = 17.069(3) Å alpha = 90 deg.
	b = 5.9278(12) Å beta = 90.54(3) deg.
	c = 7.8053(16) Å gamma = 90 deg.
Volume	789.7(3) Å <sup>3</sup>
Z, Calculated density	4, 1.389 Mg/m <sup>3</sup>
Absorption coefficient	0.096 mm <sup>-1</sup>
F(000)	352
Crystal size	0.378 x 0.314 x 0.264 mm
Theta range for data collection	3.581 to 26.792 deg.
Limiting indices	-21<=h<=21, -7<=k<=7, -9<=l<=9
Reflections collected / unique	6583 / 1666 [R(int) = 0.0435]
Completeness to theta = 25.242	99.8 %
Absorption correction	None
Refinement method	Full-matrix least-squares on F <sup>2</sup>
Data / restraints / parameters	1666 / 0 / 153
Goodness-of-fit on F <sup>2</sup>	1.007
Final R indices [I>2sigma(I)]	R1 = 0.0315, wR2 = 0.0756
R indices (all data)	R1 = 0.0459, wR2 = 0.0806
Extinction coefficient	n/a
Largest diff. peak and hole	0.192 and -0.183 e.Å <sup>-3</sup>

## X-ray structural data

Identification code	<b>12c</b>
Empirical formula	C12 H13 N3
Formula weight	199.25
Temperature	170(2) K
Wavelength	0.71073 Å
Crystal system, space group	Triclinic, P -1
Unit cell dimensions	a = 8.4766(17) Å alpha = 72.48(3) deg.
	b = 11.222(2) Å beta = 82.59(3) deg.
	c = 11.291(2) Å gamma = 85.20(3) deg.
Volume	1014.5(4) Å <sup>3</sup>
Z, Calculated density	4, 1.305 Mg/m <sup>3</sup>
Absorption coefficient	0.081 mm <sup>-1</sup>
F(000)	424
Crystal size	0.312 x 0.272 x 0.259 mm
Theta range for data collection	3.092 to 29.545 deg.
Limiting indices	-11<=h<=11, -15<=k<=14, -15<=l<=15
Reflections collected / unique	11169 / 5562 [R(int) = 0.0758]
Completeness to theta = 25.242	99.3 %
Absorption correction	None
Refinement method	Full-matrix least-squares on F <sup>2</sup>
Data / restraints / parameters	5562 / 53 / 291
Goodness-of-fit on F <sup>2</sup>	0.863
Final R indices [I>2sigma(I)]	R1 = 0.0667, wR2 = 0.1632
R indices (all data)	R1 = 0.1259, wR2 = 0.2048
Extinction coefficient	0.047(7)
Largest diff. peak and hole	0.314 and -0.279 e.Å <sup>-3</sup>
<hr/>	
Identification code	<b>12e</b>
Empirical formula	C12 H13 N3 O
Formula weight	215.25
Temperature	298(2) K
Wavelength	0.71073 Å
Crystal system, space group	Monoclinic, P 21/c
Unit cell dimensions	a = 9.829(2) Å alpha = 90 deg.
	b = 10.473(2) Å beta = 97.36(3) deg.
	c = 10.464(2) Å gamma = 90 deg.
Volume	1068.2(4) Å <sup>3</sup>
Z, Calculated density	4, 1.338 Mg/m <sup>3</sup>
Absorption coefficient	0.089 mm <sup>-1</sup>
F(000)	456
Crystal size	0.234 x 0.137 x 0.124 mm
Theta range for data collection	3.310 to 25.377 deg.
Limiting indices	-11<=h<=11, -12<=k<=12, -11<=l<=12
Reflections collected / unique	7776 / 1954 [R(int) = 0.0573]
Completeness to theta = 25.000	99.6 %
Absorption correction	None
Refinement method	Full-matrix least-squares on F <sup>2</sup>
Data / restraints / parameters	1954 / 0 / 146
Goodness-of-fit on F <sup>2</sup>	0.881
Final R indices [I>2sigma(I)]	R1 = 0.0414, wR2 = 0.0902
R indices (all data)	R1 = 0.0972, wR2 = 0.1109
Extinction coefficient	0.022(3)
Largest diff. peak and hole	0.150 and -0.114 e.Å <sup>-3</sup>

## X-ray structural data

Identification code	<b>14a</b>
Empirical formula	C <sub>8</sub> H <sub>10</sub> ClN <sub>3</sub>
Formula weight	183.64
Temperature	298(2) K
Wavelength	0.71073 Å
Crystal system, space group	Monoclinic, P 21/n
Unit cell dimensions	a = 7.7830(16) Å alpha = 90 deg.
	b = 9.4940(19) Å beta = 102.90(3) deg.
	c = 12.123(2) Å gamma = 90 deg.
Volume	873.1(3) Å <sup>3</sup>
Z, Calculated density	4, 1.397 Mg/m <sup>3</sup>
Absorption coefficient	0.383 mm <sup>-1</sup>
F(000)	384
Crystal size	0.484 x 0.376 x 0.224 mm
Theta range for data collection	3.437 to 29.419 deg.
Limiting indices	-10<=h<=10, -13<=k<=11, -16<=l<=15
Reflections collected / unique	9298 / 2395 [R(int) = 0.1004]
Completeness to theta = 25.000	99.5 %
Absorption correction	None
Refinement method	Full-matrix least-squares on F <sup>2</sup>
Data / restraints / parameters	2395 / 0 / 120
Goodness-of-fit on F <sup>2</sup>	0.920
Final R indices [I>2sigma(I)]	R1 = 0.0544, wR2 = 0.1579
R indices (all data)	R1 = 0.0842, wR2 = 0.1796
Extinction coefficient	0.049(9)
Largest diff. peak and hole	0.328 and -0.266 e.Å <sup>-3</sup>
<hr/>	
Identification code	<b>14b</b>
Empirical formula	C <sub>8</sub> H <sub>10</sub> ClN <sub>3</sub> O
Formula weight	199.64
Temperature	298(2) K
Wavelength	0.71073 Å
Crystal system, space group	Monoclinic, P 21/c
Unit cell dimensions	a = 12.414(3) Å alpha = 90 deg.
	b = 9.854(2) Å beta = 100.97(3) deg.
	c = 7.5667(15) Å gamma = 90 deg.
Volume	908.7(3) Å <sup>3</sup>
Z, Calculated density	4, 1.459 Mg/m <sup>3</sup>
Absorption coefficient	0.382 mm <sup>-1</sup>
F(000)	416
Crystal size	0.379 x 0.057 x 0.055 mm
Theta range for data collection	3.435 to 26.376 deg.
Limiting indices	-15<=h<=12, -12<=k<=12, -9<=l<=9
Reflections collected / unique	8152 / 1804 [R(int) = 0.1014]
Completeness to theta = 25.000	96.6 %
Absorption correction	Numerical
Max. and min. transmission	0.8595 and 0.5728
Refinement method	Full-matrix least-squares on F <sup>2</sup>
Data / restraints / parameters	1804 / 0 / 119
Goodness-of-fit on F <sup>2</sup>	0.939
Final R indices [I>2sigma(I)]	R1 = 0.0441, wR2 = 0.0903
R indices (all data)	R1 = 0.1013, wR2 = 0.1129
Extinction coefficient	0.041(5)
Largest diff. peak and hole	0.170 and -0.172 e.Å <sup>-3</sup>

## X-ray structural data

Identification code	<b>12u</b>
Empirical formula	C <sub>20</sub> H <sub>31</sub> N <sub>7</sub> O <sub>3</sub>
Formula weight	417.52
Temperature	298(2) K
Wavelength	0.71073 Å
Crystal system, space group	Triclinic, P -1
Unit cell dimensions	a = 6.2319(12) Å    alpha = 102.01(3) deg.
	b = 8.8799(18) Å    beta = 91.63(3) deg.
	c = 20.568(4) Å    gamma = 92.50(3) deg.
Volume	1111.4(4) Å <sup>3</sup>
Z, Calculated density	2, 1.248 Mg/m <sup>3</sup>
Absorption coefficient	0.087 mm <sup>-1</sup>
F(000)	448
Crystal size	0.477 x 0.140 x 0.095 mm
Theta range for data collection	3.275 to 29.528 deg.
Limiting indices	-8<=h<=8, -12<=k<=12, -23<=l<=28
Reflections collected / unique	12507 / 6092 [R(int) = 0.1192]
Completeness to theta = 25.242	99.2 %
Absorption correction	Numerical
Max. and min. transmission	0.9297 and 0.7199
Refinement method	Full-matrix least-squares on F <sup>2</sup>
Data / restraints / parameters	6092 / 209 / 344
Goodness-of-fit on F <sup>2</sup>	0.770
Final R indices [I>2sigma(I)]	R1 = 0.0667, wR2 = 0.1303
R indices (all data)	R1 = 0.3597, wR2 = 0.2273
Extinction coefficient	n/a
Largest diff. peak and hole	0.122 and -0.145 e.Å <sup>-3</sup>
<hr/>	
Identification code	<b>12i</b>
Empirical formula	C <sub>11</sub> H <sub>12</sub> N <sub>2</sub> O
Formula weight	188.23
Temperature	170(2) K
Wavelength	0.71073 Å
Crystal system, space group	Monoclinic, P 21/n
Unit cell dimensions	a = 6.0392(12) Å    alpha = 90 deg.
	b = 15.518(3) Å    beta = 91.61(3) deg.
	c = 9.833(2) Å    gamma = 90 deg.
Volume	921.1(3) Å <sup>3</sup>
Z, Calculated density	4, 1.357 Mg/m <sup>3</sup>
Absorption coefficient	0.089 mm <sup>-1</sup>
F(000)	400
Crystal size	0.294 x 0.283 x 0.113 mm
Theta range for data collection	3.345 to 29.454 deg.
Limiting indices	-8<=h<=8, -21<=k<=21, -13<=l<=12
Reflections collected / unique	10230 / 2546 [R(int) = 0.0394]
Completeness to theta = 25.242	99.8 %
Absorption correction	None
Refinement method	Full-matrix least-squares on F <sup>2</sup>
Data / restraints / parameters	2546 / 0 / 146
Goodness-of-fit on F <sup>2</sup>	1.054
Final R indices [I>2sigma(I)]	R1 = 0.0449, wR2 = 0.1264
R indices (all data)	R1 = 0.0617, wR2 = 0.1355
Extinction coefficient	n/a
Largest diff. peak and hole	0.241 and -0.236 e.Å <sup>-3</sup>



## X-ray structural data

Identification code	<b>25</b>
Empirical formula	C <sub>20</sub> H <sub>22</sub> F <sub>3</sub> N <sub>5</sub> O <sub>4</sub>
Formula weight	453.42
Temperature	170(2) K
Wavelength	0.71073 Å
Crystal system, space group	Orthorhombic, P 21 21 21
Unit cell dimensions	a = 8.2836(17) Å alpha = 90 deg.
	b = 16.672(3) Å beta = 90 deg.
	c = 18.679(4) Å gamma = 90 deg.
Volume	2579.6(9) Å <sup>3</sup>
Z, Calculated density	4, 1.168 Mg/m <sup>3</sup>
Absorption coefficient	0.097 mm <sup>-1</sup>
F(000)	944
Crystal size	0.463 x 0.431 x 0.055 mm
Theta range for data collection	3.276 to 20.810 deg.
Limiting indices	-8<=h<=8, -15<=k<=16, -18<=l<=18
Reflections collected / unique	11433 / 2692 [R(int) = 0.1803]
Completeness to theta = 20.810	99.5 %
Absorption correction	None
Refinement method	Full-matrix least-squares on F <sup>2</sup>
Data / restraints / parameters	2692 / 147 / 314
Goodness-of-fit on F <sup>2</sup>	0.926
Final R indices [I>2sigma(I)]	R1 = 0.0868, wR2 = 0.2011
R indices (all data)	R1 = 0.1110, wR2 = 0.2177
Absolute structure parameter	?
Extinction coefficient	n/a
Largest diff. peak and hole	0.337 and -0.446 e.Å <sup>-3</sup>
<hr/>	
Identification code	<b>28a</b>
Empirical formula	C <sub>15</sub> H <sub>12</sub> N <sub>2</sub> O <sub>2</sub>
Formula weight	252.27
Temperature	170(2) K
Wavelength	0.71073 Å
Crystal system, space group	Monoclinic, P 21/c
Unit cell dimensions	a = 5.3010(4) Å alpha = 90 deg.
	b = 9.2387(5) Å beta = 90.116(6) deg.
	c = 24.657(2) Å gamma = 90 deg.
Volume	1207.57(15) Å <sup>3</sup>
Z, Calculated density	4, 1.388 Mg/m <sup>3</sup>
Absorption coefficient	0.094 mm <sup>-1</sup>
F(000)	528
Crystal size	0.444 x 0.413 x 0.197 mm
Theta range for data collection	3.305 to 29.447 deg.
Limiting indices	-6<=h<=7, -12<=k<=12, -33<=l<=34
Reflections collected / unique	12712 / 3336 [R(int) = 0.0475]
Completeness to theta = 25.242	99.9 %
Absorption correction	Numerical
Max. and min. transmission	0.9907 and 0.8688
Refinement method	Full-matrix least-squares on F <sup>2</sup>
Data / restraints / parameters	3336 / 0 / 173
Goodness-of-fit on F <sup>2</sup>	1.033
Final R indices [I>2sigma(I)]	R1 = 0.0420, wR2 = 0.1100
R indices (all data)	R1 = 0.0603, wR2 = 0.1258
Extinction coefficient	n/a
Largest diff. peak and hole	0.262 and -0.242 e.Å <sup>-3</sup>

## X-ray structural data

Identification code	<b>28o</b>
Empirical formula	C <sub>14</sub> H <sub>5</sub> F <sub>5</sub> N <sub>2</sub> O
Formula weight	312.20
Temperature	170(2) K
Wavelength	0.71073 Å
Crystal system, space group	Triclinic, P -1
Unit cell dimensions	a = 6.5650(6) Å alpha = 76.752(8) deg. b = 7.4590(7) Å beta = 85.465(7) deg. c = 12.7782(13) Å gamma = 84.582(7) deg.
Volume	605.29(10) Å <sup>3</sup>
Z, Calculated density	2, 1.713 Mg/m <sup>3</sup>
Absorption coefficient	0.163 mm <sup>-1</sup>
F(000)	312
Crystal size	0.461 x 0.283 x 0.253 mm
Theta range for data collection	3.282 to 29.416 deg.
Limiting indices	-9<=h<=9, -10<=k<=10, -15<=l<=17
Reflections collected / unique	6664 / 3296 [R(int) = 0.0418]
Completeness to theta = 25.242	99.1 %
Absorption correction	Numerical
Max. and min. transmission	0.9209 and 0.7760
Refinement method	Full-matrix least-squares on F <sup>2</sup>
Data / restraints / parameters	3296 / 0 / 199
Goodness-of-fit on F <sup>2</sup>	1.105
Final R indices [I>2sigma(I)]	R1 = 0.0611, wR2 = 0.1411
R indices (all data)	R1 = 0.0958, wR2 = 0.1564
Extinction coefficient	n/a
Largest diff. peak and hole	0.266 and -0.249 e.Å <sup>-3</sup>
Identification code	<b>28i</b>
Empirical formula	C <sub>14</sub> H <sub>9</sub> N <sub>3</sub> O <sub>3</sub>
Formula weight	267.24
Temperature	170(2) K
Wavelength	0.71073 Å
Crystal system, space group	Monoclinic, P 21
Unit cell dimensions	a = 6.0770(12) Å alpha = 90 deg. b = 5.3497(11) Å beta = 91.47(3) deg. c = 18.327(4) Å gamma = 90 deg.
Volume	595.6(2) Å <sup>3</sup>
Z, Calculated density	2, 1.490 Mg/m <sup>3</sup>
Absorption coefficient	0.108 mm <sup>-1</sup>
F(000)	276
Crystal size	0.110 x 0.084 x 0.080 mm
Theta range for data collection	3.336 to 26.352 deg.
Limiting indices	-7<=h<=7, -6<=k<=6, -19<=l<=22
Reflections collected / unique	5069 / 2444 [R(int) = 0.1095]
Completeness to theta = 25.242	99.8 %
Absorption correction	None
Refinement method	Full-matrix least-squares on F <sup>2</sup>
Data / restraints / parameters	2444 / 1 / 181
Goodness-of-fit on F <sup>2</sup>	1.010
Final R indices [I>2sigma(I)]	R1 = 0.0628, wR2 = 0.1516
R indices (all data)	R1 = 0.1167, wR2 = 0.1871
Absolute structure parameter	?
Extinction coefficient	n/a
Largest diff. peak and hole	0.220 and -0.249 e.Å <sup>-3</sup>

## X-ray structural data

Identification code	<b>28f</b>
Empirical formula	C <sub>18</sub> H <sub>18</sub> N <sub>2</sub> O
Formula weight	278.34
Temperature	170(2) K
Wavelength	0.71073 Å
Crystal system, space group	Monoclinic, P 2 <sub>1</sub> /n
Unit cell dimensions	a = 12.0330(10) Å alpha = 90 deg.
	b = 6.0968(4) Å beta = 100.626(6) deg.
	c = 19.8777(15) Å gamma = 90 deg.
Volume	1433.28(19) Å <sup>3</sup>
Z, Calculated density	4, 1.290 Mg/m <sup>3</sup>
Absorption coefficient	0.081 mm <sup>-1</sup>
F(000)	592
Crystal size	0.484 x 0.073 x 0.072 mm
Theta range for data collection	1.841 to 26.372 deg.
Limiting indices	-15<=h<=15, -7<=k<=7, -24<=l<=24
Reflections collected / unique	11681 / 2931 [R(int) = 0.1285]
Completeness to theta = 25.242	100.0 %
Absorption correction	Numerical
Max. and min. transmission	0.8400 and 0.2755
Refinement method	Full-matrix least-squares on F <sup>2</sup>
Data / restraints / parameters	2931 / 0 / 194
Goodness-of-fit on F <sup>2</sup>	0.964
Final R indices [I>2sigma(I)]	R1 = 0.0636, wR2 = 0.1545
R indices (all data)	R1 = 0.0945, wR2 = 0.1771
Extinction coefficient	0.022(4)
Largest diff. peak and hole	0.333 and -0.329 e.Å <sup>-3</sup>
Identification code	<b>28k</b>
Empirical formula	C <sub>17</sub> H <sub>10</sub> N <sub>2</sub> O <sub>3</sub>
Formula weight	290.27
Temperature	170(2) K
Wavelength	0.71073 Å
Crystal system, space group	Triclinic, P -1
Unit cell dimensions	a = 3.7974(8) Å alpha = 89.92(3) deg.
	b = 6.6994(13) Å beta = 89.92(3) deg.
	c = 25.734(5) Å gamma = 74.78(3) deg.
Volume	631.7(2) Å <sup>3</sup>
Z, Calculated density	2, 1.526 Mg/m <sup>3</sup>
Absorption coefficient	0.107 mm <sup>-1</sup>
F(000)	300
Crystal size	0.463 x 0.458 x 0.048 mm
Theta range for data collection	3.166 to 26.369 deg.
Limiting indices	-4<=h<=4, -8<=k<=7, -28<=l<=32
Reflections collected / unique	5237 / 2590 [R(int) = 0.1004]
Completeness to theta = 25.242	99.8 %
Absorption correction	Numerical
Max. and min. transmission	0.9807 and 0.8154
Refinement method	Full-matrix least-squares on F <sup>2</sup>
Data / restraints / parameters	2590 / 0 / 202
Goodness-of-fit on F <sup>2</sup>	0.960
Final R indices [I>2sigma(I)]	R1 = 0.0625, wR2 = 0.1237
R indices (all data)	R1 = 0.1684, wR2 = 0.1703
Extinction coefficient	n/a
Largest diff. peak and hole	0.230 and -0.259 e.Å <sup>-3</sup>

## X-ray structural data

Identification code	<b>28h</b>
Empirical formula	C17 H16 N2 O
Formula weight	264.32
Temperature	170(2) K
Wavelength	0.71073 Å
Crystal system, space group	Monoclinic, P 21/n
Unit cell dimensions	a = 15.1180(13) Å alpha = 90 deg.
	b = 4.9468(3) Å beta = 104.553(7) deg.
	c = 19.2855(16) Å gamma = 90 deg.
Volume	1396.01(19) Å <sup>3</sup>
Z, Calculated density	4, 1.258 Mg/m <sup>3</sup>
Absorption coefficient	0.079 mm <sup>-1</sup>
F(000)	560
Crystal size	0.488 x 0.083 x 0.063 mm
Theta range for data collection	1.972 to 26.378 deg.
Limiting indices	-18<=h<=18, -5<=k<=6, -24<=l<=24
Reflections collected / unique	11507 / 2856 [R(int) = 0.1388]
Completeness to theta = 25.242	100.0 %
Absorption correction	Numerical
Max. and min. transmission	0.8637 and 0.5769
Refinement method	Full-matrix least-squares on F <sup>2</sup>
Data / restraints / parameters	2856 / 0 / 185
Goodness-of-fit on F <sup>2</sup>	0.912
Final R indices [I>2sigma(I)]	R1 = 0.0451, wR2 = 0.1007
R indices (all data)	R1 = 0.0942, wR2 = 0.1189
Extinction coefficient	0.012(2)
Largest diff. peak and hole	0.200 and -0.201 e.Å <sup>-3</sup>
<hr/>	
Identification code	<b>31b</b>
Empirical formula	C11 H9 Cl N2 O2
Formula weight	236.65
Temperature	170(2) K
Wavelength	0.71073 Å
Crystal system, space group	Monoclinic, P 21/c
Unit cell dimensions	a = 9.6161(19) Å alpha = 90 deg.
	b = 9.1313(18) Å beta = 98.97(3) deg.
	c = 12.110(2) Å gamma = 90 deg.
Volume	1050.3(4) Å <sup>3</sup>
Z, Calculated density	4, 1.497 Mg/m <sup>3</sup>
Absorption coefficient	0.348 mm <sup>-1</sup>
F(000)	488
Crystal size	0.212 x 0.141 x 0.035 mm
Theta range for data collection	2.144 to 29.488 deg.
Limiting indices	-12<=h<=13, -12<=k<=12, -16<=l<=16
Reflections collected / unique	11644 / 2913 [R(int) = 0.1054]
Completeness to theta = 25.242	100.0 %
Absorption correction	Numerical
Max. and min. transmission	0.9922 and 0.8666
Refinement method	Full-matrix least-squares on F <sup>2</sup>
Data / restraints / parameters	2913 / 0 / 147
Goodness-of-fit on F <sup>2</sup>	1.005
Final R indices [I>2sigma(I)]	R1 = 0.0508, wR2 = 0.1124
R indices (all data)	R1 = 0.1312, wR2 = 0.1508
Extinction coefficient	0.024(4)
Largest diff. peak and hole	0.332 and -0.416 e.Å <sup>-3</sup>

## X-ray structural data

Identification code	<b>31c</b>
Empirical formula	C13 H8 Cl N3 O
Formula weight	257.67
Temperature	170(2) K
Wavelength	0.71073 Å
Crystal system, space group	Triclinic, P -1
Unit cell dimensions	a = 7.8520(9) Å    alpha = 105.429(9) deg.
	b = 8.2413(10) Å    beta = 98.805(9) deg.
	c = 9.9554(10) Å    gamma = 111.433(9) deg.
Volume	555.11(12) Å <sup>3</sup>
Z, Calculated density	2, 1.542 Mg/m <sup>3</sup>
Absorption coefficient	0.333 mm <sup>-1</sup>
F(000)	264
Crystal size	0.222 x 0.154 x 0.107 mm
Theta range for data collection	3.678 to 29.461 deg.
Limiting indices	-10<=h<=10, -11<=k<=11, -12<=l<=13
Reflections collected / unique	6290 / 3039 [R(int) = 0.0838]
Completeness to theta = 25.242	98.9 %
Absorption correction	Numerical
Max. and min. transmission	0.9780 and 0.8822
Refinement method	Full-matrix least-squares on F <sup>2</sup>
Data / restraints / parameters	3039 / 0 / 163
Goodness-of-fit on F <sup>2</sup>	0.866
Final R indices [I>2sigma(I)]	R1 = 0.0519, wR2 = 0.1280
R indices (all data)	R1 = 0.0998, wR2 = 0.1505
Extinction coefficient	n/a
Largest diff. peak and hole	0.299 and -0.421 e.Å <sup>-3</sup>
<hr/>	
Identification code	<b>31d</b>
Empirical formula	C22 H23 Cl N2 O2
Formula weight	382.87
Temperature	170(2) K
Wavelength	0.71073 Å
Crystal system, space group	Triclinic, P 1
Unit cell dimensions	a = 6.5780(13) Å    alpha = 96.85(3) deg.
	b = 7.3496(15) Å    beta = 97.83(3) deg.
	c = 19.890(4) Å    gamma = 99.42(3) deg.
Volume	929.9(3) Å <sup>3</sup>
Z, Calculated density	2, 1.367 Mg/m <sup>3</sup>
Absorption coefficient	0.226 mm <sup>-1</sup>
F(000)	404
Crystal size	0.313 x 0.174 x 0.107 mm
Theta range for data collection	3.135 to 26.372 deg.
Limiting indices	-8<=h<=8, -9<=k<=9, -24<=l<=24
Reflections collected / unique	7483 / 6069 [R(int) = 0.0737]
Completeness to theta = 25.242	99.0 %
Absorption correction	Numerical
Max. and min. transmission	0.9751 and 0.8859
Refinement method	Full-matrix least-squares on F <sup>2</sup>
Data / restraints / parameters	6069 / 3 / 489
Goodness-of-fit on F <sup>2</sup>	0.932
Final R indices [I>2sigma(I)]	R1 = 0.0621, wR2 = 0.1313
R indices (all data)	R1 = 0.1432, wR2 = 0.1688
Absolute structure parameter	-0.18(17)
Extinction coefficient	n/a
Largest diff. peak and hole	0.306 and -0.387 e.Å <sup>-3</sup>

## X-ray structural data

Identification code	<b>41f</b>
Empirical formula	C14 H10 N2 S
Formula weight	238.30
Temperature	170(2) K
Wavelength	0.71073 Å
Crystal system, space group	Orthorhombic, P n a 21
Unit cell dimensions	a = 16.601(3) Å alpha = 90 deg.
	b = 12.379(3) Å beta = 90 deg.
	c = 5.5695(11) Å gamma = 90 deg.
Volume	1144.5(4) Å <sup>3</sup>
Z, Calculated density	4, 1.383 Mg/m <sup>3</sup>
Absorption coefficient	0.258 mm <sup>-1</sup>
F(000)	496
Crystal size	0.289 x 0.089 x 0.069 mm
Theta range for data collection	3.513 to 29.461 deg.
Limiting indices	-19<=h<=22, -17<=k<=17, -7<=l<=7
Reflections collected / unique	12817 / 3138 [R(int) = 0.0512]
Completeness to theta = 25.242	99.7 %
Absorption correction	None
Refinement method	Full-matrix least-squares on F <sup>2</sup>
Data / restraints / parameters	3138 / 1 / 194
Goodness-of-fit on F <sup>2</sup>	1.094
Final R indices [I>2sigma(I)]	R1 = 0.0402, wR2 = 0.0848
R indices (all data)	R1 = 0.0635, wR2 = 0.1031
Absolute structure parameter	0.00(4)
Extinction coefficient	n/a
Largest diff. peak and hole	0.217 and -0.380 e.Å <sup>-3</sup>
Identification code	<b>41i</b>
Empirical formula	C16 H12 N2 S2
Formula weight	296.40
Temperature	170(2) K
Wavelength	0.71073 Å
Crystal system, space group	Triclinic, P -1
Unit cell dimensions	a = 7.7620(16) Å alpha = 111.03(3) deg.
	b = 10.205(2) Å beta = 106.70(3) deg.
	c = 10.415(2) Å gamma = 96.14(3) deg.
Volume	717.0(3) Å <sup>3</sup>
Z, Calculated density	2, 1.373 Mg/m <sup>3</sup>
Absorption coefficient	0.361 mm <sup>-1</sup>
F(000)	308
Crystal size	0.156 x 0.149 x 0.064 mm
Theta range for data collection	3.501 to 29.480 deg.
Limiting indices	-10<=h<=10, -14<=k<=12, -14<=l<=14
Reflections collected / unique	8139 / 3932 [R(int) = 0.0212]
Completeness to theta = 25.242	99.4 %
Absorption correction	Numerical
Max. and min. transmission	0.9909 and 0.9711
Refinement method	Full-matrix least-squares on F <sup>2</sup>
Data / restraints / parameters	3932 / 0 / 181
Goodness-of-fit on F <sup>2</sup>	1.040
Final R indices [I>2sigma(I)]	R1 = 0.0331, wR2 = 0.0821
R indices (all data)	R1 = 0.0479, wR2 = 0.0879
Extinction coefficient	n/a
Largest diff. peak and hole	0.285 and -0.222 e.Å <sup>-3</sup>

## X-ray structural data

Identification code	<b>42b</b>
Empirical formula	C11 H8 N4 S
Formula weight	228.27
Temperature	170(2) K
Wavelength	0.71073 Å
Crystal system, space group	Monoclinic, P 21/c
Unit cell dimensions	a = 11.113(2) Å alpha = 90 deg. b = 7.1958(14) Å beta = 93.19(3) deg. c = 12.597(3) Å gamma = 90 deg.
Volume	1005.8(3) Å <sup>3</sup>
Z, Calculated density	4, 1.507 Mg/m <sup>3</sup>
Absorption coefficient	0.295 mm <sup>-1</sup>
F(000)	472
Crystal size	0.465 x 0.192 x 0.145 mm
Theta range for data collection	3.262 to 29.422 deg.
Limiting indices	-15<=h<=13, -9<=k<=9, -17<=l<=16
Reflections collected / unique	10884 / 2766 [R(int) = 0.0393]
Completeness to theta = 25.242	99.5 %
Absorption correction	Numerical
Max. and min. transmission	0.9936 and 0.8383
Refinement method	Full-matrix least-squares on F <sup>2</sup>
Data / restraints / parameters	2766 / 0 / 149
Goodness-of-fit on F <sup>2</sup>	1.036
Final R indices [I>2sigma(I)]	R1 = 0.0316, wR2 = 0.0859
R indices (all data)	R1 = 0.0354, wR2 = 0.0884
Extinction coefficient	n/a
Largest diff. peak and hole	0.444 and -0.251 e.Å <sup>-3</sup>

### 3.9. References

1. Jacob, C., A scent of therapy: pharmacological implications of natural products containing redox-active sulfur atoms. *Natural Product Reports* **2006**, *23* (6), 851-863.
2. Giles, G. I. J., C., Reactive Sulfur Species: An Emerging Concept in Oxidative Stress. *Biological Chemistry*. **2002**, *383*, 375 – 388.
3. Jacob, C.; Giles, G. I.; Giles, N. M.; Sies, H., Sulfur and Selenium: The Role of Oxidation State in Protein Structure and Function. *Angewandte Chemie International Edition* **2003**, *42* (39), 4742-4758.
4. Klamann, D., *Schmierstoffe und verwandte Produkte*;. VCH: Weinheim, Germany, 1982.
5. K.J., S., Sulphur-containing polymers. *Organic Polymer Chemistry*, Springer, Dordrecht: New york, 1973.
6. Faulkner, D. J., Marine natural products. *Natural Product Reports* **2002**, *19* (1), 1-49.
7. Mussinan, C. J. K., M. E., Sulfur Compounds in Foods. *American Chemical Society*: Washington, D. C., 1994.
8. Anthoni, U.; Christophersen, C.; Madsen, J. Ø. r.; Wium-Andersen, S.; Jacobsen, N., Biologically active sulphur compounds from the green alga *Chara globularis*. *Phytochemistry* **1980**, *19* (6), 1228-1229.
9. Anthoni, U.; Christophersen, C.; Jacobsen, N.; Svendsen, A., Synthesis of 4-methylthio-1,2-dithiolane and 5-methylthio-1,2,3-trithiane. Two naturally occurring bioactive compounds. *Tetrahedron* **1982**, *38* (15), 2425-2427.
10. Kasai, T.; Sakamura, S., 1,2,3-Trithiane-5-carboxylic Acid in Raw Asparagus Shoots. *Agricultural and Biological Chemistry* **1982**, *46* (3), 821-822.
11. Copp, B. R.; Blunt, J. W.; Munro, M. H. G.; Pannell, L. K., A biologically active 1,2,3-trithiane derivative from the New Zealand ascidain *Aplidium* sp. D. *Tetrahedron Letters* **1989**, *30* (28), 3703-3706.
12. Wratten, S. J.; Faulkner, D. J., Cyclic polysulfides from the red alga *Chondria californica*. *The Journal of Organic Chemistry* **1976**, *41* (14), 2465-2467.
13. Gmelin, R.; Susilo, R.; Fenwick, G. R., Cyclic polysulphides from *Parkia speciosa*. *Phytochemistry* **1981**, *20* (11), 2521-2523.
14. Morita, K.; Kobayashi, S.; Isolation, Structure, and Synthesis of Lenthionine and Its Analogs. *Chemical & Pharmaceutical Bulletin* **1967**, *15* (7), 988-993.
15. Morita, K.; Kobayashi, S., Isolation and synthesis of lenthionine, an odorous substance of shiitake, an edible mushroom. *Tetrahedron Letters* **1966**, *7* (6), 573-577.
16. Chen, C. C.; Ho, C. T., Identification of sulfurous compounds of Shiitake mushroom (*Lentinus edodes* Sing.). *Journal of Agricultural and Food Chemistry* **1986**, *34* (5), 830-833.
17. Francis, E.; Rahman, R.; Safe, S.; Taylor, A., Sporidesmins. Part XII. Isolation and structure of sporidesmin G, a naturally-occurring 3,6-epitetrathiopiperazine-2,5-dione. *Journal of the Chemical Society, Perkin Transactions 1* **1972**, (0), 470-472.
18. Brewer, D.; Rahman, R.; Safe, S.; Taylor, A., A new toxic metabolite of *Pithomyces chartarum* related to the sporidesmins. *Chemical Communications* **1968**, (24), 1571-1571.
19. K. H. Michel; Jones, M.O.C; Hoehn, M.M; Nagarajan, R; Epipolythiopiperazinedione antibiotics from *penicillium turbatum*. *The Journal of Antibiotics* **194**, *27* (1), 57-64.
20. Litaudon, M.; Guyot, M., Lissoclinotoxin A, an antibiotic 1,2,3-trithiane derivative from the tunicate *Lissoclinum perforatum*. *Tetrahedron Letters* **1991**, *32* (7), 911-914.



## References

21. Davidson, B. S.; Molinski, T. F.; Barrows, L. R.; Ireland, C. M., Varacin: a novel benzopentathiepin from *Lissoclinum vareau* that is cytotoxic toward a human colon tumor. *Journal of the American Chemical Society* **1991**, *113* (12), 4709-4710.
22. Behar, V.; Danishefsky, S. J., Total synthesis of the novel benzopentathiepin varacinium trifluoroacetate: the viability of "varacin-free base". *Journal of the American Chemical Society* **1993**, *115* (15), 7017-7018.
23. Ford, P. W.; Davidson, B. S., Synthesis of varacin, a cytotoxic naturally occurring benzopentathiepin isolated from a marine ascidian. *The Journal of Organic Chemistry* **1993**, *58* (17), 4522-4523.
24. Litaudon, M.; Trigalo, F.; Martin, M.-T.; Frappier, F.; Guyot, M., Lissoclinotoxins: Antibiotic polysulfur derivatives from the tunicate *Lissoclinum perforatum*. Revised structure of lissoclinotoxin A. *Tetrahedron* **1994**, *50* (18), 5323-5334.
25. Rajanikanth, B.; Ravindranath, B.; Shankaranarayana, M. L., Volatile polysulphides of *asafoetida*. *Phytochemistry* **1984**, *23* (4), 899-900.
26. Lee, M. D.; Dunne, T. S.; Siegel, M. M.; Chang, C. C.; Morton, G. O.; Borders, D. B., Calichemicins, a novel family of antitumor antibiotics. 1. Chemistry and partial structure of calichemicin .gamma.II. *Journal of the American Chemical Society* **1987**, *109* (11), 3464-3466.
27. Golik, J.; Dubay, G.; Groenewold, G.; Kawaguchi, H.; Konishi, M.; Krishnan, B.; Ohkuma, H.; Saitoh, K.; Doyle, T. W., Esperamicins, a novel class of potent antitumor antibiotics. 3. Structures of esperamicins A1, A2, and A1b. *Journal of the American Chemical Society* **1987**, *109* (11), 3462-3464.
28. Searle, P. A.; Molinski, T. F., Five new alkaloids from the tropical ascidian, *Lissoclinum* sp. lissoclinotoxin A is chiral. *The Journal of Organic Chemistry* **1994**, *59* (22), 6600-6605.
29. Makarieva, T. N.; Stonik, V. A.; Dmitrenok, A. S.; Grebnev, B. B.; Isakov, V. V.; Rebachyk, N. M.; Rashkes, Y. W., Varacin and Three New Marine Antimicrobial Polysulfides from the Far-Eastern Ascidian *Polycitorsp.* *Journal of Natural Products* **1995**, *58* (2), 254-258.
30. Steudel, R., The Chemistry of Organic Polysulfanes R-Sn-R (n > 2). *Chemical Reviews* **2002**, *102* (11), 3905-3946.
31. Chatterji, T.; Keerthi, K.; Gates, K. S., Generation of reactive oxygen species by a persulfide (BnSSH). *Bioorganic & Medicinal Chemistry Letters* **2005**, *15* (17), 3921-3924.
32. Lee, A. H. F.; Chen, J.; Liu, D.; Leung, T. Y. C.; Chan, A. S. C.; Li, T., Acid-Promoted DNA-Cleaving Activities and Total Synthesis of Varacin C. *Journal of the American Chemical Society* **2002**, *124* (47), 13972-13973.
33. Tsao, S.-m.; Yin, M.-c., In vitro activity of garlic oil and four diallyl sulphides against antibiotic-resistant *Pseudomonas aeruginosa* and *Klebsiella pneumoniae*. *Journal of Antimicrobial Chemotherapy* **2001**, *47* (5), 665-670.
34. TSAO, S.-M.; YIN, M.-C., In-vitro antimicrobial activity of four diallyl sulphides occurring naturally in garlic and Chinese leek oils. *Journal of Medical Microbiology* **2001**, *50* (7), 646-649.
35. O'Gara, E. A.; Hill, D. J.; Maslin, D. J., Activities of Garlic Oil, Garlic Powder, and Their Diallyl Constituents against "*Helicobacter pylori*". *Applied and Environmental Microbiology* **2000**, *66* (5), 2269-2273.
36. Ha, M.-W.; Ma, R.; Shun, L.-P.; Gong, Y.-H.; Yuan, Y., Effects of allitridi on cell cycle arrest of human gastric cancer cells. *World Journal of Gastroenterology* **2005**, *11* (35), 5433-5437.

## References

37. Liu, K.-L.; Chen, H.-W.; Wang, R.-Y.; Lei, Y.-P.; Sheen, L.-Y.; Lii, C.-K., DATS Reduces LPS-Induced iNOS Expression, NO Production, Oxidative Stress, and NF- $\kappa$ B Activation in RAW 264.7 Macrophages. *Journal of Agricultural and Food Chemistry* **2006**, *54* (9), 3472-3478.
38. Fehér, F.; Langer, M., Contribution to the chemistry of sulfur, no. 104 Synthesis of pentathiepin and benzopentathiepin. *Tetrahedron Letters* **1971**, *12* (24), 2125-2126.
39. Fehér, F.; Degen, B., Neue schwefelhaltige Ringverbindungen. *Angewandte Chemie* **1967**, *79* (15), 689-690.
40. Konstantinova, L. S.; Rakitin, O. A.; Rees, C. W., Pentathiepins. *Chemical Reviews* **2004**, *104* (5), 2617-2630.
41. Khomenko, T. M.; Korchagina, D. V.; Baev, D. S.; Vassiliev, P. M.; Volcho, K. P.; Salakhutdinov, N. F., Antimicrobial Activity of Substituted Benzopentathiepin-6-amines. *The Journal of Antibiotics* **2019**, *72* (8), 590-599.
42. Compagnone, R. S.; Faulkner, D. J.; Carté, B. K.; Chan, G.; Freyer, A.; Hemling, M. E.; Hofmann, G. A.; Mattern, M. R., Pentathiepins and trithianes from two *Lissoclinum* species and a *Eudistoma* sp.: inhibitors of protein kinase C. *Tetrahedron* **1994**, *50* (45), 12785-12792.
43. Moberg, W. K., E. I. Du Pont de Nemours and Company. Pentathiepinopyrazoles and pyrazolotrithiocarbonates, such as 7-methyl-7H-1,2,3,4,5-pentathiepin-6,7-cpyrazole, useful for the control of fungi., United States patent US 4,275,073, **1981** Jun. 23.
44. Khomenko, T. M.; Tolstikova, T. G.; Bolkunov, A. V.; Dolgikh, M. P.; Pavlova, A. V.; Korchagina, D. V.; Volcho, K. P.; Salakhutdinov, N. F., 8-(Trifluoromethyl)-1,2,3,4,5-benzopentathiepin-6-amine: Novel Aminobenzopentathiepine having In Vivo Anticonvulsant and Anxiolytic Activities. *Letters in Drug Design & Discovery* **2009**, *6* (6), 464-467.
45. Nagahora, N.; Ogawa, S.; Kawai, Y.; Sato, R., First synthesis and structure of sulfur-containing heterocycles fused to ferrocene. *Tetrahedron Letters* **2002**, *43* (33), 5825-5828.
46. Janosik, T.; Stensland, B.; Bergman, J., Sulfur-Rich Heterocycles from 2-Metalated Benzo[b]thiophene and Benzo[b]furan: Synthesis and Structure. *The Journal of Organic Chemistry* **2002**, *67* (17), 6220-6223.
47. Chatterji, T.; Gates, K. S., DNA cleavage by 7-methylbenzopentathiepin: A simple analog of the antitumor antibiotic varacin. *Bioorganic & Medicinal Chemistry Letters* **1998**, *8* (5), 535-538.
48. Chatterji, T.; Gates, K. S., Reaction of Thiols with 7-Methylbenzopentathiepin. *Bioorganic & Medicinal Chemistry Letters* **2003**, *13* (7), 1349-1352.
49. Lee, A. H. F.; Chan, A. S. C.; Li, T., Acid-accelerated DNA-cleaving activities of antitumor antibiotic varacin. *Chemical Communications* **2002**, (18), 2112-2113.
50. Brzostowska, E. M.; Greer, A., The Role of Amine in the Mechanism of Pentathiepin (Polysulfur) Antitumor Agents. *Journal of the American Chemical Society* **2003**, *125* (2), 396-404.
51. Asquith, C. R. M.; Laitinen, T.; Konstantinova, L. S.; Tizzard, G.; Poso, A.; Rakitin, O. A.; Hofmann-Lehmann, R.; Hilton, S. T., Investigation of the Pentathiepin Functionality as an Inhibitor of Feline Immunodeficiency Virus (FIV) via a Potential Zinc Ejection Mechanism, as a Model for HIV Infection. *ChemMedChem* **2019**, *14* (4), 454-461.
52. Sato, R. O., T.; Ogawa, S., Efficient Synthesis and Biological Properties of new Benzopentathiepins. *Heterocycles* **1995**, *41*, 893-896.

## References

53. Morris, J. L.; Rees, C. W., Organic heterocyclothiazenes. Part 3. Synthesis and structure of 1,3,5,2,4-trithiadiazepines. *Journal of the Chemical Society, Perkin Transactions 1* **1987**, (0), 211-215.
54. Steudel, R.; Hassenberg, K.; Münchow, V.; Schumann, O.; Pickardt, J., Preparation of Organic Polysulfanes R<sub>2</sub>Sn (n = 5, 7, 8, 9) from Sulfenyl Chlorides, RSCl, and Transition Metal Polysulfido Complexes. *European Journal of Inorganic Chemistry* **2000**, 2000 (5), 921-928.
55. Chenard, B. L.; Harlow, R. L.; Johnson, A. L.; Vladuchick, S. A., Synthesis, structure, and properties of pentathiepins. *Journal of the American Chemical Society* **1985**, 107 (13), 3871-3879.
56. Rewcastle, G. W.; Janosik, T.; Bergman, J., Reactions of 2-lithiated indoles with elemental sulfur. Formation of pentathiepino[6,7-b]indoles and indoline-2-thiones. *Tetrahedron* **2001**, 57 (33), 7185-7189.
57. Zubair, M.; Ghosh, A. C.; Schulzke, C., The unexpected and facile molybdenum mediated formation of tri- and tetracyclic pentathiepins from pyrazine-alkynes and sulfur. *Chemical Communications* **2013**, 49 (39), 4343-4345.
58. Dinsmore, A.; David Garner, C.; Joule, J. A., 4-(2,2-Dimethyldioxalan-4-yl)-5-(pterin-6-yl)-1,3-dithiol-2-ones proligands relating to the cofactor of the oxomolybdoenzymes. *Tetrahedron* **1998**, 54 (33), 9559-9568.
59. Bae, G. H.; Kim, S.; Lee, N. K.; Dagar, A.; Lee, J. H.; Lee, J.; Kim, I., Facile approach to benzo[d]imidazole-pyrrolo[1,2-a]pyrazine hybrid structures through double cyclodehydration and aromatization and their unique optical properties with blue emission. *RSC Advances* **2020**, 10 (12), 7265-7288.
60. Mitchell, S. A.; Danca, M. D.; Blomgren, P. A.; Darrow, J. W.; Currie, K. S.; Kropf, J. E.; Lee, S. H.; Gallion, S. L.; Xiong, J.-M.; Pippin, D. A.; DeSimone, R. W.; Brittelli, D. R.; Eustice, D. C.; Bourret, A.; Hill-Drzewi, M.; Maciejewski, P. M.; Elkin, L. L., Imidazo[1,2-a]pyrazine diaryl ureas: Inhibitors of the receptor tyrosine kinase EphB4. *Bioorganic & Medicinal Chemistry Letters* **2009**, 19 (24), 6991-6995.
61. Murray, M. F., Nicotinamide: An Oral Antimicrobial Agent with Activity against Both Mycobacterium tuberculosis and Human Immunodeficiency Virus. *Clinical Infectious Diseases* **2003**, 36 (4), 453-460.
62. McKenzie, D.; Malone, L.; Kushner, S.; Oleson, J. J.; SubbaRow, Y., The effect of nicotinic acid amide on experimental tuberculosis of white mice. *The Journal of Laboratory and Clinical Medicine* **1948**, 33 (10), 1249-1253.
63. J R DiPalma, a.; Thayer, W. S., Use of Niacin as a Drug. *Annual Review of Nutrition* **1991**, 11 (1), 169-187.
64. Lange, P. P.; Bogdan, A. R.; James, K., A New Flow Methodology for the Expedient Synthesis of Drug-Like 3-Aminoindolizines. *Advanced Synthesis & Catalysis* **2012**, 354 (13), 2373-2379.
65. Coleman, R. S.; Berg, M. A.; Murphy, C. J., Coumarin base-pair replacement as a fluorescent probe of ultrafast DNA dynamics. *Tetrahedron* **2007**, 63 (17), 3450-3456.
66. Mettey, Y.; Gompel, M.; Thomas, V.; Garnier, M.; Leost, M.; Ceballos-Picot, I.; Noble, M.; Endicott, J.; Vierfond, J.-m.; Meijer, L., Aloisines, a New Family of CDK/GSK-3 Inhibitors. SAR Study, Crystal Structure in Complex with CDK2, Enzyme Selectivity, and Cellular Effects. *Journal of Medicinal Chemistry* **2003**, 46 (2), 222-236.
67. Lu, J.-J.; Meng, L.-H.; Cai, Y.-J.; Chen, Q.; Tong, L.-J.; Lin, L.-P.; Ding, J., Dihydroartemisinin induces apoptosis in HL-60 leukemia cells dependent of iron and p38 mitogen-activated protein kinase activation but independent of reactive oxygen species. *Cancer Biology & Therapy* **2008**, 7 (7), 1017-1023.

## References

68. Afzal, O.; Kumar, S.; Haider, M. R.; Ali, M. R.; Kumar, R.; Jaggi, M.; Bawa, S., A review on anticancer potential of bioactive heterocycle quinoline. *European Journal of Medicinal Chemistry* **2015**, *97*, 871-910.
69. Montoya, A.; Quiroga, J.; Abonia, R.; Derita, M.; Sortino, M.; Ornelas, A.; Zacchino, S.; Insuasty, B., Hybrid Molecules Containing a 7-Chloro-4-aminoquinoline Nucleus and a Substituted 2-Pyrazoline with Antiproliferative and Antifungal Activity. *Molecules* **2016**, *21* (8), 969.
70. Firestone, G. L.; Sundar, S. N., Anticancer activities of artemisinin and its bioactive derivatives. *Expert Reviews in Molecular Medicine* **2009**, *11*, e32.
71. Zhuang, L.; Wai, J. S.; Embrey, M. W.; Fisher, T. E.; Egbertson, M. S.; Payne, L. S.; Guare, J. P.; Vacca, J. P.; Hazuda, D. J.; Felock, P. J.; Wolfe, A. L.; Stillmock, K. A.; Witmer, M. V.; Moyer, G.; Schleif, W. A.; Gabryelski, L. J.; Leonard, Y. M.; Lynch, J. J.; Michelson, S. R.; Young, S. D., Design and Synthesis of 8-Hydroxy-[1,6]Naphthyridines as Novel Inhibitors of HIV-1 Integrase in Vitro and in Infected Cells. *Journal of Medicinal Chemistry* **2003**, *46* (4), 453-456.
72. Bakker, P. A. H. M.; Ran, L.; Mercado-Blanco, J., Rhizobacterial salicylate production provokes headaches! *Plant and Soil* **2014**, *382* (1), 1-16.
73. Shaw, A. Y.; Chang, C.-Y.; Hsu, M.-Y.; Lu, P.-J.; Yang, C.-N.; Chen, H.-L.; Lo, C.-W.; Shiau, C.-W.; Chern, M.-K., Synthesis and structure-activity relationship study of 8-hydroxyquinoline-derived Mannich bases as anticancer agents. *European Journal of Medicinal Chemistry* **2010**, *45* (7), 2860-2867.
74. Acosta, E. J.; Nguyen, T.; Witthayapanyanon, A.; Harwell, J. H.; Sabatini, D. A., Linker-Based Bio-compatible Microemulsions. *Environmental Science & Technology* **2005**, *39* (5), 1275-1282.
75. Gu, W.; Jin, X.-Y.; Li, D.-D.; Wang, S.-F.; Tao, X.-B.; Chen, H., Design, synthesis and in vitro anticancer activity of novel quinoline and oxadiazole derivatives of ursolic acid. *Bioorganic & Medicinal Chemistry Letters* **2017**, *27* (17), 4128-4132.
76. Moret, V.; Laras, Y.; Cresteil, T.; Aubert, G.; Ping, D. Q.; Di, C.; Barthélémy-Requin, M.; Béclin, C.; Peyrot, V.; Allegro, D.; Rolland, A.; De Angelis, F.; Gatti, E.; Pierre, P.; Pasquini, L.; Petrucci, E.; Testa, U.; Kraus, J.-L., Discovery of a new family of bis-8-hydroxyquinoline substituted benzylamines with pro-apoptotic activity in cancer cells: Synthesis, structure-activity relationship, and action mechanism studies. *European Journal of Medicinal Chemistry* **2009**, *44* (2), 558-567.
77. Weinberg, E. D.; Moon, J., Malaria and iron: history and review. *Drug Metabolism Reviews* **2009**, *41* (4), 644-662.
78. Jampilek, J.; Dolezal, M.; Kunes, J.; Buchta, V.; Silva, L.; Kralova, K., Quinaldine Derivatives: Preparation and Biological Activity. *Medicinal Chemistry* **2005**, *1* (6), 591-599.
79. Li, F.; Jiang, T.; Li, Q.; Ling, X., Camptothecin (CPT) and its derivatives are known to target topoisomerase I (Top1) as their mechanism of action: did we miss something in CPT analogue molecular targets for treating human disease such as cancer? *American Journal of Cancer Research* **2017**, *7* (12), 2350-2394.
80. Haesslein, J. I.; Jullian, N., Recent Advances in Cyclin-Dependent Kinase Inhibition. Purine-Based Derivatives as Anti-Cancer Agents. Roles and Perspectives for the Future. *Current Topics in Medicinal Chemistry* **2002**, *2* (9), 1037-1050.
81. Actor, P.; Chow, A. W.; Dutko, F. J.; McKinlay, M. A., Chemotherapeutics. **2000**.
82. Balci, M., Basic <sup>1</sup>H- and <sup>13</sup>C-NMR Spectroscopy. *Elsevier* **2005**, *First edition*, 308.
83. Konstantinova, L. S.; Amelichev, S. A.; Rakitin, O. A., 1,2,3,4,5-Pentathiepinines and 1,2,3,4,5-pentathiepanes. *Russian Chemical Review*. **2007**, *76* (3), 195-211

## References

84. Medhe, S., Ionization Techniques in Mass Spectrometry: A Review. *Mass Spectrometry & Purification Techniques* **2018**, *04* (01).
85. Steudel, R.; Eckert, B., Elemental Sulfur and Sulfur-Rich Compounds I. *Topics in Current Chemistry* **2003**, *230*, 23.
86. Zubair, M.; Ghosh, A. C.; Schulzke, C., The unexpected and facile molybdenum mediated formation of tri- and tetracyclic pentathiepins from pyrazine-alkynes and sulfur. *Chemical communications* **2013**, *49* (39), 4343-5.
87. Tripathi, K. M.; Begum, A.; Sonkar, S. K.; Sarkar, S., Nanospheres of copper(III) 1,2-dicarbomethoxy-1,2-dithiolate and its composite with water soluble carbon nanotubes. *New Journal of Chemistry* **2013**, *37* (9), 2708-2715.
88. Duan, X.; Wen, Z.; Shen, H.; Shen, M.; Chen, G., Intracerebral Hemorrhage, Oxidative Stress, and Antioxidant Therapy. *Oxidative Medicine and Cellular Longevity* **2016**, *2016*, 1203285-1203285.
89. Eletto, D.; Chevet, E.; Argon, Y.; Appenzeller-Herzog, C., Redox controls UPR to control redox. *Journal of Cell Science* **2014**, *127* (17), 3649-3658.
90. Lloret, A.; Fuchsberger, T.; Giraldo, E.; Vina, J., Reductive Stress: A New Concept in Alzheimer's Disease. *Current Alzheimer Research* **2016**, *13* (2), 206-211.
91. Narasimhan, M.; Rajasekaran, N. S., Reductive potential — A savior turns stressor in protein aggregation cardiomyopathy. *Biochimica et Biophysica Acta (BBA) - Molecular Basis of Disease* **2015**, *1852* (1), 53-60.
92. Kaczanowski, S., Apoptosis: its origin, history, maintenance and the medical implications for cancer and aging. *Physical Biology* **2016**, *13* (3), 031001.
93. Cerutti, P., Prooxidant states and tumor promotion. *Science* **1985**, *227* (4685), 375-381.
94. Allen, R. G., Oxidative stress and superoxide dismutase in development, aging and gene regulation. *Age (Omaha)* **1998**, *21* (2), 47-76.
95. Scandalios, J. G., Oxidative stress: molecular perception and transduction of signals triggering antioxidant gene defenses. *Brazilian Journal of Medical and Biological Research* **2005**, *38*, 995-1014.
96. Lo, Y. Y. C.; Wong, J. M. S.; Cruz, T. F., Reactive Oxygen Species Mediate Cytokine Activation of c-Jun NH2-terminal Kinases. *Journal of Biological Chemistry* **1996**, *271* (26), 15703-15707.
97. Kovac, S.; Angelova, P. R.; Holmström, K. M.; Zhang, Y.; Dinkova-Kostova, A. T.; Abramov, A. Y., Nrf2 regulates ROS production by mitochondria and NADPH oxidase. *Biochimica et Biophysica Acta (BBA) - General Subjects* **2015**, *1850* (4), 794-801.
98. Griffiths, H. R.; Gao, D.; Pararasa, C., Redox regulation in metabolic programming and inflammation. *Redox Biology* **2017**, *12*, 50-57.
99. Paracha, U. Z.; Fatima, K.; Alqahtani, M.; Chaudhary, A.; Abuzenadah, A.; Damanhour, G.; Qadri, I., Oxidative stress and hepatitis C virus. *Virology Journal* **2013**, *10* (1), 251.
100. Bickers, D. R.; Athar, M., Oxidative Stress in the Pathogenesis of Skin Disease. *Journal of Investigative Dermatology* **2006**, *126* (12), 2565-2575.
101. Weydert, C. J.; Cullen, J. J., Measurement of superoxide dismutase, catalase and glutathione peroxidase in cultured cells and tissue. *Natural Protocols* **2010**, *5* (1), 51-66.
102. Payne, M. E.; Steck, S. E.; George, R. R.; Steffens, D. C., Fruit, vegetable, and antioxidant intakes are lower in older adults with depression. *Journal of the Academy Nutrition and Dietetics* **2012**, *112* (12), 2022-2027.
103. Lubos, E.; Loscalzo, J.; Handy, D. E., Glutathione peroxidase-1 in health and disease: from molecular mechanisms to therapeutic opportunities. *Antioxidants & redox signaling* **2011**, *15* (7), 1957-97.

## References

104. Rocher, C.; Lalanne, J. L.; Chaudiere, J., Purification and properties of a recombinant sulfur analog of murine selenium-glutathione peroxidase. *European journal of biochemistry* **1992**, *205* (3), 955-60.
105. Ho, Y. S.; Magnenat, J. L.; Bronson, R. T.; Cao, J.; Gargano, M.; Sugawara, M.; Funk, C. D., Mice deficient in cellular glutathione peroxidase develop normally and show no increased sensitivity to hyperoxia. *The Journal of biological chemistry* **1997**, *272* (26), 16644-51.
106. Klivenyi, P.; Andreassen, O. A.; Ferrante, R. J.; Dedeoglu, A.; Mueller, G.; Lancelot, E.; Bogdanov, M.; Andersen, J. K.; Jiang, D.; Beal, M. F., Mice deficient in cellular glutathione peroxidase show increased vulnerability to malonate, 3-nitropropionic acid, and 1-methyl-4-phenyl-1,2,5,6-tetrahydropyridine. *The Journal of neuroscience : the official journal of the Society for Neuroscience* **2000**, *20* (1), 1-7.
107. Seiler, A.; Schneider, M.; Forster, H.; Roth, S.; Wirth, E. K.; Culmsee, C.; Plesnila, N.; Kremmer, E.; Radmark, O.; Wurst, W.; Bornkamm, G. W.; Schweizer, U.; Conrad, M., Glutathione peroxidase 4 senses and translates oxidative stress into 12/15-lipoxygenase dependent- and AIF-mediated cell death. *Cell metabolism* **2008**, *8* (3), 237-48.
108. Brutsch, S. H.; Wang, C. C.; Li, L.; Stender, H.; Neziroglu, N.; Richter, C.; Kuhn, H.; Borchert, A., Expression of inactive glutathione peroxidase 4 leads to embryonic lethality, and inactivation of the Alox15 gene does not rescue such knock-in mice. *Antioxidants & redox signaling* **2015**, *22* (4), 281-93.
109. Ratnasinghe, D.; Tangrea, J. A.; Andersen, M. R.; Barrett, M. J.; Virtamo, J.; Taylor, P. R.; Albanes, D., Glutathione peroxidase codon 198 polymorphism variant increases lung cancer risk. *Cancer research* **2000**, *60* (22), 6381-3.
110. Blein, S.; Berndt, S.; Joshi, A. D.; Campa, D.; Ziegler, R. G.; Riboli, E.; Cox, D. G.; Breast, N. C. I.; Prostate Cancer Cohort, C., Factors associated with oxidative stress and cancer risk in the Breast and Prostate Cancer Cohort Consortium. *Free radical research* **2014**, *48* (3), 380-6.
111. Wickremasinghe, D.; Peiris, H.; Chandrasena, L. G.; Senaratne, V.; Perera, R., Case control feasibility study assessing the association between severity of coronary artery disease with Glutathione Peroxidase-1 (GPX-1) and GPX-1 polymorphism (Pro198Leu). *BMC cardiovascular disorders* **2016**, *16*, 111.
112. Lee, J. R.; Roh, J. L.; Lee, S. M.; Park, Y.; Cho, K. J.; Choi, S. H.; Nam, S. Y.; Kim, S. Y., Overexpression of glutathione peroxidase 1 predicts poor prognosis in oral squamous cell carcinoma. *Journal of cancer research and clinical oncology* **2017**, *143* (11), 2257-2265.
113. Wieczorek, E.; Jablonowski, Z.; Tomasik, B.; Gromadzinska, J.; Jablonska, E.; Konecki, T.; Fendler, W.; Sosnowski, M.; Wasowicz, W.; Reszka, E., Different Gene Expression and Activity Pattern of Antioxidant Enzymes in Bladder Cancer. *Anticancer research* **2017**, *37* (2), 841-848.
114. Schulz, R.; Emmrich, T.; Lemmerhirt, H.; Leffler, U.; Sydow, K.; Hirt, C.; Kiefer, T.; Link, A.; Bednarski, P. J., Identification of a glutathione peroxidase inhibitor that reverses resistance to anticancer drugs in human B-cell lymphoma cell lines. *Bioorganic Medicinal Chemistry Letters* **2012**, *22* (21), 6712-5.
115. Yang, W. S.; Stockwell, B. R., Ferroptosis: Death by Lipid Peroxidation. *Trends in cell biology* **2016**, *26* (3), 165-76.
116. Chaudiere, J.; Wilhelmsen, E. C.; Tappel, A. L., Mechanism of selenium-glutathione peroxidase and its inhibition by mercaptocarboxylic acids and other mercaptans. *The Journal of biological chemistry* **1984**, *259* (2), 1043-50.
117. Hall, M. D.; Marshall, T. S.; Kwit, A. D.; Miller Jenkins, L. M.; Dulcey, A. E.; Madigan, J. P.; Pluchino, K. M.; Goldsborough, A. S.; Brimacombe, K. R.; Griffiths,

## References

- G. L.; Gottesman, M. M., Inhibition of glutathione peroxidase mediates the collateral sensitivity of multidrug-resistant cells to tiopronin. *The Journal of biological chemistry* **2014**, 289 (31), 21473-89.
118. Chaudiere, J.; Tappel, A. L., Interaction of gold(I) with the active site of selenium-glutathione peroxidase. *Journal of inorganic biochemistry* **1984**, 20 (4), 313-25.
119. Carvalho, C. M.; Chew, E. H.; Hashemy, S. I.; Lu, J.; Holmgren, A., Inhibition of the human thioredoxin system. A molecular mechanism of mercury toxicity. *Journal of Biological Chemistry* **2008**, 283 (18), 11913-23.
120. Gandin, V.; Fernandes, A. P.; Rigobello, M. P.; Dani, B.; Sorrentino, F.; Tisato, F.; Bjornstedt, M.; Bindoli, A.; Sturaro, A.; Rella, R.; Marzano, C., Cancer cell death induced by phosphine gold(I) compounds targeting thioredoxin reductase. *Biochem Pharmacol* **2010**, 79 (2), 90-101.
121. Chatterji, T.; Gates, K. S., DNA cleavage by 7-methylbenzopentathiepin: a simple analog of the antitumor antibiotic varacin. *Bioorganic & medicinal chemistry letters* **1998**, 8 (5), 535-8.
122. Lee, A. H.; Chan, A. S.; Li, T., Acid-accelerated DNA-cleaving activities of antitumor antibiotic varacin. *Chemical communications* **2002**, (18), 2112-3.
123. Lee, A. H.; Chen, J.; Liu, D.; Leung, T. Y.; Chan, A. S.; Li, T., Acid-promoted DNA-cleaving activities and total synthesis of varacin C. *Journal of American Chemical Society* **2002**, 124 (47), 13972-3.
124. Duffus, J. H., Glossary for Chemists of Terms Used in Toxicology (IUPAC Recommendations 1993). *Pure & Applied Chemistry* **1993**, 65 (9), 2068.
125. Sonoda, K.; Nakashima, M.; Saito, T.; Amada, S.; Kamura, T.; Nakano, H.; Watanabe, T., Establishment of a new human uterine cervical adenocarcinoma cell line, SiSo, and its reactivity to anti-cancer reagents. *International Journal of Oncology*. **1995**, 6 (5), 1099-1104.
126. Davidson, B. S.; Molinski, T. F.; Barrows, L. R.; Ireland, C. M., Varacin: A Novel Benzopentathiepin from *Lissoclinum vareau* that Is Cytotoxic toward a Human Colon Tumor. *J. Am. Chem. Soc.* **1991**, 113, 4709-4710.
127. Wiegand, I.; Hilpert, K.; Hancock, R. E., Agar and broth dilution methods to determine the minimal inhibitory concentration (MIC) of antimicrobial substances. *Nature protocols* **2008**, 3 (2), 163-75.
128. Ghai, I.; Ghai, S., Understanding antibiotic resistance via outer membrane permeability. *Infection and drug resistance* **2018**, 11, 523-530.
129. Nikaido, H., Preventing drug access to targets: cell surface permeability barriers and active efflux in bacteria. *Seminars in cell & developmental biology* **2001**, 12 (3), 215-23.
130. Litaudon, M.; Trigalo, F.; Martin, M.; Frappier, F.; Guyot, M., Lissoclinotoxins: Antibiotic Polysulfur Derivatives From The Tunicate *Lissoclinum perforatum*. Revised Structure of Lissoclinotoxin A. *Tetrahedron* **1994**, 50 (18), 5323-5334.
131. Chen, K.-L.; Liu, L.-C.; Chen, W.-R., Adsorption of sulfamethoxazole and sulfapyridine antibiotics in high organic content soils. *Environmental Pollution* **2017**, 231, 1163-1171.
132. Prasad, R.; Kapoor, K., Multidrug Resistance in Yeast *Candida*. *International Review of Cytology* **2004**, 242, 215-248.
133. Dantas Ada, S.; Day, A.; Ikeh, M.; Kos, I.; Achan, B.; Quinn, J., Oxidative stress responses in the human fungal pathogen, *Candida albicans*. *Biomolecules* **2015**, 5 (1), 142-65.
134. McAtee, J. J.; Dodson, J. W.; Dowdell, S. E.; Girard, G. R.; Goodman, K. B.; Hilfiker, M. A.; Schon, C. A.; Sha, D.; Wang, G. Z.; Wang, N.; Viet, A. Q.; Zhang, D.; Aiyar,

## References

- N. V.; Behm, D. J.; Carballo, L. H.; Evans, C. A.; Fries, H. E.; Nagilla, R.; Roethke, T. J.; Xu, X.; Yuan, C. C. K.; Douglas, S. A.; Neeb, M. J., Development of potent and selective small-molecule human Urotensin-II antagonists. *Bioorganic & Medicinal Chemistry Letters* **2008**, *18* (12), 3500-3503.
135. Landge, S. M.; Török, B., Synthesis of Condensed Benzo[N,N]-Heterocycles by Microwave-Assisted Solid Acid Catalysis. *Catalysis Letters* **2008**, *122* (3), 338-343.
136. Bandgar, B. P.; Bettigeri, S. V., Direct Synthesis of N-Acylalkylenediamines from Carboxylic Acids Under Mild Conditions. *Synthetic Communications* **2004**, *34* (16), 2917-2924.
137. Srimani, D.; Balaraman, E.; Gnanaprakasam, B.; Ben-David, Y.; Milstein, D., Ruthenium Pincer-Catalyzed Cross-Dehydrogenative Coupling of Primary Alcohols with Secondary Alcohols under Neutral Conditions. *Advanced Synthesis & Catalysis* **2012**, *354* (13), 2403-2406.
138. Simpson, I.; St-Gallay, S. A.; Stokes, S.; Whittaker, D. T. E.; Wiewiora, R., An efficient one-pot synthesis of 2-bromo-6-aryl[5H]pyrrolo[2,3-b]pyrazines. *Tetrahedron Letters* **2015**, *56* (12), 1492-1495.
139. Chakka, N.; Bregman, H.; Du, B.; Nguyen, H. N.; Buchanan, J. L.; Feric, E.; Ligutti, J.; Liu, D.; McDermott, J. S.; Zou, A.; McDonough, S. I.; Dimauro, E. F., Discovery and hit-to-lead optimization of pyrrolopyrimidines as potent, state-dependent Na(v)1.7 antagonists. *Bioorganic Medicinal Chemistry Letters* **2012**, *22* (5), 2052-62.
140. Zhang, X.; Zhang, N.; Chen, G.; Turpoff, A.; Ren, H.; Takasugi, J.; Morrill, C.; Zhu, J.; Li, C.; Lennox, W.; Paget, S.; Liu, Y.; Almstead, N.; Njoroge, F. G.; Gu, Z.; Komatsu, T.; Clausen, V.; Espiritu, C.; Graci, J.; Colacino, J.; Lahser, F.; Risher, N.; Weetall, M.; Nomeir, A.; Karp, G. M., Discovery of novel HCV inhibitors: synthesis and biological activity of 6-(indol-2-yl)pyridine-3-sulfonamides targeting hepatitis C virus NS4B. *Bioorganic Medicinal Chemistry Letters* **2013**, *23* (13), 3947-53.
141. Aasini, A.; Andrea S.; Antonio M.; Claudiu T., Sulfonamides and Sulfonylated Derivatives as Anticancer Agents. *Current Cancer Drug Targets* **2002**, *55*.
142. Zhang, W.; Zhang, D.; Stashko, M. A.; DeRyckere, D.; Hunter, D.; Kireev, D.; Miley, M. J.; Cummings, C.; Lee, M.; Norris-Drouin, J.; Stewart, W. M.; Sather, S.; Zhou, Y.; Kirkpatrick, G.; Machius, M.; Janzen, W. P.; Earp, H. S.; Graham, D. K.; Frye, S. V.; Wang, X., Pseudo-cyclization through intramolecular hydrogen bond enables discovery of pyridine substituted pyrimidines as new Mer kinase inhibitors. *Journal of medicinal chemistry* **2013**, *56* (23), 9683-92.
143. Gazit, A.; Yaish, P.; Gilon, C.; Levitzki, A., Tyrphostins I: synthesis and biological activity of protein tyrosine kinase inhibitors. *Journal of Medicinal Chemistry* **1989**, *32* (10), 2344-2352.
144. Lemhadri, M.; Doucet, H.; Santelli, M., Sonogashira reaction of aryl halides with propionaldehyde diethyl acetal catalyzed by a tetracosphosphine/palladium complex. *Tetrahedron* **2005**, *61* (41), 9839-9847.
145. Ritzén, A.; Sindet, R.; Hentzer, M.; Svendsen, N.; Brodbeck, R. M.; Bundgaard, C., Discovery of a potent and brain penetrant mGluR5 positive allosteric modulator. *Bioorganic & Medicinal Chemistry Letters* **2009**, *19* (12), 3275-3278.
146. Siemsen, P.; Livingston, R. C.; Diederich, F., Acetylenic Coupling: A Powerful Tool in Molecular Construction. *Angewandte Chemie International Edition* **2000**, *39* (15), 2632-2657.
147. Miyaura, N.; Suzuki, A., Palladium-Catalyzed Cross-Coupling Reactions of Organoboron Compounds. *Chemical Reviews* **1995**, *95* (7), 2457-2483.



## References

148. Saito, S.; Yamamoto, Y., Recent Advances in the Transition-Metal-Catalyzed Regioselective Approaches to Polysubstituted Benzene Derivatives. *Chemical Reviews* **2000**, *100* (8), 2901-2916.
149. Chinchilla, R.; Nájera, C., Recent advances in Sonogashira reactions. *Chemical Society Reviews* **2011**, *40* (10), 5084-5121.
150. Smidt, J.; Hafner, W.; Jira, R.; Sedlmeier, J.; Sieber, R.; Rüttinger, R.; Kojer, H., Katalytische Umsetzungen von Olefinen an Platinmetall-Verbindungen Das Consortium-Verfahren zur Herstellung von Acetaldehyd. *Angewandte Chemie* **1959**, *71* (5), 176-182.
151. Smidt, J.; Hafner, W., Eine Reaktion von Palladiumchlorid mit Allylalkohol. *Angewandte Chemie* **1959**, *71* (8), 284-284.
152. Tsuji, J.; Takahashi, H.; Morikawa, M., Organic syntheses by means of noble metal compounds XVII. Reaction of  $\pi$ -allylpalladium chloride with nucleophiles. *Tetrahedron Letters* **1965**, *6* (49), 4387-4388.
153. Tsuji, J., Recollections of organopalladium chemistry. *Pure and Applied Chemistry*, **1999**, *71*, 1539.
154. Magano, J.; Dunetz, J. R., Large-Scale Applications of Transition Metal-Catalyzed Couplings for the Synthesis of Pharmaceuticals. *Chemical Reviews* **2011**, *111* (3), 2177-2250.
155. Torborg, C.; Beller, M., Recent Applications of Palladium-Catalyzed Coupling Reactions in the Pharmaceutical, Agrochemical, and Fine Chemical Industries. *Advanced Synthesis & Catalysis* **2009**, *351* (18), 3027-3043.
156. Nicolaou, K. C.; Bulger, P. G.; Sarlah, D., Palladium-Catalyzed Cross-Coupling Reactions in Total Synthesis. *Angewandte Chemie International Edition* **2005**, *44* (29), 4442-4489.
157. Corbet, J.P.; Mignani, G., Selected Patented Cross-Coupling Reaction Technologies. *Chemical Reviews* **2006**, *106* (7), 2651-2710.
158. Roughley, S. D.; Jordan, A. M., The Medicinal Chemist's Toolbox: An Analysis of Reactions Used in the Pursuit of Drug Candidates. *Journal of Medicinal Chemistry* **2011**, *54* (10), 3451-3479.
159. Negishi, E.-i., Magical Power of Transition Metals: Past, Present, and Future (Nobel Lecture). *Angewandte Chemie International Edition* **2011**, *50* (30), 6738-6764.
160. Suzuki, A., Cross-Coupling Reactions Of Organoboranes: An Easy Way To Construct C-C Bonds (Nobel Lecture). *Angewandte Chemie International Edition* **2011**, *50* (30), 6722-6737.
161. Johansson Seechurn, C. C. C.; Kitching, M. O.; Colacot, T. J.; Snieckus, V., Palladium-Catalyzed Cross-Coupling: A Historical Contextual Perspective to the 2010 Nobel Prize. *Angewandte Chemie International Edition* **2012**, *51* (21), 5062-5085.
162. Diederich, P. D. A., **2004 WILEY-VCH Verlag GmbH & Co. KGaA: 25 August 2004.**
163. Synthesis by Metal-Mediated Coupling Reactions. In *Category 6, Compounds with All-Carbon Functions*, 1st Edition ed.; Rawal, V. H.; Kozmin, S. A., Eds. Georg Thieme Verlag: Stuttgart, **2009**; Vol. 46.
164. Taylor, J. G.; Moro, A. V.; Correia, C. R. D., Evolution and Synthetic Applications of the Heck–Matsuda Reaction: The Return of Arenediazonium Salts to Prominence. *European Journal of Organic Chemistry* **2011**, *2011* (8), 1403-1428.
165. Bonin, H.; Fouquet, E.; Felpin, F.-X., Aryl Diazonium versus Iodonium Salts: Preparation, Applications and Mechanisms for the Suzuki–Miyaura Cross-Coupling Reaction. *Advanced Synthesis & Catalysis* **2011**, *353* (17), 3063-3084.

## References

166. Roglans, A.; Pla-Quintana, A.; Moreno-Mañas, M., Diazonium Salts as Substrates in Palladium-Catalyzed Cross-Coupling Reactions. *Chemical Reviews* **2006**, *106* (11), 4622-4643.
167. Suzuki, A., Cross-coupling reactions via organoboranes. *Journal of Organometallic Chemistry* **2002**, *653* (1), 83-90.
168. Curtis, M. D.; Epstein, P. S., Redistribution Reactions on Silicon Catalyzed by Transition Metal Complexes. *Advances in Organometallic Chemistry*, Stone, F. G. A.; West, R., Eds. Academic Press: **1981**, *19*, 213-255.
169. Azarian, D.; Dua, S. S.; Eaborn, C.; Walton, D. R. M., Reactions of organic halides with R<sub>3</sub>MMR<sub>3</sub> compounds (M = Si, Ge, Sn) in the presence of tetrakis(triarylphosphine)palladium. *Journal of Organometallic Chemistry* **1976**, *117* (3), C55-C57.
170. Bariwal, J.; Van der Eycken, E., C–N bond forming cross-coupling reactions: an overview. *Chemical Society Reviews* **2013**, *42* (24), 9283-9303.
171. Ishiyama, T.; Matsuda, N.; Miyaura, N.; Suzuki, A., Platinum(0)-catalyzed diboration of alkynes. *Journal of the American Chemical Society* **1993**, *115* (23), 11018-11019.
172. Murata, M.; Watanabe, S.; Masuda, Y., Novel Palladium(0)-Catalyzed Coupling Reaction of Dialkoxyborane with Aryl Halides: Convenient Synthetic Route to Arylboronates. *The Journal of Organic Chemistry* **1997**, *62* (19), 6458-6459.
173. Schlummer, B.; Scholz, U., Palladium-Catalyzed C-N and C-O Coupling—A Practical Guide from an Industrial Vantage Point†. *Advanced Synthesis & Catalysis* **2004**, *346* (13-15), 1599-1626.
174. Surry, D. S.; Buchwald, S. L., Dialkylbiaryl phosphines in Pd-catalyzed amination: a user's guide. *Chemical Science* **2011**, *2* (1), 27-50.
175. Hartwig, J. F., Carbon–heteroatom bond formation catalysed by organometallic complexes. *Nature* **2008**, *455*, 314.
176. Lundgren, R. J.; Stradiotto, M., Addressing Challenges in Palladium-Catalyzed Cross-Coupling Reactions Through Ligand Design. *Chemistry – A European Journal* **2012**, *18* (32), 9758-9769.
177. Ullmann, F., Ueber eine neue Bildungsweise von Diphenylaminderivaten. *Berichte der deutschen chemischen Gesellschaft* **1903**, *36* (2), 2382-2384.
178. Sharif, S.; Rucker, R. P.; Chandrasoma, N.; Mitchell, D.; Rodriguez, M. J.; Froese, R. D. J.; Organ, M. G., Selective Monoarylation of Primary Amines Using the Pd-PEPPSI-IPentCl Precatalyst. *Angewandte Chemie International Edition* **2015**, *54* (33), 9507-9511.
179. Guram, A. S.; Rennels, R. A.; Buchwald, S. L., A Simple Catalytic Method for the Conversion of Aryl Bromides to Arylamines. *Angewandte Chemie International Edition in English* **1995**, *34* (12), 1348-1350.
180. Louie, J.; Hartwig, J. F., Transmetalation, Involving Organotin Aryl, Thiolate, and Amide Compounds. An Unusual Type of Dissociative Ligand Substitution Reaction. *Journal of the American Chemical Society* **1995**, *117* (46), 11598-11599.
181. Hartwig, J. F., Evolution of a Fourth Generation Catalyst for the Amination and Thioetherification of Aryl Halides. *Accounts of Chemical Research* **2008**, *41* (11), 1534-1544.
182. Sunesson, Y.; Limé, E.; Nilsson Lill, S. O.; Meadows, R. E.; Norrby, P.-O., Role of the Base in Buchwald–Hartwig Amination. *The Journal of Organic Chemistry* **2014**, *79* (24), 11961-11969.
183. Fleckenstein, C. A.; Plenio, H., Sterically demanding trialkylphosphines for palladium-catalyzed cross coupling reactions—alternatives to PtBu<sub>3</sub>. *Chemical Society Reviews* **2010**, *39* (2), 694-711.

## References

184. Wolfe, J. P.; Wagaw, S.; Marcoux, J.-F.; Buchwald, S. L., Rational Development of Practical Catalysts for Aromatic Carbon–Nitrogen Bond Formation. *Accounts of Chemical Research* **1998**, *31* (12), 805-818.
185. Yin, J.; Buchwald, S. L., Palladium-Catalyzed Intermolecular Coupling of Aryl Halides and Amides. *Organic Letters* **2000**, *2* (8), 1101-1104.
186. Artamkina, G. A.; Sergeev, A. G.; Beletskaya, I. P., Palladium-catalyzed reaction of aryl halides with ureas. *Tetrahedron Letters* **2001**, *42* (26), 4381-4384.
187. Mann, G.; Hartwig, J. F.; Driver, M. S.; Fernández-Rivas, C., Palladium-Catalyzed C–N(sp<sup>2</sup>) Bond Formation: N-Arylation of Aromatic and Unsaturated Nitrogen and the Reductive Elimination Chemistry of Palladium Azolyl and Methyleneamido Complexes. *Journal of the American Chemical Society* **1998**, *120* (4), 827-828.
188. Crawford, S. M.; Lavery, C. B.; Stradiotto, M., BippyPhos: A Single Ligand With Unprecedented Scope in the Buchwald–Hartwig Amination of (Hetero)aryl Chlorides. *Chemistry – A European Journal* **2013**, *19* (49), 16760-16771.
189. Tardiff, B. J.; McDonald, R.; Ferguson, M. J.; Stradiotto, M., Rational and Predictable Chemoselective Synthesis of Oligoamines via Buchwald–Hartwig Amination of (Hetero)Aryl Chlorides Employing Mor-DalPhos. *The Journal of Organic Chemistry* **2012**, *77* (2), 1056-1071.
190. Marion, N.; Ecarnot, E. C.; Navarro, O.; Amoroso, D.; Bell, A.; Nolan, S. P., (IPr)Pd(acac)Cl: An Easily Synthesized, Efficient, and Versatile Precatalyst for C–N and C–C Bond Formation. *The Journal of Organic Chemistry* **2006**, *71* (10), 3816-3821.
191. Gildner, P. G.; Colacot, T. J., Reactions of the 21st Century: Two Decades of Innovative Catalyst Design for Palladium-Catalyzed Cross-Couplings. *Organometallics* **2015**, *34* (23), 5497-5508.
192. Li, H.; Johansson Seechurn, C. C. C.; Colacot, T. J., Development of Preformed Pd Catalysts for Cross-Coupling Reactions, Beyond the 2010 Nobel Prize. *ACS Catalysis* **2012**, *2* (6), 1147-1164.
193. Herrmann, W. A.; Brossmer, C.; Öfele, K.; Reisinger, C. P.; Priermeier, T.; Beller, M.; Fischer, H., Palladacycles as Structurally Defined Catalysts for the Heck Olefination of Chloro- and Bromoarenes. *Angewandte Chemie International Edition in English* **1995**, *34* (17), 1844-1848.
194. Marion, N.; Nolan, S. P., Well-Defined N-Heterocyclic Carbenes–Palladium(II) Precatalysts for Cross-Coupling Reactions. *Accounts of Chemical Research* **2008**, *41* (11), 1440-1449.
195. Zim, D.; Buchwald, S. L., An Air and Thermally Stable One-Component Catalyst for the Amination of Aryl Chlorides. *Organic Letters* **2003**, *5* (14), 2413-2415.
196. Schnyder, A.; Indolese, A. F.; Studer, M.; Blaser, H.-U., A New Generation of Air Stable, Highly Active Pd Complexes for C–C and C–N Coupling Reactions with Aryl Chlorides. *Angewandte Chemie International Edition* **2002**, *41* (19), 3668-3671.
197. Valente, C.; Pompeo, M.; Sayah, M.; Organ, M. G., Carbon–Heteroatom Coupling Using Pd-PEPSSI Complexes. *Organic Process Research & Development* **2014**, *18* (1), 180-190.
198. Johansson Seechurn, C. C. C.; Parisel, S. L.; Colacot, T. J., Air-Stable Pd(R-allyl)LCl (L= Q-Phos, P(t-Bu)<sub>3</sub>, etc.) Systems for C–C/N Couplings: Insight into the Structure–Activity Relationship and Catalyst Activation Pathway. *The Journal of Organic Chemistry* **2011**, *76* (19), 7918-7932.
199. DeAngelis, A. J.; Gildner, P. G.; Chow, R.; Colacot, T. J., Generating Active “L-Pd(0)” via Neutral or Cationic  $\pi$ -Allylpalladium Complexes Featuring Biaryl/Bipyrazolylphosphines: Synthetic, Mechanistic, and Structure–Activity Studies

## References

- in Challenging Cross-Coupling Reactions. *The Journal of Organic Chemistry* **2015**, *80* (13), 6794-6813.
200. Damon, D. B.; Dugger, R. W.; Hubbs, S. E.; Scott, J. M.; Scott, R. W., Asymmetric Synthesis of the Cholesteryl Ester Transfer Protein Inhibitor Torcetrapib. *Organic Process Research & Development* **2006**, *10* (3), 472-480.
201. Christensen, H.; Schjøth-Eskesen, C.; Jensen, M.; Sinning, S.; Jensen, H. H., Synthesis of 3,7-Disubstituted Imipramines by Palladium-Catalysed Amination/Cyclisation and Evaluation of Their Inhibition of Monoamine Transporters. *Chemistry – A European Journal* **2011**, *17* (38), 10618-10627.
202. Gopalsamy, A.; Shi, M.; Golas, J.; Vogan, E.; Jacob, J.; Johnson, M.; Lee, F.; Nilakantan, R.; Petersen, R.; Svenson, K.; Chopra, R.; Tam, M. S.; Wen, Y.; Ellingboe, J.; Arndt, K.; Boschelli, F., Discovery of Benzisoxazoles as Potent Inhibitors of Chaperone Heat Shock Protein 90. *Journal of Medicinal Chemistry* **2008**, *51* (3), 373-375.
203. Birch, A. M.; Birtles, S.; Buckett, L. K.; Kemmitt, P. D.; Smith, G. J.; Smith, T. J. D.; Turnbull, A. V.; Wang, S. J. Y., Discovery of a Potent, Selective, and Orally Efficacious Pyrimidinooxazinyl Bicyclooctaneacetic Acid Diacylglycerol Acyltransferase-1 Inhibitor. *Journal of Medicinal Chemistry* **2009**, *52* (6), 1558-1568.
204. George, D. M.; Breinlinger, E. C.; Friedman, M.; Zhang, Y.; Wang, J.; Argiriadi, M.; Bansal-Pakala, P.; Barth, M.; Duignan, D. B.; Honore, P.; Lang, Q.; Mittelstadt, S.; Potin, D.; Rundell, L.; Edmunds, J. J., Discovery of Selective and Orally Bioavailable Protein Kinase C $\theta$  (PKC $\theta$ ) Inhibitors from a Fragment Hit. *Journal of Medicinal Chemistry* **2015**, *58* (1), 222-236.
205. Fan, Y.; Xia, Y.; Tang, J.; Ziarelli, F.; Qu, F.; Rocchi, P.; Iovanna, J. L.; Peng, L., An Efficient Mixed-Ligand Pd Catalytic System to Promote C-N Coupling for the Synthesis of N-Arylamino-1,2,4-triazole Nucleosides. *Chemistry – A European Journal* **2012**, *18* (8), 2221-2225.
206. Pitsinos, E. N.; Vidali, V. P.; Couladouros, E. A., Diaryl Ether Formation in the Synthesis of Natural Products. *European Journal of Organic Chemistry* **2011**, *2011* (7), 1207-1222.
207. Zhang, H.; Ruiz-Castillo, P.; Buchwald, S. L., Palladium-Catalyzed C–O Cross-Coupling of Primary Alcohols. *Organic Letters* **2018**, *20* (6), 1580-1583.
208. Shibatomi, K.; Kotozaki, M.; Sasaki, N.; Fujisawa, I.; Iwasa, S., Williamson Ether Synthesis with Phenols at a Tertiary Stereogenic Carbon: Formal Enantioselective Phenoxylation of  $\beta$ -Keto Esters. *Chemistry – A European Journal* **2015**, *21* (40), 14095-14098.
209. Swamy, K. C. K.; Kumar, N. N. B.; Balaraman, E.; Kumar, K. V. P. P., Mitsunobu and Related Reactions: Advances and Applications. *Chemical Reviews* **2009**, *109* (6), 2551-2651.
210. Caron, S. G., A, *Nucleophilic Aromatic Substitution*. In *Practical Synthetic Organic Chemistry*. John Wiley & Sons: Hoboken, NJ: **2011**.
211. Whitesides, G. M.; Sadowski, J. S.; Lilburn, J., Copper(I) alkoxides. Synthesis, reactions, and thermal decompositions. *Journal of the American Chemical Society* **1974**, *96* (9), 2829-2835.
212. Lindley, J., Tetrahedron report number 163: Copper assisted nucleophilic substitution of aryl halogen. *Tetrahedron* **1984**, *40* (9), 1433-1456.
213. Palucki, M.; Wolfe, J. P.; Buchwald, S. L., Synthesis of Oxygen Heterocycles via a Palladium-Catalyzed C–O Bond-Forming Reaction. *Journal of the American Chemical Society* **1996**, *118* (42), 10333-10334.

## References

214. Torraca, K. E.; Kuwabe, S.-I.; Buchwald, S. L., A High-Yield, General Method for the Catalytic Formation of Oxygen Heterocycles. *Journal of the American Chemical Society* **2000**, *122* (51), 12907-12908.
215. Karpf, M.; Trussardi, R., New, Azide-Free Transformation of Epoxides into 1,2-Diamino Compounds: Synthesis of the Anti-Influenza Neuraminidase Inhibitor Oseltamivir Phosphate (Tamiflu). *The Journal of Organic Chemistry* **2001**, *66* (6), 2044-2051.
216. Navarro, O.; Kaur, H.; Mahjoor, P.; Nolan, S. P., Cross-Coupling and Dehalogenation Reactions Catalyzed by (N-Heterocyclic carbene)Pd(allyl)Cl Complexes. *The Journal of Organic Chemistry* **2004**, *69* (9), 3173-3180.
217. Mann, G.; Incarvito, C.; Rheingold, A. L.; Hartwig, J. F., Palladium-Catalyzed C–O Coupling Involving Unactivated Aryl Halides. Sterically Induced Reductive Elimination To Form the C–O Bond in Diaryl Ethers. *Journal of the American Chemical Society* **1999**, *121* (13), 3224-3225.
218. Torraca, K. E.; Huang, X.; Parrish, C. A.; Buchwald, S. L., An Efficient Intermolecular Palladium-Catalyzed Synthesis of Aryl Ethers. *Journal of the American Chemical Society* **2001**, *123* (43), 10770-10771.
219. Kuwabe, S.I.; Torraca, K. E.; Buchwald, S. L., Palladium-Catalyzed Intramolecular C–O Bond Formation. *Journal of the American Chemical Society* **2001**, *123* (49), 12202-12206.
220. Vorogushin, A. V.; Huang, X.; Buchwald, S. L., Use of Tunable Ligands Allows for Intermolecular Pd-Catalyzed C–O Bond Formation. *Journal of the American Chemical Society* **2005**, *127* (22), 8146-8149.
221. Wu, X.; Fors, B. P.; Buchwald, S. L., A Single Phosphine Ligand Allows Palladium-Catalyzed Intermolecular C-O Bond Formation with Secondary and Primary Alcohols. *Angewandte Chemie International Edition* **2011**, *50* (42), 9943-9947.
222. Milton, E. J.; Fuentes, J. A.; Clarke, M. L., Palladium-catalysed synthesis of aryl-alkyl ethers using alkoxy silanes as nucleophiles. *Organic & Biomolecular Chemistry* **2009**, *7* (12), 2645-2648.
223. Bhadra, S.; Dzik, W. I.; Goossen, L. J., Decarboxylative Etherification of Aromatic Carboxylic Acids. *Journal of the American Chemical Society* **2012**, *134* (24), 9938-9941.
224. Gowrisankar, S.; Neumann, H.; Beller, M., A Convenient and Practical Synthesis of Anisoles and Deuterated Anisoles by Palladium-Catalyzed Coupling Reactions of Aryl Bromides and Chlorides. *Chemistry – A European Journal* **2012**, *18* (9), 2498-2502.
225. Dash, P.; Janni, M.; Peruncheralathan, S., Trideuteriomethoxylation of Aryl and Heteroaryl Halides. *European Journal of Organic Chemistry* **2012**, *2012* (26), 4914-4917.
226. Wolter, M.; Nordmann, G.; Job, G. E.; Buchwald, S. L., Copper-Catalyzed Coupling of Aryl Iodides with Aliphatic Alcohols. *Organic Letters* **2002**, *4* (6), 973-976.
227. Zhang, H.; Ma, D.; Cao, W., N,N-Dimethylglycine-Promoted Ullmann-Type Coupling Reactions of Aryl Iodides with Aliphatic Alcohols. *Synlett* **2007**, *2007* (02), 0243-0246.
228. Altman, R. A.; Shafir, A.; Choi, A.; Lichtor, P. A.; Buchwald, S. L., An Improved Cu-Based Catalyst System for the Reactions of Alcohols with Aryl Halides. *The Journal of Organic Chemistry* **2008**, *73* (1), 284-286.
229. Zeng, H.; Qiu, Z.; Domínguez-Huerta, A.; Hearne, Z.; Chen, Z.; Li, C.-J., An Adventure in Sustainable Cross-Coupling of Phenols and Derivatives via Carbon–Oxygen Bond Cleavage. *ACS Catalysis* **2017**, *7* (1), 510-519.
230. Gowrisankar, S.; Sergeev, A. G.; Anbarasan, P.; Spannenberg, A.; Neumann, H.; Beller, M., A General and Efficient Catalyst for Palladium-Catalyzed C–O Coupling

## References

- Reactions of Aryl Halides with Primary Alcohols. *Journal of the American Chemical Society* **2010**, *132* (33), 11592-11598.
231. Harkal, S.; Kumar, K.; Michalik, D.; Zapf, A.; Jackstell, R.; Rataboul, F.; Riermeier, T.; Monsees, A.; Beller, M., An efficient catalyst system for diaryl ether synthesis from aryl chlorides. *Tetrahedron Letters* **2005**, *46* (18), 3237-3240.
232. Scott Sawyer, J., Recent Advances in Diaryl Ether Synthesis. *Tetrahedron* **2000**, *56* (29), 5045-5065.
233. Varela-Fernández, A.; Varela, J. A.; Saá, C., Ruthenium-Catalyzed Cycloisomerization of Aromatic Homo- and Bis-Homopropargylic Amines/Amides: Formation of Indoles, Dihydroisoquinolines and Dihydroquinolines. *Advanced Synthesis & Catalysis* **2011**, *353* (11-12), 1933-1937.
234. Lindstedt, E.; Stridfeldt, E.; Olofsson, B., Mild Synthesis of Sterically Congested Alkyl Aryl Ethers. *Organic Letters* **2016**, *18* (17), 4234-4237.
235. Liang, L.; Yuqiang, D., Recent Advances in the Synthesis of Thioether. *Mini-Reviews in Organic Chemistry* **2017**, *14* (5), 407-431.
236. Xia, C.; Wei, Z.; Yang, Y.; Yu, W.; Liao, H.; Shen, C.; Zhang, P., Palladium-Catalyzed Thioetherification of Quinolone Derivatives via Decarboxylative C–S Cross-Couplings. *Chemistry – An Asian Journal* **2016**, *11* (3), 360-366.
237. Leroux, F.; Jeschke, P.; Schlosser, M.,  $\alpha$ -Fluorinated Ethers, Thioethers, and Amines: Anomerically Biased Species. *Chemical Reviews* **2005**, *105* (3), 827-856.
238. Cheng, J.H.; Ramesh, C.; Kao, H.L.; Wang, Y.J.; Chan, C.C.; Lee, C.F., Synthesis of Aryl Thioethers through the N-Chlorosuccinimide-Promoted Cross-Coupling Reaction of Thiols with Grignard Reagents. *The Journal of Organic Chemistry* **2012**, *77* (22), 10369-10374.
239. Kosugi, M.; Shimizu, T.; Migita, T., Reactions of aryl halides with thiolate anions in the presence of catalytic amounts of tetrakis(triphenylphosphine)palladium preparation of aryl sulfides. *Chemistry Letters* **1978**, *7* (1), 13-14.
240. Toshihiko, M.; Tomiya, S.; Yoriyoshi, A.; Jun-ichi, S.; Yasuki, K.; Masanori, K., The Palladium Catalyzed Nucleophilic Substitution of Aryl Halides by Thiolate Anions. *Bulletin of the Chemical Society of Japan* **1980**, *53* (5), 1385-1389.
241. Murata, M.; Buchwald, S. L., A general and efficient method for the palladium-catalyzed cross-coupling of thiols and secondary phosphines. *Tetrahedron* **2004**, *60* (34), 7397-7403.
242. Fernández-Rodríguez, M. A.; Shen, Q.; Hartwig, J. F., Highly Efficient and Functional-Group-Tolerant Catalysts for the Palladium-Catalyzed Coupling of Aryl Chlorides with Thiols. *Chemistry – A European Journal* **2006**, *12* (30), 7782-7796.
243. Fernández-Rodríguez, M. A.; Shen, Q.; Hartwig, J. F., A General and Long-Lived Catalyst for the Palladium-Catalyzed Coupling of Aryl Halides with Thiols. *Journal of the American Chemical Society* **2006**, *128* (7), 2180-2181.
244. Bryan, C. S.; Braunger, J. A.; Lautens, M., Efficient Synthesis of Benzothiophenes by an Unusual Palladium-Catalyzed Vinylic C-S Coupling. *Angewandte Chemie International Edition* **2009**, *48* (38), 7064-7068.
245. Jiang, Z.; She, J.; Lin, X., Palladium on Charcoal as a Recyclable Catalyst for C–S Cross-Coupling of Thiols with Aryl Halides under Ligand-Free Conditions. *Advanced Synthesis & Catalysis* **2009**, *351* (16), 2558-2562.
246. Moreau, X.; Campagne, J. M.; Meyer, G.; Jutand, A., Palladium-Catalyzed C–S Bond Formation: Rate and Mechanism of the Coupling of Aryl or Vinyl Halides with a Thiol Derived from a Cysteine. *European Journal of Organic Chemistry* **2005**, *2005* (17), 3749-3760.

## References

247. Alvaro, E.; Hartwig, J. F., Resting State and Elementary Steps of the Coupling of Aryl Halides with Thiols Catalyzed by Alkylbisphosphine Complexes of Palladium. *Journal of the American Chemical Society* **2009**, *131* (22), 7858-7868.
248. Herrin, T. R.; Fairgrieve, J. S.; Bower, R. R.; Shipkowitz, N. L.; Mao, J. C. H., Synthesis and anti-herpes simplex activity of analogs of phosphonoacetic acid. *Journal of Medicinal Chemistry* **1977**, *20* (5), 660-663.
249. Harnden, M. R.; Parkin, A.; Parratt, M. J.; Perkins, R. M., Novel acyclonucleotides: synthesis and antiviral activity of alkenylphosphonic acid derivatives of purines and a pyrimidine. *Journal of Medicinal Chemistry* **1993**, *36* (10), 1343-1355.
250. Aarestrup, F. M.; Seyfarth, A. M.; Emborg, H.-D.; Pedersen, K.; Hendriksen, R. S.; Bager, F., Effect of Abolishment of the Use of Antimicrobial Agents for Growth Promotion on Occurrence of Antimicrobial Resistance in Fecal Enterococci from Food Animals in Denmark. *Antimicrobial Agents and Chemotherapy* **2001**, *45* (7), 2054-2059.
251. Freedman, L. D.; Doak, G. O., The Preparation And Properties Of Phosphonic Acids. *Chemical Reviews* **1957**, *57* (3), 479-523.
252. Minowa, N.; Fukatu, S.; Niida, T.; Takada, M.; Sato, K., A practical synthesis of (+)-phosphinothricine. *Tetrahedron Letters* **1983**, *24* (23), 2391-2392.
253. Toshikazu, H.; Toshio, M.; Naoto, Y.; Yoshiki, O.; Toshio, A., Palladium-catalyzed New Carbon-Phosphorus Bond Formation. *Bulletin of the Chemical Society of Japan* **1982**, *55* (3), 909-913.
254. Hirao, T.; Masunaga, T.; Ohshiro, Y.; Agawa, T., A Novel Synthesis of Dialkyl Arenephosphonates. *Synthesis* **1981**, *1981* (01), 56-57.
255. Holt, D. A.; Erb, J. M., Palladium-catalyzed phosphorylation of alkenyl triflates. *Tetrahedron Letters* **1989**, *30* (40), 5393-5396.
256. Xu, Y.; Zhang, J. I. N. G., Palladium-Catalysed Synthesis of Functionalised Alkyl Alkylarylphosphinates. *Synthesis* **1984**, *1984* (09), 778-780.
257. Xu, Y.; Li, Z. H. O. N. G.; Xia, J. I. A. Z. H. I.; Guo, H. U. I. J. U.; Huang, Y., Palladium-Catalysed Synthesis of Alkylarylphenylphosphine Oxides. *Synthesis* **1984**, *1984* (09), 781-782.
258. Montchamp, J. L.; Dumond, Y. R., Synthesis of Monosubstituted Phosphinic Acids: Palladium-Catalyzed Cross-Coupling Reactions of Anilinium Hypophosphite. *Journal of the American Chemical Society* **2001**, *123* (3), 510-511.
259. Gilbertson, S. R.; Fu, Z.; Starkey, G. W., Palladium-catalyzed synthesis of vinyl phosphines from ketones. *Tetrahedron Letters* **1999**, *40* (49), 8509-8512.
260. Oshiki, T.; Imamoto, T., Unprecedented stereochemistry of the electrophilic arylation at chiral phosphorus. *Journal of the American Chemical Society* **1992**, *114* (10), 3975-3977.
261. Tappe, F. M. J.; Trepohl, V. T.; Oestreich, M., Transition-Metal-Catalyzed C-P Cross-Coupling Reactions. *Synthesis* **2010**, *2010* (18), 3037-3062.
262. Montchamp, J. L., Recent advances in phosphorus-carbon bond formation: synthesis of H-phosphinic acid derivatives from hypophosphorous compounds. *Journal of Organometallic Chemistry* **2005**, *690* (10), 2388-2406.
263. Schwan, A. L., Palladium catalyzed cross-coupling reactions for phosphorus-carbon bond formation. *Chemical Society Reviews* **2004**, *33* (4), 218-224.
264. Toshihiko, M.; Tohru, N.; Kazuhiko, K.; Masanori, K., Convenient Preparation of Tetraarylphosphonium Halides. *Bulletin of the Chemical Society of Japan* **1983**, *56* (9), 2869-2870.

## References

265. Abbas, S.; Hayes, C. J., A Novel Palladium-Catalysed Coupling Strategy for the Rapid Synthesis of Nucleic Acid Analogues Bearing Modified Backbones. *Synlett* **1999**, 1999 (07), 1124-1126.
266. Gooßen, L. J.; Dezfuli, M. K., Practical Protocol for the Palladium-Catalyzed Synthesis of Arylphosphonates from Bromoarenes and Diethyl Phosphite. *Synlett* **2005**, 2005 (03), 445-448.
267. Zmudzka, K.; Johansson, T.; Wojcik, M.; Janicka, M.; Nowak, M.; Stawinski, J.; Nawrot, B., Novel DNA analogues with 2-, 3- and 4-pyridylphosphonate internucleotide bonds: synthesis and hybridization properties. *New Journal of Chemistry* **2003**, 27 (12), 1698-1705.
268. Kurz, L.; Lee, G.; Morgans, D.; Waldyke, M. J.; Ward, T., Stereospecific functionalization of (R)-(-)-1,1'-bi-2-naphthol triflate. *Tetrahedron Letters* **1990**, 31 (44), 6321-6324.
269. Yan, Y. Y.; RajanBabu, T. V., Highly Flexible Synthetic Routes to Functionalized Phospholanes from Carbohydrates. *The Journal of Organic Chemistry* **2000**, 65 (3), 900-906.
270. Abbas, S.; Hayes, C. J., An improved procedure for the synthesis of vinylphosphonate-linked nucleic acids. *Tetrahedron Letters* **2000**, 41 (22), 4513-4517.
271. Hirao, T.; Masunaga, T.; Ohshiro, Y.; Agawa, T., Stereoselective synthesis of vinylphosphonate. *Tetrahedron Letters* **1980**, 21 (37), 3595-3598.
272. Kalek, M.; Jezowska, M.; Stawinski, J., Preparation of Arylphosphonates by Palladium(0)-Catalyzed Cross-Coupling in the Presence of Acetate Additives: Synthetic and Mechanistic Studies. *Advanced Synthesis & Catalysis* **2009**, 351 (18), 3207-3216.
273. Kalek, M.; Stawinski, J., Pd(0)-Catalyzed Phosphorus–Carbon Bond Formation. Mechanistic and Synthetic Studies on the Role of the Palladium Sources and Anionic Additives. *Organometallics* **2007**, 26 (24), 5840-5847.
274. Kohler, M. C.; Grimes, T. V.; Wang, X.; Cundari, T. R.; Stockland, R. A., Arylpalladium Phosphonate Complexes as Reactive Intermediates in Phosphorus–Carbon Bond Forming Reactions. *Organometallics* **2009**, 28 (4), 1193-1201.
275. Rulev, A. Y., Serendipity or the art of making discoveries. *New Journal of Chemistry* **2017**, 41 (11), 4262-4268.
276. Werner, H., At Least 60 Years of Ferrocene: The Discovery and Rediscovery of the Sandwich Complexes. *Angewandte Chemie International Edition* **2012**, 51 (25), 6052-6058.
277. Roberts, R. M., Serendipity: Accidental Discoveries in Science. Wiley Science Editions: **1989**; 288.
278. Nicolaou, K. C.; Snyder, S. A.; Montagnon, T.; Vassilikogiannakis, G., The Diels–Alder Reaction in Total Synthesis. *Angewandte Chemie International Edition* **2002**, 41 (10), 1668-1698.
279. Kapdi, A. R.; Prajapati, D., Regioselective palladium-catalysed cross-coupling reactions: a powerful synthetic tool. *RSC Advances* **2014**, 4 (78), 41245-41259.
280. Gayakhe, V.; Ardhapure, A. V.; Kapdi, A. R.; Sanghvi, Y. S.; Serrano, J. L.; Schulzke, C., C-C Bond Formation: Synthesis of C5 Substituted Pyrimidine and C8 Substituted Purine Nucleosides Using Water Soluble Pd-imidate Complex. *Current Protocols in Nucleic Acid Chemistry* **2016**, 65 (1), 1.37.1-1.37.15.
281. Gayakhe, V. B., S.; Yashmeen, A.; Kapdi, A. R.; Fairlamb, I. J. S., *Palladium-Catalyzed Modification of Nucleosides, Nucleotides and Oligonucleotides*. Elsevier: 6th June 2018; 358.



## References

282. Seggio, A.; Chevallier, F.; Vaultier, M.; Mongin, F., Lithium-Mediated Zincation of Pyrazine, Pyridazine, Pyrimidine, and Quinoxaline. *The Journal of Organic Chemistry* **2007**, *72* (17), 6602-6605.
283. Murthy Bandaru, S. S.; Bhilare, S.; Chrysochos, N.; Gayakhe, V.; Trentin, I.; Schulzke, C.; Kapdi, A. R., Pd/PTABS: Catalyst for Room Temperature Amination of Heteroarenes. *Organic Letters* **2018**, *20* (2), 473-476.
284. Bhilare, S.; Bandaru, S. S. M.; Kapdi, A. R.; Sanghvi, Y. S.; Schulzke, C., Pd/PTABS: An Efficient Water-Soluble Catalytic System for the Amination of 6-Chloropurine Ribonucleoside and Synthesis of Alogliptin. *Current Protocols in Nucleic Acid Chemistry* **2018**, *74* (1), e58.
285. Bhilare, S.; Bandaru, S. S. M.; Shah, J.; Chrysochos, N.; Schulzke, C.; Sanghvi, Y. S.; Kapdi, A. R., Pd/PTABS: Low Temperature Etherification of Chloroheteroarenes. *The Journal of Organic Chemistry* **2018**.
286. Bandaru, S. S. M.; Bhilare, S.; Cardozo, J.; Chrysochos, N.; Schulzke, C.; Sanghvi, Y. S.; Gunturu, K. C.; Kapdi, A. R., Pd/PTABS: Low-Temperature Thioetherification of Chloro(hetero)arenes. *The Journal of Organic Chemistry* **2019**, *84* (14), 8921-8940.
287. Lamberth, C. D., Jürgen, Bioactive Heterocyclic Compound Classes. Wiley-VCH, Weinheim: **2012**, *2*, 670.
288. Sirohi, B.; Rastogi, S.; Dawood, S., Buparlisib in breast cancer. *Future Oncology* **2015**, *11* (10), 1463-1470.
289. Speranza, M. C.; Nowicki, M. O.; Behera, P.; Cho, C. F.; Chiocca, E. A.; Lawler, S. E., BKM-120 (Buparlisib): A Phosphatidyl-Inositol-3 Kinase Inhibitor with Anti-Invasive Properties in Glioblastoma. *Scientific Reports* **2016**, *6*, 20189.
290. Cope, C. L.; Gilley, R.; Balmanno, K.; Sale, M. J.; Howarth, K. D.; Hampson, M.; Smith, P. D.; Guichard, S. M.; Cook, S. J., Adaptation to mTOR kinase inhibitors by amplification of eIF4E to maintain cap-dependent translation. *Journal of Cell Science* **2014**, *127* (4), 788-800.
291. Sitbon, O.; Morrell, N., Pathways in pulmonary arterial hypertension: the future is here. *European Respiratory Review* **2012**, *21* (126), 321-327.
292. Mahmood, I.; Sahajwalla, C., Clinical Pharmacokinetics and Pharmacodynamics of Buspirone, an Anxiolytic Drug. *Clinical Pharmacokinetics* **1999**, *36* (4), 277-287.
293. Ruiz-Castillo, P.; Buchwald, S. L., Applications of Palladium-Catalyzed C–N Cross-Coupling Reactions. *Chemical Reviews* **2016**, *116* (19), 12564-12649.
294. Ehrentraut, A.; Zapf, A.; Beller, M., A new improved catalyst for the palladium-catalyzed amination of aryl chlorides. *Journal of Molecular Catalysis A: Chemical* **2002**, *182-183*, 515-523.
295. Neumann, H.; Brennfürer, A.; Groß, P.; Riermeier, T.; Almena, J.; Beller, M., Efficient Carbonylation of Aryl and Heteroaryl Bromides using a Palladium/Diadamantylbutylphosphine Catalyst. *Advanced Synthesis & Catalysis* **2006**, *348* (10-11), 1255-1261.
296. Michalik, D.; Kumar, K.; Zapf, A.; Tillack, A.; Arlt, M.; Heinrich, T.; Beller, M., A short and efficient synthesis of N-aryl- and N-heteroaryl-N'-(arylalkyl)piperazines. *Tetrahedron Letters* **2004**, *45* (10), 2057-2061.
297. Fleckenstein, C. A.; Plenio, H., 9-Fluorenylphosphines for the Pd-Catalyzed Sonogashira, Suzuki, and Buchwald–Hartwig Coupling Reactions in Organic Solvents and Water. *Chemistry – A European Journal* **2007**, *13* (9), 2701-2716.
298. Roiban, G. D.; Mehler, G.; Reetz, M. T., Palladium-Catalysed Amination of Aryl- and Heteroaryl Halides Using tert-Butyl Tetraisopropylphosphorodiamidite as an Easily Accessible and Air-Stable Ligand. *European Journal of Organic Chemistry* **2014**, *2014* (10), 2070-2076.

## References

299. Organ, M. G.; Abdel-Hadi, M.; Avola, S.; Dubovyk, I.; Hadei, N.; Kantchev, E. A. B.; O'Brien, C. J.; Sayah, M.; Valente, C., Pd-Catalyzed Aryl Amination Mediated by Well Defined, N-Heterocyclic Carbene (NHC)–Pd Precatalysts, PEPPSI. *Chemistry – A European Journal* **2008**, *14* (8), 2443-2452.
300. Lombardi, C.; Day, J.; Chandrasoma, N.; Mitchell, D.; Rodriguez, M. J.; Farmer, J. L.; Organ, M. G., Selective Cross-Coupling of (Hetero)aryl Halides with Ammonia To Produce Primary Arylamines using Pd-NHC Complexes. *Organometallics* **2017**, *36* (2), 251-254.
301. Wolfe, J. P.; Buchwald, S. L., A Highly Active Catalyst for the Room-Temperature Amination and Suzuki Coupling of Aryl Chlorides. *Angewandte Chemie International Edition* **1999**, *38* (16), 2413-2416.
302. Hartwig, J. F.; Kawatsura, M.; Hauck, S. I.; Shaughnessy, K. H.; Alcazar-Roman, L. M., Room-Temperature Palladium-Catalyzed Amination of Aryl Bromides and Chlorides and Extended Scope of Aromatic C–N Bond Formation with a Commercial Ligand. *The Journal of Organic Chemistry* **1999**, *64* (15), 5575-5580.
303. Walsh, K.; Sneddon, H. F.; Moody, C. J., Amination of Heteroaryl Chlorides: Palladium Catalysis or SNAr in Green Solvents? *ChemSusChem* **2013**, *6* (8), 1455-1460.
304. Bhilare, S.; Gayakhe, V.; Ardhapure, A. V.; Sanghvi, Y. S.; Schulzke, C.; Borozdina, Y.; Kapdi, A. R., Novel water-soluble phosphatriazenes: versatile ligands for Suzuki–Miyaura, Sonogashira and Heck reactions of nucleosides. *RSC Advances* **2016**, *6* (87), 83820-83830.
305. Bergamini, P.; Marvelli, L.; Marchi, A.; Bertolasi, V.; Fogagnolo, M.; Formaglio, P.; Sforza, F., New PTA (1,3,5-triaza 7-phosphaadamantane) derivatives associating zwitterionic structure and coordinative ability. *Inorganica Chimica Acta* **2013**, *398*, 11-18.
306. Mínguez, J. M.; Castellote, M. I.; Vaquero, J. J.; García-Navio, J. L.; Alvarez-Builla, J.; Castaño, O.; Andrés, J. L., Pyrrolodiazines. 2. Structure and Chemistry of Pyrrolo[1,2-a]pyrazine and 1,3-Dipolar Cycloaddition of Its Azomethine Ylides. *The Journal of Organic Chemistry* **1996**, *61* (14), 4655-4665.
307. Goyal, D.; Kaur, A.; Goyal, B., Benzofuran and Indole: Promising Scaffolds for Drug Development in Alzheimer's Disease. *ChemMedChem* **2018**, *13* (13), 1275-1299.
308. Chauhan, M.; Kumar, R., A comprehensive review on bioactive fused heterocycles as purine-utilizing enzymes inhibitors. *Medicinal Chemistry Research* **2015**, *24* (6), 2259-2282.
309. Nxumalo, W.; Dinsmore, A., Negishi coupling of pteridine-O-sulfonates. *South African Journal of Chemistry* **2013**, *66*, 00-00.
310. Barends, J.; der Linden, J. B. v.; Delft, F. L. V.; Koomen, G.-J., Palladium-Catalyzed Animation of 6-Chloropurine. Synthesis of N6-Substituted Adenosine Analogues. *Nucleosides and Nucleotides* **1999**, *18* (9), 2121-2126.
311. Lanver, A. S., H.-G., Microwave-Assisted Amination of a Chloropurine Derivative in the Synthesis of Acyclic Nucleoside Analogues. *Molecules* **2005**, *10*, 508-510.
312. Thomson, P. F.; Lagisetty, P.; Balzarini, J.; De Clercq, E.; Lakshman, M. K., Palladium-Catalyzed Aryl Amination Reactions of 6-Bromo- and 6-Chloropurine Nucleosides. *Advanced Synthesis & Catalysis* **2010**, *352* (10), 1728-1735.
313. Champeil, E.; Pradhan, P.; Lakshman, M. K., Palladium-Catalyzed Synthesis of Nucleoside Adducts from Bay- and Fjord-Region Diol Epoxides. *The Journal of Organic Chemistry* **2007**, *72* (14), 5035-5045.
314. Feng, J.; Zhang, Z.; Wallace, M. B.; Stafford, J. A.; Kaldor, S. W.; Kassel, D. B.; Navre, M.; Shi, L.; Skene, R. J.; Asakawa, T.; Takeuchi, K.; Xu, R.; Webb, D. R.; Gwaltney,

## References

- S. L., Discovery of Alogliptin: A Potent, Selective, Bioavailable, and Efficacious Inhibitor of Dipeptidyl Peptidase IV. *Journal of Medicinal Chemistry* **2007**, *50* (10), 2297-2300.
315. Awada, A.; Hendlisz, A.; Gil, T.; Bartholomeus, S.; Mano, M.; de Valeriola, D.; Strumberg, D.; Brendel, E.; Haase, C. G.; Schwartz, B.; Piccart, M., Phase I safety and pharmacokinetics of BAY 43-9006 administered for 21 days on/7 days off in patients with advanced, refractory solid tumours. *British Journal of Cancer* **2005**, *92* (10), 1855-1861.
316. Kantarjian, H. M.; Schuster, M. W.; Jain, N.; Advani, A.; Jabbour, E.; Gamelin, E.; Rasmussen, E.; Juan, G.; Anderson, A.; Chow, V. F.; Friberg, G.; Vogl, F. D.; Sekeres, M. A., A phase 1 study of AMG 900, an orally administered pan-aurora kinase inhibitor, in adult patients with acute myeloid leukemia. *American Journal of Hematology* **2017**, *92* (7), 660-667.
317. Sinha, B. K.; Kumar, A.; Mason, R. P., Nitric oxide inhibits ATPase activity and induces resistance to topoisomerase II-poisons in human MCF-7 breast tumor cells. *Biochemistry and Biophysics Reports* **2017**, *10*, 252-259.
318. Jabran, K.; Ehsanullah; Hussain, M.; Farooq, M.; Babar, M.; Dogan, M. N.; Lee, D. J., Application of bispyribac-sodium provides effective weed control in direct-planted rice on a sandy loam soil. *Weed Biology and Management* **2012**, *12* (3), 136-145.
319. Cristau, H. J.; Cellier, P. P.; Hamada, S.; Spindler, J. F.; Taillefer, M., A General and Mild Ullmann-Type Synthesis of Diaryl Ethers. *Organic Letters* **2004**, *6* (6), 913-916.
320. Marcum, J. S.; McGarry, K. A.; Ferber, C. J.; Clark, T. B., Synthesis of Biaryl Ethers by the Copper-Catalyzed Chan–Evans–Lam Etherification from Benzylic Amine Boronate Esters. *The Journal of Organic Chemistry* **2016**, *81* (17), 7963-7969.
321. Burgos, C. H.; Barder, T. E.; Huang, X.; Buchwald, S. L., Significantly Improved Method for the Pd-Catalyzed Coupling of Phenols with Aryl Halides: Understanding Ligand Effects. *Angewandte Chemie International Edition* **2006**, *45* (26), 4321-4326.
322. Anderson, K. W.; Ikawa, T.; Tundel, R. E.; Buchwald, S. L., The Selective Reaction of Aryl Halides with KOH: Synthesis of Phenols, Aromatic Ethers, and Benzofurans. *Journal of the American Chemical Society* **2006**, *128* (33), 10694-10695.
323. Parrish, C. A.; Buchwald, S. L., Palladium-Catalyzed Formation of Aryl tert-Butyl Ethers from Unactivated Aryl Halides. *The Journal of Organic Chemistry* **2001**, *66* (7), 2498-2500.
324. Lindstedt, E.; Ghosh, R.; Olofsson, B., Metal-Free Synthesis of Aryl Ethers in Water. *Organic Letters* **2013**, *15* (23), 6070-6073.
325. Platon, M.; Cui, L.; Mom, S.; Richard, P.; Saeys, M.; Hierso, J.-C., Etherification of Functionalized Phenols with Chloroheteroarenes at Low Palladium Loading: Theoretical Assessment of the Role of Triphosphane Ligands in C–O Reductive Elimination. *Advanced Synthesis & Catalysis* **2011**, *353* (18), 3403-3414.
326. Chen, G.; Chan, A. S. C.; Kwong, F. Y., Palladium-catalyzed C–O bond formation: direct synthesis of phenols and aryl/alkyl ethers from activated aryl halides. *Tetrahedron Letters* **2007**, *48* (3), 473-476.
327. Chen, Y. J.; Chen, H. H., 1,1,1-Tris(hydroxymethyl)ethane as a New, Efficient, and Versatile Tripod Ligand for Copper-Catalyzed Cross-Coupling Reactions of Aryl Iodides with Amides, Thiols, and Phenols. *Organic Letters* **2006**, *8* (24), 5609-5612.
328. Liu, Z.; Larock, R. C., Facile N-Arylation of Amines and Sulfonamides and O-Arylation of Phenols and Arenecarboxylic Acids. *The Journal of Organic Chemistry* **2006**, *71* (8), 3198-3209.
329. Ma, D.; Cai, Q., N,N-Dimethyl Glycine-Promoted Ullmann Coupling Reaction of Phenols and Aryl Halides. *Organic Letters* **2003**, *5* (21), 3799-3802.

## References

330. Takise, R.; Isshiki, R.; Muto, K.; Itami, K.; Yamaguchi, J., Decarbonylative Diaryl Ether Synthesis by Pd and Ni Catalysis. *Journal of the American Chemical Society* **2017**, *139* (9), 3340-3343.
331. Murthy Bandaru, S. S.; Bhilare, S.; Chrysochos, N.; Gayakhe, V.; Trentin, I.; Schulzke, C.; Kapdi, A. R., Pd/PTABS: Catalyst for Room Temperature Amination of Heteroarenes. *Organic Letters* **2018**, *20* (2), 473-476.
332. Sherwood, J.; Clark, J. H.; Fairlamb, I. J. S.; Slattery, J. M., Solvent effects in palladium catalysed cross-coupling reactions. *Green Chemistry* **2019**, *21* (9), 2164-2213.
333. Ramachandran, P. V.; Padiya, K. J.; Rauniyar, V.; Reddy, M. V. R.; Brown, H. C., Asymmetric synthesis of 6-(2',3',4',5',6'-pentafluorophenyl)- $\delta$ -lactones via "allyl"boranes: application for the synthesis of fluorinated analog of key pharmacophore of statin drugs. *Journal of Fluorine Chemistry* **2004**, *125* (4), 615-620.
334. Park, C.-K.; Kim, K.; Jung, S. J.; Kim, M. J.; Ahn, D. K.; Hong, S.-D.; Kim, J. S.; Oh, S. B., Molecular mechanism for local anesthetic action of eugenol in the rat trigeminal system. *PAIN* **2009**, *144* (1), 84-94.
335. Chen, G.; Feng, J.; Qiu, W.; Zhao, Y., Eugenol-modified polysiloxanes as effective anticorrosion additives for epoxy resin coatings. *RSC Advances* **2017**, *7* (88), 55967-55976.
336. Jagtap, S. A.; Monflier, E.; Ponchel, A.; Bhanage, B. M., Highly regio-selective hydroformylation of biomass derived eugenol using aqueous biphasic Rh/TPPTS/CDs as a greener and recyclable catalyst. *Molecular Catalysis* **2017**, *436*, 157-163.
337. Trita, A. S.; Over, L. C.; Pollini, J.; Baader, S.; Riegsinger, S.; Meier, M. A. R.; Gooßen, L. J., Synthesis of potential bisphenol A substitutes by isomerising metathesis of renewable raw materials. *Green Chemistry* **2017**, *19* (13), 3051-3060.
338. Kam, P. C. A.; Yarrow, M., Anabolic steroid abuse: physiological and anaesthetic considerations. *Anaesthesia* **2005**, *60* (7), 685-692.
339. Krause, A.; Hertl, A.; Muttach, F.; Jäschke, A., Phosphine-Free Stille–Migita Chemistry for the Mild and Orthogonal Modification of DNA and RNA. *Chemistry – A European Journal* **2014**, *20* (50), 16613-16619.
340. Ardhapure, A. V.; Gholap, A. K., A. R.; Schulzke, C., In Stille Cross-Coupling Reaction: Early Years to the Current State of the Art. In *Palladium-Catalyzed Modification of Nucleosides, Nucleotides and Oligonucleotides*; Kapdi, A. R., Maiti, D., Sanghvi, Y. S., Ed. Elsevier: New York, **2018**, 19-36.
341. Lorion, M. M.; Maindan, K.; Kapdi, A. R.; Ackermann, L., Heteromultimetallic catalysis for sustainable organic syntheses. *Chemical Society Reviews* **2017**, *46* (23), 7399-7420.
342. Lohr, T. L.; Marks, T. J., Orthogonal tandem catalysis. *Nature Chemistry* **2015**, *7*, 477.
343. Fogg, D. E.; dos Santos, E. N., Tandem catalysis: a taxonomy and illustrative review. *Coordination Chemistry Reviews* **2004**, *248* (21), 2365-2379.
344. Aziz, M. A.; Serya, R. A. T.; Lasheen, D. S.; Abdel-Aziz, A. K.; Esmat, A.; Mansour, A. M.; Singab, A. N. B.; Abouzid, K. A. M., Discovery of Potent VEGFR-2 Inhibitors based on Furopyrimidine and Thienopyrimidine Scaffolds as Cancer Targeting Agents. *Scientific Reports* **2016**, *6*, 24460.
345. Giofrè, S. V.; Romeo, R.; Carnovale, C.; Mancuso, R.; Cirimi, S.; Navarra, M.; Garozzo, A.; Chiacchio, M. A., Synthesis and Biological Properties of 5-(1H-1,2,3-Triazol-4-yl)isoxazolidines: A New Class of C-Nucleosides. *Molecules* **2015**, *20* (4), 5260-5275.
346. Altomare, A.; Cascarano, G.; Giacobuzzo, C.; Guagliardi, A.; Burla, M. C.; Polidori, G.; Camalli, M., SIR92 – a program for automatic solution of crystal structures by direct methods. *Journal of Applied Crystallography* **1994**, *27* (3), 435-435.

## References

347. Sheldrick, G., A short history of SHELX. *Acta Crystallographica Section A* **2008**, *64* (1), 112-122.
348. Ding, Z.; Parchment, R. E.; LoRusso, P. M.; Zhou, J.-Y.; Li, J.; Lawrence, T. S.; Sun, Y.; Wu, G. S., The Investigational New Drug XK469 Induces G2M Cell Cycle Arrest by p53-dependent and -independent Pathways. *Clinical Cancer Research* **2001**, *7* (11), 3336-3342.
349. Xia, Q. H.; Hu, W.; Li, C.; Wu, J. F.; Yang, L.; Han, X. M.; Shen, Y. M.; Li, Z. Y.; Li, X., Design, synthesis, biological evaluation and molecular docking study on peptidomimetic analogues of XK469. *European Journal of Medicinal Chemistry* **2016**, *124*, 311-325.
350. Lee, C. F.; Liu, Y. C.; Badsara, S. S., Transition-Metal-Catalyzed Coupling Reaction. *Chemistry – An Asian Journal* **2014**, *9* (3), 706-722.
351. Irshad, A.; Shagufta, Sulfones: an important class of organic compounds with diverse biological activities. *International Journal of Pharmacy and Pharmaceutical Sciences* **2015**, *7* (3).
352. Gómez, J. E.; Guo, W.; Kleij, A. W., Palladium-Catalyzed Stereoselective Formation of Substituted Allylic Thioethers and Sulfones. *Organic Letters* **2016**, *18* (23), 6042-6045.
353. Sirvent, J. A.; Lücking, U., Novel Pieces for the Emerging Picture of Sulfoximines in Drug Discovery: Synthesis and Evaluation of Sulfoximine Analogues of Marketed Drugs and Advanced Clinical Candidates. *ChemMedChem* **2017**, *12* (7), 487-501.
354. Liu, H.; Jiang, X., Transfer of Sulfur: From Simple to Diverse. *Chemistry – An Asian Journal* **2013**, *8* (11), 2546-2563.
355. Arndt, K. E.; Bland, D. C.; Irvine, N. M.; Powers, S. L.; Martin, T. P.; McConnell, J. R.; Podhorez, D. E.; Renga, J. M.; Ross, R.; Roth, G. A.; Scherzer, B. D.; Toyzan, T. W., Development of a Scalable Process for the Crop Protection Agent Isoclast. *Organic Process Research & Development* **2015**, *19* (3), 454-462.
356. Guo, Y.; Wang, X.; Fan, J.; Zhang, Q.; Wang, Y.; Zhao, Y.; Huang, M.; Ding, M.; Zhang, Y., Semisynthesis and insecticidal activity of some novel fraxinellone-based thioethers containing 1,3,4-oxadiazole moiety. *Royal Society Open Science* **2017**, *4* (12), 171053.
357. Vendetti, F. P.; Leibowitz, B. J.; Barnes, J.; Schamus, S.; Kiesel, B. F.; Abberbock, S.; Conrads, T.; Clump, D. A.; Cadogan, E.; O'Connor, M. J.; Yu, J.; Beumer, J. H.; Bakkenist, C. J., Pharmacologic ATM but not ATR kinase inhibition abrogates p21-dependent G1 arrest and promotes gastrointestinal syndrome after total body irradiation. *Scientific Reports* **2017**, *7*, 41892.
358. Honorato Pérez, J., Selexipag, a selective prostacyclin receptor agonist in pulmonary arterial hypertension: a pharmacology review. *Expert Review of Clinical Pharmacology* **2017**, *10* (7), 753-762.
359. Kuhn, M.; Falk, F. C.; Paradies, J., Palladium-Catalyzed C–S Coupling: Access to Thioethers, Benzo[b]thiophenes, and Thieno[3,2-b]thiophenes. *Organic Letters* **2011**, *13* (15), 4100-4103.
360. Herriott, A. W.; Picker, D., The Phase-Transfer Synthesis of Sulfides and Dithioacetals. *Synthesis* **1975**, *1975* (07), 447-448.
361. Ham, J.; Yang, I.; Kang, H., A Facile One-Pot Synthesis of Alkyl Aryl Sulfides from Aryl Bromides. *The Journal of Organic Chemistry* **2004**, *69* (9), 3236-3239.
362. Feng, J.; Lu, G. P.; Cai, C., Selective approach to thioesters and thioethers via sp<sup>3</sup> C–H activation of methylarenes. *RSC Advances* **2014**, *4* (97), 54409-54415.

## References

363. Nguyen, K. N.; Duus, F.; Luu, T. X. T., Benign and efficient preparation of thioethers by solvent-free S-alkylation of thiols with alkyl halides catalyzed by potassium fluoride on alumina. *Journal of Sulfur Chemistry* **2016**, *37* (3), 349-360.
364. Santoro, F.; Mariani, M.; Zaccheria, F.; Psaro, R.; Ravasio, N., Selective synthesis of thioethers in the presence of a transition-metal-free solid Lewis acid. *Beilstein Journal of Organic Chemistry* **2016**, *12*, 2627-2635.
365. Masanori, K.; Toshimi, O.; Masahiro, T.; Hiroshi, S.; Toshihiko, M., Palladium-catalyzed Reaction of Stannyl Sulfide with Aryl Bromide. Preparation of Aryl Sulfide. *Bulletin of the Chemical Society of Japan* **1985**, *58* (12), 3657-3658.
366. Eichman, C. C.; Stambuli, J. P., Transition Metal Catalyzed Synthesis of Aryl Sulfides. *Molecules* **2011**, *16* (1), 590-608.
367. Feuerstein, M.; Doucet, H.; Santelli, M., Efficient coupling of heteroaryl halides with arylboronic acids in the presence of a palladium-tetraphosphine catalyst. *Journal of Organometallic Chemistry* **2003**, *687* (2), 327-336.
368. Itoh, T.; Mase, T., A General Palladium-Catalyzed Coupling of Aryl Bromides/Triflates and Thiols. *Organic Letters* **2004**, *6* (24), 4587-4590.
369. Banerjee, S.; Das, J.; Alvarez, R. P.; Santra, S., Silica nanoparticles as a reusable catalyst: a straightforward route for the synthesis of thioethers, thioesters, vinyl thioethers and thio-Michael adducts under neutral reaction conditions. *New Journal of Chemistry* **2010**, *34* (2), 302-306.
370. Kataoka, N.; Shelby, Q.; Stambuli, J. P.; Hartwig, J. F., Air Stable, Sterically Hindered Ferrocenyl Dialkylphosphines for Palladium-Catalyzed C-C, C-N, and C-O Bond-Forming Cross-Couplings. *The Journal of Organic Chemistry* **2002**, *67* (16), 5553-5566.
371. Kondo, T.; Mitsudo, T. A., Metal-Catalyzed Carbon-Sulfur Bond Formation. *Chemical Reviews* **2000**, *100* (8), 3205-3220.
372. Cai, L.; Cuevas, J.; Peng, Y. Y.; Pike, V. W., Rapid palladium-catalyzed cross-coupling in the synthesis of aryl thioethers under microwave conditions. *Tetrahedron Letters* **2006**, *47* (26), 4449-4452.
373. Al-Mamun, M.; Zhu, Z.; Yin, H.; Su, X.; Zhang, H.; Liu, P.; Yang, H.; Wang, D.; Tang, Z.; Wang, Y.; Zhao, H., The surface sulfur doping induced enhanced performance of cobalt catalysts in oxygen evolution reactions. *Chemical Communications* **2016**, *52* (60), 9450-9453.
374. Kolpin, A.; Jones, G.; Jones, S.; Zheng, W.; Cookson, J.; York, A. P. E.; Collier, P. J.; Tsang, S. C. E., Quantitative Differences in Sulfur Poisoning Phenomena over Ruthenium and Palladium: An Attempt To Deconvolute Geometric and Electronic Poisoning Effects Using Model Catalysts. *ACS Catalysis* **2017**, *7* (1), 592-605.
375. Mandal, B.; Basu, B., Recent advances in S-S bond formation. *RSC Advances* **2014**, *4* (27), 13854-13881.
376. Siedle, G.; Kersting, B., Synthesis and Crystal Structures of Palladium(II) Complexes of Macrobicyclic Azathiaether Ligands. *Zeitschrift für anorganische und allgemeine Chemie* **2003**, *629* (12-13), 2083-2090.
377. Anilkumar, A. S. A. M. T. A. P. T. G., Recent advances in copper-catalyzed C-S cross-coupling reactions. *ARKIVOC* **2005**, (1), 1-28.
378. Yang, B.; Wang, Z.-X., Transition-Metal-Free Cross-Coupling of Aryl and Heteroaryl Thiols with Arylzinc Reagents. *Organic Letters* **2017**, *19* (22), 6220-6223.
379. Mandal, B.; Basu, B., Recent advances in S-S bond formation. *RSC Advances* **2016**, *4* (27), 1375-1381.

## References

380. Mu, S.; Liu, H.; Zhang, L.; Wang, X.; Xue, F.; Zhang, Y., Synthesis and Biological Evaluation of Novel Thioether Pleuromutilin Derivatives. *Biological and Pharmaceutical Bulletin* **2017**, *40* (8), 1165-1173.
381. Bhilare, S.; Murthy Bandaru, S. S.; Shah, J.; Chrysochos, N.; Schulzke, C.; Sanghvi, Y. S.; Kapdi, A. R., Pd/PTABS: Low Temperature Etherification of Chloroheteroarenes. *The Journal of Organic Chemistry* **2018**, *83* (21), 13088-13102.
382. Bhujabal, Y. B.; Vadagaonkar, K. S.; Kapdi, A. R., Pd/PTABS: Catalyst for Efficient C–H (Hetero)Arylation of 1,3,4-Oxadiazoles Using Bromo(Hetero)Arenes. *Asian Journal of Organic Chemistry* **2019**, *8* (2), 289-295.
383. Guilbaud, J.; Labonde, M.; Selmi, A.; Kammoun, M.; Cattey, H.; Pirio, N.; Roger, J.; Hierso, J. C., Palladium-catalyzed heteroaryl thioethers synthesis overcoming palladium dithiolate resting states inertness: Practical road to sulfones and NH-sulfoximines. *Catalysis Communications* **2018**, *111*, 52-58.
384. Malyshev, D. A.; Scott, N. M.; Marion, N.; Stevens, E. D.; Ananikov, V. P.; Beletskaya, I. P.; Nolan, S. P., Homogeneous Nickel Catalysts for the Selective Transfer of a Single Arylthio Group in the Catalytic Hydrothiolation of Alkynes. *Organometallics* **2006**, *25* (19), 4462-4470.
385. Mann, G.; Baranano, D.; Hartwig, J. F.; Rheingold, A. L.; Guzei, I. A., Carbon–Sulfur Bond-Forming Reductive Elimination Involving sp-, sp<sup>2</sup>-, and sp<sup>3</sup>-Hybridized Carbon. Mechanism, Steric Effects, and Electronic Effects on Sulfide Formation. *Journal of the American Chemical Society* **1998**, *120* (36), 9205-9219.
386. Eichman, C. C.; Stambuli, J. P., Zinc-Mediated Palladium-Catalyzed Formation of Carbon–Sulfur Bonds. *The Journal of Organic Chemistry* **2009**, *74* (10), 4005-4008.
387. Lücking, U.; Jautelat, R.; Krüger, M.; Brumby, T.; Lienau, P.; Schäfer, M.; Briem, H.; Schulze, J.; Hillisch, A.; Reichel, A.; Wengner, A. M.; Siemeister, G., The Lab Oddity Prevails: Discovery of Pan-CDK Inhibitor (R)-S-Cyclopropyl-S-(4-[[4-[[[(1R,2R)-2-hydroxy-1-methylpropyl]oxy]-5-(trifluoromethyl)pyrimidin-2-yl]amino}phenyl)sulfoximide (BAY 1000394) for the Treatment of Cancer. *ChemMedChem* **2013**, *8* (7), 1067-1085.
388. Yoneda, F.; Tsukuda, K.; Kawazoe, M.; Sone, A.; Koshiro, A., Synthesis and properties of 1-Benzothiopyrano[2,3-d]-pyrimidine-2,4-(3H)diones (10-thia-5-deazaflavins). *Journal of Heterocyclic Chemistry* **1981**, *18* (7), 1329-1334.
389. Agrofoglio, L. A.; Gillaizeau, I.; Saito, Y., Palladium-Assisted Routes to Nucleosides. *Chemical Reviews* **2003**, *103* (5), 1875-1916.
390. Bookser, B. C.; Matelich, M. C.; Ollis, K.; Ugarkar, B. G., Adenosine Kinase Inhibitors. 4. 6,8-Disubstituted Purine Nucleoside Derivatives. Synthesis, Conformation, and Enzyme Inhibition. *Journal of Medicinal Chemistry* **2005**, *48* (9), 3389-3399.
391. Tuncbilek, M.; Kucukdumlu, A.; Guven, E. B.; Altiparmak, D.; Cetin-Atalay, R., Synthesis of novel 6-substituted amino-9-(β-d-ribofuranosyl)purine analogs and their bioactivities on human epithelial cancer cells. *Bioorganic & Medicinal Chemistry Letters* **2018**, *28* (3), 235-239.
392. Laufer, S. A.; Domeyer, D. M.; Scior, T. R. F.; Albrecht, W.; Hauser, D. R. J., Synthesis and Biological Testing of Purine Derivatives as Potential ATP-Competitive Kinase Inhibitors. *Journal of Medicinal Chemistry* **2005**, *48* (3), 710-722.
393. Jacobson, K. A.; van Galen, P. J.; Williams, M., Adenosine receptors: pharmacology, structure-activity relationships, and therapeutic potential. *Journal of medicinal chemistry* **1992**, *35* (3), 407-422.
394. Wang, M.; Qiao, Z.; Zhao, J.; Jiang, X., Palladium-Catalyzed Thiomethylation via a Three-Component Cross-Coupling Strategy. *Organic Letters* **2018**, *20* (19), 6193-6197.

## References

395. Eyer, L.; Nencka, R.; Huvarová, I.; Palus, M.; Joao Alves, M.; Gould, E. A.; De Clercq, E.; Růžek, D., Nucleoside Inhibitors of Zika Virus. *The Journal of Infectious Diseases* **2016**, *214* (5), 707-711.
396. House, H. O.; Larson, J. K., The use of .beta.-ketone sulfones as synthetic intermediates. *The Journal of Organic Chemistry* **1968**, *33* (1), 61-65.
397. Md. Ashraful Alam, K. S., Aklima Jahan, Md. Wahab Khan, Md. Mosharef H Bhuiyan, Mohammad Sayed Alam and Mohammed Mahbubul Matin, Synthesis, Reactions and Medicinal Importance of Cyclic Sulfone Derivatives: A Review. *Nat Prod Chem Res* **2018**, *6* (6), 350.
398. Kotha, S.; Khedkar, P.; Ghosh, A. K., Synthesis of Symmetrical Sulfones from Rongalite: Expansion to Cyclic Sulfones by Ring-Closing Metathesis. *European Journal of Organic Chemistry* **2005**, *2005* (16), 3581-3585.
399. García Mancheño, O.; Bistri, O.; Bolm, C., Iodinane- and Metal-Free Synthesis of N-Cyano Sulfilimines: Novel and Easy Access of NH-Sulfoximines. *Organic Letters* **2007**, *9* (19), 3809-3811.
400. Degennaro, L.; Tota, A.; De Angelis, S.; Andresini, M.; Cardellicchio, C.; Capozzi, M. A.; Romanazzi, G.; Luisi, R., A Convenient, Mild, and Green Synthesis of NH-Sulfoximines in Flow Reactors. *European Journal of Organic Chemistry* **2017**, *2017* (44), 6486-6490.
401. Bull, J. A.; Degennaro, L.; Luisi, R., Straightforward Strategies for the Preparation of NH-Sulfox-imines: A Serendipitous Story. *Synlett* **2017**, *28* (19), 2525-2538.
402. Tota, A.; Zenzola, M.; Chawner, S. J.; John-Campbell, S. S.; Carlucci, C.; Romanazzi, G.; Degennaro, L.; Bull, J. A.; Luisi, R., Synthesis of NH-sulfoximines from sulfides by chemoselective one-pot N- and O-transfers. *Chemical Communications* **2017**, *53* (2), 348-351.
403. Kiesel, B. F.; Shogan, J. C.; Rachid, M.; Parise, R. A.; Vendetti, F. P.; Bakkenist, C. J.; Beumer, J. H., LC-MS/MS assay for the simultaneous quantitation of the ATM inhibitor AZ31 and the ATR inhibitor AZD6738 in mouse plasma. *Journal of Pharmaceutical and Biomedical Analysis* **2017**, *138*, 158-165.
404. Jones, B. C.; Markandu, R.; Gu, C.; Scarfe, G., CYP-Mediated Sulfoximine Deimination of AZD6738. *Drug Metabolism and Disposition* **2017**, *45* (11), 1133-1138.
405. Terrier, B.; Pagnoux, C.; Perrodeau, É.; Karras, A.; Khouatra, C.; Aumaître, O.; Cohen, P.; Decaux, O.; Desmurs-Clavel, H.; Maurier, F.; Gobert, P.; Quémeneur, T.; Blanchard-Delaunay, C.; Bonnotte, B.; Carron, P.-L.; Daugas, E.; Ducret, M.; Godmer, P.; Hamidou, M.; Lidove, O.; Limal, N.; Puéchal, X.; Mouthon, L.; Ravaud, P.; Guillevin, L., Long-term efficacy of remission-maintenance regimens for ANCA-associated vasculitides. *Annals of the Rheumatic Diseases* **2018**, *77* (8), 1150-1156.
406. Axelrad, J. E.; Lichtiger, S.; Yajnik, V., Inflammatory bowel disease and cancer: The role of inflammation, immunosuppression, and cancer treatment. *World Journal of Gastroenterology* **2016**, *22* (20), 4794-4801.
407. Frisch, M. J.; Trucks, G. W.; Schlegel, H. B.; Scuseria, G. E.; Robb, M. A.; Cheeseman, J. R.; Scalmani, G.; Barone, V.; Petersson, G. A.; Nakatsuji, H.; Li, X.; Caricato, M.; Marenich, A. V.; Bloino, J.; Janesko, B. G.; Gomperts, R.; Mennucci, B.; Hratchian, H. P.; Ortiz, J. V.; Izmaylov, A. F.; Sonnenberg, J. L.; Williams; Ding, F.; Lipparini, F.; Egidi, F.; Goings, J.; Peng, B.; Petrone, A.; Henderson, T.; Ranasinghe, D.; Zakrzewski, V. G.; Gao, J.; Rega, N.; Zheng, G.; Liang, W.; Hada, M.; Ehara, M.; Toyota, K.; Fukuda, R.; Hasegawa, J.; Ishida, M.; Nakajima, T.; Honda, Y.; Kitao, O.; Nakai, H.; Vreven, T.; Throssell, K.; Montgomery Jr., J. A.; Peralta, J. E.; Ogliaro, F.; Bearpark, M. J.; Heyd, J. J.; Brothers, E. N.; Kudin, K. N.; Staroverov, V. N.; Keith, T. A.;



## References

- Kobayashi, R.; Normand, J.; Raghavachari, K.; Rendell, A. P.; Burant, J. C.; Iyengar, S. S.; Tomasi, J.; Cossi, M.; Millam, J. M.; Klene, M.; Adamo, C.; Cammi, R.; Ochterski, J. W.; Martin, R. L.; Morokuma, K.; Farkas, O.; Foresman, J. B.; Fox, D. J. *Gaussian 16 Rev. C.01*, Wallingford, CT, **2016**.
408. Zhou, Y.-p.; Wang, M.-y.; Fang, S.; Chen, Y.; Liu, J.-y., DFT studies on the mechanism of palladium catalyzed arylthiolation of unactive arene to diaryl sulfide. *RSC Advances* **2016**, *6* (22), 18300-18307.
409. Yang, Y.-M.; Dang, Z.-M.; Yu, H.-Z., Density functional theory investigation on Pd-catalyzed cross-coupling of azoles with aryl thioethers. *Organic & Biomolecular Chemistry* **2016**, *14* (19), 4499-4506.
410. Guerriero, A.; Peruzzini, M.; Gonsalvi, L., Coordination chemistry of 1,3,5-triaza-7-phosphatricyclo[3.3.1.1]decane (PTA) and derivatives. Part III. Variations on a theme: Novel architectures, materials and applications. *Coordination Chemistry Reviews* **2018**, 328-361.
411. 1,3,5-Triaza-7-Phosphatricyclo[3.3.1.1,3,7]Decane and Derivatives. In *Inorganic Syntheses*, 40-45.
412. Schäfer, S.; Frey, W.; Hashmi, A. S. K.; Cmrecki, V.; Luquin, A.; Laguna, M., Synthesis, characterization and solubility studies of four new highly water soluble 1,3,5-triaza-7-phosphaadamantane (PTA) salts and their gold(I) complexes. *Polyhedron* **2010**, *29* (8), 1925-1932.
413. Gandy, M. N.; Raston, C. L.; Stubbs, K. A., Towards aryl C–N bond formation in dynamic thin films. *Organic & Biomolecular Chemistry* **2014**, *12* (26), 4594-4597.
414. Ho, L. A.; Raston, C. L.; Stubbs, K. A., Transition-Metal-Free Cross-Coupling Reactions in Dynamic Thin Films To Access Pyrimidine and Quinoxaline Analogues. *European Journal of Organic Chemistry* **2016**, *2016* (36), 5957-5963.
415. Lester, R. P.; Bham, T.; Bousfield, T. W.; Lewis, W.; Camp, J. E., Exploring the Reactivity of 2-Trichloromethylbenzoxazoles for Access to Substituted Benzoxazoles. *The Journal of Organic Chemistry* **2016**, *81* (24), 12472-12477.
416. Cioffi, C. L.; Lansing, J. J.; Yüksel, H., Synthesis of 2-Aminobenzoxazoles Using Tetramethyl Orthocarbonate or 1,1-Dichlorodiphenoxymethane. *The Journal of Organic Chemistry* **2010**, *75* (22), 7942-7945.
417. Wang, Q.; Schreiber, S. L., Copper-Mediated Amidation of Heterocyclic and Aromatic C–H Bonds. *Organic Letters* **2009**, *11* (22), 5178-5180.
418. Lahm, G.; Opatz, T., Unique Regioselectivity in the C(sp<sup>3</sup>)–H  $\alpha$ -Alkylation of Amines: The Benzoxazole Moiety as a Removable Directing Group. *Organic Letters* **2014**, *16* (16), 4201-4203.
419. Kallitsakis, M. G.; Hadjipavlou-Litina, D. J.; Peperidou, A.; Litinas, K. E., Synthesis of 4-hydroxy-3-[(E)-2-(6-substituted-9H-purin-9-yl)vinyl]coumarins as lipoxxygenase inhibitors. *Tetrahedron Letters* **2014**, *55* (3), 650-653.
420. A. M. Ahmed, S. M. A. E.-H., M. G. A. Saleah, A. A. H. Abdel-Rahman, Copper Electropolishing in the Presence of Purine Derivatives. *Asian J. Chem* **2013**, *25* (3), 1512-1520.
421. Hirokawa, Y.; Kinoshita, H.; Tanaka, T.; Nakamura, T.; Fujimoto, K.; Kashimoto, S.; Kojima, T.; Kato, S., Pleuromutilin derivatives having a purine ring. Part 1: New compounds with promising antibacterial activity against resistant Gram-positive pathogens. *Bioorganic & Medicinal Chemistry Letters* **2008**, *18* (12), 3556-3561.
422. Sengmany, S., Selective mono-amination of dichlorodiazines. *Tetrahedron* **2015**, *71*, 4859-4867..
423. Kono, M.; Matsumoto, T.; Imaeda, T.; Kawamura, T.; Fujimoto, S.; Kosugi, Y.; Odani, T.; Shimizu, Y.; Matsui, H.; Shimojo, M.; Kori, M., Design, synthesis, and biological

## References

- evaluation of a series of piperazine ureas as fatty acid amide hydrolase inhibitors. *Bioorganic & Medicinal Chemistry* **2014**, *22* (4), 1468-1478.
424. Marugan, J. J.; Zheng, W.; Motabar, O.; Southall, N.; Goldin, E.; Westbroek, W.; Stubblefield, B. K.; Sidransky, E.; Aungst, R. A.; Lea, W. A.; Simeonov, A.; Leister, W.; Austin, C. P., Evaluation of Quinazoline Analogues as Glucocerebrosidase Inhibitors with Chaperone Activity. *Journal of Medicinal Chemistry* **2011**, *54* (4), 1033-1058.
425. Qu, G. R.; Zhao, L.; Wang, D. C.; Wu, J.; Guo, H. M., Microwave-promoted efficient synthesis of C6-cyclo secondary amine substituted purine analogues in neat water. *Green Chemistry* **2008**, *10* (3), 287-289.
426. Raouf, A.; Depledge, P.; Hamilton, N. M.; Hamilton, N. S.; Hitchin, J. R.; Hopkins, G. V.; Jordan, A. M.; Maguire, L. A.; McGonagle, A. E.; Mould, D. P.; Rushbrooke, M.; Small, H. F.; Smith, K. M.; Thomson, G. J.; Turlais, F.; Waddell, I. D.; Waszkowycz, B.; Watson, A. J.; Ogilvie, D. J., Toxoflavins and Deazaflavins as the First Reported Selective Small Molecule Inhibitors of Tyrosyl-DNA Phosphodiesterase II. *Journal of Medicinal Chemistry* **2013**, *56* (16), 6352-6370.
427. Dudkin, S.; Iaroshenko, V. O.; Sosnovskikh, V. Y.; Tolmachev, A. A.; Villinger, A.; Langer, P., Synthesis and reactivity of 5-polyfluoroalkyl-5-deazaalloxazines. *Organic & Biomolecular Chemistry* **2013**, *11* (32), 5351-5361.
428. Zhang, Z.; Wallace, M. B.; Feng, J.; Stafford, J. A.; Skene, R. J.; Shi, L.; Lee, B.; Aertgeerts, K.; Jennings, A.; Xu, R.; Kassel, D. B.; Kaldor, S. W.; Navre, M.; Webb, D. R.; Gwaltney, S. L., Design and Synthesis of Pyrimidinone and Pyrimidinedione Inhibitors of Dipeptidyl Peptidase IV. *Journal of Medicinal Chemistry* **2011**, *54* (2), 510-524.
429. Cuenca, A., Micellar effects upon the alkaline hydrolysis of 2-(3-nitrophenoxy)quinoxaline. Effects of cationic head groups. *Tetrahedron* **1997**, *53* (37), 12361-12368.
430. Egi, M.; Liebeskind, L. S., Heteroaromatic Thioether–Organostannane Cross-Coupling. *Organic Letters* **2003**, *5* (6), 801-802.
431. Novakova, V.; Miletin, M.; Filandrová, T.; Lenčo, J.; Růžička, A.; Zimcik, P., Role of Steric Hindrance in the Newman-Kwart Rearrangement and in the Synthesis and Photophysical Properties of Arylsulfanyl Tetrapyrazinoporphyrazines. *The Journal of Organic Chemistry* **2014**, *79* (5), 2082-2093.
432. Haider, N.; van der Plas, H. C., Intramolecular diels-alder reactions of pyrazines with alkynylphenyl moieties as side-chain dienophiles. *Tetrahedron* **1990**, *46* (10), 3641-3650.
433. Juntae, M.; Dahan, E.; Hong, K. S.; Ho, L. P., Palladium-catalyzed Carbon–Sulfur Cross-coupling Reactions of Aryl Chlorides with Indium Tris(organothioliates). *Chemistry Letters* **2011**, *40* (9), 980-982.
434. Sreedhar, B.; Reddy, P. S.; Reddy, M. A., Catalyst-Free and Base-Free Water-Promoted S<sub>N</sub>Ar Reaction of Heteroaryl Halides with Thiols. *Synthesis* **2009**, *2009* (10), 1732-1738.
435. Anderson, R. G.; Jett, B. M.; McNally, A., Selective formation of heteroaryl thioethers via a phosphonium ion coupling reaction. *Tetrahedron* **2018**, *74* (25), 3129-3136.
436. Delia, T. J.; Kanaar, J. B.; Knefelkamp, E., Diarylthiopyrimidines and pyridines: Synthesis and biological activity. *Journal of Heterocyclic Chemistry* **2002**, *39* (2), 347-350.
437. Huang, L.-K.; Cherng, Y.-C.; Cheng, Y.-R.; Jang, J.-P.; Chao, Y.-L.; Cherng, Y.-J., An efficient synthesis of substituted cytosines and purines under focused microwave irradiation. *Tetrahedron* **2007**, *63* (24), 5323-5327.

## References

438. Daniela, U.; Carlo, F. M.; Marco, R.; Giulia, C.; Immacolata, S.; Teodora, B.; Alessandra, M. A.; Giovanna, S., Substrate Specificity of a Purine Nucleoside Phosphorylase from *Aeromonas hydrophila* Toward 6-Substituted Purines and its Use as a Biocatalyst in the Synthesis of the Corresponding Ribonucleosides. *Current Organic Chemistry* **2015**, *19* (22), 2220-2225.
439. Maloney, K. M.; Kuethe, J. T.; Linn, K., A Practical, One-Pot Synthesis of Sulfonylated Pyridines. *Organic Letters* **2011**, *13* (1), 102-105.
440. Yrowell, H. N.; Elion, G. B., Synthesis of 6(1-Methyl-4-nitro-5-[4,5-14 C]imidazolyl)thiopurinc (azathioprine). *Journal of Heterocyclic Chemistry* **1973**, *10* (6), 1017-1019.

## List of Scientific Contributions

**Book Chapter:** Phosphine Ligands Bearing the Ferrocenyl Skeleton: Advances in Catalytic Cross-couplings. **Siva Sankar Murthy Bandaru**,\* Jean-Cyrille Hierso,\* Anant R. Kapdi, Carola Schulzke, Shatrughn Bhilare, Jagruth Shah, Julien Roger in “**Ligands for Cross-Coupling Reactions**”. WILEY-VCH.

## Publications

1. “1,3,5-Triaza-7- phosphadamantane (PTA) derived caged phosphines for palladium-catalyzed selective functionalization of nucleosides and heteroarenes”, **Siva Sankar Murthy Bandaru**, S. Bhilare, C. Schulzke, A. R. Kapdi. *Chem. Rec.* **2021**, *21*, 188.
2. “Pentathiepins: A Novel Class of Glutathione Peroxidase 1 Inhibitors That Induce Oxidative Stress, Loss of Mitochondrial Membrane Potential and Apoptosis in Human Cancer Cells”. Steven Behnisch-Cornwell, **Siva Sankar Murthy Bandaru**, Martin Napierkowski, Lisa Wolff, Muhammad Zubair, Claudia Urbainsky, Christopher Lillig, Carola Schulzke, Patrick J Bednarski. *ChemMedChem* 2020 published ASAP (*Very Important Paper, selected for journal cover page*)
3. “Carbazole-Based N-Heterocyclic Carbenes for the Promotion of Copper-Catalyzed Palladium-Free Homo-/Hetero-Coupling of Alkynes and Sonogashira Reactions”. Tejpalsingh Ramsingh Girase, Shatrughn Bhilare, **Siva Sankar Murthy Bandaru** Nicolas Chrysochos Prof. Carola Schulzke Dr. Yogesh S. Sanghvi Dr. Anant R. Kapdi; *Asian J. Org. Chem.* 2020, *9*, 274–291.
4. “Pd/PTABS: Low Temperature Thioetherification of Chloro(Hetero)Arenes”. **Siva Sankar Murthy Bandaru**, Shatrughn Bhilare, Nicolas Chrysochos, Carola Schulzke, Anant R. Kapdi; *J. Org. Chem.* 2019, *84*, 14, 8921–8940.
5. “Pd/PTABS: Catalyst for Room Temperature Amination of Heteroarenes”. **Siva Sankar Murthy Bandaru**, Shatrughn Bhilare, Nicolas Chrysochos, Vijay Gayakhe, Ivan Trentin, Carola Schulzke, and Anant R. Kapdi; *Org. Lett.* 2018, *20*, 473–476.
6. “Crystal structure of 4-(pyrazin-2-yl)morpholine”. **Siva Sankar Murthy Bandaru**, Anant Ramakant Kapdi and Carola Schulzke; *Acta Cryst.* 2018. E74, 137–140.
7. “Synthesis of 9-arylalkynyl- and 9-aryl-substituted benzo[b]quinolizinium derivatives by Palladium-mediated cross-coupling reactions”. **Siva Sankar Murthy Bandaru**, Darinka Dzubiel, Heiko Ihmels, Mohebodin Karbasiyou, Mohamed M. A. Mahmoud and Carola Schulzke; *Beilstein J. Org. Chem.* 2018, *14*, 1871– 1884.

8. “Pd/PTABS: An Efficient Water-Soluble Catalytic System for the Amination of 6-Chloropurine Ribonucleoside and Synthesis of Alogliptin”. Shatrughn Bhilare, **Siva Sankar Murthy Bandaru**, Anant R. Kapdi, Yogesh S. Sanghvi, and Carola Schulzke; *Current Protocols in Nucleic Acid Chemistry*, 2018, 58.
9. “Pd/PTABS: Low Temperature Etherification of Chloroheteroarenes”. Shatrughn Bhilare, **Siva Sankar Murthy Bandaru**, Jagrut Shah, Nicolas Chrysochos, Carola Schulzke, Yogesh S. Sanghvi, and Anant R. Kapdi; *J. Org. Chem.* 2018, 83, 13088–13102.

#### Scientific conferences: Posters and Talk

- **Talk:** Presented the results of “*Pd/PTABS: A Potent Catalyst for C-N and C-O Cross Coupling with Heteroarenes*” in conference “Norddeutsche Doktorandenkolloquium NDDK 2018” at TU Braunschweig on September 3<sup>rd</sup> 2018.
- **Poster presentation** on “*Mo (IV) Mono (dithiolen) complexes derived through oxidative ageing of bis(dithiolene) molybdenum complexes*”; **Siva Sankar Murthy Bandaru**, Yulia Borozdina, Carola Schulzke in “FEBS Combined & Practical and Lecture Course Chemistry of Metals in Biological Systems”, at LOUVAIN-LA-NEUVE, Belgium – May 2017- Best concept award for green chemistry.
- **Poster presentation** on “*Pd/PTABS: Potent and Selective Catalyst for C-X (X = C, N, O, and S) Cross-Coupling with Heteroarenes*”. **Bandaru S.S.M.**, Schulzke C. , Bhilare S., Kapdi A. at OMCOS catalysis conference at Heidelberg 2019.

Eigenständigkeitserklärung

Hiermit erkläre ich, dass diese Arbeit bisher von mir weder an der Mathematisch-Naturwissenschaftlichen Fakultät der Universität Greifswald noch einer anderen wissenschaftlichen Einrichtung zum Zwecke der Promotion eingereicht wurde.

Ferner erkläre ich, dass ich diese Arbeit selbstständig verfasst und keine anderen als die darin angegebenen Hilfsmittel und Hilfen benutzt und keine Textabschnitte eines Dritten ohne Kennzeichnung übernommen habe.

Unterschrift des Promovenden

## Lebenslauf

### Lebenslauf

Name Siva Sankar Murthy Bandaru

Geboren 5<sup>th</sup> August 1985

Stattsangehörigkeit Indisch

#### Schulbesuch

1990-1999 Primary School (I-IX)

1999-2000 Secondary School Examination (X level)

2000-2002 Higher Secondary School Examination (10+2 level)

#### Studium

2002-2005 B.Sc in Chemie, Andhra University, Visakhapatnam, Indien.

2005-2007 M.Sc in Organische Chemie, Andhra University, Visakhapatnam, Indien.

2009-2010 P.G. Diploma in Clinical Research, Institute of Clinical Research India, Hyderabad, Indien.

2012-2015 M.Sc in Bioorganische Chemie, University Siegen, Deutschland.

#### Arbeitserfahrung

2007-2009 Scientific Manager, Abbott Pharmaceuticals, GOA & Hyderabad, Indien.

2009-2010 Business Manager, Astra Zeneca Pharmaceuticals, Hyderabad, Indien.

2010-2012 Scientific Manager, Merck Sharp & Dohme Pharmaceuticals, Hyderabad, Indien.

#### Promotion

10.2015-...2020 Institut für Biochemie, University Greifswald, Deutschland unter der Leitung von Prof. Dr Carola Schulzke.

PhD Thesis Title: **“Molybdenum Mediated Synthesis of Pentathiepins – Potent Cytotoxic and Antimicrobial agents and Discovery of Novel Pd/PTABS Catalyst for The Synthesis of Pharmaceutically Relevant Drug Molecules via C–N, C–O, and C–S Cross-coupling”**.

## ACKNOWLEDGEMENT

*Dreaming and desiring to reach significant milestones in life is not sufficient enough, there should be someone who foresees your aspirations, believes and give an opportunity. I would like to express my most profound appreciation to my supervisor prof. Dr. rer. nat. Carola Schulzke for showing such belief and great support. During my tenure of PhD, in her guidance, I got a chance to learn commitment towards science, planning, organization and most importantly, being composed and patience in every situation. I deeply indebted to her, the completion of my dissertation would not have been possible without the support and nurturing of prof. Dr. rer. nat. Carola Schulzke.*

*In modern-day science, collaborations are critical ingredients of success. I am incredibly grateful to work with Prof. Dr Patrick J. Bednarski (pharmacy), Dr. med. Jürgen Bohnert (Klinikum) from University Greifswald and for their support. I would also like to extend my deepest gratitude to Dr Anant R. Kapdi from ICT Mumbai, India. Beyond the cooperation partner, he inspired me in many ways via his discussions, ideology and approach towards science and academics. I thank his PhD students Dr Shatrughn A. Bhilare, Dr Vijay Gayakhe, for their knowledge sharing and constructive criticism.*

*A healthy working environment is quite essential for anyone to succeed, especially for international students. I would like to extend my sincere thanks to all my working colleagues Dr Yulia Borozdina, Dr Ashta C. Ghosh, Dr Christian Fischer, Lina Fischer, Dr Claudia Schindler, Dr Nicolas Chrysochos, Dr Ivan Trentin, Dr Mohsen Ahmadi, and students from Prof. Dr Patrick J. Bednarski's group Dr Steven Behnisch-Cornwell, Martin Napierkowski, Lisa Wolff. Special thanks to Dr Christian Fischer for his assistance in practical courses. I also had the great pleasure of working with our young colleagues Jevy Correia, Benedict Elvers, Maryam Khosraneh, and Sebastian Pättsch, and I wish them all the best for their future endeavours.*

*I would like to recognize the effort that I received from my Master and Bachelor students Jo Henry Judernatz, Hanna Marutz. On this occasion, I would like to thank our technical staff, Gabriele Thede, Marlen Redies, Johanna Möller, Anke Grünert, and Hoffmann, who never wavered in their support.*

*Finally, my deep and sincere gratitude to my family, my wife Ashwani, my little hero Shivansh and my parents and sister for their continuous and unparalleled love, help and support. A special thanks to my forever friend Vishnu Srinivas Murthy for his extended moral and scientific support (Thanks macha).*

*Thank you every one!*

*Siva Sankar Murthy Bandaru*